THE UNIVERSITY OF CHICAGO

CONDENSED PHASE ADSORPTION AND REACTIVITY: EXTRATERRESTRIAL ICES, ISOTOPIC ENRICHMENT, OLEFIN OXIDATION, AND NERVE AGENT SIMULANTS

A DISSERTATION SUBMITTED TO
THE FACULTY OF THE DIVISION OF THE PHYSICAL SCIENCES
IN CANDIDACY FOR THE DEGREE OF
DOCTOR OF PHILOSOPHY

DEPARTMENT OF CHEMISTRY

BY
MICHELLE BRANN

CHICAGO, ILLINOIS
AUGUST 2022

Table of Contents

List of Figures

List of Tables

Acknowledgments

Thank you to my committee members Sarah and Andrei, for supporting me in my scientific and departmental endeavors.

Thank you to Maria, Melinda, Vera, Tanya, and Vera for everything you do behind the scenes so that I'm able to focus on my research.

Thank you to Bentley and John for keeping the lights on and ensuring that my chamber bounces back from any building irregularities.

Thank you to the Sibener group (Sibener-ites, Sibe-nerds): Kevin, Grant, Kevin (K2), Jon, Darren, Jeff, Jacob, Becca, Ross, Tim, Sarah B., Ali, Julia, Rachael, Sarah W., Caleb, Josh, Stephen, Blake, Jasper, Mark, and Michael. What a group of absolute winners and I'm glad we shared time in the windowless basement together.

Thank you to Becca, for teaching about our instrument and all of its quirks in such good spirits. You allowed me to fail and learn in an encouraging environment. I couldn't have asked for a better lab partner or afternoon walking buddy.

Thank you Tim and Rachael, for appreciating my sass and always providing life and experimental wisdom.

Thank you Ali, for being my first graduate school (and Sibener group) friend and making the first year coursework bearable.

Thank you to my advisor Steve Sibener, who immediately convinced me to move to Chicago and join the group. You've given me the space to grow as an independent scientist while also providing life and experimental advice while needed.

Thank you to Cece, Maria, and Milena. You've made Chicago feel like home and I always look forward to our camping trips and overly competitive game nights.

Thank you to the movie night crew (Baroui, Fauzia, Josh, Kim) for making me an honorary Park group member and providing enough commentary that I can follow a Marvel movie. I'm glad we

encourage each other to take breaks and enjoy good food.

Thank you to Addie, Diana, Korin, Olivia, Raji, Rebecca, Regan, Sinead, and Teddy for accepting me with all my quirks. You've all kept me sane from afar and I'm fortunate that our deep conversations have continued beyond high school and college.

Thank you to my dad for always being so proud, providing freedom to explore, and teaching me the art of working hard and playing hard.

Thank you to my mom for encouraging my curiosity, to read, and go after opportunities you never dreamed possible. Although you won't have the opportunity to read this thesis, I know that you never doubted that I would finish my PhD.

Thank you to David for being competitive, but also a built in friend and comrade. I'm so lucky to have a twin to go through the world of science with.

Thank you Prajwal for always being my number one fan even from across an ocean. I love that you never doubt what I'm capable of and are always encouraging me to go after my dreams. I'm so grateful for our life together and look forward to the future.

Abstract

This thesis probes interfacial dynamics of complex molecular thin films. This work is focused on sticking and hydrogen bonding of small molecules on and in astrophysical ices, differential condensation of isotopologues, oxidation of an important industrial alkene, and thermal destruction of a chemical warfare agent. While these systems vary greatly, they all focus on elucidating how film structure and morphology impact adsorption and reactivity. When examining different astrophysical ices (crystalline, non-porous amorphous solid water, and porous amorphous-solid water), we find that ice morphology vastly changed the interaction with small hydrocarbons. Not only do the pores allow more multiple collisions yielding a higher sticking probability for methane, the undercoordinated water molecules in the porous films form more hydrogen bonds with acetone. When switching away from ices to methane isotopologues, we determine that film composition vastly impacts adsorption behavior. By making a small mass adjustment from methane to heavy methane, we find that there is preferential condensation for heavy methane (CD_4). This finding, confirmed from both experimental as well as novel theoretical gas-surface chemical trajectory simulations indicates a better energy transfer for the heavier isotopologue. We next focus on a larger hydrocarbon (propene) to facilitate increased chemical complexity upon exposure to oxygen. We conclude that oxygen is only able to diffuse through and react with the ordered film indicating the important role that film structure and morphology play in limiting reactivity even for reactions with low barriers. Lastly, we determined the mechanism for the destruction of the nerve agent simulant, diisopropyl methylphosphonate (DIMP), under atmospheric and oxygen depleted conditions which can directly inform chemical warfare mitigation strategies.

Chapter 1

Introduction

The studies in this thesis all probe condensed phase chemistry occurring on a surface ∼crystal∼ under ultra high vacuum. The low pressure ultra high vacuum environment (**Chapter 2**) ensures that the surface is free from other gases that could interfere with the system of interest. Condensed phase systems are ubiquitous in nature and have important applications in astrophysical, isotopic enrichment, industrial chemical production, and national defense, but are also much more complicated than their gas phase counter parts. For condensed phase systems, the neighboring molecules may impact reaction barriers and branching ratios. Additionally, the film structure can vary in morphology to allow or impede reactant diffusion thereby changing sticking probability and reactivity. As evident throughout the chapters in this thesis the condensed phase systems all vastly impact the reaction dynamics in a manner that would not be present in the gas phase.

In **Chapter 3** we examine how water ice morphology can impact the initial adsorption and embedding behavior for gaseous high energy projectiles. Measuring sticking probability is important since it is often the first step before any recombination or addition reactions can occur resulting in more complex organic molecules. We find that more methane ended up sticking onto the porous amorphous solid water films compared to nonporous or crystalline films and that this sticking probability is not dependent on the pore size or orientation relative to the substrate. This indicates that that porous films are more efficient at dissipating energy and that the morphology of frozen films may greatly impact the uptake and thus subsequent concentration and reactivity of adsorbates, outgassing of comets, and thermal and electrical processing.

In **Chapter 4**, we examine how water ice morphology impacts substrate interactions and hydrogen bonding. We find that there is increased hydrogen bonding interactions between acetone and porous amorphous solid water films as compared to acetone and the nonporous or crystalline films. Since there was a reduction of hydrogen bonding that occurs for even more porous films, we conclude that acetone is unable to diffuse within the water structure and access surface sites with dangling bonds in the pores. This is further evidence that morphology of the ice critically impacts not only adsorption behavior, but also the strength of surface-adsorbate interactions and thus, subsequent reactivity of incident molecules.

In addition to film structure impacting impacting adsorption and surface-adsorption interactions, there can also be differential condensation due to slight mass differences between the condensate and projectile. As discussed in **Chapter 5**, we examine the initial sticking probabilities for methane and heavy methane on methane and heavy methane surfaces using both experimental as well as numerical simulations. We find that preferential sticking and condensation occurs for heavy methane when striking the surface in comparison to the outcome for methane. We concluded this from both experimental as well as theoretical gas-surface chemical trajectory simulations. Ongoing work (**Appendix Subsection A4.2**) is exploring this model system in more detail to provide insight into energy transfer and lattice vibrations. Aside from astrophysical applications, this result offers a new method for isotope enrichment via preferential condensation of heavier isotopes and isotopes and formed the basis for a patent application.

To further understand how order and structure in condensed films can impact reactivity, we next examine the oxidative reactivity of thin films of propene in **Chapter 6**. There is a particular interest towards propene epoxidation due to its industrial importance. We found that propene readily reacts with ground state atomic oxygen ($O(^3P)$), to form the epoxide and propanal. Moreover, propene film thickness and ordering in the multilayer does influence oxygen penetration and mobility within the film, and therefore the resulting product formation. This emphasizes the limitations of condensed-phase astrophysical reactions that rely on reactant diffusion; film composition, morphology, and thickness can significantly limit reactivity despite low reaction barriers.

Finally, in **Chapter 7** we employ a novel setup to explore the destruction of the nerve agent simulant DIMP under atmospheric conditions. This work is connected to ongoing efforts within the Defense Threat Reduction Agency to detect and remove dangerous organophosphonate compounds such as Sarin and previous studies in the Sibener Group under vacuum conditions.[1,2] We found that under rapid laser heating conditions, that smaller products are more abundant at higher ablation temperatures. Additionally, oxygen plays a significant role in simulant degredation and is incorporated directly into the product of the fragmented simulant. Such knowledge can be implemented into chemical warfare agent mitigation strategies.

Chapter 2

Experimental Methods

2.1 Main UHV Chamber

All experiments in this thesis except for those in **Chapter 7** are performed in an ultrahigh vacuum (UHV) chamber (TNB-X, Perkin Elmer) with a base pressure of 10^{-10} Torr as measured by a Baynard-Alpert nude ion gauge. This base pressure was slightly higher (10^{-9}) Torr for the ice experiments in **Chapter 3** and **Chapter 4** due to frequent dosing of water. The chamber pressure is maintained by 260 L s $^{-1}$ turbomolecular pump (HiPace 300, Pfeiffer Vacuum), backed by a 3 L s^{-1} dry scroll pump (nXDS10i, Edwards Vacuum). There is also additional cryopumping due to a cold sample manipulator (down to 18 K) that increases the chamber's pumping capacity and helps to keep a low base pressure.

As shown in **Figure 2.1**, the UHV chamber contains a suite of different analytical techniques and sample configures *in situ*. In the center is a 1 cm^2 Au(111) single-crystal, the sample substrate for all experiments performed in this chamber. The crystal is mounted on a five-axis manipulator (x-, y-, and z-translation, polar rotation, and precession around a small internal diameter). The chamber is divided into two vertical levels. The lower level (**Figure 2.1, left**), is situated so that the crystal is aligned to allow for concurrent exposure to the supersonic molecular beam and analysis via Reflection Absorption Infrared Spectroscopy (RAIRS, **Subsection 2.2**)). This is the default crystal configuration since it enables collection of detailed, time-resolved data of dynamics occurring on the surface. Also on this level is a quadrupole mass spectrometer (QMS; QMG 112, Balzers) for performing time-of-flight analysis and characterizing the molecular beam (**Subsection 2.3.1**). Aside from the beam there are two ports to introduce gases into the chamber: the directed doser (MDC), and the leak valve (Varian). The directed doser is the main method of depositing water onto the crystal. The leak valve, located at the back of the chamber, is commonly used to backfill the chamber with Ar during sputtering (**Subsection 2.4.2**), but also saw use in **Chapter 3** as an additional method to dose water with a unique morphology onto the crystal. The details of

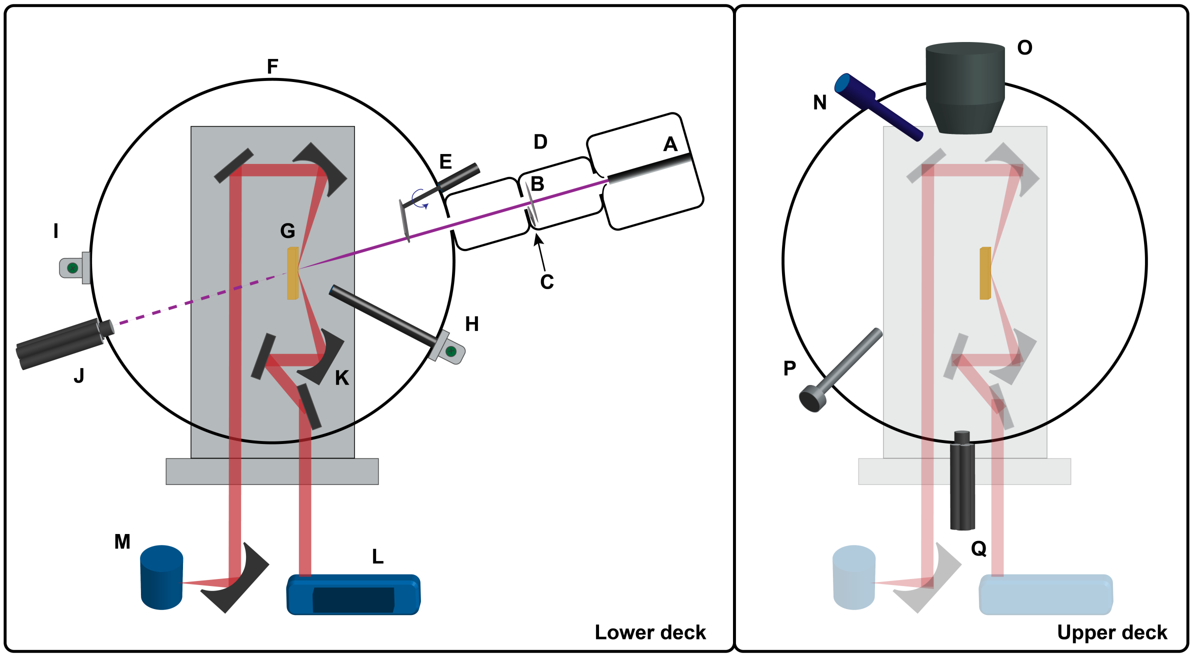

Figure 2.1: Schematic of the main chamber. The instrumentation in the main chamber is in two vertical levels. The lower layer (left) is used for RAIRS and molecular beam exposure. The upper level (right) is used for XPS, sputtering, and mass spectrometry.

A - Molecular beam source
B - Chopper (beam modulation)
C - Flag for timing exposure
D - Differential pumping stages
E - Rotatable flag
F - UHV chamber
G - Au(111) sample
H - Directed doser
I - Leak valve
J - Inline QMS
K - RAIRS optics
L - FTIR spectrometer
M - MCT/A detector
N - X-ray source
O - Cylindrical mirror analyzer
P - Ion gun for sputtering
Q - Residual gas analyzer

film preparation are discussed in more detail in **Subsection 2.4.3**.

The upper level (**Figure 2.1, right**), is used for X-ray photoelectron spectroscopy (XPS, **Subsection 2.2.2**) and sample cleaning via Ar^+ ion sputtering (**Subsection 2.4.2**). It also contains a second mass spectrometer (RGA 300, Sanford Research Systems) that is used for residual gas monitoring, temperature programmed desorption, and the King and Wells measurements (**Subsection 2.2.3**).

2.2 Chamber Instrumentation

As discussed in the previous section (**Section 2.1**), the UHV chamber contains optics for RAIRS, a flag for King and Wells, an X-ray source, and a differentially pumped supersonic molecular beamline. These components work in concert to analyze species entering the chamber, and probe reaction dynamics of films on the surface of the Au(111) crystal. RAIRS and King and Wells are used throughout this thesis to fully characterize adsorption and reactivity of these films and will be discussed below. XPS is also briefly discussed although it is not the main analytical technique of choice.

2.2.1 Reflection Absorption Infrared Spectroscopy (RAIRS)

Reflection Absorption Infrared Spectroscopy (RAIRS) follows the principles as Fourier Transform Infrared Spectroscopy (FT-IR), but uses a highly reflective-metallic surface and glancing angle IR to probe thin films. In addition to providing spectroscopic information for films down to a monolayer thickness, RAIRS also provides orientation of molecules on the substrate.

In general, the intensity of an IR absorption band increases with the strength of the electric field causing that absorption.[3] However, for a highly reflective-metallic surface, the incident IR wave combines with the reflective wave from the electric field at the surface, producing a standing wave that induces the IR absorption.[4] The strength of this standing wave on the surface is a result of the polarization of the incident light beam as well as the incident angle. In order to get significant signal, RAIRS requires p-polarized radiation. The phase shift for s-polarized light is always 180 degrees regardless of the incident angle resulting in no standing wave at the surface (**Figure 2.2a**).[4] However, for p-polarized radiation there is constructive interference for the electric field components which results in a net signal enhancement.[5]

Greenler[6] mathematically solved boundary conditions of the electric and magnetic field for both s and p-polarization radiation for a metal covered by a thin isotropic, homogenous adlayer. As shown in (**Figure 2.2c**) below[7] for p-polarized radiation, the reflectance changes as a function

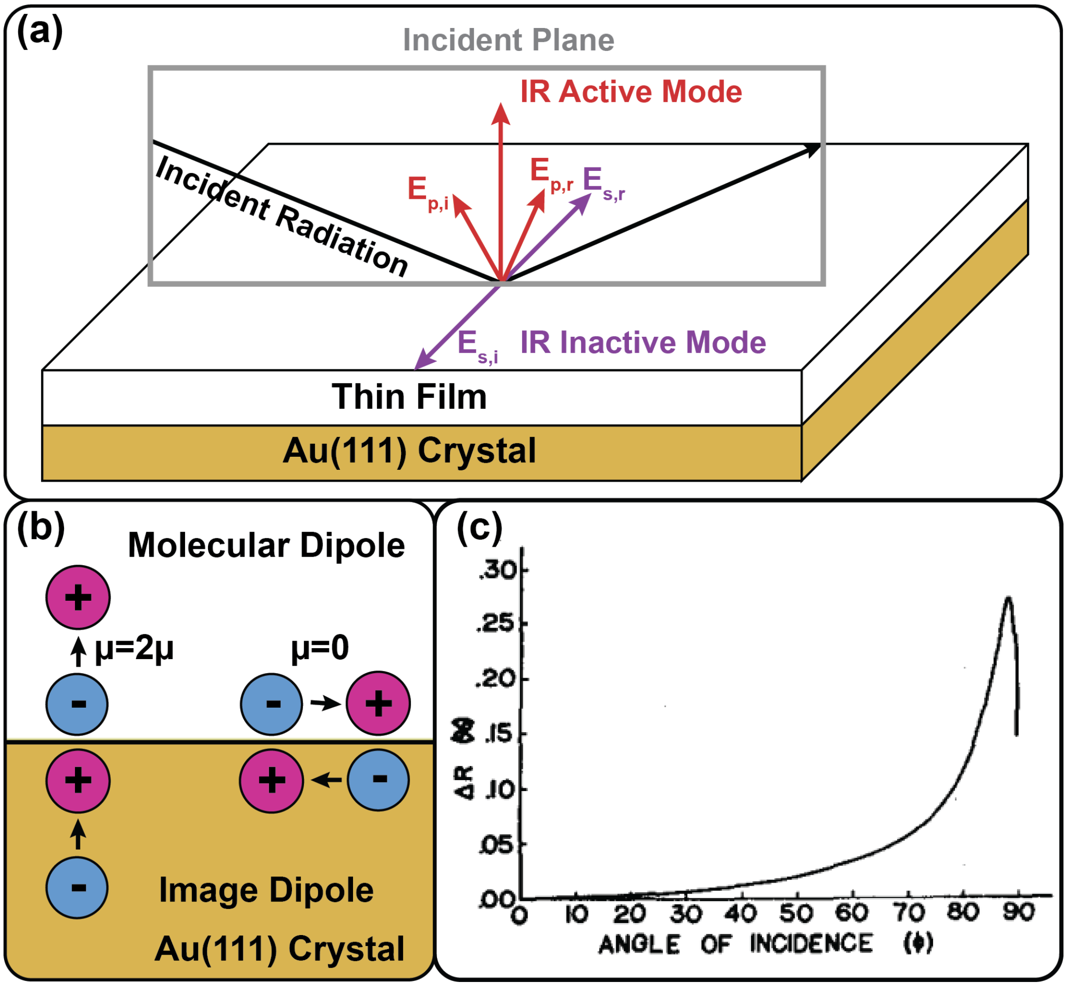

Figure 2.2: Theoretical description of RAIRS. (a) Only p-polarized light can generate an appreciable standing wave at the surface of a reflective substrate. (b) Dipoles must be oriented perpendicular to the surface in order to be detected by RAIRS. (c) Maximum reflectance is observed when using p-polarized radiation at oblique incident angles (reproduced from ref. [6]).

of incident angle by the following **Equation 2.1**:

$$\frac{\triangle R_P}{R_P} = \frac{8\pi l}{\lambda} \; sin\phi \; tan\phi \; Im\left\{ -\frac{1}{\epsilon_2} \right\} \tag{2.1}$$

In **Equation 2.1** l is the thickness of the adlayer, λ is the wavelength of the radiation, ϕ is the angle of incidence, and ϵ_2 is the complex dielectric constant of the adsorbed layer. This expression verifies (**Figure 2.2c**) and confirms that when using p-polarized radiation, the max signal enhancement occurs when ϕ the angle of incidence, is $\sim 87°$.[8]

One consequence of using a metallic substrate and examining solid adsorbates is that the radiation by a molecule adsorbed on a metal surface is also influenced by the dielectric behavior of the metal as well as an interaction between the electric field and molecule's dipole moment.[9] A metal requires that the potential is equivalent across the surface since the electric field inside a perfect conductor is zero at electrostatic equilibrium.[10] To maintain this behavior, we can imagine that a molecular dipole appearing on the surface induces an equal and opposite image dipole below the surface. This leads to screening and cancelling out of dipole moments parallel to the surface, and imposes a strict surface selection rule (**Figure 2.2b**).[11]

Second, the RAIRS surface selection rule is confirmed when considering the absorption intensity:[12]

$$E \bullet \mu = \mid E \mid \mid \mu \mid cos\theta \tag{2.2}$$

In **Equation 2.2** above, θ is the angle between the direction of polarization of the electric field vector (E) and the direction of the dipole vector (μ). Due to this cos θ term parallel vectors ($\theta = 0$) result in a maximum absorption intensity, while perpendicular vectors ($\theta = 90^\circ$) result in zero absorption intensity. When employing p-polarized light, the incident electric field is normal to the surface; therefore, dipoles that are aligned with the surface (90° relative to the incident light) will result in no absorption intensity (**Figure 2.2b**). RAIRS can only detect modes that are IR active and have component of their dipole perpendicular to the surface.[13] Thus, RAIRS uniquely allows for identification of different average molecular orientations within the film in addition to chemical species identification and environmental interaction discernible from FT-IR.

The RAIRS setup takes into account these considerations by using a reflective Au(111) substrate, and optics in order to get maximum signal enhancement by employing p-polarized light that is perpendicular to the substrate prior to incidence at a glancing angle. As shown in **Figure 2.3** Infrared light from a commercial FT-IR spectrometer (Nicolet 6700, Thermo Fischer Scientific) is polarized and focused in a nitrogen-purged area outside of the UHV chamber. Afterwards, the light enters the UHV chamber where custom parabolic mirrors on the diving board direct the polarized light so that the beam is focused onto the crystal at incident angle of 75°. The reflected light is

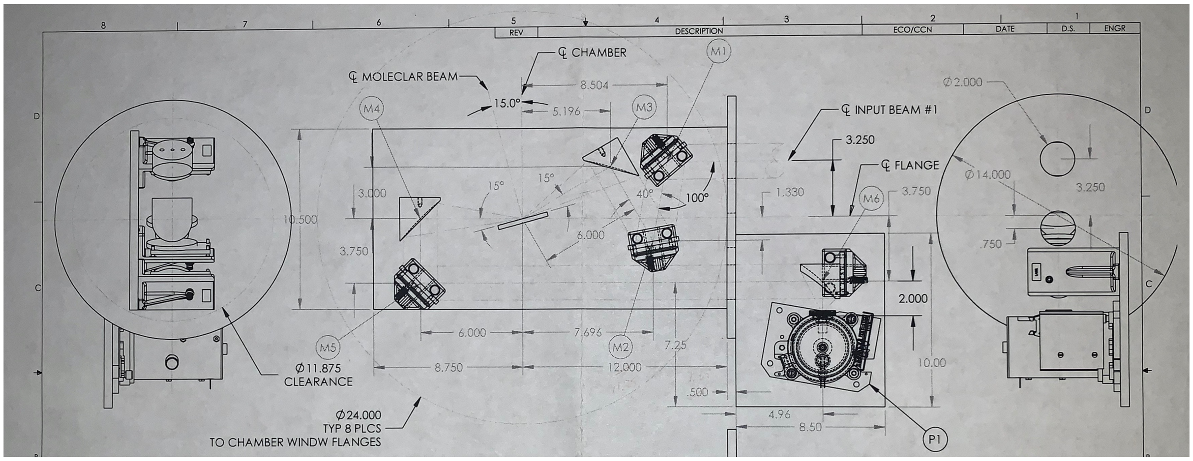

Figure 2.3: RAIRS schematic. Infrared light is polarized and focused (Input Beam #1) where it enters the UHV Chamber. Inside there are a series of parabolic mirrors (M1-M5) that direct the light to the center of the crystal and back out of the chamber into the MCT/A detector (P1).

directed outside of the chamber and detected using a liquid-nitrogen cooled mercury cadmium telluride detector (MCT/A) which provides high signal intensity over the 4000 - 650 cm^{-1} spectral range. For this thesis, spectra are averages of 50-500 scans obtained using 2 or 4 cm^{-1} resolution.

2.2.2 X-ray Photoelectron Spectroscopy (XPS)

We primarily use XPS to qualitatively obtain chemical composition information about the thin films studied and to check for crystal cleanliness after sputtering. XPS is a surface-sensitive technique based on the photoelectric effect. In general, a beam of X-ray photons bombards the surface with enough energy to eject core electrons from the first 10-20 angstroms of the sample into vacuum. Due to energy conservation, the measured kinetic energy (KE_{elec}) of the ejected electrons can be used to determine the characteristic binding energies (E_B).[14,15] Although the work function (ϕ_{spec}) is unknown, we take that into account by normalizing all spectra to the assignment of the $4f_{5/2}$ and $4f_{7/2}$ photoemission peaks of gold at 87.63 and 83.95 eV, respectively:[16]

$$KE_{elec} = hv - E_B - \phi_{spec} \tag{2.3}$$

Each element has unique core electron binding energies, so XPS can provide a complete elemental analysis of the surface. Additionally, chemical bonding and other such molecular interactions can change these binding energies, which makes XPS data useful in characterizing a molecule's chemical environment.

For XPS, we expose the sample to X-rays with an average energy of 1486.6 eV from a Al Kα X-ray source (04-153, Perkin Elmer) positioned at 45° from the sample. We detect the energy of ejected electrons by a cylindrical mirror analyzer (15-255G, Perklin Elmer) approximately 1-2 inches from the crystal surface. It is important to note that X-ray irradiation can damage thin films. Thus, XPS was primarily used to confirm initial characterization for films that were subsequently discarded or for reacted films at the end of an experiment and is often not presented in this thesis. XPS, however, was commonly employed after sputtering (**Subsection 2.4.2**) to check for the presence of impurities on the Au(111) crystal.

2.2.3 King and Wells

King and Wells is a standard vacuum technique that measures the sticking probability for a gaseous molecule onto a surface of interest.[17,18] King and Well is the main method of data collection for the methane study in **Chapter 3**. Generally, this beam reflectivity technique is used to accurately measure coverage-dependent sticking probabilities as well as provide information about binding affinity.[19] As will be discussed later on in **Chapters 3 and 5**, we employed King and Wells to gain information about initial sticking for the first few molecules incident on to the D_2O substrate or CH_4 or CD_4 substrate.

We conduct a typical King and Wells experiment using a RGA out of line with the beam to collect signal intensity for the desired mass as a function of time. A representative trial for CH_4 on top of D_2O is shown in **Figure 2.4** where m/z=15 for CH_4. The experiment begins with monitoring the background signal prior to introducing any CH_4 into the chamber (P_1). Next, the CH_4 beam is introduced into the chamber, but with a flag in front of the substrate. This pressure rise is the full indirect CH_4 flux (P_2). Then the flag is removed, at which point CH_4 molecules begin sticking to the surface (P_3). The initial sticking probability (S) is thus calculated as:

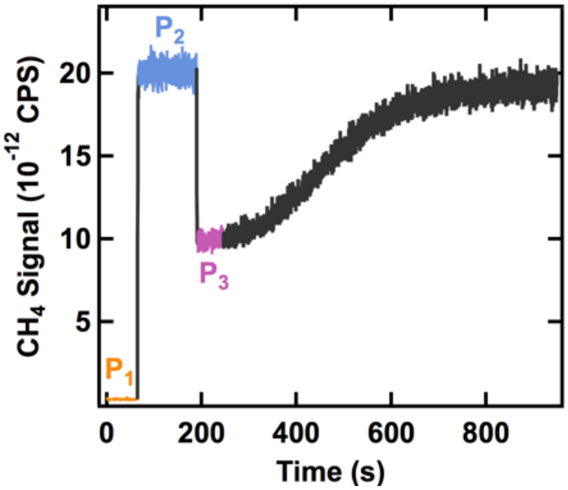

Figure 2.4: Representative King and Wells experiment. CH_4 signal (m/z=15) monitored with the RGA during a representative King and Wells experiment conducted at a surface temperature of 33.5 K. P_1 (orange) is the background CH_4 signal; P_2 (blue) is the full CH_4 flux with flag blocking the substrate; P_3 (pink) is CH_4 adsorption with flag removed.

$$S = \frac{(P_2 - P_3)}{(P_2 - P_1)} \tag{2.4}$$

Over time, the CH_4 signal rises back up to the blocked value as the available surface sites become filled and CH_4 can no longer adsorb onto the surface. More specific details about this type of measurement on the CH_4/ice system will be discussed in **Chapter 3** and the CH_4/CD_4 ice system will be discussed in **Chapter 5**.

2.3 The Supersonic Beamline

The main UHV chamber is connected via a manually operated gate valve to a triply-differentiated pumped supersonic molecular beamline. The supersonic beamline is technique commonly used in both gas and condensed phase research[20] and generates collimated, collision-free atoms or molecules with well-defined kinetic energies. Additionally, supersonic beamlines are highly customizable with regards to the molecule and energy of interest.

Our particular setup, shown in **Figure 2.5**, consists of one source chamber followed by two additional chambers of differential pumping. The beam first expands into the source chamber and

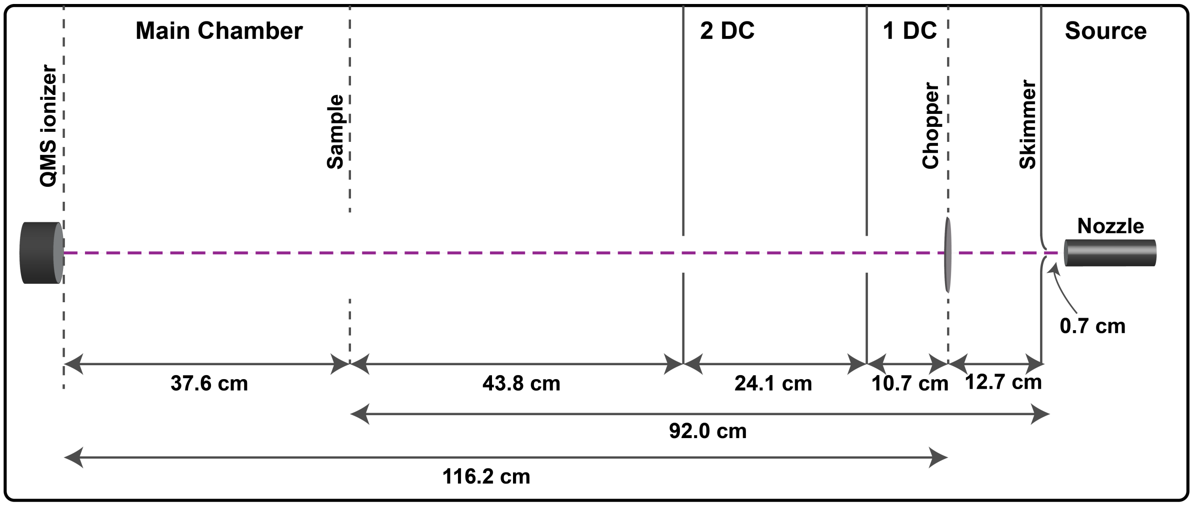

Figure 2.5: Schematic of the supersonic molecular beamline. The gas in the beamline expands through the nozzle to travel through a skimmer, two differentially pumped chambers, and into the main UHV chamber. The chopper in the 1DC modulates the beam for time-of-flight analysis by the in-line QMS.

passes through conical skimmer (0.5 mm, Gentry) that is located 7 mm from the beam nozzle exit aperature. The source chamber contains a 8000 L s^{-1} diffusion pump (VHS-400, Varian) that is backed by a 19 L s^{-1} single-stage rotary vane pump (Duo 65 MC, Pfeiffer Vacuum) coupled to a 175 L s^{-1} Roots blower (WKP 500AM, Pfeiffer Vacuum) to maintain a base pressure of 5×10^{-7} Torr with the beam off (no gas flow). After passing through the skimmer which selects for the centerline of the beam, the gas travels through the first and second differential chambers (1DC and 2DC). In the 1 DC, there is a 1200 L s^{-1} diffusion pump (VHS-4, Varian), while the 2DC has a 200 L s^{-1} turbomolecular pump (TPU-240, Pfeiffer Vacuum). Both chambers are backed together by 7 L s^{-1} dual stage rotary vane pump (Duo 20 M, Pfeiffer Vacuum) which maintain base pressures of 2×10^{-8} and 3×10^{-9} for the 1DC and 2DC respectively. Lastly, the beam travels through a 2.3 mm aperature into the main chamber where the beam spot size on the crystal is approximately 2 mm.

2.3.1 *Time-of-Flight (TOF) Analysis*

For each experiment involving beam exposure, we characterize the velocity and energy distributions of the gas species with a standard time-of-flight (TOF) techniques using an in-line quadrupole mass spectrometer (QMS, QMG 112, Balzers). Beam modulation occurs by a variable-speed, mechanical shopping wheel located in the 1DC. The chopper rotates at a frequency of 100 Hz. Such modulation is from a RC circuit that splits the output from a frequency signal generator (651A Test Oscillator, Hewlett-Packard) into two 90° out-of-phase signals. After amplification by a stereo receiver (XGA-3000, Gemini), the signals travel to a hystersis-synchronous motor that drives the chopper. The chopper is mounted on a linear motion vacuum feedthrough that can be manually adjusted with a micrometer to easily adjust into patterns for for beam modulation or out of the beam's path during experiments. Although there are multiple patterns, the work in this thesis only uses the 50% duty-cycle square waveform, and the 1% duty cycle single shot waveform.

For TOF studies of the beam's component's, the 1% duty cycle modulation chops the beam into packets that travel 116.2 cm downstream into the QMS detector in-line with the beam in the back of the UHV chamber. The signal then passes through a 90° off-axis secondary electron multiplier (SEM; QMA 120), a pre-amplification stage (VT120, Ortec), and additional amplification (Model 771, Phillips Scientific) and discrimination stages (Model 123, LRS), prior to being counted with a multi-channel analyzer (MCS-PLUS-OPT2, Ortec) in the computer. Counting is triggered by an infrared LED passing through the same chopper slit as the beam and and is detected with a photodiode (United Detector Technologies).

As seen in **Figure 2.6**, the QMS collects raw signal intensity as a function of time. The first step to get a velocity distribution is to convert the time data on the x-axis to velocity by dividing the beam path distance (L, 116.2 cm) by the time. The raw signal intensity in counts must be converted to counts per second (cps) based on the known counting bin's size set by the MCA. Next, the signal is converted from the time (t) to the velocity (v) domain using the Jacobian transformation:

$$n(t)dt = n\left(\frac{L}{t}\right)dv(t) = -\frac{L}{t^2}n(v)dt \tag{2.5}$$

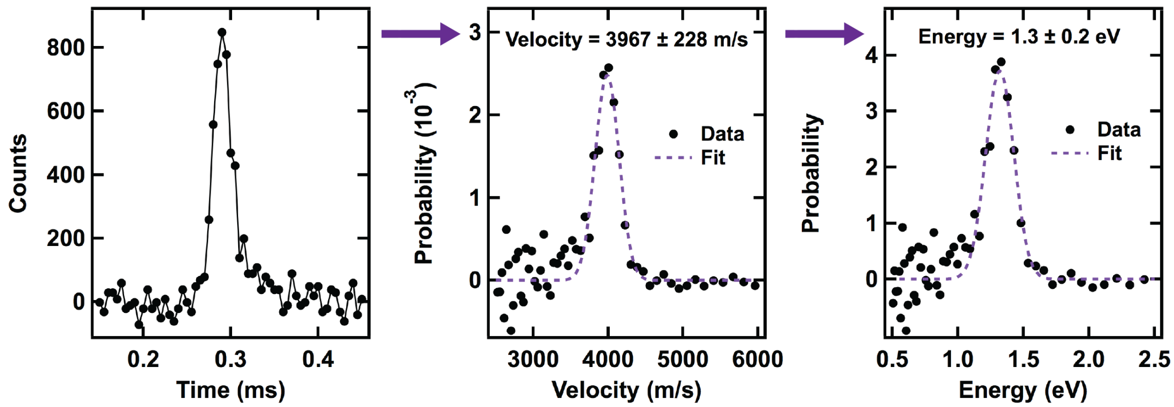

Figure 2.6: Representative TOF-MS. Raw signal intensity is converted to the velocity domain, plotted as a function of beam velocity and energy, and fit to the appropriate theoretical probability distribution (see text). 1% CH_4 seeded in H_2 at 400 K is chosen as an example.

$$n(v) \sim \frac{n(t)}{v^2} \tag{2.6}$$

We then divide this value by velocity a third time to account for the inverse proportionally between the QMA's detector ionization efficiency and velocity. This is due to the factor that the detector measures particle number density which varies with velocity.

$$n(v) \sim \frac{n(t)}{v^2} = \frac{\left[n_{den}(t)/v^2\right]}{v} = \left[n_{den}(t)/v^3\right] \tag{2.7}$$

Following this processing, the data are ultimately fit to the theoretical velocity distribution for a supersonic molecular beam,[21] to determine the average velocity. It is important to note that the above analysis does not include deconvolution for the finite width of the chopper slit. Since the slit width is much smaller than the measured beam distribution widths, it is appropriate to neglect.

$$n(v) \sim v^3 exp\left[\frac{(v - {v_0}^2)}{a^2}\right] \tag{2.8}$$

2.3.2 *Beam Flux Analysis*

In addition to knowing the beam velocity, it is also necessary to calculate the flux (# of molecules) in the beam hitting the surface per second in order to accurately determine kinetic processes on the surface during exposure. Since we often use seeded, multi-component beams, we have to first calibrate to a neat beam containing the gas of interest. To do so, we monitor the pressure rise in the chamber with a nude Bayard-Albert ion gauge calibrated to N_2. After waiting for the pressure to reach a steady value, we can assume that molecular flow into and out of the chamber (by pumping) are equivalent.Then, the gas flow rate (Q) can be defined as the change in pressure volume over the change in time:[22]

$$Q = \frac{d(PV)}{dt} \tag{2.9}$$

Assuming constant pressures, the flow rate can be simplified and rearranged using the ideal gas law. The volumetric flow rate $\frac{dV}{dt}$ is equivalent to the pumping speed S, a known value for any commercial pump on our instrument.

$$Q = \frac{dV}{dt} = \frac{dN}{dt}\frac{1}{kT} = P \cdot S \tag{2.10}$$

Additionally, the flux into the chamber (Φ, cm^{-2}, s^{-1}) is defined as the change in number of molecules per unit time per unit area ($\frac{dN}{dt}\frac{1}{A}$), so that **Equation 2.10** can be written as:

$$\Phi = \frac{P \cdot S}{kT \cdot A} \tag{2.11}$$

Here, P is the change in pressure upon introduction of the beam into the chamber, and A is the beam spot size on our crystal. However, in order to get a quantitative value for Φ, we still need to make two additional corrections. We have to take into account for the variable sensitivity of the ion gauge (using the ratio of the ionization cross sections for N_2 and the gas of interest). Then, we change S into an "effective pumping speed" that accounts for the conductance (C) of the chamber geometry leading to the pump inlet:

$$\frac{1}{EPS} = \frac{1}{C} + \frac{1}{S} \tag{2.12}$$

Our chamber is connected to the turbomolecular pump via one cylindrical tube, so C under molecular flow conditions is:[23,24]

$$C(L\,s^{-1}) = 3.81\left(\frac{T}{m}\right)^{1/2}\left(\frac{D^3}{L}\right)^{1/2} \tag{2.13}$$

In **Equation 2.13** m is the molar mass of the species of interest, and D and L are the diameter and length of the cylindrical tube, both in cm.

$$\Phi\,(molecules\,cm^{-2}\,s^{-1}) = \frac{EPS \cdot P \cdot \frac{\sigma N_2}{\sigma gas/N_2}}{kT \cdot A} \tag{2.14}$$

Once we establish these values, we calculate the flux using **Equation 2.14** for a range of beam pressures and relate them linearly to either RGA- measured pressure values at the component's parent mass or the integrated area of a TOF curve. An example of this calibration is shown in **Figure 2.7** for a beam of O_2.

2.3.3 Stainless Steel Source

The instrument's beamline has two interchangeable beam sources. The first beam source used in **Chapter 3**, **Chapter 4**, and **Chapter 5** is a traditional supersonic source able to produce intense, tunable, high-energy beams of small molecules. The beam nozzle is machined from a $\frac{1}{4}$" VCR gland and has an exit aperture customized from Mo or Pt pinholes ranging from 15 - 30 μm (3.04 mm O.D. electron microscope apertures, Ted Pella). Our nozzle is setup for resistively heating to reach beam temperatures of 1000-1100 K. We wrap the entire nozzle in a tight coil of thermocoax ((1 Nc I 10) and cover it with tantalum sheet secured by copper ties to ensure even, efficient heating. We monitor and control the temperature via a Type K thermocuple spot-welded on the front of the

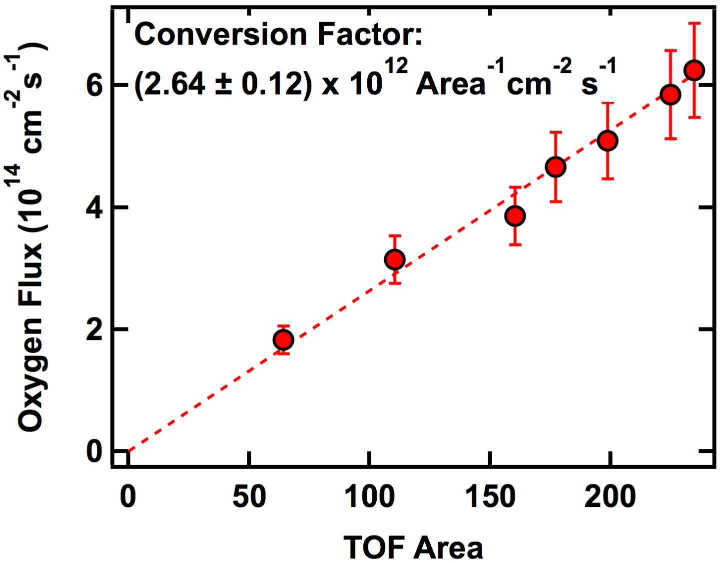

Figure 2.7: Representative beam flux calibration for a neat O_2 beam. The calculated flux (see text for the full details) is plotted against the TOF peak area (collected experimentally with the QMS) for a particular gas. We use this linear relationship to calculate flux for experiments using seeded beams where flux cannot be determined directly from the pressure rise in the chamber.

nozzle next to the aperture. The output of this thermocouple is fed into a feedback loop with a temperature controller (CN76000, Omega) and DC power supply.

2.3.4 Radio Frequency (RF) Plasma Source

Aside from the traditional beam source, there is a second source, used in **Chapter 6**, that generates intense beams of ground state atomic oxygen (O^3P). To produce a high flux of these species, a gas mixture of 5% O_2 in Ne travels through a custom-designed, water-cooled quartz nozzle of the plasma source.[25] Prior to exiting the nozzle and traveling downstream into the chamber, a radio frequency discharge ignites the gas, causing dissociation from O_2 in $O(^3P)$. Additional ionic species (O^{2+}, O^+, Ne^+) are removed from the beam by a pair of 2000 V cm^{-1} deflecting plates located in the 1DC chamber. Under all conditions of this thesis, we do not detect these species downstream in the beam. We also note that upon dissociation there is the possibility to produce other neutral species in the beam (O^1D_2), but we select against that by using relatively low RF powers (100-200 W) and stagnation pressures (<100 Torr).[26] For each experiment, we also perform a blank trial with a neat Ne beam in which we observe no reactivity, indicating that there isn't any metastable Ne. Thus, the only components of our beam source are Ne, O_2, and the desired $O(^3P)$.

During typical operation, the beam source routinely produces discharges that contain 25-40% O_2 dissociation to $O(^3P)$. To determine the extent of dissociation we monitor the relative QMS signal intensities (square-wave modulation) of O_2 (m/z = 32) and atomic oxygen (m/z = 16) in the beam with the plasma on and off. The reason that we collect both is that even with the plasma off, there is still some signal of m/z=16 that results from the dissociation detachment of O_2 in the QMS. The relative intensities with the plasma off can calculated by taking the ratio of 16/32 in the following equation:

$$\eta_L = \frac{I_{16}}{I_{32}} = \frac{CQ_{16}[N_{O_2}\sigma_D]}{CQ_{32}[N_{O_2}\sigma_{O_2}]} \tag{2.15}$$

In **Equation 2.15** above, N_{O_2} and N_O are the number densities of O_2 and O, respectively. Q_{32} and Q_{16} are the quadrupole transmission coefficients at those masses, and C is an unknown empirical constant related to our experimental setup. The two cross-sections refer to the ionization of O_2 (σ_{O_2} , 1.52 Å^2) and the dissociative detachment of O_2 (σ_D, 0.88 AA^2):[27]

$$O_2 + e^- \xrightarrow{\sigma_D} O^+ + O + 2e^- \tag{2.16}$$

$$O_2 + e^- \xrightarrow{\sigma_{O_2}} O_2^+ + 2e^- \tag{2.17}$$

With the plasma on, atomic oxygen is a second source of signal intensity for m/z =16. Thus, the relative intensities with the plasma can be calculated as such:

$$\eta_H = \frac{I_{16}}{I_{32}} = \frac{CQ_{16}[N_{O_2}\sigma_D] + CQ_{16}[N_O\sigma_O]}{CQ_{32}[N_{O_2}\sigma_{O_2}]} \tag{2.18}$$

A third cross section is introduced, corresponding to the ionization of O (σ_O, 1,15 AA^2):[27]

$$O + e^- \xrightarrow{\sigma_O} O^+ + 2e^- \tag{2.19}$$

To ultimately calculate the dissociation, we are interested in the relative number density between O and O_2. This quantity is called R and can be solved for by dividing **Equation 2.15** by **Equation 2.18** and rearranging:

$$R = \frac{N_{16}}{N_{32}} = \left(\frac{\eta_H}{\eta_L} - 1\right)\left(\frac{\sigma_D}{\sigma_O}\right) \tag{2.20}$$

The percent dissociation is then just $\frac{R}{R+1}$, and we can use this relationship to convert the measured O_2 flux (see **Subsection 2.3.2** for more details about this procedure) to O(^{3}P) flux.

2.4 Sample Manipulation and Preparation

In general for the studies in this thesis, the substrate is passive participant in the observed chemistry. During our experimental preparation, we are mainly concerned with making sure that the crystal is clean, doesn't contain impurities, and that its temperature is easily controlled. As mentioned in **Section 2.2**, all experiments (aside from those in **Chapter 7**) are performed using a single-crystal Au(111). Au(111) was chosen for being highly reflective (important for RAIRS), oxidation resistant, and unreactive in vacuum under our experimental conditions. We deposited multilayer films of interest such as water, methane, and propene on top of the substrate.

2.4.1 He-cooled Sample Manipulator

The main chamber contains a recently upgraded custom-designed manipulator and commercial recirculating liquid helium cryostat (204P, Advanced Research Systems). With this setup, the sample can reach temperatures as low as 18 K and as high as 800 K which enables deposition of p-ASW (see **Section 3.2**) and sputter/anneal cycles to clean to substrate (see **Subsection 2.4.2**). The cold head of the cryostat can easily be removed for bake out without disrupting the manipulator in vacuum. The assembly is connected to the chamber via differentially-pumped rotary seal (RNN-400, Thermionics Vacuum Products) to enable polar rotation of the sample. The cryostat itself is also mounted above a low-vibration interface, which reduces movement at the sample caused by the circulating cryostat (DMX-20B, Advanced Research Systems) and allows for RAIR spectra collection.

2.4.2 Surface Preparation

Between oxidation experiments in **Chapter 6**, cleaning of the Au(111) substrate occurred in vacuum to ensure homogeneity and maintenance of the 111 structure. Specifically, the crystal temperature was raised to 770 K while backfilling the chamber with $1 - 2 \times 10^{-5}$ Torr Ar. The substrate was then bombarded with 1 kV Ar^+ ions for 15 minutes by an ion source directed at the crystal. Following sputtering, we confirm crystal cleanliness by the absence of carbon or oxygen in XPS traces.

2.4.3 Thin Film Deposition and Characterization

For our setup, there are multiple ways to dose a thin film on the Au(111) substrate each with its own benefits and tradeoffs. The first method, used in **Chapter 4** and **Chapter 6** is beam dosing. Beam dosing is the most precise method since with a cold enough crystal (making the sticking co-efficient of the gas = 1). the dosed gas will only be on the crystal and not elsewhere in the chamber. Dosing this way enables more precise temperature programed desorption (TPD) experiments and quantifiable kinetic analysis. However, a challenge with beam dosing is that it can be quite slow (on the order of hours) especially when using small beam pinhole sizes (necessary for good beam expansions) and low volatility gases. When we needed thick water films ($>$ 200 ML) in **Chapter 3** and **Chapter 4**, it made sense to switch to directed dosing. Our doser is approximately 4 cm from the crystal so although this dosing method gave us thick, even films after only a few minutes, it negatively added more water into the chamber. Thus, not only did we have to wait for water to pump out prior to starting an experiment, we also increased our chamber water background pressure requiring more frequent chamber bakes.

Our last dosing method, background dosing, is employed infrequency since it leaks even more gas into the chamber resulting in chamber contamination and higher base pressures. Commonly used for backfilling Ar in sputtering cycles (**Subsection 2.4.2**), the leak valve located at the back of the chamber is easily customizable to leak in other molecules of interest. For instance, we background dosed water in **Chapter 3** to gain a film with a desired morphology. More generally, however, we use background dosing to quantify the deposition rate for molecules that cannot be used via the beam. We want to use RAIR signal intensity as a measure for film thickness, but first have to calibrate the signal to a controlled dose at a known flux. For instance, we know that a monolayer of water is 1.06×10^{15} molecules.[28] Thus, if we cool the crystal to a temperature at which water sticks with unit and backfill the chamber to a constant background pressure of 1×10^{-7} Torr, we know that our growth rate is roughly 0.1 layers of water per second.[29–31] Then, we can easily compare this with the growth of RAIR signal intensity, for daily film thickness quantification.

Chapter 3

Sticking Probability of High-Energy Methane on Crystalline, Amorphous, and Porous-Amorphous Ice Films

We present research detailing the sticking probability of CH_4 on various D_2O ices of terrestrial and astrophysical interest using a combination of time-resolved, in situ reflection absorption infrared spectroscopy (RAIRS) and King and Wells mass spectrometry techniques. As the incident translational energy of CH_4 increases (up to 1.8 eV), the sticking probability decreases for all ice films studied, which include high-density, non-porous amorphous (np-ASW) and crystalline (CI) films as well as porous amorphous (p-ASW) films with various pore morphologies. Importantly, sticking probabilities for all p-ASW films diverge and remain higher than either np-ASW or CI films at the highest translational energies studied. This trend is consistent across all porous morphologies studied and does not depend on pore size or orientation relative to the substrate. It is proposed that in addition to offering slightly higher binding energies, the porous network in the D_2O film is very efficient at dissipating the energy of the incident CH_4 molecule. These results offer a clear picture of the initial adsorption of small molecules on various icy interfaces; a quantitative understanding of these mechanisms is essential for the accurate modeling of many astrophysical processes occurring on the surface of icy dust particles.

3.1 Introduction

Examining molecular and atomic adsorption onto frozen water ices is necessary to create accurate models of the chemical and physical processes occurring in atmospheric and terrestrial environments.[32,33] Furthermore, understanding the interactions between gas molecules and different molecular ices can help to classify the composition and the history of complex multicomponent ices.[34] Adsorption on icy surfaces, in astrophysical environments for instance, is a critical first step in a variety of recombination and addition reactions, some resulting in the formation of small organic molecules.[35,36]

Ice can exist in a variety of crystalline and amorphous forms. Crystalline (CI) water ice with its hexagonal lattice is the most common form of snow and ice on Earth[37] and can also be found in warmer astrophysical environments.[38] Amorphous solid water (ASW), on the other hand, is the most abundant form of water in astrophysical environments .[39] and is present in comets, planetary rings, and interstellar clouds.[29] ASW can be classified into two types: high-density nonporous (np-ASW) and low-density porous (p-ASW) based on its pore structure.[40] In general, ASW morphology plays a significant role in the adsorption of volatile gas species within astrophysical ices.[41–43] Although not yet found in such environments, p-ASW can exist as the result of heterogeneous molecular synthesis occurring on dust grains in the interstellar medium (ISM).[44] Exposure to ultraviolet light, x-rays, cosmic radiation, or thermal processing can also induce morphological changes in astrophysical ices.[33,42,44,45] Over time and as a result of these processes, ASW ices can become CI and vice versa. Because of this, there is interest in understanding the precise role of surface morphology in gaseous adsorption.[46]

Ice can exist in a variety of crystalline and amorphous forms. Crystalline (CI) water ice with its hexagonal lattice is the most common form of snow and ice on Earth[37] and can also be found in warmer astrophysical environments.[38] Amorphous solid water (ASW), on the other hand, is the most abundant form of water in astrophysical environments .[39] and is present in comets, planetary rings, and interstellar clouds.[29] ASW can be classified into two types: high-density nonporous (np-ASW) and low-density porous (p-ASW) based on its pore structure.[40] In general, ASW morphol-

ogy plays a significant role in the adsorption of volatile gas species within astrophysical ices.[41–43] Although not yet found in such environments, p-ASW can exist as the result of heterogeneous molecular synthesis occurring on dust grains in the interstellar medium (ISM).[44] Exposure to ultraviolet light, x-rays, cosmic radiation, or thermal processing can also induce morphological changes in astrophysical ices.[33,42,44,45] Over time and as a result of these processes, ASW ices can become CI and vice versa. Because of this, there is interest in understanding the precise role of surface morphology in gaseous adsorption.[46]

This work uses high-energy projectiles to examine adsorption mechanisms on various astrophysical ices. A particular focus is on porous amorphous water ices, and how the pore structure influences the energy accommodation and uptake of incident molecules. In general, a molecule impacting a surface adsorbs if it loses enough of its kinetic energy to the lattice upon impact.[47] Accurate measurements of sticking probabilities are essential because a higher sticking probability can lead to greater observed reactivity as has been shown for a variety of molecules on amorphous ices.[48]

We present the first study examining the sticking probability of CH_4 as a function of translational beam energy on p-ASW of varying porosities, np-ASW, and CI D_2O ice films under ultrahigh vacuum (UHV) using the King and Wells method and molecular beam techniques.[17] Molecular beams enable tunable control of incident energy, and thus precise knowledge of the sticking process.[49] CH_4 was chosen primarily due to its known presence in many astrophysical environments, including its potential incorporation in icy clathrates found in outer solar system bodies such as Titan.[44,50,51] Within those environments, reactions involving CH_4 can be a significant contributor to the formation of complex organic molecules.[52] Additionally, CH_4 will hopefully allow us to exclusively probe adsorption phenomena, because its light mass and lower momenta may preclude direct embedding underneath the surface.[30,53,54] We demonstrate that for the highest energy beam (1.8 eV), the sticking probability is higher for p-ASW than np-ASW and CI ices. For the p-ASW ices, we also determine that there is no difference in sticking probability as a result of increased porosity.

Our results build upon previous work in our group focused on the sticking probability of D_2O and H_2O on CI for incident translation energies ranging from 0.3 to 0.7 eV.[55] The sticking probability was near unity for those measurements and did not change as a function of water ice morphology or surface temperatures ranging from 140 to 155 K. By using CH_4 and expanding the water ice morphology to include amorphous water ices with and without pores as well as higher incident translational energies, our measurements provide a more complete understanding of the dynamics of sticking between projectiles and water ices. Such work is critical to creating accurate models of these processes occurring in atmospheric and terrestrial environments between water ices and CH_4. By examining the initial part of the uptake process, these results provide insight into the adsorption-desorption equilibrium for ices in the troposphere.[56] Beyond these astrophysical and environmental applications, the adsorption of molecules into solid materials is an important first step in many dynamic processes at interfaces in fields such as photo-catalysis, radiation chemistry, waste processing, and advanced materials synthesis.[41] Many commercial catalysts are porous within these fields; these pore structures enable efficient sticking and transport of molecules.[57]

3.2 Experimental

All experiments were conducted in a molecular beam scattering instrument that was previously discussed in full detail.[55] Generally, this instrument consists of a UHV chamber with base pressures of 10^{-10} Torr connected to a triply differentially pumped molecular beamline. Inside the chamber, a state-of-the-art helium-cooled sample manipulator (Advanced Research Systems) enables precise and accurate temperature control of the Au(111) sample substrate between 20 K and 800 K. The crystal is exposed to the beam and monitored in real time with optics for in-situ reflection absorption infrared spectroscopy (RAIRS). Gas scattering and incident flux is also monitored with a residual gas analyzer (RGA).

All RAIR spectra are analyzed with Gaussian peaks atop either linear or cubic baselines, depending on the region. Spectra were acquired with a Nicolet 6700 infrared spectrophotometer (Thermo Fisher) using incident p-polarized IR radiation at an angle of 75° to the Au(111) crystal and a liquid nitrogen cooled mercury cadmium telluride (MCT/A) detector. Each RAIR spectrum is an average of 70-200 scans taken using 4 cm^{-1} resolution with a clean Au(111) sample for the background. For ice preparation, D_2O was chosen (rather than H_2O) due to its preferable O-D stretch frequency that avoids overlap with the ν_3 methane mode.[58–60]

D_2O films were produced via directed doser at a 30° angle and approximately 4 cm from the Au(111) crystal. D_2O was typically leaked in at a pressure of 2.0×10^{-9} Torr, leading to an average growth rate of 0.5 ML/min.[28] The ice films used in this study were between 150 and 300 layers thick. Film thickness was determined by backfilling the UHV chamber to a pressure of 1.0×10^{-7} Torr D_2O, which corresponds to a growth rate of 0.1 ML/s. RAIR spectra were collected at regular time intervals during exposure, which allowed for direct quantification of film thickness from integrated intensity of the large O-D stretch between 3600 cm^{-1} and 2800 cm^{-1}.[61,62] **Figure 3.1** shows a typical normalized O-D stretch for the three different ice films used in this study. Following literature precedent and as a result of D_2O molecule coordination differences among these films, this region can be used to distinguish p-ASW, np-ASW, and CI films.[63] In particular, the interface of p-ASW films contains a significant fraction of three- and two-coordinated surface D_2O molecules ("dangling bonds") that can be clearly resolved spectroscopically at 2725 cm^{-1} and 2740 cm^{-1} respectively. Though also present in the np-ASW film, this dangling bond region is much lower intensity, reflecting the large difference in surface areas between porous and nonporous films.[59,64–66] The temperature of the substrate during dosing dictates the water ice morphology; the substrate temperatures used for ice growth were 150 K for CI, 107 K for np-ASW, and 25 K for p-ASW.[38,39]

ASW films with increased porosity were produced by changing the angle of the directed doser relative to surface normal.[29,67,68] The films used in this study were produced at 30°, 60°, or 70° as well as via background deposition. As characterized by Stevenson et. al.,[29] porosity increases with deposition angle, so the D_2O films dosed at 30º are less porous than those grown at 60° or 70°.[69] The pores also grow with an orientation that matches deposition angle.[67] Although films produced via background deposition (backfilling the chamber with water vapor) are as porous as

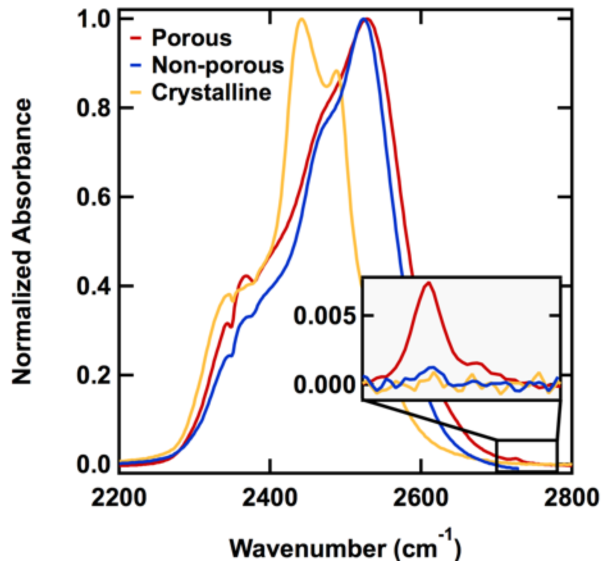

Figure 3.1: Infrared spectra of D_2O ices. Normalized infrared spectra of the O-D stretch distinguish porous amorphous (p-ASW, red), non-porous amorphous (np-ASW, blue), and crystalline (CI, yellow) D_2O ices on Au(111) dosed at 25 K, 107 K, and 150 K, respectively. The inset demonstrates that while dangling O-D modes are observed for both ASW films, they are significantly more intense in the p-ASW films.

those grown at 70°, the water molecules approach the surface with thermal energy and random angular orientation resulting in non-uniform pore orientation and size.[67,68] The intensities of the dangling bond spectroscopic signals are known to roughly scale with porosity, so RAIR spectra can be used to qualitatively confirm that ices with different porosities have been formed.[70,71] Unless otherwise specified in this work, "p-ASW" refers to our default porous film grown at 30°, and porous films grown at other deposition angles (60, 70 and background) will be identified as such.

CH_4 beams were produced by expanding 1% CH_4 in H_2 or neat CH_4 at stagnation pressures of 200-400 psi through a 10 µM molybdenum pinhole. Resistively heating the beam nozzle from room temperature to 970 K resulted in CH_4 translational energies of up to 0.3 eV for the neat CH_4 beam and up to 1.8 eV for the CH_4 beam seeded in H_2. The translational energy distribution widths ($\Delta E/E$) ranged from 12% to 21%. Translational energies were measured by time-of-flight (TOF) using a mechanical chopper (a rotating slotted disk) to modulate the beam prior to detection with an in-line quadrupole mass spectrometer (QMS). For one experiment (investigating the impact of embedding phenomena), CF_4 beams were produced by expanding 1% CF_4 in H2 at stagnation pressures of 300-500 psi through a 20 μM molybdenum pinhole. Resistively heating the beam nozzle temperature to over 950 K resulted in a CF_4 translational energy of 5.3 eV with a ΔE/E$\approx$40%.

The CH_4 or CF_4 flux was determined by first measuring the pressure rise with a nude Bayard-Albert ion gauge calibrated to N_2 for a neat CH_4 or CF_4 beam open to the chamber.[72] The flux was then calculated by taking into account the relative gauge sensitivity to CH_4 and N_2[73,74] or CF_4 and N_2,[73,75] along with the chamber pumping speed, and the spot size of the beam on the Au(111) crystal. Using neat beams at varied stagnation pressures the calculated fluxes were correlated to a pressure rise for m/z=15 (CH_4) or for m/z=69 (CF_4) measured by a RGA not in line with the beam. A linear regression then enabled a conversion between measured RGA pressure and total CH_4 and CF_4 flux. Typical beam fluxes for the CH_4 and CF_4 beams were 2.21×10^{13} atoms cm^{-2} s^{-1} and 1.27×10^{14} atoms cm^{-2} s^{-1}, respectively. All beam exposures in this study were performed at normal incidence.

As described in **Subsection 2.2.3**, sticking probability was determined using the King and Wells technique.[17,18] In order to conduct multiple trials with a given film, the ice was first annealed to 70 K for 30 minutes. While this reduced porosity slightly, it ensured that repeated King and Wells cycles did not further alter the film morphology throughout the day.[57,67,76] To explore the generalizability of our results, the sticking probabilities for CH_4 on np-ASW, p-ASW, and CI H_2O films were also examined. We note that for all the CH_4 translational energies studied, the sticking probability values were the same as those observed for D_2O ices; we did not observe any significant isotopic effect at our experimental resolution, as has been previously detected between D_2O impinging on H_2O and D_2O ices.[77]

3.3 Results

3.3.1 King and Wells

King and Wells measurements of initial sticking probabilities were performed on a prepared ice substrate held at 33.5 K for all results presented in this study. This temperature choice reflects a number of important considerations related to both the nature of the CH_4/D_2O interaction and the King and Wells method itself. As discussed by He et al., there are three potential challenges with performing King and Wells measurements for this ice system.[46] First, the liquid helium cooling of the sample manipulator may impact the pumping speed of the chamber, thereby altering the reflected portion of the beam at different sample temperatures. We avoid this by taking all measurements at a single sample temperature, where the unknown improvement in chamber pumping speed is consistent across experiments. Second, because CH_4 interacts with the ice surface via weak dispersion forces rather than direct chemisorption, these experiments require low surface temperatures. Furthermore, ice surfaces have a wide range of binding sites and binding energies.[66,67,78,79] These two factors present a second challenge; a well-defined saturation of the CH_4 reflected signal might be difficult to observe over short exposure time scales. And although full reflection may ultimately be observed with long exposures, CH_4 desorption as well as finite adsorption of background H_2O and D_2O at these low temperatures over long timescales compete to prevent signal saturation. As such, all initial sticking probability measurements referenced herein are calculated using the initial CH_4 indirect flux rather than the value at saturation (after surface sites are filled). These considerations, therefore, are mitigated by our experimental setup.

Beyond the aforementioned considerations, we are also specifically interested in quantifying the initial sticking probabilities in the low coverage, sub-monolayer regime. This is desirable because the concentrations of small molecules in the ISM are typically quite low.[80] Moreover, we want to eliminate any contribution from multilayer sticking, which occurs more readily in porous films, even at higher surface temperatures.[57,69] As such, the desired temperature regime should be high enough to restrict all sticking to sub-monolayer.[67] In light of these considerations, 33.5 K was selected as the surface temperature of interest. At this temperature, however, the monolayer is not perfectly stable on the surface. While this does not impact the measurements of initial sticking probabilities, CH_4 surface coverage at long exposure timescales will reflect contributions from both adsorption and desorption. By explicitly quantifying and accounting for the rates of desorption, we also account for the third concern with King and Wells measurements, which is that they typically do not have the time resolution to distinguish between molecules that are directly reflected from the surface and those that adsorb for a short time and then desorb again.

As shown in the top panels of **Figure 3.2a-c**, quantification of the monolayer was established via isothermal desorption experiments for each ice film. After dosing a multilayer film of CH_4 at 20 K, the integrated area of the degenerate ν_4 mode was tracked over time at an elevated temperature.[60,81–83] A distinct slope change is observed when multilayer desorption changes to monolayer, thereby allowing for an approximate quantification of monolayer thickness. The bottom panels of **Figure 3.2a-c** show that when the surface is held at 33.5 K (as during a King and Wells experiment), the total amount of adsorbed CH_4 reaches a maximum far below the respective monolayer thickness for each type of ice film. Measured desorption rates for all films at 33.5 K are similar in magnitude to the incident CH_4 flux, so this steady-state maximum indicates that only a small fraction of the monolayer is stable on the surface over long timescales (as shown in **Figure 3.2c** in pink).

Figure 3.2 highlights another important feature of this system, which is that the monolayer thickness (and uptake at 33.5 K) on the porous film is significantly higher than uptake on either CI or np-ASW films (likely due to the increased surface area).[84] This effect has been well-documented previously – Kimmel et. al. demonstrated, for example, that a 50 layer film of p-ASW deposited at 30° sees a total CH_4 adsorption of 2 monolayer equivalents.[67] On this basis one might expect, therefore, that a 185 layer film (as used in Figure 3c) would likewise adsorb roughly 7-8 monolayers of CH_4. Indeed, the data show that the p-ASW monolayer adsorption is almost exactly 8 times that of the CI and np-ASW films. Similarly, steady-state adsorptions at 33.5 K are on the order of 10^{14} CH_4 cm^{-2} on the porous films and 10^{13} CH_4 cm^{-2} on crystalline and non-porous films.

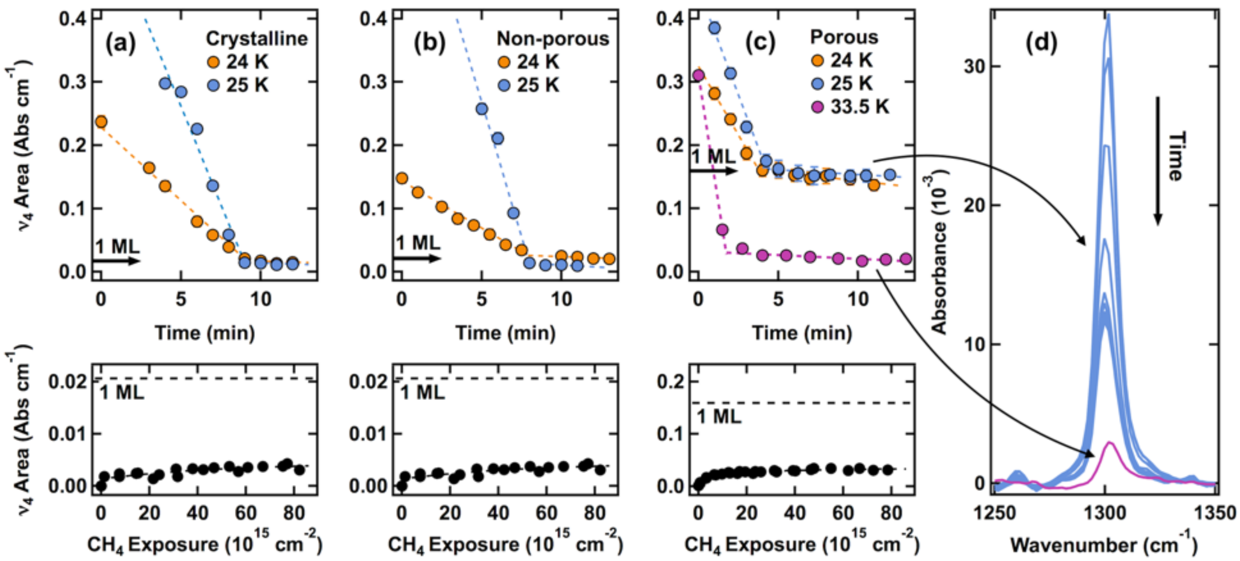

Figure 3.2: Isothermal desorption of CH_4 from crystalline, non-porous amorphous, and porous amorphous ice films Isothermal desorption of CH_4 from crystalline (CI, a), non-porous amorphous (np-ASW, b) and porous amorphous (185 layers, c) ice films (top) allows for quantitative estimation of monolayer thickness, as measured via the integrated absorbance of the ν_4 mode. Growth of the same peak area during exposure at 33.5 K (bottom) confirms that the amount of adsorbed CH_4 is significantly less than a full monolayer for each type of ice. This is also demonstrated in the corresponding RAIR spectra for desorption a 25 K (blue, d) and 33.5 K (pink, d)

3.3.2 Sticking Probabilities for CI, np-ASW, and p-ASW

Measured sticking probabilities for CH_4 on crystalline (CI), non-porous (np-ASW), and porous (p-ASW) D_2O films are displayed in **Figure 3.3**. Clearly, as the CH_4 incident energy increases, the observed trend on the porous film diverges from both CI and np-ASW; sticking probabilities remain significantly higher for the porous film. This divergence will be discussed in further detail below. First, however, it is important to note that crystalline and non-porous films display nearly identical sticking probability trends throughout the range of incident energies studied. This insensitivity to morphology (CI versus np-ASW) has been observed in other experimental and theoretical systems, including D_2O sticking on H_2O and D_2O,50 H_2O sticking on H_2O,[47] and CO sticking on H_2O.[37,85] The theoretical work of Al-Halabi et. al., for example shows not only that the sticking of CO is nearly equal between np-ASW and CI H_2O films, but also an exponential decay of sticking probability with incident translational energy that is roughly comparable to that measured in this study.[76]

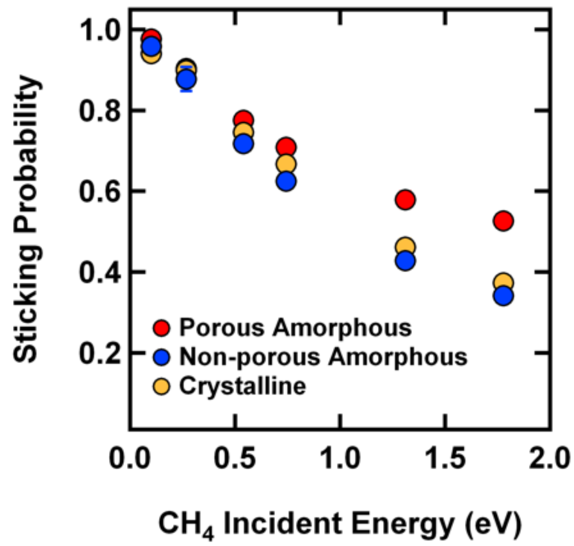

Figure 3.3: Sticking probabilities for CH_4 on porous, non-porous, and crystalline D_2O films. Sticking probability decreases for all films as incident CH_4 energy increases, but remains higher for the porous (red) film (films held at 33.5 K). Error bars represent the standard deviation of at least three measurements on at least two different days.

It is important, when discussing adsorption to both porous and non-porous films, to elucidate the contribution of any penetration of the incident CH_4 into the bulk ice. Previous work in this lab has identified a significant activated uptake channel for incident projectiles in the ice bulk (termed "embedding").[37] After investigating this process for a range of molecules in np-ASW H_2O, a clear momentum barrier for this channel was established (embedding probabilities in CI films were significantly lower than those observed for np-ASW). In general, the momenta reached in the current study (using the relatively light CH_4) are well below this barrier, so no embedding is expected in either np-ASW or CI films. There is, however, the question of whether the use of D_2O (rather than H_2O) or a more porous ice morphology will effectively lower this barrier, making direct comparisons of sticking probabilities across films more challenging. To examine this, both porous and non-porous D_2O ice films were exposed to beams of 5.3 eV CF_4. CF_4 was selected because it has a higher mass and has been successfully used in previous embedding experiments in this lab. All such ballistic embedding experiments were performed with the films held at 70

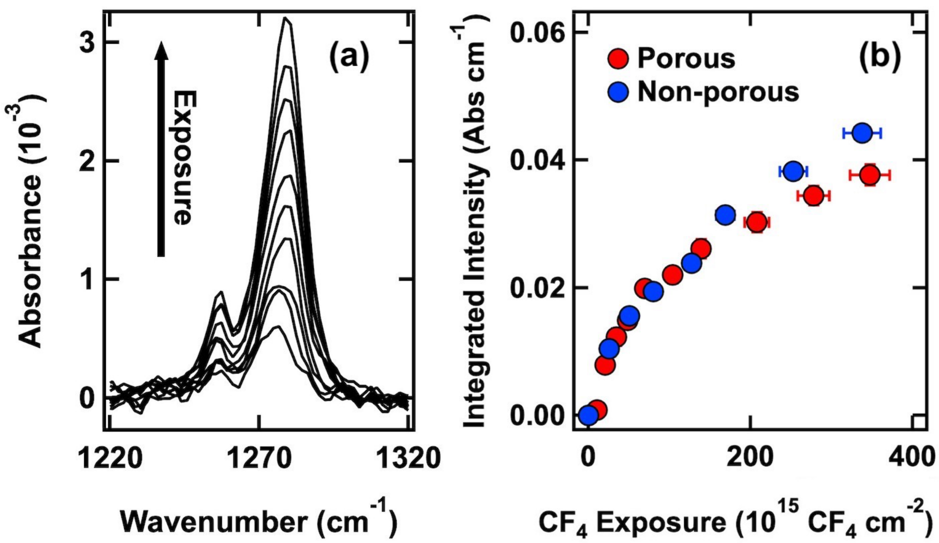

Figure 3.4: Ballistic embedding barrier for porous films. a) RAIR spectra collected throughout CF_4 exposure show clear signal growth at 1276 and 1257 cm^{-1}. (b) The integrated area of these CF_4 peaks is proportional to the amount of CF_4 that remains embedded in the surface. Both p-ASW and np-ASW films show similar rates of uptake, indicating that the barrier for ballistic embedding into porous films matches that established in previous works for non-porous films. This figure highlights the trend for a porous film deposited at 30° from surface normal, but there are no significant differences in embedding rates for any of the porous films studied in this work.

K so as to mimic ice preparation conditions used during sticking probability experiments and to preclude a significant surface adsorption channel for CF_4 on the ice. RAIR spectra were collected at regular intervals during exposure to quantify the increase in stable, embedded CF_4 within the ice film (**Figure 3.4a**). These growth rates closely match data collected in previous works, indicating no major differences between D_2O and H_2O ice films (**Figure 3.4b**). Furthermore, the rates of embedding are nearly identical for both p-ASW and np-ASW. Therefore, we expect the previously reported momentum barrier for np-ASW to hold for p-ASW, preventing CH_4 embedding in all of the ice films discussed herein. Indeed, RAIR spectra collected during anneal cycles to 70 K after King and Wells experiments (as well as RGA monitoring of ice desorption at the end of the day) confirm that there is no discernible uptake of CH_4 into the ice bulk; all CH_4 is surface adsorbed.

Though we have demonstrated that there are no differences in embedding phenomena, there are other ways in which CH_4 may interact differently with the p-ASW structure, thereby impacting the observed sticking probability. First, we observe no discernible sputtering of the water film by the

CH_4 beam. Though sputtering of astrophysical ices has been reported, the impinging species in these works are typically either charged and/or significantly higher in energy.[30,53] In other words, we don't expect the momentum transfer for the CH_4/D_2O system to be significant enough to desorb water molecules from the surface, nor is there any possibility for electronic sputtering. Secondly, there is also a large body of research investigating the impact of fast, heavy ions on the morphology of ice films. Specifically, high energy ions (mimicking the effect of cosmic rays) have been shown to compact the pores of vapor-deposited ices.[86–90] Even the relatively low energy release of H_2 recombination (4.5 eV) on the surface of ice can have a similar compaction effect.[91–94] Though it appears unlikely, it is important to investigate the possible impact that CH_4 may have on the morphology of the porous D_2O films used in this study. **Figure 3.5** depicts representative regions from RAIR spectra of the film before, during, and following CH_4 exposure. Upon exposure to CH_4 (**Figure 3.5a**), there is a slight red shift in intensity of the dangling O-D mode (**Figure 3.5b**). This shift is well documented in FTIR studies of sequential CH_4/H_2O depositions, and indicates that some of the surface D_2O molecules are coordinating with the adsorbed CH_4.[64] After annealing the sample back to 70 K following the experiment, however, all CH_4 desorbs and there are no lasting changes in the O-D stretch or the dangling O-D peaks. This indicates that the water film height, morphology, and porosity are not impacted by CH_4 sticking experiments, even at the highest energies studied (1.8 eV).

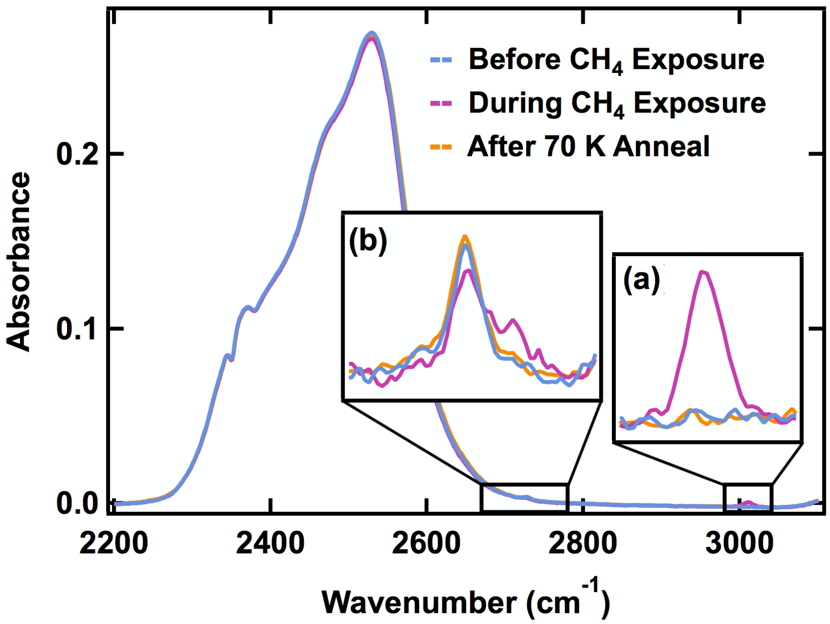

Figure 3.5: D_2O RAIR spectra during CH_4 exposure and anneal. RAIR spectra of D_2O films are unchanged by CH_4 exposure and subsequent anneal. During exposure, some CH_4 adsorbs to the surface (a) and the dangling O-D stretching mode is slightly red-shifted (b). Annealing to 70 K removes all CH_4 and leaves the original D_2O film unchanged.

3.3.3 Amorphous Films, Varied Porosity

In the previous section, we established that sticking probabilities of CH_4 are higher for p-ASW films than either np-ASW or CI films at high incident energies. This comparison, however, only includes porous films deposited at 30° relative to surface normal. **Figure 3.6** depicts the sticking probabilities for CH_4 on a variety of porous films, including those deposited via directed doser (at 30°, 60°, and 70° from surface normal) as well as via background deposition. Surprisingly, there is no strong variation in sticking probabilities for CH_4 on any of these films, despite the expected differences in pore orientation and film density.[58,66]

To further understand these results, it is possible to quantify CH_4 coverage on a given surface during a period of exposure and compare it across films. We can estimate the amount of adsorbed

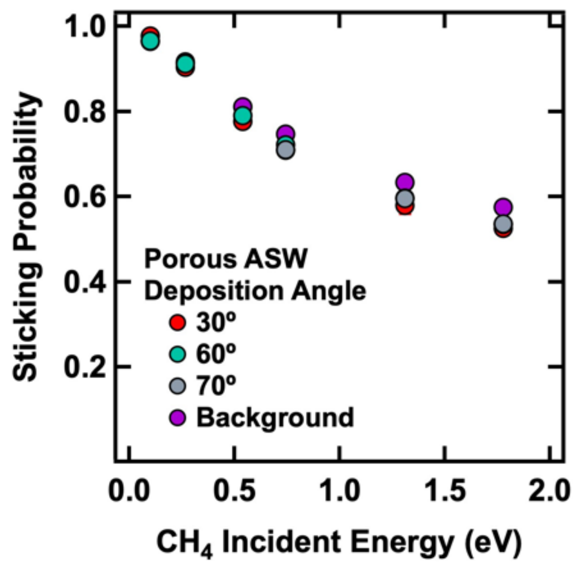

Figure 3.6: Sticking probabilities for CH_4 impinging on porous D_2O films. Sticking probabilities are shown for CH_4 impinging on porous D_2O films held at 33.5 K, deposited via directed doser at 30° (red), 60° (green), and 70° (gray) relative to surface normal as well as via background deposition (purple). For the incident energies studied, there are no clear differences in sticking probabilities for these films. Error bars represent the standard deviation of at least three measurements on at least two different days.

CH_4 at a given time t_1 using the following equation:

$$N_{CH_4} = (P_2 - P_1)(t_1 - t_0) - \int_{t_0}^{t_1} P(t) \tag{3.1}$$

In **Equation 3.1**, P_2 is the indirect CH_4 flux when the beam is blocked from the substrate, P_1 is the background CH_4 pressure when the beam is closed, and t_0 is the time at which the flag is removed and the film is fully exposed to CH_4. The last term is a simple numerical integration of the raw King and Wells pressure reading between those two time values. In doing this analysis for high translational energy CH_4 beams (1.8 eV), we find that in the first seconds of exposure (corresponding to a total exposure of $(5.0 \pm 0.4) \times 10^{14} \frac{CH_4}{cm^2}$), CI and np-ASW films have adsorbed $(1.0 \pm 0.1) \times 10^{14} \frac{CH_4}{cm^2}$, while 200 ML porous films (at all deposition angles) have accumulated $(1.8 \pm 0.3) \times 10^{14} \frac{CH_4}{cm^2}$. This increase is the result of both increased surface area and higher initial sticking probabilities on porous films at these beam energies, and the difference only widens as exposure continues. The difference in uptake is illustrated qualitatively in **Figure 3.7a**, which

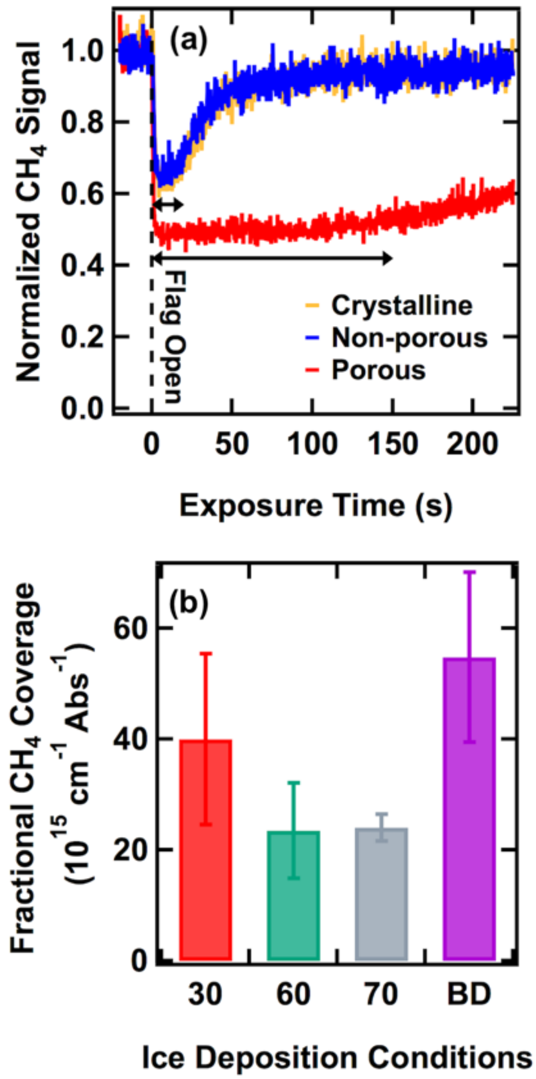

Figure 3.7: CH_4 uptake and fractional coverage on porous films. Representative, normalized King and Wells data for all films studied show a clear increase in CH_4 uptake on porous films relative to CI and np-ASW. (a) Total uptake on a porous film (p-ASW, red) is nearly an order of magnitude higher than on either crystalline (CI, yellow) or non-porous (np-ASW, blue). Time and intensity axes are normalized to the incident flux. (b) Fractional CH_4 coverage is higher for porous films deposited at 30° or via background deposition (red, purple) than for those deposited at 60° or 70° (green, gray). Fractional coverage is defined as the total adsorbed CH_4 scaled by the integrated areas of the dangling bond feature. All data was selected from trials using 1.8 and CH_4 beams.

depicts normalized King and Wells data for representative trials on np-ASW, CI, and p-ASW films. To aid in visual comparison, the data have been normalized in both axes by incident flux. Clearly, the porous film adsorbs more CH_4 before desorption takes over.

In **Figure 3.7b** the results of a similar coverage analysis are displayed for all porous ices. In this depiction, total coverage is scaled further by surface area to give an approximate "fractional coverage". Relative surface area is defined via the integrated intensity of the dangling O-D feature. As discussed in **Figure 3.1**, this feature provides a reasonable measure of porosity and is related to the total surface area of the film.[68,95] Though the initial sticking probability is consistent across porous films, the relative accumulation of CH_4 is 1-2 times higher for films deposited at 30° and via background deposition than those deposited at 60° or 70°. The roots of this behavior will be addressed further in the Discussion section below.

3.4 Discussion

There are two new, significant findings to come out of this work. The first is that the sticking probability of CH_4 on p-ASW D_2O films does not decay as fast as it does on CI and np-ASW D_2O films. The second is that under our energetic conditions, the sticking probability trend does not depend on the type of porous ice film used. What follows is a qualitative discussion of why these trends occur and how future studies might further refine the proposed conclusions.

Sticking probabilities for a particular system are known to depend both on the binding energy between the surface and the adsorbate as well as the surface conditions (morphology, temperature, etc).[71,93] Binding energies for a variety of molecules on different ices of astrochemical interest have been widely reported. As discussed, the low-coverage binding energy for CH_4 on np-ASW ice has been reported in the range of 0.06 – 0.14 eV.[36] Additionally, differences in binding energy for CO (CH_4 and CO are expected to have similar binding interactions on ice)[66,76,80,96] between CI and np-ASW are small and on the order of 0.01 eV at most.[76] This suggests a partial explanation for the similarity in sticking probabilities between these two ice films. Binding energies on porous films, on the other hand, may be higher than those for either np-ASW or CI ice interfaces.

Many studies assert that the binding energy distribution for molecules on porous films is wider and peaks at higher values.[37,97] This idea is refined by Zubkov et al., who concluded that while the distribution of binding sites on the surface is independent of film thickness and porosity, the lower fractional coverages of adsorbates on porous films (due to their increased surface area) leads to adsorbates interacting with more higher energy binding sites.[35,80,98,99] In short, it is likely that at the low coverages investigated here, CH_4 binds somewhat more strongly to the porous films.

Binding energy, however, is not a sufficient explanation on its own. Whatever the variation may be for the different ice films, all available reported binding energies for CO and CH_4 are less than 0.2 eV. This is significantly lower than most of the incident energies studied here, suggesting that there must be an additional mechanism for energy accomodation by the surface. Indeed, theoretical work has been done to show that energy dissipation into ice films is incredibly facile under similar conditions.[57] *We suggest, therefore, that it is the distinct morphology of the porous films that is largely responsible for the observed divergence in sticking probabilities at high incident energies.* Desorption studies from a variety of porous substrates have found that desorption kinetics are governed by diffusive motion within pores and multiple collisions with pore walls.[37,100] Indeed, the energy-dissipating effects of these pore wall collisions have been previously cited in studies of molecular or atomic interactions with ice;[101,102] Vidali et al. aslo found that prior to desorption, molecules on porous ice experience hundreds of desorption-readsorption attempts (as compared to just one attempt on non-porous).[103] Perhaps the most significant evidence of this energy accommodation by pore walls was demonstrated in a study of HD recombination. Hornekaer et al. found that on porous ice, a significant fraction of newly formed HD remained adsorbed to the surface, indicating that the porous network was extremely efficient at dissipating the 4.5 eV recombination energy.[99] This is in contrast to a non-porous film, which saw almost zero retention of the HD molecules following recombination. In summary, the higher sticking probabilities for CH_4 on p-ASW relative to np-ASW and CI likely result from diffusion on and multiple collisions with pore walls, leading to a more efficient dissipation of incident translational energy. It is possible, then, that the sticking probability as discussed here on porous films is more of an uptake coefficient; a measure of advantageous decelleration induced by the physical pore structure, rather than a higher capacity for site-specfic energy accomodation on different types of icy surfaces.

In order to discuss CH_4 coverage, it is important to mention the impact of desorption. As mentioned previously, only a fraction of a CH_4 monolayer can remain stably adsorbed on the surface at 33.5 K. Therefore, we expect the increase in reflected signal after the first few seconds (after initial sticking is measured) to be a result of both directly reflected CH_4 and steadily desorbing CH_4. Ultimately, when the reflected signal levels off at long exposure timescales, adsorption and desorption are occuring at equal rates. Measured isothermal, low-coverage desorption rates for all porous films studied here are roughly equivalent and comparable in magnitude to the incident flux, making it possible to compare coverages across these films despite the competing rates of adsorption and desorption.

At normal incidence, this study showed that porous films of any orientation are equally efficient at dissipating the energy of impinging CH_4, but these films adsorb relatively different amounts of CH_4, depending on deposition conditions. The invariance in sticking probability across films of different porosities suggests that the D_2O pore surface is equally efficient at accomodating the incident energy of the CH_4 molecules, regardless of how that pore is oriented relative to the incident beam. These results also suggest, however, that incident CH_4 is not sampling the full surface area of the pore network of 60° and 70° films before beginning to desorb. This can perhaps be understood in terms of pore geometry and size. Films deposited at 30° have lower total surface areas, but they also have pores that are closer to perpendicular to the substrate.[29,104] Relatively more of the pore surface area, therefore, is accessible to the incident beam. Likewise background deposited films have a distribution of pore sizes and orientations; some fraction of which will be perpendicular or near-perpendicular to the substrate. On the other hand, the more tilted, wider pores of the 60° and 70° films present fewer surface sites for the incident beam. So while CH_4 may undergo multiple collisions with the pore structure before sticking, these covereage results indicate that adsorbed CH_4 is not necessarily diffusing fully into the pore structure and filling up all available surface sites, particularly on the more angled porous film structures. A future experiment that explores the angular dependance of sticking and uptake on these porous films would be a significant step towards identifying the relative importance of factors such as pore orientation and size.

3.5 Conclusion

In this work we present detailed sticking probability measurements for high translational energy CH_4 impinging on a variety of D_2O ice films at 33.5 K. We confirm that at the energies studied, CH_4 is unable to either embed in the bulk or significantly impact the morphology of any ice, including low-density porous films. As incident translational energy increases, the sticking probability decreases for all films. However, CH_4 sticks with greater probability to p-ASW films than it does to either CI or np-ASW films at the same energies. Furthermore, we observe no substantial changes in sticking probability when changing the exact morphology (pore orientation and size) of the porous film used. Even though there may be slight changes in binding energies between CH_4 and the different films, we propose that the porous morphology is largely responsible for this observed divergence. Multiple collisions with pore walls are likely efficient at dissipating the incident energy of the CH_4 projectile. This conclusion is supported by the fact that porous films with more beam-accesible pore surfaces (films deposited at 30° and via background deposition) accumulate relatively more CH_4 during exposure than do films with fewer accesible pore surfaces (deposited at 60° and 70°).

These results are further evidence that the morphology of ice films (and other industrial substrates) critically influences the adsorption and subsequent reactivity of incident molecules. Even if not universally porous, small cracks, fissures, and other morphological deformities in the surface of astrophysical ices may lead to an increased uptake of gaseous molecules, thereby impacting phenomena including the outgassing of comets, chemical reactions in the ISM, and thermal and electrical processing of icy dust grains.[29,95]

Chapter 4

Acetone-Water Interactions in Crystalline and Amorphous Ice Environments

We present research that systematically examines acetone interacting with various D_2O ices of terrestrial and astrophysical interest using time-resolved, in situ reflection absorption infrared spectroscopy (RAIRS). We examine acetone deposited on top of different D_2O ice films: high-density, non-porous amorphous (np-ASW), and crystalline (CI) films as well as porous amorphous (p-ASW) with various pore morphologies. Analysis of RAIR spectra changes after acetone exposure, we find that more hydrogen bonding occurs between acetone and p-ASW ices as compared to acetone and np-ASW or CI ices. Hydrogen bonding quantification occurred by two independent RAIR spectral changes: a greater relative intensity of the 1703 cm^{-1} feature at low acetone coverage as part of a 14 cm^{-1} shift in the C=O region, and a $\sim$30% integrated dangling bond area reduction after acetone exposure. Interestingly, when changing the water structure to be more porous (deposited at 70º compared to 30º), there is a further reduction in the amount of hydrogen bonding that occurs. This suggests that there is a lack of access to surface sites with dangling bonds in the pores as initial layers of acetone block the pores and acetone is unable to diffuse within the structure at low temperatures. In general, these results offer a clearer picture of the mechanisms that can occur when small organic hydrocarbons interact with various icy interfaces; a quantitative understanding of these interactions is essential for the accurate modeling of many astrophysical processes occurring on the surface of icy dust particles.

4.1 Introduction

Surface chemistry interactions between ices and small molecules are not as well understood as those that occur between adsorbates and metals.[105] These interactions are important for many atmospheric processes – such as reactions occurring on stratospheric cloud particles that can result in the seasonal ozone hole in Antarctica.[106,107] Additionally, bromine-induced tropospheric scavenging of ozone occurs on aerosols,[108–110] as well as mid-latitude ozone depletion from volcanic eruptions.[111] Aside from atmospheric sciences, understanding chemical interactions and properties of astrophysical ices is important to help classify the composition and history of complex multi-component ices.[34] Many interstellar dust grains are coated with thin ice films. Exposure to ultraviolet light, x-rays, cosmic radiation, or thermal processing can induce morphological changes resulting in novel molecules and increased chemical complexity.[33,91]

This work focuses on the interaction between acetone and astrophysical ices of varying morphologies: crystalline ice (CI), nonporous amorphous solid water (np-ASW), and porous amorphous solid water (p-ASW). CI ice in a hexagonal lattice is the most common form of snow and ice on Earth,[37] but is also present in warmer astrophysical environments.[38] ASW, on the other hand, is the most abundant form of water in astrophysical environments[39] and is present in comets, planetary rings, and interstellar clouds.[29] ASW can be further classified into two types: high-density nonporous (np-ASW) and low-density porous (p-ASW) based on its pore structure.[40] In general, ASW morphology and accessibility to dangling bonds play a significant role in the adsorption and subsequent reactivity of volatile gas species within astrophysical ices.[41,42,112,113]

Acetone was chosen due to its relative abundance as a volatile organic in the troposphere,[105] its importance in organic chemistry, and its presence in the interstellar medium.[114] Acetone formation occurs on grain mantles where after gaseous CO molecules condense, they undergo hydrogen addition, resulting in formyl radicals.[115] These radicals can rapidly undergo addition reactions yielding methanol and acetaldehyde which upon reaction produce acetone. Thus, in order to quantify the role that acetone plays in icy dust grain mantles, it is necessary to classify how strongly acetone and water films interact.

More specifically, our work systematically probes acetone deposited on top of ice films of varying thicknesses as well as within a water matrix. This uniquely enables us to examine how the C=O moiety changes and therefore provides information about the film's orientation as well as hydrogen bonding effects. Our work builds upon experimental studies[116–120] as well as molecular dynamics simulations and ab initio calculations of the acetone-water system.[105,121] When investigating acetone adsorption on thin films (10-15 ML) of np-ASW and CI ices, Temperature Programmed Desorption (TPD) measurements yielded two desorption states from the np-ASW film: a hydrogen bonded and a physiosorbed state. This is in contrast to only a physiosorbed state from the CI ice films. Therefore, acetone interacts with the np-ASW film more strongly than with CI ice due to the prevalence of hydrogen bonds. This is thought to be due to a structural difference between the np-ASW and CI ice films that impacts the ice's ability to form hydrogen bonds.[117]

Note that the surface chemistry of amorphous films is more complicated due to the presence of microscopic pores. Not only can species be trapped,[34] but the deposition angle dictates the pore orientation and density.[67,95] Although there are many studies focused on adsorption into pores[29,41,95] to understand how pore morphology depends on the growth angle, little is known about how the pore morphology can impact hydrogen bonding sites and accessibility for adsorbed species to these sites.[122] Herein, we employ RAIRS to examine p-ASW and how its structure impacts diffusion, and chemical interactions between acetone and the underlying film structure. We demonstrate that there are increased hydrogen bonding interactions between acetone and the p-ASW films as compared to acetone and the np-ASW or CI films. Hydrogen bonding quantification occurred by observing two RAIR spectral changes: a greater relative intensity of the 1703 cm^{-1} feature at low acetone coverage as part of a 14 cm^{-1} shift in the C=O region and a $\sim$30% integrated dangling bond area reduction following exposure. Interestingly, when changing the water structure to be more porous (deposited at 70º compared to 30º), there is a further reduction in the amount of hydrogen bonding that occurs. Additionally, when examining dilute acetone inside a np-ASW matrix, we are able to tease apart peaks due to acetone interacting with water in the acetone-water interfacial region.

Overall, this work demonstrates that not only is there a difference in the ability to form hydrogen bonds between crystalline and amorphous water ices, but that such differences occur for porous amorphous water ices. Our work, therefore, demonstrates the importance of ice morphology in facilitating hydrogen bonding between interfacial undercoordinated water molecules and the C=O moiety. The demonstrated spectroscopic differences, particularly at sub-monolayer abundances, may guide the search for porous ices in the interstellar medium or on icy bodies in our solar system. Additionally, the prevalence of hydrogen bonds between acetone and crystalline and amorphous ices of varying porosity may impact subsequent reactivity and thus, molecular complexity and gas phase abundances of hydrocarbons. Aside from astrophysical environments, this work can also be applied more broadly to understand water and solid interfaces and transport of these molecules into frozen media.

4.2 Experimental

All experiments were conducted in a molecular beam gas-surface scattering ultra-high vacuum instrument that was previously discussed in detail.[55] This instrument consists of a UHV chamber with a base pressure of 10-10 torr connected to a triply differentially pumped molecular beamline. In the main chamber, a He cooled manipulator (Advanced Research Systems) enables precise and accurate temperature control of the Au(111) sample between 16 K and 800 K. The crystal is exposed to the beam and monitored in real time with optics for in situ reflection absorption infrared spectroscopy (RAIRS). Gas scattering and incident flux are monitored with a residual gas analyzer (RGA).

All RAIR spectra were analyzed using Gaussian peaks atop cubic baselines. Spectra were acquired with a Nicolet 6700 infrared spectrophotometer (Thermo Fisher) using incident p-polarized IR radiation at an angle of 75° to the Au(111) crystal and a liquid nitrogen cooled mercury cadmium telluride (MCT/A) detector. Each RAIR spectrum is an average of 200-300 scans taken using 2 cm^{-1} resolution with a clean Au(111) sample or a D_2O underlayer for the background reference spectra.

D_2O films were produced via directed doser at a 30º angle with respect to the surface normal and approximately 4 cm from the Au(111) crystal. The ice films used in this study varied between 100-600 layers thick. D_2O film thickness was determined by backfilling the UHV chamber to a chamber pressure of 1×10^{-7} torr, which corresponds to a growth rate of 0.05 ML/s.[28] The D_2O growth and film thickness were monitored using RAIRS and integrated intensity of the O-D stretch between 3000 and 2000 cm^{-1}.[61] The deposition temperature of the Au(111) crystal determined the ice film coordination.[113,123] The D_2O films used in this study were np-ASW, p-ASW or CI dosed at 108, 20, and 150 K, respectively. D_2O was typically leaked into the chamber at a pressure of 4×10^{-10} Torr, resulting in an average growth rate of $\sim$ 0.25 ML/s. ASW films with increased porosity were produced by increasing the angle of the directed doser relative to surface normal from 30º to 70º.[68] The intensities of the dangling bond spectroscopic signals roughly scale with porosity so RAIR spectra can be used to qualitatively confirm that ices with different porosities have been formed.[70,71]

Figure 4.1 gives the normalized O-D stretch between 2200 and 2800 cm^{-1} for the three different ice films used in this study: np-ASW, p-ASW and CI deposited at 108, 20, and 150 K, respectively and collected at 68 K. When comparing acetone interacting with np-ASW, p-ASW and CI D_2O films, it was necessary to anneal the films to a middle temperature of 68 K. This ensured that amorphous D_2O did not deposit on top of crystalline ice films during a lengthy cooling process to 20 K and that the porous film structure did not collapse and become non-porous at 108 K. As a result of D_2O molecule coordination differences among the films, we can easily distinguish p-ASW, np-ASW, and CI films.[63] Additionally, the p-ASW interface contains a significant fraction of three and two-coordinated surface D_2O molecules ("dangling bonds") that are spectroscopically identified at 2725 cm^{-1} and 2745 cm^{-1}, respectively.[124] Undercoordinated D_2O molecules not only change the density of the ASW structure, but can also form hydrogen bonds with deposited acetone. On p-ASW films there are two different surface sites that contain these dangling bonds: one on the top of the ice film and one decorating the pores. Annealing to 68 K for these experiments significantly reduced the number of two-coordinated surface molecules, but does not change

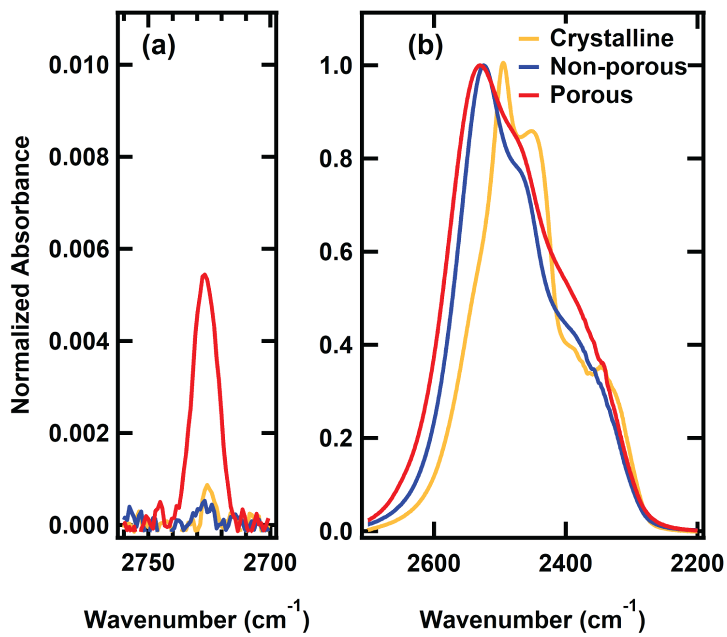

Figure 4.1: Crystalline (CI), non-porous amorphous (np-ASW) and porous amorphous (p-ASW) D_2O ices. Normalized infrared spectra of 150 ML crystalline (CI, yellow), non-porous amorphous (np-ASW, blue) and porous amorphous (p-ASW, red) D_2O ices in the O-D stretch region between 2760 and 2700 cm^{-1} (a) and 2700 and 2200 (b) cm^{-1} dosed at 150 K, 108 K, and 20 K respectively and collected at 68 K. The region between 2760 and 2700 cm^{-1} (a) demonstrates that while dangling O-D are observed for all films, the intensity is greatest for the p-ASW films.

the number of three-coordinated molecules.

Although previous studies by Kimmel *et al* demonstrated that N_2 TPD spectra obtained from films before and after annealing to ~60 K differed in their line shape,[67] the total amount of N_2 adsorption was similar for both the deposited and annealed water film. This suggests that while annealing does result in some rearrangement of the molecules on the surface of the pores, this does not significantly adjust the overall porosity.[125] The np-ASW and CI ices also contain dangling bonds from surface molecules that are not fully participating in the hydrogen bonding network,[59] but at a lower intensity compared to the p-ASW ice[95] (**Figure 4.1a**). On CI and np-ASW ices there are only surface sites that contain dangling bonds available for hydrogen bonding on top of the ice film due to the lack of a pore structure. Due to the agreement in the integrated area of the 2730 cm^{-1} peak for the np-ASW and CI ices, the amount of dangling bonds of the surface of these two ices are similar, but less than that of on the surface of the p-ASW ice. Unless otherwise stated, p-ASW refers to the default porous film deposited at 30º and other porous films (70º) will be labeled as such. When examining acetone interacting with p-ASW films of varying porosity, acetone exposure occurred at the deposition temperature (20 K). ‘

Acetone (Sigma-Aldrich 99.5%, 5ºC) was bubbled through the molecular beam at a typical flux of 5.4×10^{14} molecules cm^{-2} s^{-1} that resulted in an average growth rate of 3 ML/min onto the Au(111) substrate or the D_2O ice film (assuming that one monolayer (ML) is $\sim 10^{15}$ molecules cm^{-2}).[28] The acetone molecular flux was determined by measuring the pressure rise using a nude Bayard-Albert ion gauge for an acetone beam open to the chamber. The flux was calculated by accounting for the relative gauge sensitivities to acetone and N_2,[73,126] the chamber pumping speed at different temperatures and the beam spot size on the Au(111) crystal. By varying the pressure of the beam and monitoring the pressure rise for m/z = 43 amu measured by a RGA not in line with the beam and fitting to a linear regression we determined the total acetone flux. The default acetone exposure was performed at normal incidence unless otherwise indicated.

For co-dosing experiments of D_2O and acetone, a 100-layer D_2O film was initially grown on the surface before D_2O was dosed through the directed doser while the acetone was dosed through the supersonic molecular beam. Four different acetone film compositions were produced: 1%, 1.5%, 2%, and 25% where the acetone film percentage is calculated from the 1700 cm^{-1} C=O stretch for acetone and the 2200-2800 cm^{-1} OD stretch for D_2O. The acetone incident flux was reduced by employing a mechanical chopper (a rotating slotted disk). Concurrently, the directed doser's leak valve was adjusted to increase the D_2O growth rate. The final mixed D_2O and acetone film were comprised of 400 layers of D_2O and between 4-50 layers of acetone. After dosing the mixed acetone and D_2O film, each RAIR spectrum is an average of 3000 scans.

4.3 Results

4.3.1 Acetone Spectra

RAIR spectra of condensed amorphous acetone on Au(111) at 70 K is shown in **Figure 4.2**. In the condensed phase acetone spectra red-shifts as compared to liquid and gas phase spectra[127,128] and are comprised of many spectral features. The most intense spectral feature (in the 1700 region, **Figure 4.2a**) is assigned to the C=O stretch.[129–132] There are additional major spectral features corresponding to δ_a asymmetric methyl bending (1420 cm^{-1}), δ_s symmetric methyl bending (1371 cm^{-1}), ν_a asymmetric C-C-C stretching (1239 cm^{-1}), and ρ methyl rocking (1097 cm^{-1}, 901 cm^{-1}) modes (Figure 2b).46 Condensed phase acetone spectral features are red shifted compared to the liquid features which are: 1712 cm^{-1} (CO stretch), 1438 cm^{-1} (asymmetric methyl bending), 1420 cm^{-1} (asymmetric methyl bending), 1362 cm^{-1} (symmetric methyl bending), and 1092.5 cm^{-1} (methyl rocking). Unless otherwise stated, changes in the intensity and specific peak locations within the C=O region will be used to characterize acetone-substrate interactions.

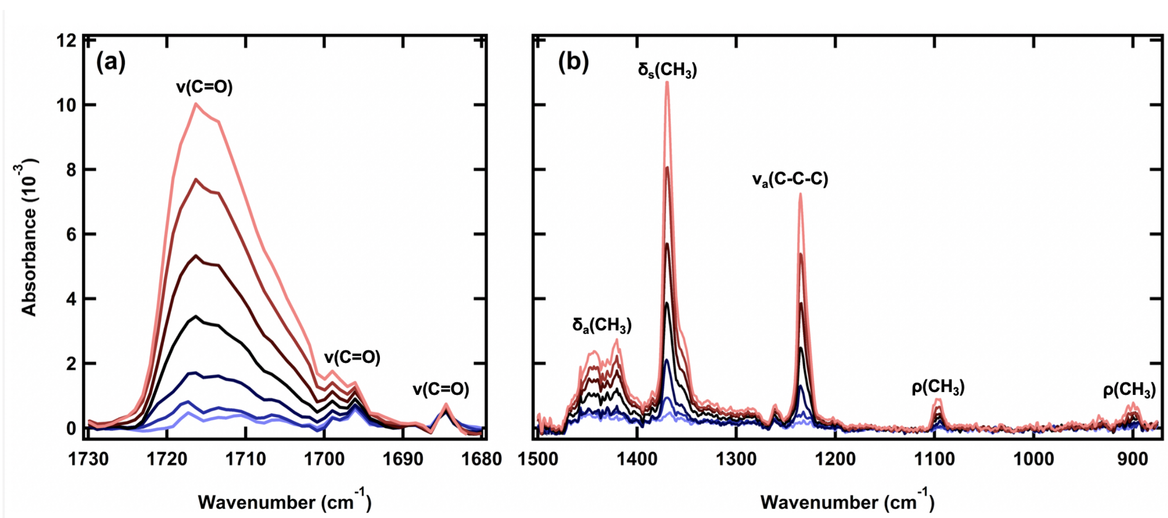

Figure 4.2: RAIR spectra of 1-24 ML acetone adsorbed on Au(111) at 68 K. The RAIR spectra are separated into two wavenumber regimes: (a) C=O stretching between 1680-1720 cm^{-1} and (b) CH3 deformation and rocking modes between 875-1500 cm^{-1}. The spectra correspond to 1, 1.7, 4.2, 8.3, 13, 19 and 24 ML of acetone.

As shown in **Figure 4.2a**, as layers of acetone grow in at 68 K, the C=O stretch splits into multiple peaks and the peaks less than 1700 cm^{-1} saturate at low coverage while the 1716 and 1708 components increase significantly with increasing acetone film thickness. These results show good agreement with previous RAIRS studies of acetone on Au(111) at 90 K[129] and FTIR studies of amorphous and crystalline acetone.[130] Therefore, this indicates that peaks at 1708 cm^{-1} and 1716 cm^{-1} correspond to acetone-acetone bulk interactions[117,120,133] whereas the 1694 cm^{-1} and 1698 cm^{-1} peaks correspond to interfacial acetone.[132] It is important to note for our future analysis of acetone on top of and within water matrices that since the 1698-1708 cm^{-1} peaks are present in bulk condensed acetone, these features cannot be attributed to H-bonded CO as in liquid spectra of acetone and water mixtures.[127]

4.3.2 Low Coverage Acetone on Water Films of Varying Thickness

Next, we examined low coverage (<1 ML) of acetone dosed on top np-ASW D_2O films of varying thickness (100, 300, 600 ML) at 108 K. All acetone films are between 0.74 ML and 0.94 ML of acetone. As shown in **Figure 4.3**, acetone on top of a 100 ML np-ASW D_2O film contains two features: a main acetone monolayer peak[117,129] at 1702 cm^{-1} and a shoulder at 1711 cm^{-1}. Since the 1711 cm^{-1} peak is attributed to multilayer acetone or acetone-acetone interactions,[134] this suggests that when the ASW film is thinner, fewer acetone molecules interact with water in the acetone-water interfacial region and that the water film is not yet self-similar; by self-similarity we mean that the structure of the interface is no longer varying with changes in thickness. Films less than 100 layers contain small islands that with increasing thickness converge to form a uniform film structure.[19,29,54,61,135] Thus, in contrast to the ultrathin films grown in previous studies[116–118] we chose to grow ice films of at least 150 layers to ensure that any differences observed with how acetone interacts with the CI, np-ASW, and p-ASW D_2O ices are due to the underlying water coordination and not simply a film thickness effect.

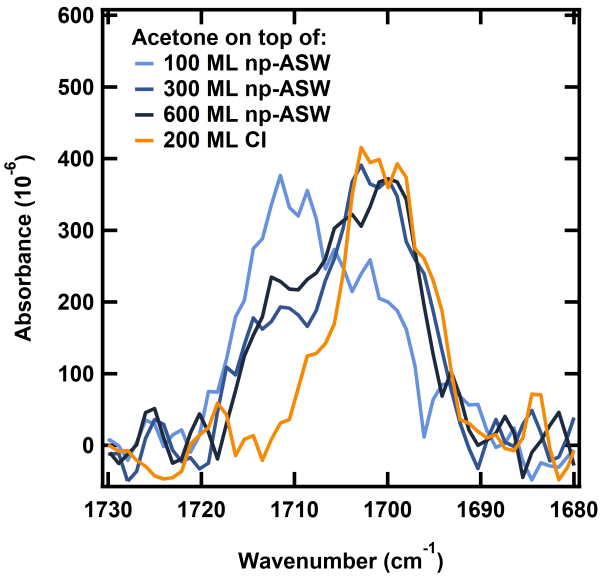

Figure 4.3: Representative RAIR spectra of the ν(CO) region of sub-monolayer acetone on top of np-ASW (blue) and CI (orange) D_2O films of varying thicknesses at 108 K. The thinnest np-ASW film (100 layers) has increased acetone spectral intensity at 1711 cm^{-1} indicating less interaction with the underlying water film.

4.3.3 Acetone Interaction with CI, np-ASW, and p-ASW Ice Films

To understand the interaction between acetone and our different astrophysical ices, we dosed layers of acetone on top of 150 layers p-ASW, np-ASW and CI at 68 K and collected RAIR spectra. At 68 K, acetone and water desorption are unlikely to occur and acetone is likely amorphous.[114,122,130] As seen in **Figure 4.4** focused on the C=O region, each spectrum is normalized to the intensity at 1711.5 cm^{-1}, the amorphous multilayer carbonyl band,[130] to examine peak widths and shape as a function of exposure.

For all three of the molecular ices, there is a blue-shift as a function of increasing exposure. This shift is consistent with acetone-acetone interactions in addition to the initial acetone-water substrate interactions. With increasing acetone exposure, the relative intensity of these low-frequency modes saturates as there is a larger growth of the bulk carbonyl modes ($>$ 1711 cm^{-1}). As an example, for acetone on p-ASW ices, the initial 2.6 ML spectra contains no spectra features greater than 1711.5 cm^{-1}. However, with increasing acetone exposure, new features grow in at 1712 cm^{-1} and 1716 cm^{-1}. By 25 ML (spectra 6), the integrated area from the multilayer features

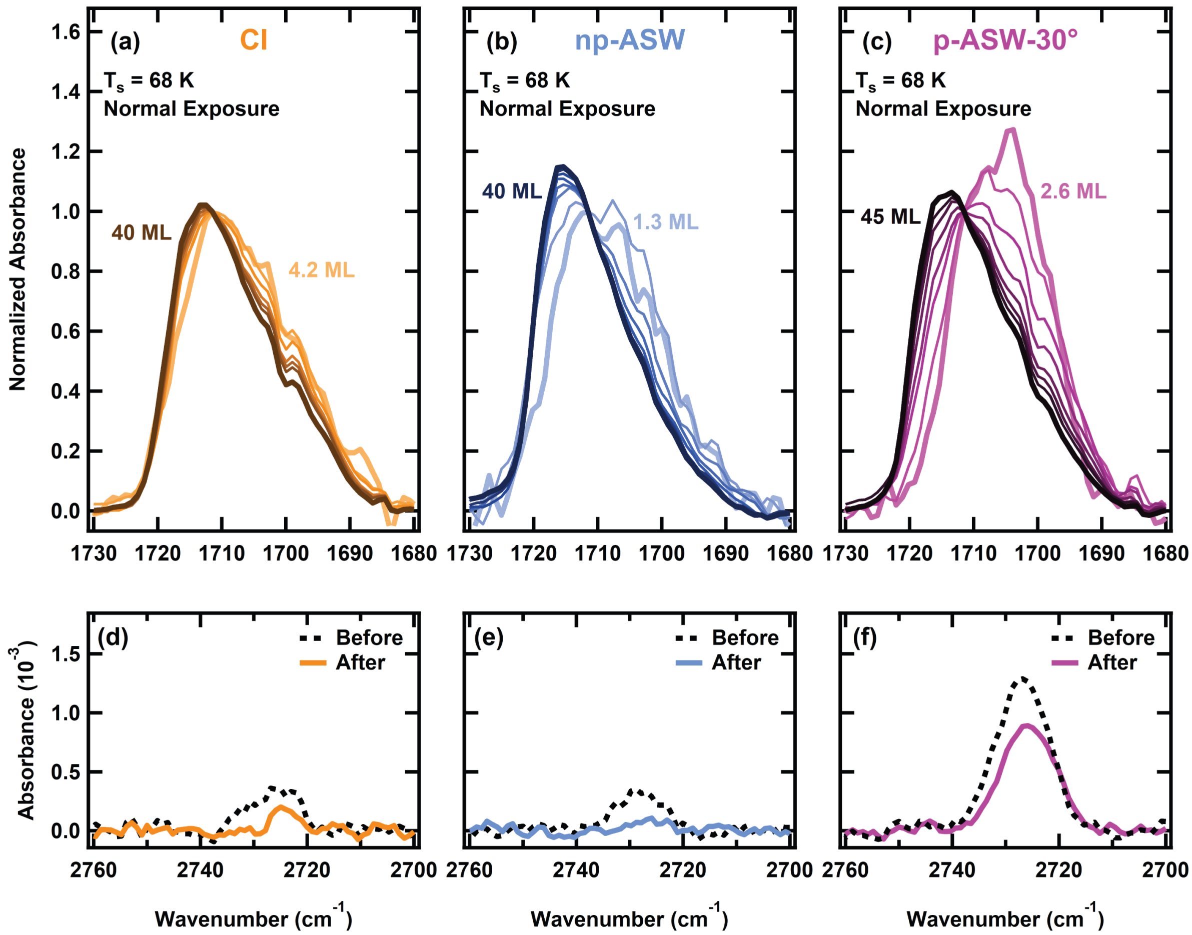

Figure 4.4: Representative RAIR spectra of the ν(CO) region of acetone on top of 150 layers of CI (a), np-ASW (b) and p-ASW (c) D_2O films at 68 K. Acetone exposure was normal. All acetone spectra are normalized to the intensity at 1711.5 cm^{-1}, the amorphous multilayer carbonyl band. The initial and final acetone spectra for each D_2O film are slightly thicker and with increasing acetone exposure, the spectra darken in color. Additional RAIR spectra (d-f) provides the corresponding OD dangling bond intensity before and after acetone exposure for the corresponding CI (d), np-ASW (e) and p-ASW (f) D_2O films. The 14 cm^{-1} shift (c) and decrease in dangling bond intensity (f) indicates increased hydrogen bonding occurs between uncoordinated D_2O molecules in the pores of p-ASW and the acetone.

(>1711.5 cm^{-1}) reaches ~50% of that of the entire C=O region from 1680 to 17230 cm^{-1}. The relative ratio of ~50% for the integrated area of features < 1711.5 cm^{-1} and ~ 50% for integrated area of features >1711.5 cm^{-1} remains relatively consistent throughout the rest of the exposure. In other words, with more than 25 ML of acetone, there is no change to the normalized acetone spectra for acetone on p-ASW, np-ASW and CI ice films at 68 K with increasing exposure (**Figure**

4.4a-c). As shown in **Figure 4.4c**, for the p-ASW ices at low coverage, there is a 14 cm^{-1} shift to $\sim$1703 cm^{-1} when compared to the bulk value of 1717 cm^{-1}, indicative of hydrogen bonding between the ice to the carbonyl oxygen on the acetone.25 This spectroscopic shift is also identified for acetone on top of np-ASW and CI ices. However, at low coverages of acetone, the relative intensity of the 1703 cm^{-1} mode is greatest for acetone on top of the p-ASW film followed by acetone on np-ASW and lastly acetone on CI.

We examine this further by focusing on the uncoordinated OD dangling bonds (**Figure 4.4d-f**) both after deposition and following acetone adsorption. After exposure to acetone, in the RAIR spectra between 2700 cm^{-1} and 2800 cm^{-1}, there is a decrease in intensity of the OD dangling bond for all three ice films (CI, np-ASW and p-ASW), with the largest drop for the p-ASW films. Quenching of the dangling bond intensity occurs when the undercoordinated OD molecules hydrogen bond to the acetone. For CI and np-ASW films, this drop in dangling bond intensity results from acetone adsorbing onto available surface sites on top of the film. However, for p-ASW films, this drop in dangling bond intensity results from both acetone adsorbing onto available surface sites on top of the film as well as onto available sites that decorate the pore structure. In general, uncoordinated water molecules on the surface of the water film and within the open pore structure are necessary for hydrogen bonding to occur.[136,137] The larger drop in the higher wavenumber shoulder (2725 cm^{-1}) of the dangling bond peak for the p-ASW film after exposure suggests that acetone is more easily able to hydrogen bond to the less coordinated water molecules, possibly due geometric presentation of the pores to the direction of the incident acetone beam.

Quantifying this further, we also focus on the integrated intensity of the OD dangling bonds between 2700 cm^{-1} and 2800 cm^{-1} (**Figure 4.5**). For the np-ASW and CI films, the integrated OD dangling bond area after deposition is identical such that both films have the same number of dangling surface molecules.[120] After exposure to acetone at 68 K, this dangling bond feature diminishes slightly more for the acetone on top of np-ASW films as compared to acetone on top of CI films. Due to the fact that the CI dangling bond intensity does decrease after adsorption of acetone coupled with the presence of the 1703 cm^{-1} feature at low coverages of acetone, we conclude that hydrogen-bonding does occur between the crystalline ice surface and acetone. However, since the relative intensity of the 1703 cm^{-1} feature for acetone on CI ices is less than that for acetone on np-ASW ices, and more dangling bonds remain uncoordinated following exposure, fewer hydrogen bonds form between CI ices and acetone as compared to np-ASW ices and acetone.

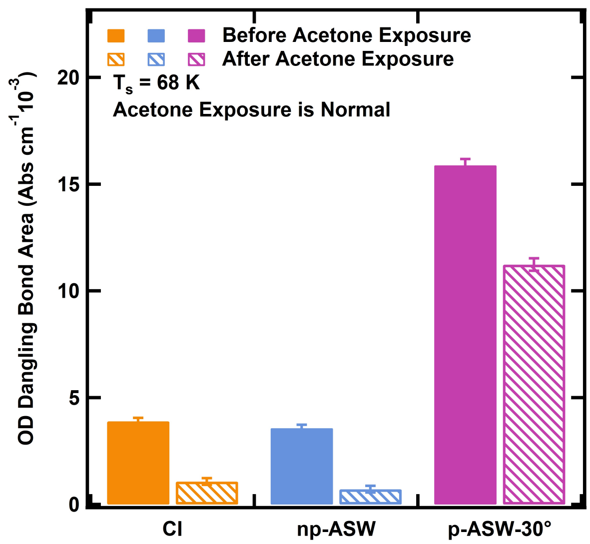

Figure 4.5: Integrated OD dangling bond intensity for CI, np-ASW, and p-ASW D_2O before and after exposure to 40-45 ML of acetone at 68 K. Due to its increased porosity, p-ASW films have more uncoordinated dangling bonds throughout the water film and thus form more hydrogen bonds with the underlying structure.

We suggest that the structural features of the CI surface are such that some of the uncoordinated OD molecules are not accessible for hydrogen bonding due to the rigid structure and the adsorption temperature. The np-ASW ice surface is rough on the length scale of several molecules, while the CI surface is much smoother. One possibility is that on CI ice films, the available surface sites with dangling bonds are oriented such that acetone is unable to form a linear bond with the planar ice surface and also experience significant van der Waals and electrostatic interactions with the film.[117] For low coverages of acetone at 68 K (**Figure 4.4a-c**), the spectroscopic feature at 1709 cm^{-1} is assigned to Van der Waals interactions[120] that occur between carbon atoms and all three difference D_2O films. Since additional electrostatic interactions occurs between acetone and surface water molecules, not all free OD molecules may be able to form hydrogen bonds with acetone.

Regardless of the slight surface structural differences that occur between CI and np-ASW that dictate the amount of hydrogen bonds that can form, the p-ASW film has many more dangling bonds both on the surface and in the pores resulting in the largest integrated area compared among the three films (**Figure 4.5**). In other words, the p-ASW film has more available surface sites for hydrogen bonding. Upon exposure to acetone, the integrated area decreases by ~30% as acetone decorates the pore structure and adsorbs on top of the film. *Thus, we confirm due to the greatest relative intensity for the 1703 cm^{-1} feature (**Figure 4.4c**) and the largest titration of free OD molecules (**Figure 4.5**) that more hydrogen bonds occur between the p-ASW film and acetone as compared to acetone and the np-ASW or CI films.*

4.3.4 Acetone Interaction with p-ASW Films, Increased Porosity

To further probe the role that surface and pore sites with dangling bonds play in facilitating hydrogen bonds, we examined acetone dosed on top of 150 layers of p-ASW at 20 K (**Figure 4.6a,d**). We also examined acetone on top of p-ASW films with increased porosity (panels b-c for the acetone RAIR spectra and corresponding e-f for the OD dangling bonds).

First, we can see in the **Figure 4.6d** inset that as a result of not annealing the p-ASW D_2O film to 68 K, there is a new spectroscopic feature at 2748 cm^{-1} attributed to two coordinated D_2O molecules.[70] Additionally, the overall dangling bond surface area is greater than that of the p-ASW film annealed to 68 K. Similarly to the p-ASW film at 68 K (**Figure 4.4d**), upon exposure to acetone at 20 K, there is a decrease in dangling bond intensity as acetone is able to hydrogen bond to the ice surface. The hydrogen bonding is confirmed by the 14 cm^{-1} shift to 1703 cm^{-1} when compared to the bulk value of 1717 cm^{-1}. When further examining the intensity of the OD dangling bonds before and after exposure to acetone (**Figure 4.6d**), it is apparent that there is a greater decrease in the intensity of the higher wavenumber (2748 cm^{-1}), two coordinated D_2O molecules. This indicates that accessibility of free OD is necessary to facilitate the hydrogen bonding. The unannealed p-ASW film contains a larger integrated dangling bond intensity and thus, has more sites available on the surface of the ice and within the pores structure that are

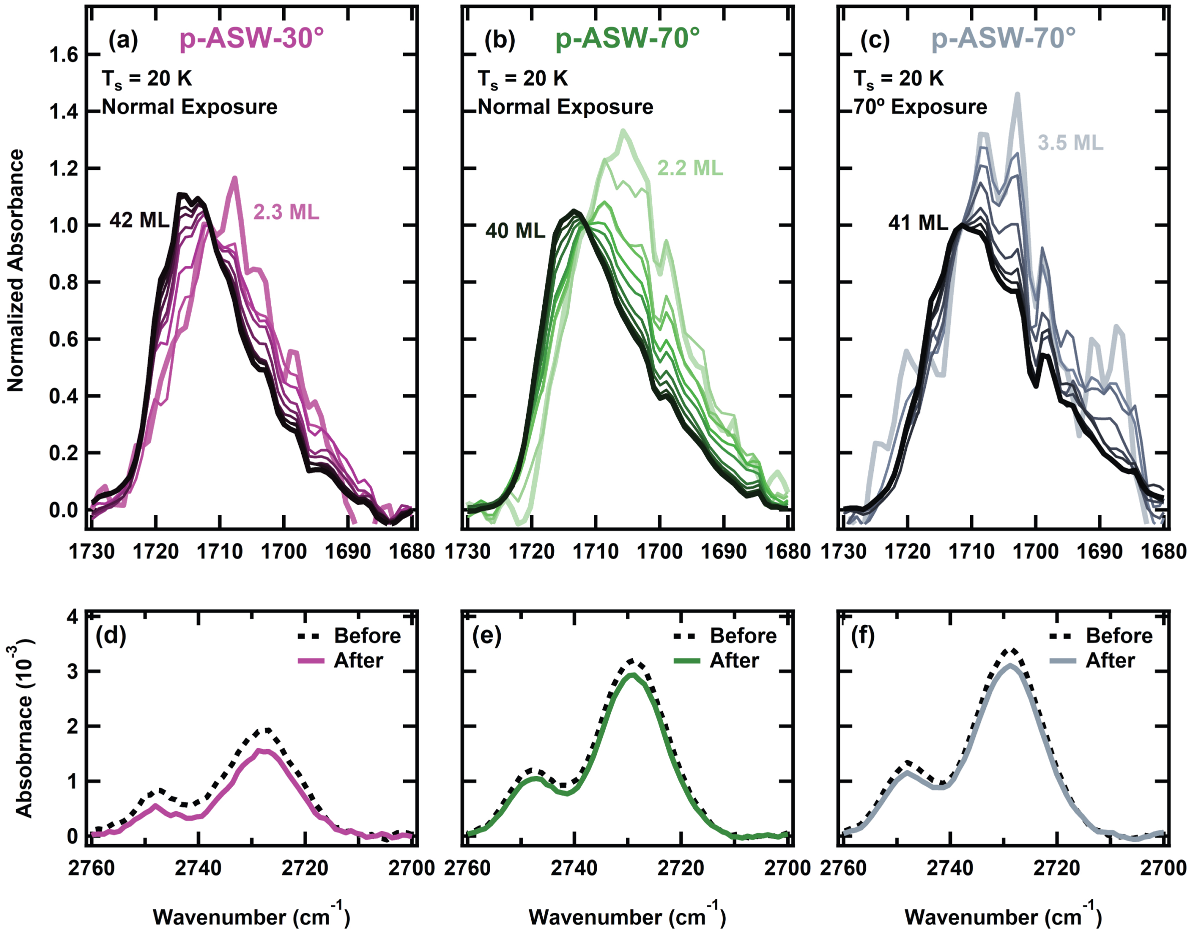

Figure 4.6: Representative RAIR spectra of the ν(CO) region of acetone on top of 150 layers of p-ASW D_2O film (a) deposited at 30º and p-ASW D_2O films deposited at 70º (b, c) at 20 K. Acetone exposure was normal for a and b and 70º for c. All acetone spectra are normalized to the intensity at 1711.5 cm^{-1}, the amorphous multilayer carbonyl band. The initial and final acetone spectra for each D_2O film are slightly thicker and with increasing acetone exposure, the spectra darken in color. Additional RAIR spectra (d-f) provides the corresponding OD dangling bond intensity before and after acetone exposure for the p-ASW D_2O films.

available for hydrogen bonding. Interestingly, when comparing between the p-ASW at 20 K to the film annealed to 68 K, the same percentage (∼30%) of dangling bonds participate in hydrogen bonding to acetone molecules (**Figure 4.7**). We suggest then, that acetone is unable to fully access the full canted pore structure[95] and is limited by the dangling bonds that are accessible on the interfacial region. Since O-O distances in amorphous water samples deposited at 77 K can be 2.7 Å,[138,139] while acetone is closer to 3 Å it is possible that acetone's size as well as the cryogenic experimental temperature (20 K) limits its mobility within the pore structure. To confirm this, we examined acetone on top of ASW films with increased porosity.

The ASW films with increased porosity were produced by changing the angle of the directed doser relative to surface normal.[29,67,68] As we demonstrated previously[113] and characterized by Stevenson et al.[29] porosity increases with deposition angle such that D_2O films dosed at 30° are less porous than those grown at 60° or 70°.[69]58 These pores grow in at an orientation dictated by the deposition angle.[67] Additionally, since the intensities of the dangling bond spectroscopic signals scale with porosity, RAIR spectra can be used to qualitatively confirm that ices with different porosities have been formed.[70,71] p-ASW-70º films still contain the two different surface sites with dangling bonds available for hydrogen bonding: one on top of the ice film and one decorating the pores. However, since the p-ASW-70º film structure has larger pores, there are fewer surface sites on top of the ice film and more surface sites decorating the pores. To highlight the effect that pore structure has on hydrogen bonding, we choose to focus on acetone deposited on top of p-ASW films dosed at 70° since these films have the largest percentage of available undercoordinated surface sites that could hydrogen bond to the acetone.

We first compare the C=O RAIR stretch for acetone on top of p-ASW deposited at 70º to that deposited at 30º (**Figure 4.6a,b**). There are two noticeable spectral differences: the presence of the shoulder at 1720 cm^{-1} for high acetone coverages on the p-ASW-30º film and the higher relative broad intensity of the 1705 cm^{-1} feature for low coverages on the p-ASW-70º film. Both differences are attributed to the increased surface area of the 70º film.

Adjusting the dosing angle for the p-ASW from 30° to 70°, also significantly increases the integrated area of the dangling bonds (**Figure 4.7**). Upon exposure of the p-ASW dosed at 70º to acetone at 20 K, the integrated OD dangling area decrease (and thus the amount of hydrogen bonding that occurs) is less than half that for the p-ASW dosed at 30° (**Figure 4.5**). This finding is supported by our previous work examining methane sticking probability on p-ASW of varying morphologies (30°, 60°, 70°, and background deposited).[113] When examining total coverage scaled by the dangling bond surface are to give an approximate "fractional coverage", we deter-

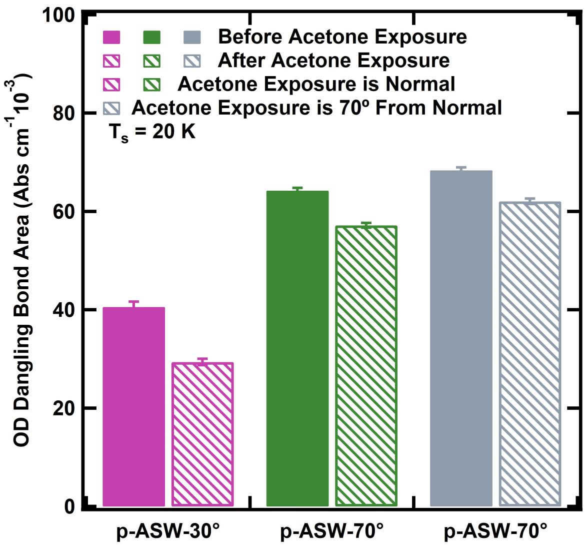

Figure 4.7: Integrated OD dangling bond intensity for p-ASW D_2O deposited at 30º, and p-ASW deposited at 70º before and after exposure to 40-42 ML of acetone at 20 K. Acetone exposure occurred at normal incidence and at 70º. Although there is a greater number of dangling OD molecules for films deposited at 70º, less overall hydrogen bonding occurs.

mined that although the initial sticking probability was the consistent across the different porous films, the relative methane accumulation was 1-2 times higher for background deposited and 30° films compared to those deposited at 60° or 70°. Although films deposited at 30° have less total surface area (from the integrated dangling bond intensity), their pores are closer to perpendicular to the substrate.[29,104] We suggest then that the difference in the number of hydrogen bonds that form results from the accessibility of different surface sites for hydrogen bonding. Since the p-ASW-70º films contain less surface sites on the top of the ice film and also form fewer hydrogen bonds as compared to the p-ASW-30º film, this indicates that these sites are readily available to the beam and extremely important for hydrogen bonding.

To test whether accessible surface sites to the beam are responsible for this difference, we deposited p-ASW films at 70º prior to acetone exposure also at 70º from surface normal. As shown in **Figure 4.7**, the integrated dangling bond intensity decrease following exposure at 70º is comparable to the decrease that occurs from after exposure to an acetone beam normal to the surface. Thus, the same number of hydrogen bonds form between acetone and the p-ASW-70º film regardless of the angle of the incident acetone beam. In sum, this behavior results from a lack of access to available sites within the pores, but *not* because of surface sites available to the beam. Since there was no difference in the number of hydrogen bonds that occur as a function of incident beam deposition angle, it is likely that acetone covering the ice surface prevents additional acetone molecules from being able to access the entire pore structure. Since N_2 only readily diffuses into the pore structure at 23 K,[140] and NH_3 and CH_3OH are unable to diffuse into the pore structure,[141] it is not expected that acetone would diffuse at 20 K. Regardless of the beam's incident angle, once an acetone molecule adsorbs onto the surface, the surface temperature does not provide enough mobility to the molecule.

We conclude that increasing the surface dangling bonds for p-ASW films compared to CI and np-ASW films increases the number of hydrogen bonds occurring between acetone and the underlying p-ASW surface. When increasing the porosity of film (deposited at 70º compared to 30º), there is a further reduction in the number of hydrogen bonds, but this effect is not dependent on the angle of the incident acetone beam. Therefore, this results from a lack of access to available surface sites decorating the pores. Initial layers of acetone block the pores and acetone is unable to diffuse through the structure at low temperatures. Overall, our results highlight the important role that interfacial uncoordinated OD dangling bonds play in facilitating hydrogen bonding especially between porous amorphous ices and acetone.

4.3.5 Acetone in a Non-Porous Water Matrix, Concentration Effects

In order to examine individual acetone RAIR spectra features, we also focused on acetone condensed in a np-ASW matrix. For these experiments, we first dosed 100 layers of np-ASW on the Au(111) before co-dosing acetone and np-ASW through both the beam and directed doser, respectively, at 108 K. By varying the incident acetone and water fluxes, this produces mixed films that ranged from 1-25% acetone. As shown in **Figure 4.8**, there are distinct RAIR spectral differences due to acetone concentration. There is a greater intensity of the 1698 cm^{-1} peak in the 1-2% acetone mixed films compared to the 25% acetone film due to isolation of individual acetone molecules. The relative intensity of this peak (1698 cm^{-1}) also decreases with increasing acetone percentage. There is also a red-shift of the 1711.5 cm^{-1} mode in the 25% acetone film when compared to the 1-2% films. Since the OH stretch band of liquid water surrounded by acetone was less redshifted compared to pure liquid water[127] this suggests that the acetone-water hydrogen bonding is weaker than the water-water hydrogen bonding in the mixed matrix.

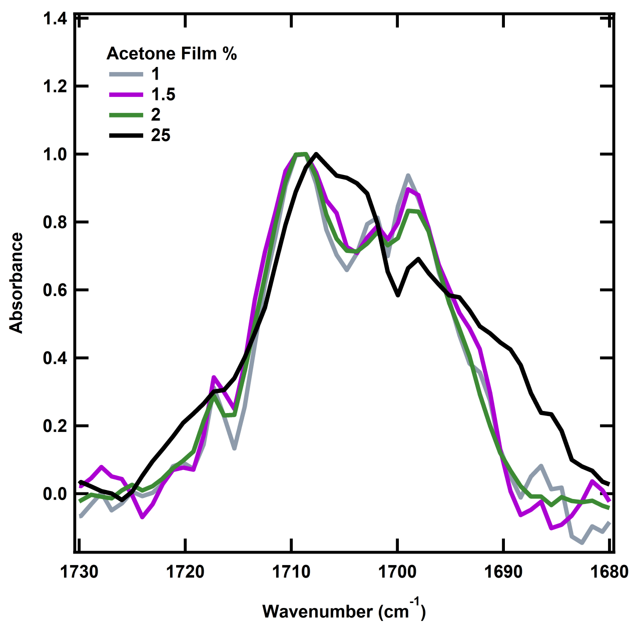

Figure 4.8: RAIR spectra of the ν(CO) region of acetone diluted in a np-ASW matrix at 108 K. The percentage of acetone in each mixture ranges from 1% to 25%. All acetone spectra are normalized to the intensity at 1708 cm^{-1}.

4.4 Conclusion

In this work we present RAIR spectra analyses for acetone on top of D_2O ice films of varying morphologies and for acetone within an ice matrix. When first examining acetone on Au(111), we determine that the acetone spectra are comprised of both bulk (1708 cm^{-1}, 1716 cm^{-1}) and interfacial (1694 cm^{-1}, 1698 cm^{-1}) signatures that can be used to probe the strength and interaction between acetone and D_2O ice films. For low coverages (<1 ML) of acetone deposited on top of np-ASW and CI films, we determine that when the np-ASW film is thinner, less of the acetone molecules are interacting with water in the acetone-water interfacial region and that films are not structurally self-similar until 150 layers. Importantly, when increasing the underlying D_2O surface thickness and examining acetone on top of p-ASW, np-ASW and CI films at 68 K, we conclude that more hydrogen bonding occurs between acetone and p-ASW ices as compared to acetone and np-ASW or CI films. Hydrogen bonding quantification occurred by two independent RAIR spectral changes: a greater relative intensity of the 1703 cm^{-1} feature at low acetone coverage as part of a 14 cm^{-1} shift in the C=O region, and by a $\sim$30% integrated dangling bond area reduction following exposure. Interestingly, when changing the water structure to be more porous (deposited at 70º compared to 30º), there is a further reduction in the amount of hydrogen bonding that occurs. However, when adjusting the acetone deposition angle to match that of the angled pore structure, the number of hydrogen bonds formed is the same as that from a normal incidence beam striking the same surface (p-ASW-70º). Therefore, acetone is unable to access available surface sites in the pores due to initial adsorption blocking the pore structure at temperatures where acetone cannot diffuse.

In general, these results are further evidence that the morphology of the ice critically impacts the strength of the surface-adsorbate interactions and thus subsequent reactivity of incident molecules. Even if not fully porous, small cracks and morphological deformities in the surface of the astrophysical ices can lead to uncoordinated water molecules that hydrogen bond to incident projectiles. Strong hydrogen bonding between adsorbates and p-ASW ices may result in a higher desorption temperature of these molecules[142] thereby impacting comet outgassing, chemical abundances due to reactions in the ISM, and thermal and electrical processing of icy dust grains.[67]

Chapter 5

Differential Condensation of Methane Isotopologues Leading to Isotopic Enrichment Under Non-equilibrium Gas-Surface Collision Conditions

In this paper we examine the initial differential sticking probability of CH_4 and CD_4 on CH_4 and CD_4 ices under non-equilibrium flow conditions using a combination of experimental methods and numerical simulations. The experimental methods include time-resolved *in-situ* reflection-absorption infrared spectroscopy (RAIRS) for monitoring on-surface gaseous condensation and complementary King and Wells mass spectrometry techniques for monitoring sticking probabilities that provide confirmatory results via a second independent measurement method. Seeded supersonic beams are employed so that the entrained CH_4 and CD_4 have the same incident velocity but different kinetic energies and momenta. We found that as the incident velocity of CH_4 and CD_4 increases, the sticking probabilities for both molecules on a CH_4 condensed film decrease systematically, but that preferential sticking and condensation occurs for CD_4. These observations differ when condensed CD_4 is used as the target interface, indicating that the film's phonon and rovibrational densities of states, and collisional energy transfer cross sections, have a role in differential energy accommodation between isotopically substituted incident species. Lastly, we employed a mixed incident supersonic beam comprised of both CH_4 and CD_4 in a 3:1 ratio and measured the condensate composition as well as the sticking probability. When doing so, we see the same effect in the condensed mixed film, supporting an isotopic enrichment of the heavier isotope. We propose that enhanced multi-phonon interactions and inelastic cross sections between the incident CD_4 projectile and the CH_4 film allow for more efficacious gas-surface energy transfer. VENUS code MD simulations show the same sticking probability differences between isotopologues as observed in the gas-surface scattering experiments. Ongoing analyses of these trajectories will provide additional insights into energy and momentum transfer between the incident species and the interface. These results offer a new route for isotope enrichment via preferential condensation of heavier isotopes and isotopologues during gas-surface collisions under specifically selected substrate, gas-mixture, and incident velocity conditions. They also yield valuable insights into gaseous condensation under non-equilibrium conditions such as occur in aircraft flight in low temperature environments. Moreover, these results can help to explain the increased abundance of deuterium in solar system planets, and can be incorporated into astrophysical models of interstellar icy dust grain surface processes.

5.1 Introduction

Adsorption is a key process in both astrophysical and terrestrial environments as it serves as the first step in many gas-surface interactions.[33,36,48] In extraterrestrial environments where chemical species are scarce, adsorption onto an interstellar grain, planetesimal, or other larger body controls many combinatorial reactions. The formation of larger organic molecules becomes more feasible when species can engage on a surface rather than the void of space.[143–148] In addition, the astrophysical environment is abundant with isotopes of many chemical species.[149] In order to accurately model the chemical abundances, we need to better understand how differences in mass can influence the ability of a species to adsorb under specified conditions, and thus lead to observed relative isotope abundances.[150,151]

Interstellar methane is the most common hydrocarbon, existing both in the gaseous and the solid form.[152–158] Methane is commonly found in the gaseous planetary atmospheres or as molecular ices intermixed with water ice matrices.[51,159] As the most basic hydrocarbon, CH_4 serves as a base for addition reactions which form larger hydrocarbon species.[160] Additionally, the isotopic twin of CH_4, CD_4, can serve as a model for understanding the effects and the abundance of deuterium within these environments.[151,161] Theoretical methods and gas chromatography have found that the isotopic difference in CH_4 and CD_4 stems from the difference in polarizability and length of the C-H and C-D bonds, however, no studies have reported how this difference might translate into its sticking probability.[151,162,163] Studying CH_4 and CD_4 adsorption is an excellent model system to determine how slight mass differences in the condensate and projectile can impact adsorption and surface abundance of isotopic species.

Here we present the first study of the isotopic sticking probability of CH_4 and CD_4 as a function of translational beam energy on CH_4 and CD_4 thin films under ultrahigh vacuum (UHV) conditions at low temperatures using the King and Wells method[17] complemented by in situ infrared spectroscopic studies of gaseous condensation. VENUS code molecular dynamics (MD) simulations show the same sticking probability differences between isotopologues as were observed in the gas-surface scattering experiments. Taken together, these results accurately and independently determine the sticking probability, allowing us to explore how differences in isotopic composition of the surface and incident molecular mass can impact the overall energy accommodation, and thus adsorption of the gaseous species onto the film. Key to these studies is the use of essentially monoenergetic seeded supersonic beams so that the CH_4 and CD_4 have the same incident velocity but different kinetic energies and momenta. It is shown that as the incident velocity of CH_4 and CD_4 increases, the sticking probabilities for both molecules on a CH_4 condensed film decrease systematically, but that preferential sticking and condensation occurs for CD_4. These observations differ when condensed CD_4 is used as the target interface, indicating that the film's phonon and rovibrational densities of states, and collisional energy transfer cross sections, play a role in differential energy accommodation between isotopically substituted incident species. In addition, a mixture of gaseous CH_4 and CD_4 was grown on a methane thin film. While both species adsorbed creating a mixed isotopologue condensate, we saw an increased abundance of CD_4 vs. CH_4 within the film as opposed to initial beam concentration. We demonstrate an isotopic enrichment for CD_4 in our mixed surface based on the difference in sticking probabilities between CH_4 and CD_4.

This experiment builds on previous work by our group where CH_4 sticking was investigated on the surfaces of D_2O of varying morphologies and where H_2O and D_2O sticking on their own films were studied.[17,55,113] In particular, we consider a similar isotopic experiment as the H_2O and D_2O sticking but expand to study CH_4 and CD_4 sticking on both films rather than only their own films.[113] Additionally, previous work examined the sticking of only CH¬4 on H_2O which we expand to include CH_4 and CD_4 sticking onto both CH_4 and CD_4 ices to examine how the mass difference can affect the overall sticking.[55] We examine how these differences in mass, energy, and surface composition can affect the ability of the film to absorb and dissipate energy from the impinging molecules to allow adsorption onto the film structure.

Our work demonstrates differential condensation between methane isotopologues under specifically selected substrate, gas-mixture, and incident velocity conditions. The demonstrated outcomes have obvious implications for the development of novel isotopic enrichment and separation techniques. These results also provide new insights into gaseous condensation under non-equilibrium conditions such as occur in aircraft flight in low temperature environments. More broadly, this work is critical to understanding the nature of methane adsorption within astrophysical environments. Our sticking probability differences can be incorporated into astrophysical models to explain molecular abundances and increased deuterium abundance in cometary ices and outer solar system planets. Aside from astrophysical environments, adsorption has implications into fields such as heterogenous catalysis or thin film growth where the adsorption process serves as the first step in film formation.[55]

5.2 Experimental

All experiments were conducted in a molecular beam scattering instrument previously discussed in full detail.[55] Briefly, this instrument consists of a UHV chamber with base pressures of 10^{-10} Torr connected to a triply differentially pumped molecular beamline. In the main chamber, a state-of-the-art closed-cycle helium-cooled sample manipulator (Advanced Research Systems) enables precise and accurate temperature control of the Au(111) sample substrate between 16 and 800 K. The crystal is exposed to the impinging beam at normal incident angle and monitored in real time with optics for *in situ* reflection absorption infrared spectroscopy (RAIRS). Gas scattering and incident flux monitoring occurs with a residual gas analyzer (RGA).

All RAIR spectra are analyzed with Gaussian peak fitting atop cubic baselines. Spectra were acquired with a Nicolet 6700 infrared spectrophotometer (Thermo Fischer) using incident p-polarized IR radiation at an angle of 75° to the Au(111) crystal and a liquid nitrogen-cooled mercury cadmium telluride (MCT/A) detector. Each RAIR spectrum is an average of 25-200 scans taken using 4 cm^{-1} resolution with a clean Au(111) sample used for the background correction.

CH_4 or CD_4 was dosed on the Au(111) substrate via beam deposition at 18 K prior to measurements at 20 K. Dosing conditions resulted in a deposition rate of 0.5 layers per second.

CH_4 and CD_4 beams were produced by expanding 1% CH_4 in H2 or 1% CD_4 in H2 at stagnation pressures of 150-400 psi through a 15 µm platinum pinhole. Resistively heating the beam nozzle from room temperature up to 1100 K resulted in beam velocities of up to 4600 m/s and rotationally cold molecules resulting from the seeded expansion. The translational energy distribution widths (Δv/v) ranged from 5 to 24%. We note that the velocity slip between the two isotopologues varied between 0 and at most 100 m/s with velocities spanning 2400 to 4600 m/s, therefore the incident velocities of the two isotopologues were essentially identical for the purposes of a given experiment. Incident velocities were measured by time-of-flight methods using a mechanical chopper to modulate the beam prior to detection with an in-line quadrupole mass spectrometer. To confirm all the results and further understand phonon interactions at cold temperatures, a mixed beam was produced by expanding 1% CD_4, 3% CH_4 in H2.

As described in **Subsection 2.2.3** and **Chapter 3**, sticking probability was determined using the King and Wells technique.[17,18] King and Wells measurements were performed at 20 K for all results presented in this study. This temperature was carefully chosen due to the methane surface interaction and the King and Wells method itself. UHV conditions at 20 K accurately model astrophysical chemistry rich environments such as dense molecular clouds.1 Additionally, at 20 K, multilayer CH_4 is stable on a gold substrate and frozen ice films which enables measuring the condensate via RAIRS. As mentioned in He et al.,[46] and detailed in **Chapter 3** examining the initial sticking probability of CH_4 on D_2O ices,[113] the liquid helium cooling of the sample manipulator could impact the pumping speed and thus the reflected portion of the beam, therefore we take all measurements at a single sample temperature. This ensures that the unknown pumping speed remains consistent across measurements. We also calculate sticking probability by using the initial CH_4 indirect flux instead of the value at saturation.

5.3 Results and Discussion

To fully understand the role that mass matching and pre-adsorbed hydrocarbons play in trapping dynamics for CH_4 and CD_4, we examined sticking probability on top of amorphous CH_4 and CD_4. Although sticking probability was previously found to be independent of ice film thickness,[47] we choose to grow films for ∼80 layers to achieve self-similarity in film structure.[29,54,135] The measured sticking probabilities for CH_4 and CD_4 on a CD_4 substrate are shown in **Figure 5.1**.

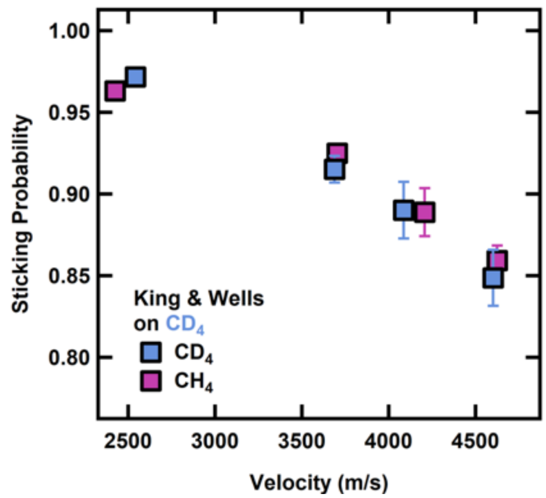

Figure 5.1: Sticking probabilities for CH_4 and CD_4 on a CD_4 film at 20 K. Sticking probability decreases with increasing velocity. Error bars represent the standard deviation of at least three measurements on at least three different days.

For physisorption trapping to occur, the CH_4 or CD_4 molecule must lose some initial kinetic energy when impinging upon the surface. If the energy loss is not efficient enough, the impactor molecule just bounces back. As expected the sticking probability decreases with an increase in energy as more energy must be lost in the initial condensation in order for sticking to occur.[164,165] The corrugation of the gas-surface potential for CH_4 and CD_4 is greater on the alkane-covered surface[166] than it is on a bare metal substrate.[167,168] Although our films are thicker than one monolayer, previous rare gas and alkene studies demonstrate that sticking probabilities are enhanced by such adlayers that allow for enhanced energy accommodation.[166,169] Sticking probabilities are close to unity at low incident velocities for both incident isotopologues before decaying down to 0.85 for both CH_4 and CD_4. There was no strong variation in sticking probabilities between the CH_4 and CD_4 projectiles indicating, overall, very similar energy accommodation.43 This suggests that both phonon creation and translational to intramolecular energy transfer are essentially the same for both CH_4 and CD_4 on the condensed CD_4 film.

*However, we note a higher sticking coefficient for CD_4 on CH_4 ice than for CH_4 on CH_4 ice particularly at high incident translational energies, **Figure 5.2***. We monitored the amount of adsorbed CH_4 and CD_4 via the intensity of the degenerate ν_4 bending mode[60,81–83,170] to calculate

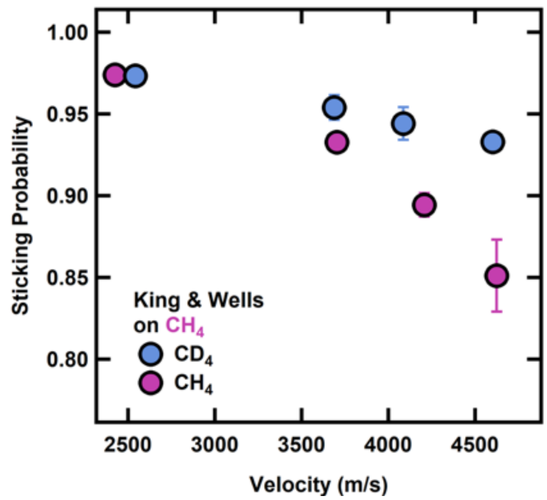

Figure 5.2: Sticking probabilities for CH_4 and CD_4 on a CH_4 film at 20 K. Sticking probability decreases with increasing velocity. Error bars represent the standard deviation of at least three measurements on at least three different days.

the initial growth rate. To ensure that these measurements were taken during an essentially constant film thickness regime, the IR measurements were completed by adding no more than an additional 0.75 MLs of condensate over the less than 4 minutes.

As shown in **Figure 5.3** for CH_4 and CD_4 beams at 4600 m/s, sticking probability differences between the CH_4 and CD_4 result in a larger amount of CD_4 stuck on the surface after exposure and therefore a higher initial growth rate. Based on the total spectral intensity vs. time and thus, condensed projectile on the surface, we calculated the initial growth rate for each incident velocity. As a consistency check, at the end of the growth exposure, we took an additional King and Wells measurement, which matched the initial sticking probability at the beginning. Taken together, this indicates that the coverage following the growth rate is not enough to change the underlying film structure and that RAIRS allows us to determine the amount of CH_4 or CD_4 on the surface. When overlaying this with the initial sticking probability, **Figure 5.4**, we confirm that both the King and Wells measurements and infrared spectroscopy of the condensate demonstrate an increased condensation of CD_4 on CH_4 compared to CH_4 on CH_4.

This isotopic effect increases with increasing translational energy. To understand this, we start by examining the Baule model,[171] which predicts that a more efficient collision occurs when the

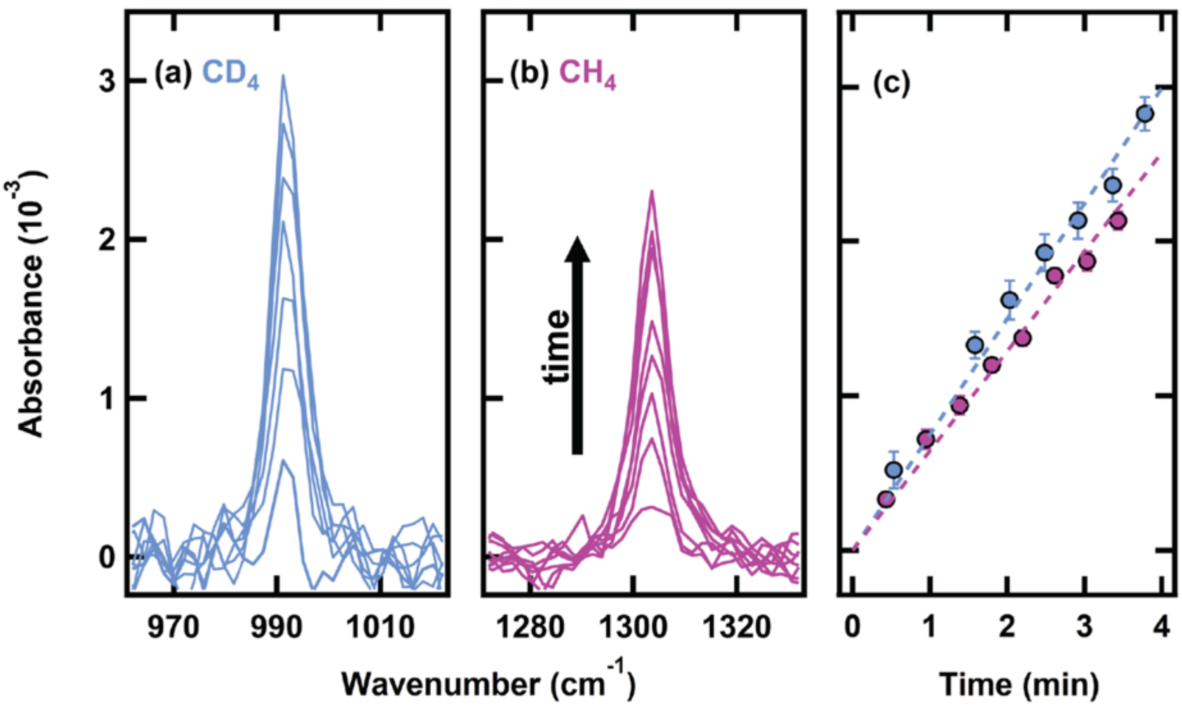

Figure 5.3: Representative RAIR spectra of CD_4 (a) and CH_4 (b) ν_4 bending mode as a function of exposure time for the highest energy beam (4600 m/s) on a CH_4 surface at 20 K. Spectra taken $\sim$ every 25 seconds (c) as a function of intensity to get the initial growth rate. Differences in sticking probability result in an increased amount of CD_4 on the surface and thus a higher growth rate.

gas and surface masses match due the singularity in the momentum case. An incident molecule containing mass m and energy E encounters a square well potential of depth D and a surface species of mass M, resulting in an energy transfer (Δ) in the collision:[167]

$$\Delta = \frac{4mM(E + D)}{(M + m)^2} \tag{5.1}$$

For this, we assume that the energy of the incoming molecule is much greater than the well depth of the potential. Thus, for the CH_4 film, the energy transfer for the CD_4 projectile is greater than that of the CH_4, which would generally indicate a higher sticking probability. This model does not account for the density of states of the film nor the internal modes of the molecule, as discussed later. These contributions can influence sticking probabilities.[77,172] Due to the role of

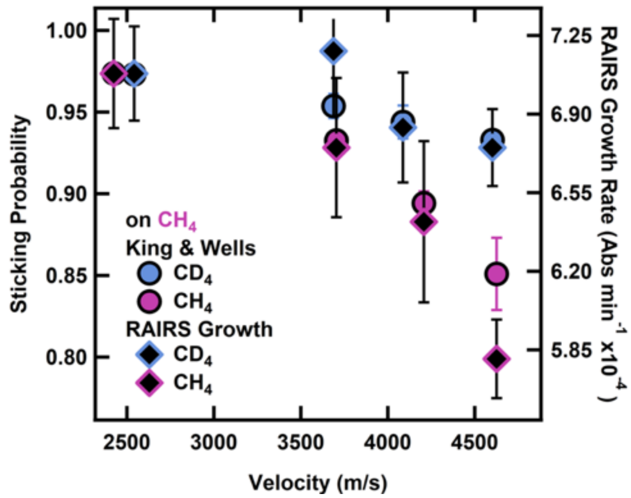

Figure 5.4: Confirmation of increased condensation of CD_4 on CH_4 as a function of incident methane velocity. Monitoring of the amount of adsorbed methane via the intensity of the ν_4 bending mode for CH_4 and CD_4 by RAIRS, we calculate the initial growth rate to overlay with the sticking probability. Error bars represent the standard deviation of at least three measurements on at least three different days.

these molecular degrees of freedom, complex and multi-phonon interactions[173,174] between the surface and the incident projectiles CH_4 film and CD_4 clearly need to be taken into consideration, as they are in the MD simulations shown herein.

We performed chemical dynamics simulations using the VENUS MD computer program.[175,176] Classical trajectories simulated collisions of a beam of CH_4 or CD_4 with the CH_4 or CD_4 surface at a surface temperature of 20 K. Initial conditions for the trajectories were selected to sample the experimental beam's translational and vibrational energy. After collision the trajectories were terminated at 50 picoseconds; CH_4 and CD_4 remaining on the surface were considered trapped. The scattered trajectories are dominated at the level of 99% by direct scattering rather than those that trap and then desorb.

5.3.1 Computational Details

The potential energy function for the $(CH_4)_{beam}$ and $(CH_4)_{surface}$ on top of a Au(111) crystal is given by:

$$V = V_{beam} + V_{surface} + V_{beam+surface} \tag{5.2}$$

where V_{beam} is the beam CH_4 intramolecular potential. $V_{surface}$ is comprised of intramolecular CH_4 potentials (same as V_{beam}) as well as the intermolecular CH_4—CH_4 and Au—CH_4 potentials using the 6-12 Lennard-Jones fashion. Lastly, $V_{beam+surface}$ is the intermolecular CH_4—CH_4 potential. Each intramolecular CH_4 potential is expressed as a sum of Morse potentials for the C-H stretches and quadratic potentials for the H-C-H bends: the Morse parameters are D = 112.5 kcal/mol, β = 1.86 Å^{-1} and $r_0 = 1.086$ Å,[177] and each HCH quadratic bend has $f = 0.585$ mdyn Å/rad^2 and $\theta = 109.47°$.[177,178] The methane harmonic frequencies are 3193, 3021, 1583, and 1413 cm^{-1}.

The surface model consists of 6 methane layers stacked in an AB sequence on top of a layer of gold to form a cubic close packed structure.[179] There are 789 CH_4 molecules in alternating layers of 120/143 molecules to so that x and y are each 40 Åfor an area of 800 Å for each layer. The total surface height of all the stacked layers is 18 Å including the gold layer on the bottom. All intermolecular potentials are written as sums of Lennard-Jones two body potentials with a cut-off distance of 10 Å and are summarized in **Table 5.1**. For the Au (111) base, ϵ_0 = 5.29 kcal/mol and σ_0 = 2.951 Å[180] were used to give an atomic spacing of 2.93 Å, closely matching that determined from STM images of the reconstructed (111) surface.[181] Our surface contains CH_4 spaced by 3.8 Åwhich is comparable to calculated CH_4 intermolecular potentials.[182] CH_4—CH_4 intermolecular potentials among all methane molecules (including those in different layers) are written as sums of 6-12 Lennard-Jones two-body potentials and include interactions between carbons and hydrogens.[183,184] To calculate the Au—CH_4 interaction, we employ standard mixing rules[180,185] and assume a geometric mean between C and Au to get a ϵ_0 = 0.7336 kcal/mol and σ_0 = 2.99 Å. Geometry optimization of the surface occurred prior to trajectory simulations to obtain a potential energy minima configuration. Additionally, we note that this is a flat crystalline surface, which a model representation of a local section in the experimental surface topology which in reality may contain domains of small, imperfect crystallites. However, even with this difference, there is qualitatively

	ϵ_0 kcal/mol	σ_0 Å
Au-Au	5.29	2.951
C-C	0.1017	3.35
C-H	0.473	2.99
H-H	0.0097	2.61
Au-C	0.7337	2.99
Au-H	0	0

Table 5.1: Parameters of the Lennard Jones 12-6 atom-atom interactions

similar energy-transfer dynamics and thus is appropriate to use for our study.[186]

A microcanonical ensemble averaged intermolecular potential curve for CH_4 approaching to the surface is obtained by averaging the potential energies of randomly oriented CH_4 as a function of CH_4-surface center-of-mass separation parallel to the surface norm.[187] Such potential energy minimum is -0.07 eV at a center-of-mass separation of 4.25 Å.

5.3.2 Procedure for the Chemical Dynamics Simulations

Chemical dynamics simulations were performed using the VENUS general chemical dynamics computer program.[175,176] Classical trajectories were used to simulate collisions of a beam of CH_4 or CD_4 with the CH_4 or CD_4 surface. Simulations at each collision energy were carried out using a surface temperature of 20 K. Initial conditions for the trajectories were selected to sample the beam's translational and vibrational energy at the experimental conditions. The selection of initial conditions follows from previous VENUS studies.[188,189] For each simulation, a beam of colliding molecules was aimed within a circular area. Each trajectory was initialized with a separation of 10 Å between the center of the beam and surface aiming point. For each beam, the initial vibrational quantum states were sampled from Boltzmann distributions at 300, 700, 900, or 1100 K and the translational energies were determined from the molecular beam velocity distributions (Figure 1). Using the experimental velocities, the CH_4 translational energies were 0.49, 1.16, 1.48 and 1.79 eV and the CD_4 translation energies were 0.67, 1.41, 1.74, and 2.19 eV. Zero-point energy was included in these samplings and the rotational energy was set to 0 K to match the experimental supersonic molecular beam conditions.

For each trajectory, the gold and bottom three layers were held rigid and acted as anchor layers. Additionally, the mass of carbon atoms in rim CH_4 molecules was artificially increased by 10000 to truncate the surface. Initial conditions for this surface were selected by assigning velocities to the carbon atoms of these layers, sampled from a Maxwell-Boltzmann distribution at 20 K. The surface was equilibrated by a 50 ps molecular dynamics simulation with velocity scaling every 1000 steps and another equilibration without velocity scaling. The trajectories were propagated with a Velocity-Verlet integrator, with a time step of 0.01 fs. Trajectories were terminated either when the distance between the central methane molecule and outgoing product exceeds 30 Å or the total integration exceeds 50 ps. Typically, 750-2000 trajectories were calculated for each ensemble of initial conditions including the surface composition and beam conditions.

5.3.3 Simulation Results

Overall, we find that there is nice agreement between the chemical trajectory simulation results and the experimentally determined sticking probabilities.

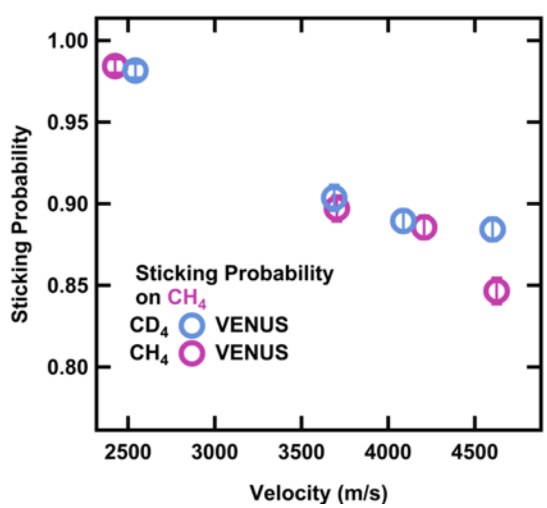

Figure 5.5: Sticking probabilities calculated from the number of CH_4 and CD_4 direct and physisorption scattering trajectories on a CH_4 layered surface at 20 K. Error bars represent the standard error of at least 750 trajectories for each velocity. An updated version of figure with refined potentials is in the Appendix as **Figure A4.20**.

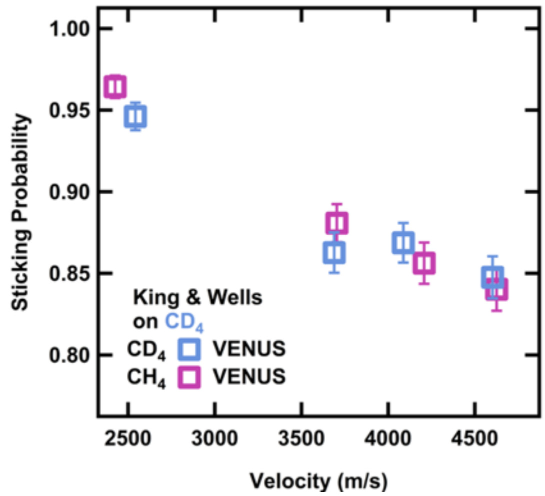

Figure 5.6: Sticking probabilities calculated from the number of CH_4 and CD_4 direct and physisorption scattering trajectories on a CD_4 layered surface at 20 K Error bars represent the standard error of at least 750 trajectories for each velocity.

The VENUS calculations demonstrate a decrease in sticking probability with increasing incident velocity as well as a difference between CH_4 and CD_4 on a CH_4 surface (**Figure 5.5**). Additionally, for the simulated collisions on a CD_4 surface (**Figure 5.6**), there is no difference in sticking probability, again in agreement with our experimental results. In a more careful comparison to the results shown in **Figure 5.2**, the theoretical sticking probability for the CD_4 on the CH_4 surface is slightly lower than the experimental value. This could arise from various effects; e.g. Lennard-Jones potentials are not optimized for the repulsive region.[190]

Full details of the energy transfer and chemical dynamics simulations will be discussed in a forthcoming manuscript to provide a molecular-level understanding of the mechanisms occurring between the methane projectile and the methane surface. When examining phonon dispersion curves for CH_4 and CD_4,[191] not only are the CD_4 phonon modes at a lower energy, but there is enhanced translational-rotational coupling.[192] In addition to this coupling, local corrugation of the surface can also influence trajectory paths and therefore energy flow.[193,194] Full analysis of our molecular dynamics studies will provide necessary insight into lattice vibrations and how energy is efficiently dissipated to trap the methane isotopologues.

To further explore and confirm our experimental results, we consider a beam comprised of both CH_4 and CD_4 in a 3:1 ratio; this ratio was not selected to optimize condensation differences, but rather to demonstrate the robust nature of differential sticking. This allows us to quantify the sticking probability as well as condensate composition. While dosing a multilayer film of both CH_4 and CD_4 at 20 K, the integrated area of the degenerate ν_4 mode was tracked over time using RAIRS.[60,81–83,170] Once the condensate reached a self-similar structural steady state of at least 100 layers, at least 10 spectra per experiment on at least three different days were averaged to determine the film composition.

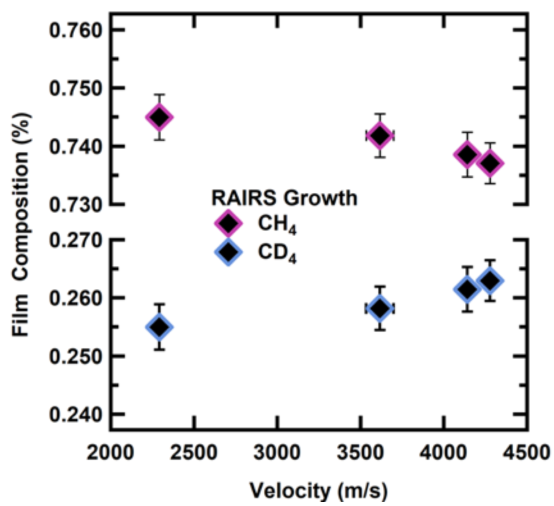

Figure 5.7: Enrichment of the heavier isotope (CD_4) into a mixed condensed film at higher beam velocities. Integrated area of the ν_4 mode for CD_4 and CH_4 to calculate the film composition and determine the enrichment of the heavier isotope (CD_4) at each velocity. Error bars represent the standard deviation of at least 35 steady-state films on at least three different days.

As depicted in **Figure 5.7**, the condensate composition for the room temperature beam (2200 m/s) is 74.5% CH_4 and 25.5% CD_4. However, as the beam velocities increase, the heavier isotope (CD_4) becomes preferentially adsorbed into the film. Due to increased adsorption into the film, the condensate film structure changed to 73.7% CH_4 and 23.6% CD_4. Overall, by measuring the condensate with RAIRS, we confirm that due to the increased sticking probability of CD_4 on a CH_4 film, we see an increased affinity for CD_4. We demonstrate for our fastest beam (4400 m/s), that there is a 3.12 ± 0.06 % enrichment of CD_4 compared to the room temperature beam (2200 m/s). When taking the individual King and Wells values (**Figure 5.1 and 5.2**) and combining that with the film composition determined from the RAIR spectra, we calculate the sticking probabilities for CH_4 and CD_4 on the mixed film. For the highest velocity beam, these sticking probabilities also result in a CD_4 enrichment of 3.9% $\pm$ 0.02 indicating excellent agreement with the observed condensate enrichment.

5.4 Conclusion

We examined the differential sticking probability of CH_4 and CD_4 on CH_4 and CD_4 ices using RAIRS for measuring on-surface gaseous condensation and complementary King and Wells mass spectrometry techniques for monitoring sticking probabilities. We found that as the incident translational energy of CH_4 and CD_4 increases (up to 2 eV), the sticking probability decreases for both films. Interestingly, we conclude that preferential sticking and condensation occurs for CD_4 when striking the surface in comparison to the outcome for CH_4. This observation was confirmed both experimentally from infrared spectroscopy of the condensation and via mass spectrometric detection of the reflected molecules, as well as theoretically from the gas-surface chemical trajectory simulations. This theoretical model system will be explored in more detail to provide insight in energy transfer and lattice vibrations. Next, we employed a mixed incident supersonic beam comprised of both CH_4 and CD_4 in a 3:1 ratio to measure the condensate as well as the sticking probability. When doing so, we see the same effect in the condensed mixed film, supporting an isotopic enrichment of the heavier isotope. Since the Baule model[77] does not accurately represent this condensed phase system due to its molecular complexity, we propose that enhanced multi-phonon interactions attributable to the film's phonon and rovibrational densities of states and inelastic cross sections including intermolecular energy exchange between the incident CD_4 projectile and the CH_4 film allow for more efficacious gas-surface energy transfer.

In general, these results indicate the importance of understanding gas-surface energy exchange under non-equilibrium conditions at cold substrate temperatures, and have important astrophysical and terrestrial implications. Our work demonstrates the importance of film structure and surface lattice coupling to allow for efficient energy transfer and an isotopic enrichment of the heavier isotope (CD_4) The insights gained from gaseous condensation under non-equilibrium conditions are also important for understanding aircraft flight in low temperature environments. These results also offer a new route for isotope enrichment via the preferential condensation of heavier isotopes and isotopologues during gas-surface collisions under carefully selected substrate, gas-mixture, and incident velocity conditions.

Importantly, our experiments are conducted at low temperature astrophysical conditions. By experimentally determining initial sticking probability differences between methane and its heavier isotopologue as a function of incident energy, we find that the film composition is important, especially for high energy projectiles bombarding icy-dust grains. Since adsorption is often a first step for many cold temperature reactions occurring on these grains, differences in sticking probabilities have notable implications for allowed reaction probabilities and follow-on events leading to increased molecular complexity. Our work, therefore, can not only explain increased abundance of deuterium in solar system planets[195,196] but can also be incorporated into astrophysical models of the icy dust grain processes including those in the interstellar region.[36]

Chapter 6

Reaction Kinetics and Influence of Film Morphology on the Oxidation of Propene Thin Films by O(^{3}P) Atomic Oxygen

We present results detailing the oxidative reactivity of condensed propene thin films, with particular attention to epoxide product formation due to its importance in the industrial production of polyurethane plastics and trace presence of these species in the interstellar medium. These studies were conducted in a state-of-the-art ultra-high vacuum scattering instrument equipped for operation with cryogenic substrate temperatures. After exposing films to a supersonic beam of ground state atomic oxygen, O(^{3}P), generated from a radio frequency plasma source, reflection absorption infrared (RAIR) spectra confirm significant propene reactivity yielding products including propylene oxide, propanal, and a small amount of acetone. In addition to identifying these primary products, we discuss experimentally-determined activation energy barriers for reaction in the condensed propene system. Interestingly, we identify significant differences in propene film crystallinity as a result of substrate deposition temperature; lower deposition temperatures (<44 K) yield a more amorphous film, whereas higher temperatures (>59 K) yield a more ordered, crystalline film. Very little oxidative reactivity is observed in the amorphous propene film, suggesting that film structure has a substantial impact on observed reactivity by impeding or allowing efficient O(^{3}P) diffusion. Overall, this work provides fundamental mechanistic insight into the diffusion and reactivity of atomic oxygen in condensed films of small, unsaturated hydrocarbons. The results also emphasize limitations of condensed phase reactions that rely on reactant diffusion; film composition, morphology, and thickness can significantly limit reactivity despite low reaction barriers.

6.1 Introduction

The reaction of atomic oxygen, $O(^3P)$, with small alkenes is important across many fields including smog formation in the atmosphere, combustion processes and chemical complexity in astrophysical ices.[197,198] These reactions also play a critical role in the formation of polycyclic aromatic hydrocarbons and soot.[199] Additionally, the products formed from oxygen addition across double bonds are often significant industrial intermediates. Propylene oxide, for example, is a key intermediate in the manufacturing of polyurethane plastics and other products.[200,201] It is one of the top chemicals produced worldwide by mass,[202] and there is immense interest in optimizing the economic and environmental efficiency of its production.[203–205]

The gas phase reaction between alkenes (including propene) and oxygen has been well-studied, beginning as early as the 1950's.[206–210] It is well established, for example, that the reaction begins with oxygen addition across the double bond, forming a triplet biradical intermediate. This primary product species then progresses through a number of reaction channels including intersystem crossing (ISC) from the triplet to the singlet potential energy surface (PES) to form singlet products. Recently, a comprehensive study from Leonori et al. used crossed molecular beams and complementary ab initio electronic structure calculations to identify complete branching ratios, energetic barriers, and potential energy surfaces for the $O(^3P)$ + propene reaction.[211,212] This study and others have highlighted the temperature dependent role of ISC in the gas phase reaction; the fraction of products formed via ISC decreases with increasing temperature.[208,211,212] Despite this rigorous work in the gas phase, however, there still remains limited mechanistic and kinetic data available for the oxidation of condensed alkene films. In the few early studies of this system,[213–216] primary products and reaction rates were identified, but the experimental conditions utilized thick, uncharacterized propene films and were limited to temperatures above 70 K (propene phase may have been unclear).

Understanding reactions between condensed alkenes and oxygen at cold temperatures is also important for astrophysical applications due to the trace presence of these species in the interstellar medium.[217] It is thought that reactions on interstellar dust grains below 77 K facilitate the formation of many such molecules with abundances that cannot be explained by gas phase chemistry alone.[33,218,219] To date, only gaseous propene has been observed in a dark interstellar cloud[220] and on Titan,[221] but molecules formed on dust grains (possibly due to exposure to ionizing radiation)[222] could desorb and contribute to these measured gas phase concentrations.[223] Additionally, propylene oxide, one of the major products in the O(^{3}P) + propene reaction, has been detected spectroscopically in the interstellar medium[224] as well as produced in a laboratory simulation experiment by exposure of propylene ices at 5 K to energetic electrons.[225] Such studies indicate that oxygen atom addition and insertion reaction pathways could activate a novel channel for chemical complexity in ices that are too cold for radicals to diffuse and react.[226,227]

In this work a radio frequency plasma source is used to generate a supersonic expansion of ground state atomic oxygen, O(^{3}P), which is then exposed to condensed propene films under ultra-high vacuum (UHV) conditions. We track reaction product formation in real time with in situ reflection absorption infrared spectroscopy (RAIRS), which allows us to determine the activation energy for this process. We find that in the condensed phase, propene reacts readily with O(^{3}P) to form primarily the singlet partial oxidation products propylene oxide and propanal. Additionally, we present the first study highlighting the specific impact of alkene film morphology on oxidative reactivity. Specifically, oxygen is unable to react with more disordered, amorphous propene films.

Overall, this work provides fundamental insight into the diffusion and reactivity of ground state atomic oxygen in condensed films of small, unsaturated hydrocarbons. By employing cryogenic conditions and thin films of propene, we can simulate interstellar conditions which can aid in modeling reactivity on interstellar dust grains. Additionally, the kinetic and mechanistic detail gained from this reaction will inform polyurethane plastic manufacturing. This work also broadly highlights the possible challenges with condensed phase reactivity in which film structure and morphology may significantly limit reactant diffusion and reactivity in thicker films.

6.2 Experimental

All experiments were conducted in a molecular beam scattering instrument that has been previously discussed in detail.[55] Briefly, this instrument consists of a UHV chamber with base pressures of 10^{-10} Torr connected to a triply differentially pumped molecular beamline. Inside the chamber, a state-of-the-art, helium-cooled, and vibrationally isolated sample manipulator (Advanced Research Systems) enables precise and accurate temperature control of the Au(111) sample substrate between 20 K and 800 K. The crystal is exposed to the beam and monitored in real time with in situ RAIRS.

All RAIR spectra were analyzed with Gaussian peaks atop cubic baselines. Spectra were acquired with a Nicolet 6700 infrared spectrophotometer (Thermo Fisher) using p-polarized IR radiation incident at 75° from the surface of a Au(111) sample substrate and collected in a liquid nitrogen cooled mercury cadmium telluride (MCT/A) detector. Each RAIR spectrum is an average of 300-500 scans taken using 4 cm^{-1} resolution with a clean Au(111) sample used as a reference background. Between experiments, the Au(111) crystal was sputtered and thermally annealed in vacuum using 1 kV Ar^+ ions ($1-2\times10^{-5}$ Torr Ar backfill into the chamber) directed at the crystal by an ion gun while the surface temperature was held at 770 K for 15 minutes.

Propene was dosed on the Au(111) substrate via beam deposition at surface temperatures ranging from 44 K to 59 K, where propene desorption is negligible. Dosing conditions resulteItd in a typical incident propene flux of 2.6×10^{15} molecules cm^{-2} s^{-1}, corresponding to a deposition rate of approximated 2.4 layers s^{-1} (assuming one monolayer is roughly 10^{15} molecules cm^{-2}).[28] Propene flux was initially determined by measuring the pressure rise with a nude Bayard-Albert ion gauge calibrated to N_2 for a neat propene beam open to the chamber. The flux was then calculated by taking into account the relative gauge sensitivity to propene[228] and N_2[73] along with the chamber pumping speed, and the spot size of the beam on the Au(111) crystal. We performed this measurement and calculation at room temperature to ensure no additional pumping capacity was added by the cold sample manipulator. Following this measurement, we used the same beam to establish a conversion to propene film thickness by monitoring propene growth on the cold crystal via RAIRS as a function of exposure and calculating an absorption cross-section for the $=CH_2$ wagging mode (γ_w), comprised of two peaks: a large, sharp peak at 919 cm^{-1} and a smaller shoulder at 914 cm^{-1}. Our calculated cross-section is in good agreement with previously reported values.[229–232] Propene film thicknesses are herein reported in layers; films throughout this study ranged from 10 to 240 layers (specific thicknesses are specified in the text). The beam source was thoroughly pumped out and purged prior to turning on the oxygen source to avoid trace propene contaminants during exposure.

A radio frequency plasma source described in detail previously[27] was used to generate atomic oxygen in its ground state, $O(^3P)$. Igniting and expanding a 5% O_2 in Ne mixture through a water-cooled quartz nozzle led to 25-40% O_2 dissociation to $O(^3P)$. We note that by selecting a low backing pressure (60 Torr), low RF power (100 W), and employing a 2000 V/cm deflecting plate region in the second differential beam chamber, our beam is essentially devoid of O^+ and $O(^1D)$[233,234] and is primarily comprised of $O(^3P)$, non-dissociated O_2, and Ne. The beam is characterized using time-of-flight (TOF) techniques to determine the flux and average kinetic energy. O_2 flux was determined in a similar manner to that of propene (see above), using a neat O_2 beam and the relative ionization sensitivity to O_2 and N_2.[235,236] O_2 flux is further scaled to reflect dissociation into $O(^3P)$ using the relative intensities of m/z=16 to m/z=32 established from square wave modulated time-of-flight spectra of the incident beam.[27] Typical experimental conditions result in an $O(^3P)$ flux of 8.4×10^{14} atoms cm^{-2} s^1 and translational energies of 0.12 eV. The beam energy widths are approximately 0.06 eV. While it would be desirable to explore the reaction with higher incident translational energies by substituting a seeded mixture of O_2 in He, doing so would reduce O_2 dissociation and introduce $O(^1D)$ to the beam, which is a more reactive species.[26] Thus, for this experiment, 5% O_2 in Ne remains the optimal gas mixture.

6.3 Results and Discussion

6.3.1 Spectral Evidence of Reactivity and Product Formation

Condensed propene is observed to react readily with $O(^3P)$. **Figure 6.1** shows typical RAIR spectra of a 66-layer propene film adsorbed on Au(111) at 54 K before and after extended exposure to $O(^3P)$. Prior to exposure, spectral features are easily correlated with gas-phase and condensed-phase propene peak assignments.[170,231,232,237–240] As shown by the dashed line in **Figure 6.1a**, the most intense features at 919 cm^{-1} and 914 cm^{-1} are assigned to the $=CH_2$ wagging mode of propene (γ_W) with a smaller feature at 1003 cm^{-1} corresponding to the CC bend.[239–241] Unless otherwise stated, changes in the integrated areas of the features at 914 cm^{-1} and 919 cm^{-1} are used throughout the rest of this study to track propene reaction progress (generally corresponding to reaction of the propene double bond). A second region is highlighted in **Figure 6.1b** at 1643 cm^{-1}, corresponding to the propene C=C stretch.[242] A third region highlighted **Figure 6.1c** shows additional CH, CH_2 and CH_3 stretching modes that are smaller in intensity.[243] The two largest peaks at 3075 cm^{-1} and 2977 cm^{-1} correspond to the CH_2 and CH_2 + CH stretching modes, respectively.48,53 Other notable features in this stretching region are peaks at 2939 cm^{-1} and 2964 cm^{-1} assigned to CH_3 stretching,,[237,239] and a peak at 3009 cm^{-1} assigned to CH stretching.[238]

Following 1×10^{18} atoms cm^{-2} of oxygen exposure, the aforementioned propene peaks change dramatically, many of them decaying in intensity. At the same time, there is significant growth of novel features that represent oxygenated products. Most notably in the solid line in **Figure 6.1a**, the spectral signature at 830 cm^{-1} is assigned to the ring deformation mode of propylene oxide (δ_{C_2O}).[244–247] New peaks (1730 cm^{-1} and 1693 cm^{-1}) in **Figure 6.1b** are similarly assigned to the C=O stretching frequency of propanal ($\nu_{C=O}$).[248–250] Additionally, there is a small amount of acetone produced, confirmed spectroscopically by growth of a new peak at 1709 cm^{-1}, corresponding to its C=O stretching mode.[129,134]

In order to determine the role of film thickness in product formation and oxidative reactivity, propene films of increasing thickness ranging from 12 to 66 layers were dosed at 59 K and exposed

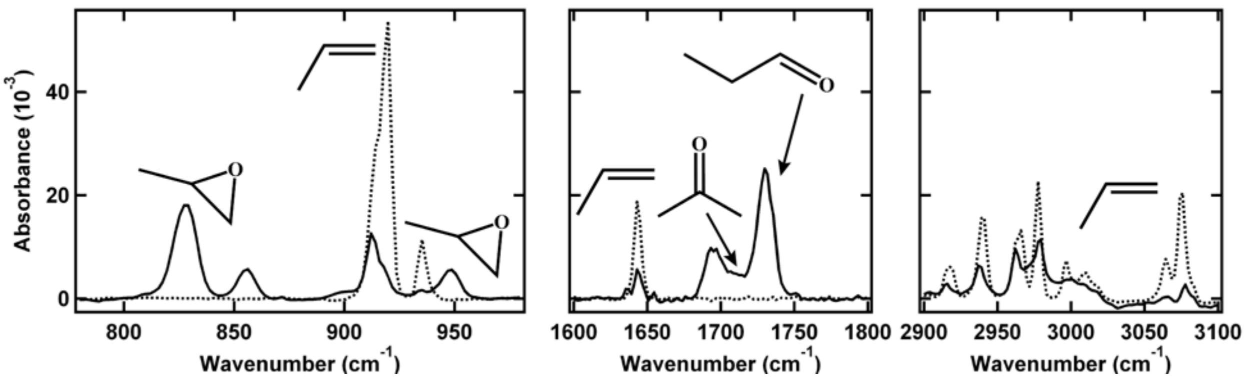

Figure 6.1: RAIR spectra of a 66-layer propene film before and after exposure to O(^{3}P). As a result of exposure, (solid line, total exposure $\sim 1 \times 10^{18}$ atoms cm^{-2}) the total signal intensity is observed to decrease for the CH_2 wagging (919 cm^{-1} and 914 cm^{-1}, a), C=C stretching (1643 cm^{-1}, b), and CH, CH_2 and CH_3 stretching (3009 cm^{-1}, 3075 cm^{-1} 2977 cm^{-1}, 2939 cm^{-1}, and 2964 cm^{-1}, c) modes of propene. New peaks grow in upon exposure corresponding to propylene oxide (830 cm^{-1}, a), acetone (1709 cm^{-1}, b), and propanal (1730 cm^{-1} and 1693 cm^{-1}, b).

to O(^{3}P) at 54 K. **Figure 6.2** depicts the decrease in the integrated area of the γ_w peak as propene films of varying thicknesses are exposed to O(^{3}P). There is a clear period of initial linear reactivity for all films with a rate that is independent of the starting thickness. From these initial reactivity measurements, we estimate that 1 propene molecule reacts for every 100 oxygen atoms reaching the film surface. Given the observed rate of reaction and calculated barriers (below), this low reaction probability is perhaps surprising. We estimate, however, that at our surface temperatures, the sticking probability of oxygen atoms is on the order of 20% or less. This estimate was performed using the basic King and Wells technique[17] and thus explains why not every oxygen atom reaching the film is able to react with the propene film. **Figure 6.2** also shows that after this initial period of exposure there is a stark drop in reactivity. In the 12 and 24 layer films, the reaction tails off because oxygen reacts with propene completely down to the Au(111) substrate. In thicker films, however, oxygen is unable to fully react with the propene in more buried layers. Moreover, the total reacted depth is inconsistent for both the 46 and 66-layer films (reaction complete at 4 layers and 23 layers remaining, respectively). This suggests that oxygen reactivity is connected to initial propene film thickness and that the reaction does not progress by simple layer-by-layer consumption of propene.

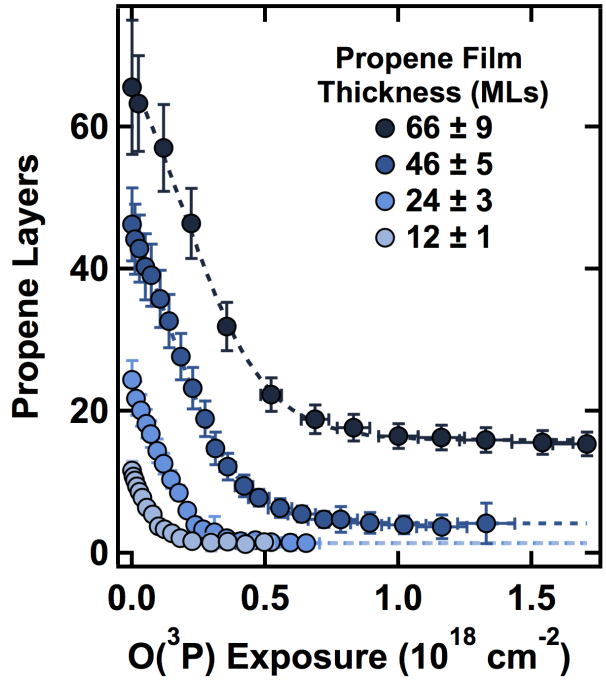

Figure 6.2: Decrease in the integrated area of the γ_w peak upon exposure to O(^{3}P). Changes in the number of propene layers on the surface when exposed to O(^{3}P) at 54 K demonstrate initial reactivity that slows upon extended exposure. O(^{3}P) is only able to fully react the film when the initial film has 24 layers of propene or fewer. Dotted lines are drawn to guide the eye.

These results indicate that for films less than 70 layers thick (**Figure 6.2**), the initial reactivity of O(^{3}P) + propene is linear and independent of film thickness. However, when examining thicker propene films (70 – 240 layers), the initial linear rate slows slightly (**Figure 6.3a**). When plotting the initial rates as a function of propene film thickness in layers, we see that initial propene reactivity plateaus for films greater than 150 layers (**Figure 6.3b**). We note that frequencies of the γ_w mode do not shift upon increased propene deposition, confirming that there are no major changes in film structure or optical effects as coverage increases.[251] Rather, we propose that these changes in initial reaction rates can be attributed to increased barriers for oxygen diffusion within the film, as discussed in the following section, Effect of Surface Temperature.

Throughout oxygen exposure, propene disappearance is coupled to the growth of new spectral features corresponding to propylene oxide, propanal, and a small amount of acetone (**Figure 6.1**). Product growth is immediately observed upon O(^{3}P) exposure by monitoring the integrated areas

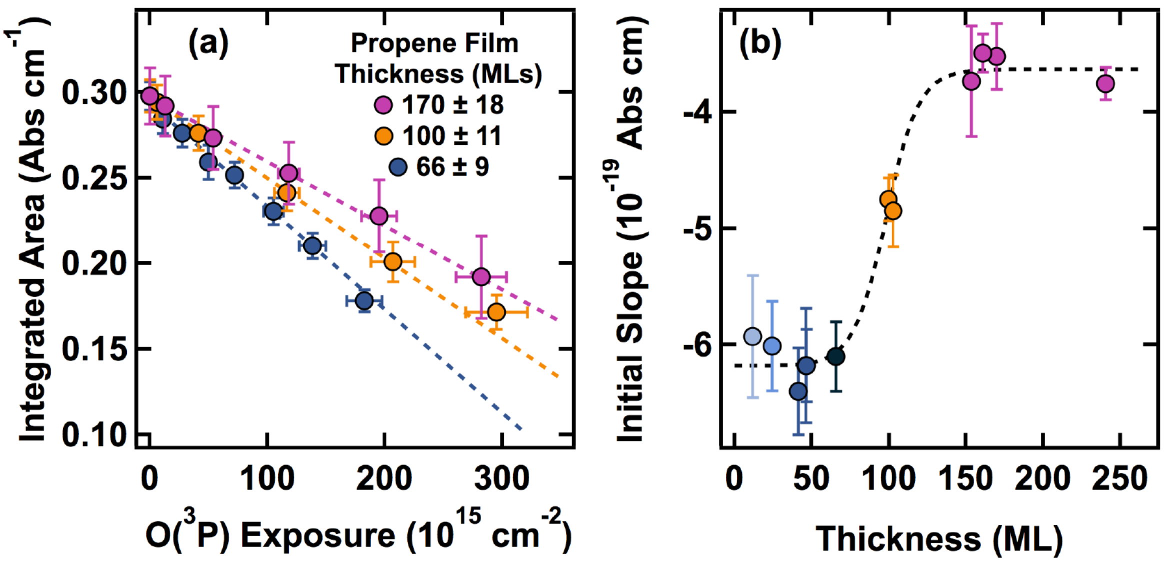

Figure 6.3: Integrated areas of the γ_W peak corresponding to 66, 100, and 170-layer thick propene films. (a) Initial O(^{3}P) reactivity is linear with rates that depend on thickness. Taking these initial rates from (a) and including rates for films up to 240 layers (b) demonstrates that that this initial rate slows for films greater than 70 layers, but reaches a steady value for films greater than 150 layers. Dotted line in (b) is drawn to guide the eye.

of propylene oxide's δ_{C_2O} mode (**Figure 6.4a**) and propanal's $\nu_{C=O}$ mode ((**Figure 6.4b**). We see that not only is there more propylene oxide and propanal formed in thicker films, but that the rate of formation of these products does not change with increasing film thickness (up to 70 ML). During exposure at 54 K, the Au(111) substrate temperature is such that propene and our products (propanal and propylene oxide) are stable on the surface.[225,242,250] Even though our film composition changes (decrease in propene, increase in propanal and propylene oxide), there is limited desorption of products, and thus our overall film thickness is likely comparable throughout. We detect no distortion or shifting of RAIR peaks as exposure continues and products form. Additionally, we expect that the index of refraction is comparable for alkene ices and oxygen hydrocarbons,[252] so we primarily attribute changes in peak intensity to reactivity and possibly molecular orientation, rather than optical effects as our films are likely less than 100 nm thick.[120]

In addition to RAIRS, temperature programmed desorption (TPD) data can help to confirm product identities and their relative stabilities on the surface (**Figure 6.5**). For the 46-layer film, O(^{3}P) is unable to fully react the film down to the substrate (**Figure 6.2**), and there are correspond-

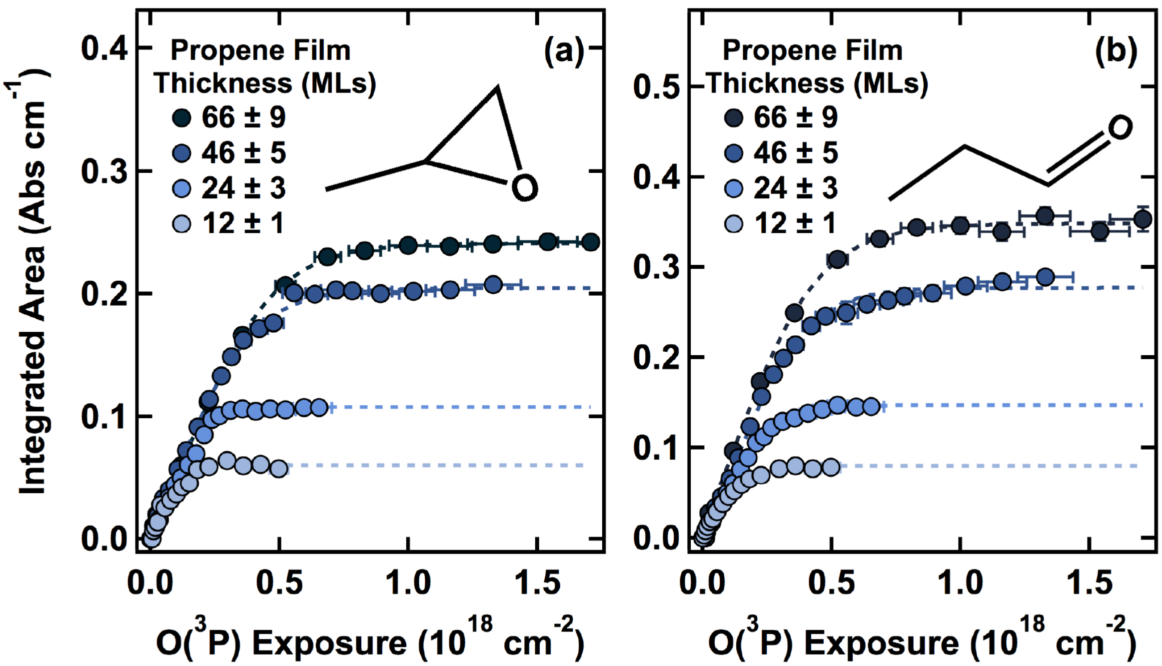

Figure 6.4: Increase in the integrated area of the propylene oxide and propanal peaks upon exposure to O(^{3}P). Integrated area of the propylene oxide ring deformation peak (δ_{C_2O}, a) and propanal C=O peak ($\nu_{C=O}$, b) for propene films of varying thickness exposed to O(3P) at 54 K demonstrate that the primary products grow in with a similar linear rate. More product is formed in reactions with thicker films. Dotted lines are drawn to guide the eye.

ingly low-temperature desorption features for propene at m/z = 39 and 41. As shown in **Figure 6.5**, these first desorption features peak at 119 K, closely matching previous studies for propene on Au(111).[242] Although it is difficult to quantitatively differentiate our products due to significantly overlapping cracking patterns, we can assign m/z = 43 to acetone and propylene oxide, m/z=26 to propanal and propylene oxide, and m/z = 58 to propanal, propylene oxide, and acetone. As shown in **Figure 6.5**, acetone appears to be the least stable with a small desorption feature at 78 K, while propanal and propylene oxide have major desorption features at 175 K.[250,253] From this analysis, it is clear that propanal and propylene oxide are not only our major products in the condensed phase, but also more stable on the surface. It is possible that these products are in weakly bound multilayer films, while there is less than a monolayer of acetone.[129] We also note that we do not identify any high-molecular weight polymeric or oligomeric species which suggests that our intermediate product species are not long lived on the surface.

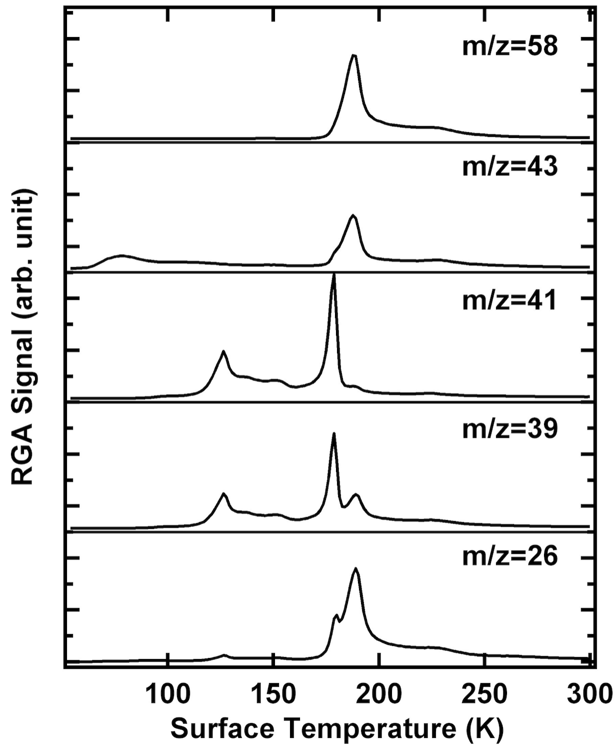

Figure 6.5: TPD of a 46-layer propene film after O(^{3}P) exposure. After exposure to $\sim 1 \times 10^{18}$ atoms cm^{-2} of (O^{3}P) TPD confirms the presence of propanal (m/z = 26, 58), propylene oxide (m/z = 26, 43, 58), and acetone (m/z = 43, 58). There is also some propene left on the surface (m/z = 39, 41)

6.3.2 Effect of Surface Temperature

In addition to characterizing film reactivity and product formation, we can use the initial reaction rates at surface temperatures ranging from 44 K to 59 K to calculate the activation energy for the disappearance of propene (films of 30 layers thick). The =CH_2 wagging mode of propene (γ_w) is comprised of two features at 919 cm^{-1} and 914 cm^{-1} (Figure 1). Upon exposure to O(^{3}P), **Figure 6.6a** depicts the loss of integrated area of 919 cm^{-1} peak for four different surface temperatures (all films dosed at 59 K). A corresponding Arrhenius plot is shown in **Figure 6.6b**; the calculated activation energy for the removal of propene's double bond is 0.41 $\pm$ 0.05 kcal mol^{-1}. Under our experimental conditions, this activation energy is similar to or less than those reported in gas phase studies of the same system.[254–256] However, because this value is calculated simply from the disappearance of propene, it is possibly a convolution of three different reaction steps,

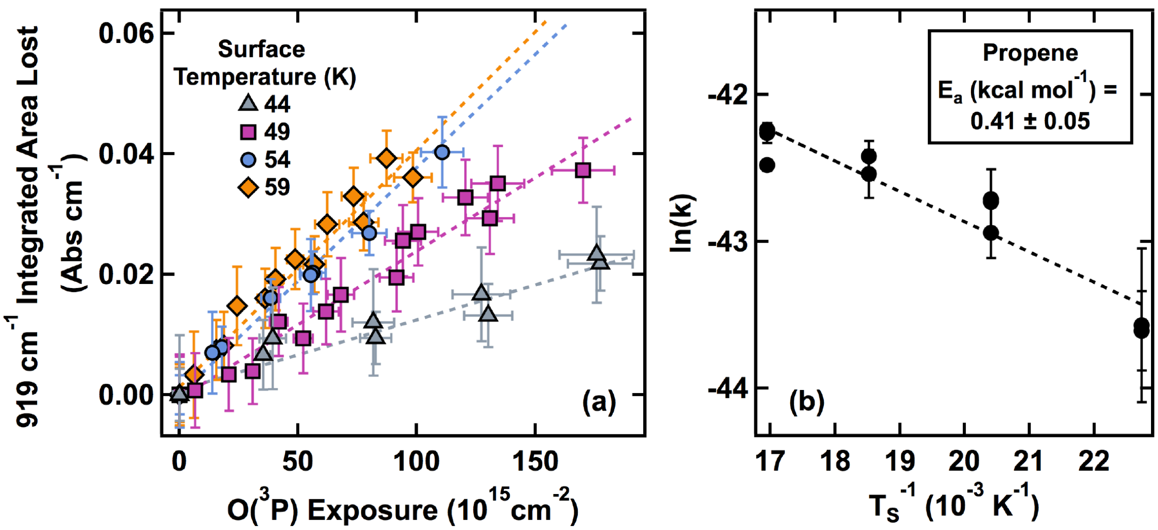

Figure 6.6: Initial reaction rates and activation energy for the disappearance of propene. Integrated area lost from the 919 cm^{-1} peak (part of the =CH_2 wagging mode, γ_W) corresponding to 30-layer thick propene films exposed to $O(^3P)$ (a) provides initial linear reaction rates for surface temperatures ranging from 44 K to 59 K. These rates are fit to an Arrhenius model (b), giving an experimental activation energy of 0.41 $\pm$ 0.05 kcal mol^{-1}

each of which will be explored in detail below.

The first challenge hidden within the measured activation energy is a question of product formation and reaction mechanism. The observed product distribution for the $O(^3P)$ + propene reaction is well supported by a mechanism[257,258] (**Figure 6.7**) in which $O(^3P)$ attacks the double bond to form a triplet biradical intermediate. It is important to note that our reaction products (acetone, propanal, and propylene oxide) are singlet species. As outlined by the PES in Leonori et al,[211] it is clear that our reaction proceeds almost 100% via ISC to the singlet surface, leading to our observed products. This can be accounted for by recent studies[211,259] demonstrating that ISC and nonadiabatic effects become increasingly important as reaction temperature decreases.[260]

As mentioned above, however, the measured activation energy for propene oxidation may include barrier contributions for oxygen addition to *either side* of the double bond (**Figure 6.7**). To parse these contributions, we perform the same Arrhenius analysis on product formation, using the integrated area of propylene oxide's δ_{C_2O} mode and propanal's $\nu_{C=O}$mode as a function of $O(^3P)$ exposure. Propylene oxide is a major product in both addition channels, while propanal should

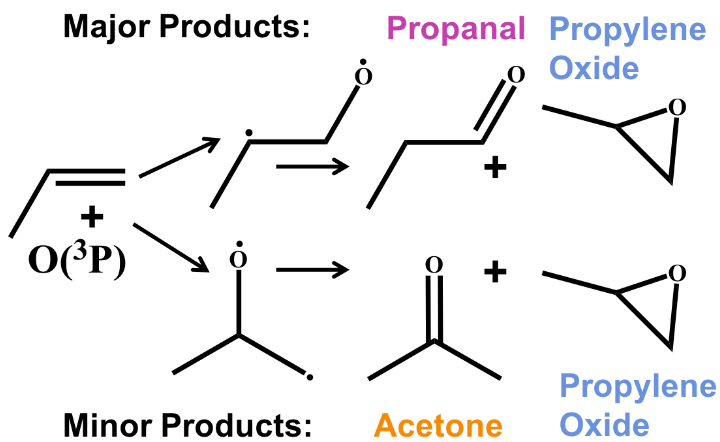

Figure 6.7: Reported mechanism for the O(^{3}P) reaction with condensed propene. O(^{3}P) is expected to preferentially attack the least substituted side of the double bond to form a triplet biradical intermediate that progresses, via ISC, to the final products propylene oxide and propanal.

only be formed from addition of oxygen to the terminal propene carbon.

The results of this analysis show that the activation energy for propylene oxide formation is 0.36 ±0.03 kcal mol^{-1} (**Figure 6.8a**) and 0.34 ± 0.06 kcal mol^{-1} for propanal formation (**Figure 6.8b**). These values are in good agreement with one another, and they are also within error of the measured activation energy for destruction of propene's double bond (0.41 ± 0.05 kcal mol^{-1}). This suggests that not only is oxygen addition to the terminal carbon the dominating pathway obeying Cvetanovic's rules for oxygen addition to alkenes,[257] but the addition step itself is rate limiting.[214] This makes sense for our low temperature, condensed phase environment given that in the gas phase the barrier for O(^{3}P) addition is three times higher for the central carbon compared to the terminal carbon.[211]

To further assess the mechanism, we examine changes in the CH region associated with the terminal and central carbons. This analysis is shown for a representative 46-layer film, but these trends are consistent for films of varying thicknesses. In particular, as shown in **Figure 6.9a**, we track changes in peaks at 2977 cm^{-1} (CH_2 + CH stretching) and 3075 cm^{-1} (CH_2 stretching). We integrated these two peaks as a function of O(^{3}P) exposure and normalized their intensity to the pristine film (**Figure 6.9b**). When oxygen atoms are introduced into the film, there is a clear decay in intensity for both peaks, again supporting that atomic oxygen is easily able to react with

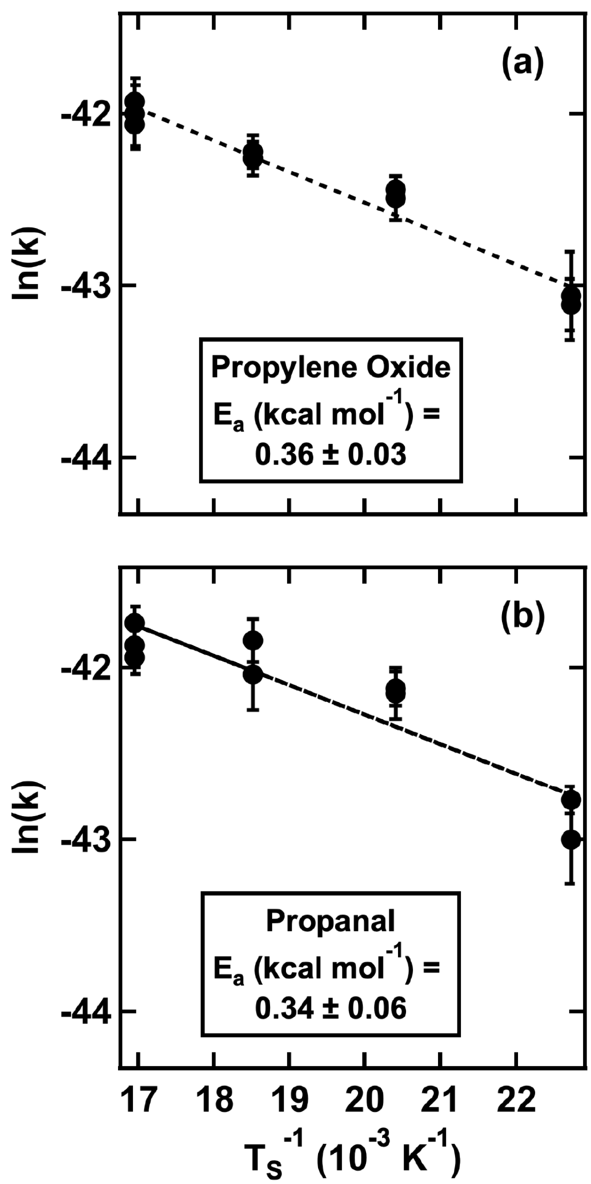

Figure 6.8: Initial reaction rates and activation energy for propylene oxide and propanal formation. Initial rate constants of propylene oxide (a) and propanal (b) formation from 30-layer thick propene films exposed to O(3P) over temperatures ranging from 44 to 59 K are fit to an Arrhenius model. The experimental activation energies are 0.36 $\pm$ 0.03 kcal mol^{-1} and 0.34 $\pm$ 0.06 kcal mol^{-1} for propylene oxide and propanal formation respectively.

the condensed propene. The relative reaction rates in **Figure 6.9b** suggest that reactivity is greater for the 3075 cm^{-1} peak corresponding to only CH_2 stretches (green) compared to the 2977 cm^{-1} peak corresponding to CH_2 + CH stretches (orange). This can be interpreted as again reinforcing that oxygen addition to the terminal carbon is the dominant pathway. We also note that because we are using RAIRS, this trend may also be linked to a change in average molecular orientation; this is, however, unlikely to be a significant contribution due to the thick, polycrystalline nature of the film.[170]

Also complicating this analysis is a small decrease in intensity of the peaks at 2939 cm^{-1} and 2964 cm^{-1} corresponding to the CH_3 stretching modes. This suggests that although oxygen addition is the dominant mechanism, hydrogen abstraction may be a minor secondary pathway. Gas phase studies found that H abstraction was unable to compete with oxygen addition,[261] and although barriers in the condensed phase are often lower, we do not expect that H abstraction is a significant contribution to the overall reaction mechanism. H abstraction would necessarily yield a highly reactive hydroxyl radical,[199] which we see no evidence for in our product analysis. Moreover, abstraction leaves behind a carbon-centered radical that could easily continue to react with other molecules in the film or with oxygen species in the beam. It is possible that a small amount of acrolein is formed through this channel, but it is certainly only a minor contribution.

The second challenge with quantifying a reaction barrier for this system in the condensed phase is the potential contribution of oxygen diffusion. To untangle this contribution, we return to the difference in initial reaction rates observed between thin (<70 layer) and thick (>150 layer) films). By performing the same Arrhenius analysis again on 150 ML films, we find that the activation energy for the reaction of propene's double bond is 1.06 ± 0.11 kcal mol^{-1}. This is significantly higher than the calculated barrier for 30-layer propene films (0.41 kcal mol^{-1}), suggesting that oxygen diffusion through the film plays a significant role in the observed reaction in thicker films.[257,262–264] The thinnest propene films (<70 layers) may contain more small defects, grain boundaries, and islands that allow oxygen more ready access to the bulk. In other words, the reaction is not diffusion controlled for thin films because there is less need for diffusion: the surface

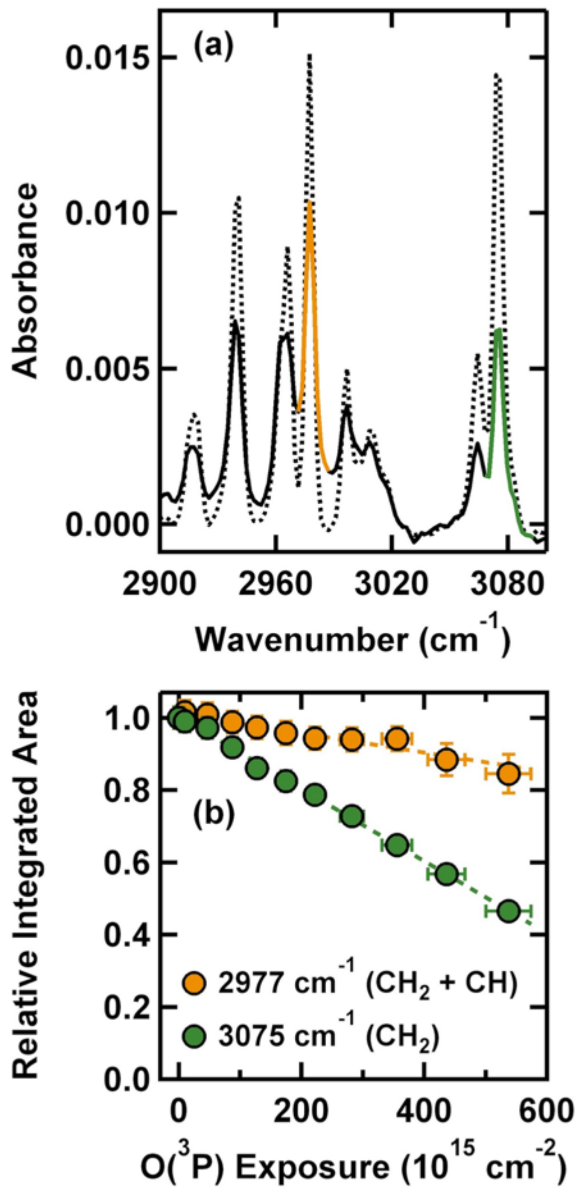

Figure 6.9: Changes in the CH region associated with terminal and central carbons. (a) RAIR spectra of the CH region of a 46-layer propene film before (dashed line) and after exposure to $O(^3P)$ (solid line, total exposure $\sim 5 \times 10^{17}$ atoms cm^{-2}) at 54 K shows significant reactivity. (b) Normalized intensities as a function of exposure demonstrate different rates of reaction for peaks at 2977 cm^{-1} (orange, CH_2 + CH stretching mode) and 3075 cm^{-1} (green, CH_2 stretching mode).

is likely inhomogeneous with exposed propene islands.[265] Higher reactivity at defects and grain boundaries is well documented,[266,267] and as with other thick molecular films, self-similarity may not be achieved until a certain thickness is reached (often $>$100 layers).[19,29,54,61] Our results, therefore, suggest that propene films reach self-similarity at approximately 150 layers, at which point oxygen diffusion becomes limiting.

6.3.3 Effect of Propene Film Structure

For all experiments mentioned thus far, propene films were deposited at a surface temperature of 59 K and exposed to oxygen at temperatures between 44 and 59 K. However, as shown in **Figure 6.10**, the deposition substrate temperature has a profound impact on the RAIR spectra of the pristine propene film, indicating a significant difference in film morphology. This is true regardless of film thickness. The spectral differences between a propene film produced at 59 K and one produced at 44 K can be summarized as follows: The γ_w peak broadens and red shifts by 2 cm^{-1} to 918 cm^{-1}, the C=C wagging mode red shifts by 2 cm^{-1} to 933 cm^{-1}, the CH_2 twisting + CH out of plane bending mode red shifts by 7 cm^{-1} to 995 cm^{-1}, and the CH_3 rock + CH out of plane bending mode red shifts by 4 cm^{-1} to 1043 cm^{-1}. These alkene modes are known to be sensitive to the conformation of the molecule and local changes within the environment.[268] In general, the peak shifts and broadening observed for the propene film dosed at 44 K compared to the propene film at 59 K are attributed to increased film disorder.[237,242,269] Red shifts may also be a result of increased intermolecular interactions with surrounding propene molecules, resulting in a slight weakening of the $=CH_2$ bond.

Although this is, to our knowledge, the first spectral evidence of differing morphologies of condensed propene, it is not unusual for deposition conditions to influence mobility during film deposition, leading to different film phases at different temperatures and dosing rates. There is vast literature, for example, on the growth of amorphous solid water and crystalline water ice films whereby crystalline films are only possible at higher substrate temperatures where there is enough mobility for water molecules to rearrange during dosing or upon annealing.[29,67,95,113]

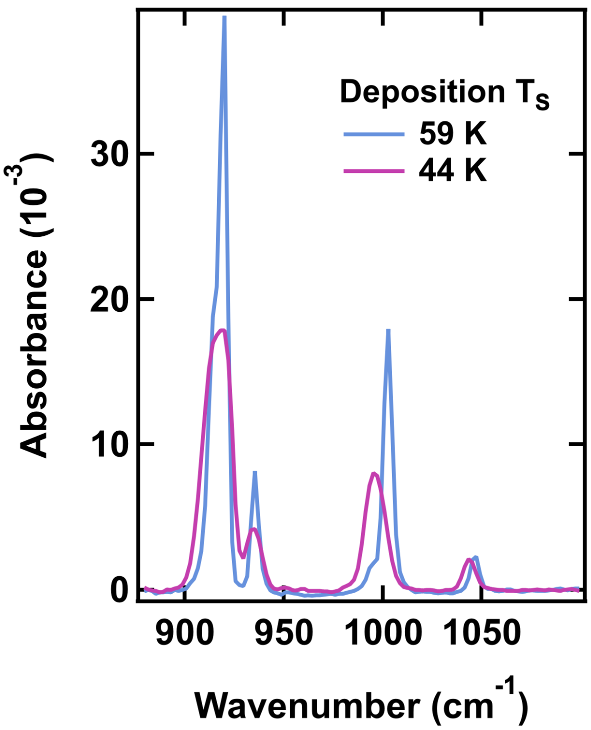

Figure 6.10: Spectral differences between amorphous and crystalline propene films. RAIR spectra of characteristic regions of 46-layer condensed propene films demonstrate that films deposited at 44 K (pink) are significantly different than films deposited at 59 K (blue). The peaks corresponding to the γ_W mode, the C=C wagging mode, the CH_2 twisting + CH out of plane bending mode, and the CH_3 rock + CH out of plane mode in the low-temperature film are generally broader and red-shifted from the analogous high-temperature film. Such shifts indicate a more disordered and amorphous film.

Similarly for alkenes, amorphous (produced at 12 K) and crystalline (produced at 70 K) acetylene have been clearly identified spectroscopically.[270] Upon warming the amorphous acetylene from 12 K, an irreversible change was detected in the spectra between 40 K and 50 K indicating that the amorphous acetylene ice had crystallized. Such spectral changes between amorphous and crystalline have also been detected for ethane and ethylene;[252] warming films to 60 K always resulted in crystallization. Based on the similarities between our observations and these studies, we will use the terms "amorphous" and "crystalline" to differentiate the films deposited below 44 K or at 59 K, respectively as propene films are less ordered when deposited below 44 K and more highly ordered at 59 K.

In order to determine how propene structure impacts oxidative reactivity, a crystalline film dosed at 59 K and an amorphous film dosed at 44 K were exposed to O(^{3}P) at an intermediate temperature of 49 K (**Figure 6.11**). At 49 K, both propene films remain structurally the same as when deposited, the amorphous film is unable to irreversibly change to a crystalline structure and vice versa. As expected, the reaction rate for the crystalline film (blue) is linear as oxygen reacts with the film. On the other hand, the amorphous film grown at 44 K is largely unreactive. There is a very short initial period of reactivity, which we attribute to O(^{3}P) reacting with the disordered propene surface layers at the vacuum interface. After this, however, there is little to no reaction despite extended exposure; this is true for all RAIR spectral regions, including the CH. It is interesting to note that the initial reaction rate of the amorphous film is faster than the rate in the crystalline film. This may further support the "amorphous" vs. "crystalline" designation of the two films. A more amorphous film typically presents a larger exposed surface area (due to islands, microporous pockets, and under-coordinated surface molecules) than the crystalline film.[71,96] A larger surface area would provide more accessible surface propene molecules and thus a faster observable rate of initial reaction before oxygen penetration into the bulk becomes necessary for continued reaction.

Beyond the first seconds of reactivity, it is quite surprising that reactivity plateaus so drastically for the amorphous film. These results suggest that oxygen is unable to diffuse into the propene bulk when the film has a more amorphous structure. This behavior is supported by previous studies examining oxidative reactivity of self-assembled monolayers (SAMs)[271–273] that found that a more compact and less mobile film structure was not as reactive. Additionally, it has been suggested that film density plays a role in observed spectroscopic band strengths, as is the case for amorphous methane.[274] Thus, the lower intensity of the peaks corresponding to amorphous propene could indicate increased density compared to the crystalline propene film. Although larger diffusion barriers in amorphous films are less common, there are polymer films where the amorphous regions are denser and this trend has been observed.[275,276] This suggests that our amorphous propene film may be packed more closely, making it less accessible to the permeating oxygen. We know from previous studies that monolayer propene molecules organize with the double bond nearly paral-

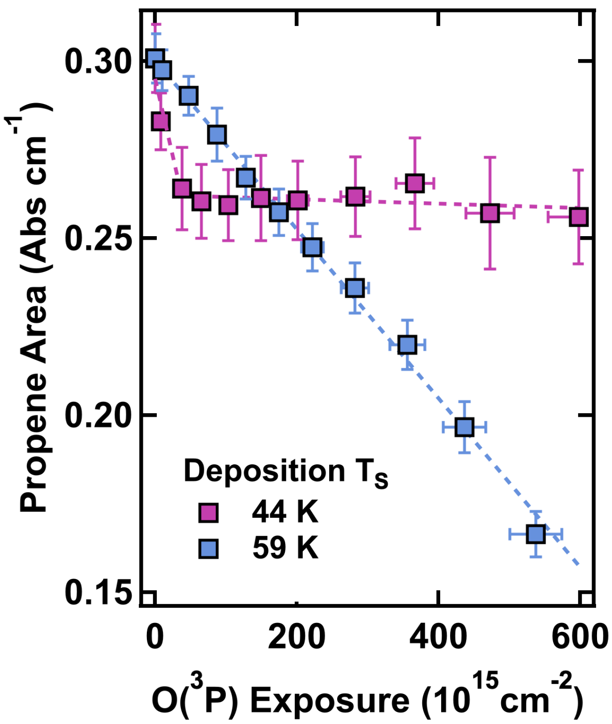

Figure 6.11: Oxidative reactivity of amorphous and crystalline propene films. Changes in the integrated area of the γ_W mode for a 46-layer propene film dosed at 44 K (pink) and 59 K (blue) and exposed to $O(^3P)$ at 49 K demonstrate that while films dosed at 44 K do experience some initial reactivity, $O(^3P)$ is unable to penetrate into the bulk of the film; diffusion and reaction occurs more readily for propene films deposited at 59 K.

lel to the Au(111) substrate.[242] This molecular orientation also appears to propagate to thicker multilayer crystalline propene films as well.[241] Thus, it is possible that in this crystalline propene structure, the molecules are organized in such a way that intermolecular-spacing affords easy access for oxygen to diffuse into the film and encounter propene's double bond.[277] It is also likely that our propene films are polycrystalline, and that grain boundaries further facilitate diffusion.[273]

RAIR spectra of the amorphous and crystalline forms of propene are easily differentiated, allowing us to probe the amorphous to crystallization transition directly and extract an activation energy for the process. Amorphous propene films (70-layers thick) were dosed at 44 K and subjected to isothermal annealing at 50, 51, 51.5, 52, 53, 54, and 55 K. Spectra collected every 60-90 seconds during the anneal clearly demonstrate a sharp phase transition (**Figure 6.12a**), evidenced by a sharpening of the peak at 919 cm^{-1} and a decrease in relative intensity of the 914 cm^{-1}

shoulder. The crystallization process occurs over a time scale of 5-30 minutes, depending on the temperature.

Rate constants for the crystallization were established by tracking the change in intensity at 919 cm^{-1} throughout the anneal. As shown in **Figure 6.12a**, the crystallizing spectra have multiple isobectic points where the spectra overlap, indicating a linear combination of crystalline and amorphous states.[278] Thus, the relative intensity of this point to both the starting fully amorphous film and the ending fully crystalline film can be used to establish the crystalline fraction of the film at any point in time.

This analysis is shown for a representative trial at each temperature by the dotted data in **Figure 6.12b**. The corresponding fit (illustrated by a dashed line) is the integrated form of the Avrami[279–281] equation:

$$x(t) = 1 - e^{(-kt)^n} \tag{6.1}$$

This form of the Avrami equation is commonly used to describe phase transformation by nucleation and gives the crystallized fraction of a material ($x(t)$) as a function of time during isothermal annealing. In **Equation 6.1**, k is the crystallization rate constant (experimental fit parameter) and n is a parameter related to the crystallization mechanism.[278] A value of n = 4 fits the data well, suggesting that the nucleation rate is constant and that there is isotropic three-dimensional growth of the crystalline phase.[282,283] We note, however, that the value of n has little impact on the calculated activation energy for propene crystallization, which is the focus of this analysis.

An activation energy for the crystallization was calculated by assuming that the crystallization rate constants have an Arrhenius-like temperature dependence. This plot is shown in **Figure 6.12c**; the corresponding analysis gives an activation energy of 1.61 $\pm$ 0.16 kcal mol^{-1}. This activation energy is much lower than those reported for water[278] or methanol[284] ices ($\sim$ 17-23 kcal mol^{-1}) indicating a low barrier for this irreversible change to crystalline propene. One possible explanation for this low value is that our amorphous propene is in a metastable state, similar to what has been observed in ethane, ethylene, and acetylene ices.[252,270] Even though we do not observe any additional spectral differences between propene deposited between 20 K and 44 K,

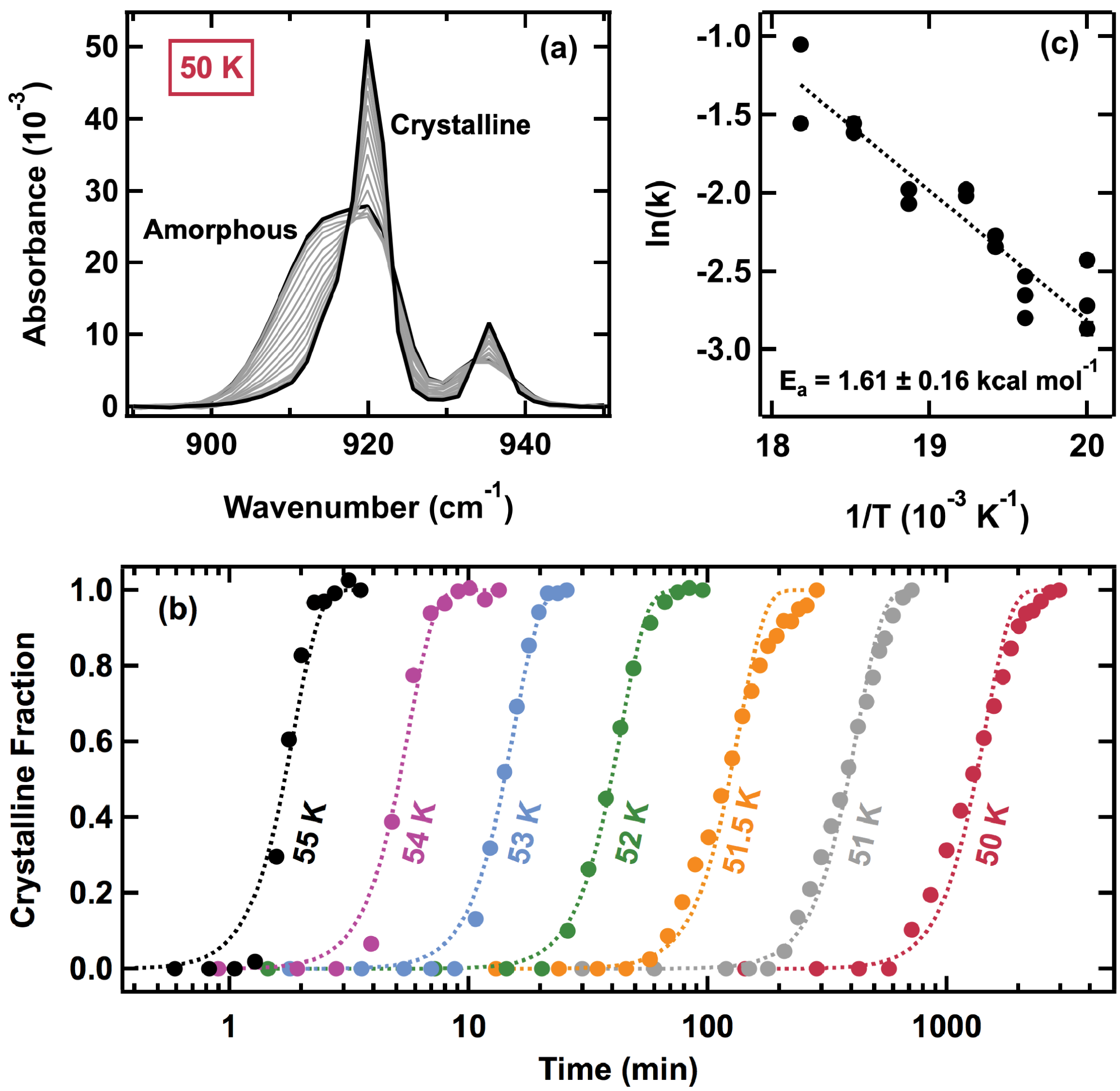

Figure 6.12: Activation energy for the propene amorphous to crystalline transition. (a) Time-resolved RAIR spectra of a 70-layer propene film isothermally annealed at 50 K indicate a transition from amorphous to crystalline propene. (b) Representative crystalline fractions versus annealing time are fit to the Avrami equation (**Equation 6.1**, dashed lines), using k as a fit parameter and a n value of 4 (see text for details). Crystalline fractions are established using the relative intensities of the corresponding spectra at 919 cm^{-1}. (c) Rate constants (k) are fit to an Arrhenius equation, yielding an activation of 1.61 ± 0.16 kcal mol^{-1} for the crystallization of propene.

amorphous solid water ices are known to be metastable compared to crystalline ices.[30] A second, explanation for the difference may be that the propene films used are thin (∼70-layers); water film crystallization kinetics, for example, are only independent of thickness for films greater than 300 layers.[285]

Regardless, this analysis highlights a number of interesting features of the propene system. First, the Avrami fitting procedure and low activation energy barrier suggests that crystallization occurs rapidly, with nucleation occurring randomly (i.e. the weak physisorption interaction between propene and the Au(111) substrate is not the dominating factor in crystallization nucleation). Additionally, we demonstrate the general feasibility of using isothermal annealing and corresponding spectra to determine alkene crystalline activation energies, which can be useful in discussing the relative stabilities of solids, liquids, and supercooled liquids.[284]

The discovery of multiple propene phases may also help to explain the observations from **Figure 6.2**, in which $O(^3P)$ is unable to fully erode thicker films and the total reacted depth is inconsistent among thicker films. When propene films crystallize (**Figure 6.12a**), RAIR spectra show a dramatic change in the relative intensity of the γ_W mode; the 914 cm^{-1} shoulder decreases in intensity while the 919 cm^{-1} peak increases. During oxidation, this bluer peak (919 cm^{-1}) is consumed more readily (**Figure 6.13**). This may indicate that within "crystalline" films, there is not uniform $O(^3P)$ reactivity within the film. Instead, it is possible that due to inhomogeneity in film organization, there are certain domains of increased order or accessibility where oxygen diffusion and reaction occurs more readily. *Our results, therefore, show broadly that film structure can have a dramatic impact on observed reactivity by impeding or allowing efficient reactant diffusion.*

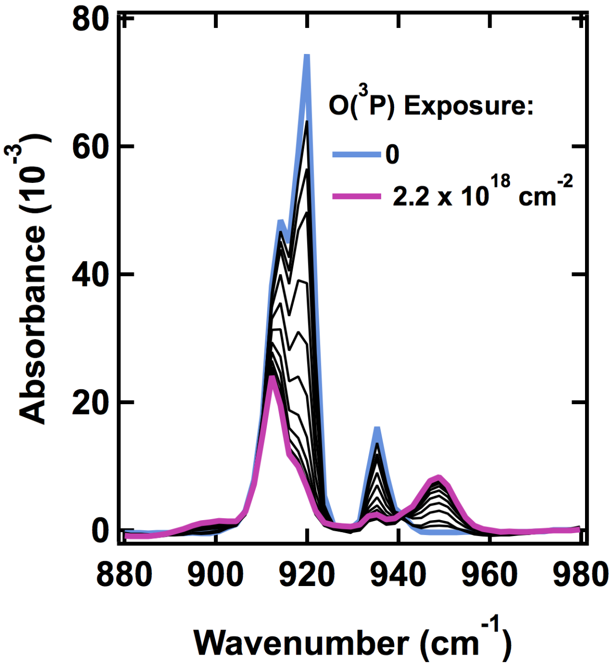

Figure 6.13: Consumption of the γ_w mode during O(^{3}P) exposure. (Upon exposure to O(^{3}P), RAIR spectra of the γ_w propene mode shows a faster rate of intensity decrease for the higher wavenumber peak (919 cm^{-1}), indicating that there may be multiple domains within the propene film and that some of them are more accessible to O(^{3}P) reactivity.

6.4 Conclusion

The oxidative reactivity of condensed propene films at cryogenic surface temperatures has been characterized using time resolved RAIRS. We find that in the condensed phase, propene reacts readily with O(^{3}P) to form primarily propylene oxide and propanal, supporting a mechanism where oxygen almost always preferentially adds to the least substituted side of the double bond. Following addition, the triplet biradical intermediate undergoes ISC at a likelihood of close to 100% to form the singlet products: propanal, propylene oxide, and a small amount of acetone. The activation energy for the loss of propene in the O(^{3}P) + propene reaction for 30-layer thick films is 0.41 $\pm$ 0.05 kcal mol^{-1} while the activation energy for propylene oxide formation is 0.36 $\pm$ 0.03 kcal mol^{-1} and 0.34 $\pm$ 0.06 kcal mol^{-1} for propanal formation. When examining thicker films (150 ML), we find that the activation energy for the reaction of propene's double bond is

1.06 ± 0.11 kcal mol^{-1} which suggests that oxygen diffusion through the film plays a significant role in the observed reaction. Interestingly, it is possible to spectroscopically differentiate two forms of propene: an amorphous form present at lower deposition temperatures (<44 K) and a crystalline form present at 59 K. Little reactivity is observed when the propene film is more disordered. Additionally, since RAIR spectra of the amorphous and crystalline forms of propene are easily differentiated, it is possible probe the amorphous to crystallization transition directly and extract an activation energy for this process.

Overall, this work provides fundamental mechanistic insight into the diffusion and reactivity of ground state atomic oxygen in condensed films of small, unsaturated hydrocarbons. Our results indicate that despite low reaction barriers for oxygen diffusion, film composition and morphology can have significant impact on reactant diffusion and subsequent reactivity. In general, such work informs the development of novel industrial processes used in the production of polyurethane plastics as well as shed light on possible chemical pathways in frozen astrophysical environments. In addition to these applications, an important future extension of this work may be to consider conformationally ordered, vinyl-containing films in which molecular orientation relative to the impinging oxygen atom can be controlled, allowing for precise, stereodynamic tuning of reaction kinetics.

Chapter 7

Rapid Laser-Induced Temperature Jump Decomposition of the Nerve Agent Simulant Diisopropyl Methylphosphonate under Atmospheric Conditions

We present work detailing the destruction of the nerve agent simulant diisopropyl methylphosphonate (DIMP) via rapid laser heating under atmospheric conditions. Following Nd:YAG laser ablation of liquid DIMP deposited on a graphite substrate, both parent and product fragments are transmitted via capillary from an atmospheric chamber to a vacuum chamber containing a high-resolution mass spectrometer. This allows for real time measurements of product distributions under a variety of temperature and atmospheric conditions. Ex situ Fourier transform infrared (FTIR) spectroscopy analysis of the same chamber contents provides complementary information about product identities and fragmentation pathways. Results demonstrate that product distributions depend on heating rate, surface temperature, and atmospheric oxygen content. In the destruction of the DIMP, the relative production of alkene products depends significantly on laser power; smaller products are relatively more abundant at higher ablation temperatures. We also show that in the absence of atmospheric oxygen, the concentration of oxygenated products decreases sharply relative to alkene and alkane products. This suggests that under high-temperature conditions atmospheric oxygen is incorporated directly into the products of the fragmented simulant. This project extends significantly our understanding of the fundamental chemistry of these dangerous compounds under atmospheric and rapidly changing thermal conditions. The results have critical implications for the development of effective chemical warfare agent decontamination and destruction strategies.

7.1 Introduction

Due to the threat chemical warfare agents (CWAs) pose to the global community, there is considerable interest in detecting, destroying existing stockpiles, and decontaminating areas affected by these compounds.[286,287] Current large-scale destruction techniques include incineration[288] and neutralization by base hydrolysis, but these strategies come with additional challenges regarding safe transport and toxic byproducts.[289] Therefore, it remains critical to continue developing new strategies and to understand the exact chemistry of agents' destruction in both vapor and condensed phases. Of particular interest are the extremely dangerous organophosphonate nerve agents Soman and Sarin.[290] Sarin, for example, has a high estimated toxicity of 35 mg min m^{-3} in humans via vapor inhalation.[291] Even beyond these dangerous compounds, many less toxic organophosphonates have found widespread industrial use as plasticizers, flame retardants, fire-resistant fluids and lubricants, and pesticides.[292,293] It is therefore important to characterize environmental impacts and remediation strategies for organophosphonate contaminants more broadly. This study adds to our fundamental understanding of the primary chemical kinetics and physical processes occurring when these compounds are exposed to rapid heating under atmospheric conditions.

The current work presents a detailed investigation of the laser-induced, high temperature rapid heating destruction of the nerve agent simulant diisopropyl methylphosphonate (DIMP, **Figure 7.1**).[294–296] DIMP was selected from among the class of organophosphonate simulants for two reasons. First, DIMP shares key structural similarities with the nerve agent Sarin, which is a compound of particular interest due in part to its use in urban terror attacks in Japan and its exposure to US troops abroad.[289,294] Second, it has been shown in a number of pyrolytic and thermal studies that a significant organophosphonate destruction channel yields substituted and unsubstituted carbon products resulting from the alkoxy moiety.[296–302] This gaseous product array is easily detectible and differentiable via mass spectrometry and FTIR analyses, which enables a robust investigation of the impact of laser heating rate, surface temperature, and atmospheric pressure on simulant destruction.

In addition to experimental and theoretical work on the thermal decomposition and combus-

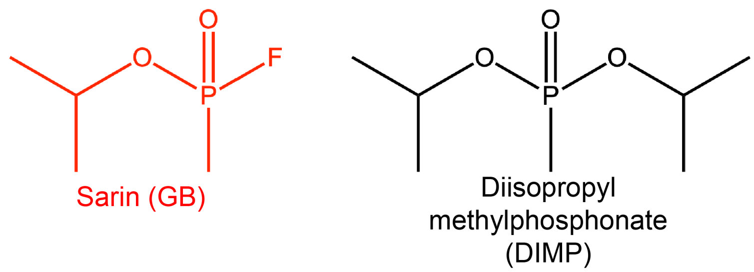

Figure 7.1: Sarin and diisopropyl methylphosphonate chemical structures. The chemical structures of the nerve agent sarin (red) and the simulant diisopropyl methylphosphonate (black) differ only in the replacement of fluorine with an additional oxygen and isopropyl group.

tion of these compounds,[296,301,303–305] this work is an extension of previous studies examining oxidative[306,307] and laser destruction[308] of adsorbed chemical nerve agent simulants under ultra-high vacuum conditions. The oxidative destruction of DIMP and dimethyl methylphosphonate (DMMP) progresses at similar rates and yields oxygen- and carbonyl-containing oligomeric product species.[306,307] Laser desorption and destruction studies of a number of Sarin simulants (DIMP, DMMP, and diethyl ethylphosphonate), demonstrated lower temperature thresholds for destruction of simulants with relatively larger phosphonate side chains.[308] On the basis of these results, we again expect that the majority of gas phase products in this study will include a variety of 1, 2, and 3-carbon products generated from the DIMP isopropyl group, with possible incorporation of atmospheric oxygen.

Using a unique atmospheric pressure ablation chamber, rapid laser heating of 1011 K s^{-1}, and in situ mass spectrometry, this work probes the reaction products in the prompt destruction of DIMP under atmospheric and, for the first time, oxygen-depleted atmospheric conditions. In addition to identifying product branching ratios as a function of laser power, the manipulation of oxygen content allows us to elucidate the mechanistic role of oxygen in simulant destruction. This basic understanding is critical for practical decontamination strategies that involve, for example, flame incineration, as those conditions often lead to significant oxygen depletion in the local environment.[309]

In the laser-induced thermal destruction of DIMP, we demonstrate that the resulting product distribution is dependent on both surface temperature rise and atmospheric oxygen composition.

More specifically, the relative production of small alkene products depends significantly on laser power; the relative yield of smaller substituted products is higher when the sample is ablated with higher laser powers. Likewise, under oxygen-depleted conditions, the relative amount of oxygenated products decreases sharply relative to alkene and alkane products. This suggests that under extreme high-temperature conditions atmospheric oxygen is incorporated directly into the products of the fragmented simulant. Such findings are directly relevant to producing novel chemical warfare agent mitigation strategies and maintaining national security.

7.2 Experimental

All experiments were conducted in a newly constructed atmospheric-mass spectrometry apparatus, shown in **Figure 7.2**. Additional measurements were collected via ex situ FT-IR analysis. In short, a UTI 100 quadrupole mass spectrometer (QMS) occupies a high-vacuum chamber reaching base pressures of 10^{-9} Torr. This chamber samples, via a 20 cm fused silica capillary with a 25-μm inner diameter, the gaseous products produced in a small, adjacent atmospheric chamber used for laser ablation trials. A second identical inlet capillary in the atmospheric chamber ensures that atmospheric pressure is maintained during experimental sampling. The volume of the atmospheric sampling chamber is small (approximately 40 cm^3), which enables rapid diffusion of vapor products; changes in chamber contents are detected by the mass spectrometer within 300 ms. We do note that the capillary is not heated, so there is a possibility for vapor condensation of DIMP or associated products during transport. Gas phase products are, however, expected to thermalize rapidly in the atmospheric chamber, so we do not expect condensation in the capillary to be a major pathway. The large pressure differential between the two chambers also ensured consistent gas flow through the capillary, and repeated use of the same capillary showed no blockage, indicating that condensation was not happening on a large scale.

In order to prepare DIMP samples for ablation, the atmospheric chamber was routinely purged and re-opened to atmosphere between trials. The substrate for all experiments was a highly ordered pyrolytic graphite crystal (HOPG, Bruker). In addition to chamber purging, the HOPG surface was

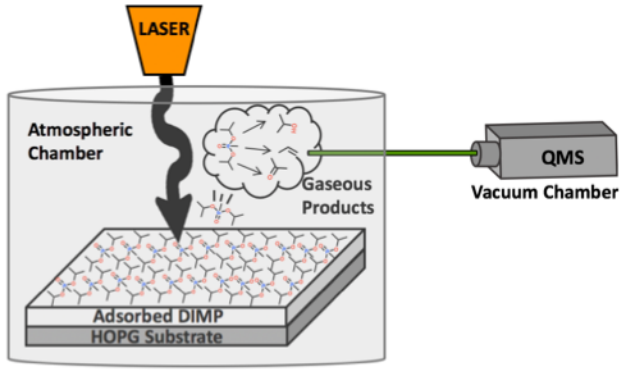

Figure 7.2: Joint atmospheric and high-vacuum apparatus. Laser ablation experiments are conducted in a joint atmospheric and high vacuum apparatus. A Nd:YAG laser is used to ablate DIMP simulant films in an atmospheric chamber (purple). Gaseous products are transported via capillary (green) to a high vacuum chamber containing a UTI QMS for analysis.

exfoliated between trials to ensure reproducible surface quality and composition. To begin each experiment, 10 µL of DIMP (Alfa Aesar) was deposited on the HOPG surface and the chamber was sealed. A background mass scan was then collected; final product analysis was performed on the background-subtracted spectra collected following ablation.

DIMP films were ablated with a Nd:YAG laser (Quanta-Ray GCR 130) producing near-IR photons at 1064 nm. To estimate the surface temperature on the HOPG substrate induced by the laser pulse, the following calculation was carried out for one-dimensional heat flow into a semi-infinite slab of material (transverse propagation of the beam is large compared to the depth of heat conduction into the film). Assuming that the optical absorption coefficient of HOPG is large (on the order of 104 – 106 cm^{-1}),[310–313] the surface temperature of the HOPG surface at time t can be calculated as:[314]

$$T(0,t) = \frac{2F_0}{K}(\frac{kt}{\pi})^{\frac{1}{2}} \tag{7.1}$$

In **Equation 7.1**, F_0 is the absorbed incident flux from the laser, K is the thermal conductivity of HOPG and k is the thermal diffusivity (reported as 290 W m^{-1} K^{-1} and 0.000165 m^2 s, respectively).[315] In practice, the total pulsed laser power is first measured with a Scientech calorimeter (Model 38-0101). This output is then converted to pulse energy by incorporating the pulse frequency (20 Hz) and scaling to the duration of individual pulses (8 ns). Pulse energies in this study range from 0.103 to 0.244 J. This total flux is further scaled to the reflection coefficient of HOPG (reported as 0.21 at 300 K).[310] With this model, peak laser powers raise the crystal temperature to approximately 2830 ± 110 K at a heating rate of 3.2 x 1011 K s^{-1}. The error cited for temperature is a standard propagation including error from the calorimeter measurement, pulse width, and HOPG reflection coefficient. We note that simulant films were ablated for 2 minutes at 20 Hz in order to generate sufficient product signal for analysis. However, product signals (propene at m/z = 41, for example) were detected for single pulse ablations and thermocouple measurements of the HOPG crystal show a steady-state temperature rise of only approximately 350 K as a result of the extended ablation. We therefore assume that the modest temperature rise caused by extended ablation is negligible compared to the high temperatures during each individual pulse.

Mass spectra analyses involved a series of steps illustrated with representative data in **Figure 7.3**. To begin, background spectra were subtracted from post-ablation spectra (**Figure 7.3, a**). Next, the MALDIquant R package was used for data smoothing (using a 7-point Savitzky-Golay-filter, **Figure 7.3, b**) and peak detection.[316,317] In order to deconvolve the spectra into individual product contributions, it was first necessary to build a library of fragmentation patterns for the proposed products. To this end, mass spectra were collected for propene (Sigma Aldrich), acetone, and isopropyl alcohol (IPA, both from Fisher Scientific). The spectra for additional products, ethylene and acetylene, were obtained from reference data from the National Institute of Standards and Technology (NIST).[229] Once this library was complete, the relative product contributions for the ablated spectra were determined using a least-squares analysis (**Figure 7.3, c**). We note that though present in the background-subtracted spectra, large peaks associated with atmospheric gases like N2, O_2, Ar, etc were excluded from this deconvolution procedure due to the difficulty separating trace product signals from atmospheric contributions. The omission of m/z = 27 and 28 in particular made it difficult to distinguish ethylene and acetylene. Therefore, all discussions herein will group these two-carbon products together.

In addition to mass spectrometry, a second modular chamber was used for concurrent ex situ

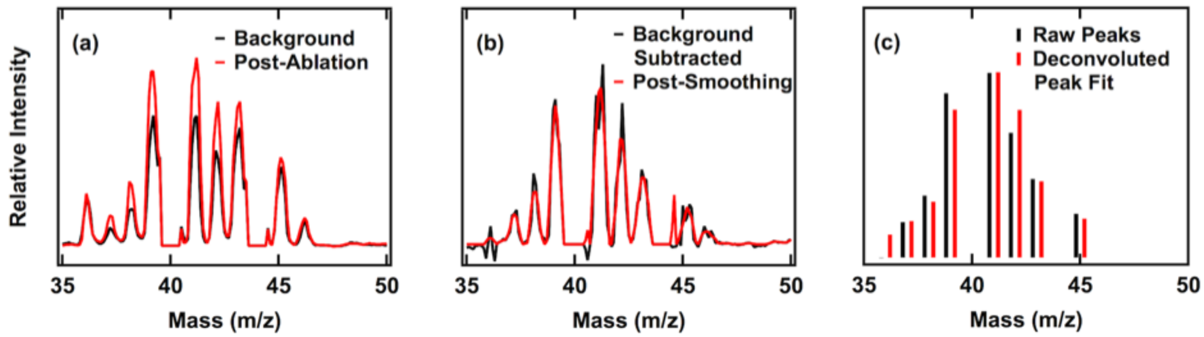

Figure 7.3: Processing of representative ablated DIMP mass spectra. Background spectra are subtracted from post-ablation spectra (a). These background-subtracted spectra are smoothed (red, b) and peaks are detected (black bars, c). A least-squares procedure is used to determine relative product yields and reproduce the ablated spectra (red bars, c).

FTIR analysis of ablated products. To begin these experiments, a 150 cm^3 IR cell with ZnSe windows was purged to approximately 25 mTorr. This chamber was connected via leak valve to an analogous atmospheric chamber for simulant ablation. Following the ablation procedure, the valve was opened, allowing the evolved gaseous products to escape into the purged chamber. The contents of the unheated chamber were analyzed using a Nicolet iS50 infrared spectrophotometer (Thermo Fisher) and a liquid-nitrogen-cooled MCT/A detector. All such FTIR spectra were averaged over 200 scans at 4 cm^{-1} resolution; peak fitting analysis utilized Gaussian peaks atop cubic baselines.

7.3 Results and Discussion

7.3.1 FTIR Product Analysis

Previous investigations into the thermal destruction of DIMP have consistently identified a number of products including propene, IPA, and ethylene. These studies include destruction via pyrolysis, combustion, exposure to a corona discharge, dissociative adsorption, laser ablation, etc.[286,296,318–320] While this provides a reasonable set of products to look for, the current work represents the first direct study of rapid laser heating (on the order of 1011 K s^{-1}) of adsorbed liquid DIMP under atmospheric pressure and oxygen depleted conditions. It is therefore neces-

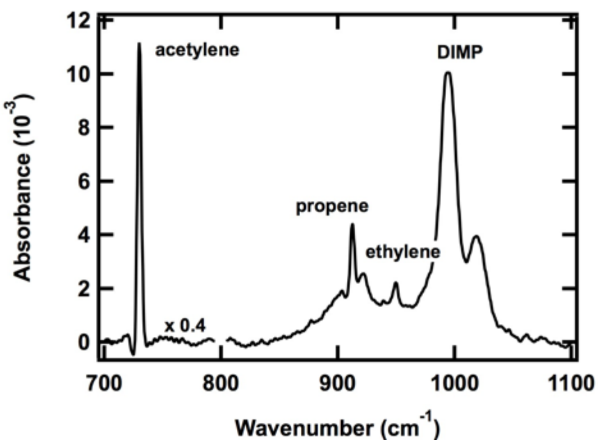

Figure 7.4: Representative ablated DIMP spectra. A representative FTIR spectra of DIMP ablated to approximately 2720 K shows clear evidence of residual DIMP as well as acetylene, propene, and ethylene products.

sary to firmly establish the full range of products before attempting to assess branching ratios; this was done using ex situ FTIR. Representative spectra of ablated DIMP in **Figure 7.4** show clear evidence of propene, ethylene, acetylene, as well as contributions from unreacted DIMP or other partially decomposed organophosphonate fragments such as isopropyl methylphosphonate (IMP). In addition to the prominent phosphonate P-O-C stretching modes at 995 and 1020 cm^{-1}, we observe significant signal intensity from propene's =CH_2 wagging mode (912 cm^{-1}) and the bending modes of acetylene and ethylene (730 cm^{-1} and 949 cm^{-1}, respectively). All peaks referenced herein are consistent with those reported for the corresponding molecules in the gas phase.[229,231,240,295,321–324] CO is also observed, but this is difficult to uniquely assign to either DIMP or HOPG ablation. Additionally, other small product peaks are observed in the spectra beyond those highlighted in **Figure 7.4**, but we were not able to clearly establish their identities using FTIR alone.

In both FTIR and the following MS analyses, we note that the scope of our experiment did not include direct quantification of condensed-phase products or parent molecules remaining on the HOPG substrate or in the atmospheric chamber. Similar to other studies, however, our gas-phase product analysis suggests that it is primarily phosphorus-containing products that remain following thermal destruction.[296,325] In addition to unreacted DIMP, these products likely include IMP and methylphosphonic acid (MPA).

As laser power (and thereby HOPG surface temperature) is increased, an interesting trend emerges in the relative distribution of products. When spectra are normalized to the height of the propene peak, there is a corresponding relative increase in the height of ethylene (**Figure 7.5, a**). If the relative areas of these two peaks are plotted as a function of HOPG surface temperature (**Figure 7.5, b**), it becomes clear that as the ablation temperature increases, ethylene production increases relative to propene. The same trend is observed for relative propene and acetylene production. Without precise absorption cross-sections for these compounds it is difficult to quantify the absolute amount of each product formed. It is clear, however, that higher temperatures lead to a higher yield of smaller substituted carbon products.

7.3.2 Effects of Varying Surface Temperature

The results described in the preceding section were easily replicated with in situ mass spectrometry. However, it is important to note that the mass spectra data reveal some additional minor products unidentified in the FTIR data. FTIR spectra provided no conclusive evidence of oxygenated ablation products, despite their suggested presence in other pyrolytic and thermal decomposition studies of DIMP.[296,318,319] Background subtracted mass spectra of ablated DIMP, however, show clear increases in m/z = 43 and m/z = 45 (acetone and IPA, respectively). The yield of both of these products is consistently small relative to propene and ethylene/acetylene, so their absence in FTIR spectra may simply be due to lack of sensitivity. Therefore, mass spectra are deconvoluted into contributions from four observed products: propene, ethylene/acetylene, acetone, and IPA. **Figure 7.6** shows the least-squares fit for the data collected in three representative trials at different ablation powers. When the data are normalized to propene signal (m/z = 41), there is a clear corresponding relative increase in the amount of the smaller acetylene and ethylene products. In other words, these results again suggest that peak surface temperatures impact the extent of bond cleavage and identity of destruction products.

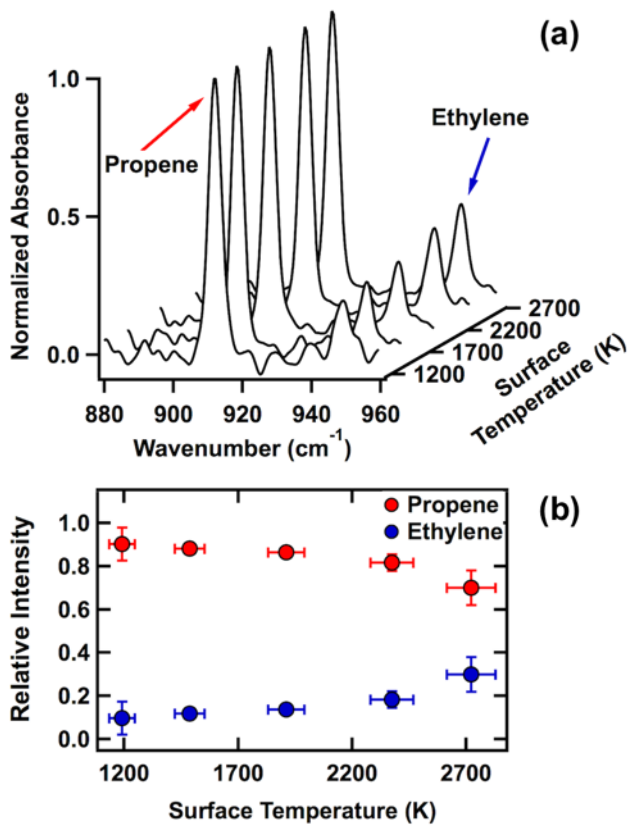

Figure 7.5: Relative production of ethylene and propene as a function of laser ablation power. FTIR spectra normalized to propene height (a) demonstrate increases in relative ethylene production as surface ablation temperature increases. Baseline and other product peaks have been subtracted for clarity. The relative integrated area of the associated peaks (b) shows that this trend is observed throughout the temperature range explored in this study (error bars represent the standard deviation of at least three trials at each ablation temperature).

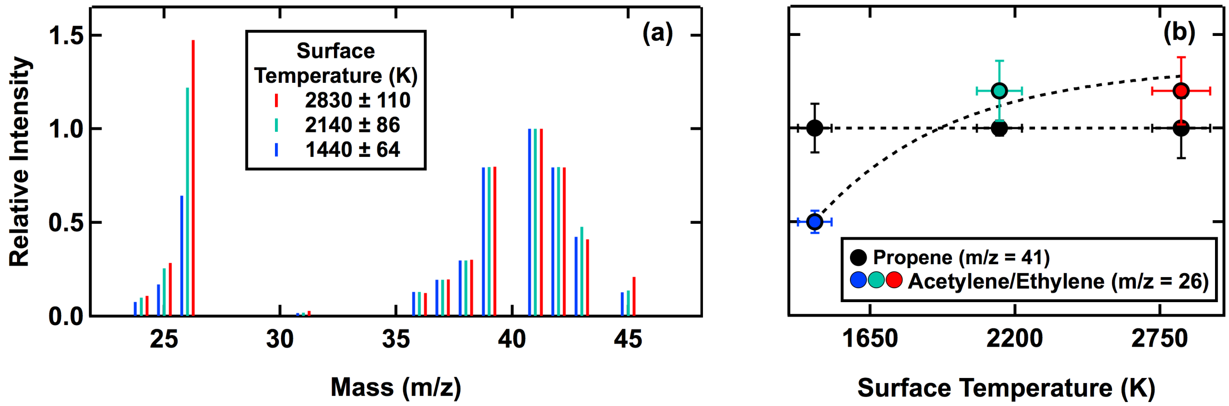

Figure 7.6: Increase in ethylene and acetylene production at higher laser powers. Reproduced representative mass spectra (a) from a least-squares fit of the data (normalized to propene signal at m/z = 41) show an increase in low molecular weight products (ethylene and acetylene) as laser power is increased. This can also be seen in the normalized relative intensities of propene and acetylene/ethylene (m/z=26) averaged across all trials (b). Ablation surface temperatures are 1440 K (blue), 2140 K (green), and 2830 K (red). Dotted line is drawn to guide the eye.

7.3.3 Effects of Varying Atmospheric Oxygen

In order to probe the role of atmospheric oxygen in DIMP destruction, we performed a series of experiments with variable partial pressures of oxygen. Following simulant deposition, the sampling chamber was carefully purged with N_2 until a desired oxygen pressure was reached (as measured with the QMS). The chamber, however, was still maintained at atmospheric pressure. After ablation at the highest laser powers, the results in **Figure 7.7** show that the presence of oxygenated products plummets nearly to zero when atmospheric oxygen is reduced. Signals associated with both acetone (m/z = 43) and IPA (m/z = 45) decrease sharply relative to propene (m/z = 41). *This observation is of critical importance; it demonstrates clearly that atmospheric oxygen is incorporated directly into the fragmenting DIMP molecule.*

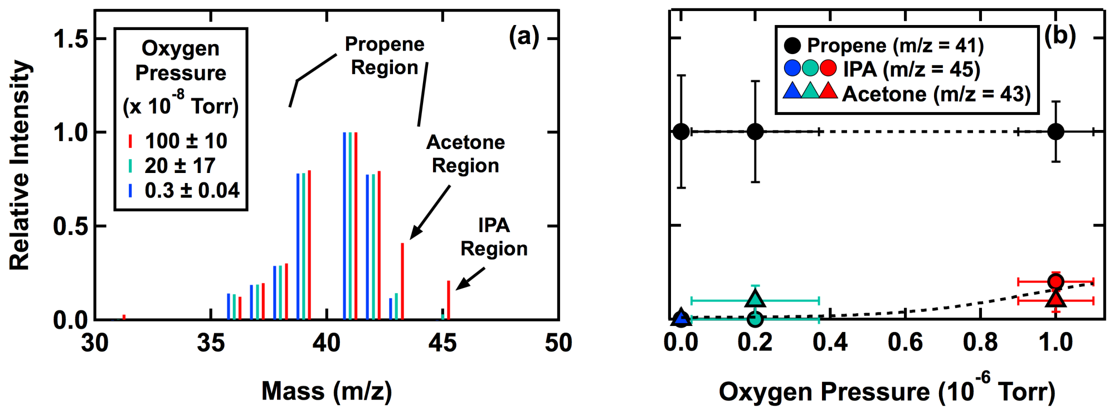

Figure 7.7: Decrease in oxygenated products as available oxygen decreases. Reproduced representative mass spectra (a) from a least-squares fit of the data (normalized to propene signal at m/z = 41) show a sharp decrease in oxygenated products as available oxygen decreases. This can also be seen in the normalized relative intensities of propene, IPA (m/z=45) and acetone (m/z=43) averaged across all trials (b). Recorded oxygen pressures in the QMS chamber were 1×10^{-6} Torr under atmospheric ablation conditions (red), 2×10^{7} under low oxygen conditions (green), and 3×10^{-9} Torr under oxygen-depleted conditions (blue). Dotted line is drawn to guide the eye.

7.3.4 Mechanism of Destruction

The effects of varying both ablation surface temperature and atmospheric composition are summarized in **Table 7.1**. Each entry represents the average of at least three similar trials. In brief, we observe that higher ablation temperatures lead to an increase in the relative production of shorter chain substituted products (ethylene/acetylene vs. propene). Additionally, a reduction in available atmospheric oxygen leads to a decrease in the relative production of oxygenated products (acetone and IPA vs. propene). These results inform the following discussion of the mechanisms underlying the thermal destruction of condensed-phase DIMP.

To begin, it has been proposed experimentally and theoretically that that the primary pyrolytic destruction step for DIMP and other similar molecules is a unimolecular decomposition to IMP and propene via a six-membered ring transition state.[296,326–328] Moreover, propene production has been observed under a variety of high temperature conditions, beginning with temperatures as low as 700 K, which is lower than the ablation range studied here.[296,308] In vacuum studies, propene is also produced as a result of dissociative adsorption of DIMP.[297,301] Essentially, many studies agree that a major step in DIMP destruction involves the formation of propene. On the other hand, few studies have identified direct mechanisms that yield smaller substituted products from DIMP's initial dissociation (and indeed no single initial bond scission is enough to yield a two-carbon product from DIMP directly). Instead, it is likely that the smaller products (ethylene, acetylene, methane, etc) are produced as secondary destruction products of propene.[197,329] The results of this work present evidence that indeed propene is likely one of the first products, and that higher ablation temperatures increase the relative extent of further fragmentation.

The results of the oxygen study add interesting detail to the existing mechanistic picture. Zegers and Fisher proposed a two-step pyrolysis mechanism for DIMP, beginning with the unimolecular decomposition that yields propene. The second step involves transfer of a hydrogen from the phosphorous hydroxyl group to the oxygen of the isopropoxy group, yielding IPA and methyl dioxophosphorane.[296] Our observations suggest, however, that this intermolecular step may not be the primary mechanism for IPA formation at these high-temperature, fast-heating, and condensed-phase conditions. Instead, atmospheric O_2 or radicals formed from thermal dissociation may abstract hydrogens or break bonds in the DIMP molecule directly. For example, if an alkyl radical forms upon scission of the P-O-C bond, atmospheric O_2 can readily add to generate an alkoxy radical. This species, in turn, is expected to react or decompose readily to form both the observed acetone and IPA.[330–332] The direct incorporation of oxygen from the atmosphere in this proposed mechanism would account for the observed dependence on oxygen pressure in the ablation chamber in the production of oxygenated products.

7.4 Conclusion

Building on work investigating pyrolysis, dissociative adsorption, and laser ablation of chemical warfare agents and their simulants, this study presents a comprehensive look at rapid thermal ablation of condensed DIMP, a simulant of Sarin, under atmospheric pressure conditions. Decomposition products observed include propene, ethylene, acetylene, IPA, and acetone, which are well in line with existing literature on thermal destruction of organophosphonates. Product distribu-

Chamber Conditions		Relative Product Contributions			
Oxygen (Torr)	***T_s(K)***	***IPA***	***Acetone***	***Propene***	***Ethylene/Acetylene***
$(1 \pm 0.1) \times 10^{-6}$	2830 ± 110	0.2 ± 0.05	0.1 ± 0.06	1 ± 0.16	1.2 ± 0.18
$(1 \pm 0.1) \times 10^{-6}$	2140 ± 86	0.2 ± 0.03	0.1 ± 0.12	1 ± 0.04	1.2 ± 0.16
$(1 \pm 0.1) \times 10^{-6}$	1440 ± 64	0.1 ± 0.08	0.4 ± 0.13	1 ± 0.13	0.5 ± 0.06
$(1 \pm 0.1) \times 10^{-6}$	2830 ± 110	0.2 ± 0.05	0.1 ± 0.06	1 ± 0.16	1.2 ± 0.18
$(2 \pm 1.7) \times 10^{-7}$	2830 ± 110	0 ± 0.03	0.1 ± 0.08	1 ± 0.27	4.2 ± 0.86
$(3 \pm 0.4) \times 10^{-9}$	2830 ± 110	0 ± 0.0	0 ± 0.0	1 ± 0.3	7 ± 1.49

Table 7.1: Normalized product ratios following DIMP ablation. Summary of all DIMP ablation experiments performed, normalized to propene production. As surface temperature is increased, the relative ratio of ethylene and acetylene to propene increases. As available oxygen is decreased, the relative production of IPA and acetone decreases.

tions varied significantly when both laser power (HOPG surface temperature) and oxygen content were altered; higher ablation powers led to higher temperatures, which increased the extent of secondary fragmentation in alkene and alkyne products observed. Lower oxygen partial pressures led to a sharp decrease in oxygenated products, suggesting that a dominating mechanism in this system involves direct incorporation of atmospheric oxygen into product fragments.

Though Sarin, unlike DIMP, includes a fluorine substituent on the central phosphorus atom, there is reason to believe the results highlighted here have direct relevance for Sarin's thermal destruction. Experimental work with simulants and nerve agents has shown significant correlation between bond frequency and desorption energies, suggesting that simulants like DIMP are indeed appropriate for modeling the chemistry of toxic agents.[294] Perhaps more importantly, pyrolytic simulations of Sarin have confirmed that thermal destruction begins with the same six-center intermediate that leads to propene elimination.[305] Therefore we expect that the chemistry observed in these temperature-jump experiments is relatively generalizable to Sarin and other large organophosphonates.

In addition to validating the applicability of these results on live nerve agents, extensions of this work may include tracking the destruction temperature thresholds and product distributions for additional simulants and simulant mixtures, as well as the impact of incorporating less absorptive or reactive substrates. In general, this work continues to shed light on the basic mechanisms of organophosphonate thermal destruction, related to those encountered under high temperature rapid heating blast conditions. These results are critical for the accurate modeling of environmental persistence and implementation of mitigation strategies for chemical warfare agents and other organophosphonate pesticides.

Appendix A

Appendix

Appendices **A1-A6** contain figures with the raw data as collected for figures throughout this thesis. Since not every figure in this thesis has corresponding raw data, the numbers may not match up exactly to the associated figure in the thesis, but will be marked accordingly.

Appendix **A7** contains the copyright attribution for all work reproduced in this thesis that has been published.

A1 Experimental Section (Chapter 2)

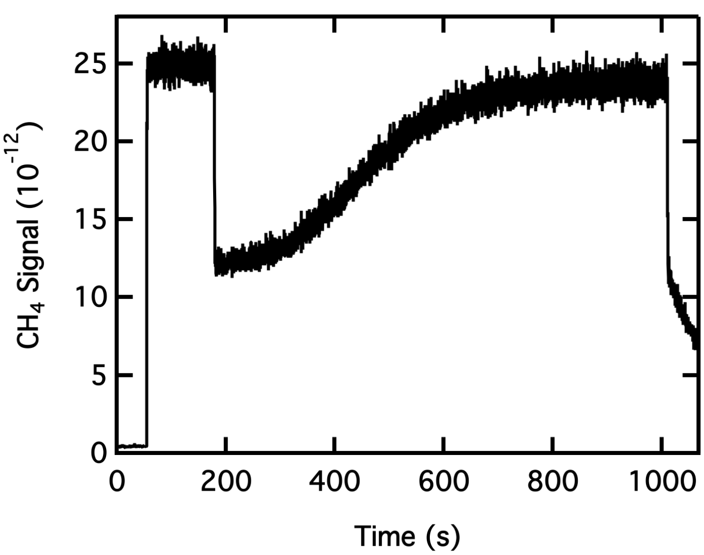

Figure A1.1: Raw RGA data for Figure 2.4. Signal intensity for a beam of CH_4 (seeded in H_2) exposed to a thick film of p-ASW D_2O at 33.5 K. The beam nozzle is heated to 970 K, resulting in an energy of 1.8 eV (*Data file: 040619.R05)*

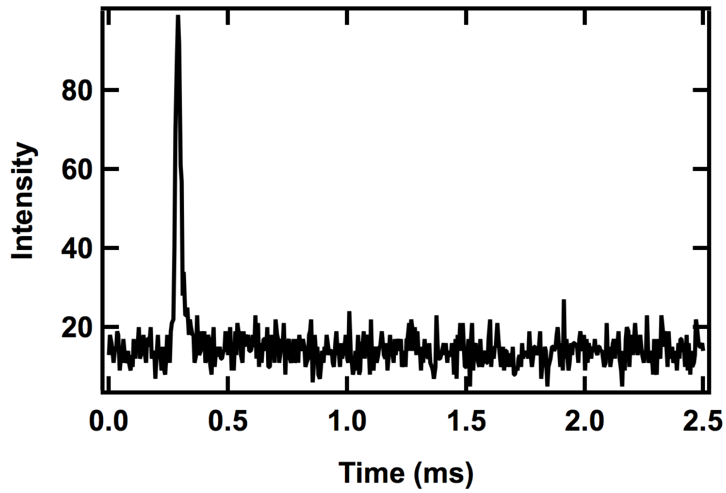

Figure A1.2: Raw TOF data for Figure 2.6. QMS intensity for a seeded CH_4 beam at 400 K collected as a function of time. The beam passes through the rotating chopper slit at 1% duty-cycle modulation to trigger at t= 0. (*Data file: 040918T.F05*)

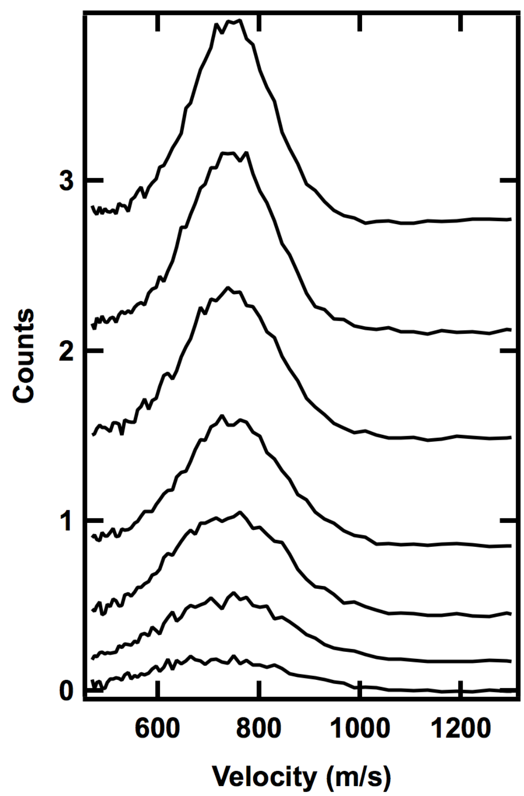

Figure A1.3: Raw TOF data for Figure 2.7. We collect a series of TOF spectra for a neat beam (for instance O_2) at various backing pressures and find the linear relationship between the integrated areas of these curves and the calculated beam flux. We then use the slope of this fit to convert TOF peak to absolute flux for seeded beams. (*Data files: 071519T.F01-7*)

A2 Sticking Probability of High-Energy Methane on Crystalline, Amorphous, and Porous-Amorphous Ice Films (Chapter 3)

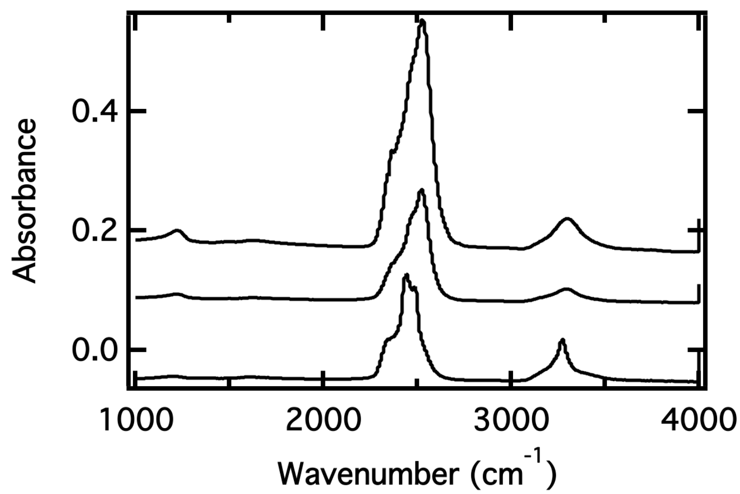

Figure A2.1: Raw RAIR spectrum for Figure 3.1. In addition to integrating the O-D stretching region to gain information about film thickness, the shape of the O-D stretching region also provides details about the ice morphology (p-ASW, np-ASW, and CI). We can compare the integrated area of the small dangling bond region between 2700 and 2780 cm^{-1} to gain information about the ice surface area and porosity. Each spectrum is representative of each film type, deposited via directed doser at a crystal temperature of 25 K, 107, and 150 K for p-ASW, np-ASW, and CI respectively. These films are between 150 and 250 layers thick. (*Data files: 040218A.IR06 (p-ASW, top), 042018A.IR01 (np-ASW, middle), 050918A.IR36 (CI, bottom)*)

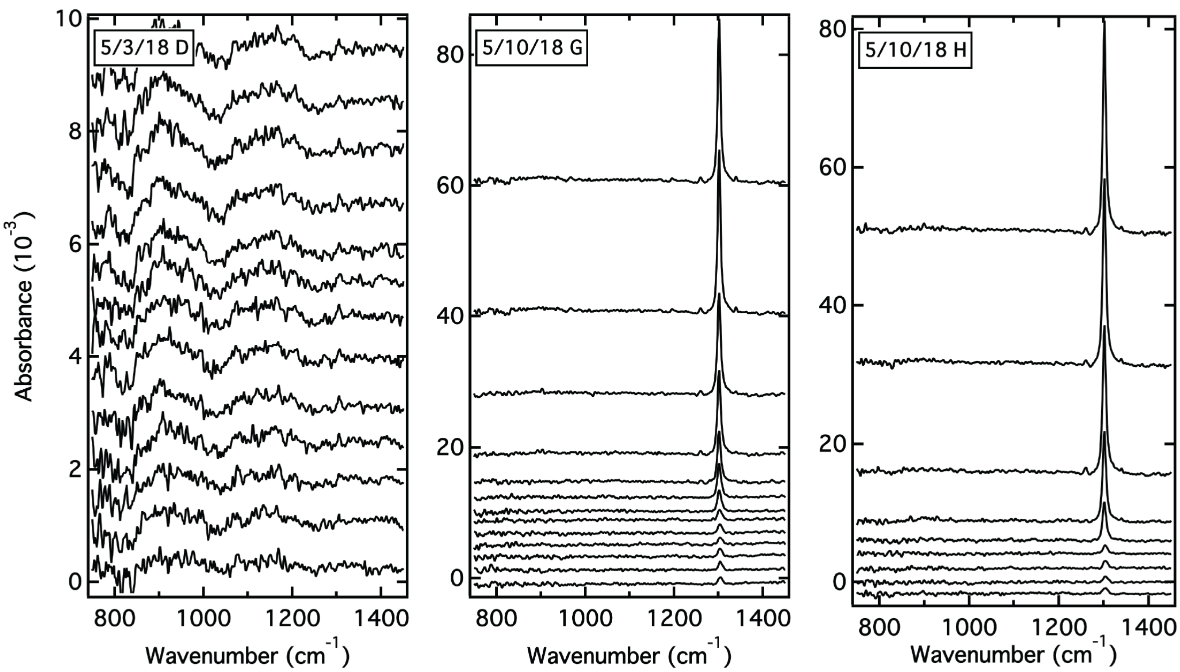

Figure A2.2: Raw RAIR spectrum for Figure 3.2a - CI Films.We tracked the integrated area of methane's ν_4 mode (1305 cm^{-1}) during adsorption and desorption experiments. In the top panel of **Figure 3.2a**, we isothermally desorb a multilayer film of methane on a CI film at 24 and 25 K to determine the height of the monolayer. In the bottom panel, we see a small amount of methane grow in on a CI film held at 33.5 K .(*Data files: 051018G.IR01-16 (desorption, 24 K), 051018H.IR01-09 (desorption, 25 K), 050318D.IR01-13 (adsoprtion, 33.5 K)*)

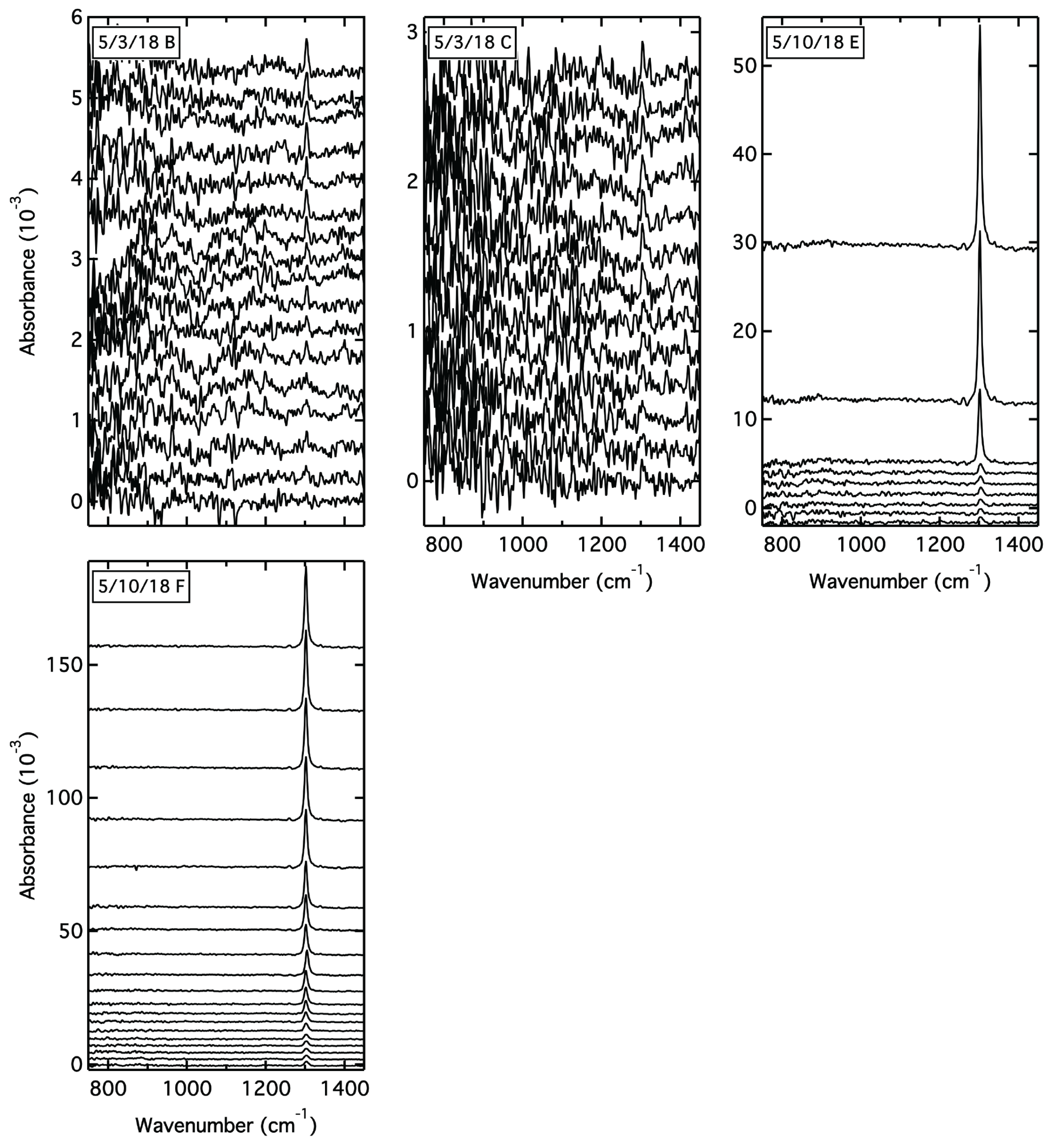

Figure A2.3: Raw RAIR spectrum for Figure 3.2b - np-ASW Films. We tracked the integrated area of methane's ν_4 mode (1305 cm^{-1}) during adsorption and desorption experiments. In the top panel of **Figure 3.2b**, we isothermally desorb a multilayer film of methane on a np-ASW film at 24 and 25 K to determine the height of the monolayer. In the bottom panel, we see a small amount of methane grow in on a np-ASW film held at 33.5 K. (*Data files: 051018F.IR09-29 (desorption, 24 K), 051018E.IR01-10 (desorption, 25 K), 050318B.IR01-17 (adsoprtion, 33.5 K), 050318C.IR01-13 (adsoprtion, 33.5 K)*)

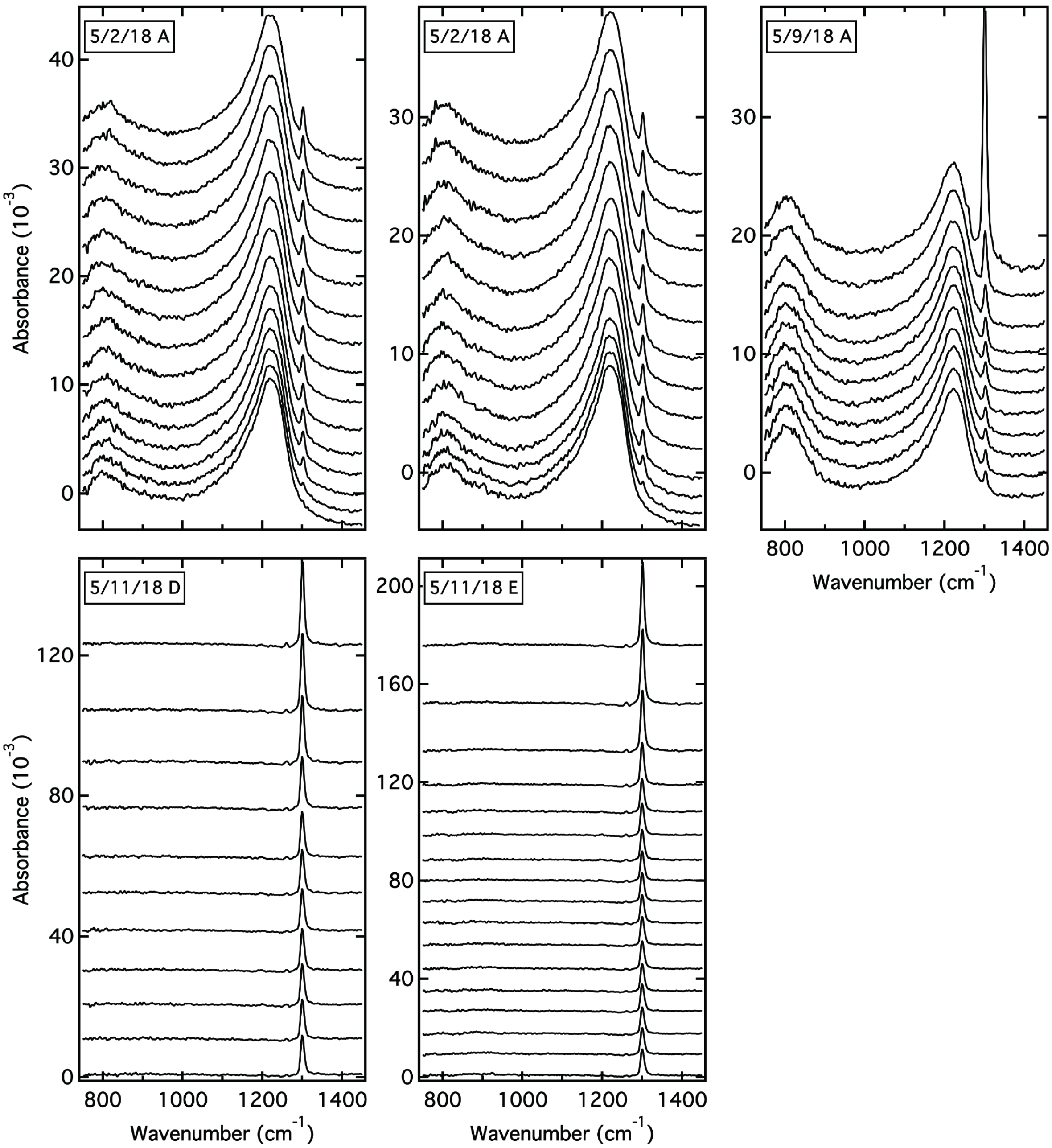

Figure A2.4: Raw RAIR spectrum for Figure 3.2c and d - p-ASW Films.We tracked the integrated area of methane's ν_4 mode (1305 cm^{-1}) during adsorption and desorption experiments. In the top panel of **Figure 3.2c**, we isothermally desorb a multilayer film of methane on a p-ASW film at 24 and 25 K to determine the height of the monolayer. In the bottom panel, we see a small amount of methane grow in on a p-ASW film held at 33.5 K. The spectra in **Figure 3.2d** are from the same data sets. (*Data files: 051118D.IR01-11 (desorption, 24 K), 051118E.IR01-17 (desorption, 25K), 050918A.IR25-35 (desorption, 33.6 K), 050218A.IR18-32 (adsoprtion, 33.5 K), 050218A.IR33-45 (adsoprtion, 33.5 K)*)

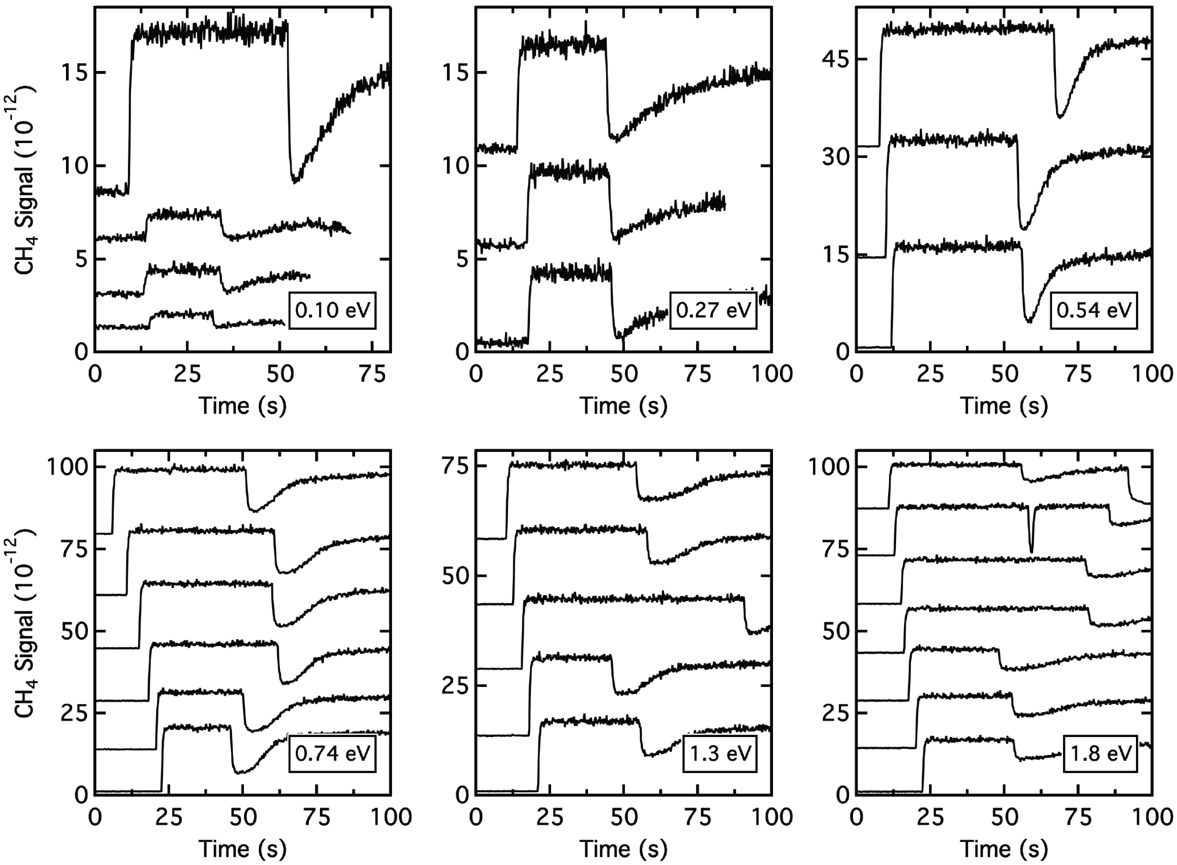

Figure A2.5: Raw King and Wells data for Figure 3.3 - CI films. We collect the RGA signal at m/z = 15 as a CI film is exposed to a heated beam of CH_4 (0.10 and 0.27 eV) or CH_4 seeded in H_2 (0.54, 0.74, 1.3, 1.8 eV). We use the drop in intensity to calculate the initial sticking probability; each yellow data point in **Figure 3.3** represents the average value across all trials with a particular beam energy.

0.10 eV	**0.27 eV**	**0.54 eV**	**0.74 ev**	**1.3 eV**	**1.8 eV**
060818.R07	042418.R08	050218.R05	041818.R02	041818.R04	041818.R03
061118.R04	060818.R05	050218.R06	041818.R05	042518.R13	041918.R03
061118.R09	060818.R06	050318.R06	042318.R11	042518.R14	041918.R04
061118.R10			043018.R07	043018.R05	042718.R05
			043018.R08	043018.R06	042718.R06
			043018.R09		042718.R10
					043018.R04

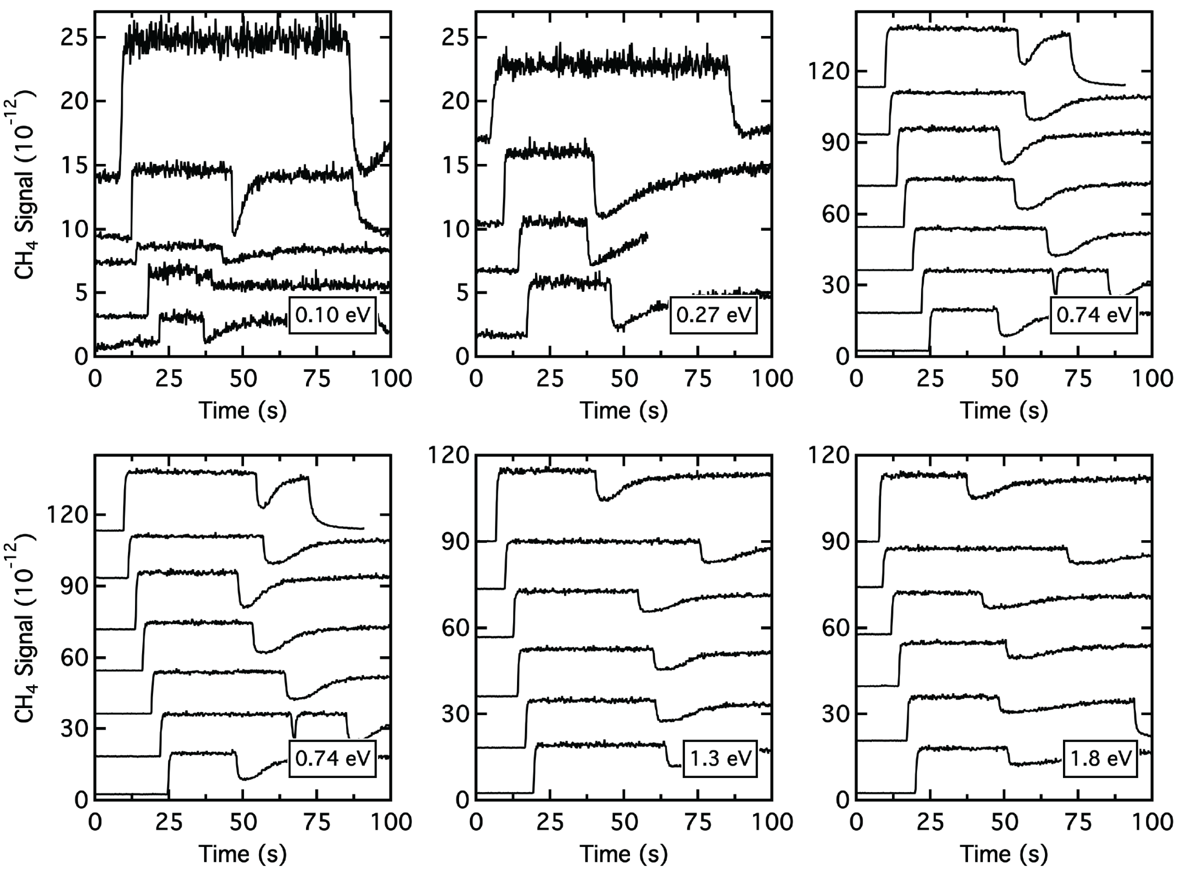

Figure A2.6: Raw King and Wells data for Figure 3.3 - np-ASW films. We collect the RGA signal at m/z = 15 as a np-ASW film is exposed to a heated beam of CH_4 (0.10 and 0.27 eV) or CH_4 seeded in H_2 (0.54, 0.74, 1.3, 1.8 eV). We use the drop in intensity to calculate the initial sticking probability; each blue data point in **Figure 3.3** represents the average value across all trials with a particular beam energy.

0.10 eV	**0.27 eV**	**0.54 eV**	**0.74 ev**	**1.3 eV**	**1.8 eV**
040518.R05	042418.R06	050318.R02	041518.R02	041718.R04	041718.R03
040518.R06	042418.R07	050318.R03	041718.R02	041718.R07	041718.R06
040518.R08	060818.R02	050318.R04	041718.R05	042318.R05	042018.R02
042418.R04	060818.R03	050318.R05	042318.R02	042318.R06	042018.R03
042418.R05			042318.R03	042318.R07	042018.R04
			042318.R04	042718.R03	042718.R04
			042718.R02		

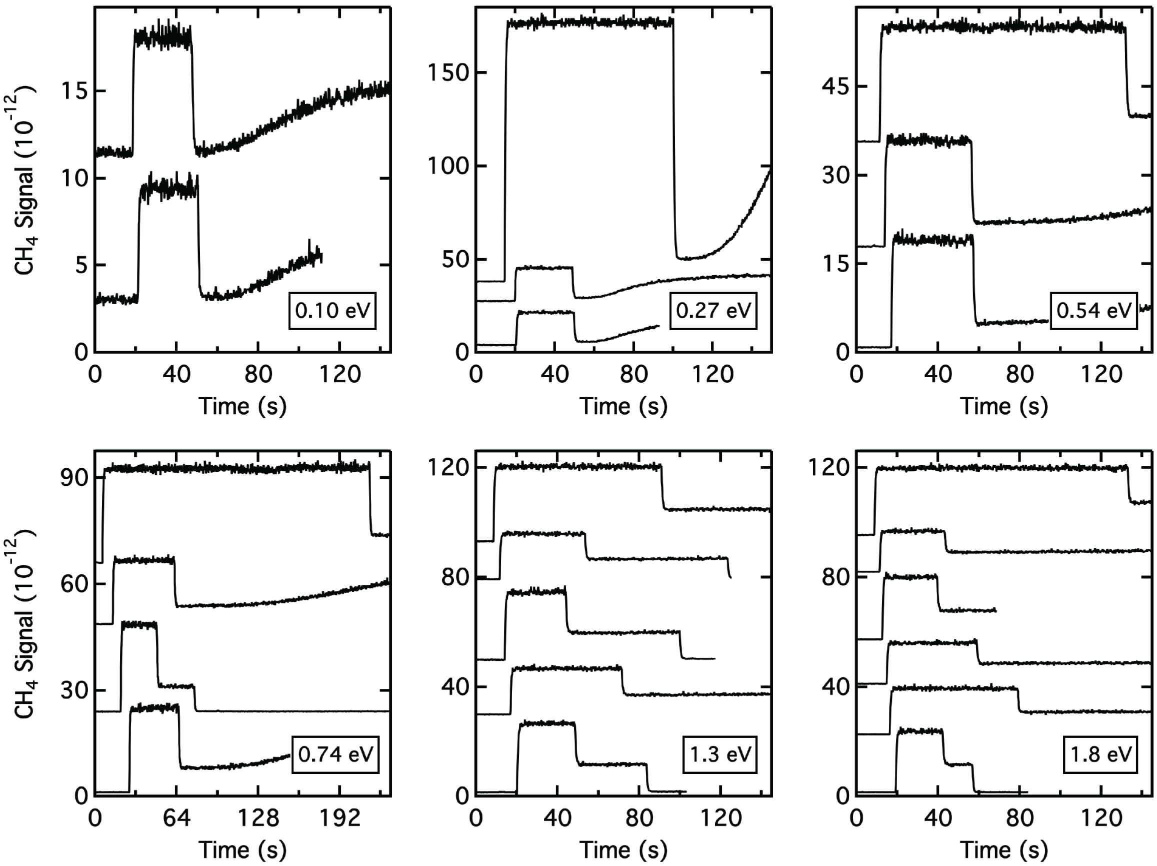

Figure A2.7: Raw King and Wells data for Figure 3.3 - p-ASW films. We collect the RGA signal at m/z = 15 as a p-ASW (30° deposition) film is exposed to a heated beam of CH_4 (0.10 and 0.27 eV) or CH_4 seeded in H_2 (0.54, 0.74, 1.3, 1.8 eV). We use the drop in intensity to calculate the initial sticking probability; each red data point in **Figure 3.3** represents the average value across all trials with a particular beam energy. This data set is also in **Figure 3.6**.

0.10 eV	**0.27 eV**	**0.54 eV**	**0.74 ev**	**1.3 eV**	**1.8 eV**
042518.R02	040618.R09	050218.R02	040618.R03	040618.R07	040618.R05
042518.R03	042518.R04	050218.R03	041318.R02	041318.R09	041318.R04
	042518.R05	050218.R04	042518.R07	041318.R12	041318.R08
			042518.R08	042518.R11	042518.R09
				042518.R12	042518.R10
					043018.R02

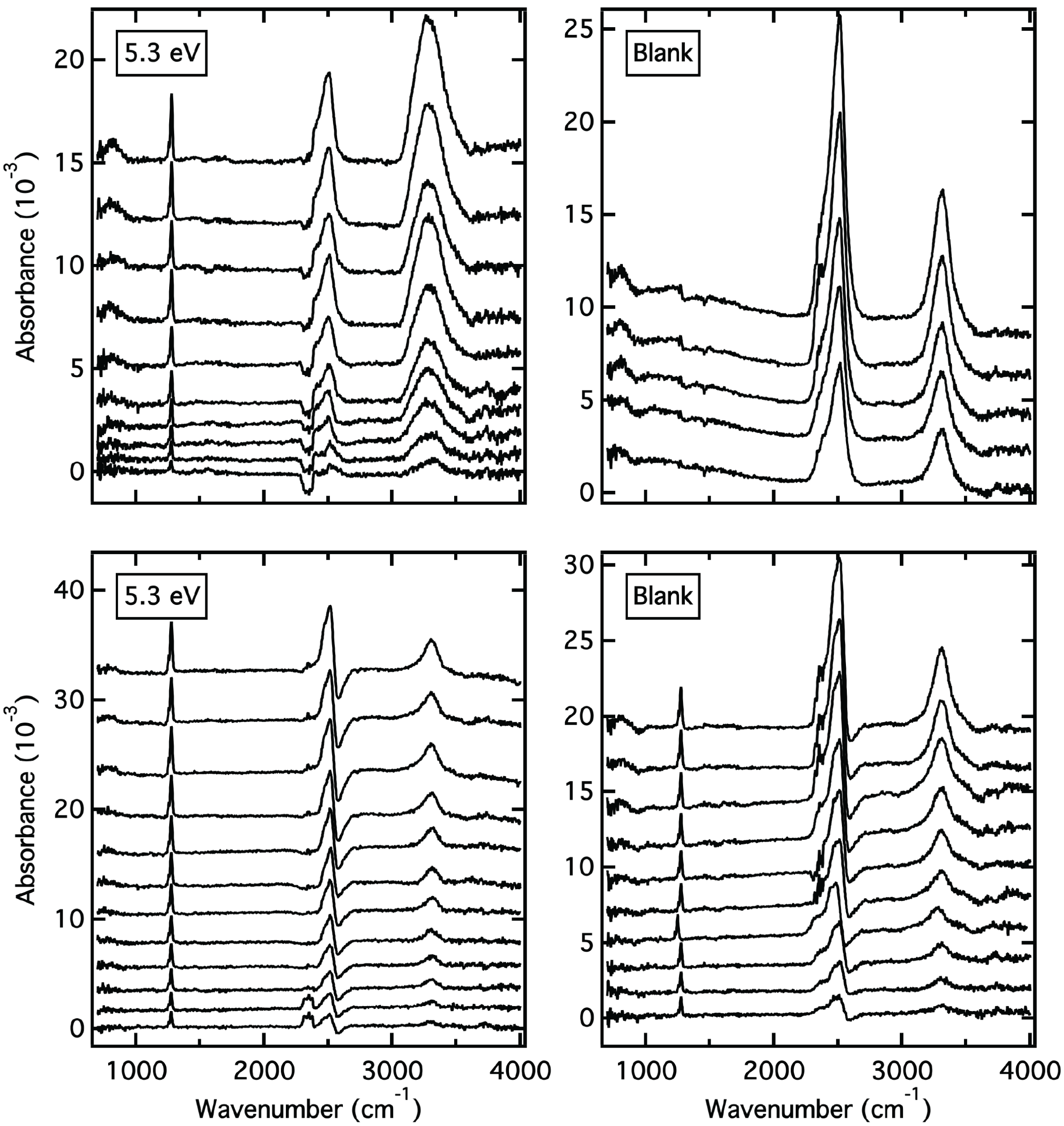

Figure A2.8: Raw RAIR spectrum for Figure 3.4. We tracked the growth rate of CF_4 embedded in np-ASW (top) and p-ASW (bottom) films via the integrated area of modes at 1276 and 1257 cm^{-1}. We performed embedding experiments using a heated beam of CF_4 seeded in H_2 (5.3 eV) and with the ice film held at 70 K. We also performed corresponding blank trials with a room temperature beam (≈0.11 eV) to quantify any small contributions to the signal from CF_4 surface adsorption. (*Data files: 031218B.IR01-10 (np-ASW, 5.3 eV), 013118B.IR04-08 (np-ASW, blank), 031418B.IR01-12 (p-ASW, 5.3 eV),031518B.IR01-10 (p-ASW, blank)*)

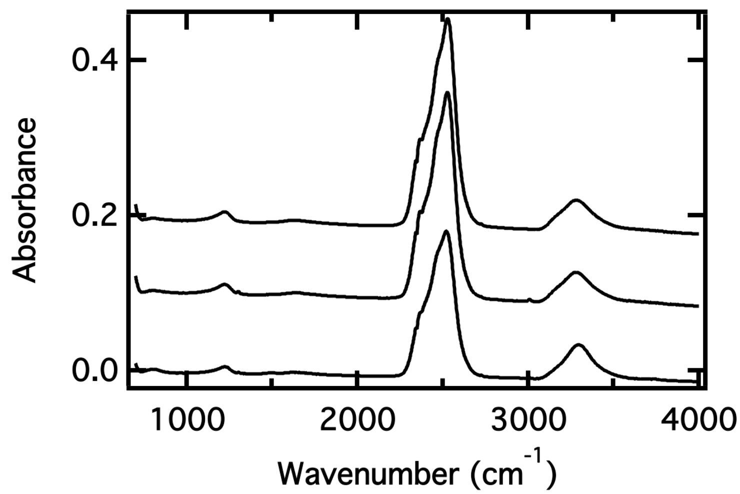

Figure A2.9: Raw RAIR spectrum for Figure 3.5. Spectra collected before, during, and after exposure to a seeded, 0.54 eV CH_4/H_2 beam illustrate little change in the underlying water structure as a result of CH_4 exposure. (*Data files: 050218A.IR33 (before CH_4 exposure), 050218A.IR45 (during CH_4 exposure), 050218A.IR46 (after anneal)*)

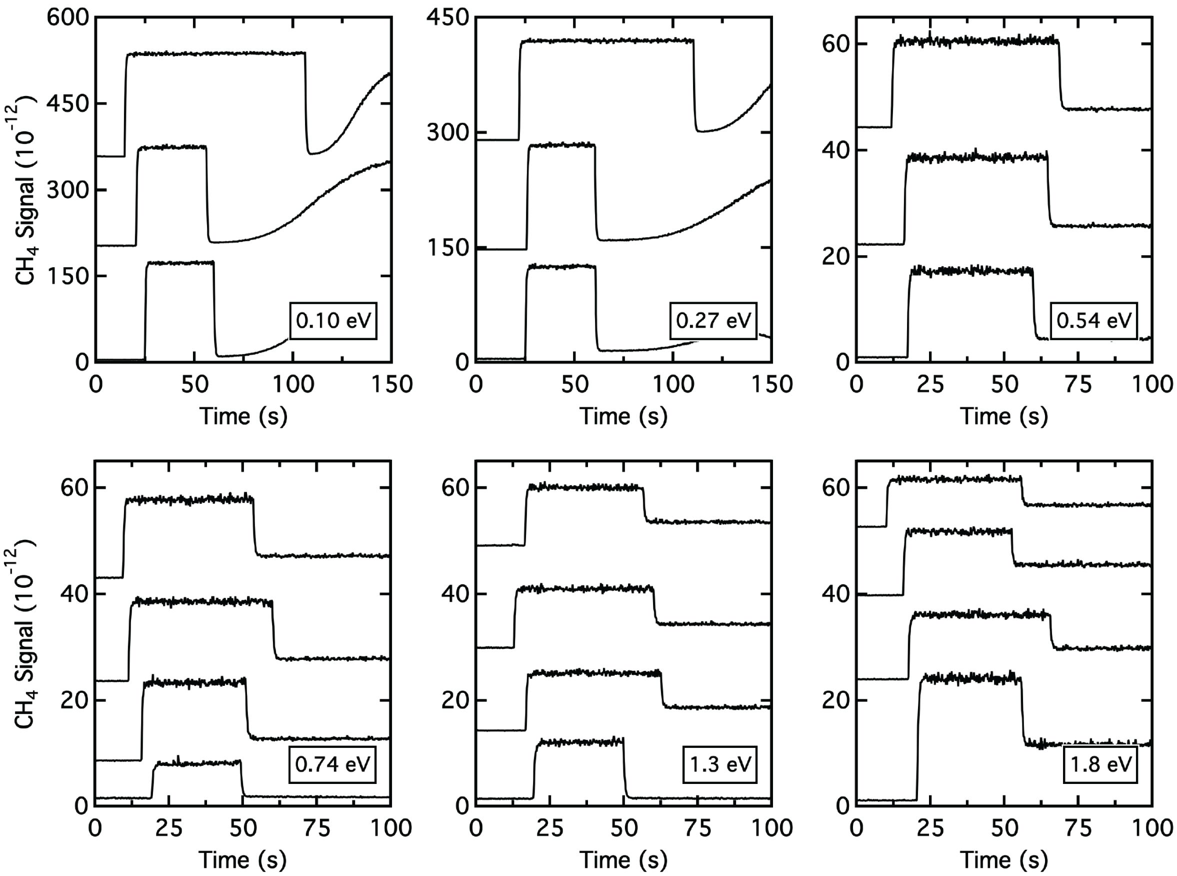

Figure A2.10: Raw King and Wells data for Figure 3.6 - 60° films. We collect the RGA signal at m/z = 15 as a p-ASW (60° deposition) film is exposed to a heated beam of CH_4 (0.10 and 0.27 eV) or CH_4 seeded in H_2 (0.54, 0.74, 1.3, 1.8 eV). We use the drop in intensity to calculate the initial sticking probability; each green data point in **Figure 3.6** represents the average value across all trials with a particular beam energy.

0.10 eV	**0.27 eV**	**0.54 eV**	**0.74 ev**	**1.3 eV**	**1.8 eV**
040818.R02	050718.R14	050718.R02	040918.R02	040918.R04	040918.R03
050718.R16	050718.R15	050718.R03	050718.R05	050718.R08	050718.R11
050718.R17	040818.R03	050718.R04	050718.R06	050718.R09	050718.R12
			050718.R07	050718.R10	050718.R13

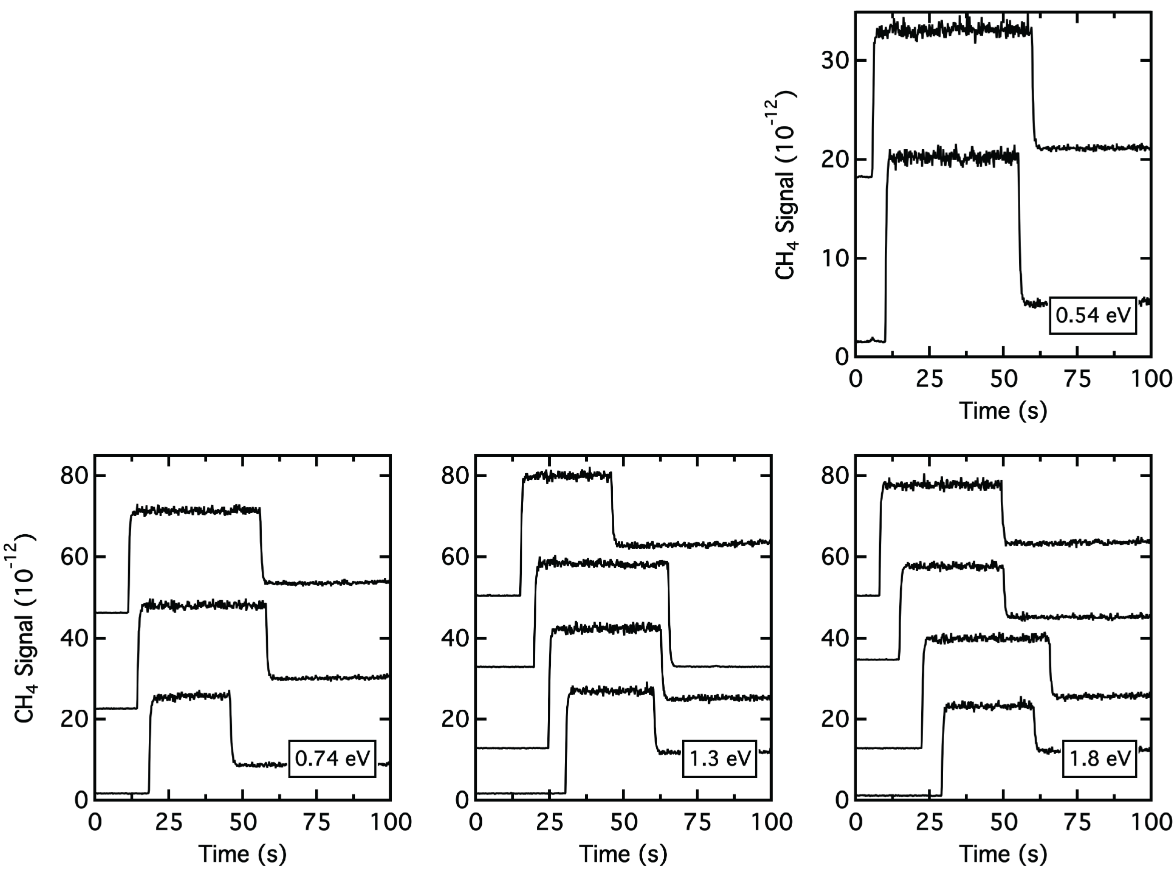

Figure A2.11: Raw King and Wells data for Figure 3.6 - 70° films. We collect the RGA signal at m/z = 15 as a p-ASW (70° deposition) film is exposed to a heated beam of CH_4 (0.10 and 0.27 eV) or CH_4 seeded in H_2 (0.54, 0.74, 1.3, 1.8 eV). We use the drop in intensity to calculate the initial sticking probability; each grey data point in **Figure 3.6** represents the average value across all trials with a particular beam energy.

0.54 eV	**0.74 ev**	**1.3 eV**	**1.8 eV**
051418.R02	041118.R02	041118.R04	041118.R03
051418.R03	051518.R02	041118.R04	041118.R06
	051518.R03	051518.R05	051518.R07
		051518.R06	051518.R08

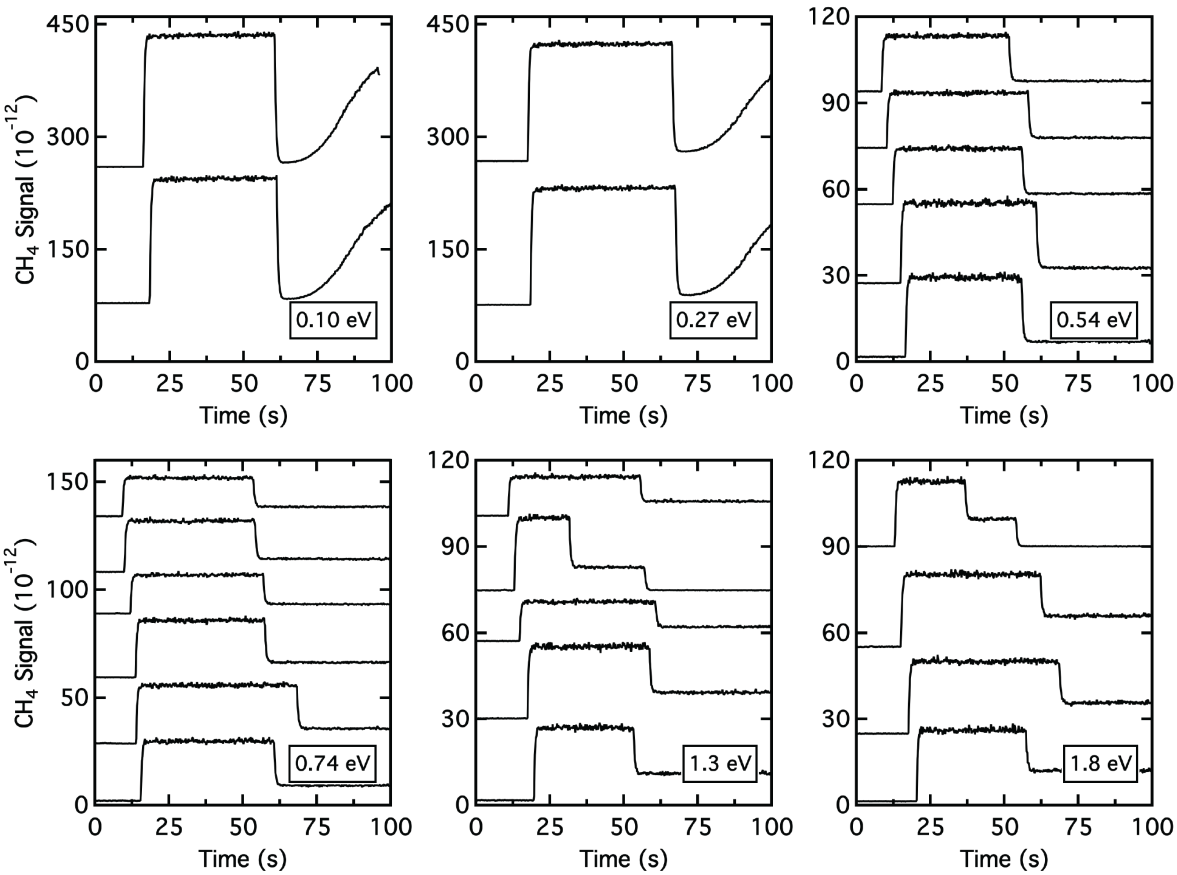

Figure A2.12: Raw King and Wells data for Figure 3.6 - Background films. We collect the RGA signal at m/z = 15 as a p-ASW (Background deposition) film is exposed to a heated beam of CH_4 (0.10 and 0.27 eV) or CH_4 seeded in H_2 (0.54, 0.74, 1.3, 1.8 eV). We use the drop in intensity to calculate the initial sticking probability; each purple data point in **Figure 3.6** represents the average value across all trials with a particular beam energy.

0.10 eV	0.27 eV	0.54 eV	0.74 ev	1.3 eV	1.8 eV
050818.R11	050818.R09	050818.R02	041218.R02	041218.R04	041218.R03
050818.R12	050818.R10	050818.R03	050818.R05	050818.R07	051618.R09
		050818.R04	050818.R06	050818.R08	051618.R10
		051618.R02	051618.R04	051618.R07	051618.R11
		051618.R03	051618.R05	051618.R08	
			051618.R06		

Figure A2.13: Raw King and Wells data for Figure 3.7. All the data listed here already appears in **Figures A2.5 - A2.7** and **A2.10 - A2.12**. The files below were used to calculate the values in **Subsection 3.3.3** and are part of **Figure 3.6**.

Panel A	**Panel B - 30°**	**Panel B - 60°**	**Panel B - 70°**	**Panel B - BD**
041818.R03	050218.R02	050718.R11	041118.R03	051618.R02
042518.R09	050218.R03	040918.R03	051518.R07	051618.R03
041718.R06	050218.R04	050718.R02	051518.R08	051618.R09
	040618.R05		051418.R03	051618.R10
	042518.R09			050818.R02
	043018.R02			

A3 Acetone-Water Interactions in Crystalline and Amorphous Ice Environments (Chapter 4)

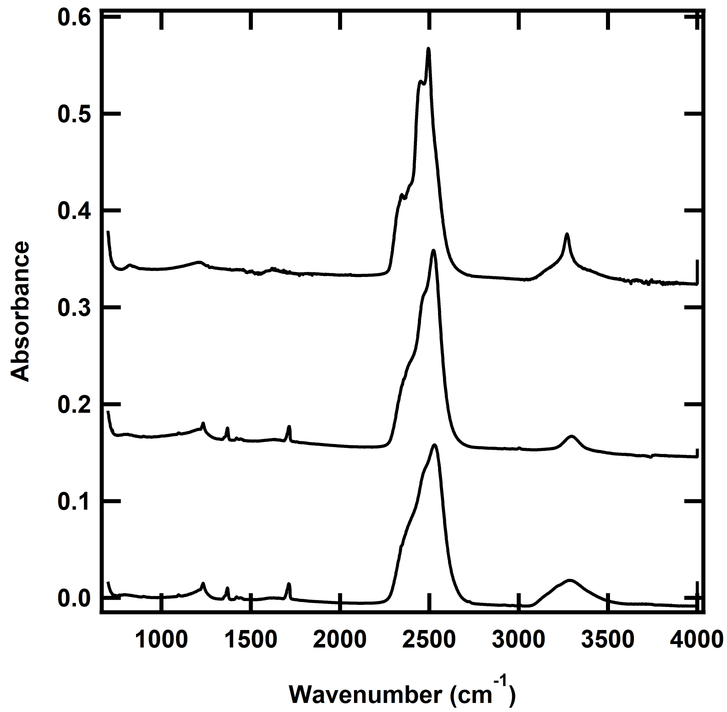

Figure A3.1: Raw RAIR spectrum for Figure 4.1. In addition to integrating the O-D stretching region to gain information about film thickness, the shape of the O-D stretching region also provides details about the ice morphology (p-ASW, np-ASW, and CI). We can compare the integrated area of the small dangling bond region between 2700 and 2780 cm^{-1} to gain information about the ice surface area and porosity. Each spectrum is representative of each film type, deposited via directed doser at a crystal temperature of 20 K, 107, and 150 K for p-ASW, np-ASW, and CI respectively collected at 70 K. These films are 150 layers thick. (*Data files: 120221A.IR13 (CI, top), 120721A.IR12 (np-ASW, middle), 120621A.IR04 (p-ASW, bottom)*)

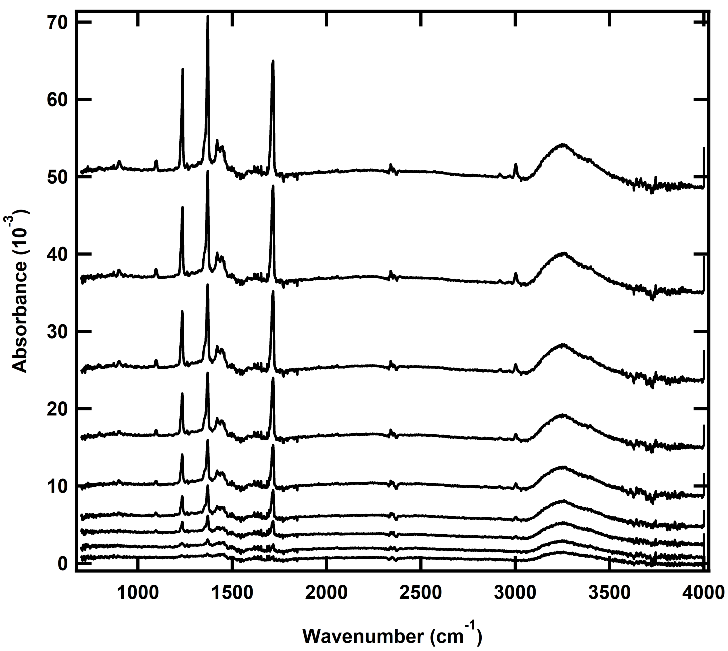

Figure A3.2: Raw RAIR spectrum for Figure 4.2. These spectra correspond to acetone exposure on the Au(111) substrate at 70 K via the molecular beam. (*Data files: 121621A01-08)*)

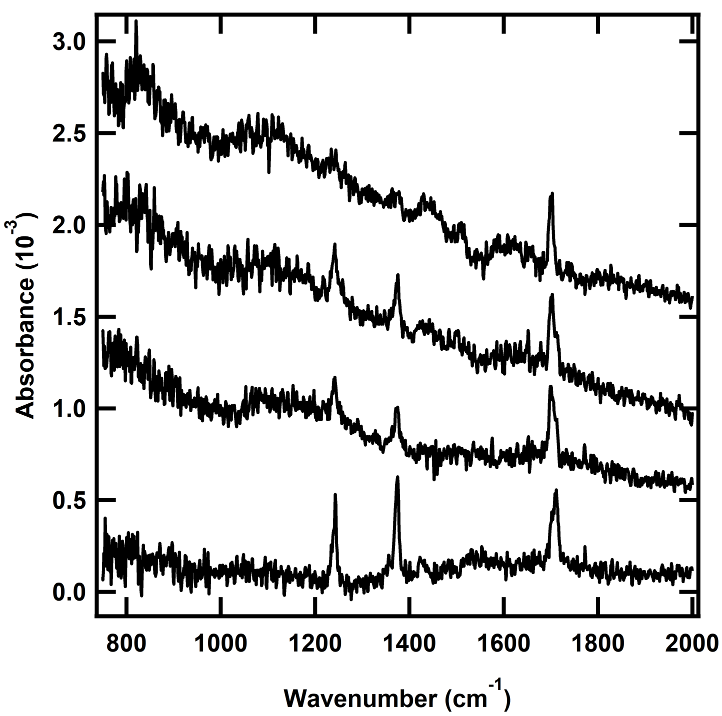

Figure A3.3: Raw RAIR spectrum for Figure 4.3. These spectra correspond to sub-monolayer acetone deposited on top of an ice film (np-ASW or CI) at 110 K. (*Data files from top to bottom: 082721B.IR02 (230 ML CI), 111121B.IR03 (330 ML np-ASW), 101221C.IR02 (588 ML np-ASW), 051721C.IR01(111 ML np-ASW)*)

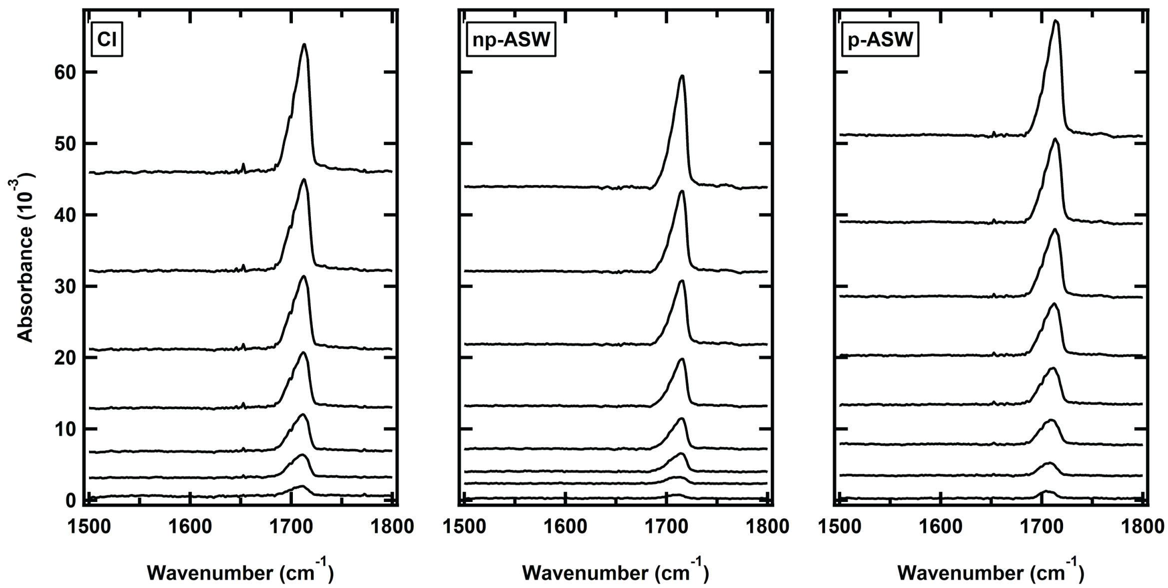

Figure A3.4: Raw RAIR spectrum for Figure 4.4a-c. These spectra correspond to acetone deposited at 70 K on top of the D_2O films of varying morphologies (CI, np-ASW, p-ASW deposited at 150, 107, and 20 K respectively). All spectra in **Figure 4.4a-c** are normalized to the intensity at 1711 cm^{-1}. (*Data files: CI:120221B.IR01-07, np-ASW:120721B.IR01-08, p-ASW: 120621B.IR01-08*)

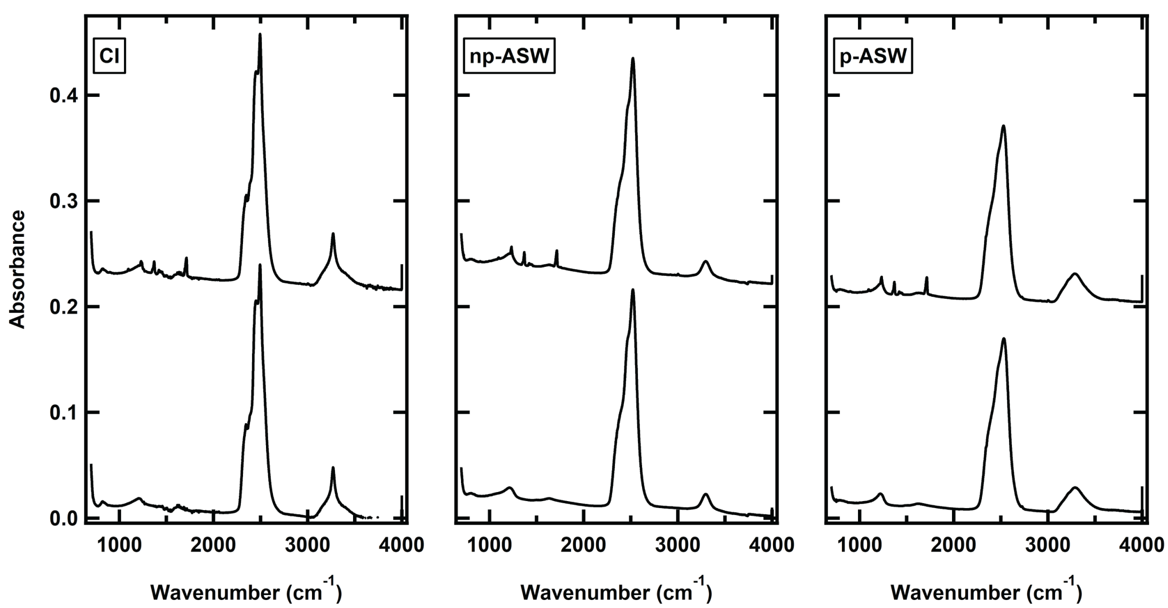

Figure A3.5: Raw RAIR spectrum for Figure 4.4d-f. These spectra correspond to the D_2O Films before (bottom) and after (top) exposure to 40-45 ML of acetone at 70 K. CI, np-ASW, p-ASW films were deposited at 150, 107, and 20 K respectively (*Data files: CI:120221A.IR13-14, np-ASW:120721A.IR11-12, p-ASW: 120621A.IR03-04 where the first spectra is before and the second is after exposure*)

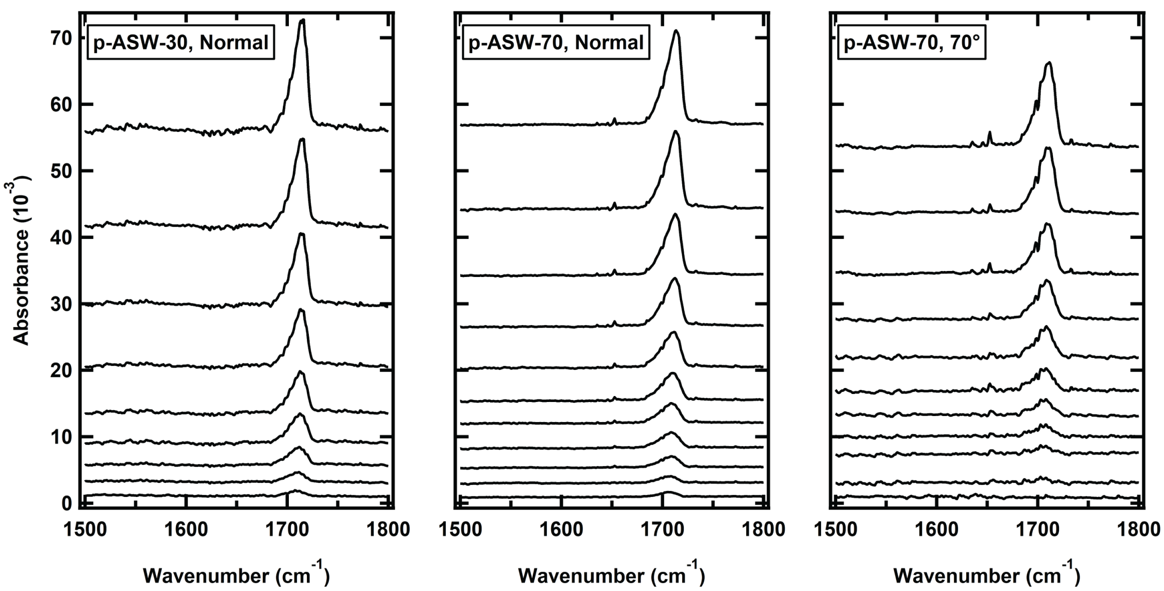

Figure A3.6: Raw RAIR spectrum for Figure 4.6a-c. These spectra correspond to acetone deposited at 20 K on top of p-ASW D_2O films of varying porosity (30º and 70º) also deposited at 20 K. Acetone exposure was either normal or at 70º from normal. All spectra in **Figure 4.6a-c** are normalized to the intensity at 1711 cm^{-1}. (*Data files: p-ASW-30, normal:120821B.IR01-09, p-ASW-70, normal: 021822B.IR02-12, p-ASW-70, 70º: 022222B.IR01-11*)

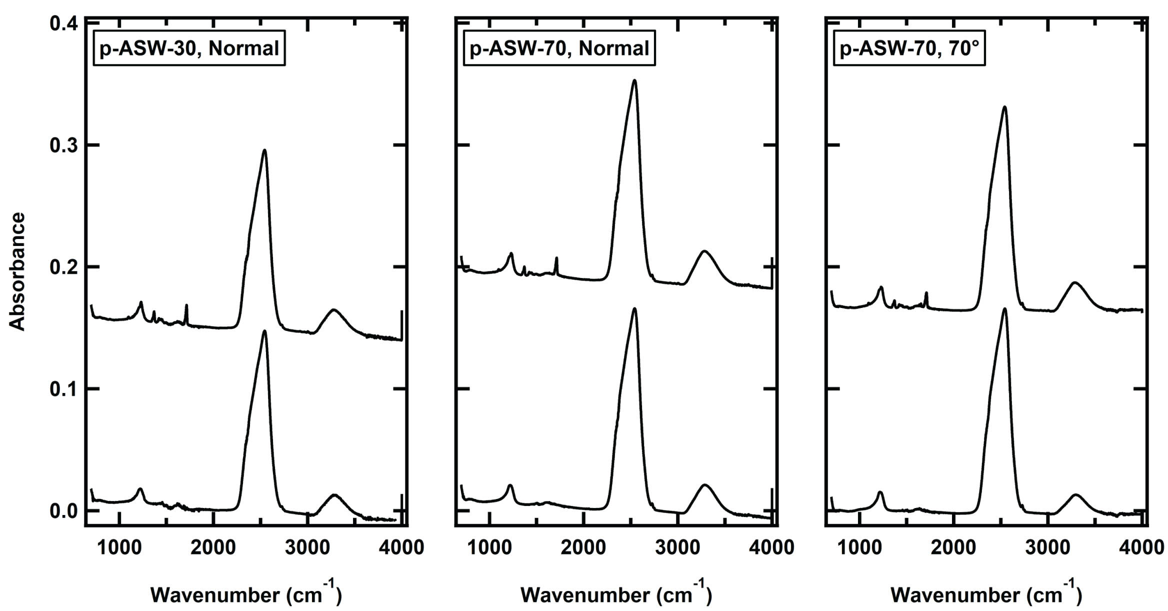

Figure A3.7: Raw RAIR spectrum for Figure 4.6. These spectra correspond to the D_2O Films before (bottom) and after (top) exposure to 40-45 ML of acetone at 20 K. Acetone exposure was either normal or at 70º from normal. (*Data files: p-ASW-30, normal:120821A.IR02-03, p-ASW-70, normal: 021822A.IR05-06, p-ASW-70, 70º: 022222A.IR06-07 where the first spectra is before and the second is after exposure*)

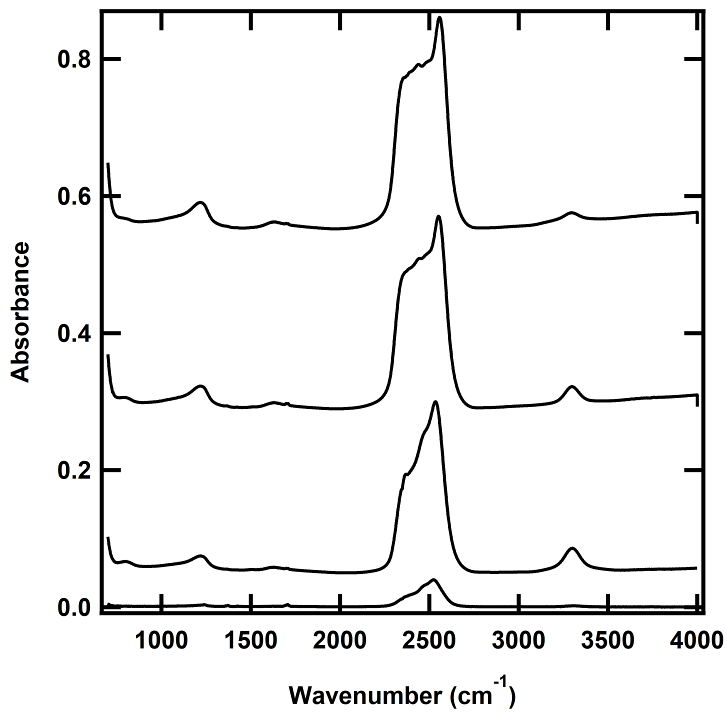

Figure A3.8: Raw RAIR spectrum for Figure 4.8. Initially a 100-layer D_2O film was grown on the surface, prior to creating a mixture of acetone and D_2O by dosing np-ASW D_2O through the directed doser and acetone through the beam at 107 K . These spectra were taken at the end when the mixed film thickness had ∼400 layers of D_2O. The overall film percentage was taken from integrated area of the 1700 cm^{-1} C=O stretch for acetone and the 2200-2800 cm^{-1} OD stretch for D_2O. (*Data files from top to bottom: 1%: 071222B10, 2%: 071621B.IR18, 1.5%: 072821B.IR15, 25%: 060221D.IR01*)

A4 Differential Condensation of Methane Isotopologues Leading to Isotopic Enrichment Under Non-equilibrium Gas-Surface Collision Conditions (Chapter 5)

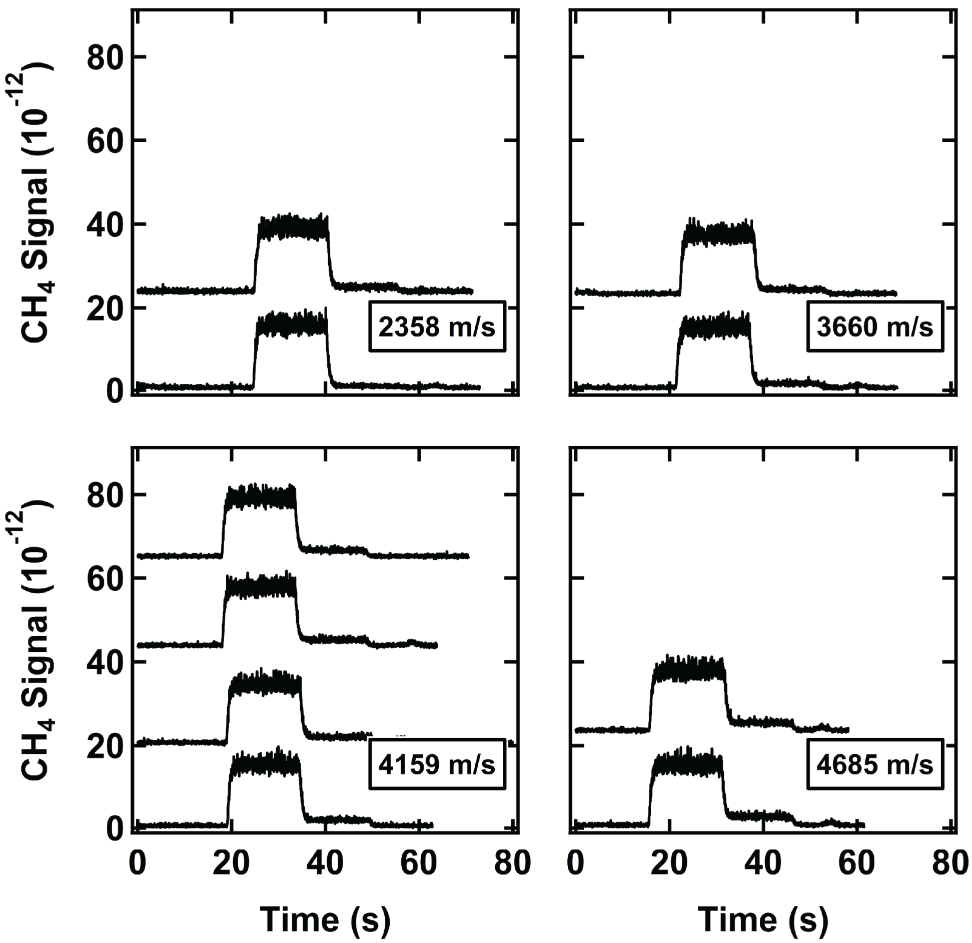

Figure A4.1: Raw King and Wells data for Figure 5.1 - CH_4 on CD_4. We collect the RGA signal at m/z = 15 as a CD_4 film at 20 K is exposed to a heated beam of CH_4 seeded in H_2 (2358 m/s, 3660 m/s, 4159 m/s, 4685 m/s). We use the drop in intensity to calculate the initial sticking probability; each pink data point in **Figure 5.1** represents the average value across all trials with a particular beam velocity.

2358 m/s	3660 m/s	4159 m/s	4685 m/s
120420.R01	120420.R02	120420.R03	120320.R12
120720.R01	120920.R02	120920.R03	120920.R03
		121020.R07	
		121520.R09	

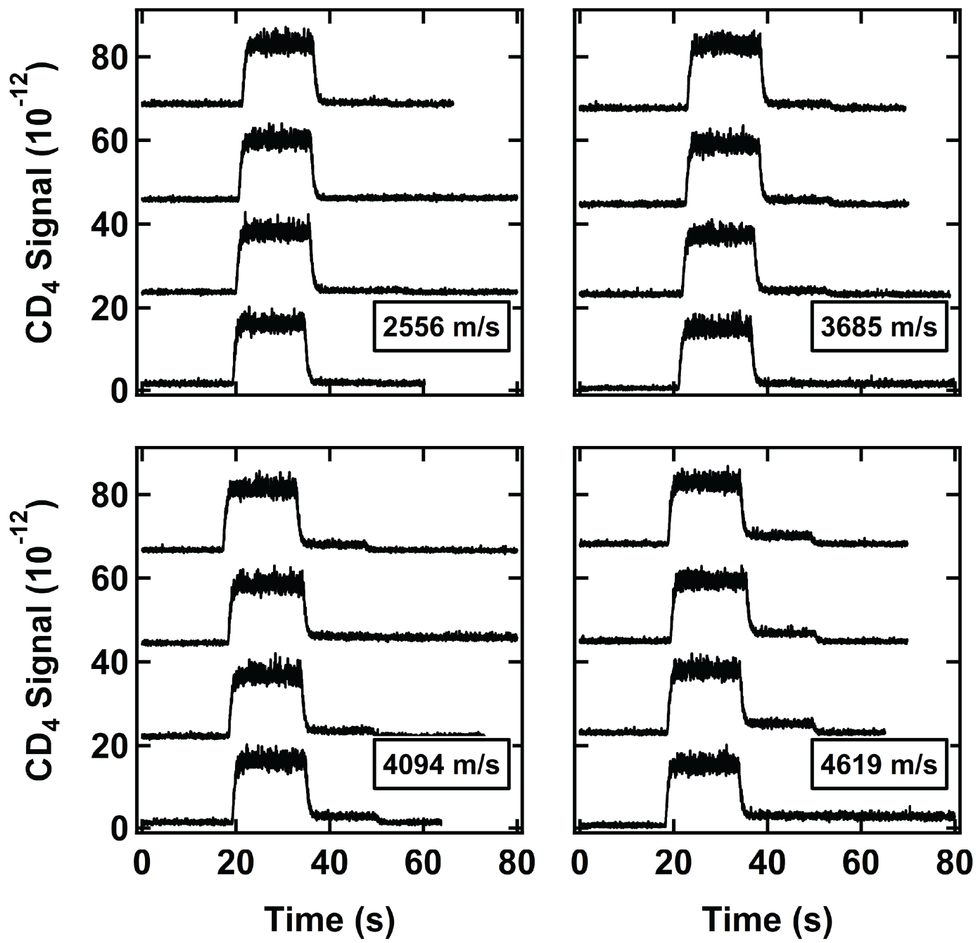

Figure A4.2: Raw King and Wells data for Figure 5.1 - CD_4 on CD_4. We collect the RGA signal at m/z = 20 as a CD_4 film at 20 K is exposed to a heated beam of CD_4 seeded in H_2 (2556 m/s, 3685 m/s, 4094 m/s, 4619 m/s). We use the drop in intensity to calculate the initial sticking probability; each blue data point in **Figure 5.1** represents the average value across all trials with a particular beam velocity.

2556 m/s	3685 m/s	4094 m/s	4619 m/s
102520.R01	102520.R03	102520.R04	102520.R05
102520.R02	120320.R03	120320.R06	120320.R09
120320.R02	120320.R04	120320.R07	120320.R10
120320.R03	120320.R05	120320.R08	120320.R11

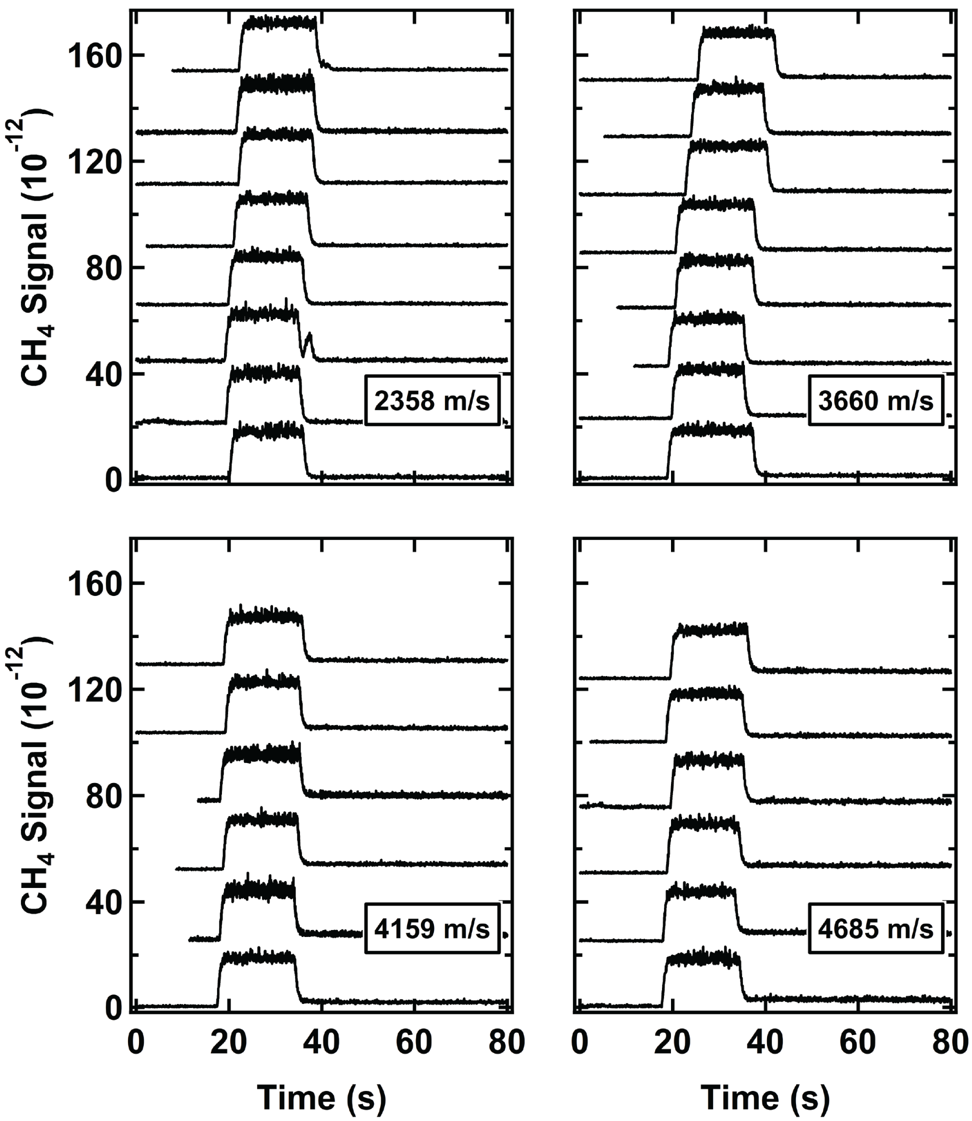

Figure A4.3: Raw King and Wells data for Figure 5.2 - CH_4 on CH_4. We collect the RGA signal at m/z = 15 as a CH_4 film at 20 Kis exposed to a heated beam of CH_4 seeded in H_2 (2358 m/s, 3660 m/s, 4159 m/s, 4685 m/s). We use the drop in intensity to calculate the initial sticking probability; each pink data point in **Figure 5.2** represents the average value across all trials with a particular beam velocity.

2358 m/s	3660 m/s	4159 m/s	4685 m/s
092120.R09	092720.R04	092820.R01	092220.R09
092120.R10	092720.R05	092820.R02	092220.R10
092220.R03	092820.R04	092920.R06	092620.R03
092620.R01	092820.R05	092920.R07	092620.R04
092620.R02	092920.R04	101120.R03	092820.R06
092920.R03	092920.R05	101120.R06	092820.R07
100520.R01	100520.R03		
101120.R01	100520.R04		

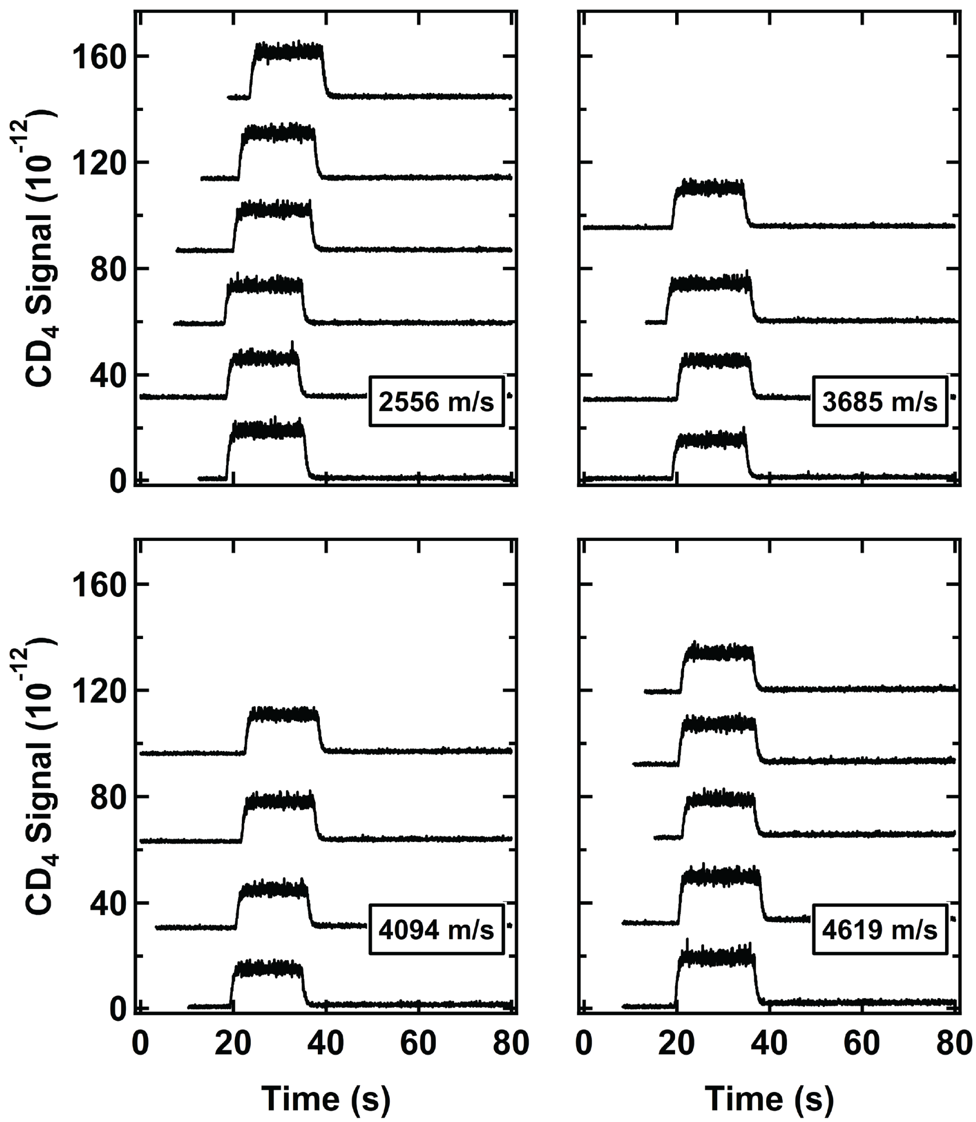

Figure A4.4: Raw King and Wells data for Figure 5.2 - CD_4 on CH_4. We collect the RGA signal at m/z = 20 as a CH_4 film at 20 K is exposed to a heated beam of CD_4 seeded in H_2 (2556 m/s, 3685 m/s, 4094 m/s, 4619 m/s). We use the drop in intensity to calculate the initial sticking probability; each blue data point in **Figure 5.2** represents the average value across all trials with a particular beam velocity.

2556 m/s	3685 m/s	4094 m/s	4619 m/s
101220.R01	102020.R01	102020.R02	101220.R03
101220.R02	102420.R01	102020.R03	101320.R02
101320.R01	102420.R03	102420.R02	101820.R03
101820.R01	102620.R01	102620.R01	101920.R02
101820.R02			101920.R03
101920.R01			

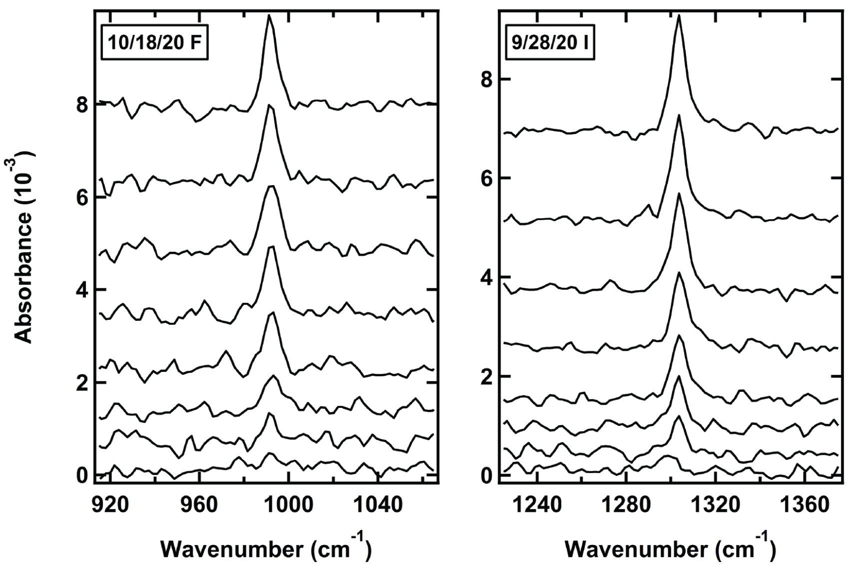

Figure A4.5: Raw RAIR spectrum for Figure 5.3 - CD_4 and CH_4. We tracked the growth of methane's ν_4 mode (992 cm^{-1} (CD_4, right and **Figure 5.3a**) and 1305 cm^{-1} (CH_4, left and **Figure 5.3b**)) during initial adsorption onto the CH_4 film at 20 K. The third panel (**Figure 5.3c**) shows the amplitude plotted as a function of time to get the initial growth rate. We note that in order to directly compare between CD_4 and CH_4, we use the infrared cross section and multiply the CD_4 absorbance by 1.55. (*Data files: 101820F.IR01-08 (CD_4) 092820I.IR01-08 (CH_4)*)

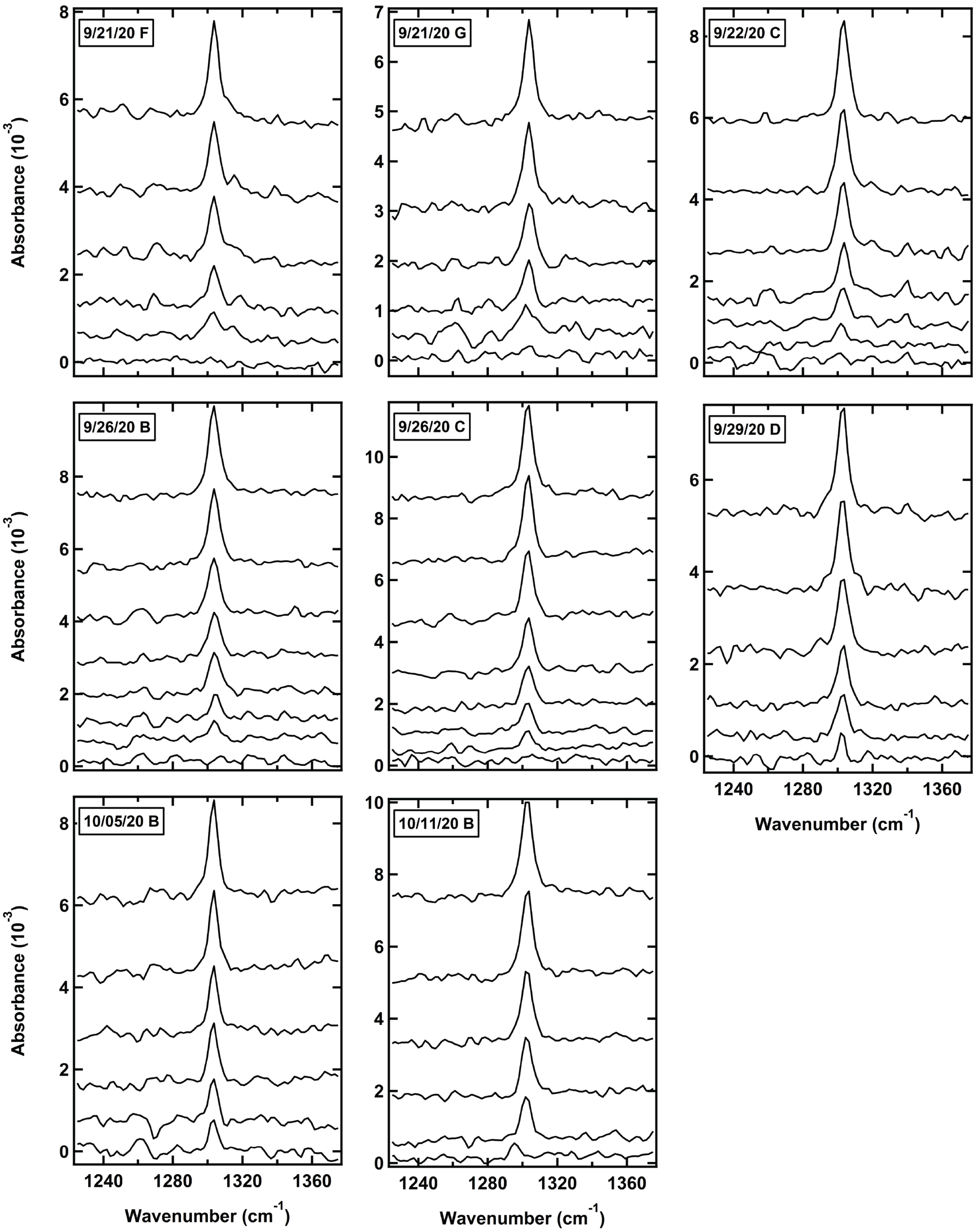

Figure A4.6: Raw RAIR spectrum for Figure 5.4 - CH_4 at 2358 m/s. We tracked the growth of methane's ν_4 mode (1305 cm^{-1}) during initial adsorption onto the CH_4 film at 20 K. We use a least squares regression to calculate the initial growth rate or the 2358 m/s CH_4 beam to overlay with the Sticking Probability in **Figure 5.4**. (*Data files: 092120F.IR01-06, 092120G.IR01-06, 092220C.IR01-07, 092620B.IR01-08, 092620C.IR01-08, 092920D.IR01-06, 100520B.IR01-06, 101120B.IR01-06*)

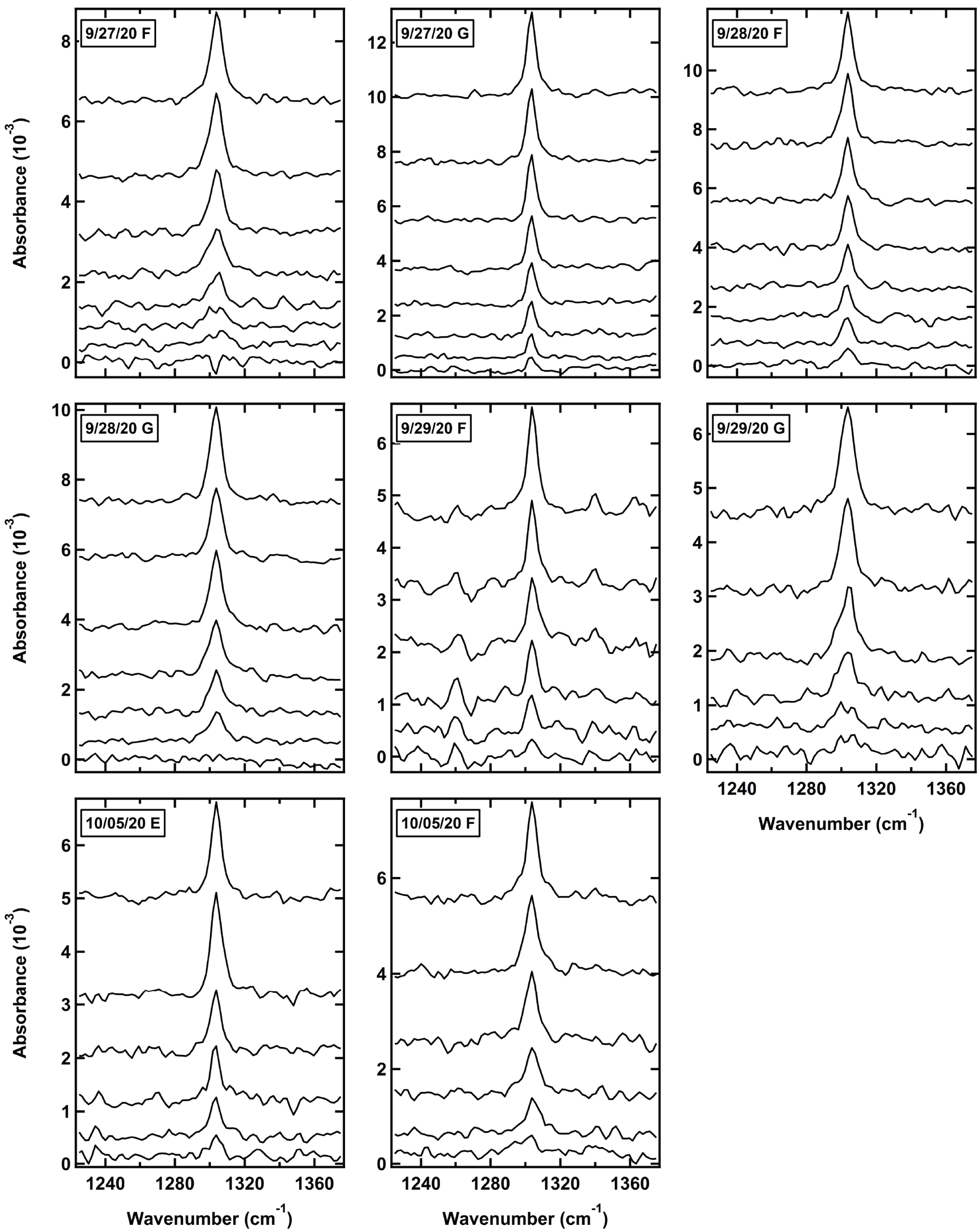

Figure A4.7: Raw RAIR spectrum for Figure 5.4 - CH_4 at 3660 m/s. We tracked the growth of methane's ν_4 mode (1305 cm^{-1}) during initial adsorption onto the CH_4 film at 20 K.We use a least squares regression to calculate the initial growth rate or the 3660 m/s CH_4 beam to overlay with the Sticking Probability in **Figure 5.4**. (*Data files: 092920F.IR01-08, 092720G.IR01-08, 092820F.IR01-08, 092820G.IR01-07, 092920F.IR01-06, 092920G.IR01-06, 100520E.IR01-06, 100520F.IR01-06*)

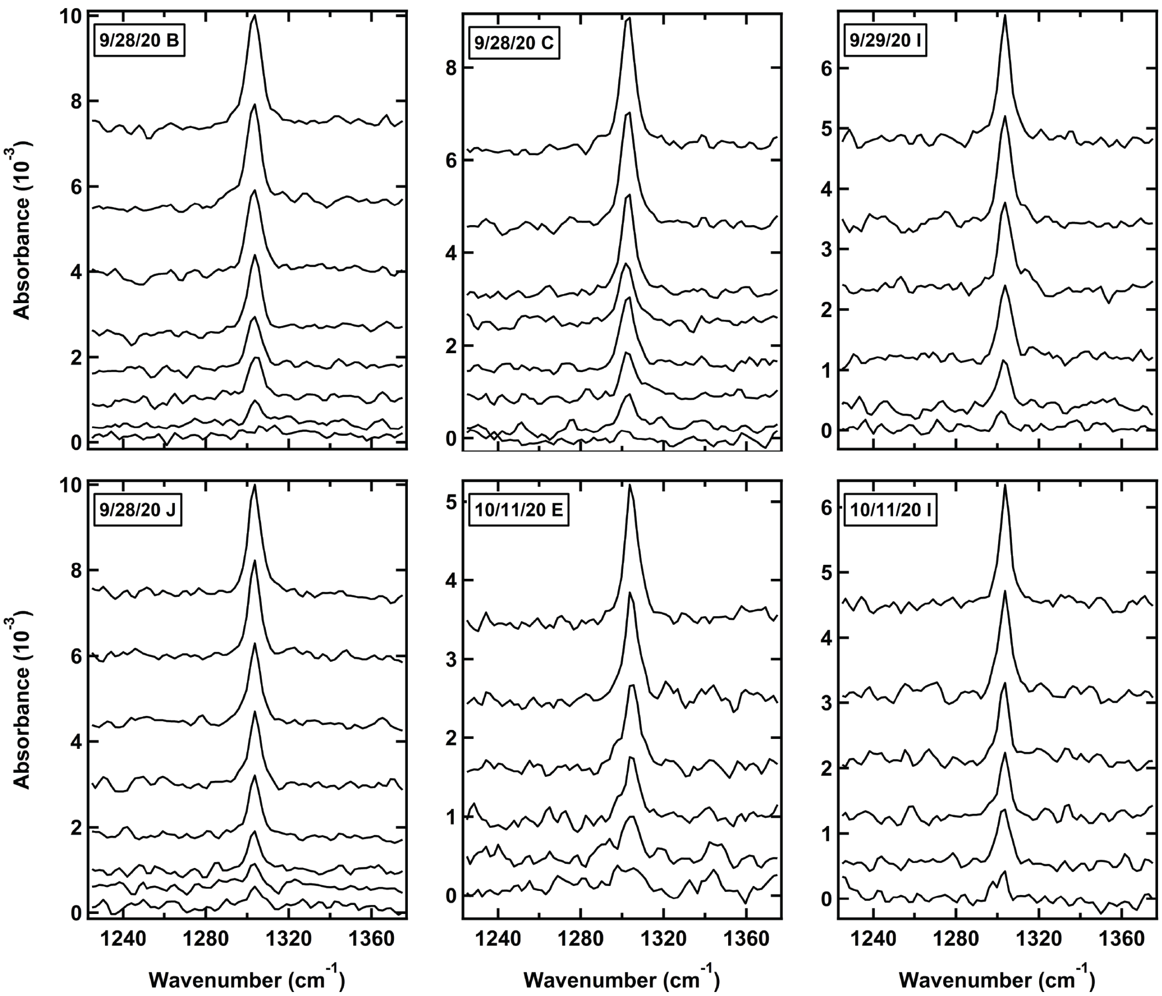

Figure A4.8: Raw RAIR spectrum for Figure 5.4 - CH_4 at 4159 m/s. We tracked the growth of methane's ν_4 mode (1305 cm^{-1}) during initial adsorption onto the CH_4 film at 20 K. We use a least squares regression to calculate the initial growth rate or the 4159 m/s CH_4 beam to overlay with the Sticking Probability in **Figure 5.4**. (*Data files: 092820B.IR01-08, 092820C.IRIR01-08, 092920I.IR01-06, 092820J.IR01-08, 101120E.IR01-06, 101120I.IR01-06*)

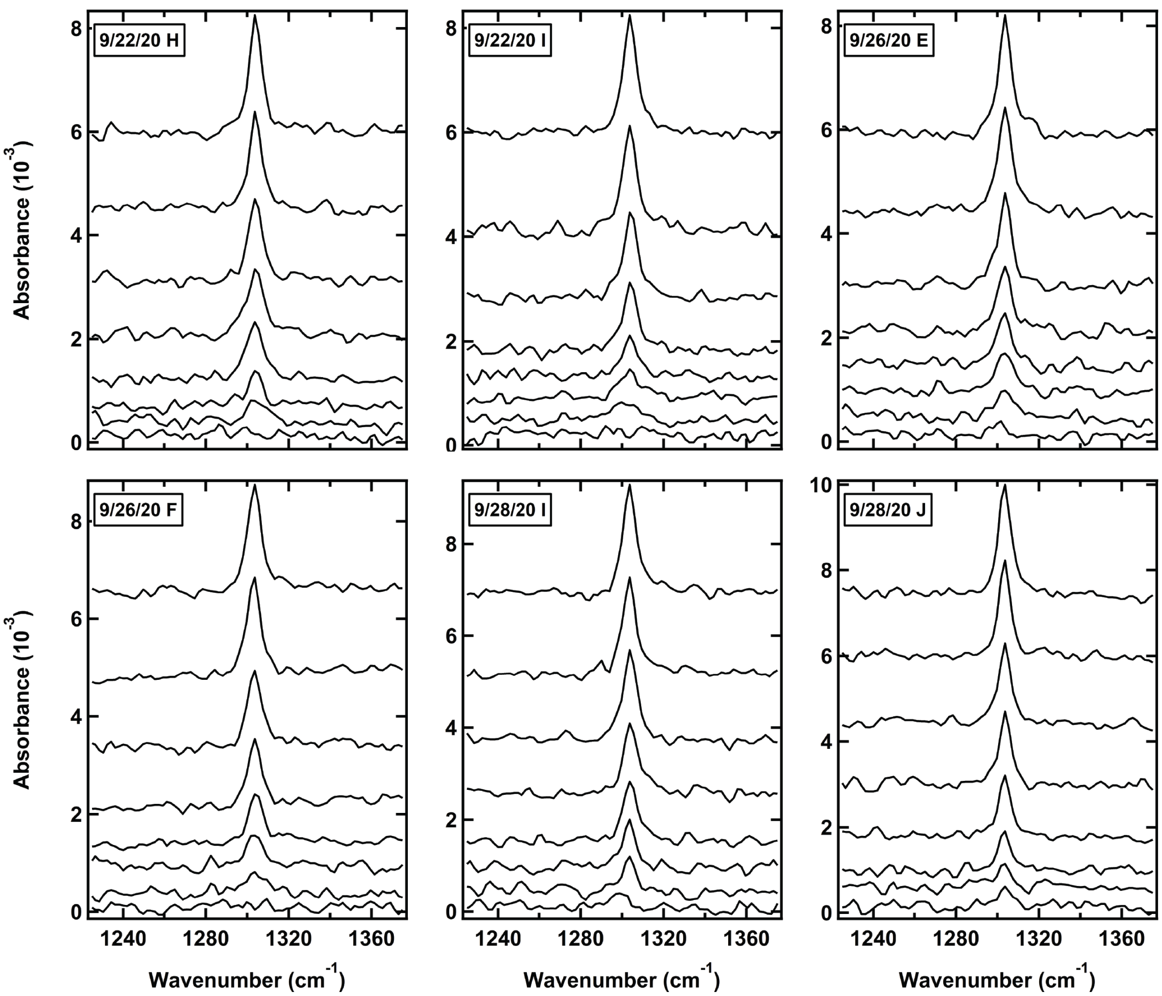

Figure A4.9: Raw RAIR spectrum for Figure 5.4 - CH_4 at 4685 m/s. We tracked the growth of methane's ν_4 mode (1305 cm^{-1}) during initial adsorption onto the CH_4 film at 20 K. We use a least squares regression to calculate the initial growth rate or the 4685 m/s CH_4 beam to overlay with the Sticking Probability in **Figure 5.4**. (*Data files: 09220H.IR01-08, 092220I.IR01-08, 092620.IR01-08, 092620F.IR01-08, 092820I.IR01-08, 092820J.IR01-08*)

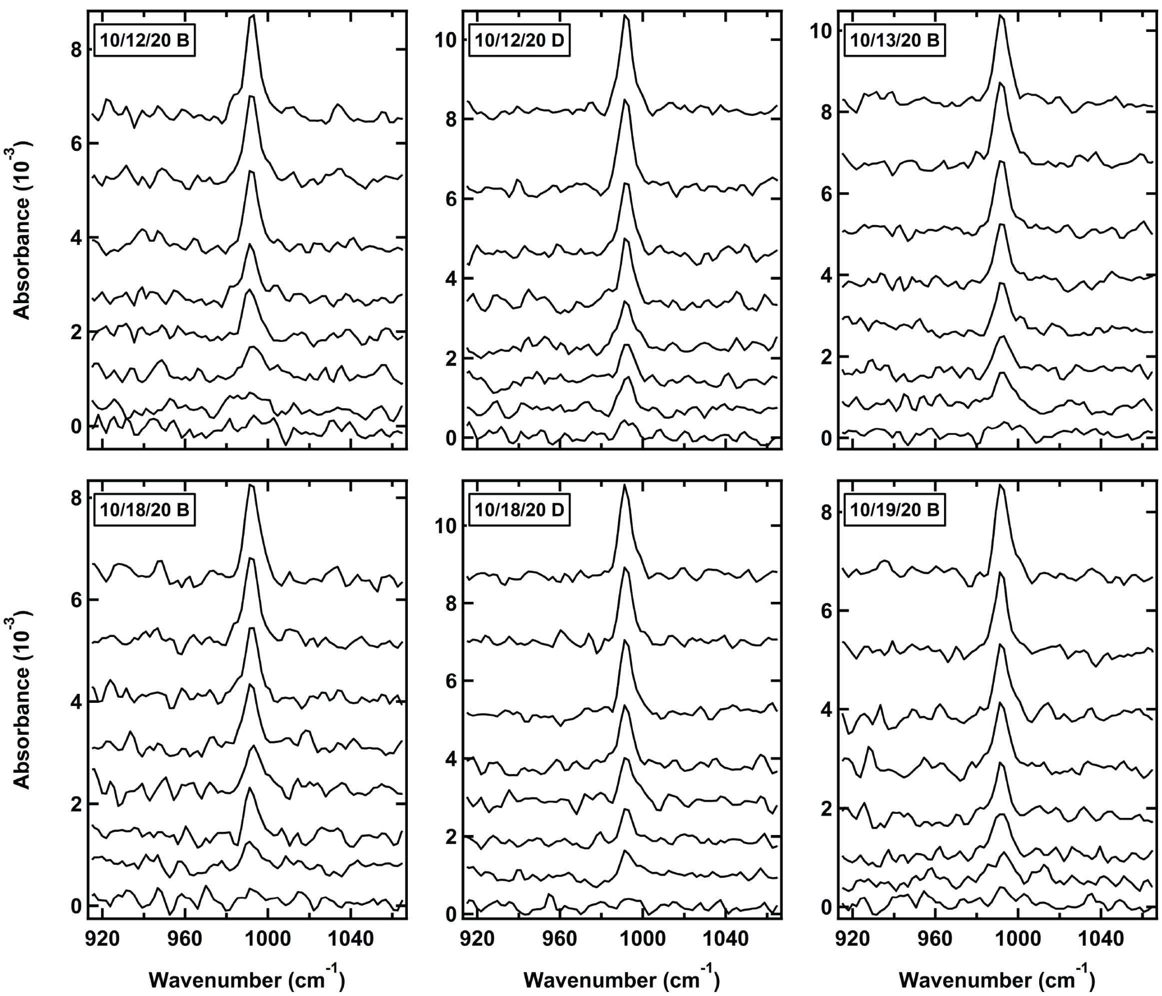

Figure A4.10: Raw RAIR spectrum for Figure 5.4 - CD_4 at 2556 m/s. We tracked the growth of deuterated methane's ν_4 mode (992 cm^{-1}) during initial adsorption onto the CH_4 film at 20 K. We use a least squares regression to calculate the initial growth rate or the 2556 m/s CD_4 beam to overlay with the Sticking Probability in **Figure 5.4**. (*Data files: 101220B.IR01-08, 101220D.IR01-08, 101320B.IR01-08, 101820B.IR01-08, 101820D.IR01-08, 101920B.IR01-08*)

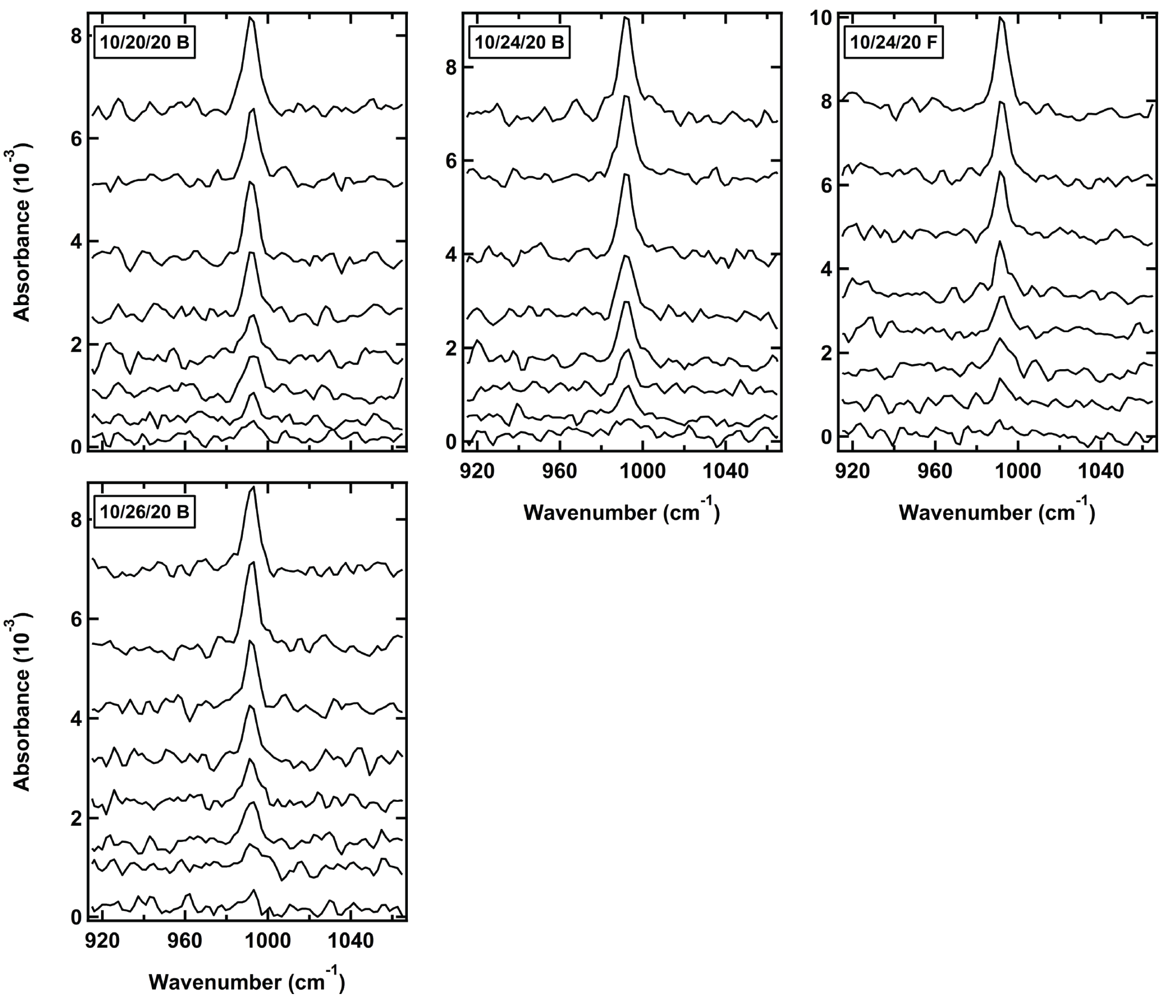

Figure A4.11: Raw RAIR spectrum for Figure 5.4 - CD_4 at 3685 m/s. We tracked the growth of deuterated methane's ν_4 mode (992 cm^{-1}) during initial adsorption onto the CH_4 film at 20 K. We use a least squares regression to calculate the initial growth rate or the 3685 m/s CD_4 beam to overlay with the Sticking Probability in **Figure 5.4**. (*Data files: 102020B.IR01-08, 102420B.IR01-08, 102420F.IR01-08, 102620B.IR01-08*)

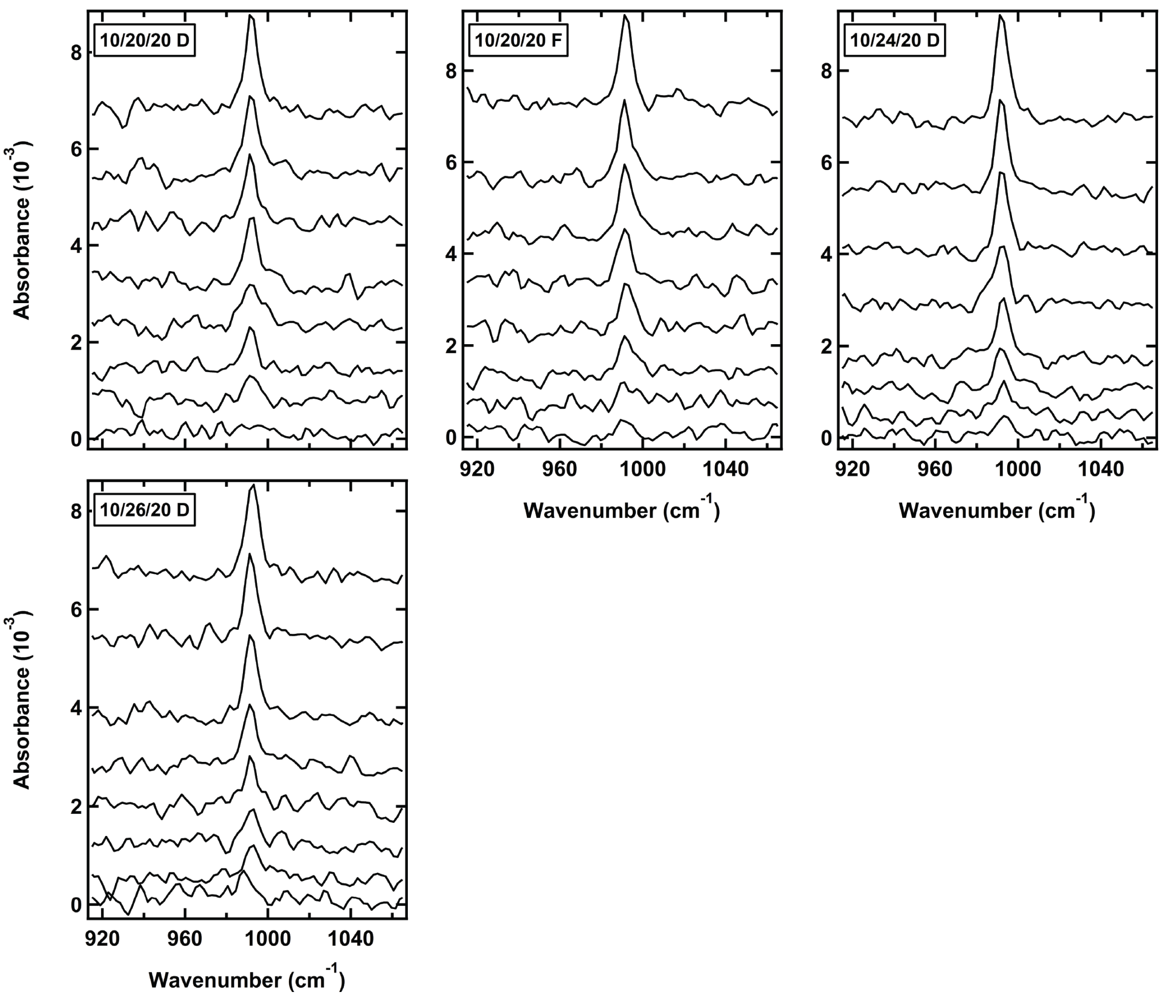

Figure A4.12: Raw RAIR spectrum for Figure 5.4 - CD_4 at 4159 m/s. We tracked the growth of deuterated methane's ν_4 mode (992 cm^{-1}) during initial adsorption onto the CH_4 film at 20 K. We use a least squares regression to calculate the initial growth rate for the 4159 m/s CD_4 beam to overlay with the Sticking Probability in **Figure 5.4**. (*Data files: 102020D.IR01-08, 102020F.IR01-08, 102420D.IR01-08, 102620D.IR01-08*)

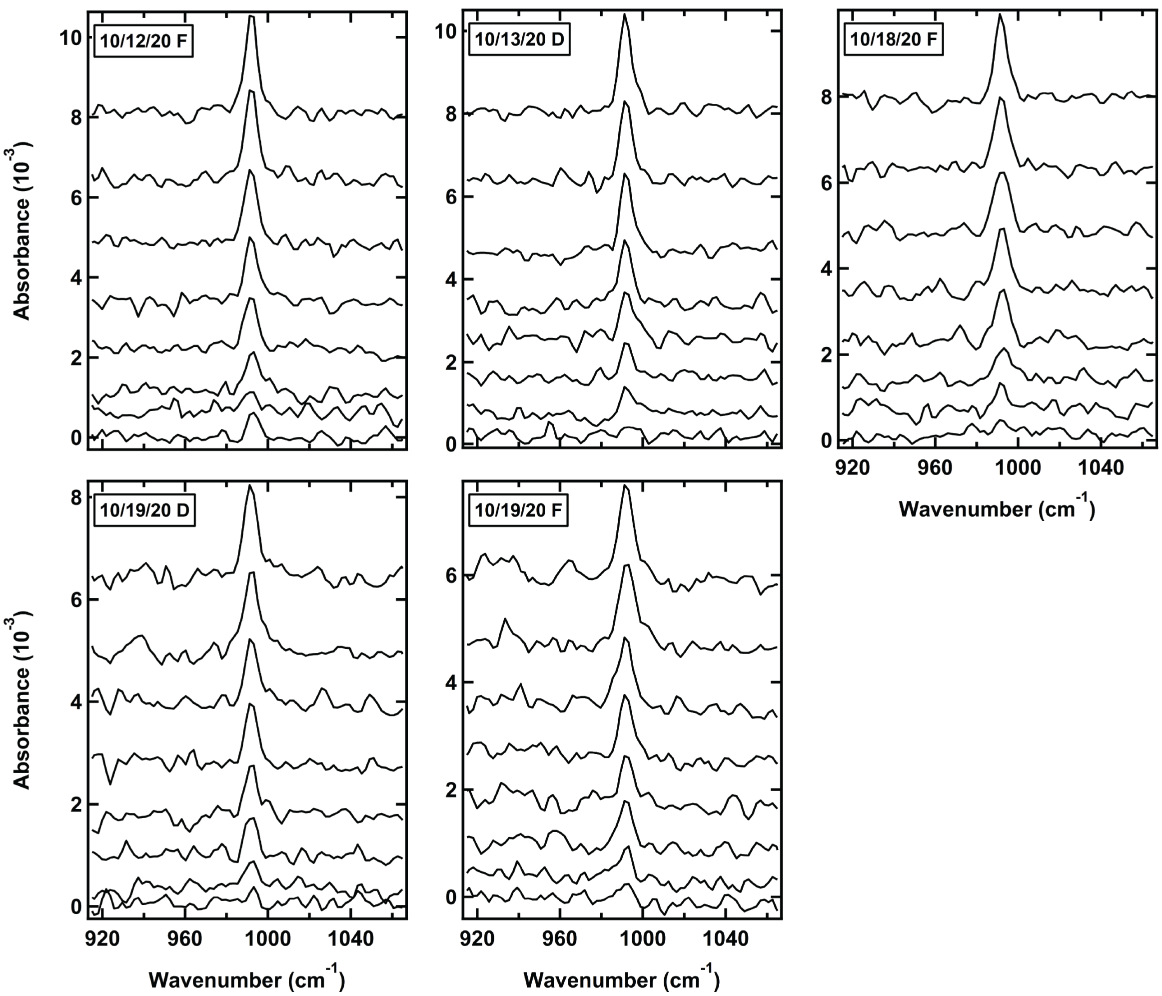

Figure A4.13: Raw RAIR spectrum for Figure 5.4 - CD_4 at 4619 m/s. We tracked the growth of deuterated methane's ν_4 mode (992 cm^{-1}) during initial adsorption onto the CH_4 film at 20 K. We use a least squares regression to calculate the initial growth rate or the 4619 m/s CD_4 beam to overlay with the Sticking Probability in **Figure 5.4**. (*Data files: 101220F.IR01-08, 101320D.IR01-08, 101820F.IR01-08, 101920D.IR01-08, 101920F.IR01-08*)

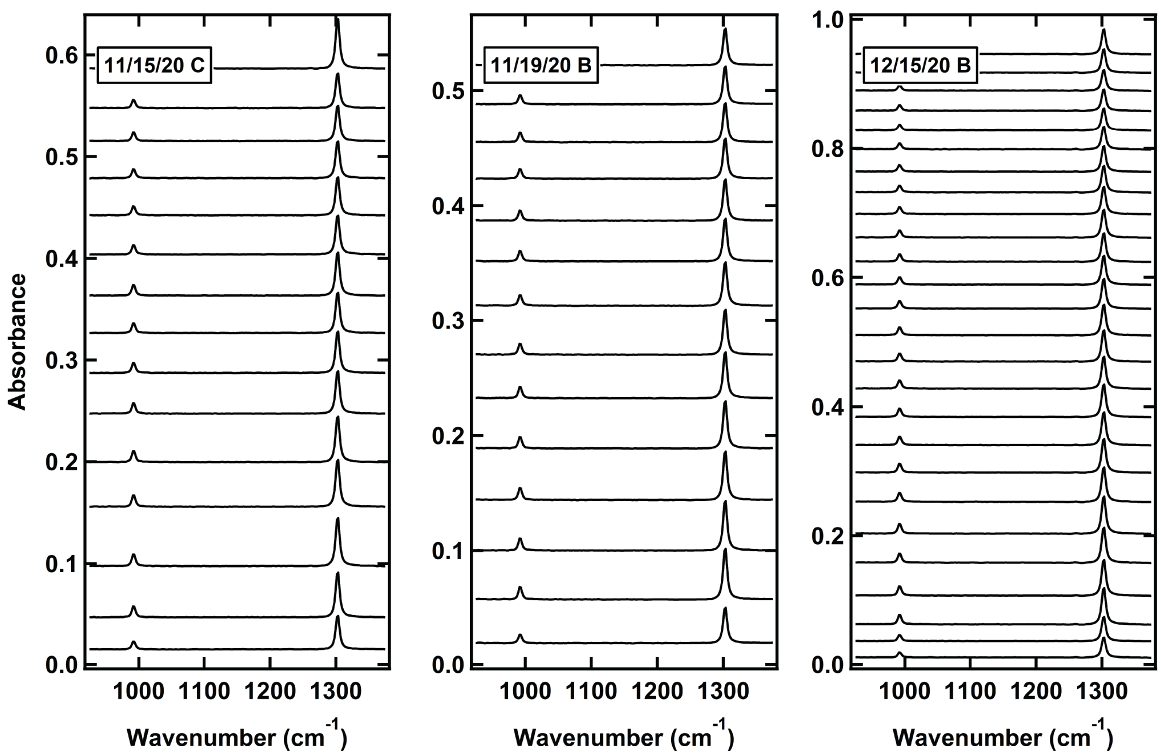

Figure A4.14: Raw RAIR spectrum for Figure 5.7 - CH_4 and CD_4 at 2293 m/s. We tracked methane's ν_4 mode (992 cm^{-1} (CD_4) and 1305 cm^{-1} (CH_4)) once the film reached a steady state. We use the integrated area with the appopriate infrared cross sections to calculate the percentage of CD_4 and CH_4 for each spectra. We average all spectra taken for the beam at 2293 m/s to get the film composition % in **Figure 5.7**. (*Data files: 111520C.IR26-40 111920B.IR27-40, 121520B.IR25-50*)

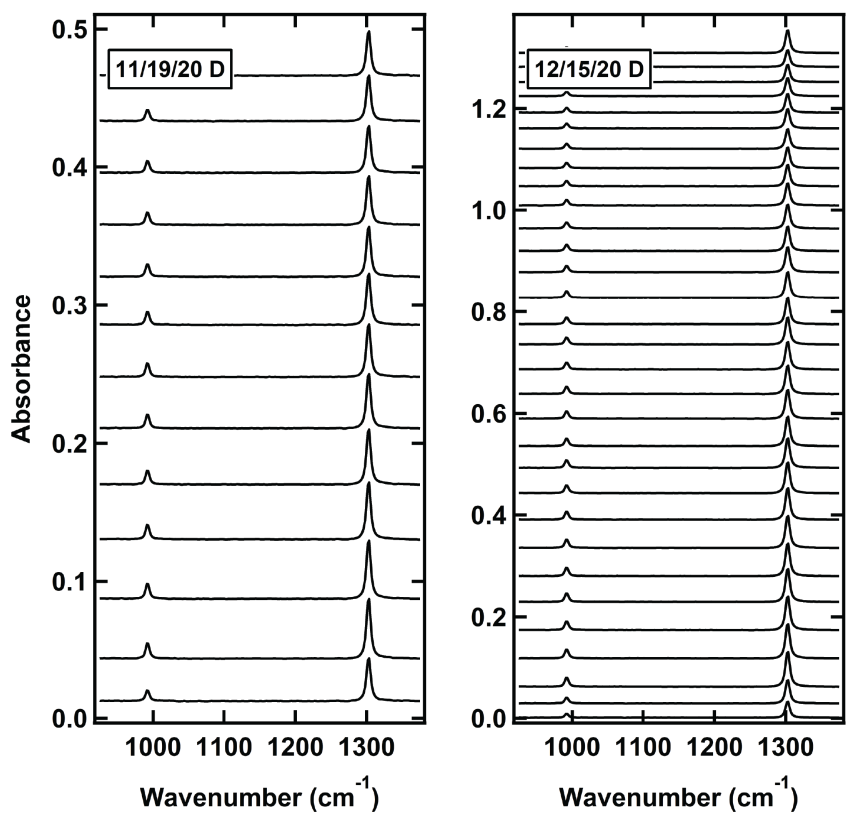

Figure A4.15: Raw RAIR spectrum for Figure 5.7 - CH_4 and CD_4 at 3595 m/s. We tracked methane's ν_4 mode (992 cm^{-1} (CD_4) and 1305 cm^{-1} (CH_4)) once the film reached a steady state. We use the integrated area with the appopriate infrared cross sections to calculate the percentage of CD_4 and CH_4 for each spectra. We average all spectra taken for the beam at 3595 m/s to get the film composition % in **Figure 5.7**. (*Data files: 111920D.IR28-40, 121520D.IR20-50*)

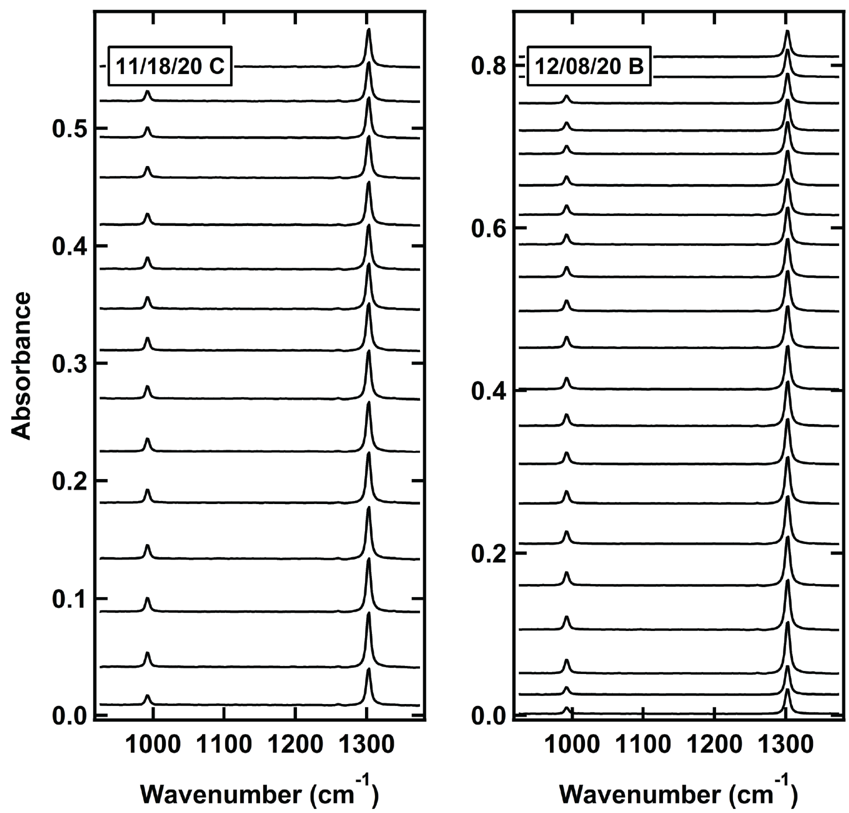

Figure A4.16: Raw RAIR spectrum for Figure 5.7 - CH_4 and CD_4 at 4123 m/s. We tracked methane's ν_4 mode (992 cm^{-1} (CD_4) and 1305 cm^{-1} (CH_4)) once the film reached a steady state. We use the integrated area with the appopriate infrared cross sections to calculate the percentage of CD_4 and CH_4 for each spectra. We average all spectra taken for the beam at 4123 m/s to get the film composition % in **Figure 5.7**. (*Data files: 111820C.IR26-40, 120820B.IR20-42*)

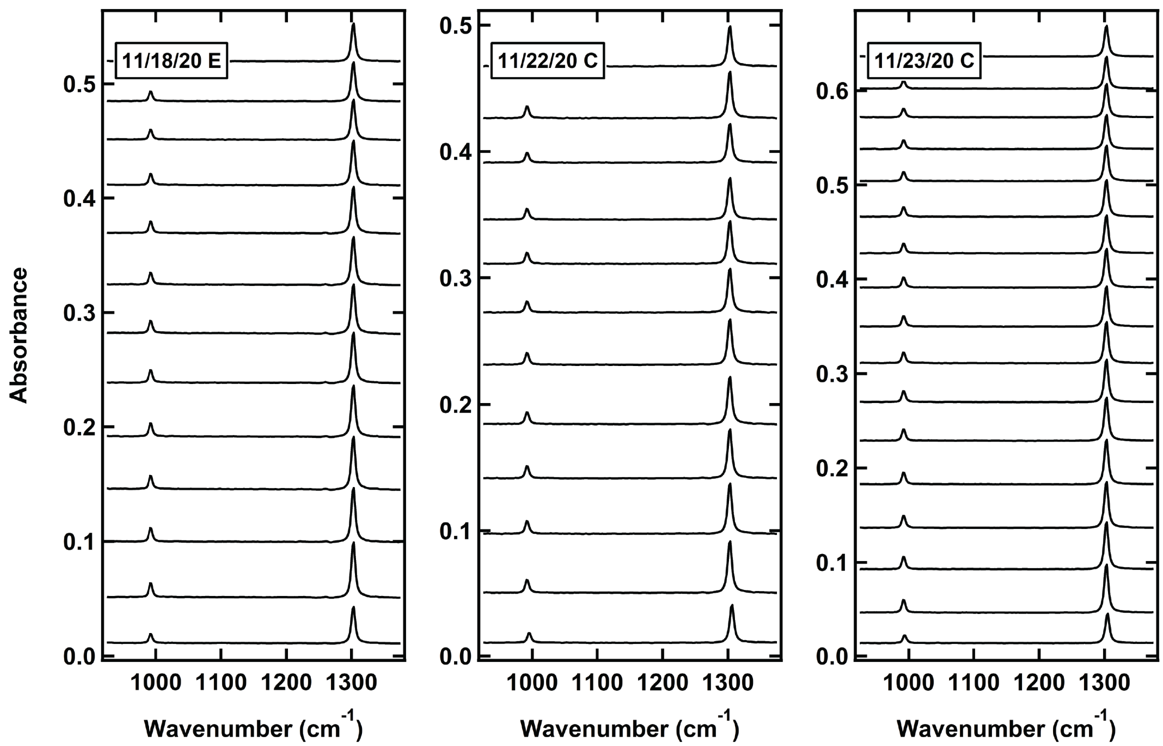

Figure A4.17: Raw RAIR spectrum for Figure 5.7 - CH_4 and CD_4 at 4276 m/s. We tracked methane's ν_4 mode (992 cm^{-1} (CD_4) and 1305 cm^{-1} (CH_4)) once the film reached a steady state. We use the integrated area with the appopriate infrared cross sections to calculate the percentage of CD_4 and CH_4 for each spectra. We average all spectra taken for the beam at 4276 m/s to get the film composition % in **Figure 5.7**.(*Data files: 111820E.IR26-40, 112220C.IR29-40, 112320C.IR24-40*)

A4.1 VENUS Input Information

The following input file was used to create **Figures 5.5 and 5.6**. For brevity, in the example input files (**Subsection A4.1.1**), the potential energy parameters include examples instead of listing the million lines of code and the surface coordinates (**Subsection A4.1.3**) are only listed once at the end. Additionally, for each trajectory to not take days to run on the Midway, the Lennard Jones potentials were cutoff at 10 Å. During additional analysis after publishing **Chapter 5**, the Lennard Jones parameters as part of the potential were further refined to correct a transcription error. To avoid confusion, those that are reproduced below are the most up to date values, but a comparison will occur when discussing the surface (**Subsection A4.1.2**) and the preliminary analysis of the VENUS trajectories (**Subsection A4.2**).

A4.1.1 Example Input File

In the following input file, the **bold** text are the numbers that differ between the 300 K, 700 K, 900 K, and 1100 K CH_4 and CD_4 beams and CH_4 and CD_4 surfaces. There are a total 16 different input files with the following conditions where at a specific temperature and vibrational energy, the CH_4 and CD_4 beams were at the same velocities, but different energies:

Surface Molecule	Beam Molecule	Beam Vibrational Temperature (K)	Beam Rotational Temperature (K)	Beam Energy (eV)
CH_4	CH_4	300	0	0.41
CD_4	CH_4	300	0	0.67
CH_4	CD_4	300	0	0.41
CD_4	CD_4	300	0	0.67
CH_4	CH_4	700	0	1.14
CD_4	CH_4	700	0	1.41
CH_4	CD_4	700	0	1.14
CD_4	CD_4	700	0	1.41
CH_4	CH_4	900	0	1.45
CD_4	CH_4	900	0	1.75
CH_4	CD_4	900	0	1.45
CD_4	CD_4	900	0	1.75
CH_4	CH_4	1100	0	1.85
CD_4	CH_4	1100	0	2.20
CH_4	CD_4	1100	0	1.85
CD_4	CD_4	1100	0	2.20

Table A.1: VENUS Input File Parameters

For 789 methane surface at 20 K (2285 rigid atoms) with a 300 K CD_4 beam
Trajectory
4205,0,3160,4740,0,841053,0,0,0,0,0,0,0,0,0,0,0,0,0,0,0,0,0,0,0,0,0
%Potential Energy Parameters%
1,2,1.086,1.863,112.45, → Morse stretch between carbon and hydrogen
2,3,1,109.471221,0.585,1.086,2,1.086,2, → Harmonic bend between carbon and hydrogen
1,6,12,6,0,812999.79,-575.20,0, → Carbon-Carbon LJ (beam with top two layers)
1,7,12,6,0,96581.62,-135.16,0, → Carbon-Hydrogen LJ(beam with top two layers)
2,7,12,6,0,3868.24,-12.24,0, → Hydrogen-Hydrogen LJ (beam with top two layers)
3951,6,12,6,0,1498264.42,-2096.82,0, → Au-C LJ
6,11,12,6,0,812999.79,-575.20,0,→ Carbon-Carbon LJ for Surface
452,3891,12,6,0,96581.62,-135.16,0, → Carbon-Hydrogen LJ for Surface
4204,4205,12,6,0,2307000,-6987,0, → Hydrogen-Hydrogen LJ for Surface
%Calculating the Trajectories and Selecting Initial Conditions%
999, → Zero vibrational energy
2,1,0, → Trajectory, Beam-Surface Collision
12.0,**2.01565,2.01565,2.01565,2.01565**, → Beam Carbon Mass (CD_4)
120000.0,**1.007825,1.007825,1.007825,1.007825**, → Example Surface Mass, heavy for rim
1969600.0 → Au Mass
3,1,0, → Velociy-Verlet Integrator
1,500000.0,1000,50, → 1 trajectory, Number of Steps, Printout details
0.01, → Time Step
5,7,1077835661, → Boltzmann Distribution of Normal Modes, MD sampling for surface
0.001,2, → Cartesian Coordinate Displacement, Number of Displacements
5,0, → Number atoms in the beam
0.000006, -0.000000, 0.000006,
-0.000006, 0.000000, 1.086006,
1.023901, 0.000000, -0.361982,
-0.511935, -0.886715, -0.362000,
-0.511935, 0.886715, -0.362000,→ Beam Coordinates
300, 1,0, → Beam vibrational temperature, rotational energy,
1,0,0,0, → Average and print rotational energy
4200,0, → Number Atoms in the Surface
Surface Coordinates (**Subsection A4.1.3**)
20,5000,0,1,2285, → MD Parameters: Surface Temp, Number of Steps, Number of Rigid Atoms
1, 1591, 0, 0, → Aim at center carbon
40, 30, -2320.0, → Halt trajectory at 40 A, Potential Energy at Equilibrium Position
1,**15.536205565**, → Fixed beam, initial energy in kcal/mol to match experimental data
10, 0, 4, → Start at 10 Å away, sample input parameter randomly
1376,1411,1846, → Reference Place of the Surface
1591,0,0,1,0, → Beam is normal to surface, aim at center carbon

A4.1.2 Methane Surface

As mentioned in **Subsection 5.3.1**, the surface model is comprised of six layers of methane stacked in an AB sequence to form a cubic closed packed structure[179] on top of an Au crystal. Between the six layers there are a total of 789 CH_4 molecules in alternating layers of 120/143 molecules. The CH_4 molecules are spaced 3.8 Å apart in plane and 3.4 Å apart between layers. The surface was optimized to find the minimum energy and geometry prior to running all the trajectories.The methane harmonic frequencies are 3193, 3021, 1583, and 1413 cm^{-1}.

Additionally, we calculated the orientation averaged CH_4 (beam) – CH_4 (surface) intermolecular potential versus the CH_4-CH_4 center-of-mass separation (**Figure A4.18**). Each distance was averaged over 1000 orientations. Thus, the incident methane experiences a different potential based on where it hits in the unit cell. The direct site corresponds to an impact parameter equal to 0, while the one methane away site corresponds to an impact parameter of 4. This information was used to select the approximate impact parameter, BMAX, (4 Å) in order to randomly sample directly hitting the methane, hitting one methane, and the 3 fold site. These are the conditions used in **Figures 5.5 and 5.6**.

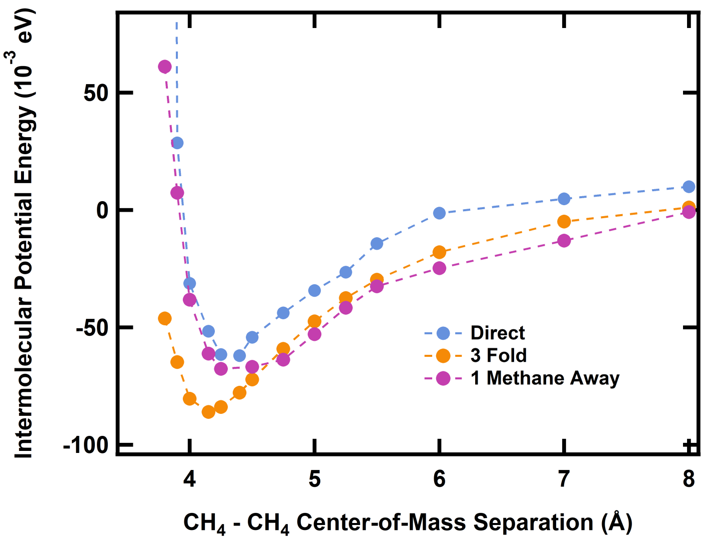

Figure A4.18: Orientation averaged CH_4 (beam) – CH_4 (surface) intermolecular potential

After refining the Lennard Jones Potentials, we recalculated the orientation average CH_4 (beam) – CH_4 (surface) intermolecular potential versus the CH_4-CH_4 center-of-mass separation (**Figure A4.19**. Additionally, there was concern that due to not having a fully periodic surface and after seeing variation in the sticking probabilities when preliminarily testing a variety of BMAX values (2,4,6, and 8), we decided to increase the impact parameter to 8 Å to avoid under-sampling the surface and repeatedly hitting a ”special” area.

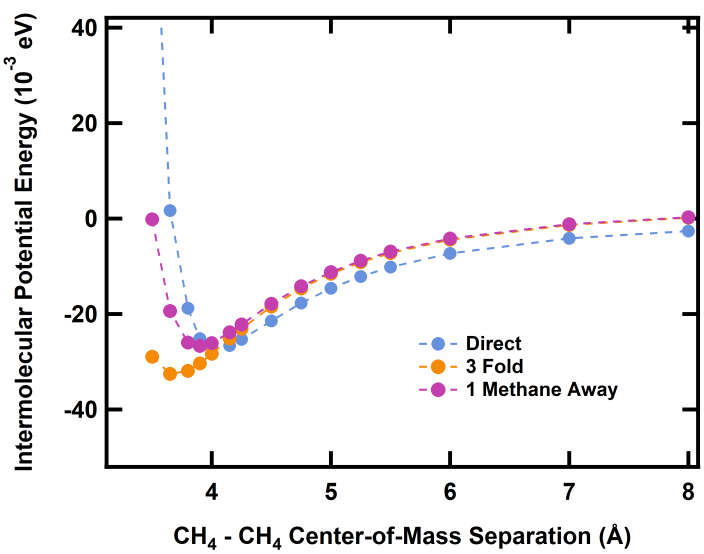

Figure A4.19: Orientation averaged CH_4 (beam) – CH_4 (surface) intermolecular potential, refined potential

A4.1.3 Surface Coordinates

The exact coordinates shown below are x,y,z for all methane (789) molecules and Au (255) atoms that are part of the surface. Each methane is listed as one carbon first and then its corresponding four hydrogens for a total of 3945 lines of coordinates. The top three layers are listed first (Z≅12, 15, 18 Å), before the bottom three (Z≅3, 6, 9 Å) layers that are held rigid during the trajectory. The Au atoms are at the very end (Z=0 Å).

Layer	**Molecule / Atom**	**# of Molecules / Atoms**	**# per Row**	**# Columns**	**∼Z Height (Å)**
4	CH_4	120	10	12	12
5	CH_4	143	11	13	15
6	CH_4	120	10	12	18
1	CH_4	143	11	13	3
2	CH_4	120	10	12	6
3	CH_4	143	11	13	9
0	Au(111)	255	15	17	0

Table A.2: Methane Surface Structure

The coordinates listed start in the top left of the surface and go across for the number of molecules per row (10-15) prior to starting the next row. For brevity, the coordinates are listed in two columns (starting with the column on the left) and the carbons will be denoted in **bold** to differentiate them from the hydrogens.

C1: 9.67156100000000519e+00,1.23220849999999951e+01,1.23670200000000012e+01,
9.27805599999999415e+00,1.33336679999999941e+01,1.23383699999999939e+01,
8.86436400000000132e+00,1.16257950000000010e+01,1.25736500000000066e+01,
1.04227179999999971e+01,1.22477040000000059e+01,1.31476179999999958e+01,
1.01223550000000066e+01,1.20787289999999916e+01,1.14109130000000075e+01,
C2: 1.38070950000000034e+01,1.21175219999999924e+01,1.23684100000000079e+01,
1.28658230000000068e+01,1.25324889999999999e+01,1.20213120000000000e+01,
1.44185739999999956e+01,1.18432639999999957e+01,1.15146390000000073e+01,
1.36129590000000003e+01,1.12364969999999996e+01,1.29728739999999913e+01,
1.43302300000000025e+01,1.28579050000000058e+01,1.29661620000000063e+01,
C3: 1.76416240000000019e+01,1.19796669999999918e+01,1.24328330000000047e+01,
1.73796779999999841e+01,1.09299619999999973e+01,1.25251920000000055e+01,
1.69294520000000128e+01,1.24751809999999919e+01,1.17808309999999916e+01,
1.86393740000000011e+01,1.20682720000000033e+01,1.20136459999999960e+01,
1.76182830000000169e+01,1.24441089999999920e+01,1.34137330000000057e+01,
C4: 2.19641519999999857e+01,1.22035079999999936e+01,1.23860299999999987e+01,
2.15149389999999826e+01,1.16014090000000030e+01,1.16024229999999993e+01,
2.25895170000000073e+01,1.29700059999999970e+01,1.19411880000000036e+01,
2.25695000000000145e+01,1.15691279999999919e+01,1.30260479999999940e+01,
2.11815689999999965e+01,1.26689489999999957e+01,1.29771280000000044e+01,
C5: 2.57029339999999906e+01,1.19935810000000071e+01,1.23660610000000019e+01,
2.62873330000000028e+01,1.23038579999999996e+01,1.32272680000000047e+01,
2.63706670000000097e+01,1.16475130000000001e+01,1.15832230000000027e+01,
2.51227480000000141e+01,1.28356040000000001e+01,1.20025449999999958e+01,
2.50346210000000135e+01,1.11880760000000058e+01,1.26549209999999986e+01,
C6: 3.00391100000000087e+01,1.21937650000000085e+01,1.24061009999999960e+01,
3.00894089999999985e+01,1.31062089999999978e+01,1.29900050000000002e+01,
3.08866920000000004e+01,1.21506270000000007e+01,1.17291450000000082e+01,
2.91152920000000017e+01,1.21822569999999989e+01,1.18359260000000061e+01,
3.00629549999999876e+01,1.13359690000000041e+01,1.30711400000000079e+01,
C7: 3.43665129999999765e+01,1.19668890000000011e+01,1.23385580000000080e+01,
3.49642040000000228e+01,1.26750199999999995e+01,1.17731040000000001e+01,
3.39321369999999733e+01,1.24669039999999954e+01,1.31991080000000073e+01,
3.49959410000000196e+01,1.11486239999999987e+01,1.26754440000000060e+01,
3.35727479999999715e+01,1.15776380000000032e+01,1.17084019999999953e+01,
C8: 3.80407679999999992e+01,1.22356709999999996e+01,1.24088189999999938e+01,
3.77874029999999763e+01,1.31577909999999957e+01,1.29214000000000022e+01,
3.90735489999999986e+01,1.22765550000000011e+01,1.20770560000000068e+01,
3.73887420000000059e+01,1.21066439999999929e+01,1.15513100000000085e+01,
3.79129020000000254e+01,1.13987750000000055e+01,1.30889269999999998e+01,
C9: 4.22805320000000089e+01,1.20930540000000041e+01,1.24124400000000014e+01,
4.18417519999999961e+01,1.26681700000000018e+01,1.32215100000000009e+01,
4.29935299999999980e+01,1.27081219999999947e+01,1.18733459999999973e+01,
4.14974679999999780e+01,1.17684789999999925e+01,1.17342829999999957e+01,
4.27885029999999862e+01,1.12240479999999980e+01,1.28194999999999967e+01,
C10: 4.60496219999999939e+01,1.18626079999999982e+01,1.23199930000000019e+01,
4.55069069999999822e+01,1.26904450000000042e+01,1.27667719999999957e+01,
4.60868779999999868e+01,1.19935180000000915e+01,1.12434510000000031e+01,
4.55443339999999921e+01,1.09303220000000032e+01,1.25540509999999941e+01,
4.70602469999999683e+01,1.18368439999999926e+01,1.27166320000000060e+01,
C11: 1.15021350000000089e+01,1.55598980000000045e+01,1.24841490000000038e+01,
1.15212710000000048e+01,1.51378059999999943e+01,1.34841689999999963e+01,
1.20889720000000005e+01,1.64733750000000077e+01,1.24671549999999999e+01,
1.04768570000000075e+01,1.57810290000000020e+01,1.22030150000000061e+01,
1.19239979999999921e+01,1.48448259999999941e+01,1.17858450000000013e+01,
C12: 1.61499570000000056e+01,1.53898440000000008e+01,1.25030110000000076e+01,
1.51985340000000043e+01,1.58611579999999965e+01,1.27313810000000072e+01,
1.60241100000000030e+01,1.47115109999999978e+01,1.16651900000000084e+01,
1.64953770000000129e+01,1.48345789999999974e+01,1.33706589999999985e+01,
1.68776820000000007e+01,1.61531079999999958e+01,1.22459460000000000e+01,
C13: 1.97936450000000149e+01,1.52719919999999912e+01,1.23674199999999919e+01,
1.93437270000000123e+01,1.62385899999999853e+01,1.25719429999999920e+01,
1.90958049999999859e+01,1.44843790000000056e+01,1.26299639999999930e+01,
2.06986099999999862e+01,1.51630760000000022e+01,1.29546349999999968e+01,
2.00346040000000163e+01,1.52016209999999938e+01,1.13146170000000015e+01,
C14: 2.35512319999999883e+01,1.56507880000000037e+01,1.25710200000000075e+01,
2.31935059999999929e+01,1.51066149999999968e+01,1.34396029999999997e+01,
2.27160979999999879e+01,1.61300689999999888e+01,1.20703779999999983e+01,
2.40349100000000000e+01,1.49630589999999944e+01,1.18844499999999929e+01,
2.42652059999999916e+01,1.64062640000000018e+01,1.28850460000000089e+01,
C15: 2.81275639999999957e+01,1.53689859999999959e+01,1.24400490000000013e+01,
2.72640799999999987e+01,1.60256380000000072e+01,1.23884500000000063e+01,
2.79132590000000004e+01,1.45397829999999990e+01,1.31068379999999977e+01,
2.89828030000000054e+01,1.59233379999999933e+01,1.28132199999999939e+01,
2.83500140000000160e+01,1.49833060000000068e+01,1.14513069999999990e+01,
C16: 3.19792440000000134e+01,1.53024869999999928e+01,1.24498999999999952e+01,
3.15352010000000070e+01,1.52848749999999955e+01,1.34403380000000056e+01,
3.28686170000000042e+01,1.59254289999999939e+01,1.24638130000000003e+01,
3.12634459999999829e+01,1.57097920000000020e+01,1.17437629999999951e+01,
3.22486469999999829e+01,1.42930189999999925e+01,1.21566930000000064e+01,
C17: 3.61145240000000296e+01,1.55622869999999954e+01,1.26316179999999957e+01,
3.70804660000000126e+01,1.56023650000000071e+01,1.31253209999999957e+01,
3.62128760000000140e+01,1.50600550000000019e+01,1.16745380000000008e+01,
3.57465959999999671e+01,1.65718800000000017e+01,1.24751600000000069e+01,
3.54135160000000133e+01,1.50158260000000056e+01,1.32554809999999963e+01,
C18: 4.00449979999999965e+01,1.52396869999999998e+01,1.23723690000000084e+01,
3.97610219999999698e+01,1.47944469999999990e+01,1.33180809999999939e+01,
3.91526349999999652e+01,1.55561500000000059e+01,1.18439510000000056e+01,
4.05775259999999887e+01,1.45042190000000086e+01,1.17807539999999995e+01,
4.06823150000000267e+01,1.60997890000000124e+01,1.25517369999999926e+01,
C19: 4.36680429999999728e+01,1.55449710000000032e+01,1.24519549999999988e+01,
4.45972739999999875e+01,1.59335679999999929e+01,1.28579399999999926e+01,
4.38829190000000112e+01,1.49337099999999960e+01,1.15810990000000003e+01,
4.30264069999999896e+01,1.63719450000000019e+01,1.21654389999999923e+01,
4.31692570000000177e+01,1.49427690000000019e+01,1.32040819999999965e+01,
C20: 4.80402449999999875e+01,1.51480270000000080e+01,1.25025289999999912e+01,
4.80851290000000201e+01,1.62267900000000116e+01,1.26194059999999968e+01,
4.84699949999999728e+01,1.48697330000000009e+01,1.15456599999999981e+01,
4.70051589999999903e+01,1.48234040000000002e+01,1.25451949999999965e+01,
4.86007430000000136e+01,1.46734299999999975e+01,1.33019660000000018e+01,
C21: 9.82647000000000482e+00,1.89461629999999853e+01,1.23712940000000068e+01,
1.04395159999999935e+01,1.90819760000000094e+01,1.32572860000000057e+01,
1.04654690000000058e+01,1.87420639999999917e+01,1.15188349999999927e+01,
9.25044300000000637e+00,1.98479250000000004e+01,1.21867520000000025e+01,
9.15068699999999571e+00,1.81102600000000025e+01,1.25250950000000031e+01,
C22: 1.38805110000000027e+01,1.94172699999999848e+01,1.25428709999999988e+01,
1.47439429999999980e+01,1.92068159999999989e+01,1.19202919999999989e+01,
1.39163639999999973e+01,2.04497290000000138e+01,1.28728139999999998e+01,
1.38898510000000017e+01,1.87579749999999829e+01,1.34052299999999954e+01,
1.29703350000000039e+01,1.92509920000000010e+01,1.19750770000000064e+01,
C23: 1.80352099999999930e+01,1.91468530000000012e+01,1.24283830000000018e+01,
1.79711460000000095e+01,2.02291419999999951e+01,1.23916679999999924e+01,
1.70349690000000025e+01,1.87255220000000155e+01,1.24330259999999991e+01,
1.85546499999999876e+01,1.88477390000000069e+01,1.33338450000000017e+01,
1.85776870000000095e+01,1.87805830000000003e+01,1.15638020000000080e+01,
C24: 2.15641800000000035e+01,1.89107699999999941e+01,1.24415030000000087e+01,
2.14871620000000143e+01,1.97679940000000162e+01,1.31025240000000073e+01,
2.26045720000000100e+01,1.87539709999999995e+01,1.21745400000000036e+01,
2.09820869999999993e+01,1.90939909999999905e+01,1.15448140000000058e+01,
2.11835290000000005e+01,1.80290779999999838e+01,1.29476800000000008e+01,
C25: 2.59959670000000027e+01,1.94986679999999856e+01,1.25087799999999979e+01,
2.59893719999999947e+01,2.05268540000000016e+01,1.28541000000000075e+01,
2.50793700000000083e+01,1.92919729999999871e+01,1.19650459999999918e+01,
2.60649349999999841e+01,1.88309120000000143e+01,1.33622739999999932e+01,
2.68512820000000120e+01,1.93381800000000126e+01,1.18609799999999963e+01,
C26: 3.00242490000000108e+01,1.89695290000000142e+01,1.23412380000000060e+01,
2.97958069999999993e+01,1.93896949999999968e+01,1.33161609999999925e+01,
3.07570790000000095e+01,1.95927800000000119e+01,1.18397400000000082e+01,
2.91194789999999834e+01,1.89239180000000046e+01,1.17443310000000074e+01,
3.04268280000000043e+01,1.79692049999999876e+01,1.24656749999999917e+01,
C27: 3.39285029999999919e+01,1.93997220000000058e+01,1.25210129999999995e+01,
3.30995139999999921e+01,1.91879880000000071e+01,1.18536210000000041e+01,
3.38711320000000290e+01,1.87429340000000176e+01,1.33832450000000050e+01,
3.38783820000000199e+01,2.04318050000000066e+01,1.28503399999999921e+01,
3.48693499999999718e+01,1.92301619999999998e+01,1.20068409999999965e+01,
C28: 3.83792749999999981e+01,1.89046640000000036e+01,1.24384160000000014e+01,
3.88628870000000063e+01,1.92631459999999899e+01,1.33420249999999958e+01,
3.89046450000000214e+01,1.92890230000000025e+01,1.15699780000000076e+01,
3.73489709999999881e+01,1.92462499999999986e+01,1.24200970000000016e+01,
3.83995790000000279e+01,1.78196909999999884e+01,1.24236660000000076e+01,
C29: 4.19510149999999817e+01,1.92041660000000074e+01,1.24489859999999966e+01,
4.29567830000000149e+01,1.92321910000000026e+01,1.20411120000000004e+01,
4.13096120000000133e+01,1.86246660000000128e+01,1.17938559999999990e+01,
4.15671070000000003e+01,2.02144489999999834e+01,1.25390789999999920e+01,
4.19741069999999650e+01,1.87389000000000100e+01,1.34299049999999976e+01,
C30: 4.62451780000000278e+01,1.93494770000000026e+01,1.25432000000000057e+01,
4.54470320000000010e+01,1.89608239999999879e+01,1.19183730000000077e+01,
4.71732069999999789e+01,1.93758289999999952e+01,1.19798939999999982e+01,
4.63689639999999829e+01,1.87031950000000090e+01,1.34067430000000052e+01,
4.59917099999999765e+01,2.03506929999999970e+01,1.28728569999999977e+01,
C31: 1.16379880000000000e+01,2.23403619999999894e+01,1.24306610000000063e+01,
1.22017640000000072e+01,2.28368499999999832e+01,1.32144639999999954e+01,
1.08706180000000034e+01,2.30117019999999966e+01,1.20572099999999954e+01,
1.11746580000000087e+01,2.14459650000000106e+01,1.28332209999999999e+01,
1.23101810000000004e+01,2.20700959999999949e+01,1.16227409999999954e+01,
C32: 1.58814209999999957e+01,2.25666870000000172e+01,1.23858660000000004e+01,
1.48737069999999957e+01,2.27830610000000001e+01,1.27265250000000053e+01,
1.64239630000000053e+01,2.34951599999999849e+01,1.22412259999999927e+01,
1.58360249999999935e+01,2.20204370000000115e+01,1.14495199999999970e+01,
1.63908370000000121e+01,2.19638719999999851e+01,1.31308799999999944e+01,
C33: 1.99976139999999867e+01,2.23416339999999911e+01,1.24091140000000064e+01,
2.07886009999999989e+01,2.30685129999999938e+01,1.22546829999999999e+01,
2.00715940000000105e+01,2.15575490000000163e+01,1.16628460000000005e+01,
1.90339950000000089e+01,2.28342099999999879e+01,1.23207710000000058e+01,
2.00924839999999890e+01,2.19087950000000135e+01,1.34006360000000044e+01,
C34: 2.37547099999999933e+01,2.24771609999999884e+01,1.23637540000000013e+01,
2.35721470000000107e+01,2.32633009999999845e+01,1.30886060000000041e+01,
2.47859599999999933e+01,2.25255749999999990e+01,1.20282610000000054e+01,
2.30905950000000043e+01,2.26119850000000067e+01,1.15164500000000074e+01,
2.35658400000000145e+01,2.15109320000000039e+01,1.28215740000000003e+01,
C35: 2.81879419999999961e+01,2.23897639999999956e+01,1.24090450000000077e+01,
2.75559079999999874e+01,2.21062800000000171e+01,1.15733800000000022e+01,
2.87578470000000171e+01,2.32765750000000113e+01,1.21490779999999938e+01,
2.88656340000000001e+01,2.15763390000000082e+01,1.26430509999999982e+01,
2.75672959999999891e+01,2.26016860000000083e+01,1.32744990000000049e+01,
C36: 3.18261819999999931e+01,2.23876379999999904e+01,1.24351780000000051e+01,
3.26965300000000276e+01,2.27358730000000155e+01,1.29831020000000059e+01,
3.21497730000000326e+01,2.18478490000000007e+01,1.15509719999999980e+01,
3.12214230000000148e+01,2.32400459999999954e+01,1.21412049999999936e+01,
3.12433930000000108e+01,2.17285989999999911e+01,1.30705910000000029e+01,
C37: 3.59798970000000113e+01,2.25097559999999943e+01,1.23483119999999995e+01,
3.55119169999999685e+01,2.25323540000000155e+01,1.33276629999999937e+01,
3.66859979999999789e+01,2.33296059999999829e+01,1.22655740000000086e+01,
3.52160200000000032e+01,2.26078079999999857e+01,1.15841759999999936e+01,
3.65020340000000187e+01,2.15667539999999954e+01,1.22213879999999925e+01,
C38: 3.97335459999999692e+01,2.23947450000000035e+01,1.23963049999999991e+01,
4.07034900000000217e+01,2.26041239999999877e+01,1.28367459999999977e+01,
3.91199289999999906e+01,2.18592779999999976e+01,1.31143289999999968e+01,
3.98615250000000032e+01,2.17887459999999973e+01,1.15051500000000043e+01,
3.92473939999999989e+01,2.33289170000000057e+01,1.21324240000000032e+01,
C39: 4.39572620000000006e+01,2.23379450000000127e+01,1.23806560000000011e+01,
4.30055580000000062e+01,2.27584400000000023e+01,1.20724359999999972e+01,
4.38384509999999917e+01,2.18370670000000112e+01,1.33368120000000011e+01,
4.46903980000000184e+01,2.31318200000000116e+01,1.24765420000000024e+01,
4.42895979999999802e+01,2.16220649999999920e+01,1.16359580000000047e+01,
C40: 4.77406399999999908e+01,2.26478150000000136e+01,1.23524279999999974e+01,
4.71556989999999848e+01,2.27028840000000095e+01,1.32657159999999940e+01,
4.83991410000000019e+01,2.35091129999999926e+01,1.22933839999999965e+01,
4.70734980000000073e+01,2.26404679999999848e+01,1.14967570000000056e+01,
4.83341959999999861e+01,2.17387429999999948e+01,1.23589490000000085e+01,
C41: 1.03808860000000028e+01,2.64330080000000095e+01,1.25125299999999993e+01,
1.09492650000000047e+01,2.63100990000000101e+01,1.34292390000000081e+01,
1.10476139999999938e+01,2.67485800000000047e+01,1.17166209999999995e+01,
9.61053800000000025e+00,2.71841270000000015e+01,1.26584979999999981e+01,
9.91902100000000754e+00,2.54876679999999932e+01,1.22440870000000039e+01,
C42: 1.39298780000000043e+01,2.55706580000000166e+01,1.23844960000000039e+01,
1.33987020000000011e+01,2.65171969999999946e+01,1.23809570000000043e+01,
1.48593949999999924e+01,2.56767579999999953e+01,1.18351349999999929e+01,
1.33172720000000089e+01,2.48042499999999969e+01,1.19226390000000021e+01,
1.41503169999999937e+01,2.52844450000000161e+01,1.34065969999999965e+01,
C43: 1.78395870000000164e+01,2.60984960000000081e+01,1.26283989999999993e+01,
1.69026229999999840e+01,2.61060850000000021e+01,1.31765450000000084e+01,
1.81553690000000031e+01,2.71191870000000015e+01,1.24365179999999952e+01,
1.77035809999999979e+01,2.55764870000000019e+01,1.16863480000000062e+01,

1.859828100000000006e+01,2.559002399999999966e+01,1.321587800000000001e+01,
C44: 2.236843100000000106e+01,2.615472300000000061e+01,1.246574900000000063e+01,
2.152356199999999831e+01,2.682147099999999895e+01,1.260926100000000005e+01,
2.310897200000000140e+01,2.663759599999999850e+01,1.183646099999999990e+01,
2.202995999999999910e+01,2.523980900000000105e+01,1.198948700000000045e+01,
2.281064100000000039e+01,2.591857999999999862e+01,1.342858599999999925e+01,
C45: 2.595606300000000033e+01,2.540117000000000047e+01,1.240377699999999983e+01,
2.535296800000000061e+01,2.627353499999999897e+01,1.263417500000000082e+01,
2.700728900000000010e+01,2.566254400000000047e+01,1.247687700000000000e+01,
2.573835400000000107e+01,2.506226500000000001e+01,1.139818200000000026e+01,
2.573469499999999854e+01,2.460751399999999833e+01,1.310979700000000037e+01,
C46: 3.027366100000000060e+01,2.661670099999999906e+01,1.259708299999999959e+01,
2.990834999999999866e+01,2.759116099999999960e+01,1.290326899999999988e+01,
3.112102700000000155e+01,2.674132900000000035e+01,1.193043199999999970e+01,
2.948337499999999878e+01,2.607630199999999832e+01,1.208508600000000044e+01,
3.058647099999999952e+01,2.605227299999999957e+01,1.347025499999999987e+01,
C47: 3.414572799999999830e+01,2.561194100000000162e+01,1.240866100000000039e+01,
3.479592399999999941e+01,2.541205799999999826e+01,1.325346500000000027e+01,
3.465929299999999813e+01,2.625680600000000098e+01,1.170273300000000027e+01,
3.324447899999999834e+01,2.610463700000000031e+01,1.275871300000000019e+01,
3.388453499999999963e+01,2.467702600000000146e+01,1.192461899999999986e+01,
C48: 3.769537199999999899e+01,2.620068200000000047e+01,1.249604000000000070e+01,
3.700775099999999895e+01,2.688552100000000067e+01,1.298140199999999922e+01,
3.859670500000000004e+01,2.673226500000000172e+01,1.220768200000000014e+01,
3.722387899999999661e+01,2.577561700000000044e+01,1.161687000000000047e+01,
3.795620699999999914e+01,2.540281299999999831e+01,1.318468599999999924e+01,
C49: 4.213753700000000180e+01,2.555339599999999933e+01,1.257830399999999926e+01,
4.263922300000000121e+01,2.505781500000000150e+01,1.340404700000000027e+01,
4.255268099999999976e+01,2.520415799999999962e+01,1.163832799999999956e+01,
4.228097499999999798e+01,2.662665399999999849e+01,1.265986599999999918e+01,
4.107596499999999651e+01,2.532775399999999877e+01,1.261172700000000013e+01,
C50: 4.594468100000000277e+01,2.580719099999999955e+01,1.240402399999999972e+01,
4.675150099999999753e+01,2.652671799999999891e+01,1.230395299999999992e+01,
4.585149200000000036e+01,2.523674700000000115e+01,1.148663999999999952e+01,
4.501445400000000063e+01,2.632969200000000143e+01,1.260158599999999929e+01,
4.616226699999999994e+01,2.513295000000000101e+01,1.322548300000000054e+01,
C51: 1.211475199999999930e+01,2.956677000000000177e+01,1.240974399999999989e+01,
1.228728399999999965e+01,2.896265199999999851e+01,1.329554500000000061e+01,
1.275122400000000056e+01,2.921535300000000035e+01,1.160489100000000029e+01,
1.234371200000000002e+01,3.060358300000000042e+01,1.263195299999999932e+01,
1.107381600000000077e+01,2.948221900000000062e+01,1.211270000000000024e+01,
C52: 1.567335399999999979e+01,2.921572499999999906e+01,1.235550300000000057e+01,
1.524107500000000037e+01,2.947120299999999915e+01,1.331841000000000008e+01,
1.672589599999999876e+01,2.948013299999999859e+01,1.235044599999999981e+01,
1.515832100000000082e+01,2.976029099999999872e+01,1.157101399999999991e+01,
1.556741599999999970e+01,2.814939800000000147e+01,1.218350099999999969e+01,
C53: 1.998354700000000150e+01,2.966799100000000067e+01,1.249301200000000023e+01,
1.906342199999999920e+01,2.950296900000000022e+01,1.194160199999999961e+01,
2.001483699999999999e+01,3.069111499999999992e+01,1.285005800000000065e+01,
2.083964599999999834e+01,2.948048400000000058e+01,1.185277100000000061e+01,
2.001517600000000030e+01,2.899133199999999988e+01,1.334118800000000071e+01,
C54: 2.406160900000000069e+01,2.948147200000000012e+01,1.235170800000000035e+01,
2.463903200000000027e+01,2.876458900000000085e+01,1.292745599999999939e+01,
2.460687700000000078e+01,3.041680600000000112e+01,1.228294700000000006e+01,
2.311048200000000108e+01,2.965357200000000049e+01,1.284596799999999917e+01,
2.388501000000000118e+01,2.908651199999999903e+01,1.135648699999999955e+01,
C55: 2.751894599999999969e+01,2.933786999999999896e+01,1.239293900000000015e+01,
2.712378100000000103e+01,2.976915599999999884e+01,1.330752599999999930e+01,
2.856813400000000058e+01,2.959822300000000084e+01,1.229402100000000075e+01,
2.696812699999999907e+01,2.972487800000000036e+01,1.154161999999999999e+01,
2.741568799999999939e+01,2.825746799999999936e+01,1.242913800000000002e+01,
C56: 3.216063700000000125e+01,2.977956899999999862e+01,1.243016599999999983e+01,
3.286723099999999675e+01,2.977372700000000094e+01,1.160724599999999995e+01,
3.238489299999999815e+01,2.895694100000000049e+01,1.310177200000000042e+01,
3.115296000000000021e+01,2.966438499999999934e+01,1.204315599999999975e+01,
3.223853499999999883e+01,3.071866699999999994e+01,1.296774600000000000e+01,
C57: 3.581076199999999687e+01,2.948981600000000114e+01,1.235172799999999960e+01,
3.647937100000000044e+01,2.997312300000000107e+01,1.305751199999999912e+01,
3.639306100000000299e+01,2.900060699999999869e+01,1.157806700000000077e+01,
3.515961800000000181e+01,3.023173999999999850e+01,1.190273400000000059e+01,
3.520977400000000301e+01,2.875069600000000136e+01,1.287307900000000060e+01,
C58: 3.968622700000000236e+01,2.956740699999999933e+01,1.248973900000000015e+01,
3.938410199999999861e+01,2.904269499999999837e+01,1.339064800000000055e+01,
3.881936699999999973e+01,2.972525699999999915e+01,1.185600699999999996e+01,
4.042274900000000315e+01,2.897389000000000081e+01,1.195731400000000022e+01,
4.011917300000000353e+01,3.052587499999999920e+01,1.275682800000000050e+01,
C59: 4.403240300000000218e+01,2.937337300000000084e+01,1.244163700000000006e+01,
4.403831699999999927e+01,3.029931699999999850e+01,1.300696300000000072e+01,
4.470337700000000325e+01,2.946030899999999875e+01,1.159344199999999958e+01,
4.302575099999999964e+01,2.917191700000000054e+01,1.208797500000000014e+01,
4.435943400000000025e+01,2.856001499999999993e+01,1.308162399999999960e+01,
C60: 4.767155400000000043e+01,2.949388400000000132e+01,1.233301999999999943e+01,
4.846871500000000310e+01,2.876153599999999955e+01,1.224671400000000077e+01,
4.810052000000000305e+01,3.047748500000000149e+01,1.249939200000000028e+01,
4.703058899999999909e+01,2.923296600000000112e+01,1.316986900000000027e+01,
4.708855299999999744e+01,2.950231199999999987e+01,1.141729100000000052e+01,
C61: 1.002269500000000058e+01,3.270457199999999887e+01,1.239597900000000053e+01,
1.077934600000000032e+01,3.334960099999999983e+01,1.195945099999999961e+01,
9.063874000000000208e+00,3.321424600000000282e+01,1.238840199999999925e+01,
1.029863300000000059e+01,3.246755499999999728e+01,1.341849900000000062e+01,
9.950055000000000760e+00,3.178748900000000077e+01,1.182059699999999935e+01,
C62: 1.432071000000000005e+01,3.268676500000000118e+01,1.243863999999999947e+01,
1.483615200000000023e+01,3.359941800000000001e+01,1.215485199999999999e+01,
1.422579799999999928e+01,3.204075699999999927e+01,1.157179600000000086e+01,
1.333317100000000011e+01,3.293336999999999648e+01,1.281708800000000004e+01,
1.488720200000000027e+01,3.217639599999999689e+01,1.321164199999999944e+01,
C63: 1.807744800000000041e+01,3.277984299999999962e+01,1.235258299999999920e+01,
1.854917599999999922e+01,3.285054499999999678e+01,1.332787399999999955e+01,
1.883446999999999960e+01,3.286738499999999874e+01,1.158021800000000034e+01,
1.735311300000000045e+01,3.358120199999999755e+01,1.224448000000000022e+01,
1.757499100000000070e+01,3.182184499999999971e+01,1.226430200000000070e+01,
C64: 2.194866899999999887e+01,3.280028000000000077e+01,1.243556500000000042e+01,
2.114229800000000026e+01,3.314911899999999889e+01,1.307319900000000068e+01,
2.257564599999999899e+01,3.364029899999999884e+01,1.215229500000000051e+01,
2.153234600000000043e+01,3.233872099999999961e+01,1.154633100000000034e+01,
2.254484000000000066e+01,3.207123500000000149e+01,1.297444600000000037e+01,
C65: 2.618960999999999828e+01,3.287490199999999874e+01,1.248304899999999940e+01,
2.692785900000000154e+01,3.366287700000000171e+01,1.237195499999999981e+01,
2.620264200000000088e+01,3.223943799999999982e+01,1.160317399999999921e+01,
2.520409099999999825e+01,3.331682800000000100e+01,1.259565500000000071e+01,
2.642255899999999968e+01,3.228192700000000315e+01,1.336229999999999940e+01,
C66: 2.993620900000000162e+01,3.275727899999999693e+01,1.235977899999999963e+01,
2.988240400000000108e+01,3.167917500000000075e+01,1.246909699999999965e+01,
3.095439000000000007e+01,3.305212499999999665e+01,1.212720500000000001e+01,
2.962667799999999829e+01,3.322870699999999999e+01,1.328635700000000064e+01,
2.927178100000000072e+01,3.307308700000000101e+01,1.156331999999999915e+01,
C67: 3.413797999999999888e+01,3.295801900000000018e+01,1.254564500000000038e+01,
3.322488299999999839e+01,3.326594399999999752e+01,1.304596300000000042e+01,
3.472469199999999745e+01,3.383561499999999711e+01,1.229090500000000041e+01,
3.388970900000000341e+01,3.241266499999999695e+01,1.164026299999999914e+01,
3.471356300000000061e+01,3.231938199999999739e+01,1.320888599999999968e+01,
C68: 3.821120599999999712e+01,3.291248800000000330e+01,1.243101099999999981e+01,
3.896661399999999986e+01,3.304158699999999982e+01,1.320010800000000017e+01,
3.867268899999999832e+01,3.250950999999999880e+01,1.153536000000000072e+01,
3.775279599999999647e+01,3.387120500000000334e+01,1.220876900000000020e+01,
3.745043100000000180e+01,3.222382199999999841e+01,1.278477400000000053e+01,
C69: 4.203512099999999663e+01,3.276946000000000225e+01,1.236881799999999920e+01,
4.117027000000000214e+01,3.307476199999999977e+01,1.178896899999999981e+01,
4.284113099999999719e+01,3.348057699999999670e+01,1.221854500000000066e+01,
4.235270299999999821e+01,3.178218100000000135e+01,1.205195999999999934e+01,
4.176898700000000275e+01,3.274026099999999673e+01,1.342079900000000059e+01,
C70: 4.579671900000000306e+01,3.269469200000000342e+01,1.246537099999999931e+01,
4.522289800000000071e+01,3.354823900000000236e+01,1.211857299999999960e+01,
4.681931999999999761e+01,3.300358700000000312e+01,1.266089799999999954e+01,
4.579313599999999695e+01,3.192070199999999858e+01,1.170437199999999933e+01,
4.535551499999999692e+01,3.230917199999999667e+01,1.337932900000000025e+01,
C71: 1.151938700000000004e+01,3.674749700000000274e+01,1.245093999999999923e+01,
1.193093600000000087e+01,3.774645000000000294e+01,1.255026400000000031e+01,
1.229640200000000050e+01,3.606678899999999999e+01,1.211669400000000074e+01,
1.071033899999999939e+01,3.675872100000000131e+01,1.172736500000000071e+01,
1.113879500000000000e+01,3.641617200000000310e+01,1.341234500000000018e+01,
C72: 1.618990000000000151e+01,3.678598600000000118e+01,1.252298399999999923e+01,
1.526762399999999964e+01,3.645650799999999947e+01,1.205424299999999960e+01,
1.700379099999999966e+01,3.672954500000000166e+01,1.180760800000000010e+01,
1.641173099999999963e+01,3.614517500000000183e+01,1.337090000000000067e+01,
1.607795300000000083e+01,3.781002900000000011e+01,1.286154699999999984e+01,
C73: 1.988251700000000000e+01,3.595725000000000193e+01,1.241829500000000053e+01,
1.946101000000000170e+01,3.695738099999999804e+01,1.240150200000000069e+01,
2.093365999999999971e+01,3.601211099999999732e+01,1.268393900000000052e+01,
1.978005100000000027e+01,3.550123299999999915e+01,1.144004200000000004e+01,
1.935610199999999992e+01,3.535534599999999728e+01,1.315104499999999987e+01,
C74: 2.412147200000000069e+01,3.692217699999999780e+01,1.259657499999999963e+01,
2.427310599999999852e+01,3.625967899999999844e+01,1.344292800000000021e+01,
2.495997699999999853e+01,3.682598600000000033e+01,1.191413400000000067e+01,
2.405409399999999920e+01,3.794706999999999653e+01,1.294514000000000031e+01,
2.320070799999999878e+01,3.664756299999999811e+01,1.209140000000000015e+01,
C75: 2.825461500000000115e+01,3.648894500000000107e+01,1.242916999999999916e+01,
2.722359600000000057e+01,3.621766699999999872e+01,1.222642899999999955e+01,
2.871207300000000018e+01,3.572512100000000146e+01,1.305054100000000084e+01,
2.828086300000000008e+01,3.744123199999999940e+01,1.294889599999999952e+01,
2.879862299999999919e+01,3.656908599999999865e+01,1.149354199999999970e+01,
C76: 3.181602499999999978e+01,3.633286900000000230e+01,1.244138599999999961e+01,
3.267254799999999904e+01,3.697904499999999928e+01,1.260482799999999948e+01,
3.215562599999999804e+01,3.536520900000000012e+01,1.208571700000000071e+01,
3.116161999999999921e+01,3.678132500000000249e+01,1.170142700000000069e+01,
3.127665899999999866e+01,3.620648400000000322e+01,1.337481400000000065e+01,
C77: 3.581788800000000350e+01,3.704096499999999992e+01,1.256476699999999980e+01,
3.671090199999999726e+01,3.667649999999999721e+01,1.206643700000000052e+01,
3.558546799999999877e+01,3.638715599999999739e+01,1.339964100000000080e+01,
3.497637300000000238e+01,3.704723200000000105e+01,1.187957300000000060e+01,
3.598927900000000335e+01,3.804519499999999965e+01,1.293733699999999942e+01,
C78: 4.009629999999999939e+01,3.606404899999999714e+01,1.244659300000000002e+01,
4.061240000000000094e+01,3.701744200000000262e+01,1.248886599999999980e+01,
4.051961899999999872e+01,3.538913300000000106e+01,1.318281400000000048e+01,
4.021063199999999682e+01,3.563061499999999882e+01,1.145916199999999918e+01,
3.904184200000000260e+01,3.621408199999999766e+01,1.265652000000000044e+01,
C79: 4.372715999999999781e+01,3.668901499999999771e+01,1.245727100000000043e+01,
4.323633699999999891e+01,3.630439700000000158e+01,1.334595500000000001e+01,
4.419253299999999740e+01,3.764304099999999664e+01,1.268299999999999983e+01,
4.299280499999999705e+01,3.682237899999999797e+01,1.166938799999999965e+01,
4.448624999999999829e+01,3.598512199999999694e+01,1.212994199999999978e+01,
C80: 4.822145199999999932e+01,3.638015800000000155e+01,1.257512200000000036e+01,
4.881732900000000086e+01,3.727970899999999688e+01,1.269773400000000052e+01,
4.864445599999999814e+01,3.576973100000000017e+01,1.178333300000000072e+01,
4.720205500000000143e+01,3.665277700000000038e+01,1.231798900000000074e+01,
4.822072399999999703e+01,3.581549799999999806e+01,1.350244600000000084e+01,
C81: 9.754901000000000266e+00,3.989938999999999680e+01,1.236312399999999911e+01,
9.257438999999999751e+00,4.086257499999999965e+01,1.230190299999999937e+01,
1.033226299999999931e+01,3.972884400000000227e+01,1.146041899999999991e+01,
9.012479000000000795e+00,3.911450399999999661e+01,1.247214499999999937e+01,
1.041850999999999949e+01,3.989018399999999787e+01,1.322287299999999988e+01,
C82: 1.396552400000000027e+01,3.993995000000000317e+01,1.242151699999999970e+01,
1.299654100000000057e+01,4.001369400000000098e+01,1.193765299999999918e+01,
1.403015300000000032e+01,3.899940999999999747e+01,1.295890400000000042e+01,
1.408471800000000052e+01,4.076287899999999809e+01,1.311733199999999933e+01,
1.474966799999999978e+01,3.998571299999999695e+01,1.167281799999999947e+01,
C83: 1.812262899999999988e+01,3.980747600000000119e+01,1.236378999999999984e+01,
1.869276100000000085e+01,4.070410400000000095e+01,1.214282799999999973e+01,
1.807805799999999863e+01,3.917792000000000030e+01,1.148068800000000067e+01,
1.711651200000000017e+01,4.008591200000000043e+01,1.266206900000000068e+01,
1.860098999999999947e+01,3.926382999999999868e+01,1.317305200000000021e+01,
C84: 2.167642999999999986e+01,3.968345599999999962e+01,1.238210199999999972e+01,
2.131764199999999931e+01,3.978423599999999993e+01,1.340206200000000081e+01,
2.269987199999999916e+01,4.004048800000000341e+01,1.232204300000000075e+01,
2.104749800000000093e+01,4.026768400000000270e+01,1.171876800000000074e+01,
2.163787100000000052e+01,3.863954300000000330e+01,1.208750799999999970e+01,
C85: 2.613430400000000020e+01,4.006445500000000237e+01,1.240501199999999926e+01,
2.520682400000000101e+01,3.998864199999999869e+01,1.184593300000000049e+01,
2.607541499999999957e+01,4.090237900000000337e+01,1.309039800000000042e+01,
2.696019499999999880e+01,4.021990300000000218e+01,1.171842799999999940e+01,
2.629582100000000011e+01,3.914693799999999868e+01,1.296104899999999915e+01,
C86: 3.006792899999999946e+01,3.974187599999999776e+01,1.232378699999999938e+01,
3.043876900000000063e+01,4.075331500000000062e+01,1.218878699999999959e+01,
3.001210000000000022e+01,3.924343199999999854e+01,1.136094600000000021e+01,

2.908168399999999920e+01,3.977713800000000077e+01,1.277521400000000007e+01,
3.074180399999999835e+01,3.919487600000000072e+01,1.297623199999999954e+01,
C87: 3.374243799999999993e+01,4.013108799999999832e+01,1.241319799999999951e+01,
3.385162700000000058e+01,4.106568899999999900e+01,1.295268800000000020e+01,
3.467570800000000020e+01,3.989067299999999960e+01,1.191360399999999942e+01,
3.295112799999999709e+01,4.023192900000000094e+01,1.167750299999999974e+01,
3.349009199999999709e+01,3.933801400000000115e+01,1.310927299999999995e+01,
C88: 3.834050100000000327e+01,3.984926300000000055e+01,1.236346900000000026e+01,
3.864038099999999787e+01,4.056744199999999978e+01,1.311999699999999969e+01,
3.895530699999999769e+01,3.997818099999999930e+01,1.147839100000000023e+01,
3.729739500000000163e+01,4.000693600000000316e+01,1.210751300000000086e+01,
3.847133399999999881e+01,3.884308200000000255e+01,1.275006899999999987e+01,
C89: 4.186326999999999998e+01,3.976581900000000047e+01,1.238279299999999949e+01,
4.131035899999999828e+01,4.069212799999999675e+01,1.226286200000000015e+01,
4.181370400000000132e+01,3.918963099999999855e+01,1.146503900000000087e+01,
4.143160199999999804e+01,3.919105700000000070e+01,1.319658100000000012e+01,
4.290013299999999674e+01,3.999114000000000146e+01,1.261263100000000037e+01,
C90: 4.611902099999999649e+01,4.004332800000000248e+01,1.239350600000000036e+01,
4.527609300000000303e+01,3.976461499999999916e+01,1.176905000000000001e+01,
4.593246700000000260e+01,4.101290300000000144e+01,1.284158099999999969e+01,
4.702112400000000036e+01,4.008934899999999857e+01,1.179120299999999943e+01,
4.624828800000000228e+01,3.930258800000000008e+01,1.317657200000000017e+01,
C91: 1.189279699999999984e+01,4.301524200000000064e+01,1.245017099999999921e+01,
1.259753599999999985e+01,4.374949099999999902e+01,1.282750599999999963e+01,
1.215841700000000003e+01,4.274355099999999652e+01,1.143505000000000031e+01,
1.089306799999999953e+01,4.343901000000000323e+01,1.246079800000000048e+01,
1.191623599999999961e+01,4.213271300000000252e+01,1.308190600000000003e+01,
C92: 1.561405300000000018e+01,4.323646500000000259e+01,1.239709399999999917e+01,
1.643350300000000175e+01,4.394388699999999659e+01,1.248361300000000007e+01,
1.529044999999999987e+01,4.293482300000000151e+01,1.338749600000000051e+01,
1.594669000000000025e+01,4.236242000000000019e+01,1.184767699999999913e+01,
1.478608499999999992e+01,4.370356799999999708e+01,1.187453600000000087e+01,
C93: 2.040989799999999832e+01,4.320679799999999915e+01,1.252360499999999988e+01,
2.085042400000000029e+01,4.418220199999999664e+01,1.234388700000000050e+01,
2.022402999999999906e+01,4.271206999999999709e+01,1.157532899999999998e+01,
1.947133099999999928e+01,4.332732800000000140e+01,1.305647599999999997e+01,
2.108876700000000071e+01,4.260595699999999653e+01,1.312030200000000058e+01,
C94: 2.404419700000000049e+01,4.311841900000000294e+01,1.237797300000000078e+01,
2.493698799999999949e+01,4.353574900000000270e+01,1.192481300000000033e+01,
2.371142899999999898e+01,4.225756400000000212e+01,1.180891100000000016e+01,
2.326432399999999845e+01,4.387273499999999871e+01,1.239201399999999964e+01,
2.426678300000000021e+01,4.280971900000000119e+01,1.339369699999999952e+01,
C95: 2.783236099999999880e+01,4.331046700000000271e+01,1.252742800000000045e+01,
2.703226599999999991e+01,4.368771499999999719e+01,1.315665399999999963e+01,
2.852463799999999949e+01,4.411550499999999886e+01,1.229973700000000036e+01,
2.741573700000000002e+01,4.291693300000000022e+01,1.160599099999999950e+01,
2.835983699999999885e+01,4.251895100000000127e+01,1.305127300000000012e+01,
C96: 3.221536100000000147e+01,4.357912100000000066e+01,1.256236900000000034e+01,
3.182264899999999841e+01,4.278192899999999810e+01,1.318628799999999934e+01,
3.303687299999999993e+01,4.406696600000000075e+01,1.307680599999999949e+01,
3.143025799999999848e+01,4.430331100000000077e+01,1.236654500000000034e+01,
3.256715100000000263e+01,4.316153400000000000e+01,1.162457799999999963e+01,
C97: 3.594912099999999811e+01,4.314372099999999932e+01,1.236230800000000052e+01,
3.595105199999999712e+01,4.310555599999999998e+01,1.344511299999999920e+01,
3.676229500000000172e+01,4.377635200000000282e+01,1.202342100000000080e+01,
3.500903100000000023e+01,4.355606499999999670e+01,1.201438600000000001e+01,
3.607732000000000028e+01,4.214235899999999901e+01,1.196409599999999962e+01,
C98: 3.960470500000000271e+01,4.344920400000000171e+01,1.256307699999999983e+01,
4.052322300000000155e+01,4.385314699999999988e+01,1.297789999999999999e+01,
3.984422599999999903e+01,4.267772999999999683e+01,1.183757499999999929e+01,
3.904990399999999795e+01,4.424401900000000154e+01,1.207596400000000081e+01,
3.900403399999999721e+01,4.302450699999999983e+01,1.336107299999999931e+01,
C99: 4.376658700000000124e+01,4.300804899999999975e+01,1.249587999999999965e+01,
4.397499200000000030e+01,4.407198700000000002e+01,1.255699399999999955e+01,
4.429586199999999963e+01,4.258386500000000296e+01,1.164884099999999911e+01,
4.269922700000000049e+01,4.285546200000000283e+01,1.237202100000000016e+01,
4.409783399999999887e+01,4.252186700000000030e+01,1.340747600000000084e+01,
C100: 4.750563199999999853e+01,4.345481099999999941e+01,1.236544600000000038e+01,
4.716292500000000132e+01,4.320770900000000125e+01,1.336501600000000067e+01,
4.821245100000000150e+01,4.427732699999999966e+01,1.241969899999999960e+01,
4.665645500000000112e+01,4.374686899999999667e+01,1.175610099999999925e+01,
4.799090400000000045e+01,4.258914699999999698e+01,1.192599599999999960e+01,
C101: 1.027508699999999919e+01,4.707920800000000128e+01,1.248306799999999939e+01,
9.721140999999999366e+00,4.625974099999999822e+01,1.203511699999999962e+01,
1.070786799999999950e+01,4.674991200000000191e+01,1.342210999999999999e+01,
9.604729000000000738e+00,4.791427399999999892e+01,1.266203299999999921e+01,
1.106956500000000077e+01,4.738888000000000034e+01,1.181152999999999942e+01,
C102: 1.393525299999999945e+01,4.663082599999999900e+01,1.244448399999999921e+01,
1.490974300000000063e+01,4.682706199999999797e+01,1.201394900000000021e+01,
1.348466999999999949e+01,4.756495799999999718e+01,1.276590400000000081e+01,
1.404412899999999986e+01,4.596919900000000325e+01,1.329809299999999972e+01,
1.329891399999999990e+01,4.615682600000000235e+01,1.170455699999999943e+01,
C103: 1.772977900000000062e+01,4.731067399999999878e+01,1.249506500000000031e+01,
1.875308599999999970e+01,4.705943700000000263e+01,1.223202200000000062e+01,
1.707433999999999941e+01,4.708561699999999917e+01,1.166092199999999934e+01,
1.766613800000000012e+01,4.836607399999999757e+01,1.273762499999999953e+01,
1.742456699999999969e+01,4.672310699999999883e+01,1.335557799999999951e+01,
C104: 2.232735100000000017e+01,4.694599399999999889e+01,1.242066799999999915e+01,
2.210855400000000159e+01,4.796198600000000312e+01,1.273329700000000031e+01,
2.312189000000000050e+01,4.695709300000000042e+01,1.168164499999999961e+01,
2.143580400000000097e+01,4.650246899999999783e+01,1.198830500000000043e+01,
2.264016900000000021e+01,4.636136700000000133e+01,1.328049700000000044e+01,
C105: 2.594682999999999851e+01,4.662880899999999684e+01,1.248438900000000018e+01,
2.691214499999999887e+01,4.623060799999999659e+01,1.278061100000000039e+01,
2.602882999999999925e+01,4.770230600000000010e+01,1.235202499999999937e+01,
2.521597699999999875e+01,4.641538500000000056e+01,1.325699799999999939e+01,
2.563493499999999869e+01,4.616496500000000225e+01,1.155423299999999998e+01,
C106: 2.993164499999999961e+01,4.737062499999999687e+01,1.252266700000000021e+01,
2.907339800000000096e+01,4.716475599999999702e+01,1.189103300000000019e+01,
3.086691599999999980e+01,4.728491499999999803e+01,1.197860200000000042e+01,
2.994359800000000149e+01,4.665226200000000034e+01,1.333634499999999967e+01,
2.984691899999999976e+01,4.836094500000000096e+01,1.295346600000000059e+01,
C107: 3.414560199999999668e+01,4.686596699999999771e+01,1.241456400000000038e+01,
3.481823599999999885e+01,4.702650799999999975e+01,1.157884800000000070e+01,
3.398514300000000077e+01,4.780425199999999819e+01,1.293568400000000018e+01,
3.458173299999999983e+01,4.614336500000000285e+01,1.309754099999999966e+01,
3.319422999999999746e+01,4.649128799999999728e+01,1.205105400000000060e+01,
C108: 3.773608800000000230e+01,4.688932799999999901e+01,1.246744799999999920e+01,
3.741546600000000211e+01,4.788425999999999760e+01,1.275660300000000014e+01,
3.879544400000000337e+01,4.690644000000000347e+01,1.222982799999999948e+01,
3.717416699999999707e+01,4.655971199999999754e+01,1.160002000000000066e+01,
3.756371500000000196e+01,4.620088400000000206e+01,1.328907799999999995e+01,
C109: 4.227532200000000273e+01,4.708331199999999939e+01,1.250707700000000067e+01,
4.305194800000000299e+01,4.709433800000000048e+01,1.174944600000000072e+01,
4.201447399999999988e+01,4.810193100000000044e+01,1.277418100000000045e+01,
4.263746600000000342e+01,4.655878599999999778e+01,1.338631200000000021e+01,
4.139790299999999945e+01,4.657465499999999992e+01,1.211892699999999934e+01,
C110: 4.603649399999999758e+01,4.681418699999999689e+01,1.238427599999999984e+01,
4.547121500000000083e+01,4.609222400000000164e+01,1.180357399999999934e+01,
4.624341900000000294e+01,4.640282700000000204e+01,1.336738099999999996e+01,
4.546021100000000104e+01,4.772727900000000290e+01,1.249004399999999926e+01,
4.697409499999999838e+01,4.703165599999999813e+01,1.188189099999999954e+01,
C111: 1.156505899999999976e+01,5.046834100000000234e+01,1.238103800000000021e+01,
1.173581899999999933e+01,4.987681200000000104e+01,1.327576600000000084e+01,
1.215967200000000048e+01,5.137571799999999911e+01,1.242934999999999945e+01,
1.051258299999999934e+01,5.072733999999999810e+01,1.231369800000000048e+01,
1.185246500000000047e+01,4.989197200000000265e+01,1.150690900000000028e+01,
C112: 1.533641599999999983e+01,5.008720199999999778e+01,1.236064900000000044e+01,
1.538250999999999991e+01,5.109186400000000106e+01,1.277017400000000080e+01,
1.440939700000000023e+01,4.996356699999999762e+01,1.181043900000000058e+01,
1.537760600000000011e+01,4.936483400000000188e+01,1.317023499999999991e+01,
1.617645200000000116e+01,4.993115800000000348e+01,1.169068599999999947e+01,
C113: 1.996429099999999934e+01,5.027452799999999655e+01,1.237859000000000087e+01,
2.026214200000000076e+01,4.951124000000000080e+01,1.166719999999999935e+01,
1.897989000000000104e+01,5.065095300000000123e+01,1.211663099999999993e+01,
2.068229399999999885e+01,5.108893199999999979e+01,1.235887100000000061e+01,
1.993239000000000161e+01,4.984501699999999857e+01,1.337486600000000081e+01,
C114: 2.423198700000000017e+01,5.006548500000000246e+01,1.236217700000000086e+01,
2.480368700000000004e+01,5.089130300000000062e+01,1.195082400000000078e+01,
2.409658800000000056e+01,4.930390500000000031e+01,1.160148799999999980e+01,
2.326098400000000055e+01,5.042599500000000035e+01,1.268826600000000049e+01,
2.476268800000000047e+01,4.964300599999999974e+01,1.320997999999999983e+01,
C115: 2.788054299999999941e+01,5.034209800000000001e+01,1.242827199999999976e+01,
2.881805900000000165e+01,5.079390000000000072e+01,1.273621400000000037e+01,
2.804935100000000148e+01,4.969820200000000199e+01,1.157072800000000079e+01,
2.717614299999999972e+01,5.112415299999999974e+01,1.216280800000000006e+01,
2.747609200000000129e+01,4.975475099999999884e+01,1.324721100000000007e+01,
C116: 3.176704600000000056e+01,5.050055199999999900e+01,1.236776099999999978e+01,
3.137262700000000137e+01,5.027230699999999952e+01,1.335314299999999932e+01,
3.216208499999999759e+01,5.151193500000000114e+01,1.236275599999999919e+01,
3.097343400000000102e+01,5.041523800000000222e+01,1.163225800000000021e+01,
3.256093800000000016e+01,4.980068299999999937e+01,1.212640799999999963e+01,
C117: 3.578191000000000344e+01,5.017431799999999953e+01,1.238442700000000052e+01,
3.672412200000000126e+01,5.071319799999999844e+01,1.235505299999999984e+01,
3.577776000000000067e+01,4.941080900000000042e+01,1.161329500000000081e+01,
3.496367399999999748e+01,5.086700700000000097e+01,1.221210800000000063e+01,
3.566209700000000282e+01,4.970802700000000129e+01,1.335793699999999973e+01,
C118: 3.991642399999999924e+01,5.025313700000000239e+01,1.237922200000000039e+01,
4.090342199999999906e+01,5.020296199999999942e+01,1.193152000000000063e+01,
3.985490200000000272e+01,4.954334999999999667e+01,1.319834400000000052e+01,
3.916392499999999899e+01,5.001141400000000203e+01,1.163570600000000077e+01,
3.974096699999999771e+01,5.125648000000000337e+01,1.275505099999999992e+01,
C119: 4.394961099999999732e+01,5.035107200000000205e+01,1.241793200000000041e+01,
4.479964499999999816e+01,5.095598400000000083e+01,1.211853299999999933e+01,
4.358913900000000297e+01,4.978532100000000327e+01,1.156441200000000080e+01,
4.315776799999999724e+01,5.099823700000000315e+01,1.278305399999999992e+01,
4.424914799999999815e+01,4.966876700000000255e+01,1.320708899999999986e+01,
C120: 4.765114499999999964e+01,5.012534999999999741e+01,1.239237100000000069e+01,
4.734826199999999830e+01,5.116706800000000044e+01,1.234522499999999923e+01,
4.872957399999999950e+01,5.006666100000000341e+01,1.250550100000000064e+01,
4.735579299999999847e+01,4.961983399999999733e+01,1.147830399999999962e+01,
4.717210500000000195e+01,4.964814200000000000e+01,1.324221600000000088e+01,
C121: 8.192358999999999725e+00,1.055196199999999962e+01,1.587200600000000072e+01,
8.735481999999999303e+00,1.002499000000000073e+01,1.665077700000000149e+01,
8.860647999999999413e+00,1.075859200000000016e+01,1.504164100000000026e+01,
7.806363000000000163e+00,1.148635999999999946e+01,1.626830700000000007e+01,
7.366661999999999821e+00,9.936816999999999567e+00,1.552701500000000046e+01,
C122: 1.194894999999999996e+01,1.059152100000000019e+01,1.608517799999999909e+01,
1.185940199999999933e+01,1.167324699999999993e+01,1.608452399999999827e+01,
1.299903800000000054e+01,1.031600800000000007e+01,1.610882300000000100e+01,
1.148963999999999963e+01,1.019067000000000078e+01,1.518649199999999944e+01,
1.144863100000000067e+01,1.018678500000000042e+01,1.695984400000000036e+01,
C123: 1.635057400000000172e+01,1.060106599999999943e+01,1.596265600000000084e+01,
1.648898200000000003e+01,9.869070999999999927e+00,1.517255600000000015e+01,
1.545701200000000064e+01,1.118431999999999960e+01,1.576184499999999922e+01,
1.721116400000000013e+01,1.126102999999999987e+01,1.599705900000000014e+01,
1.624426499999999862e+01,1.009020199999999967e+01,1.691487899999999911e+01,
C124: 1.996916200000000075e+01,1.017341300000000004e+01,1.583892400000000045e+01,
2.097292300000000154e+01,9.762432999999999694e+00,1.588909899999999986e+01,
1.936743299999999834e+01,9.577436999999999756e+00,1.515921999999999947e+01,
2.001440200000000047e+01,1.119682399999999944e+01,1.547845799999999983e+01,
1.952193300000000065e+01,1.015694300000000005e+01,1.682822099999999921e+01,
C125: 2.396314999999999884e+01,1.105430300000000088e+01,1.611625700000000094e+01,
2.493579499999999882e+01,1.080130499999999927e+01,1.570553199999999983e+01,
2.319895999999999958e+01,1.088674199999999992e+01,1.536347600000000035e+01,
2.395644199999999913e+01,1.209906999999999933e+01,1.640969899999999981e+01,
2.376088899999999882e+01,1.043062699999999943e+01,1.698176499999999933e+01,
C126: 2.802255999999999858e+01,1.021403300000000058e+01,1.592909700000000051e+01,
2.867692600000000169e+01,1.041582900000000045e+01,1.677147499999999880e+01,
2.857469599999999943e+01,9.681931999999999761e+00,1.516071000000000006e+01,
2.765236399999999861e+01,1.115153399999999984e+01,1.552485899999999930e+01,
2.718511300000000119e+01,9.606794999999999973e+00,1.625945499999999910e+01,
C127: 3.174800199999999961e+01,1.034607500000000080e+01,1.587026299999999956e+01,
3.138839499999999916e+01,1.012613799999999920e+01,1.687093199999999982e+01,
3.257532299999999936e+01,1.104696900000000070e+01,1.592808899999999994e+01,
3.094571600000000089e+01,1.078269399999999933e+01,1.528409800000000018e+01,
3.208409699999999987e+01,9.428658999999999679e+00,1.539640400000000042e+01,
C128: 3.594458699999999851e+01,1.031033299999999997e+01,1.609121800000000135e+01,
3.581979900000000328e+01,1.138529699999999956e+01,1.600186599999999970e+01,
3.629075100000000020e+01,9.907396000000000313e+00,1.514403800000000011e+01,
3.499351300000000009e+01,9.856021999999999395e+00,1.635247299999999981e+01,
3.667452099999999859e+01,1.009369399999999928e+01,1.686548000000000158e+01,
C129: 4.000768300000000011e+01,1.010644300000000051e+01,1.585479600000000033e+01,
4.029422300000000234e+01,1.100523699999999927e+01,1.531678400000000018e+01,

4.077092300000000336e+01,9.345504999999999285e+00,1.572226399999999913e+01,
3.906132099999999951e+01,9.740883999999999432e+00,1.546767299999999956e+01,
3.990258999999999645e+01,1.033439699999999917e+01,1.691116099999999989e+01,
C130: 4.362367199999999912e+01,1.077008400000000066e+01,1.595866299999999960e+01,
4.415474900000000247e+01,1.161399699999999946e+01,1.638715300000000141e+01,
4.429631899999999689e+01,1.020881800000000084e+01,1.531694700000000076e+01,
4.278547700000000020e+01,1.113372500000000009e+01,1.537298599999999915e+01,
4.326016700000000270e+01,1.012634500000000060e+01,1.675396800000000042e+01,
C131: 4.812526799999999838e+01,1.049188700000000019e+01,1.608136500000000169e+01,
4.865448200000000156e+01,1.105201300000000053e+01,1.684661600000000092e+01,
4.884257499999999652e+01,1.000215900000000069e+01,1.542953499999999956e+01,
4.751005800000000079e+01,1.117042999999999964e+01,1.549759199999999915e+01,
4.749296900000000221e+01,9.744605999999999213e+00,1.655160300000000007e+01,
C132: 9.667030000000000456e+00,1.403629699999999936e+01,1.581772300000000087e+01,
8.714173000000000613e+00,1.404433299999999996e+01,1.633826600000000084e+01,
9.638308000000000320e+00,1.475147199999999970e+01,1.500146600000000063e+01,
9.855700000000000571e+00,1.304397100000000087e+01,1.542127900000000018e+01,
1.045995600000000003e+01,1.430370500000000078e+01,1.650773900000000083e+01,
C133: 1.379030799999999957e+01,1.436256400000000077e+01,1.600686800000000076e+01,
1.385717099999999924e+01,1.508614299999999986e+01,1.681353700000000018e+01,
1.393682000000000087e+01,1.486577600000000032e+01,1.505573500000000031e+01,
1.281147099999999917e+01,1.389410099999999915e+01,1.602034599999999998e+01,
1.455869200000000063e+01,1.360215499999999977e+01,1.613609500000000097e+01,
C134: 1.804283900000000074e+01,1.416239200000000054e+01,1.582919799999999988e+01,
1.708549899999999866e+01,1.388455500000000065e+01,1.561160199999999953e+01,
1.853946799999999939e+01,1.448897900000000050e+01,1.492199300000000051e+01,
1.857580300000000051e+01,1.331654699999999991e+01,1.625134999999999863e+01,
1.802749199999999874e+01,1.497713199999999922e+01,1.654517699999999891e+01,
C135: 2.157231799999999922e+01,1.406383600000000023e+01,1.585609299999999955e+01,
2.228029599999999988e+01,1.347307099999999913e+01,1.528351299999999924e+01,
2.091867299999999830e+01,1.340282099999999943e+01,1.641503399999999857e+01,
2.098156799999999933e+01,1.466844500000000018e+01,1.517778099999999952e+01,
2.211246699999999876e+01,1.470814599999999928e+01,1.654197699999999926e+01,
C136: 2.626338600000000056e+01,1.431221799999999966e+01,1.595415700000000037e+01,
2.605376800000000159e+01,1.505238499999999924e+01,1.672006599999999921e+01,
2.690518000000000143e+01,1.474649800000000077e+01,1.519557499999999983e+01,
2.533170300000000097e+01,1.399272999999999989e+01,1.549690099999999937e+01,
2.675966700000000031e+01,1.345668399999999920e+01,1.640124899999999997e+01,
C137: 2.998297300000000121e+01,1.380758100000000077e+01,1.580354799999999926e+01,
2.917882099999999923e+01,1.312028100000000030e+01,1.604541199999999890e+01,
2.962991399999999942e+01,1.453731600000000057e+01,1.508194100000000049e+01,
3.081442499999999995e+01,1.325510000000000055e+01,1.537789899999999932e+01,
3.031040700000000143e+01,1.431692100000000067e+01,1.670277899999999960e+01,
C138: 3.369392299999999807e+01,1.415884100000000068e+01,1.596204900000000038e+01,
3.456193700000000035e+01,1.359317700000000073e+01,1.563690599999999975e+01,
3.401011100000000198e+01,1.494280999999999970e+01,1.664336899999999986e+01,
3.299949199999999649e+01,1.349540999999999968e+01,1.646757300000000157e+01,
3.320926999999999651e+01,1.460182299999999955e+01,1.509817299999999918e+01,
C139: 3.833943599999999918e+01,1.387439200000000028e+01,1.590415400000000012e+01,
3.813199500000000342e+01,1.437006399999999928e+01,1.684566900000000089e+01,
3.864082299999999748e+01,1.461326700000000045e+01,1.517083099999999973e+01,
3.744165900000000136e+01,1.337096400000000074e+01,1.555823700000000009e+01,
3.913112999999999886e+01,1.314519100000000051e+01,1.603997700000000037e+01,
C140: 4.189191999999999894e+01,1.420743799999999979e+01,1.580554000000000059e+01,
4.187291700000000105e+01,1.503189899999999923e+01,1.651057700000000139e+01,
4.133765999999999963e+01,1.448176899999999989e+01,1.491515000000000057e+01,
4.144214699999999851e+01,1.332954800000000084e+01,1.625782900000000097e+01,
4.292020800000000236e+01,1.398587900000000062e+01,1.553681599999999996e+01,
C141: 4.623406500000000108e+01,1.441677999999999926e+01,1.597831900000000083e+01,
4.602930299999999875e+01,1.509410300000000049e+01,1.680119499999999988e+01,
4.715544100000000327e+01,1.387667199999999923e+01,1.617148699999999906e+01,
4.633155599999999907e+01,1.498500699999999952e+01,1.505842900000000029e+01,
4.541539600000000121e+01,1.371058500000000002e+01,1.587977799999999995e+01,
C142: 5.032333500000000015e+01,1.386376600000000003e+01,1.587293799999999955e+01,
5.013891600000000182e+01,1.476277100000000075e+01,1.645310100000000020e+01,
5.108400600000000225e+01,1.406577300000000008e+01,1.512473400000000012e+01,
4.940634800000000126e+01,1.355384300000000053e+01,1.538122899999999937e+01,
5.066488499999999817e+01,1.307155000000000022e+01,1.653249299999999877e+01,
C143: 8.129293000000000546e+00,1.740591799999999978e+01,1.595108699999999935e+01,
8.142887999999999238e+00,1.846644999999999825e+01,1.618393800000000127e+01,
8.684210000000000207e+00,1.722992999999999952e+01,1.503435600000000072e+01,
7.102750999999999593e+00,1.707647400000000104e+01,1.582143300000000075e+01,
8.587457999999999814e+00,1.685065399999999869e+01,1.676401500000000055e+01,
C144: 1.179675600000000024e+01,1.732867299999999844e+01,1.587049999999999983e+01,
1.240665599999999991e+01,1.751377899999999954e+01,1.674932099999999835e+01,
1.124302499999999938e+01,1.822758599999999873e+01,1.561791900000000055e+01,
1.110231300000000054e+01,1.652171699999999888e+01,1.607450499999999849e+01,
1.243825000000000003e+01,1.705526100000000156e+01,1.503842099999999959e+01,
C145: 1.600774099999999933e+01,1.737650299999999959e+01,1.587332800000000077e+01,
1.578365200000000002e+01,1.789826800000000162e+01,1.679856600000000100e+01,
1.604456199999999910e+01,1.630859600000000142e+01,1.605985499999999888e+01,
1.696703300000000070e+01,1.771054000000000173e+01,1.549001600000000067e+01,
1.523362799999999950e+01,1.758702500000000057e+01,1.514181699999999964e+01,
C146: 2.006297500000000156e+01,1.732965700000000098e+01,1.590348900000000043e+01,
1.996249299999999849e+01,1.677068799999999982e+01,1.497896399999999950e+01,
2.098718999999999824e+01,1.705079399999999978e+01,1.639895999999999825e+01,
1.921970299999999909e+01,1.711143799999999970e+01,1.655039599999999922e+01,
2.008110399999999984e+01,1.839085100000000139e+01,1.567844299999999969e+01,
C147: 2.410426999999999964e+01,1.745049600000000112e+01,1.582743600000000050e+01,
2.384840799999999916e+01,1.801567299999999960e+01,1.671796799999999985e+01,
2.518364800000000159e+01,1.736420299999999983e+01,1.575047400000000053e+01,
2.371995400000000132e+01,1.796184799999999981e+01,1.494998999999999967e+01,
2.366638999999999982e+01,1.645913200000000032e+01,1.588820899999999980e+01,
C148: 2.845254399999999961e+01,1.722567499999999896e+01,1.587534300000000087e+01,
2.755907699999999849e+01,1.736147100000000165e+01,1.647705000000000001e+01,
2.888401299999999949e+01,1.819574300000000022e+01,1.564726699999999937e+01,
2.819300700000000148e+01,1.672143600000000063e+01,1.495127899999999954e+01,
2.917215900000000062e+01,1.663084200000000124e+01,1.642775800000000064e+01,
C149: 3.209729999999999706e+01,1.732966100000000154e+01,1.589971399999999946e+01,
3.283373699999999928e+01,1.728976799999999869e+01,1.669642100000000084e+01,
3.260356399999999866e+01,1.740176900000000160e+01,1.494213300000000011e+01,
3.146114899999999892e+01,1.819859299999999891e+01,1.603837199999999896e+01,
3.149285799999999824e+01,1.642888900000000163e+01,1.591927599999999998e+01,
C150: 3.613353899999999896e+01,1.741951600000000155e+01,1.583539299999999983e+01,
3.606435599999999653e+01,1.791916900000000012e+01,1.679663599999999946e+01,
3.668737800000000249e+01,1.804413900000000126e+01,1.514093699999999920e+01,
3.513673800000000114e+01,1.724148999999999887e+01,1.544421900000000036e+01,
3.664628400000000141e+01,1.647044100000000100e+01,1.595677599999999963e+01,
C151: 3.978864500000000248e+01,1.728427900000000150e+01,1.588231500000000018e+01,
3.907106000000000279e+01,1.676858500000000163e+01,1.651177099999999953e+01,
3.993732399999999672e+01,1.672355999999999909e+01,1.496533499999999961e+01,
4.073355200000000309e+01,1.737391799999999975e+01,1.640748599999999868e+01,
3.941092100000000187e+01,1.827267900000000012e+01,1.564168199999999942e+01,
C152: 4.398796999999999713e+01,1.731546799999999919e+01,1.587167299999999948e+01,
4.396815200000000345e+01,1.630765600000000148e+01,1.547024799999999978e+01,
4.408321399999999812e+01,1.802525299999999930e+01,1.505547299999999922e+01,
4.483294699999999722e+01,1.742023700000000019e+01,1.654525399999999991e+01,
4.306784900000000249e+01,1.750771400000000000e+01,1.641373099999999852e+01,
C153: 4.835350999999999999e+01,1.730976199999999920e+01,1.588778100000000038e+01,
4.742802700000000016e+01,1.725391099999999867e+01,1.645271800000000084e+01,
4.852026899999999898e+01,1.637029899999999927e+01,1.537039299999999997e+01,
4.917990499999999798e+01,1.750149800000000155e+01,1.656561699999999959e+01,
4.828736800000000073e+01,1.811439800000000133e+01,1.516155700000000017e+01,
C154: 1.028778400000000026e+01,2.116890799999999828e+01,1.602697099999999963e+01,
9.678769000000000844e+00,2.045291200000000131e+01,1.548339400000000055e+01,
9.654602000000000572e+00,2.174876499999999879e+01,1.669153700000000029e+01,
1.077748199999999912e+01,2.183231999999999928e+01,1.532193700000000014e+01,
1.103647199999999984e+01,2.063783199999999951e+01,1.660569900000000132e+01,
C155: 1.392219700000000060e+01,2.050616899999999987e+01,1.576780699999999946e+01,
1.308901799999999938e+01,2.079181399999999869e+01,1.513371300000000019e+01,
1.484550600000000031e+01,2.059571100000000143e+01,1.520422499999999921e+01,
1.379507199999999933e+01,1.947842400000000040e+01,1.609018000000000015e+01,
1.396085199999999915e+01,2.116426299999999827e+01,1.662978899999999882e+01,
C156: 1.773584500000000119e+01,2.072991299999999981e+01,1.602712999999999965e+01,
1.788477100000000064e+01,2.167272099999999924e+01,1.654460699999999918e+01,
1.691735500000000059e+01,2.018759700000000024e+01,1.648902800000000113e+01,
1.864518999999999949e+01,2.014095700000000022e+01,1.608350099999999827e+01,
1.749763400000000146e+01,2.092440500000000014e+01,1.498619300000000010e+01,
C157: 2.221731000000000122e+01,2.069028799999999890e+01,1.594015100000000018e+01,
2.283871299999999849e+01,2.059676599999999880e+01,1.682461299999999937e+01,
2.270024799999999843e+01,2.135043200000000141e+01,1.522642699999999927e+01,
2.125035300000000049e+01,2.110100100000000012e+01,1.621203300000000169e+01,
2.208005500000000154e+01,1.971236499999999836e+01,1.549066400000000066e+01,
C158: 2.588393400000000000e+01,2.057256299999999882e+01,1.582502700000000040e+01,
2.555967899999999915e+01,2.110107400000000055e+01,1.671501200000000154e+01,
2.634426500000000004e+01,1.962808499999999867e+01,1.609639500000000112e+01,
2.660590300000000141e+01,2.118144399999999905e+01,1.528913999999999973e+01,
2.502826200000000156e+01,2.038540899999999922e+01,1.518450999999999951e+01,
C159: 2.991980300000000170e+01,2.142074699999999865e+01,1.607459899999999919e+01,
2.999108100000000121e+01,2.237936200000000042e+01,1.657786400000000171e+01,
2.972086799999999940e+01,2.158293499999999909e+01,1.501998399999999911e+01,
2.911150599999999855e+01,2.083885300000000029e+01,1.650644300000000086e+01,
3.085431099999999915e+01,2.088003900000000002e+01,1.618588300000000046e+01,
C160: 3.407354099999999875e+01,2.041560399999999831e+01,1.582324099999999945e+01,
3.421430900000000008e+01,2.107642500000000041e+01,1.667195999999999856e+01,
3.412143799999999771e+01,1.938163199999999975e+01,1.614348199999999878e+01,
3.484996100000000041e+01,2.060145500000000141e+01,1.508845400000000048e+01,
3.310481300000000005e+01,2.060741099999999904e+01,1.537218400000000074e+01,
C161: 3.765908000000000300e+01,2.100073799999999835e+01,1.594098699999999980e+01,
3.718513300000000044e+01,2.118710099999999841e+01,1.498217499999999980e+01,
3.862100699999999875e+01,2.052513199999999927e+01,1.577927700000000044e+01,
3.702871199999999874e+01,2.035058199999999928e+01,1.653936300000000159e+01,
3.780658900000000244e+01,2.194212800000000030e+01,1.646028199999999941e+01,
C162: 4.183187300000000164e+01,2.056178799999999995e+01,1.602861400000000103e+01,
4.172585800000000233e+01,2.094395099999999843e+01,1.501788600000000073e+01,
4.270649600000000135e+01,1.992248800000000131e+01,1.608278200000000169e+01,
4.194877300000000275e+01,2.139451999999999998e+01,1.671491299999999924e+01,
4.094543699999999831e+01,1.999560999999999922e+01,1.629384599999999850e+01,
C163: 4.601517900000000338e+01,2.038951700000000145e+01,1.578108300000000064e+01,
4.502172399999999897e+01,2.041899599999999992e+01,1.534422700000000006e+01,
4.603077600000000302e+01,2.099475500000000139e+01,1.668060399999999888e+01,
4.673027499999999890e+01,2.078851999999999833e+01,1.506940499999999972e+01,
4.627389300000000105e+01,1.936402500000000160e+01,1.602054000000000045e+01,
C164: 4.953448999999999813e+01,2.126769099999999924e+01,1.598590300000000042e+01,
4.889142499999999814e+01,2.063900399999999991e+01,1.659422700000000006e+01,
5.037441700000000111e+01,2.068168100000000109e+01,1.562497100000000039e+01,
4.990285999999999689e+01,2.209569300000000069e+01,1.658407100000000156e+01,
4.897408099999999820e+01,2.165313499999999891e+01,1.513970400000000005e+01,
C165: 7.950363000000000291e+00,2.463755400000000151e+01,1.594835999999999920e+01,
8.807767000000000124e+00,2.449034699999999987e+01,1.659849200000000025e+01,
7.351244000000000334e+00,2.546317200000000014e+01,1.632075400000000087e+01,
7.350297000000000303e+00,2.373263400000000090e+01,1.593085899999999988e+01,
8.294079999999999231e+00,2.486359399999999908e+01,1.494320699999999924e+01,
C166: 1.208965000000000067e+01,2.445758700000000019e+01,1.582570399999999999e+01,
1.121158800000000078e+01,2.423725100000000054e+01,1.522625999999999991e+01,
1.179462999999999973e+01,2.503837100000000149e+01,1.669323100000000082e+01,
1.279536000000000051e+01,2.502593200000000095e+01,1.523060000000000080e+01,
1.255115999999999943e+01,2.352909400000000062e+01,1.614721000000000117e+01,
C167: 1.567354899999999951e+01,2.416804300000000083e+01,1.582371999999999979e+01,
1.488416800000000073e+01,2.421296600000000154e+01,1.656475199999999859e+01,
1.663932199999999995e+01,2.418226900000000157e+01,1.631948500000000024e+01,
1.559833700000000078e+01,2.502095299999999867e+01,1.515735199999999949e+01,
1.557577399999999912e+01,2.325066999999999950e+01,1.525205799999999989e+01,
C168: 2.018228099999999969e+01,2.449468399999999946e+01,1.598388399999999976e+01,
2.005712799999999874e+01,2.524953800000000115e+01,1.675424299999999889e+01,
2.048703599999999980e+01,2.496841699999999875e+01,1.505549899999999930e+01,
1.924130699999999905e+01,2.397438100000000105e+01,1.583167000000000080e+01,
2.094188700000000125e+01,2.378367199999999926e+01,1.629364500000000149e+01,
C169: 2.409491099999999975e+01,2.425964199999999948e+01,1.579562100000000058e+01,
2.385024599999999850e+01,2.477781900000000093e+01,1.671688899999999833e+01,
2.447999400000000136e+01,2.497168999999999883e+01,1.507331899999999969e+01,
2.320048800000000000e+01,2.379077699999999851e+01,1.539812700000000056e+01,
2.484417200000000037e+01,2.349943299999999979e+01,1.599225099999999955e+01,
C170: 2.778553300000000092e+01,2.453727299999999900e+01,1.589545500000000011e+01,
2.802846900000000119e+01,2.516262599999999949e+01,1.674869800000000097e+01,
2.869785900000000112e+01,2.428409200000000112e+01,1.536367599999999989e+01,
2.711941399999999902e+01,2.507388999999999868e+01,1.522812300000000008e+01,
2.730094300000000018e+01,2.362736400000000003e+01,1.623505600000000015e+01,
C171: 3.246775800000000345e+01,2.428644900000000106e+01,1.588892599999999966e+01,
3.214277200000000079e+01,2.493729499999999888e+01,1.669466900000000109e+01,
3.309455299999999767e+01,2.484373199999999926e+01,1.520063500000000012e+01,
3.159852700000000070e+01,2.391239900000000063e+01,1.535666800000000087e+01,
3.302761100000000027e+01,2.345123999999999853e+01,1.629781200000000041e+01,
C172: 3.597815500000000100e+01,2.433989100000000150e+01,1.579519999999999946e+01,

3.685431299999999766e+01,2.425940599999999847e+01,1.643063899999999933e+01,
3.540446399999999727e+01,2.342005599999999887e+01,1.584981200000000001e+01,
3.629628399999999999e+01,2.450625300000000095e+01,1.477132300000000065e+01,
3.536788599999999860e+01,2.517441799999999930e+01,1.612483999999999895e+01,
C173: 4.017917099999999664e+01,2.458626900000000148e+01,1.596736800000000045e+01,
3.992237800000000192e+01,2.522170699999999854e+01,1.680925500000000028e+01,
4.116690200000000033e+01,2.416217400000000026e+01,1.612095499999999859e+01,
4.017537200000000297e+01,2.517418800000000090e+01,1.505457600000000085e+01,
3.945109000000000066e+01,2.378522999999999854e+01,1.588292500000000018e+01,
C174: 4.443119999999999692e+01,2.388247000000000142e+01,1.585281100000000087e+01,
4.482345800000000224e+01,2.415977000000000174e+01,1.487989699999999971e+01,
4.359365799999999780e+01,2.320383800000000107e+01,1.572312499999999957e+01,
4.409709399999999846e+01,2.477273399999999981e+01,1.637617499999999993e+01,
4.520798800000000028e+01,2.339136600000000143e+01,1.642933499999999825e+01,
C175: 4.800364600000000337e+01,2.459393899999999888e+01,1.583682199999999973e+01,
4.794430400000000247e+01,2.503826600000000013e+01,1.682496799999999837e+01,
4.757357600000000275e+01,2.527311900000000122e+01,1.510801000000000016e+01,
4.746085399999999765e+01,2.365429500000000118e+01,1.582235099999999939e+01,
4.904446000000000083e+01,2.441226800000000097e+01,1.558648499999999970e+01,
C176: 9.709623999999999810e+00,2.783130299999999835e+01,1.581072600000000072e+01,
1.047679499999999919e+01,2.833729599999999849e+01,1.638817200000000085e+01,
9.560508999999999702e+00,2.835546599999999984e+01,1.487159600000000026e+01,
8.780450999999999340e+00,2.782214700000000107e+01,1.637255899999999897e+01,
1.002361999999999931e+01,2.681140200000000107e+01,1.561284099999999953e+01,
C177: 1.394322200000000045e+01,2.757212000000000174e+01,1.593238999999999983e+01,
1.422449100000000044e+01,2.861696600000000146e+01,1.601826399999999850e+01,
1.385310800000000064e+01,2.731066200000000066e+01,1.488278799999999968e+01,
1.299123400000000039e+01,2.741063700000000125e+01,1.642858400000000074e+01,
1.470619399999999999e+01,2.695540000000000092e+01,1.639534499999999895e+01,
C178: 1.780503699999999867e+01,2.747594000000000136e+01,1.586118899999999954e+01,
1.872227600000000081e+01,2.747192999999999842e+01,1.644172000000000011e+01,
1.795522800000000174e+01,2.804732299999999867e+01,1.495012799999999942e+01,
1.701079500000000166e+01,2.793056100000000086e+01,1.644468900000000033e+01,
1.753426500000000132e+01,2.645576099999999897e+01,1.561081800000000008e+01,
C179: 2.180581600000000009e+01,2.767268699999999981e+01,1.585045500000000018e+01,
2.129885200000000012e+01,2.786646299999999954e+01,1.679018100000000047e+01,
2.247617400000000032e+01,2.849616200000000177e+01,1.562314100000000039e+01,
2.107010999999999967e+01,2.757610999999999990e+01,1.505798200000000087e+01,
2.237648300000000035e+01,2.675276300000000163e+01,1.592689400000000077e+01,
C180: 2.575069799999999987e+01,2.758884000000000114e+01,1.595602000000000054e+01,
2.663285000000000124e+01,2.733874899999999997e+01,1.653715299999999999e+01,
2.584119499999999903e+01,2.716876800000000003e+01,1.495919899999999991e+01,
2.566117799999999960e+01,2.866840399999999889e+01,1.588404399999999939e+01,
2.486816400000000016e+01,2.718479999999999919e+01,1.644162800000000146e+01,
C181: 2.993984999999999985e+01,2.766113899999999859e+01,1.580854500000000051e+01,
2.979098799999999869e+01,2.822218399999999860e+01,1.672574499999999986e+01,
3.056077700000000164e+01,2.823950599999999866e+01,1.513173800000000035e+01,
2.897762200000000021e+01,2.747311099999999939e+01,1.534177000000000035e+01,
3.042542999999999864e+01,2.671549200000000113e+01,1.602851499999999874e+01,
C182: 3.355408500000000060e+01,2.784585799999999978e+01,1.592684299999999986e+01,
3.289709799999999973e+01,2.736580299999999966e+01,1.664526100000000142e+01,
3.435297899999999771e+01,2.835855499999999907e+01,1.645328100000000049e+01,
3.298921500000000151e+01,2.856411500000000103e+01,1.534221600000000052e+01,
3.398061299999999818e+01,2.709841000000000122e+01,1.526521400000000028e+01,
C183: 3.781517999999999802e+01,2.752745600000000081e+01,1.586210200000000015e+01,
3.781108600000000308e+01,2.825710799999999878e+01,1.505818200000000040e+01,
3.853338899999999967e+01,2.782826499999999825e+01,1.661815700000000007e+01,
3.808996900000000352e+01,2.655525700000000100e+01,1.546709599999999973e+01,
3.682353499999999968e+01,2.747218000000000160e+01,1.630026099999999900e+01,
C184: 4.188231400000000093e+01,2.769078999999999979e+01,1.582939400000000063e+01,
4.127514999999999645e+01,2.759550300000000078e+01,1.672425899999999999e+01,
4.255177700000000129e+01,2.853881900000000016e+01,1.593322000000000038e+01,
4.123728599999999744e+01,2.784169899999999842e+01,1.496889600000000087e+01,
4.246489400000000103e+01,2.678517499999999885e+01,1.568955500000000036e+01,
C185: 4.559852800000000173e+01,2.744827199999999934e+01,1.588065399999999983e+01,
4.483810600000000335e+01,2.741619899999999888e+01,1.665427700000000044e+01,
4.543232100000000173e+01,2.663901200000000102e+01,1.517766300000000079e+01,
4.658101400000000325e+01,2.734437600000000046e+01,1.633057900000000018e+01,
4.554073799999999750e+01,2.839821299999999837e+01,1.535785399999999967e+01,
C186: 5.011434100000000313e+01,2.762201800000000063e+01,1.585638400000000026e+01,
5.077766900000000305e+01,2.848173800000000000e+01,1.586954099999999990e+01,
5.050878000000000156e+01,2.684920299999999926e+01,1.650944199999999995e+01,
5.003961900000000185e+01,2.723720799999999898e+01,1.484357600000000055e+01,
4.912915300000000229e+01,2.792005800000000093e+01,1.620280100000000090e+01,
C187: 8.216143000000000640e+00,3.111320800000000020e+01,1.587730299999999950e+01,
8.621102000000000487e+00,3.057878499999999988e+01,1.673120499999999969e+01,
9.008051999999999282e+00,3.130575500000000133e+01,1.516026300000000049e+01,
7.789283000000000179e+00,3.205478699999999748e+01,1.620909699999999987e+01,
7.443646000000000207e+00,3.051123899999999978e+01,1.540818000000000088e+01,
C188: 1.200236899999999984e+01,3.124515200000000092e+01,1.606931000000000154e+01,
1.187184700000000070e+01,3.169945399999999935e+01,1.509200500000000034e+01,
1.114781900000000014e+01,3.061526399999999981e+01,1.629208799999999968e+01,
1.208719499999999947e+01,3.202432499999999749e+01,1.681974400000000003e+01,
1.290673899999999996e+01,3.064496199999999959e+01,1.606719500000000167e+01,
C189: 1.639847500000000124e+01,3.142004499999999823e+01,1.595918099999999917e+01,
1.688637999999999906e+01,3.167127899999999840e+01,1.502265700000000059e+01,
1.545767900000000061e+01,3.091990900000000053e+01,1.575007300000000043e+01,
1.620465599999999995e+01,3.232813399999999859e+01,1.652100899999999939e+01,
1.703586800000000068e+01,3.076061199999999829e+01,1.653951899999999853e+01,
C190: 1.984309899999999871e+01,3.067493800000000093e+01,1.578085199999999944e+01,
2.084946899999999914e+01,3.062144100000000080e+01,1.537760699999999936e+01,
1.952573699999999945e+01,2.968515100000000118e+01,1.608675699999999864e+01,
1.917474800000000101e+01,3.104698000000000135e+01,1.501167300000000004e+01,
1.982808599999999899e+01,3.135184999999999889e+01,1.662818000000000040e+01,
C191: 2.380425999999999931e+01,3.152950099999999978e+01,1.608874000000000137e+01,
2.295133799999999979e+01,3.098113100000000131e+01,1.647581100000000021e+01,
2.396245899999999907e+01,3.242391099999999682e+01,1.668335899999999938e+01,
2.361690700000000120e+01,3.181035599999999874e+01,1.505722500000000075e+01,
2.469058700000000073e+01,3.090433099999999911e+01,1.613577000000000092e+01,
C192: 2.824049000000000120e+01,3.139777799999999885e+01,1.589362200000000058e+01,
2.801389400000000052e+01,3.223724599999999896e+01,1.654245699999999886e+01,
2.877768500000000174e+01,3.174821000000000026e+01,1.501825499999999991e+01,
2.731434399999999840e+01,3.092386799999999880e+01,1.558257399999999926e+01,
2.885051800000000100e+01,3.067779399999999868e+01,1.642965799999999987e+01,
C193: 3.180837100000000106e+01,3.129061099999999840e+01,1.589654999999999951e+01,
3.125758599999999987e+01,3.039416699999999949e+01,1.616137000000000157e+01,
3.284204600000000340e+01,3.103325600000000151e+01,1.568566000000000038e+01,
3.177481900000000081e+01,3.199714399999999870e+01,1.671903700000000015e+01,
3.136231099999999827e+01,3.174086000000000141e+01,1.501533599999999957e+01,
C194: 3.640897999999999968e+01,3.133107800000000154e+01,1.606972299999999976e+01,
3.723849799999999988e+01,3.083265099999999848e+01,1.656113799999999969e+01,
3.561777099999999763e+01,3.061332300000000117e+01,1.587453900000000040e+01,
3.674897399999999692e+01,3.175599000000000061e+01,1.513034299999999988e+01,
3.603101600000000104e+01,3.212315100000000001e+01,1.670884699999999867e+01,
C195: 4.016835600000000284e+01,3.083529700000000062e+01,1.582073300000000060e+01,
4.053344299999999834e+01,3.126747800000000055e+01,1.674638699999999858e+01,
3.947941600000000051e+01,3.152666699999999977e+01,1.534547700000000070e+01,
3.965627400000000335e+01,2.990175500000000142e+01,1.602783900000000017e+01,
4.100388900000000092e+01,3.064736699999999914e+01,1.515383199999999952e+01,
C196: 4.379603900000000039e+01,3.140130600000000172e+01,1.598954600000000070e+01,
4.399741600000000119e+01,3.234979400000000282e+01,1.647696300000000136e+01,
4.472115600000000057e+01,3.084125099999999975e+01,1.589097600000000021e+01,
4.337812399999999968e+01,3.158480000000000132e+01,1.500469299999999961e+01,
4.308783600000000291e+01,3.083140300000000167e+01,1.658152099999999862e+01,
C197: 4.863297000000000025e+01,3.133817399999999864e+01,1.594069499999999984e+01,
4.953662899999999780e+01,3.102379799999999932e+01,1.645431400000000011e+01,
4.889821500000000043e+01,3.185351299999999952e+01,1.502232399999999934e+01,
4.806643799999999800e+01,3.200797599999999932e+01,1.658086399999999827e+01,
4.802897099999999853e+01,3.046722600000000014e+01,1.570368200000000058e+01,
C198: 9.674531999999999243e+00,3.453676600000000008e+01,1.581247800000000048e+01,
8.713984999999999204e+00,3.443328199999999839e+01,1.630809599999999904e+01,
1.030340400000000045e+01,3.521455000000000268e+01,1.638143699999999825e+01,
9.525391000000000830e+00,3.493443899999999758e+01,1.481310099999999963e+01,
1.015601400000000076e+01,3.356646299999999883e+01,1.574736500000000028e+01,
C199: 1.363896300000000039e+01,3.490894399999999820e+01,1.590256800000000048e+01,
1.392439199999999921e+01,3.554663800000000151e+01,1.673322800000000043e+01,
1.351747499999999924e+01,3.551068200000000274e+01,1.500672400000000017e+01,
1.270301000000000080e+01,3.441091300000000075e+01,1.613498299999999830e+01,
1.441214699999999915e+01,3.416487000000000052e+01,1.573573799999999956e+01,
C200: 1.796466600000000113e+01,3.470608699999999658e+01,1.581193200000000054e+01,
1.706988600000000034e+01,3.442846600000000024e+01,1.526299700000000037e+01,
1.860482999999999976e+01,3.383636200000000116e+01,1.592046599999999934e+01,
1.768383800000000150e+01,3.507951599999999814e+01,1.679131299999999882e+01,
1.849180700000000144e+01,3.548064099999999854e+01,1.526641799999999982e+01,
C201: 2.157204400000000177e+01,3.448581000000000074e+01,1.583572500000000005e+01,
2.251052599999999870e+01,3.422289200000000164e+01,1.535716000000000037e+01,
2.103540800000000033e+01,3.358100600000000213e+01,1.610259500000000088e+01,
2.097221800000000158e+01,3.507253299999999996e+01,1.514797300000000035e+01,
2.177531700000000114e+01,3.506827899999999687e+01,1.672869999999999990e+01,
C202: 2.609778100000000123e+01,3.493709100000000234e+01,1.588815499999999936e+01,
2.519574799999999826e+01,3.509797300000000320e+01,1.647069600000000023e+01,
2.608853500000000025e+01,3.558265500000000259e+01,1.501521900000000009e+01,
2.614095100000000116e+01,3.389990300000000190e+01,1.556968499999999977e+01,
2.696695599999999970e+01,3.516387900000000144e+01,1.649706000000000117e+01,
C203: 3.007397900000000135e+01,3.466246499999999742e+01,1.581228800000000057e+01,
3.074648900000000040e+01,3.409309900000000226e+01,1.517880199999999924e+01,
2.911039500000000046e+01,3.416769200000000239e+01,1.586158999999999963e+01,
2.994522900000000121e+01,3.565770799999999952e+01,1.539801800000000043e+01,
3.049616299999999924e+01,3.474134200000000305e+01,1.680804600000000093e+01,
C204: 3.385125299999999982e+01,3.485324200000000161e+01,1.590177699999999916e+01,
3.398007299999999731e+01,3.554180000000000206e+01,1.673084100000000163e+01,
3.480613900000000172e+01,3.439732300000000009e+01,1.565799299999999938e+01,
3.347653400000000090e+01,3.539173900000000117e+01,1.503656499999999951e+01,
3.314289999999999736e+01,3.407983600000000024e+01,1.618139299999999992e+01,
C205: 3.834144799999999975e+01,3.459416399999999925e+01,1.584718699999999991e+01,
3.736133199999999732e+01,3.415888799999999748e+01,1.567994299999999974e+01,
3.867293999999999699e+01,3.508909500000000037e+01,1.494014899999999990e+01,
3.904568600000000345e+01,3.381249700000000047e+01,1.611188800000000043e+01,
3.827947499999999792e+01,3.531910999999999645e+01,1.665248700000000071e+01,
C206: 4.193555200000000127e+01,3.460161099999999834e+01,1.580869999999999997e+01,
4.276927500000000038e+01,3.447887200000000263e+01,1.512401099999999943e+01,
4.149085800000000290e+01,3.363254799999999989e+01,1.601097599999999943e+01,
4.119474499999999750e+01,3.525178900000000226e+01,1.535851000000000077e+01,
4.229150299999999874e+01,3.504158999999999935e+01,1.673469899999999910e+01,
C207: 4.598707100000000025e+01,3.478479200000000304e+01,1.591870100000000043e+01,
4.669125499999999818e+01,3.503479500000000257e+01,1.670588199999999901e+01,
4.618379199999999685e+01,3.377696600000000160e+01,1.556545000000000023e+01,
4.609611900000000162e+01,3.548402999999999707e+01,1.509512699999999974e+01,
4.497580700000000320e+01,3.483946900000000113e+01,1.630937300000000079e+01,
C208: 5.028649999999999665e+01,3.465103100000000325e+01,1.584251000000000076e+01,
5.061094400000000348e+01,3.547525600000000168e+01,1.647079199999999943e+01,
5.039667000000000030e+01,3.492673099999999664e+01,1.479791699999999999e+01,
4.924418299999999959e+01,3.442754599999999954e+01,1.604926899999999890e+01,
5.089296999999999827e+01,3.377494300000000038e+01,1.605208899999999872e+01,
C209: 8.323772999999999200e+00,3.788644899999999893e+01,1.601723499999999945e+01,
8.075189999999999202e+00,3.893048999999999893e+01,1.618276900000000040e+01,
7.440030000000000143e+00,3.735210099999999755e+01,1.568158799999999964e+01,
8.681383000000000294e+00,3.744801100000000105e+01,1.694394300000000086e+01,
9.098748000000000502e+00,3.781515199999999766e+01,1.525976499999999980e+01,
C210: 1.221252499999999941e+01,3.823533499999999918e+01,1.586620899999999956e+01,
1.295240100000000005e+01,3.816428700000000163e+01,1.665717199999999920e+01,
1.271220199999999956e+01,3.840072200000000180e+01,1.491714799999999919e+01,
1.154219200000000001e+01,3.906437100000000129e+01,1.606867799999999846e+01,
1.164213600000000071e+01,3.731293200000000354e+01,1.581801300000000055e+01,
C211: 1.590061000000000035e+01,3.790051499999999862e+01,1.582417300000000004e+01,
1.514290100000000017e+01,3.811501899999999665e+01,1.507756200000000035e+01,
1.687595800000000068e+01,3.817932799999999816e+01,1.543696399999999969e+01,
1.589253099999999996e+01,3.684015000000000128e+01,1.605282700000000062e+01,
1.569157399999999924e+01,3.847342199999999934e+01,1.672147999999999968e+01,
C212: 2.002295700000000167e+01,3.781810500000000275e+01,1.598099500000000006e+01,
2.004085299999999847e+01,3.890281300000000186e+01,1.593581999999999965e+01,
2.010325999999999880e+01,3.741596799999999945e+01,1.497625799999999963e+01,
1.909022399999999919e+01,3.749249300000000318e+01,1.643014499999999956e+01,
2.085883600000000015e+01,3.746919700000000120e+01,1.657909000000000077e+01,
C213: 2.384023399999999882e+01,3.788015200000000249e+01,1.580272000000000077e+01,
2.308987399999999823e+01,3.830437799999999982e+01,1.514239700000000077e+01,
2.478236400000000117e+01,3.780660799999999711e+01,1.527112900000000018e+01,
2.352230799999999888e+01,3.689029800000000137e+01,1.611409199999999942e+01,
2.396068800000000110e+01,3.852436800000000261e+01,1.666776499999999928e+01,
C214: 2.753618399999999866e+01,3.827341200000000043e+01,1.592145400000000066e+01,
2.681942099999999840e+01,3.799016600000000210e+01,1.668589199999999906e+01,
2.819654999999999845e+01,3.904155300000000040e+01,1.631155400000000100e+01,
2.701007299999999844e+01,3.865873100000000306e+01,1.505486800000000081e+01,
2.812246000000000024e+01,3.740629299999999802e+01,1.563317400000000035e+01,

C215: 3.251833100000000343e+01,3.823973500000000314e+01,1.591331100000000021e+01,
3.320600300000000260e+01,3.808495299999999872e+01,1.673879000000000161e+01,
3.302296499999999924e+01,3.803373299999999801e+01,1.497504499999999972e+01,
3.216617999999999711e+01,3.926649100000000203e+01,1.591888299999999923e+01,
3.167009900000000044e+01,3.756977999999999899e+01,1.601599500000000020e+01,
C216: 3.618692300000000017e+01,3.780041400000000351e+01,1.580166499999999985e+01,
3.633914099999999792e+01,3.844850499999999727e+01,1.665878000000000014e+01,
3.707468999999999681e+01,3.782362299999999777e+01,1.517691800000000057e+01,
3.534273600000000215e+01,3.816307900000000330e+01,1.522540599999999955e+01,
3.600222899999999981e+01,3.678076800000000190e+01,1.612238800000000083e+01,
C217: 4.015353300000000303e+01,3.784430600000000311e+01,1.597566100000000056e+01,
3.935299499999999995e+01,3.776662900000000178e+01,1.670458700000000007e+01,
4.028713700000000131e+01,3.888546800000000303e+01,1.569839400000000040e+01,
3.989388100000000037e+01,3.726939500000000294e+01,1.509306400000000004e+01,
4.107659699999999958e+01,3.746330400000000083e+01,1.640109199999999845e+01,
C218: 4.435774899999999832e+01,3.802880700000000047e+01,1.582724900000000012e+01,
4.515030699999999797e+01,3.787742000000000075e+01,1.655338499999999868e+01,
4.477577699999999794e+01,3.844865099999999813e+01,1.491790699999999958e+01,
4.361988099999999946e+01,3.871296199999999743e+01,1.623483299999999829e+01,
4.388309000000000282e+01,3.707835299999999989e+01,1.560462799999999994e+01,
C219: 4.810569000000000273e+01,3.780545699999999698e+01,1.586421200000000020e+01,
4.774229299999999654e+01,3.831528999999999741e+01,1.675102499999999850e+01,
4.904694700000000296e+01,3.824841599999999886e+01,1.555275900000000000e+01,
4.737690200000000118e+01,3.790779799999999966e+01,1.506609300000000040e+01,
4.825662400000000218e+01,3.675435099999999977e+01,1.608448100000000025e+01,
C220: 9.684737999999999403e+00,4.202923299999999784e+01,1.603422499999999928e+01,
9.770996000000000237e+00,4.278811000000000320e+01,1.680558900000000122e+01,
9.756104000000000553e+00,4.249593000000000131e+01,1.505631400000000042e+01,
8.725479999999999237e+00,4.152866900000000072e+01,1.612561699999999831e+01,
1.048290500000000058e+01,4.130297500000000355e+01,1.614624399999999937e+01,
C221: 1.373758199999999974e+01,4.171467400000000225e+01,1.582251600000000025e+01,
1.278182499999999955e+01,4.125801799999999986e+01,1.605580300000000094e+01,
1.412708699999999951e+01,4.220653300000000030e+01,1.670605400000000174e+01,
1.360416500000000006e+01,4.244467000000000212e+01,1.503050299999999950e+01,
1.443144799999999961e+01,4.094615699999999947e+01,1.549695200000000028e+01,
C222: 1.735462300000000013e+01,4.143698200000000043e+01,1.596455500000000072e+01,
1.660430099999999953e+01,4.090804000000000083e+01,1.653655399999999887e+01,
1.767512100000000075e+01,4.231475100000000111e+01,1.651776600000000172e+01,
1.693422100000000086e+01,4.174213600000000213e+01,1.501110599999999984e+01,
1.820807599999999837e+01,4.078857599999999906e+01,1.579007400000000061e+01,
C223: 2.219494500000000059e+01,4.165444600000000008e+01,1.594654599999999967e+01,
2.217493100000000084e+01,4.256808900000000051e+01,1.653182299999999927e+01,
2.256845799999999969e+01,4.187031000000000347e+01,1.495048099999999991e+01,
2.119008200000000031e+01,4.124918300000000215e+01,1.587441899999999961e+01,
2.284563199999999838e+01,4.092911800000000255e+01,1.642425700000000077e+01,
C224: 2.579289899999999847e+01,4.158457099999999684e+01,1.582767100000000049e+01,
2.529630900000000082e+01,4.070804900000000259e+01,1.542281099999999938e+01,
2.523598099999999889e+01,4.195050799999999924e+01,1.668062899999999971e+01,
2.584232000000000085e+01,4.235764700000000005e+01,1.506769899999999929e+01,
2.679898000000000025e+01,4.132054600000000022e+01,1.613579199999999858e+01,
C225: 3.000467400000000140e+01,4.214632600000000195e+01,1.601497399999999871e+01,
3.087761599999999973e+01,4.152285200000000032e+01,1.618034099999999853e+01,
3.009519299999999831e+01,4.265144699999999744e+01,1.505806199999999961e+01,
2.993211300000000108e+01,4.288363100000000117e+01,1.680854100000000173e+01,
2.911448800000000148e+01,4.152546699999999902e+01,1.601382399999999961e+01,
C226: 3.418292000000000286e+01,4.160502600000000228e+01,1.584644199999999969e+01,
3.459835199999999844e+01,4.064599100000000220e+01,1.613872399999999985e+01,
3.473761700000000019e+01,4.198815700000000106e+01,1.499743299999999913e+01,
3.425295400000000257e+01,4.230371499999999685e+01,1.667232299999999867e+01,
3.314223599999999692e+01,4.147914099999999848e+01,1.556588799999999928e+01,
C227: 3.778991500000000059e+01,4.171744400000000041e+01,1.591583299999999923e+01,
3.794053100000000001e+01,4.244650299999999987e+01,1.670519200000000026e+01,
3.874116300000000024e+01,4.125878999999999763e+01,1.566290399999999927e+01,
3.738331800000000271e+01,4.220983900000000233e+01,1.503881400000000035e+01,
3.709906699999999802e+01,4.095159799999999706e+01,1.625382400000000160e+01,
C228: 4.228190500000000185e+01,4.162034200000000084e+01,1.604454000000000136e+01,
4.302434699999999879e+01,4.117878799999999728e+01,1.670005700000000104e+01,
4.135562800000000294e+01,4.105845500000000214e+01,1.611431200000000175e+01,
4.264162900000000178e+01,4.159362000000000137e+01,1.502099199999999968e+01,
4.210029200000000316e+01,4.264883100000000127e+01,1.633968700000000140e+01,
C229: 4.603491799999999756e+01,4.144841999999999871e+01,1.581969400000000014e+01,
4.684184799999999882e+01,4.079591500000000082e+01,1.550130899999999912e+01,
4.515474700000000041e+01,4.085155799999999715e+01,1.602936100000000152e+01,
4.580985799999999841e+01,4.215749499999999728e+01,1.502989200000000025e+01,
4.633148500000000070e+01,4.198715899999999834e+01,1.671199700000000021e+01,
C230: 4.963797999999999888e+01,4.179574499999999659e+01,1.597680599999999984e+01,
5.051278299999999888e+01,4.125856600000000185e+01,1.562279099999999943e+01,
4.995390199999999936e+01,4.266279500000000269e+01,1.654887599999999992e+01,
4.904511999999999716e+01,4.114154200000000117e+01,1.660897999999999897e+01,
4.904395499999999686e+01,4.211675400000000025e+01,1.512641700000000000e+01,
C231: 7.674503999999999770e+00,4.505086500000000171e+01,1.588071300000000008e+01,
8.227282999999999902e+00,4.502649100000000004e+01,1.681513299999999944e+01,
8.369099000000000288e+00,4.498368299999999920e+01,1.504843800000000087e+01,
7.118093000000000004e+00,4.598102099999999837e+01,1.581348900000000057e+01,
6.985464999999999591e+00,4.421225599999999645e+01,1.584568100000000079e+01,
C232: 1.184486500000000042e+01,4.500576300000000174e+01,1.585291999999999923e+01,
1.275916899999999998e+01,4.469631700000000052e+01,1.634753699999999910e+01,
1.201229999999999976e+01,4.593686999999999898e+01,1.532173900000000089e+01,
1.106300799999999995e+01,4.514638999999999669e+01,1.659285900000000069e+01,
1.154023899999999969e+01,4.424002399999999824e+01,1.514715400000000045e+01,
C233: 1.577536800000000028e+01,4.485199800000000181e+01,1.582022199999999934e+01,
1.497046300000000052e+01,4.517418299999999931e+01,1.647145199999999932e+01,
1.579555000000000042e+01,4.547484200000000243e+01,1.493130500000000005e+01,
1.562107100000000059e+01,4.381831199999999882e+01,1.553367300000000029e+01,
1.672164499999999876e+01,4.494311299999999676e+01,1.634497700000000009e+01,
C234: 2.004221100000000177e+01,4.504898599999999931e+01,1.588490700000000011e+01,
1.940310600000000107e+01,4.541660100000000000e+01,1.668194799999999844e+01,
1.990701899999999824e+01,4.566185000000000116e+01,1.499854200000000048e+01,
1.977986599999999839e+01,4.402006000000000085e+01,1.565732500000000016e+01,
2.107861199999999968e+01,4.509555199999999786e+01,1.620306899999999928e+01,
C235: 2.407015499999999975e+01,4.486534400000000034e+01,1.581734800000000085e+01,
2.436582100000000040e+01,4.575765400000000227e+01,1.527596899999999991e+01,
2.351876499999999837e+01,4.420789899999999761e+01,1.515363699999999980e+01,
2.343851899999999944e+01,4.514634000000000214e+01,1.665353700000000003e+01,
2.495412599999999870e+01,4.435741099999999904e+01,1.618632099999999951e+01,
C236: 2.778199400000000097e+01,4.507104900000000214e+01,1.585319100000000070e+01,
2.790095300000000123e+01,4.557170099999999735e+01,1.680891099999999838e+01,
2.873178599999999960e+01,4.506786100000000062e+01,1.532684300000000022e+01,
2.704274200000000050e+01,4.559731399999999724e+01,1.525783999999999985e+01,
2.745603900000000053e+01,4.404902200000000079e+01,1.601482800000000140e+01,
C237: 3.224727899999999892e+01,4.507735499999999718e+01,1.585911399999999993e+01,
3.305948200000000270e+01,4.545046399999999664e+01,1.647383900000000168e+01,
3.214305000000000234e+01,4.570356400000000008e+01,1.497801899999999975e+01,
3.132309400000000110e+01,4.509678000000000253e+01,1.642845000000000155e+01,
3.246302800000000133e+01,4.405785900000000055e+01,1.555620200000000075e+01,
C238: 3.595759300000000280e+01,4.492669099999999816e+01,1.582689200000000085e+01,
3.597142300000000148e+01,4.579965399999999676e+01,1.518180800000000019e+01,
3.696746300000000218e+01,4.454591099999999670e+01,1.593957200000000007e+01,
3.532306200000000018e+01,4.416768799999999828e+01,1.538489200000000068e+01,
3.556325600000000264e+01,4.520655200000000207e+01,1.679779299999999864e+01,
C239: 4.013254400000000288e+01,4.512835499999999911e+01,1.586897899999999950e+01,
3.967684299999999809e+01,4.567955299999999852e+01,1.668548200000000037e+01,
4.119656899999999666e+01,4.502121400000000051e+01,1.605584800000000101e+01,
3.998116600000000176e+01,4.566778800000000160e+01,1.493866099999999975e+01,
3.967749200000000087e+01,4.414546800000000104e+01,1.579585699999999981e+01,
C240: 4.433365200000000073e+01,4.479365700000000317e+01,1.582485900000000001e+01,
4.375440100000000143e+01,4.543300200000000189e+01,1.648397699999999944e+01,
4.490660199999999946e+01,4.540678100000000228e+01,1.513646699999999967e+01,
4.366202100000000286e+01,4.415347299999999819e+01,1.526265899999999931e+01,
4.500896000000000186e+01,4.418411400000000100e+01,1.641605500000000006e+01,
C241: 4.797549000000000063e+01,4.498863099999999804e+01,1.583966999999999992e+01,
4.752595800000000281e+01,4.400865999999999900e+01,1.571953599999999973e+01,
4.889482000000000284e+01,4.490130299999999863e+01,1.641059699999999921e+01,
4.728521299999999883e+01,4.564077699999999993e+01,1.636448299999999989e+01,
4.819548699999999997e+01,4.540808200000000028e+01,1.486259100000000011e+01,
C242: 9.771810999999999581e+00,4.824163399999999768e+01,1.583923399999999937e+01,
9.103638999999999371e+00,4.851566499999999849e+01,1.664998100000000036e+01,
1.078926500000000033e+01,4.851790900000000306e+01,1.609766499999999922e+01,
9.474377999999999744e+00,4.876796099999999967e+01,1.493750299999999953e+01,
9.717950999999999340e+00,4.717121800000000320e+01,1.567027099999999962e+01,
C243: 1.398918399999999984e+01,4.808585800000000177e+01,1.597327100000000044e+01,
1.396275600000000061e+01,4.893452200000000119e+01,1.529632499999999951e+01,
1.312792299999999912e+01,4.812668299999999988e+01,1.663234999999999886e+01,
1.490313300000000041e+01,4.812100199999999717e+01,1.655773500000000098e+01,
1.396436800000000034e+01,4.716716999999999871e+01,1.539818400000000054e+01,
C244: 1.807077100000000058e+01,4.832804000000000144e+01,1.580779599999999974e+01,
1.715597700000000003e+01,4.877954799999999835e+01,1.543574399999999969e+01,
1.839990299999999834e+01,4.885929300000000097e+01,1.669449799999999939e+01,
1.883949199999999990e+01,4.839339900000000227e+01,1.504459100000000049e+01,
1.788755199999999945e+01,4.728504300000000171e+01,1.604516500000000079e+01,
C245: 2.175555800000000062e+01,4.826647200000000026e+01,1.588407499999999928e+01,
2.092424300000000059e+01,4.787304499999999763e+01,1.645979399999999870e+01,
2.227074700000000007e+01,4.902637200000000206e+01,1.646363900000000058e+01,
2.138229199999999963e+01,4.870691000000000059e+01,1.496500499999999967e+01,
2.244532099999999986e+01,4.746285400000000010e+01,1.564606700000000039e+01,
C246: 2.598171800000000076e+01,4.833507699999999829e+01,1.603930199999999928e+01,
2.683836000000000155e+01,4.790012999999999721e+01,1.654399499999999890e+01,
2.611177199999999843e+01,4.824355899999999764e+01,1.496574599999999933e+01,
2.590297999999999945e+01,4.938520499999999913e+01,1.630351999999999890e+01,
2.507553000000000054e+01,4.781826300000000174e+01,1.633889200000000130e+01,
C247: 2.995225999999999900e+01,4.810650799999999805e+01,1.574367100000000086e+01,
3.075069099999999978e+01,4.834118000000000137e+01,1.504843900000000012e+01,
2.901616299999999882e+01,4.816577300000000150e+01,1.519721599999999917e+01,
2.994375900000000001e+01,4.883991300000000280e+01,1.654317100000000096e+01,
3.007928599999999975e+01,4.709519199999999728e+01,1.611380899999999983e+01,
C248: 3.355737200000000087e+01,4.854592999999999847e+01,1.596718500000000063e+01,
3.313799699999999859e+01,4.885316699999999912e+01,1.501398200000000038e+01,
3.402250300000000038e+01,4.940132100000000293e+01,1.644681699999999935e+01,
3.430547500000000127e+01,4.777667999999999893e+01,1.580092299999999916e+01,
3.276967899999999645e+01,4.815727400000000102e+01,1.660436400000000035e+01,
C249: 3.808849099999999765e+01,4.821645900000000040e+01,1.591853099999999976e+01,
3.888795799999999758e+01,4.826865200000000300e+01,1.665005599999999930e+01,
3.835894900000000263e+01,4.880060100000000034e+01,1.504439900000000030e+01,
3.717406600000000338e+01,4.861369799999999941e+01,1.634778400000000076e+01,
3.793175899999999956e+01,4.718333100000000258e+01,1.562689400000000006e+01,
C250: 4.177460599999999857e+01,4.838439799999999735e+01,1.581008800000000036e+01,
4.130290300000000059e+01,4.860773700000000019e+01,1.676054099999999991e+01,
4.246535899999999941e+01,4.918139200000000244e+01,1.555208499999999994e+01,
4.101280200000000065e+01,4.830458900000000000e+01,1.504107699999999959e+01,
4.231396600000000063e+01,4.744511099999999715e+01,1.588173100000000026e+01,
C251: 4.541233499999999879e+01,4.835513900000000120e+01,1.598302900000000015e+01,
4.548299000000000092e+01,4.939862699999999762e+01,1.627455099999999888e+01,
4.510287600000000197e+01,4.829110500000000172e+01,1.494498899999999963e+01,
4.467945999999999884e+01,4.785345399999999927e+01,1.660559999999999903e+01,
4.638158899999999818e+01,4.788038199999999733e+01,1.609927899999999923e+01,
C252: 5.001917999999999864e+01,4.808488799999999941e+01,1.591888800000000082e+01,
5.067879599999999840e+01,4.893803400000000181e+01,1.604670000000000130e+01,
5.060655899999999718e+01,4.720551499999999834e+01,1.567190699999999914e+01,
4.931612200000000001e+01,4.828795300000000168e+01,1.511627400000000065e+01,
4.947275299999999731e+01,4.790832999999999942e+01,1.684075699999999998e+01,
C253: 7.950952000000000019e+00,5.179795200000000222e+01,1.588120800000000088e+01,
8.399326999999999543e+00,5.130223699999999809e+01,1.673724299999999943e+01,
8.375647999999999982e+00,5.139401500000000311e+01,1.496685599999999994e+01,
8.152623000000000175e+00,5.286373300000000341e+01,1.593376199999999976e+01,
6.877928999999999959e+00,5.163104700000000236e+01,1.588690199999999919e+01,
C254: 1.162236799999999981e+01,5.219877699999999976e+01,1.590582999999999991e+01,
1.105675800000000031e+01,5.274040800000000218e+01,1.665813999999999950e+01,
1.264304300000000048e+01,5.205943800000000010e+01,1.624962400000000073e+01,
1.162667399999999951e+01,5.276445999999999970e+01,1.497887500000000038e+01,
1.116327899999999929e+01,5.122950900000000019e+01,1.573516599999999954e+01,
C255: 1.612737399999999965e+01,5.217034100000000052e+01,1.595952899999999985e+01,
1.677792799999999929e+01,5.221192899999999781e+01,1.682807499999999834e+01,
1.664109600000000100e+01,5.259366500000000144e+01,1.510149099999999933e+01,
1.522279699999999991e+01,5.273775100000000293e+01,1.615700299999999956e+01,
1.586762599999999956e+01,5.113653300000000002e+01,1.575121700000000047e+01,
C256: 1.986822300000000041e+01,5.177957099999999713e+01,1.584863600000000083e+01,
2.077561700000000044e+01,5.121833900000000028e+01,1.604994500000000102e+01,
1.903785299999999836e+01,5.109321700000000277e+01,1.571821800000000025e+01,
1.999904400000000138e+01,5.236314600000000041e+01,1.494226800000000033e+01,
1.966064099999999826e+01,5.244621899999999926e+01,1.668025899999999950e+01,
C257: 2.408469200000000043e+01,5.247488500000000045e+01,1.595790700000000051e+01,
2.488091599999999914e+01,5.293942299999999790e+01,1.653195300000000145e+01,
2.385389800000000093e+01,5.309031499999999681e+01,1.509346299999999985e+01,
2.319962999999999909e+01,5.237684300000000093e+01,1.657959800000000072e+01,

2.440401200000000159e+01,5.149108499999999822e+01,1.562650000000000006e+01,
C258: 2.829472600000000071e+01,5.171016800000000302e+01,1.587061899999999959e+01,
2.888115000000000165e+01,5.205545000000000044e+01,1.671653099999999981e+01,
2.850941399999999959e+01,5.233085799999999921e+01,1.500585200000000086e+01,
2.723790500000000137e+01,5.177634799999999871e+01,1.611083700000000007e+01,
2.855039899999999875e+01,5.067955700000000263e+01,1.564742599999999939e+01,
C259: 3.187152199999999880e+01,5.209090199999999982e+01,1.586258899999999983e+01,
3.134585200000000071e+01,5.270712000000000330e+01,1.658578199999999825e+01,
3.288169599999999804e+01,5.190265399999999829e+01,1.621328600000000009e+01,
3.191030800000000056e+01,5.260695400000000177e+01,1.490795699999999968e+01,
3.134975700000000032e+01,5.114629500000000206e+01,1.574182500000000040e+01,
C260: 3.598523600000000044e+01,5.239255099999999743e+01,1.595591400000000085e+01,
3.535790399999999778e+01,5.285344099999999656e+01,1.675311100000000053e+01,
3.695827700000000249e+01,5.216484100000000268e+01,1.642105499999999907e+01,
3.610576400000000064e+01,5.307501700000000255e+01,1.515987100000000076e+01,
3.551913199999999904e+01,5.147482300000000066e+01,1.564934700000000056e+01,
C261: 4.024885199999999941e+01,5.172080199999999905e+01,1.585950099999999985e+01,
4.119639800000000207e+01,5.143738299999999697e+01,1.630724599999999924e+01,
4.043473099999999931e+01,5.229896899999999960e+01,1.495939800000000020e+01,
3.967993200000000087e+01,5.232116700000000264e+01,1.656309999999999860e+01,
3.968536100000000033e+01,5.082832200000000000e+01,1.560617200000000082e+01,
C262: 4.416973999999999734e+01,5.242877000000000010e+01,1.592851699999999937e+01,
4.354055300000000273e+01,5.285641999999999996e+01,1.670347100000000040e+01,
4.518986900000000162e+01,5.234946399999999755e+01,1.629243999999999915e+01,
4.414687800000000095e+01,5.306622900000000218e+01,1.504970999999999925e+01,
4.380154399999999981e+01,5.144086200000000275e+01,1.566789900000000024e+01,
C263: 4.852361799999999903e+01,5.182528200000000140e+01,1.595446300000000051e+01,
4.939690800000000337e+01,5.146107200000000148e+01,1.648740899999999954e+01,
4.883595199999999892e+01,5.230026500000000311e+01,1.502918299999999974e+01,
4.799639299999999764e+01,5.254637300000000266e+01,1.657200999999999880e+01,
4.786441399999999646e+01,5.099227000000000141e+01,1.572808299999999981e+01,
C264: 9.671499000000000734e+00,1.232221599999999917e+01,1.886682599999999965e+01,
9.033811999999999287e+00,1.318968300000000049e+01,1.872574600000000089e+01,
9.065573999999999799e+00,1.142124600000000001e+01,1.885561500000000024e+01,
1.018357699999999966e+01,1.240198099999999926e+01,1.982111599999999996e+01,
1.040454199999999929e+01,1.227554699999999954e+01,1.806820899999999952e+01,
C265: 1.380723799999999990e+01,1.211740499999999976e+01,1.886785100000000170e+01,
1.285740799999999950e+01,1.248027000000000086e+01,1.848796600000000012e+01,
1.445800999999999981e+01,1.186921300000000024e+01,1.803540900000000136e+01,
1.364025400000000054e+01,1.123150000000000048e+01,1.947315299999999993e+01,
1.427282199999999968e+01,1.288850700000000060e+01,1.947422999999999860e+01,
C266: 1.764162899999999823e+01,1.197991000000000028e+01,1.893258600000000058e+01,
1.725096200000000124e+01,1.099935699999999983e+01,1.918756099999999876e+01,
1.694505900000000054e+01,1.248611700000000013e+01,1.827203899999999948e+01,
1.859909499999999838e+01,1.186963199999999929e+01,1.843259899999999973e+01,
1.777193499999999915e+01,1.256442499999999995e+01,1.983836700000000164e+01,
C267: 2.196422099999999844e+01,1.220393400000000028e+01,1.888578199999999896e+01,
2.123290000000000077e+01,1.180366700000000080e+01,1.819044999999999845e+01,
2.264926499999999976e+01,1.285799399999999970e+01,1.835659199999999913e+01,
2.251887500000000131e+01,1.138617900000000027e+01,1.933576700000000059e+01,
2.145497999999999979e+01,1.276564699999999952e+01,1.966301400000000044e+01,
C268: 2.570301200000000108e+01,1.199348200000000020e+01,1.886550199999999933e+01,
2.628466299999999833e+01,1.232979399999999970e+01,1.971859999999999857e+01,
2.637300300000000064e+01,1.161823300000000003e+01,1.809811000000000042e+01,
2.512935799999999986e+01,1.282551800000000064e+01,1.847038200000000074e+01,
2.502903099999999981e+01,1.120124700000000040e+01,1.917688599999999965e+01,
C269: 3.003931599999999946e+01,1.219386199999999931e+01,1.890652400000000100e+01,
3.013788900000000126e+01,1.292529700000000048e+01,1.970290200000000169e+01,
3.086929100000000048e+01,1.229667300000000019e+01,1.821438099999999949e+01,
2.910290200000000027e+01,1.235515599999999914e+01,1.838128299999999982e+01,
3.004648600000000158e+01,1.119449200000000033e+01,1.933115600000000001e+01,
C270: 3.436633499999999941e+01,1.196684600000000032e+01,1.883809400000000167e+01,
3.492385699999999815e+01,1.267980200000000046e+01,1.823890400000000156e+01,
3.401893700000000109e+01,1.245187400000000011e+01,1.974544500000000014e+01,
3.500815200000000260e+01,1.113017600000000051e+01,1.909728799999999893e+01,
3.351309599999999733e+01,1.160669099999999965e+01,1.827135200000000034e+01,
C271: 3.804060199999999980e+01,1.223571699999999929e+01,1.890839300000000023e+01,
3.797319300000000197e+01,1.306180699999999995e+01,1.960956099999999935e+01,
3.902964500000000214e+01,1.221792600000000029e+01,1.846152199999999866e+01,
3.729346400000000017e+01,1.235734899999999925e+01,1.813109199999999888e+01,
3.786520999999999759e+01,1.130140399999999978e+01,1.943316499999999891e+01,
C272: 4.228056899999999985e+01,1.209347600000000078e+01,1.891242899999999949e+01,
4.189514599999999689e+01,1.271484899999999918e+01,1.971516099999999838e+01,
4.301077399999999784e+01,1.265437700000000021e+01,1.833818499999999929e+01,
4.146404900000000282e+01,1.179294499999999957e+01,1.826325200000000137e+01,
4.275229000000000212e+01,1.121029700000000062e+01,1.933264199999999988e+01,
C273: 4.604968300000000170e+01,1.186263800000000046e+01,1.881946100000000044e+01,
4.553497999999999735e+01,1.271298299999999948e+01,1.925687599999999833e+01,
4.612861699999999843e+01,1.200172300000000014e+01,1.774620699999999829e+01,
4.549083399999999955e+01,1.095480899999999913e+01,1.902622600000000119e+01,
4.704443899999999701e+01,1.178204200000000057e+01,1.924747099999999948e+01,
C274: 1.150184600000000046e+01,1.555989600000000017e+01,1.898376599999999925e+01,
1.131877000000000066e+01,1.523484400000000072e+01,2.000353399999999837e+01,
1.218030300000000032e+01,1.640772099999999867e+01,1.899071400000000054e+01,
1.056244500000000031e+01,1.585005800000000065e+01,1.852294900000000055e+01,
1.194553200000000004e+01,1.474567799999999984e+01,1.841969999999999929e+01,
C275: 1.615017599999999831e+01,1.538947300000000062e+01,1.900288700000000119e+01,
1.515332100000000004e+01,1.564480000000000004e+01,1.934994100000000117e+01,
1.607472999999999885e+01,1.470776099999999964e+01,1.816170199999999824e+01,
1.670328200000000152e+01,1.491466199999999986e+01,1.980755999999999872e+01,
1.666603500000000082e+01,1.629237499999999983e+01,1.869199400000000111e+01,
C276: 1.979435499999999948e+01,1.527166800000000002e+01,1.886771500000000046e+01,
1.906572999999999851e+01,1.607063099999999878e+01,1.877536999999999878e+01,
1.936340500000000020e+01,1.434034199999999970e+01,1.851574799999999854e+01,
2.008329300000000117e+01,1.516506299999999996e+01,1.990894000000000119e+01,
2.066892500000000155e+01,1.551250800000000041e+01,1.827411299999999983e+01,
C277: 2.355078800000000072e+01,1.565060599999999980e+01,1.907114199999999826e+01,
2.295476899999999887e+01,1.509851699999999930e+01,1.979151500000000041e+01,
2.289906500000000023e+01,1.624806600000000145e+01,1.844200000000000176e+01,
2.410904899999999884e+01,1.495584200000000052e+01,1.845159200000000155e+01,
2.424251599999999840e+01,1.630262899999999959e+01,1.959618400000000094e+01,
C278: 2.812720500000000001e+01,1.536945000000000050e+01,1.894099100000000035e+01,
2.729264500000000027e+01,1.603070900000000165e+01,1.872746899999999926e+01,
2.783407100000000156e+01,1.465200800000000037e+01,1.970156400000000119e+01,
2.896811800000000048e+01,1.595415799999999962e+01,1.930028899999999936e+01,
2.841070500000000010e+01,1.484076899999999988e+01,1.803748799999999974e+01,
C279: 3.197927100000000067e+01,1.530228499999999947e+01,1.894974600000000109e+01,
3.161099600000000009e+01,1.526650399999999941e+01,1.997060899999999961e+01,
3.284981499999999954e+01,1.594954700000000081e+01,1.890205800000000025e+01,
3.120332099999999897e+01,1.569358500000000056e+01,1.830016099999999923e+01,
3.225372800000000240e+01,1.430240200000000073e+01,1.862981600000000171e+01,
C280: 3.611438499999999863e+01,1.556192099999999989e+01,1.913108300000000028e+01,
3.692187599999999748e+01,1.541019200000000033e+01,1.984072600000000008e+01,
3.636600899999999825e+01,1.509283399999999986e+01,1.818523199999999918e+01,
3.596092099999999903e+01,1.662600799999999879e+01,1.897885399999999834e+01,
3.520363300000000351e+01,1.511817800000000034e+01,1.952170299999999870e+01,
C281: 4.004583099999999973e+01,1.523962099999999964e+01,1.887364000000000175e+01,
4.019913900000000240e+01,1.503395399999999960e+01,1.992872799999999955e+01,
3.900601199999999835e+01,1.549551699999999954e+01,1.870283399999999929e+01,
4.030314299999999861e+01,1.435980200000000018e+01,1.829340900000000047e+01,
4.067390000000000327e+01,1.607177199999999928e+01,1.857263800000000131e+01,
C282: 4.366772499999999724e+01,1.554480399999999918e+01,1.895195999999999970e+01,
4.459738500000000272e+01,1.596060100000000048e+01,1.932869000000000170e+01,
4.388037099999999668e+01,1.488340200000000024e+01,1.811789399999999972e+01,
4.302199199999999735e+01,1.635121099999999927e+01,1.861983499999999836e+01,
4.317425699999999722e+01,1.498736899999999928e+01,1.974225099999999955e+01,
C283: 4.804024700000000081e+01,1.514768899999999974e+01,1.900263199999999841e+01,
4.827575499999999664e+01,1.616020100000000070e+01,1.868956500000000176e+01,
4.839830800000000011e+01,1.444343300000000063e+01,1.825814799999999849e+01,
4.696513399999999905e+01,1.504352100000000014e+01,1.911276200000000003e+01,
4.852180700000000257e+01,1.494263800000000053e+01,1.995404399999999967e+01,
C284: 9.826454999999999274e+00,1.894622999999999990e+01,1.887080800000000025e+01,
1.032465900000000047e+01,1.912548900000000174e+01,1.981887400000000099e+01,
1.057001200000000019e+01,1.876872799999999941e+01,1.810090800000000044e+01,
9.228075999999999723e+00,1.981268800000000141e+01,1.860577500000000128e+01,
9.183175999999999561e+00,1.807603800000000049e+01,1.896011499999999828e+01,
C285: 1.388087900000000019e+01,1.941793099999999939e+01,1.904447899999999905e+01,
1.476238900000000065e+01,1.962987899999999897e+01,1.844772400000000090e+01,
1.380920099999999984e+01,2.014014200000000088e+01,1.985217400000000154e+01,
1.395991000000000071e+01,1.841799500000000123e+01,1.946058000000000021e+01,
1.299262300000000003e+01,1.948043300000000144e+01,1.842359400000000136e+01,
C286: 1.803500700000000023e+01,1.914693799999999868e+01,1.892762300000000053e+01,
1.801509000000000071e+01,2.023153900000000149e+01,1.893555900000000136e+01,
1.702044199999999918e+01,1.876785800000000037e+01,1.885599900000000062e+01,
1.849007999999999896e+01,1.878739799999999960e+01,1.984561199999999914e+01,
1.861144600000000082e+01,1.879659600000000097e+01,1.807855500000000148e+01,
C287: 2.156408000000000058e+01,1.891075199999999867e+01,1.894124199999999902e+01,
2.149338200000000043e+01,1.967224500000000020e+01,1.971189400000000091e+01,
2.260163000000000011e+01,1.879342000000000112e+01,1.864448900000000009e+01,
2.097223699999999980e+01,1.920906499999999895e+01,1.808241200000000148e+01,
2.118916000000000111e+01,1.796873400000000132e+01,1.932929499999999834e+01,
C288: 2.599585300000000032e+01,1.949925100000000100e+01,1.900966000000000022e+01,
2.592606500000000125e+01,2.042041599999999946e+01,1.957979800000000026e+01,
2.510163700000000020e+01,1.937595900000000171e+01,1.840661599999999964e+01,
2.608612000000000108e+01,1.866018400000000099e+01,1.969304899999999847e+01,
2.687106400000000050e+01,1.953452899999999914e+01,1.836951799999999935e+01,
C289: 3.002418899999999979e+01,1.896965300000000099e+01,1.884066899999999833e+01,
2.981287999999999982e+01,1.940154000000000067e+01,1.981420500000000118e+01,
3.072015999999999991e+01,1.960592700000000121e+01,1.830431099999999844e+01,
2.910292300000000054e+01,1.888326599999999900e+01,1.827404900000000154e+01,
3.046305100000000010e+01,1.798535700000000048e+01,1.896978000000000009e+01,
C290: 3.392832599999999843e+01,1.940023300000000006e+01,1.902225599999999872e+01,
3.309037800000000118e+01,1.936516200000000154e+01,1.833375099999999946e+01,
3.385079400000000049e+01,1.857421000000000078e+01,1.972287899999999894e+01,
3.391121900000000267e+01,2.033717199999999892e+01,1.957010700000000014e+01,
3.486154299999999751e+01,1.931838499999999925e+01,1.847372000000000014e+01,
C291: 3.837931700000000035e+01,1.890451799999999949e+01,1.893778999999999968e+01,
3.890228299999999706e+01,1.902941300000000169e+01,1.988117099999999837e+01,
3.892919499999999999e+01,1.940796800000000033e+01,1.814896099999999990e+01,
3.738431400000000338e+01,1.933148299999999864e+01,1.901592099999999874e+01,
3.830015900000000073e+01,1.784750800000000126e+01,1.870452699999999879e+01,
C292: 4.195094900000000138e+01,1.920429299999999984e+01,1.894853300000000118e+01,
4.294868499999999756e+01,1.923554599999999937e+01,1.852186000000000021e+01,
4.130501399999999990e+01,1.860506399999999871e+01,1.831555200000000028e+01,
4.155701100000000281e+01,2.021177399999999835e+01,1.902560599999999980e+01,
4.199693899999999758e+01,1.875922299999999865e+01,1.993790100000000010e+01,
C293: 4.624512000000000000e+01,1.935045300000000168e+01,1.904479800000000012e+01,
4.538366899999999760e+01,1.917835300000000132e+01,1.840711599999999848e+01,
4.712997899999999873e+01,1.950055100000000152e+01,1.843370099999999923e+01,
4.639422100000000171e+01,1.848708299999999838e+01,1.968637700000000024e+01,
4.607273699999999650e+01,2.022904799999999881e+01,1.965871200000000130e+01,
C294: 1.163788500000000070e+01,2.234039299999999884e+01,1.893057100000000048e+01,
1.212964700000000029e+01,2.289724500000000162e+01,1.972252200000000144e+01,
1.085496900000000053e+01,2.295242500000000163e+01,1.849304899999999918e+01,
1.120471399999999917e+01,2.143555200000000127e+01,1.934356100000000112e+01,
1.236576299999999939e+01,2.208102799999999988e+01,1.816845899999999858e+01,
C295: 1.588129700000000000e+01,2.256637600000000177e+01,1.888603499999999968e+01,
1.486938800000000072e+01,2.275833799999999840e+01,1.922901200000000088e+01,
1.639853499999999897e+01,2.350736500000000007e+01,1.873054000000000130e+01,
1.584630499999999920e+01,2.201133400000000151e+01,1.795436600000000027e+01,
1.641010999999999953e+01,2.198363099999999903e+01,1.963409599999999955e+01,
C296: 1.999775299999999945e+01,2.234158000000000044e+01,1.890856099999999884e+01,
2.075644399999999834e+01,2.310682500000000061e+01,1.877926100000000176e+01,
2.008387000000000100e+01,2.160522699999999929e+01,1.811643799999999871e+01,
1.901423499999999933e+01,2.279990300000000047e+01,1.886901200000000145e+01,
2.013266600000000039e+01,2.185651999999999973e+01,1.987060500000000118e+01,
C297: 2.375478400000000079e+01,2.247722999999999871e+01,1.886402100000000104e+01,
2.366946799999999840e+01,2.316462200000000138e+01,1.970016999999999996e+01,
2.476996300000000062e+01,2.249780300000000111e+01,1.848023999999999845e+01,
2.306376799999999960e+01,2.277366200000000163e+01,1.808151200000000003e+01,
2.351307800000000015e+01,2.147239899999999935e+01,1.919673900000000089e+01,
C298: 2.818780999999999892e+01,2.238955599999999890e+01,1.890878100000000117e+01,
2.761012500000000003e+01,2.203824499999999986e+01,1.805964499999999973e+01,
2.877628100000000089e+01,2.325350800000000007e+01,1.861536800000000014e+01,
2.884604200000000063e+01,2.159897000000000133e+01,1.925242199999999926e+01,
2.751230800000000087e+01,2.266984000000000066e+01,1.971142100000000141e+01,
C299: 3.182627600000000001e+01,2.238742399999999932e+01,1.893472500000000025e+01,
3.269933000000000334e+01,2.274090400000000045e+01,1.947484000000000037e+01,
3.214619700000000080e+01,2.181527099999999919e+01,1.806968900000000033e+01,
3.123501399999999961e+01,2.323820299999999861e+01,1.861017100000000113e+01,
3.123101799999999884e+01,2.175725999999999871e+01,1.958800400000000153e+01,
C300: 3.598002300000000275e+01,2.250997399999999971e+01,1.884797599999999917e+01,
3.565479200000000048e+01,2.263927299999999931e+01,1.987586500000000100e+01,
3.671586899999999787e+01,2.326936500000000052e+01,1.860426599999999908e+01,

3.512580200000000019e+01,2.260444400000000087e+01,1.818540399999999835e+01,
3.642239000000000004e+01,2.152593800000000002e+01,1.873056800000000166e+01,
C301: 3.973363100000000259e+01,2.239475300000000146e+01,1.889567800000000020e+01,
4.071329800000000176e+01,2.257364400000000160e+01,1.932799599999999884e+01,
3.912337999999999738e+01,2.183826600000000084e+01,1.960050499999999829e+01,
3.984028299999999945e+01,2.182408099999999962e+01,1.797873500000000035e+01,
3.925656000000000034e+01,2.334507199999999827e+01,1.867646200000000078e+01,
C302: 4.395748499999999837e+01,2.233787799999999990e+01,1.888039799999999957e+01,
4.304272000000000276e+01,2.276449799999999968e+01,1.848143299999999911e+01,
4.374501800000000173e+01,2.184497800000000112e+01,1.982430099999999840e+01,
4.468573899999999810e+01,2.312594500000000153e+01,1.904031600000000068e+01,
4.435237399999999752e+01,2.161368200000000073e+01,1.817549899999999852e+01,
C303: 4.774063000000000301e+01,2.264776200000000017e+01,1.885200999999999993e+01,
4.717035800000000023e+01,2.271815499999999943e+01,1.977339900000000128e+01,
4.839647200000000282e+01,2.350887300000000124e+01,1.876660800000000151e+01,
4.706002900000000011e+01,2.262443800000000138e+01,1.800726099999999974e+01,
4.833617499999999723e+01,2.174006299999999925e+01,1.886420599999999936e+01,
C304: 1.038055800000000062e+01,2.643330500000000072e+01,1.901267800000000108e+01,
1.089220500000000058e+01,2.639202799999999982e+01,1.996961299999999895e+01,
1.107576899999999931e+01,2.675679799999999986e+01,1.824477200000000110e+01,
9.555260000000000531e+00,2.713651600000000030e+01,1.907274900000000173e+01,
9.999435000000000073e+00,2.544769499999999951e+01,1.876275199999999899e+01,
C305: 1.392977600000000038e+01,2.557062799999999925e+01,1.888546600000000097e+01,
1.339907900000000041e+01,2.650506700000000038e+01,1.873423599999999922e+01,
1.491793499999999995e+01,2.564206599999999980e+01,1.844310700000000125e+01,
1.338075699999999912e+01,2.475788000000000011e+01,1.842242900000000105e+01,
1.402541199999999932e+01,2.537936900000000051e+01,1.995002799999999965e+01,
C306: 1.783958399999999855e+01,2.609889899999999940e+01,1.912859600000000171e+01,
1.711794599999999988e+01,2.599081599999999881e+01,1.993279899999999927e+01,
1.806791099999999872e+01,2.715053299999999936e+01,1.898579799999999906e+01,
1.742467999999999861e+01,2.568998399999999904e+01,1.821266599999999869e+01,
1.874923300000000026e+01,2.556304700000000096e+01,1.938310999999999851e+01,
C307: 2.236869700000000094e+01,2.615458999999999889e+01,1.896550799999999981e+01,
2.151594199999999901e+01,2.681043100000000123e+01,1.911169200000000146e+01,
2.311327100000000101e+01,2.665748500000000121e+01,1.835706000000000060e+01,
2.204526500000000055e+01,2.524761900000000026e+01,1.846417599999999837e+01,
2.280026000000000153e+01,2.590107000000000070e+01,1.992912700000000115e+01,
C308: 2.595524899999999846e+01,2.540081999999999951e+01,1.890391299999999930e+01,
2.548779700000000048e+01,2.634782900000000083e+01,1.865468600000000166e+01,
2.701536199999999965e+01,2.555706599999999895e+01,1.907907799999999909e+01,
2.582432700000000025e+01,2.470079600000000042e+01,1.808612600000000015e+01,
2.549723600000000090e+01,2.499769600000000065e+01,1.980201800000000034e+01,
C309: 3.027325199999999938e+01,2.661751500000000092e+01,1.909855400000000003e+01,
3.004897100000000165e+01,2.749038200000000032e+01,1.970414699999999897e+01,
3.110649300000000039e+01,2.683794400000000024e+01,1.843874999999999886e+01,
2.940129800000000060e+01,2.635212299999999885e+01,1.850859000000000165e+01,
3.053662399999999977e+01,2.578641000000000005e+01,1.974597899999999839e+01,
C310: 3.414584899999999834e+01,2.561168100000000081e+01,1.890886199999999917e+01,
3.480443100000000101e+01,2.538257300000000072e+01,1.974113600000000091e+01,
3.464057900000000245e+01,2.630494699999999852e+01,1.823609199999999930e+01,
3.323366800000000154e+01,2.606275700000000128e+01,1.928590099999999907e+01,
3.390593299999999743e+01,2.469741600000000048e+01,1.837693499999999958e+01,
C311: 3.769531400000000332e+01,2.620067699999999888e+01,1.899610799999999955e+01,
3.726765900000000187e+01,2.705102099999999865e+01,1.951740600000000114e+01,
3.868236699999999928e+01,2.646066799999999830e+01,1.862608600000000081e+01,
3.705574500000000171e+01,2.592228700000000075e+01,1.816559799999999925e+01,
3.777816399999999675e+01,2.536319100000000049e+01,1.968226999999999904e+01,
C312: 4.213763800000000259e+01,2.555329300000000003e+01,1.907785200000000003e+01,
4.274760299999999802e+01,2.510196300000000136e+01,1.985459600000000080e+01,
4.248812099999999958e+01,2.522484899999999897e+01,1.810447999999999880e+01,
4.221177600000000041e+01,2.663474100000000178e+01,1.914192500000000052e+01,
4.110229600000000261e+01,2.525398799999999966e+01,1.920994299999999910e+01,
C313: 4.594447600000000165e+01,2.580711200000000005e+01,1.890442799999999934e+01,
4.679634099999999819e+01,2.646433800000000147e+01,1.875858099999999951e+01,
4.592116200000000248e+01,2.506378600000000034e+01,1.811485899999999916e+01,
4.502865200000000101e+01,2.638860100000000131e+01,1.887971999999999895e+01,
4.603107899999999830e+01,2.531037600000000154e+01,1.986610500000000101e+01,
C314: 1.211487600000000064e+01,2.956675200000000103e+01,1.890918999999999883e+01,
1.230268799999999985e+01,2.895379199999999997e+01,1.978561900000000051e+01,
1.274585300000000032e+01,2.923022200000000126e+01,1.809365599999999930e+01,
1.233679399999999937e+01,3.060315599999999847e+01,1.914043399999999906e+01,
1.107178599999999946e+01,2.947591200000000100e+01,1.862171800000000133e+01,
C315: 1.567335300000000053e+01,2.921578299999999828e+01,1.885483500000000134e+01,
1.525932800000000000e+01,2.951330400000000154e+01,1.981353599999999915e+01,
1.672868199999999916e+01,2.946686800000000162e+01,1.882253199999999893e+01,
1.515257700000000085e+01,2.973667100000000119e+01,1.805808700000000044e+01,
1.555221500000000034e+01,2.814510299999999887e+01,1.872476199999999835e+01,
C316: 1.998349100000000078e+01,2.966874599999999873e+01,1.899458299999999866e+01,
1.907196799999999826e+01,2.959372700000000123e+01,1.841032200000000074e+01,
1.994395000000000095e+01,3.055765299999999840e+01,1.961637599999999892e+01,
2.084325300000000070e+01,2.972525600000000168e+01,1.833442300000000103e+01,
2.007455799999999968e+01,2.879309299999999894e+01,1.963004000000000104e+01,
C317: 2.406163799999999853e+01,2.948154999999999859e+01,1.885101200000000077e+01,
2.463241000000000014e+01,2.875830300000000150e+01,1.942542800000000014e+01,
2.461838499999999996e+01,3.040974100000000035e+01,1.877818999999999861e+01,
2.311428700000000092e+01,2.966673799999999872e+01,1.934760700000000000e+01,
2.387669500000000156e+01,2.908734300000000061e+01,1.785687400000000125e+01,
C318: 2.751930499999999924e+01,2.933766699999999972e+01,1.889244700000000066e+01,
2.715127499999999827e+01,2.980438200000000037e+01,1.980112899999999954e+01,
2.857650699999999944e+01,2.955606300000000175e+01,1.877617800000000159e+01,
2.697392800000000079e+01,2.972602099999999936e+01,1.803802100000000053e+01,
2.737696499999999844e+01,2.826304700000000025e+01,1.895387900000000059e+01,
C319: 3.216057099999999735e+01,2.977985299999999924e+01,1.893051600000000079e+01,
3.287889299999999793e+01,2.984568600000000060e+01,1.812039599999999950e+01,
3.243281700000000001e+01,2.895852000000000004e+01,1.958657300000000134e+01,
3.116961600000000132e+01,2.960398999999999958e+01,1.852335300000000018e+01,
3.216161900000000173e+01,3.070754099999999909e+01,1.949423799999999929e+01,
C320: 3.581083799999999684e+01,2.948985800000000168e+01,1.885109500000000082e+01,
3.643552300000000344e+01,2.996342800000000040e+01,1.960228400000000093e+01,
3.643883199999999789e+01,2.903835899999999981e+01,1.809020399999999995e+01,
3.516547500000000070e+01,3.023292700000000011e+01,1.839573899999999895e+01,
3.520259699999999725e+01,2.872163199999999961e+01,1.931898699999999991e+01,
C321: 3.968618200000000229e+01,2.956741699999999895e+01,1.899017000000000170e+01,
3.937606900000000110e+01,2.885125700000000037e+01,1.974494200000000177e+01,
3.884574500000000086e+01,2.979454300000000089e+01,1.834181500000000042e+01,
4.049567900000000265e+01,2.914499500000000154e+01,1.840303700000000120e+01,
4.002711200000000247e+01,3.047707000000000122e+01,1.947458999999999918e+01,
C322: 4.403257399999999677e+01,2.937357099999999832e+01,1.894132499999999908e+01,
4.392144100000000151e+01,3.029210700000000145e+01,1.950862899999999911e+01,
4.471826200000000284e+01,2.953573899999999952e+01,1.811625899999999945e+01,
4.306556599999999690e+01,2.906866700000000137e+01,1.855290499999999909e+01,
4.442334199999999811e+01,2.859584399999999960e+01,1.959010800000000074e+01,
C323: 4.767158500000000032e+01,2.949385900000000049e+01,1.883247300000000024e+01,
4.847507399999999933e+01,2.876838100000000153e+01,1.874681500000000156e+01,
4.809190199999999749e+01,3.048099500000000006e+01,1.899979400000000140e+01,
4.703085399999999794e+01,2.922680599999999984e+01,1.966741899999999887e+01,
4.709073599999999971e+01,2.949786100000000033e+01,1.791531600000000068e+01,
C324: 1.002258299999999913e+01,3.270453100000000290e+01,1.889580399999999827e+01,
1.083004399999999912e+01,3.331336199999999792e+01,1.850010800000000089e+01,
9.081452999999999776e+00,3.323449000000000098e+01,1.878344299999999834e+01,
1.020295100000000055e+01,3.250518199999999780e+01,1.994789499999999904e+01,
9.975723000000000340e+00,3.176580900000000085e+01,1.835345200000000077e+01,
C325: 1.432077600000000039e+01,3.268666300000000291e+01,1.893802900000000022e+01,
1.482169500000000006e+01,3.359862300000000346e+01,1.862721600000000066e+01,
1.422592399999999913e+01,3.201935499999999735e+01,1.808739299999999872e+01,
1.333366299999999960e+01,3.292957499999999982e+01,1.931970199999999949e+01,
1.490159799999999990e+01,3.220161699999999882e+01,1.971675600000000017e+01,
C326: 1.807755699999999877e+01,3.277970299999999781e+01,1.885226400000000169e+01,
1.847574200000000033e+01,3.288249600000000328e+01,1.985720200000000091e+01,
1.888607000000000014e+01,3.286721000000000004e+01,1.813383400000000023e+01,
1.734619199999999850e+01,3.356149099999999663e+01,1.867275700000000072e+01,
1.760312400000000110e+01,3.180883999999999905e+01,1.875015900000000002e+01,
C327: 2.194876500000000163e+01,3.280005299999999835e+01,1.893546800000000019e+01,
2.114768199999999965e+01,3.322387400000000213e+01,1.953309600000000046e+01,
2.259971699999999828e+01,3.359569700000000125e+01,1.858583499999999944e+01,
2.152678900000000084e+01,3.227384800000000098e+01,1.808548000000000044e+01,
2.252211000000000141e+01,3.210609399999999880e+01,1.954228600000000071e+01,
C328: 2.618955100000000158e+01,3.287484700000000259e+01,1.898258300000000176e+01,
2.666452200000000161e+01,3.382186800000000204e+01,1.874656699999999887e+01,
2.615423799999999943e+01,3.225587099999999907e+01,1.809160599999999874e+01,
2.517930300000000088e+01,3.305573499999999854e+01,1.933719699999999975e+01,
2.675931599999999833e+01,3.236693300000000306e+01,1.975481900000000124e+01,
C329: 2.993655800000000156e+01,3.275686600000000226e+01,1.886010599999999826e+01,
2.985557299999999969e+01,3.176397599999999954e+01,1.842974600000000152e+01,
3.092240100000000069e+01,3.316252099999999814e+01,1.865577400000000097e+01,
2.978606900000000124e+01,3.269774999999999920e+01,1.993382599999999982e+01,
2.918066999999999922e+01,3.340302799999999905e+01,1.842535799999999924e+01,
C330: 3.413796299999999917e+01,3.295795600000000292e+01,1.904498800000000003e+01,
3.324940099999999887e+01,3.336008499999999799e+01,1.952197699999999969e+01,
3.480010599999999954e+01,3.377272299999999916e+01,1.876736199999999855e+01,
3.385304000000000002e+01,3.240479200000000048e+01,1.815525399999999934e+01,
3.465032699999999721e+01,3.229557100000000247e+01,1.973611000000000004e+01,
C331: 3.821091200000000043e+01,3.291261099999999828e+01,1.893060600000000093e+01,
3.894574300000000022e+01,3.317423399999999845e+01,1.968589100000000158e+01,
3.871386799999999795e+01,3.249566599999999994e+01,1.806402599999999836e+01,
3.765769499999999681e+01,3.380067700000000031e+01,1.864049599999999884e+01,
3.752297899999999942e+01,3.217728400000000022e+01,1.933631400000000156e+01,
C332: 4.203553399999999840e+01,3.276936800000000005e+01,1.886825400000000030e+01,
4.113130100000000056e+01,3.313335200000000214e+01,1.839177400000000162e+01,
4.288808900000000079e+01,3.332980100000000334e+01,1.849866499999999903e+01,
4.216358900000000176e+01,3.171633800000000036e+01,1.864038700000000048e+01,
4.195529799999999909e+01,3.289988499999999760e+01,1.994321300000000008e+01,
C333: 4.579666000000000281e+01,3.269459100000000262e+01,1.896500100000000089e+01,
4.526607700000000278e+01,3.358338200000000029e+01,1.863789999999999836e+01,
4.681932700000000125e+01,3.295834800000000087e+01,1.921768700000000152e+01,
4.580144399999999649e+01,3.195937500000000142e+01,1.816643300000000139e+01,
4.530372700000000208e+01,3.227977800000000030e+01,1.983894300000000044e+01,
C334: 1.151956000000000024e+01,3.674771199999999993e+01,1.895072100000000148e+01,
1.178090899999999941e+01,3.767413299999999765e+01,1.945275699999999830e+01,
1.239760599999999968e+01,3.634443699999999922e+01,1.845586000000000126e+01,
1.074364600000000003e+01,3.693873800000000074e+01,1.821603700000000003e+01,
1.115605700000000056e+01,3.603074999999999761e+01,1.968080900000000000e+01,
C335: 1.618978399999999951e+01,3.678641700000000014e+01,1.902385299999999901e+01,
1.523974100000000043e+01,3.673865899999999840e+01,1.850054700000000096e+01,
1.699548800000000170e+01,3.693364100000000150e+01,1.831196200000000118e+01,
1.635122099999999890e+01,3.585664200000000079e+01,1.956109700000000018e+01,
1.617332599999999942e+01,3.761148399999999725e+01,1.972933400000000148e+01,
C336: 1.988228799999999907e+01,3.595724599999999782e+01,1.891890499999999875e+01,
1.945682899999999904e+01,3.695006200000000263e+01,1.881294000000000111e+01,
2.095041799999999910e+01,3.603800499999999829e+01,1.909498699999999971e+01,
1.970811199999999985e+01,3.538622699999999810e+01,1.801362599999999858e+01,
1.941511600000000115e+01,3.545340000000000202e+01,1.975961300000000165e+01,
C337: 2.412162199999999856e+01,3.692316399999999987e+01,1.909900700000000029e+01,
2.430977800000000144e+01,3.603879100000000335e+01,1.970046500000000123e+01,
2.494900900000000021e+01,3.707365999999999673e+01,1.841273699999999991e+01,
2.402771500000000060e+01,3.778739300000000156e+01,1.974953400000000059e+01,
2.320128800000000169e+01,3.678802499999999753e+01,1.853943699999999950e+01,
C338: 2.825455300000000136e+01,3.648915399999999920e+01,1.892873300000000114e+01,
2.721169599999999988e+01,3.632212200000000024e+01,1.867896500000000160e+01,
2.863703599999999838e+01,3.563094099999999997e+01,1.947273500000000013e+01,
2.833960000000000079e+01,3.737615900000000124e+01,1.954853900000000166e+01,
2.882775200000000027e+01,3.662469300000000061e+01,1.801712099999999950e+01,
C339: 3.181600699999999904e+01,3.633261999999999858e+01,1.894120200000000054e+01,
3.263984299999999905e+01,3.696458100000000258e+01,1.925738799999999884e+01,
3.220716999999999786e+01,3.544372299999999854e+01,1.845658299999999841e+01,
3.118811099999999925e+01,3.687820700000000329e+01,1.824474899999999877e+01,
3.122984599999999844e+01,3.604282500000000056e+01,1.980802600000000169e+01,
C340: 3.581812999999999647e+01,3.704181400000000224e+01,1.906706600000000051e+01,
3.670037200000000155e+01,3.673848900000000128e+01,1.851185699999999912e+01,
3.558248600000000295e+01,3.628366100000000216e+01,1.980791800000000080e+01,
3.497664400000000029e+01,3.715502299999999991e+01,1.839086199999999849e+01,
3.600987700000000302e+01,3.798495400000000188e+01,1.956924899999999923e+01,
C341: 4.009629499999999780e+01,3.606426700000000096e+01,1.894747699999999924e+01,
4.054739299999999957e+01,3.704905600000000021e+01,1.888645800000000108e+01,
4.050902500000000117e+01,3.553013399999999677e+01,1.979801499999999947e+01,
4.030485399999999885e+01,3.551055399999999906e+01,1.803850800000000021e+01,
3.902249700000000132e+01,3.616554299999999955e+01,1.907083700000000093e+01,
C342: 4.372730500000000120e+01,3.668907600000000002e+01,1.895735699999999824e+01,
4.328636000000000195e+01,3.606230899999999906e+01,1.972670600000000007e+01,
4.410011000000000081e+01,3.760482600000000275e+01,1.940577199999999891e+01,
4.297528400000000204e+01,3.692927999999999855e+01,1.821249900000000110e+01,
4.454794400000000110e+01,3.615748299999999915e+01,1.848521900000000073e+01,
C343: 4.822150599999999798e+01,3.638052100000000166e+01,1.907505799999999851e+01,
4.889861799999999903e+01,3.721538499999999772e+01,1.892074600000000117e+01,

4.855214000000000141e+01,3.553145399999999654e+01,1.848427600000000126e+01,
4.721903900000000220e+01,3.666554399999999703e+01,1.876949499999999915e+01,
4.821511300000000233e+01,3.610897099999999682e+01,2.012643999999999878e+01,
C344: 9.754820000000000491e+00,3.989947699999999742e+01,1.886253299999999911e+01,
9.130732999999999322e+00,4.077942500000000337e+01,1.873946499999999915e+01,
1.018646200000000057e+01,3.962229800000000068e+01,1.790642700000000076e+01,
9.151809999999999334e+00,3.907810400000000328e+01,1.923793200000000070e+01,
1.055080700000000071e+01,4.011621699999999890e+01,1.956868800000000164e+01,
C345: 1.396542600000000078e+01,3.993948600000000226e+01,1.892194999999999894e+01,
1.301355200000000067e+01,4.008976100000000287e+01,1.842203100000000049e+01,
1.400770299999999935e+01,3.893007800000000174e+01,1.931894899999999993e+01,
1.406477499999999914e+01,4.065149499999999705e+01,1.973550200000000032e+01,
1.477431999999999945e+01,4.008359899999999953e+01,1.821285800000000066e+01,
C346: 1.812255000000000038e+01,3.980728799999999978e+01,1.886331699999999856e+01,
1.864959999999999951e+01,4.073564100000000110e+01,1.866750700000000052e+01,
1.810775500000000093e+01,3.920145699999999778e+01,1.796281300000000059e+01,
1.710424599999999984e+01,4.002829499999999996e+01,1.916789299999999940e+01,
1.862713799999999864e+01,3.926423199999999980e+01,1.965674299999999874e+01,
C347: 2.167668700000000115e+01,3.968352999999999753e+01,1.888154499999999913e+01,
2.150862000000000052e+01,4.026751900000000006e+01,1.978124000000000038e+01,
2.271283100000000132e+01,3.978363199999999722e+01,1.857353799999999922e+01,
2.102580100000000130e+01,4.004084900000000147e+01,1.809025300000000058e+01,
2.145842800000000139e+01,3.863952900000000312e+01,1.908326399999999978e+01,
C348: 2.613425399999999854e+01,4.006432000000000215e+01,1.890627900000000139e+01,
2.525902800000000070e+01,3.991480599999999868e+01,1.828168099999999896e+01,
2.592735199999999907e+01,4.083459200000000067e+01,1.964285699999999935e+01,
2.697421200000000141e+01,4.036830900000000355e+01,1.829019399999999962e+01,
2.637824399999999869e+01,3.913624300000000034e+01,1.941413400000000067e+01,
C349: 3.006788200000000089e+01,3.974177600000000155e+01,1.882313399999999959e+01,
3.039272899999999922e+01,4.077165600000000012e+01,1.871203699999999870e+01,
3.005110000000000170e+01,3.925965000000000060e+01,1.785049599999999970e+01,
2.907373300000000071e+01,3.972178699999999907e+01,1.925745799999999974e+01,
3.075628599999999935e+01,3.921460499999999882e+01,1.947651199999999960e+01,
C350: 3.374245499999999964e+01,4.013109800000000149e+01,1.891390099999999919e+01,
3.391643100000000288e+01,4.096282000000000068e+01,1.958959600000000023e+01,
3.465997800000000240e+01,3.989837099999999737e+01,1.838234200000000129e+01,
3.296589099999999917e+01,4.039806000000000097e+01,1.820412299999999917e+01,
3.342642200000000230e+01,3.926376499999999936e+01,1.948516599999999954e+01,
C351: 3.834035999999999689e+01,3.984947700000000026e+01,1.886295499999999947e+01,
3.853545799999999844e+01,4.051885999999999655e+01,1.969516899999999993e+01,
3.899607499999999760e+01,4.009936100000000181e+01,1.803488899999999973e+01,
3.730573100000000153e+01,3.995224600000000237e+01,1.855051800000000028e+01,
3.852475299999999692e+01,3.882522699999999816e+01,1.917222999999999900e+01,
C352: 4.186321699999999879e+01,3.976590900000000062e+01,1.888225999999999871e+01,
4.137746400000000335e+01,4.073478599999999972e+01,1.882202300000000150e+01,
4.174101799999999685e+01,3.923792699999999911e+01,1.794267599999999874e+01,
4.141624800000000306e+01,3.918718599999999697e+01,1.968485499999999888e+01,
4.292094199999999660e+01,3.990416199999999947e+01,1.908337900000000076e+01,
C353: 4.611872900000000186e+01,4.004339099999999974e+01,1.889390699999999867e+01,
4.526438499999999721e+01,3.990751099999999951e+01,1.823832200000000014e+01,
4.595818400000000281e+01,4.091285299999999836e+01,1.952359399999999923e+01,
4.701779899999999657e+01,4.018354599999999976e+01,1.830172400000000010e+01,
4.623466700000000174e+01,3.916310299999999955e+01,1.951901600000000059e+01,
C354: 1.189322699999999955e+01,4.301482200000000233e+01,1.894986899999999963e+01,
1.234920699999999982e+01,4.396639600000000314e+01,1.869774500000000117e+01,
1.197222999999999971e+01,4.233826499999999982e+01,1.810554499999999933e+01,
1.084590700000000041e+01,4.316960900000000123e+01,1.919139399999999895e+01,
1.240240900000000046e+01,4.258592000000000155e+01,1.980756399999999928e+01,
C355: 1.561394699999999958e+01,4.323683999999999679e+01,1.889716999999999913e+01,
1.646162500000000151e+01,4.391307700000000125e+01,1.883990199999999859e+01,
1.536885099999999937e+01,4.305164400000000313e+01,1.993868099999999899e+01,
1.586743899999999918e+01,4.229894500000000335e+01,1.841411700000000096e+01,
1.475999999999999979e+01,4.368483799999999917e+01,1.840032400000000123e+01,
C356: 2.041009000000000029e+01,4.320685399999999987e+01,1.902327199999999863e+01,
2.085843799999999959e+01,4.414694099999999821e+01,1.871808199999999900e+01,
2.028758600000000101e+01,4.256552700000000300e+01,1.815599200000000124e+01,
1.943867499999999993e+01,4.339842900000000014e+01,1.946933200000000141e+01,
2.105181599999999875e+01,4.271813300000000169e+01,1.974994999999999834e+01,
C357: 2.404363899999999887e+01,4.311853200000000186e+01,1.887846599999999953e+01,
2.496861200000000025e+01,4.343286499999999961e+01,1.840741500000000030e+01,
2.374849700000000041e+01,4.214590900000000318e+01,1.849817600000000084e+01,
2.326689500000000166e+01,4.384489599999999854e+01,1.866339500000000129e+01,
2.419027300000000125e+01,4.305565399999999698e+01,1.995249799999999851e+01,
C358: 2.783239199999999869e+01,4.331049699999999802e+01,1.902699900000000000e+01,
2.708827600000000047e+01,4.368429100000000176e+01,1.972374200000000144e+01,
2.852101400000000098e+01,4.410941199999999895e+01,1.876882099999999909e+01,
2.734125200000000078e+01,4.294984699999999833e+01,1.812903700000000029e+01,
2.838251299999999944e+01,4.249599400000000315e+01,1.948856299999999919e+01,
C359: 3.221550400000000280e+01,4.357925900000000041e+01,1.906231400000000065e+01,
3.135421699999999845e+01,4.301367199999999968e+01,1.940489799999999931e+01,
3.298539699999999897e+01,4.356245400000000245e+01,1.982768899999999945e+01,
3.191807299999999969e+01,4.460540799999999706e+01,1.887023100000000042e+01,
3.259798299999999927e+01,4.313383199999999817e+01,1.814964499999999958e+01,
C360: 3.594857499999999817e+01,4.314358599999999910e+01,1.886351499999999959e+01,
3.590083299999999866e+01,4.305055500000000279e+01,1.994428500000000071e+01,
3.675551699999999755e+01,4.381600199999999745e+01,1.859339599999999848e+01,
3.501222099999999671e+01,4.354589800000000110e+01,1.849330499999999944e+01,
3.612428599999999790e+01,4.216715299999999900e+01,1.842353299999999898e+01,
C361: 3.960470899999999972e+01,4.344902299999999684e+01,1.906290600000000168e+01,
4.047566100000000233e+01,4.391312800000000038e+01,1.951590300000000155e+01,
3.992550099999999702e+01,4.267806199999999966e+01,1.836883900000000125e+01,
3.903365699999999805e+01,4.420023799999999881e+01,1.852769999999999939e+01,
3.898613699999999938e+01,4.300635199999999969e+01,1.983770399999999867e+01,
C362: 4.376645100000000355e+01,4.300802900000000051e+01,1.899628900000000087e+01,
4.431484600000000285e+01,4.386252799999999752e+01,1.938129700000000000e+01,
4.434879300000000057e+01,4.252620199999999784e+01,1.821757500000000007e+01,
4.281878199999999879e+01,4.334382599999999996e+01,1.858661199999999880e+01,
4.358395099999999900e+01,4.230292599999999936e+01,1.980153999999999925e+01,
C363: 4.750553399999999726e+01,4.345465800000000200e+01,1.886536500000000061e+01,
4.714826599999999956e+01,4.319939000000000107e+01,1.985848700000000022e+01,
4.821815200000000345e+01,4.427088799999999935e+01,1.893680900000000022e+01,
4.666668099999999697e+01,4.376025700000000285e+01,1.824838099999999841e+01,
4.798922799999999711e+01,4.259021899999999761e+01,1.842174800000000090e+01,
C364: 1.027480899999999941e+01,4.707969700000000302e+01,1.898349500000000134e+01,
9.745018999999999210e+00,4.626315199999999805e+01,1.850221099999999907e+01,
1.065390400000000071e+01,4.675886400000000265e+01,1.988108700000000084e+01,
9.590557999999999694e+00,4.790553799999999995e+01,1.915362199999999859e+01,
1.108877799999999958e+01,4.740869099999999747e+01,1.834548200000000051e+01,
C365: 1.393584500000000048e+01,4.663053800000000138e+01,1.894429999999999836e+01,
1.491520299999999999e+01,4.660076099999999855e+01,1.848016000000000147e+01,
1.363872199999999957e+01,4.766082500000000266e+01,1.911248399999999847e+01,
1.397097100000000047e+01,4.610531799999999691e+01,1.989401700000000162e+01,
1.321442900000000087e+01,4.614858199999999755e+01,1.829285499999999942e+01,
C366: 1.772939200000000071e+01,4.731154399999999782e+01,1.899577100000000129e+01,
1.868321900000000113e+01,4.714156899999999695e+01,1.850536500000000117e+01,
1.696265100000000103e+01,4.750379600000000124e+01,1.825326000000000093e+01,
1.781072199999999839e+01,4.816554299999999955e+01,1.966129400000000160e+01,
1.745878799999999842e+01,4.643130599999999930e+01,1.957126500000000036e+01,
C367: 2.232756499999999988e+01,4.694599199999999684e+01,1.892070199999999858e+01,
2.209912399999999977e+01,4.792494599999999849e+01,1.933066699999999827e+01,
2.310637499999999989e+01,4.703839099999999718e+01,1.817069899999999905e+01,
2.143448000000000064e+01,4.652699299999999738e+01,1.846733000000000047e+01,
2.266895600000000144e+01,4.629113799999999657e+01,1.971677599999999941e+01,
C368: 2.594652100000000061e+01,4.662872300000000081e+01,1.898465200000000053e+01,
2.695289199999999852e+01,4.624474699999999672e+01,1.911841000000000079e+01,
2.598532799999999909e+01,4.770787700000000342e+01,1.888241400000000070e+01,
2.534399200000000008e+01,4.636906900000000320e+01,1.984982199999999963e+01,
2.550795600000000007e+01,4.618923499999999649e+01,1.809460199999999830e+01,
C369: 2.993171800000000005e+01,4.737230100000000022e+01,1.902621200000000101e+01,
2.905417800000000028e+01,4.744424800000000175e+01,1.839154299999999864e+01,
3.083092200000000105e+01,4.758042700000000025e+01,1.845508699999999891e+01,
2.999438400000000016e+01,4.637071699999999908e+01,1.944103600000000043e+01,
2.984913399999999939e+01,4.808418999999999954e+01,1.984185700000000097e+01,
C370: 3.414578300000000155e+01,4.686601900000000143e+01,1.891436300000000159e+01,
3.484227099999999666e+01,4.711432200000000137e+01,1.812038000000000082e+01,
3.411440900000000198e+01,4.767637599999999765e+01,1.963617299999999943e+01,
3.447111999999999910e+01,4.595524000000000342e+01,1.940785599999999889e+01,
3.315477500000000077e+01,4.671712200000000337e+01,1.849803599999999904e+01,
C371: 3.773585099999999670e+01,4.688968200000000053e+01,1.896735699999999980e+01,
3.759503000000000128e+01,4.796452299999999980e+01,1.892943299999999951e+01,
3.879818699999999865e+01,4.666604000000000241e+01,1.894697999999999993e+01,
3.725246899999999783e+01,4.642625300000000266e+01,1.811351200000000006e+01,
3.730182200000000137e+01,4.649978899999999982e+01,1.988317800000000091e+01,
C372: 4.227510199999999685e+01,4.708364799999999661e+01,1.900718600000000080e+01,
4.306095499999999987e+01,4.728743899999999911e+01,1.828739900000000063e+01,
4.202520499999999970e+01,4.799531799999999748e+01,1.954103599999999830e+01,
4.261936099999999783e+01,4.633380799999999766e+01,1.971320400000000106e+01,
4.139526500000000198e+01,4.671395700000000062e+01,1.848911800000000127e+01,
C373: 4.603628199999999993e+01,4.681418399999999735e+01,1.888411599999999879e+01,
4.546039600000000291e+01,4.612635199999999713e+01,1.827311299999999861e+01,
4.619202299999999894e+01,4.637840599999999824e+01,1.986641399999999891e+01,
4.549594799999999850e+01,4.774936799999999693e+01,1.898699600000000132e+01,
4.699810699999999741e+01,4.699939599999999729e+01,1.841552499999999881e+01,
C374: 1.156516799999999989e+01,5.046840100000000007e+01,1.888044800000000123e+01,
1.168695899999999988e+01,4.989665200000000311e+01,1.979559899999999928e+01,
1.212945999999999991e+01,5.139328299999999672e+01,1.895403900000000164e+01,
1.051364200000000082e+01,5.069548900000000202e+01,1.873183600000000126e+01,
1.193120399999999925e+01,4.988659599999999728e+01,1.803993300000000133e+01,
C375: 1.533688599999999980e+01,5.008740800000000348e+01,1.886029200000000117e+01,
1.537060800000000071e+01,5.109873100000000079e+01,1.925426900000000074e+01,
1.444219299999999961e+01,4.996490299999999962e+01,1.825862100000000154e+01,
1.532303699999999935e+01,4.937921899999999908e+01,1.968318599999999918e+01,
1.621321500000000171e+01,4.991109900000000010e+01,1.824385300000000143e+01,
C376: 1.996427900000000122e+01,5.027436399999999850e+01,1.887847700000000017e+01,
2.027350099999999955e+01,4.948512999999999806e+01,1.820088099999999898e+01,
1.896443400000000068e+01,5.060696099999999831e+01,1.861551899999999904e+01,
2.065642300000000020e+01,5.110778400000000232e+01,1.880406400000000033e+01,
1.996310499999999877e+01,4.989535999999999660e+01,1.989608499999999935e+01,
C377: 2.423192999999999842e+01,5.006560600000000250e+01,1.886165300000000045e+01,
2.482317799999999863e+01,5.088375700000000279e+01,1.846264899999999898e+01,
2.410781899999999922e+01,4.930367400000000089e+01,1.809946599999999961e+01,
2.325664099999999834e+01,5.043779099999999715e+01,1.916058800000000062e+01,
2.473585900000000137e+01,4.963958600000000132e+01,1.972391500000000164e+01,
C378: 2.788096300000000127e+01,5.034175799999999867e+01,1.892810499999999863e+01,
2.881208499999999972e+01,5.076471000000000089e+01,1.929153099999999910e+01,
2.807720000000000127e+01,4.971976300000000037e+01,1.806041099999999844e+01,
2.720374100000000084e+01,5.114487400000000150e+01,1.865461499999999972e+01,
2.742958300000000094e+01,4.973806799999999839e+01,1.970971300000000070e+01,
C379: 3.176681200000000160e+01,5.050047599999999903e+01,1.886755399999999838e+01,
3.137939199999999929e+01,5.029654000000000025e+01,1.986124300000000176e+01,
3.217511100000000113e+01,5.150619499999999817e+01,1.883888299999999916e+01,
3.096433299999999988e+01,5.041172499999999701e+01,1.814203600000000094e+01,
3.254853899999999811e+01,4.978504499999999666e+01,1.863160099999999986e+01,
C380: 3.578192599999999857e+01,5.017429599999999823e+01,1.888398300000000063e+01,
3.670620000000000260e+01,5.074348400000000225e+01,1.885608999999999824e+01,
3.578291600000000017e+01,4.944472900000000237e+01,1.808077300000000065e+01,
3.493913799999999981e+01,5.084751899999999836e+01,1.875957000000000008e+01,
3.569998499999999808e+01,4.966324800000000295e+01,1.983855000000000146e+01,
C381: 3.991651800000000350e+01,5.025306199999999990e+01,1.887923100000000076e+01,
4.089791100000000057e+01,5.018154200000000031e+01,1.842183599999999899e+01,
3.981245400000000245e+01,4.947873899999999736e+01,1.963340200000000024e+01,
3.914909500000000264e+01,5.012436900000000151e+01,1.812257200000000168e+01,
3.980501399999999990e+01,5.122806500000000085e+01,1.934404299999999921e+01,
C382: 4.394964600000000132e+01,5.035086400000000140e+01,1.891762900000000158e+01,
4.479340599999999739e+01,5.095513199999999898e+01,1.859964499999999887e+01,
4.357453799999999688e+01,4.978114800000000173e+01,1.807309000000000054e+01,
4.316361700000000212e+01,5.099902099999999905e+01,1.929326800000000119e+01,
4.426469199999999660e+01,4.967211199999999849e+01,1.970428400000000124e+01,
C383: 4.765115300000000076e+01,5.012541800000000336e+01,1.889181100000000058e+01,
4.733235100000000273e+01,5.116178800000000138e+01,1.883305100000000110e+01,
4.873084399999999761e+01,5.008435300000000012e+01,1.900050200000000089e+01,
4.735999000000000336e+01,4.960487599999999730e+01,1.798480800000000102e+01,
4.718253599999999892e+01,4.965096100000000234e+01,1.974879599999999868e+01,
C384: 8.192052999999999585e+00,1.055174899999999916e+01,2.872135000000000105e+00,
8.809808000000000305e+00,1.005504700000000007e+01,3.614358999999999877e+00,
8.794912000000000063e+00,1.079330599999999940e+01,2.001857000000000220e+00,
7.782586000000000226e+00,1.146459100000000042e+01,3.294379000000000168e+00,
7.380105000000000359e+00,9.893280000000000740e+00,2.578215999999999841e+00,
C385: 1.194865599999999972e+01,1.059119300000000052e+01,3.085525000000000073e+00,
1.184077599999999997e+01,1.167023200000000038e+01,3.133728000000000069e+00,
1.300144500000000036e+01,1.033643799999999935e+01,3.008974999999999955e+00,
1.142026700000000083e+01,1.021306000000000047e+01,2.215494000000000074e+00,
1.153324199999999955e+01,1.014518299999999940e+01,3.984287999999999830e+00,
C386: 1.635128600000000176e+01,1.060067300000000046e+01,2.963208999999999982e+00,

1.648800200000000160e+01,9.887024000000000257e+00,2.156241000000000074e+00,
1.545958300000000030e+01,1.119123699999999921e+01,2.776394999999999946e+00,
1.721400099999999966e+01,1.125686100000000067e+01,3.014565999999999857e+00,
1.624253699999999867e+01,1.006739800000000074e+01,3.902813999999999783e+00,
C387: 1.996881000000000128e+01,1.017306400000000011e+01,2.839351999999999876e+00,
2.098057899999999876e+01,9.783236000000000487e+00,2.897574999999999790e+00,
1.935939199999999971e+01,9.509593999999999880e+00,2.233025000000000038e+00,
1.998651299999999864e+01,1.116107200000000077e+01,2.389000999999999930e+00,
1.954881200000000163e+01,1.023848300000000044e+01,3.838633000000000184e+00,
C388: 2.396294699999999978e+01,1.105431600000000003e+01,3.116999999999999993e+00,
2.496096700000000013e+01,1.084584899999999941e+01,2.744047000000000125e+00,
2.324256300000000053e+01,1.092237100000000005e+01,2.315298999999999996e+00,
2.391852199999999939e+01,1.207718400000000081e+01,3.476646999999999821e+00,
2.372931700000000177e+01,1.037266499999999958e+01,3.929377000000000120e+00,
C389: 2.802312999999999832e+01,1.021341999999999928e+01,2.929384999999999906e+00,
2.867125300000000010e+01,1.024563500000000005e+01,3.799742000000000175e+00,
2.858033299999999954e+01,9.839753999999999223e+00,2.075568000000000080e+00,
2.765614100000000164e+01,1.121216800000000013e+01,2.713176999999999950e+00,
2.718300100000000086e+01,9.555104999999999293e+00,3.129433000000000131e+00,
C390: 3.174735000000000085e+01,1.034556500000000057e+01,2.870389999999999997e+00,
3.124851100000000059e+01,1.009732600000000069e+01,3.802325000000000177e+00,
3.246768300000000096e+01,1.113883700000000054e+01,3.044849000000000139e+00,
3.101359300000000019e+01,1.067783299999999969e+01,2.142345000000000166e+00,
3.226177700000000215e+01,9.467800000000000438e+00,2.490798999999999985e+00,
C391: 3.594447600000000165e+01,1.030951499999999932e+01,3.091450000000000031e+00,
3.586203400000000130e+01,1.139197799999999994e+01,3.073828999999999922e+00,
3.627099400000000173e+01,9.955942000000000291e+00,2.118018000000000178e+00,
3.497697900000000004e+01,9.876972999999999558e+00,3.328249000000000013e+00,
3.666757599999999684e+01,1.001294599999999946e+01,3.845378000000000185e+00,
C392: 4.000814799999999849e+01,1.010636799999999980e+01,2.855132999999999921e+00,
4.039811999999999870e+01,1.106976099999999974e+01,2.540458999999999801e+00,
4.073113399999999729e+01,9.329454999999999387e+00,2.625182999999999822e+00,
3.907940399999999670e+01,9.903731999999999758e+00,2.330243999999999982e+00,
3.982271200000000277e+01,1.012371800000000022e+01,3.925031999999999854e+00,
C393: 4.362293100000000123e+01,1.076975299999999969e+01,2.958944999999999936e+00,
4.387654700000000219e+01,1.174953200000000031e+01,3.350985999999999798e+00,
4.453209600000000279e+01,1.025263299999999944e+01,2.666922000000000015e+00,
4.297775299999999987e+01,1.088364699999999985e+01,2.093030000000000168e+00,
4.310889499999999686e+01,1.019306300000000043e+01,3.721896000000000093e+00,
C394: 4.812569799999999987e+01,1.049150900000000064e+01,3.081458000000000030e+00,
4.865986199999999684e+01,1.083694200000000052e+01,3.961647000000000141e+00,
4.881147599999999898e+01,9.963736000000000814e+00,2.425402000000000058e+00,
4.770560400000000101e+01,1.134408299999999947e+01,2.556039999999999868e+00,
4.732516700000000043e+01,9.822578999999999283e+00,3.383274999999999810e+00,
C395: 9.667151999999999745e+00,1.403709300000000049e+01,2.817864999999999842e+00,
8.701167999999999125e+00,1.402426200000000023e+01,3.313724999999999810e+00,
9.673358999999999597e+00,1.481098899999999929e+01,2.056299000000000099e+00,
9.850243000000000748e+00,1.307351599999999969e+01,2.352740999999999971e+00,
1.044592100000000023e+01,1.424013899999999921e+01,3.544938000000000144e+00,
C396: 1.379027999999999921e+01,1.436305699999999952e+01,3.007222000000000062e+00,
1.387181400000000053e+01,1.508098700000000036e+01,3.817543999999999826e+00,
1.393868699999999983e+01,1.486974299999999971e+01,2.058354000000000017e+00,
1.280522799999999961e+01,1.390785600000000066e+01,3.024073000000000011e+00,
1.454860099999999918e+01,1.359161600000000014e+01,3.128817000000000181e+00,
C397: 1.804323000000000121e+01,1.416252500000000047e+01,2.829129000000000005e+00,
1.708931400000000167e+01,1.386113699999999938e+01,2.628347000000000211e+00,
1.853387100000000132e+01,1.444610800000000062e+01,1.903083000000000080e+00,
1.858775999999999939e+01,1.334774200000000022e+01,3.295525000000000038e+00,
1.801746500000000140e+01,1.501363199999999942e+01,3.501319000000000070e+00,
C398: 2.157213199999999986e+01,1.406432099999999963e+01,2.855237999999999943e+00,
2.237258999999999887e+01,1.353130299999999941e+01,2.352063999999999933e+00,
2.094837400000000116e+01,1.335669000000000040e+01,3.391370999999999913e+00,
2.097534999999999883e+01,1.458827400000000019e+01,2.115962999999999816e+00,
2.199918699999999916e+01,1.477796599999999927e+01,3.552582999999999824e+00,
C399: 2.626407299999999978e+01,1.431288999999999945e+01,2.954193000000000069e+00,
2.610704000000000136e+01,1.512290800000000068e+01,3.659618000000000038e+00,
2.685269800000000018e+01,1.466972799999999921e+01,2.114688999999999819e+00,
2.530309899999999956e+01,1.395698200000000000e+01,2.595387000000000111e+00,
2.679012000000000171e+01,1.350100499999999926e+01,3.446177000000000046e+00,
C400: 2.998297200000000018e+01,1.380766099999999952e+01,2.804365000000000219e+00,
2.917389599999999916e+01,1.314858699999999914e+01,3.101634999999999920e+00,
2.962206700000000126e+01,1.451005299999999920e+01,2.059562000000000115e+00,
3.079065900000000156e+01,1.321909600000000040e+01,2.381067999999999962e+00,
3.034538799999999981e+01,1.435077899999999929e+01,3.669909000000000088e+00,
C401: 3.369315900000000141e+01,1.415933399999999942e+01,2.962420999999999971e+00,
3.454711199999999849e+01,1.356691999999999965e+01,2.647943000000000158e+00,
3.403082500000000010e+01,1.495951999999999948e+01,3.614008000000000109e+00,
3.299280199999999752e+01,1.352643400000000007e+01,3.497974999999999834e+00,
3.320563899999999791e+01,1.458187299999999986e+01,2.089109000000000105e+00,
C402: 3.834134499999999690e+01,1.387473899999999993e+01,2.904278000000000137e+00,
3.799060999999999666e+01,1.462105200000000060e+01,3.608712999999999838e+00,
3.874203500000000133e+01,1.436679700000000004e+01,2.023432000000000119e+00,
3.751225800000000277e+01,1.323663699999999999e+01,2.613969999999999904e+00,
3.911546400000000290e+01,1.327144999999999975e+01,3.366759000000000057e+00,
C403: 4.189142400000000066e+01,1.420770500000000069e+01,2.804349000000000203e+00,
4.186580299999999966e+01,1.507449199999999934e+01,3.456405999999999867e+00,
4.131513000000000346e+01,1.441210200000000086e+01,1.907202000000000064e+00,
4.147022199999999970e+01,1.334971400000000052e+01,3.317917000000000005e+00,
4.291994100000000145e+01,1.399390000000000001e+01,2.530418000000000056e+00,
C404: 4.623444200000000137e+01,1.441725800000000035e+01,2.978695000000000093e+00,
4.606104799999999955e+01,1.516575199999999946e+01,3.745220999999999911e+00,
4.714368999999999943e+01,1.386878199999999950e+01,3.204750999999999905e+00,
4.633485900000000157e+01,1.490372999999999948e+01,2.013141000000000069e+00,
4.539530299999999841e+01,1.372900600000000004e+01,2.950715000000000199e+00,
C405: 5.032333700000000221e+01,1.386426100000000083e+01,2.872888999999999804e+00,
5.059989900000000063e+01,1.482812400000000075e+01,3.289801999999999893e+00,
5.119678100000000143e+01,1.339815300000000065e+01,2.426712000000000202e+00,
4.955970599999999848e+01,1.400412399999999913e+01,2.113509000000000082e+00,
4.993591200000000185e+01,1.322659100000000088e+01,3.661960999999999800e+00,
C406: 8.128918999999999784e+00,1.740530800000000156e+01,2.951332999999999984e+00,
8.037418999999999869e+00,1.844741099999999889e+01,3.242572000000000010e+00,
8.764817999999999998e+00,1.732913900000000140e+01,2.074429999999999996e+00,
7.145719999999999850e+00,1.700616700000000137e+01,2.720706999999999987e+00,
8.566307000000000116e+00,1.683860800000000069e+01,3.767851999999999979e+00,
C407: 1.179656400000000005e+01,1.732757799999999904e+01,2.870970000000000021e+00,
1.262166900000000069e+01,1.741242099999999837e+01,3.571661999999999892e+00,
1.139333799999999997e+01,1.831381999999999977e+01,2.663539999999999797e+00,
1.102120000000000033e+01,1.670261100000000098e+01,3.300888000000000044e+00,
1.215069800000000022e+01,1.688064400000000020e+01,1.946976000000000040e+00,
C408: 1.600759499999999846e+01,1.737634900000000115e+01,2.873959000000000152e+00,
1.590699700000000050e+01,1.786457199999999901e+01,3.838017999999999930e+00,
1.603530900000000159e+01,1.630126999999999882e+01,3.015179999999999971e+00,
1.692606299999999919e+01,1.770273699999999906e+01,2.395764999999999922e+00,
1.516076499999999960e+01,1.763492199999999954e+01,2.245578000000000074e+00,
C409: 2.006308200000000141e+01,1.732872400000000113e+01,2.903401999999999816e+00,
2.000018000000000029e+01,1.674165599999999898e+01,1.992442000000000046e+00,
2.093048299999999884e+01,1.701912400000000147e+01,3.477733000000000185e+00,
1.916394000000000020e+01,1.717880500000000055e+01,3.492224999999999913e+00,
2.015783499999999862e+01,1.837871799999999922e+01,2.646580999999999850e+00,
C410: 2.410411900000000074e+01,1.745064199999999843e+01,2.828202999999999800e+00,
2.327193099999999859e+01,1.785727100000000078e+01,3.393854999999999844e+00,
2.499766299999999930e+01,1.745990999999999871e+01,3.444916000000000089e+00,
2.426851299999999867e+01,1.805289399999999844e+01,1.939850000000000074e+00,
2.387682900000000075e+01,1.642978300000000047e+01,2.536224999999999952e+00,
C411: 2.845260499999999837e+01,1.722440200000000132e+01,2.875185999999999797e+00,
2.749728899999999854e+01,1.724949200000000005e+01,3.390391999999999850e+00,
2.876328900000000033e+01,1.823872199999999921e+01,2.643022999999999900e+00,
2.835485100000000003e+01,1.665717599999999976e+01,1.954661999999999900e+00,
2.919535300000000078e+01,1.675747000000000142e+01,3.513732000000000077e+00,
C412: 3.209745099999999951e+01,1.732933099999999982e+01,2.899869999999999948e+00,
3.284147300000000058e+01,1.721472999999999942e+01,3.682199000000000222e+00,
3.259439900000000279e+01,1.751451199999999986e+01,1.952355999999999980e+00,
3.144955600000000118e+01,1.816747799999999913e+01,3.137831999999999955e+00,
3.150638800000000117e+01,1.642243500000000012e+01,2.825245999999999924e+00,
C413: 3.613293800000000289e+01,1.742005299999999934e+01,2.836050999999999878e+00,
3.604889599999999916e+01,1.790203599999999895e+01,3.805139000000000049e+00,
3.676281099999999924e+01,1.802008199999999860e+01,2.186274000000000051e+00,
3.514747200000000049e+01,1.731997700000000151e+01,2.392097000000000140e+00,
3.657246399999999653e+01,1.643543499999999824e+01,2.958727000000000107e+00,
C414: 3.978878000000000270e+01,1.728361299999999900e+01,2.882601000000000191e+00,
3.896072199999999697e+01,1.700996100000000055e+01,3.527719999999999967e+00,
3.987536599999999964e+01,1.656160500000000013e+01,2.076636999999999844e+00,
4.070798099999999664e+01,1.729461600000000132e+01,3.458848000000000145e+00,
3.960961499999999802e+01,1.826903199999999927e+01,2.464331000000000049e+00,
C415: 4.398793899999999724e+01,1.731532599999999888e+01,2.872116000000000113e+00,
4.398207200000000228e+01,1.635347099999999898e+01,2.369263999999999815e+00,
4.406317500000000109e+01,1.810657899999999998e+01,2.132560999999999929e+00,
4.483662100000000095e+01,1.736647200000000169e+01,3.547212000000000032e+00,
4.306925999999999988e+01,1.743431100000000100e+01,3.437444999999999862e+00,
C416: 4.835363699999999909e+01,1.730922299999999936e+01,2.888266999999999918e+00,
4.744042000000000314e+01,1.727311500000000066e+01,3.474438000000000137e+00,
4.836558300000000088e+01,1.648484900000000053e+01,2.181805999999999912e+00,
4.921056399999999798e+01,1.723034499999999980e+01,3.550603000000000176e+00,
4.840065299999999837e+01,1.824925100000000100e+01,2.346842999999999790e+00,
C417: 1.028838400000000064e+01,2.116936899999999966e+01,3.027403000000000066e+00,
9.575806000000000040e+00,2.045576499999999953e+01,2.624919999999999920e+00,
9.768278999999999712e+00,2.187550200000000089e+01,3.667486999999999941e+00,
1.076426499999999997e+01,2.170281400000000005e+01,2.210320999999999980e+00,
1.104136399999999973e+01,2.063989400000000174e+01,3.601881000000000110e+00,
C418: 1.392231300000000083e+01,2.050511399999999895e+01,2.768028000000000155e+00,
1.310509599999999963e+01,2.076663699999999935e+01,2.103269000000000055e+00,
1.485655900000000074e+01,2.055107800000000040e+01,2.217531000000000141e+00,
1.377417100000000083e+01,1.949868700000000032e+01,3.143390000000000128e+00,
1.395453999999999972e+01,2.120597499999999869e+01,3.596156999999999826e+00,
C419: 1.773515799999999842e+01,2.072959200000000024e+01,3.027946000000000026e+00,
1.795300100000000043e+01,2.164282599999999945e+01,3.573336999999999986e+00,
1.690521899999999889e+01,2.021446900000000113e+01,3.500620000000000065e+00,
1.861169100000000043e+01,2.009021999999999863e+01,3.029783000000000115e+00,
1.747066200000000080e+01,2.097568199999999905e+01,2.003976999999999897e+00,
C420: 2.221794500000000028e+01,2.068951399999999907e+01,2.940688999999999886e+00,
2.282969299999999890e+01,2.039642399999999967e+01,3.787617000000000012e+00,
2.242264700000000133e+01,2.172445199999999943e+01,2.687161000000000133e+00,
2.116781500000000094e+01,2.058167600000000164e+01,3.192927000000000071e+00,
2.245130299999999934e+01,2.005692200000000014e+01,2.089636000000000049e+00,
C421: 2.588299500000000108e+01,2.057165000000000177e+01,2.825880999999999865e+00,
2.520066699999999926e+01,2.084630900000000153e+01,3.623205000000000009e+00,
2.631699199999999905e+01,1.959781299999999860e+01,3.028814000000000117e+00,
2.667342000000000013e+01,2.131255399999999867e+01,2.756898000000000071e+00,
2.534108000000000160e+01,2.053572099999999878e+01,1.885610000000000008e+00,
C422: 2.991967999999999961e+01,2.142094600000000071e+01,3.075763999999999943e+00,
3.001712099999999950e+01,2.237524700000000166e+01,3.582851999999999926e+00,
2.983011700000000133e+01,2.158852900000000119e+01,2.006685000000000052e+00,
2.903485200000000077e+01,2.090483000000000047e+01,3.435010000000000119e+00,
3.079593200000000053e+01,2.081204999999999927e+01,3.273069000000000006e+00,
C423: 3.407480100000000078e+01,2.041442100000000082e+01,2.823971999999999927e+00,
3.460818700000000092e+01,2.099737199999999859e+01,3.567120000000000068e+00,
3.405467199999999650e+01,1.937323699999999960e+01,3.123240000000000016e+00,
3.457767199999999974e+01,2.050409099999999896e+01,1.865817000000000059e+00,
3.305926900000000046e+01,2.078611700000000084e+01,2.733630999999999922e+00,
C424: 3.765809000000000140e+01,2.100055199999999900e+01,2.941246000000000027e+00,
3.708590499999999679e+01,2.126861900000000105e+01,2.058247999999999855e+00,
3.857298600000000022e+01,2.049998700000000085e+01,2.640344999999999942e+00,
3.706998600000000010e+01,2.033576199999999901e+01,3.565910999999999831e+00,
3.790380799999999795e+01,2.189871199999999973e+01,3.498657999999999824e+00,
C425: 4.183176699999999926e+01,2.056090000000000018e+01,3.030041000000000206e+00,
4.177601700000000307e+01,2.080470700000000051e+01,1.973408999999999969e+00,
4.265960599999999658e+01,1.988107300000000066e+01,3.199247999999999870e+00,
4.198723100000000130e+01,2.147068099999999902e+01,3.601541000000000103e+00,
4.090314800000000162e+01,2.009363000000000099e+01,3.341070999999999902e+00,
C426: 4.601581500000000347e+01,2.038829799999999892e+01,2.781397000000000119e+00,
4.494514399999999910e+01,2.055421499999999924e+01,2.845555000000000057e+00,
4.652285299999999779e+01,2.102920400000000001e+01,3.494831000000000021e+00,
4.635819399999999746e+01,2.062290399999999835e+01,1.778019000000000016e+00,
4.623590699999999742e+01,1.935008499999999998e+01,3.004484000000000155e+00,
C427: 4.953376599999999996e+01,2.126774100000000089e+01,2.985902999999999974e+00,
4.903474099999999680e+01,2.056158100000000033e+01,3.642759999999999998e+00,
5.039730899999999991e+01,2.079012600000000077e+01,2.532753000000000032e+00,
4.985805400000000276e+01,2.213021200000000022e+01,3.560394000000000059e+00,
4.884791400000000294e+01,2.158677600000000041e+01,2.206977999999999884e+00,
C428: 7.950118999999999936e+00,2.463821799999999840e+01,2.948550000000000004e+00,
8.793017000000000749e+00,2.453166200000000075e+01,3.624985999999999819e+00,
7.320739999999999803e+00,2.545832800000000162e+01,3.281108999999999831e+00,
7.373461999999999961e+00,2.371804500000000004e+01,2.941965999999999859e+00,
8.314657000000000409e+00,2.484428199999999975e+01,1.946566999999999936e+00,

C429: 1.209042900000000031e+01,2.445792399999999844e+01,2.825985999999999887e+00,
1.113239199999999940e+01,2.420333799999999869e+01,2.383195000000000174e+00,
1.194508800000000015e+01,2.522842800000000096e+01,3.575628000000000029e+00,
1.275757499999999922e+01,2.482446799999999953e+01,2.052030999999999938e+00,
1.252052100000000046e+01,2.357495099999999866e+01,3.287873999999999963e+00,
C430: 1.567243500000000012e+01,2.416879399999999833e+01,2.824247999999999870e+00,
1.485830299999999937e+01,2.390732300000000166e+01,3.491429999999999811e+00,
1.651831800000000072e+01,2.452153399999999905e+01,3.405739000000000072e+00,
1.534924600000000083e+01,2.494957000000000136e+01,2.142757000000000023e+00,
1.596658200000000072e+01,2.329224500000000120e+01,2.254948999999999870e+00,
C431: 2.018256600000000134e+01,2.449524200000000107e+01,2.984487000000000112e+00,
2.005495700000000170e+01,2.522943000000000069e+01,3.774163000000000157e+00,
2.043861000000000061e+01,2.499871399999999966e+01,2.057153000000000009e+00,
1.925689500000000010e+01,2.394277999999999906e+01,2.853003000000000178e+00,
2.097798299999999827e+01,2.380802299999999860e+01,3.256120999999999821e+00,
C432: 2.409497599999999906e+01,2.425928100000000143e+01,2.794986999999999888e+00,
2.369637600000000077e+01,2.478892199999999946e+01,3.653964999999999907e+00,
2.470746099999999856e+01,2.493196500000000171e+01,2.203590999999999855e+00,
2.327524000000000015e+01,2.389342699999999908e+01,2.184623999999999899e+00,
2.469837100000000163e+01,2.342168900000000065e+01,3.130240000000000133e+00,
C433: 2.778496499999999969e+01,2.453788799999999881e+01,2.896030999999999800e+00,
2.802984400000000065e+01,2.522474199999999911e+01,3.700004999999999988e+00,
2.870194000000000045e+01,2.415336100000000030e+01,2.460367999999999888e+00,
2.721685799999999844e+01,2.505929199999999923e+01,2.132146000000000097e+00,
2.719573199999999957e+01,2.371454900000000166e+01,3.286945000000000023e+00,
C434: 3.246875800000000112e+01,2.428702499999999986e+01,2.889558000000000071e+00,
3.212059899999999857e+01,2.493784899999999993e+01,3.685742999999999991e+00,
3.309137599999999679e+01,2.485234499999999969e+01,2.203367000000000075e+00,
3.161422599999999861e+01,2.388819300000000112e+01,2.351675000000000182e+00,
3.304290499999999753e+01,2.346891300000000058e+01,3.313127999999999851e+00,
C435: 3.597751900000000091e+01,2.433985799999999955e+01,2.795116999999999852e+00,
3.696490000000000009e+01,2.421916600000000130e+01,3.229890999999999845e+00,
3.544350399999999723e+01,2.339603100000000069e+01,2.842775000000000052e+00,
3.607517099999999743e+01,2.464722499999999883e+01,1.758288000000000073e+00,
3.543071499999999929e+01,2.509796100000000152e+01,3.345156999999999936e+00,
C436: 4.017911099999999891e+01,2.458716799999999836e+01,2.967931999999999793e+00,
3.983092099999999647e+01,2.522349600000000081e+01,3.775881000000000043e+00,
4.116987100000000055e+01,2.421106500000000139e+01,3.204673000000000105e+00,
4.021936900000000037e+01,2.515980499999999864e+01,2.046263999999999861e+00,
3.949602000000000146e+01,2.375226100000000073e+01,2.845019999999999882e+00,
C437: 4.443211300000000108e+01,2.388296899999999923e+01,2.853048999999999946e+00,
4.484708200000000033e+01,2.418938500000000147e+01,1.897578999999999905e+00,
4.362200399999999689e+01,2.317972899999999825e+01,2.686104999999999965e+00,
4.405234399999999795e+01,2.475356999999999985e+01,3.378171000000000035e+00,
4.520598999999999990e+01,2.340833800000000053e+01,3.447236000000000189e+00,
C438: 4.800301300000000282e+01,2.459405399999999986e+01,2.837334999999999940e+00,
4.795967799999999670e+01,2.511853500000000139e+01,3.786550999999999778e+00,
4.750493600000000072e+01,2.518289100000000147e+01,2.073344000000000076e+00,
4.751199900000000298e+01,2.363058699999999845e+01,2.927713999999999928e+00,
4.904118700000000075e+01,2.444480700000000084e+01,2.556324000000000041e+00,
C439: 9.709355000000000402e+00,2.783076700000000159e+01,2.810572000000000070e+00,
1.049563599999999930e+01,2.832674799999999848e+01,3.370823000000000125e+00,
9.484291000000000693e+00,2.840490499999999940e+01,1.916828999999999894e+00,
8.818523000000000778e+00,2.775421499999999853e+01,3.426820999999999895e+00,
1.004180400000000084e+01,2.683692999999999884e+01,2.527077999999999935e+00,
C440: 1.394304200000000016e+01,2.757077699999999965e+01,2.933009000000000199e+00,
1.420973599999999948e+01,2.862091799999999964e+01,2.865683000000000202e+00,
1.380743000000000009e+01,2.716826000000000008e+01,1.933743999999999907e+00,
1.301930800000000055e+01,2.746635200000000054e+01,3.493546999999999958e+00,
1.473771299999999940e+01,2.703002299999999991e+01,3.435667000000000026e+00,
C441: 1.780493500000000040e+01,2.747557600000000022e+01,2.860864999999999991e+00,
1.874608100000000022e+01,2.740948200000000057e+01,3.397299999999999986e+00,
1.789019599999999954e+01,2.821045900000000017e+01,2.066088999999999842e+00,
1.701954299999999876e+01,2.777556200000000075e+01,3.547093999999999969e+00,
1.756462300000000099e+01,2.650784799999999919e+01,2.432164999999999910e+00,
C442: 2.180528999999999940e+01,2.767225099999999927e+01,2.851204000000000072e+00,
2.114110600000000062e+01,2.765014899999999898e+01,3.709229999999999805e+00,
2.247393800000000041e+01,2.852370099999999908e+01,2.932335999999999832e+00,
2.121755100000000027e+01,2.775910599999999917e+01,1.942268000000000105e+00,
2.238751900000000106e+01,2.675697299999999856e+01,2.818454000000000015e+00,
C443: 2.575066899999999848e+01,2.758780499999999947e+01,2.957059999999999800e+00,
2.662857199999999835e+01,2.735180799999999834e+01,3.550203000000000220e+00,
2.584622200000000092e+01,2.714183399999999935e+01,1.971783000000000063e+00,
2.566202699999999837e+01,2.866532399999999825e+01,2.858334000000000152e+00,
2.486630099999999999e+01,2.719616699999999909e+01,3.449783000000000044e+00,
C444: 2.994049599999999955e+01,2.766049100000000038e+01,2.807939000000000185e+00,
3.008328200000000052e+01,2.830155799999999999e+01,3.672248999999999874e+00,
3.043667500000000103e+01,2.809896900000000031e+01,1.947407000000000110e+00,
2.887923599999999880e+01,2.756512199999999879e+01,2.600802999999999976e+00,
3.036029299999999864e+01,2.667917399999999972e+01,3.006461999999999968e+00,
C445: 3.355323599999999828e+01,2.784552499999999853e+01,2.927035000000000053e+00,
3.288897599999999954e+01,2.744023899999999827e+01,3.684051000000000187e+00,
3.420417799999999886e+01,2.858831400000000045e+01,3.377456000000000014e+00,
3.296699300000000221e+01,2.830894500000000136e+01,2.139425999999999828e+00,
3.415624900000000252e+01,2.704688200000000009e+01,2.506419000000000175e+00,
C446: 3.781560000000000343e+01,2.752652300000000096e+01,2.862331999999999876e+00,
3.774375799999999970e+01,2.836353300000000033e+01,2.174326000000000203e+00,
3.860261299999999807e+01,2.772106600000000043e+01,3.583895000000000053e+00,
3.804743500000000012e+01,2.662329000000000079e+01,2.306725999999999832e+00,
3.686731799999999737e+01,2.740207699999999846e+01,3.357792999999999822e+00,
C447: 4.188208499999999646e+01,2.769081299999999857e+01,2.830083000000000126e+00,
4.127519199999999699e+01,2.755147200000000041e+01,3.719378999999999991e+00,
4.257070999999999827e+01,2.851481100000000168e+01,2.987127000000000088e+00,
4.123853700000000089e+01,2.791146699999999825e+01,1.983749999999999902e+00,
4.244381700000000279e+01,2.678324999999999889e+01,2.630389000000000088e+00,
C448: 4.559835600000000255e+01,2.744744199999999879e+01,2.880955999999999850e+00,
4.482197800000000143e+01,2.722847700000000160e+01,3.607232999999999912e+00,
4.553763000000000005e+01,2.673877399999999938e+01,2.060709999999999820e+00,
4.657231399999999866e+01,2.737299399999999849e+01,3.354804000000000119e+00,
4.545998699999999815e+01,2.845432699999999926e+01,2.498785999999999952e+00,
C449: 5.011475699999999733e+01,2.762201400000000007e+01,2.856611000000000011e+00,
5.076384800000000297e+01,2.849258999999999986e+01,2.846722999999999892e+00,
5.043626799999999832e+01,2.693885799999999975e+01,3.637185000000000112e+00,
5.016446899999999687e+01,2.712147900000000078e+01,1.894168000000000074e+00,
4.909281399999999707e+01,2.793505800000000150e+01,3.049091999999999913e+00,
C450: 8.215808000000000888e+00,3.111324600000000018e+01,2.877613999999999894e+00,
8.648486000000000118e+00,3.056026599999999860e+01,3.705699000000000076e+00,
8.990292000000000172e+00,3.135126599999999897e+01,2.154812999999999867e+00,
7.771081999999999823e+00,3.203132599999999996e+01,3.249502000000000113e+00,
7.450579000000000285e+00,3.050818800000000053e+01,2.400600999999999985e+00,
C451: 1.200158200000000086e+01,3.124537899999999979e+01,3.070228000000000179e+00,
1.184548099999999948e+01,3.168669500000000028e+01,2.090472000000000108e+00,
1.116108200000000039e+01,3.060474599999999867e+01,3.314893000000000089e+00,
1.208621899999999982e+01,3.203388499999999794e+01,3.810991000000000017e+00,
1.291545400000000043e+01,3.065979199999999949e+01,3.059921999999999809e+00,
C452: 1.639964900000000014e+01,3.142025699999999944e+01,2.959591000000000083e+00,
1.693252899999999883e+01,3.169913100000000128e+01,2.055689999999999795e+00,
1.546911799999999992e+01,3.092862799999999979e+01,2.692489999999999828e+00,
1.618248000000000175e+01,3.231081100000000106e+01,3.540664000000000033e+00,
1.700983099999999837e+01,3.074186100000000010e+01,3.547432999999999836e+00,
C453: 1.984271499999999833e+01,3.067369800000000168e+01,2.781365000000000087e+00,
2.090368199999999987e+01,3.064617799999999903e+01,2.555626000000000175e+00,
1.952259799999999856e+01,2.969935900000000117e+01,3.131302999999999948e+00,
1.929353199999999902e+01,3.093110499999999874e+01,1.880894999999999984e+00,
1.965331199999999967e+01,3.141925700000000177e+01,3.546224000000000043e+00,
C454: 2.380385800000000174e+01,3.152987600000000157e+01,3.089303999999999828e+00,
2.298910000000000053e+01,3.099667200000000022e+01,3.568284999999999929e+00,
2.399454599999999971e+01,3.245586600000000033e+01,3.623158000000000101e+00,
2.353488499999999917e+01,3.175320100000000068e+01,2.061284999999999812e+00,
2.469859399999999994e+01,3.091514600000000002e+01,3.103543999999999858e+00,
C455: 2.824178099999999958e+01,3.139902299999999968e+01,2.893909999999999982e+00,
2.806702299999999894e+01,3.230060600000000193e+01,3.471928000000000125e+00,
2.877982300000000038e+01,3.164994199999999935e+01,1.984817000000000053e+00,
2.728931700000000049e+01,3.094542600000000121e+01,2.636610000000000120e+00,
2.882746099999999956e+01,3.069866400000000084e+01,3.480747000000000035e+00,
C456: 3.180781700000000001e+01,3.129029099999999985e+01,2.897024000000000044e+00,
3.119983999999999824e+01,3.043173200000000023e+01,3.162062000000000150e+00,
3.283774300000000324e+01,3.097542800000000085e+01,2.758284999999999876e+00,
3.176221900000000176e+01,3.202937800000000124e+01,3.689548999999999968e+00,
3.143650600000000139e+01,3.172535399999999939e+01,1.974167999999999923e+00,
C457: 3.640945299999999918e+01,3.133129299999999873e+01,3.070529000000000064e+00,
3.722026300000000276e+01,3.081584399999999846e+01,3.575594000000000161e+00,
3.558531299999999931e+01,3.064287399999999906e+01,2.909937000000000218e+00,
3.675990199999999675e+01,3.170364199999999855e+01,2.112651000000000057e+00,
3.607275099999999668e+01,3.216356499999999841e+01,3.681176999999999921e+00,
C458: 4.016856800000000050e+01,3.083463499999999868e+01,2.821730000000000071e+00,
4.063925900000000269e+01,3.119228499999999826e+01,3.731333999999999929e+00,
3.945786700000000025e+01,3.157423899999999861e+01,2.466813999999999840e+00,
3.965056500000000028e+01,2.990239100000000150e+01,3.020468999999999848e+00,
4.092617200000000111e+01,3.067095199999999977e+01,2.061497000000000135e+00,
C459: 4.379559400000000124e+01,3.140145899999999912e+01,2.990022999999999875e+00,
4.391048500000000132e+01,3.234648500000000126e+01,3.511331999999999898e+00,
4.475610300000000308e+01,3.089728500000000011e+01,2.941225000000000200e+00,
4.343221799999999888e+01,3.158603000000000094e+01,1.983570000000000055e+00,
4.308555700000000144e+01,3.077715099999999993e+01,3.521691000000000127e+00,
C460: 4.863378600000000063e+01,3.133837499999999920e+01,2.941189000000000053e+00,
4.951671499999999781e+01,3.102683400000000091e+01,3.491366999999999887e+00,
4.893502300000000105e+01,3.184776199999999946e+01,2.030715999999999966e+00,
4.804388699999999801e+01,3.201262799999999942e+01,3.555114000000000107e+00,
4.803852499999999992e+01,3.046619099999999847e+01,2.687438000000000216e+00,
C461: 9.674395999999999773e+00,3.453670100000000076e+01,2.812822000000000155e+00,
8.711418000000000106e+00,3.438929100000000005e+01,3.292406000000000166e+00,
1.032150999999999996e+01,3.510872700000000179e+01,3.470523000000000025e+00,
9.536400999999999684e+00,3.507771300000000281e+01,1.881475000000000009e+00,
1.012949099999999980e+01,3.357317900000000321e+01,2.606952999999999854e+00,
C462: 1.363874799999999965e+01,3.490961899999999929e+01,2.903172000000000086e+00,
1.387892199999999931e+01,3.559871900000000267e+01,3.706768999999999981e+00,
1.350888699999999965e+01,3.546216400000000135e+01,1.977465999999999946e+00,
1.272081400000000073e+01,3.438246399999999880e+01,3.143189000000000011e+00,
1.444670799999999922e+01,3.419342799999999727e+01,2.787628999999999913e+00,
C463: 1.796563700000000097e+01,3.470602600000000137e+01,2.812320999999999849e+00,
1.699319500000000005e+01,3.447543499999999739e+01,2.388123999999999914e+00,
1.853871699999999834e+01,3.379043999999999670e+01,2.918661999999999868e+00,
1.783244499999999988e+01,3.516884000000000299e+01,3.784244999999999859e+00,
1.849168900000000093e+01,3.538795700000000011e+01,2.151879999999999793e+00,
C464: 2.157141000000000020e+01,3.448602000000000345e+01,2.836056000000000132e+00,
2.247504899999999850e+01,3.413288299999999964e+01,2.349050999999999778e+00,
2.097178399999999954e+01,3.363688700000000154e+01,3.147853000000000012e+00,
2.100343300000000113e+01,3.509313000000000216e+01,2.138418999999999848e+00,
2.184015199999999979e+01,3.508207500000000323e+01,3.702576000000000089e+00,
C465: 2.609736499999999992e+01,3.493759599999999921e+01,2.888466000000000200e+00,
2.512209999999999965e+01,3.496501800000000060e+01,3.365307000000000048e+00,
2.610279799999999994e+01,3.560676899999999989e+01,2.033446999999999782e+00,
2.630804399999999887e+01,3.392546600000000012e+01,2.556611999999999885e+00,
2.685531699999999944e+01,3.525024700000000166e+01,3.598933000000000160e+00,
C466: 3.007349400000000017e+01,3.466085000000000349e+01,2.812786000000000008e+00,
3.016782100000000000e+01,3.391845500000000158e+01,2.026269999999999794e+00,
2.911930399999999963e+01,3.453836600000000345e+01,3.314442999999999806e+00,
3.012784699999999916e+01,3.565502800000000150e+01,2.379779000000000089e+00,
3.087836799999999826e+01,3.453471400000000102e+01,3.529681000000000068e+00,
C467: 3.385166199999999748e+01,3.485379499999999808e+01,2.902191999999999883e+00,
3.383506299999999811e+01,3.552274500000000046e+01,3.756714999999999804e+00,
3.487722200000000328e+01,3.457066900000000231e+01,2.685207999999999817e+00,
3.342388700000000057e+01,3.535505799999999965e+01,2.039235999999999827e+00,
3.327234099999999728e+01,3.396429400000000243e+01,3.128178999999999821e+00,
C468: 3.834227599999999825e+01,3.459439799999999821e+01,2.847439000000000053e+00,
3.741172300000000206e+01,3.411749499999999813e+01,2.556559000000000026e+00,
3.874741399999999913e+01,3.513830600000000004e+01,1.999691000000000107e+00,
3.905317999999999756e+01,3.383980499999999836e+01,3.166469000000000200e+00,
3.815253200000000078e+01,3.528469400000000178e+01,3.663367000000000040e+00,
C469: 4.193477599999999939e+01,3.460186999999999813e+01,2.808711999999999875e+00,
4.287890699999999811e+01,3.444265399999999744e+01,2.296990999999999783e+00,
4.145329100000000011e+01,3.364457000000000164e+01,2.980242000000000058e+00,
4.129415399999999892e+01,3.522341399999999823e+01,2.191660000000000164e+00,
4.211810799999999944e+01,3.509432100000000077e+01,3.757934000000000108e+00,
C470: 4.598715399999999676e+01,3.478565600000000302e+01,2.919604000000000088e+00,
4.680089300000000208e+01,3.500946199999999919e+01,3.602338000000000040e+00,
4.606921499999999980e+01,3.375553299999999979e+01,2.585945000000000160e+00,
4.603832100000000338e+01,3.544911400000000157e+01,2.061609999999999943e+00,
4.503956300000000113e+01,3.492553000000000196e+01,3.430489000000000122e+00,
C471: 5.028660599999999903e+01,3.465100900000000195e+01,2.842607999999999802e+00,
5.066779600000000272e+01,3.554214999999999947e+01,3.332444000000000184e+00,
5.022595499999999902e+01,3.482383099999999843e+01,1.772227999999999914e+00,
4.929774299999999698e+01,3.442182300000000339e+01,3.228130000000000166e+00,

5.095347000000000293e+01,3.381648500000000013e+01,3.037962999999999969e+00,
C472: 8.323762999999999579e+00,3.788587299999999658e+01,3.017573000000000061e+00,
7.956877999999999673e+00,3.887783699999999953e+01,3.263837000000000099e+00,
7.503694000000000308e+00,3.727735599999999749e+01,2.648213000000000150e+00,
8.744272999999999740e+00,3.742493100000000084e+01,3.906102999999999881e+00,
9.090211000000000041e+00,3.796324599999999805e+01,2.252276999999999862e+00,
C473: 1.221320099999999975e+01,3.823474699999999871e+01,2.866524000000000072e+00,
1.289670300000000047e+01,3.813293300000000130e+01,3.703183000000000114e+00,
1.278055100000000088e+01,3.837408299999999883e+01,1.951249999999999929e+00,
1.156880600000000037e+01,3.909346599999999938e+01,3.026072999999999791e+00,
1.160660799999999959e+01,3.733808899999999653e+01,2.782983000000000207e+00,
C474: 1.589973700000000001e+01,3.789931200000000189e+01,2.825232999999999883e+00,
1.545982099999999981e+01,3.816440300000000008e+01,1.868557999999999941e+00,
1.691169800000000123e+01,3.828811499999999768e+01,2.877196000000000087e+00,
1.592087599999999981e+01,3.681936400000000020e+01,2.926124000000000169e+00,
1.530640499999999982e+01,3.832782699999999920e+01,3.625903999999999794e+00,
C475: 2.002280299999999968e+01,3.781690400000000096e+01,2.981384999999999952e+00,
2.000105800000000045e+01,3.890071700000000021e+01,2.919569000000000081e+00,
2.011140299999999925e+01,3.740048699999999826e+01,1.982599000000000000e+00,
1.910541999999999874e+01,3.746452800000000138e+01,3.441555999999999838e+00,
2.087329700000000088e+01,3.750737300000000118e+01,3.580667000000000044e+00,
C476: 2.384173300000000140e+01,3.787893700000000052e+01,2.801839999999999886e+00,
2.301856700000000089e+01,3.845483699999999772e+01,2.389989999999999985e+00,
2.457226299999999952e+01,3.769001999999999697e+01,2.021307000000000187e+00,
2.346681099999999986e+01,3.693412299999999959e+01,3.182077000000000044e+00,
2.430673200000000023e+01,3.844105600000000322e+01,3.605430000000000135e+00,
C477: 2.753468799999999916e+01,3.827310800000000057e+01,2.921205000000000052e+00,
2.682562000000000069e+01,3.799439499999999725e+01,3.694456000000000184e+00,
2.810380200000000173e+01,3.913859000000000066e+01,3.246275999999999939e+00,
2.699840000000000018e+01,3.851584100000000177e+01,2.008814000000000100e+00,
2.821148700000000176e+01,3.744513599999999798e+01,2.733236000000000221e+00,
C478: 3.251999299999999948e+01,3.823987499999999784e+01,2.913352000000000164e+00,
3.322250100000000117e+01,3.801942300000000330e+01,3.710983000000000143e+00,
3.306486900000000162e+01,3.853112899999999996e+01,2.020465999999999873e+00,
3.186752999999999858e+01,3.905180699999999661e+01,3.219484000000000012e+00,
3.192297599999999846e+01,3.735828500000000219e+01,2.701719999999999899e+00,
C479: 3.618467900000000270e+01,3.779935300000000353e+01,2.800444999999999851e+00,
3.580265599999999893e+01,3.847812400000000110e+01,3.556500999999999912e+00,
3.717799999999999727e+01,3.811714200000000119e+01,2.499533000000000005e+00,
3.552879000000000076e+01,3.781690400000000096e+01,1.935362999999999944e+00,
3.623120800000000230e+01,3.678959400000000102e+01,3.194732000000000127e+00,
C480: 4.015394700000000228e+01,3.784296199999999999e+01,2.976262000000000185e+00,
3.932395000000000351e+01,3.763791799999999910e+01,3.644997000000000043e+00,
4.022375699999999910e+01,3.891324699999999837e+01,2.808660999999999852e+00,
3.998803099999999944e+01,3.734035200000000287e+01,2.028321000000000041e+00,
4.107848400000000311e+01,3.748608500000000276e+01,3.419173999999999936e+00,
C481: 4.435824499999999659e+01,3.802835400000000021e+01,2.827142999999999962e+00,
4.506085600000000113e+01,3.781334999999999980e+01,3.625455999999999790e+00,
4.489490500000000139e+01,3.842062299999999908e+01,1.968544000000000072e+00,
4.363584600000000080e+01,3.876252699999999862e+01,3.169951000000000185e+00,
4.383979699999999724e+01,3.711715600000000137e+01,2.544709000000000110e+00,
C482: 4.810571600000000103e+01,3.780455400000000310e+01,2.864498000000000211e+00,
4.736472700000000202e+01,3.779878500000000230e+01,3.657024999999999970e+00,
4.907416899999999771e+01,3.807012300000000238e+01,3.277826000000000128e+00,
4.782233699999999743e+01,3.853286599999999851e+01,2.110593999999999859e+00,
4.816368400000000349e+01,3.682009299999999996e+01,2.411148999999999987e+00,
C483: 9.684886999999999802e+00,4.202993000000000023e+01,3.034794999999999909e+00,
9.637396999999999991e+00,4.273446299999999809e+01,3.859382999999999786e+00,
9.730069000000000301e+00,4.257335400000000192e+01,2.095816999999999819e+00,
8.800053000000000125e+00,4.140058799999999906e+01,3.045958000000000165e+00,
1.057001799999999925e+01,4.141064099999999826e+01,3.136848000000000081e+00,
C484: 1.373910599999999960e+01,4.171480600000000294e+01,2.822356000000000087e+00,
1.289016299999999937e+01,4.123908200000000335e+01,3.301728000000000218e+00,
1.430780599999999936e+01,4.226912599999999998e+01,3.559807000000000166e+00,
1.338649999999999984e+01,4.239251200000000352e+01,2.050985999999999976e+00,
1.436981199999999959e+01,4.095370700000000141e+01,2.373196000000000083e+00,
C485: 1.735371299999999906e+01,4.143720499999999873e+01,2.965087000000000028e+00,
1.659233499999999850e+01,4.089032600000000173e+01,3.512204000000000104e+00,
1.777948699999999960e+01,4.220523200000000230e+01,3.603943999999999814e+00,
1.690900299999999845e+01,4.189975299999999692e+01,2.089177999999999980e+00,
1.813668099999999939e+01,4.075220099999999704e+01,2.653783999999999921e+00,
C486: 2.219532900000000097e+01,4.165486700000000297e+01,2.946693999999999924e+00,
2.216550300000000107e+01,4.257865999999999929e+01,3.515476000000000045e+00,
2.255775600000000125e+01,4.185922200000000259e+01,1.943767000000000023e+00,
2.119591000000000136e+01,4.123401499999999942e+01,2.890080000000000204e+00,
2.285932599999999937e+01,4.094783000000000208e+01,3.432751999999999803e+00,
C487: 2.579171799999999948e+01,4.158522700000000327e+01,2.828181999999999974e+00,
2.526630899999999968e+01,4.064958399999999727e+01,2.990203000000000166e+00,
2.572868199999999916e+01,4.219770400000000166e+01,3.720152000000000125e+00,
2.534001699999999957e+01,4.211270499999999828e+01,1.993643999999999972e+00,
2.683314199999999872e+01,4.137980799999999704e+01,2.602479000000000209e+00,
C488: 3.000447700000000140e+01,4.214682499999999976e+01,3.015603000000000034e+00,
3.081278999999999968e+01,4.142401699999999920e+01,2.968852000000000046e+00,
2.992478200000000044e+01,4.266478500000000196e+01,2.064578000000000024e+00,
3.020513400000000104e+01,4.286464200000000346e+01,3.804892000000000163e+00,
2.907337199999999910e+01,4.163102399999999648e+01,3.227952000000000155e+00,
C489: 3.418394200000000183e+01,4.160624099999999714e+01,2.846731000000000122e+00,
3.478636900000000054e+01,4.075389700000000204e+01,3.143661999999999956e+00,
3.450411199999999923e+01,4.195076000000000249e+01,1.868128999999999929e+00,
3.430122200000000277e+01,4.240686800000000289e+01,3.568747999999999809e+00,
3.314045500000000288e+01,4.131226999999999805e+01,2.801032000000000188e+00,
C490: 3.778916799999999654e+01,4.171833099999999916e+01,2.916084999999999816e+00,
3.790706600000000037e+01,4.251776399999999967e+01,3.640473000000000070e+00,
3.876172900000000254e+01,4.129247500000000315e+01,2.688225000000000087e+00,
3.734663199999999961e+01,4.211461700000000263e+01,2.007239000000000217e+00,
3.714500799999999714e+01,4.094707100000000111e+01,3.325825000000000031e+00,
C491: 4.228265799999999786e+01,4.162111900000000020e+01,3.045198000000000071e+00,
4.303012400000000071e+01,4.111673199999999895e+01,3.648159999999999847e+00,
4.137173099999999692e+01,4.103092199999999679e+01,3.027937999999999796e+00,
4.265503400000000056e+01,4.174031800000000203e+01,2.032204999999999817e+00,
4.207051200000000080e+01,4.259740800000000149e+01,3.470148000000000010e+00,
C492: 4.603552400000000233e+01,4.144873299999999716e+01,2.820615000000000094e+00,
4.680634500000000031e+01,4.069888999999999868e+01,2.965743999999999936e+00,
4.508622700000000094e+01,4.095548300000000097e+01,2.643911000000000122e+00,
4.628632999999999953e+01,4.206276199999999932e+01,1.960998000000000019e+00,
4.596484900000000096e+01,4.207448399999999822e+01,3.703323999999999838e+00,
C493: 4.963757900000000234e+01,4.179605200000000309e+01,2.977038999999999991e+00,
5.052099199999999968e+01,4.130002700000000004e+01,2.586240999999999790e+00,
4.993679300000000154e+01,4.267504499999999723e+01,3.539787000000000017e+00,
4.910117900000000191e+01,4.111422600000000216e+01,3.630088999999999899e+00,
4.899601599999999735e+01,4.209161399999999986e+01,2.152508999999999784e+00,
C494: 7.674336000000000269e+00,4.505127800000000349e+01,2.880977000000000121e+00,
8.175378000000000256e+00,4.500476700000000108e+01,3.843342999999999954e+00,
8.413947999999999539e+00,4.501526599999999689e+01,2.086559999999999970e+00,
7.111939999999999706e+00,4.597757399999999706e+01,2.810281999999999947e+00,
6.997627999999999737e+00,4.420749299999999948e+01,2.784123000000000125e+00,
C495: 1.184508100000000042e+01,4.500562899999999900e+01,2.853485000000000049e+00,
1.275185199999999952e+01,4.474269199999999813e+01,3.387726999999999933e+00,
1.195623699999999978e+01,4.598729300000000109e+01,2.404662000000000077e+00,
1.100879600000000025e+01,4.501681500000000113e+01,3.545859999999999790e+00,
1.165976999999999997e+01,4.427296799999999877e+01,2.074050999999999867e+00,
C496: 1.577454999999999963e+01,4.485163699999999665e+01,2.820184999999999942e+00,
1.501191900000000068e+01,4.513208300000000150e+01,3.538410999999999973e+00,
1.602410100000000170e+01,4.571132699999999716e+01,2.205814000000000163e+00,
1.540355500000000077e+01,4.405323099999999670e+01,2.185598000000000152e+00,
1.666323999999999828e+01,4.451614099999999752e+01,3.346054999999999779e+00,
C497: 2.004194100000000134e+01,4.504951100000000253e+01,2.885267999999999944e+00,
1.979911799999999999e+01,4.556975400000000320e+01,3.806869999999999976e+00,
1.942996899999999982e+01,4.543932499999999663e+01,2.077474000000000043e+00,
1.984596200000000010e+01,4.398832099999999912e+01,3.006076000000000192e+00,
2.109009100000000103e+01,4.519930500000000251e+01,2.648022000000000098e+00,
C498: 2.407067800000000091e+01,4.486430800000000119e+01,2.817466000000000026e+00,
2.428961299999999923e+01,4.579056099999999674e+01,2.295551999999999815e+00,
2.373766499999999979e+01,4.411939199999999772e+01,2.101637999999999895e+00,
2.329029299999999836e+01,4.503729400000000282e+01,3.551757999999999971e+00,
2.496576200000000156e+01,4.451177799999999962e+01,3.318214000000000219e+00,
C499: 2.778182400000000030e+01,4.507085000000000008e+01,2.853825000000000056e+00,
2.782471999999999923e+01,4.556286500000000217e+01,3.820349999999999913e+00,
2.877714299999999881e+01,4.503648700000000105e+01,2.421456000000000053e+00,
2.712095100000000159e+01,4.562391800000000330e+01,2.193531999999999815e+00,
2.740727100000000149e+01,4.405998600000000209e+01,2.976020999999999805e+00,
C500: 3.224701400000000007e+01,4.507714899999999858e+01,2.859210000000000029e+00,
3.301053100000000029e+01,4.534959500000000077e+01,3.579241000000000117e+00,
3.223491200000000134e+01,4.580317000000000149e+01,2.051908000000000065e+00,
3.127811799999999920e+01,4.506366899999999731e+01,3.348688000000000109e+00,
3.246341699999999975e+01,4.409258799999999923e+01,2.456339999999999968e+00,
C501: 3.595785999999999660e+01,4.492502999999999957e+01,2.826811000000000185e+00,
3.586036299999999954e+01,4.583191000000000059e+01,2.237999999999999989e+00,
3.697726099999999860e+01,4.483611299999999744e+01,3.188616999999999813e+00,
3.571731199999999973e+01,4.406782199999999960e+01,2.206506000000000078e+00,
3.527687699999999893e+01,4.496815000000000140e+01,3.669691999999999954e+00,
C502: 4.013245599999999769e+01,4.512858599999999853e+01,2.869435000000000180e+00,
3.929810700000000168e+01,4.545562300000000278e+01,3.481513000000000080e+00,
4.104939699999999903e+01,4.518930199999999786e+01,3.447687000000000168e+00,
4.021186099999999897e+01,4.576588100000000026e+01,1.993897000000000030e+00,
3.997005899999999912e+01,4.410156700000000285e+01,2.556372000000000089e+00,
C503: 4.433411199999999752e+01,4.479290900000000164e+01,2.825038999999999856e+00,
4.353533500000000345e+01,4.527830699999999808e+01,3.377327000000000190e+00,
4.482849499999999665e+01,4.551915400000000034e+01,2.187397999999999954e+00,
4.392078899999999919e+01,4.399868599999999930e+01,2.211343999999999976e+00,
4.505249899999999741e+01,4.437523099999999943e+01,3.522691000000000017e+00,
C504: 4.797551599999999894e+01,4.498816899999999919e+01,2.840281000000000056e+00,
4.752376799999999690e+01,4.400326600000000354e+01,2.790639999999999787e+00,
4.892603400000000136e+01,4.492777900000000102e+01,3.361587999999999798e+00,
4.731399400000000099e+01,4.566239600000000110e+01,3.374036999999999953e+00,
4.813773799999999881e+01,4.536279400000000095e+01,1.834087000000000023e+00,
C505: 9.771454000000000306e+00,4.824085300000000132e+01,2.839151000000000202e+00,
9.074436999999999642e+00,4.866678499999999730e+01,3.554691000000000045e+00,
1.077270399999999917e+01,4.860449700000000206e+01,3.048761999999999972e+00,
9.483090999999999937e+00,4.853554400000000157e+01,1.834594000000000058e+00,
9.754739000000000715e+00,4.715884899999999647e+01,2.916984999999999939e+00,
C506: 1.398907600000000073e+01,4.808487999999999829e+01,2.973930999999999880e+00,
1.399136299999999977e+01,4.905140699999999754e+01,2.478908000000000111e+00,
1.311466399999999943e+01,4.801295600000000263e+01,3.612766000000000144e+00,
1.489195699999999967e+01,4.798547899999999800e+01,3.567731000000000208e+00,
1.395958500000000058e+01,4.729862800000000078e+01,2.226074999999999804e+00,
C507: 1.807152100000000061e+01,4.832729100000000244e+01,2.809223999999999943e+00,
1.712783200000000150e+01,4.885627199999999704e+01,2.900316000000000116e+00,
1.873978400000000022e+01,4.864375799999999828e+01,3.602927999999999908e+00,
1.852137600000000006e+01,4.855407999999999902e+01,1.847299999999999942e+00,
1.789686899999999881e+01,4.725864200000000181e+01,2.882919999999999927e+00,
C508: 2.175471900000000147e+01,4.826600799999999936e+01,2.884589000000000070e+00,
2.097082199999999830e+01,4.783089400000000069e+01,3.495248999999999828e+00,
2.223878200000000049e+01,4.906829900000000322e+01,3.433247999999999855e+00,
2.132209399999999988e+01,4.866295199999999710e+01,1.971151000000000098e+00,
2.248682700000000168e+01,4.750405500000000103e+01,2.636376999999999970e+00,
C509: 2.598148399999999825e+01,4.833427300000000315e+01,3.039970999999999979e+00,
2.683877299999999977e+01,4.795472300000000132e+01,3.586383000000000099e+00,
2.612579699999999860e+01,4.816239399999999904e+01,1.977575000000000083e+00,
2.587952999999999903e+01,4.939938800000000185e+01,3.223412999999999862e+00,
2.508112099999999955e+01,4.782493699999999848e+01,3.368555999999999884e+00,
C510: 2.995311999999999841e+01,4.810531799999999691e+01,2.742268000000000150e+00,
3.056298400000000015e+01,4.818415099999999995e+01,1.847407999999999939e+00,
2.892626599999999826e+01,4.835092999999999819e+01,2.491670000000000051e+00,
3.032206299999999999e+01,4.879885300000000115e+01,3.491143999999999803e+00,
3.000217200000000162e+01,4.708963800000000077e+01,3.119527999999999857e+00,
C511: 3.355627900000000352e+01,4.854542399999999702e+01,2.968106000000000133e+00,
3.311179700000000281e+01,4.878115900000000238e+01,2.005881000000000025e+00,
3.394110500000000030e+01,4.945457300000000345e+01,3.419818999999999942e+00,
3.436837500000000034e+01,4.783872300000000166e+01,2.827145999999999937e+00,
3.280304300000000239e+01,4.811004499999999950e+01,3.616934000000000093e+00,
C512: 3.808889299999999878e+01,4.821598000000000184e+01,2.919125000000000192e+00,
3.887448899999999696e+01,4.786674200000000212e+01,3.580216000000000065e+00,
3.838729200000000219e+01,4.805447699999999855e+01,1.887640999999999902e+00,
3.792067699999999775e+01,4.927573399999999992e+01,3.085246999999999851e+00,
3.717111299999999829e+01,4.767258999999999958e+01,3.118723000000000134e+00,
C513: 4.177444400000000257e+01,4.838405300000000153e+01,2.811017999999999795e+00,
4.113785599999999931e+01,4.840764999999999674e+01,3.689102000000000103e+00,
4.247315499999999844e+01,4.921408000000000271e+01,2.849651999999999852e+00,
4.116201099999999968e+01,4.846903499999999809e+01,1.918415999999999899e+00,
4.232301300000000310e+01,4.744766200000000111e+01,2.784336999999999840e+00,
C514: 4.541181100000000015e+01,4.835485400000000311e+01,2.983912000000000120e+00,
4.551130700000000218e+01,4.934724899999999792e+01,3.412844000000000211e+00,
4.510656199999999671e+01,4.843494100000000202e+01,2.008399999999999963e+00,

4.467589799999999656e+01,4.778906200000000126e+01,3.545482999999999940e+00,
4.637073900000000037e+01,4.784747399999999828e+01,3.020916000000000157e+00,
C515: 5.001977200000000323e+01,4.808456199999999825e+01,2.918855000000000199e+00,
5.067542399999999958e+01,4.894785900000000112e+01,2.983251999999999793e+00,
5.057671500000000009e+01,4.723324099999999959e+01,2.538874999999999993e+00,
4.919444699999999671e+01,4.830596500000000049e+01,2.248536000000000090e+00,
4.963026899999999841e+01,4.785135700000000014e+01,3.905527000000000193e+00,
C516: 7.951182000000000194e+00,5.179823400000000078e+01,2.881212999999999802e+00,
8.403655999999999793e+00,5.139659499999999781e+01,3.783183000000000185e+00,
8.332642999999999134e+00,5.126296299999999917e+01,2.016694999999999904e+00,
8.196989000000000303e+00,5.285222900000000124e+01,2.791695999999999955e+00,
6.872908999999999935e+00,5.168045599999999951e+01,2.933527000000000218e+00,
C517: 1.162182600000000043e+01,5.219936599999999771e+01,2.906290999999999958e+00,
1.105573500000000031e+01,5.273214500000000271e+01,3.664581999999999784e+00,
1.263976899999999937e+01,5.204822699999999713e+01,3.253271999999999942e+00,
1.163440499999999922e+01,5.278045999999999793e+01,1.989028999999999936e+00,
1.115753400000000006e+01,5.123595900000000114e+01,2.717772000000000077e+00,
C518: 1.612782199999999833e+01,5.217105399999999804e+01,2.959760000000000169e+00,
1.676416599999999946e+01,5.220816200000000151e+01,3.839004000000000083e+00,
1.665876099999999838e+01,5.259106599999999787e+01,2.110665000000000013e+00,
1.522431399999999968e+01,5.274506099999999975e+01,3.142649000000000026e+00,
1.586396099999999976e+01,5.113925100000000157e+01,2.747326999999999853e+00,
C519: 1.986798800000000043e+01,5.177974300000000341e+01,2.849149999999999849e+00,
2.080402399999999830e+01,5.124686400000000219e+01,2.986502999999999908e+00,
1.903716999999999970e+01,5.109271100000000132e+01,2.972776000000000085e+00,
1.983809300000000064e+01,5.220665000000000333e+01,1.851150999999999991e+00,
1.979249899999999940e+01,5.257468599999999981e+01,3.585109000000000101e+00,
C520: 2.408466400000000007e+01,5.247570100000000082e+01,2.958096999999999976e+00,
2.499589599999999834e+01,5.279368699999999848e+01,3.456049999999999844e+00,
2.391598300000000066e+01,5.309356999999999971e+01,2.081158999999999981e+00,
2.324529300000000021e+01,5.257701399999999836e+01,3.639787999999999801e+00,
2.418120100000000150e+01,5.143688499999999664e+01,2.656268999999999991e+00,
C521: 2.829551700000000025e+01,5.171031800000000089e+01,2.871440000000000214e+00,
2.843846100000000021e+01,5.249252100000000354e+01,3.611032999999999937e+00,
2.853596500000000091e+01,5.209660000000000224e+01,1.885472999999999955e+00,
2.726125899999999902e+01,5.138057899999999734e+01,2.888348000000000138e+00,
2.894738200000000106e+01,5.087348000000000070e+01,3.097319999999999932e+00,
C522: 3.187094000000000094e+01,5.209139299999999650e+01,2.863001000000000129e+00,
3.121575599999999895e+01,5.261536300000000210e+01,3.552459999999999951e+00,
3.285939799999999877e+01,5.199882300000000157e+01,3.302710999999999952e+00,
3.193915000000000148e+01,5.264939100000000138e+01,1.933956999999999926e+00,
3.147105099999999922e+01,5.110206000000000159e+01,2.661805000000000199e+00,
C523: 3.598525399999999763e+01,5.239330700000000007e+01,2.959597000000000021e+00,
3.540163100000000185e+01,5.285271999999999792e+01,3.788272000000000084e+00,
3.693468699999999671e+01,5.205166700000000191e+01,3.397545000000000037e+00,
3.616490300000000246e+01,5.312034200000000084e+01,2.209633000000000180e+00,
3.543978100000000353e+01,5.154682999999999993e+01,2.589322000000000124e+00,
C524: 4.024882399999999905e+01,5.172106800000000248e+01,2.859735999999999834e+00,
4.118528599999999784e+01,5.153388900000000206e+01,3.376246000000000080e+00,
4.043767600000000328e+01,5.232847699999999946e+01,1.979656000000000082e+00,
3.956754899999999964e+01,5.224669099999999844e+01,3.522133999999999876e+00,
3.980549100000000351e+01,5.077721999999999980e+01,2.558319000000000010e+00,
C525: 4.416953900000000033e+01,5.242949999999999733e+01,2.928920999999999886e+00,
4.354688399999999859e+01,5.282490099999999700e+01,3.725989999999999839e+00,
4.519121299999999763e+01,5.232952800000000337e+01,3.283367999999999842e+00,
4.414483100000000348e+01,5.310629300000000086e+01,2.080071999999999921e+00,
4.379520399999999825e+01,5.145585400000000220e+01,2.626843000000000039e+00,
C526: 4.852433700000000272e+01,5.182571399999999784e+01,2.954763999999999946e+00,
4.938910299999999864e+01,5.144881500000000329e+01,3.492814999999999781e+00,
4.884990100000000268e+01,5.230485199999999679e+01,2.036252000000000173e+00,
4.799898199999999804e+01,5.254739000000000004e+01,3.573262999999999856e+00,
4.785881799999999942e+01,5.100110500000000258e+01,2.716537999999999897e+00,
C527: 9.671538999999999220e+00,1.232203900000000019e+01,5.866908999999999708e+00,
9.264027999999999707e+00,1.332762499999999939e+01,5.825743000000000116e+00,
8.878230999999999540e+00,1.161996800000000007e+01,6.105310000000000237e+00,
1.043997700000000073e+01,1.227381500000000081e+01,6.632601000000000191e+00,
1.010501000000000005e+01,1.206415800000000083e+01,4.906596000000000402e+00,
C528: 1.380708199999999941e+01,1.211752500000000055e+01,5.868269999999999875e+00,
1.286834999999999951e+01,1.252394400000000019e+01,5.504569000000000045e+00,
1.442601900000000015e+01,1.182598300000000080e+01,5.025711000000000261e+00,
1.360873600000000039e+01,1.124927600000000005e+01,6.489627999999999730e+00,
1.432439600000000013e+01,1.287099000000000082e+01,6.454615000000000435e+00,
C529: 1.764162999999999926e+01,1.197906999999999920e+01,5.932737999999999623e+00,
1.736382400000000104e+01,1.093514799999999987e+01,6.037415000000000198e+00,
1.693379600000000096e+01,1.247930000000000028e+01,5.279218000000000188e+00,
1.863860899999999887e+01,1.204819099999999921e+01,5.507970000000000255e+00,
1.763059099999999901e+01,1.245451100000000011e+01,6.908984000000000236e+00,
C530: 2.196413400000000138e+01,1.220356100000000055e+01,5.885945999999999678e+00,
2.148799100000000095e+01,1.162373599999999918e+01,5.101427000000000156e+00,
2.259361799999999931e+01,1.296711299999999945e+01,5.441754000000000424e+00,
2.257114299999999929e+01,1.154715299999999978e+01,6.501748000000000083e+00,
2.120244699999999938e+01,1.267181099999999994e+01,6.501636999999999666e+00,
C531: 2.570293799999999962e+01,1.199351000000000056e+01,5.865988999999999898e+00,
2.627767300000000006e+01,1.228546200000000077e+01,6.740022999999999875e+00,
2.637911300000000026e+01,1.165895300000000034e+01,5.085431999999999952e+00,
2.513064899999999824e+01,1.284447699999999948e+01,5.510877999999999943e+00,
2.502799399999999963e+01,1.118557200000000051e+01,6.131670999999999871e+00,
C532: 3.003914899999999832e+01,1.219378200000000056e+01,5.906057999999999808e+00,
3.006424900000000022e+01,1.311533000000000015e+01,6.477271000000000001e+00,
3.088329799999999992e+01,1.216806799999999988e+01,5.223983999999999739e+00,
2.911242400000000075e+01,1.214490600000000065e+01,5.342670000000000030e+00,
3.009484799999999893e+01,1.134656299999999973e+01,6.582669000000000104e+00,
C533: 3.436656899999999837e+01,1.196688200000000002e+01,5.838479999999999670e+00,
3.496523599999999732e+01,1.266448399999999985e+01,5.261086999999999847e+00,
3.394423499999999905e+01,1.247873500000000035e+01,6.698061000000000043e+00,
3.499206600000000122e+01,1.114654099999999914e+01,6.177633000000000152e+00,
3.356388799999999861e+01,1.157829899999999945e+01,5.219440999999999775e+00,
C534: 3.804066000000000258e+01,1.223573299999999975e+01,5.908686999999999578e+00,
3.783159899999999709e+01,1.320510100000000087e+01,6.348614000000000424e+00,
3.908341000000000065e+01,1.218965599999999938e+01,5.610470000000000290e+00,
3.740739200000000153e+01,1.208791100000000007e+01,5.040297999999999945e+00,
3.783937300000000192e+01,1.145777999999999963e+01,6.639160000000000394e+00,
C535: 4.228047000000000111e+01,1.209290999999999960e+01,5.912490000000000023e+00,
4.182969400000000348e+01,1.264123700000000028e+01,6.733586999999999989e+00,
4.298663400000000223e+01,1.273159300000000016e+01,5.392373000000000083e+00,
4.150505299999999664e+01,1.177349700000000077e+01,5.223125999999999713e+00,
4.279965599999999881e+01,1.122183199999999914e+01,6.300354999999999706e+00,
C536: 4.604958400000000296e+01,1.186262999999999934e+01,5.819716999999999807e+00,
4.552681799999999868e+01,1.269805500000000009e+01,6.276083999999999996e+00,
4.595062999999999676e+01,1.192006699999999952e+01,4.740453999999999724e+00,
4.561972500000000252e+01,1.093027799999999949e+01,6.173562999999999690e+00,
4.710068900000000269e+01,1.190281899999999915e+01,6.089724999999999611e+00,
C537: 1.150215999999999994e+01,1.555983699999999992e+01,5.984103000000000172e+00,
1.155252800000000057e+01,1.515879800000000088e+01,6.991709000000000174e+00,
1.207211000000000034e+01,1.648279700000000147e+01,5.933931000000000289e+00,
1.046659000000000006e+01,1.575725699999999918e+01,5.723849999999999660e+00,
1.191962799999999945e+01,1.483770200000000017e+01,5.290440000000000254e+00,
C538: 1.614999299999999849e+01,1.538983900000000027e+01,6.002880000000000216e+00,
1.518542099999999984e+01,1.585102599999999917e+01,6.193722000000000172e+00,
1.607061799999999963e+01,1.473009700000000066e+01,5.144757000000000247e+00,
1.645485599999999948e+01,1.481668299999999938e+01,6.874385000000000190e+00,
1.688492400000000160e+01,1.616245299999999929e+01,5.799985000000000390e+00,
C539: 1.979356900000000152e+01,1.527204200000000078e+01,5.867388000000000048e+00,
1.936381000000000085e+01,1.624775599999999898e+01,6.072049999999999947e+00,
1.908570200000000128e+01,1.449852899999999956e+01,6.144921000000000078e+00,
2.070450699999999955e+01,1.515054400000000001e+01,6.442821000000000353e+00,
2.001818600000000004e+01,1.519102499999999978e+01,4.811803000000000274e+00,
C540: 2.355128500000000003e+01,1.565081799999999923e+01,6.070825000000000138e+00,
2.319934999999999903e+01,1.509997500000000059e+01,6.937466999999999828e+00,
2.271145599999999831e+01,1.612493800000000022e+01,5.573178000000000409e+00,
2.404011799999999965e+01,1.497025799999999940e+01,5.380715000000000359e+00,
2.425906399999999863e+01,1.641111000000000075e+01,6.387245000000000061e+00,
C541: 2.812758900000000040e+01,1.536894400000000083e+01,5.939923000000000286e+00,
2.728560900000000089e+01,1.605131499999999889e+01,5.869918000000000191e+00,
2.786506299999999925e+01,1.453328300000000084e+01,6.580919999999999881e+00,
2.898362099999999941e+01,1.589064300000000074e+01,6.355902000000000385e+00,
2.837649599999999950e+01,1.499631600000000020e+01,4.952461999999999698e+00,
C542: 3.197924300000000031e+01,1.530250700000000030e+01,5.949872000000000050e+00,
3.153350000000000009e+01,1.528784500000000079e+01,6.939602999999999966e+00,
3.287391499999999667e+01,1.591774599999999928e+01,5.965921999999999947e+00,
3.126807799999999915e+01,1.571668400000000076e+01,5.243074000000000012e+00,
3.224048200000000008e+01,1.429099700000000084e+01,5.656513000000000346e+00,
C543: 3.611469499999999755e+01,1.556218600000000052e+01,6.131434999999999746e+00,
3.706151899999999699e+01,1.565962900000000069e+01,6.653673999999999644e+00,
3.626892300000000091e+01,1.504666800000000038e+01,5.188736999999999711e+00,
3.570291799999999682e+01,1.654900900000000163e+01,5.942466999999999722e+00,
3.542183500000000151e+01,1.499373499999999915e+01,6.744663000000000075e+00,
C544: 4.004491199999999651e+01,1.523972700000000025e+01,5.872327000000000297e+00,
3.974895999999999674e+01,1.481606200000000051e+01,6.824328999999999645e+00,
3.915930199999999672e+01,1.555500100000000074e+01,5.332177999999999862e+00,
4.057423599999999908e+01,1.448773699999999920e+01,5.298624000000000223e+00,
4.068930199999999786e+01,1.609684599999999932e+01,6.040149999999999686e+00,
C545: 4.366811100000000323e+01,1.554497699999999938e+01,5.951920000000000321e+00,
4.460253500000000315e+01,1.592257599999999940e+01,6.356347000000000413e+00,
4.387277199999999766e+01,1.494880900000000068e+01,5.068245000000000111e+00,
4.302736199999999656e+01,1.637958100000000172e+01,5.686555000000000248e+00,
4.317382400000000331e+01,1.493138500000000057e+01,6.697841000000000378e+00,
C546: 4.804021500000000344e+01,1.514804200000000023e+01,6.002365000000000173e+00,
4.810474599999999867e+01,1.622055100000000039e+01,6.160299000000000191e+00,
4.847545699999999869e+01,1.489749400000000001e+01,5.040360999999999869e+00,
4.699859399999999710e+01,1.484267499999999984e+01,6.021640999999999799e+00,
4.858219900000000280e+01,1.463263500000000050e+01,6.788997000000000170e+00,
C547: 9.826504999999999157e+00,1.894610899999999987e+01,5.871095000000000397e+00,
1.038429400000000058e+01,1.914013100000000023e+01,6.782398999999999845e+00,
1.051942900000000058e+01,1.875750700000000037e+01,5.057983000000000118e+00,
9.210471000000000075e+00,1.980773200000000145e+01,5.632056000000000395e+00,
9.192227000000000814e+00,1.807658400000000043e+01,6.014880999999999922e+00,
C548: 1.388058700000000023e+01,1.941720300000000066e+01,6.042883999999999922e+00,
1.475067999999999913e+01,1.922127800000000164e+01,5.424844000000000221e+00,
1.389767400000000031e+01,2.045035199999999875e+01,6.372141000000000055e+00,
1.389708800000000011e+01,1.875849900000000048e+01,6.905629000000000239e+00,
1.297649400000000064e+01,1.923475300000000132e+01,5.470321000000000211e+00,
C549: 1.803509000000000029e+01,1.914691799999999944e+01,5.928333000000000297e+00,
1.797709199999999896e+01,2.022954199999999858e+01,5.891233999999999860e+00,
1.703249900000000139e+01,1.873182699999999912e+01,5.951463000000000392e+00,
1.856865300000000119e+01,1.884568300000000107e+01,6.824825999999999837e+00,
1.855950400000000045e+01,1.877641399999999905e+01,5.054739999999999789e+00,
C550: 2.156432799999999972e+01,1.891068900000000141e+01,5.941480000000000317e+00,
2.157292599999999894e+01,1.981184100000000115e+01,6.546078999999999759e+00,
2.257606600000000086e+01,1.868280299999999983e+01,5.620754999999999946e+00,
2.093369099999999960e+01,1.906540999999999997e+01,5.072987999999999609e+00,
2.117658600000000035e+01,1.808430299999999846e+01,6.529072000000000209e+00,
C551: 2.599607100000000059e+01,1.949869999999999948e+01,6.008434000000000275e+00,
2.597050499999999928e+01,2.053153400000000062e+01,6.338661000000000101e+00,
2.506642099999999829e+01,1.925545500000000132e+01,5.502919000000000338e+00,
2.611827100000000002e+01,1.884609000000000023e+01,6.867665999999999826e+00,
2.683019099999999924e+01,1.935445999999999955e+01,5.329759000000000135e+00,
C552: 3.002404599999999846e+01,1.896957000000000093e+01,5.841116000000000419e+00,
2.980520699999999934e+01,1.936490999999999829e+01,6.828572999999999560e+00,
3.078794399999999953e+01,1.957733899999999849e+01,5.368066999999999922e+00,
2.912367199999999912e+01,1.898552799999999863e+01,5.235866999999999827e+00,
3.038099199999999911e+01,1.794861600000000124e+01,5.932598999999999734e+00,
C553: 3.392861400000000316e+01,1.939987599999999901e+01,6.020571000000000339e+00,
3.310294799999999782e+01,1.918346299999999971e+01,5.350706999999999880e+00,
3.387320700000000073e+01,1.874242100000000022e+01,6.882361999999999647e+00,
3.387229399999999657e+01,2.043220900000000029e+01,6.348145999999999844e+00,
3.487066300000000041e+01,1.923539999999999850e+01,5.507005999999999624e+00,
C554: 3.837933300000000258e+01,1.890471300000000099e+01,5.938475000000000392e+00,
3.884868399999999866e+01,1.930450499999999892e+01,6.832196999999999854e+00,
3.890513899999999836e+01,1.926708599999999905e+01,5.060858999999999774e+00,
3.734318999999999988e+01,1.922633799999999837e+01,5.899930999999999592e+00,
3.841952400000000267e+01,1.782050900000000127e+01,5.964050000000000296e+00,
C555: 4.195085000000000264e+01,1.920407399999999853e+01,5.949014000000000024e+00,
4.297231699999999677e+01,1.922064500000000109e+01,5.581598999999999755e+00,
4.133068699999999751e+01,1.862598099999999945e+01,5.272254000000000218e+00,
4.157311299999999932e+01,2.021833300000000122e+01,6.017865999999999715e+00,
4.193061200000000355e+01,1.874475299999999933e+01,6.932806000000000246e+00,
C556: 4.624510200000000282e+01,1.934966299999999961e+01,6.042714000000000141e+00,
4.544538699999999665e+01,1.897251100000000079e+01,5.412872000000000128e+00,
4.717535399999999868e+01,1.936636700000000033e+01,5.482789000000000357e+00,
4.635747700000000293e+01,1.869946900000000056e+01,6.904925000000000423e+00,
4.600222699999999776e+01,2.035318499999999986e+01,6.373279000000000138e+00,
C557: 1.163789799999999985e+01,2.234043600000000040e+01,5.930774000000000434e+00,
1.222695099999999968e+01,2.272115499999999955e+01,6.759586999999999790e+00,

1.101417099999999927e+01,2.313646100000000061e+01,5.535482000000000014e+00,
1.101014299999999935e+01,2.152736000000000161e+01,6.279175999999999647e+00,
1.230421899999999980e+01,2.198072300000000112e+01,5.153673000000000393e+00,
C558: 1.588155399999999950e+01,2.256654999999999944e+01,5.885799999999999699e+00,
1.487589799999999940e+01,2.279249499999999884e+01,6.226322999999999830e+00,
1.642659199999999942e+01,2.349015699999999995e+01,5.720687999999999995e+00,
1.583084700000000034e+01,2.200198200000000170e+01,4.960621999999999865e+00,
1.639234799999999836e+01,2.197673299999999941e+01,6.640228999999999715e+00,
C559: 1.999779099999999943e+01,2.234166400000000152e+01,5.908853999999999829e+00,
2.073689099999999996e+01,2.312834199999999996e+01,6.024868999999999808e+00,
2.028130700000000175e+01,2.169457900000000095e+01,5.085306000000000104e+00,
1.902872199999999836e+01,2.278583400000000125e+01,5.702509000000000050e+00,
1.994167200000000051e+01,2.176088800000000134e+01,6.824816000000000216e+00,
C560: 2.375467300000000037e+01,2.247707400000000177e+01,5.863506000000000107e+00,
2.362561699999999831e+01,2.331392900000000168e+01,6.541438999999999560e+00,
2.476455400000000040e+01,2.248597600000000085e+01,5.465238000000000262e+00,
2.304219300000000104e+01,2.256416499999999914e+01,5.049834999999999852e+00,
2.358249299999999948e+01,2.154756300000000024e+01,6.397528000000000326e+00,
C561: 2.818796700000000044e+01,2.238976800000000011e+01,5.908934999999999604e+00,
2.753232399999999913e+01,2.212086599999999947e+01,5.086748000000000047e+00,
2.875203000000000131e+01,2.327989099999999922e+01,5.647516000000000425e+00,
2.887034399999999934e+01,2.157171800000000061e+01,6.111011000000000415e+00,
2.759196199999999877e+01,2.258854300000000137e+01,6.794579999999999842e+00,
C562: 3.182627400000000151e+01,2.238771900000000059e+01,5.935061000000000142e+00,
3.268773300000000148e+01,2.274708599999999947e+01,6.489872000000000085e+00,
3.216413099999999758e+01,2.185299499999999995e+01,5.053046000000000149e+00,
3.121277399999999957e+01,2.323243199999999931e+01,5.637095999999999663e+00,
3.124743399999999838e+01,2.172054400000000030e+01,6.565559000000000367e+00,
C563: 3.597995099999999979e+01,2.250993199999999916e+01,5.847966999999999693e+00,
3.560155000000000314e+01,2.256240599999999930e+01,6.863982000000000028e+00,
3.668421200000000226e+01,2.331857899999999972e+01,5.680945000000000356e+00,
3.515151699999999835e+01,2.259894500000000050e+01,5.152823999999999849e+00,
3.647852699999999970e+01,2.155739099999999908e+01,5.699437999999999782e+00,
C564: 3.973361799999999988e+01,2.239481699999999975e+01,5.896283999999999637e+00,
4.069381099999999662e+01,2.260857599999999934e+01,6.355705000000000382e+00,
3.910662299999999902e+01,2.186120100000000122e+01,6.604026000000000174e+00,
3.988158700000000323e+01,2.178510999999999953e+01,5.010866000000000042e+00,
3.925081899999999990e+01,2.332665199999999928e+01,5.618343000000000309e+00,
C565: 4.395746900000000323e+01,2.233790600000000026e+01,5.880342999999999876e+00,
4.299564199999999659e+01,2.270476800000000139e+01,5.536588000000000065e+00,
4.382493099999999941e+01,2.179194299999999984e+01,6.809651999999999816e+00,
4.462696600000000302e+01,2.317552699999999888e+01,6.045260999999999996e+00,
4.437899000000000171e+01,2.167748100000000022e+01,5.129140999999999728e+00,
C566: 4.774053200000000174e+01,2.264802299999999846e+01,5.852479999999999905e+00,
4.724956099999999992e+01,2.270588000000000051e+01,6.819327000000000361e+00,
4.842300000000000182e+01,2.348549699999999874e+01,5.743669999999999831e+00,
4.699251999999999896e+01,2.268384599999999907e+01,5.067440999999999640e+00,
4.829565800000000309e+01,2.171751000000000076e+01,5.785446999999999562e+00,
C567: 1.038099599999999967e+01,2.643299400000000077e+01,6.012432999999999694e+00,
1.094999499999999948e+01,2.631176400000000015e+01,6.929002999999999801e+00,
1.105149600000000021e+01,2.672305000000000064e+01,5.210084000000000160e+00,
9.626955999999999847e+00,2.720204499999999825e+01,6.149964999999999904e+00,
9.898690000000000211e+00,2.549366200000000049e+01,5.759450000000000180e+00,
C568: 1.392972999999999928e+01,2.557033399999999901e+01,5.883980000000000062e+00,
1.344818500000000050e+01,2.654245500000000035e+01,5.847012000000000320e+00,
1.483389599999999930e+01,2.559081300000000070e+01,6.284822000000000131e+00,
1.325491599999999970e+01,2.481274399999999858e+01,5.500541000000000125e+00,
1.418670799999999943e+01,2.533459300000000169e+01,6.910356000000000165e+00,
C569: 1.783970199999999906e+01,2.609849799999999931e+01,6.128506999999999927e+00,
1.688262800000000041e+01,2.608094699999999833e+01,6.640465999999999980e+00,
1.813158100000000061e+01,2.712702600000000075e+01,5.940642000000000422e+00,
1.775700499999999948e+01,2.556577800000000167e+01,5.186507999999999896e+00,
1.859031099999999981e+01,2.561785100000000170e+01,6.748846000000000345e+00,
C570: 2.236847099999999955e+01,2.615477599999999825e+01,5.965514999999999901e+00,
2.153016399999999919e+01,2.683077400000000168e+01,6.103959999999999830e+00,
2.311132299999999873e+01,2.662384000000000128e+01,5.328452000000000410e+00,
2.202009299999999925e+01,2.523767399999999839e+01,5.500706000000000095e+00,
2.281178399999999939e+01,2.592536000000000129e+01,6.929520000000000124e+00,
C571: 2.595592299999999852e+01,2.540112600000000143e+01,5.903628000000000320e+00,
2.535598099999999988e+01,2.626228000000000051e+01,6.180019999999999847e+00,
2.700699399999999883e+01,2.567107999999999990e+01,5.935578999999999716e+00,
2.569566299999999970e+01,2.508241299999999896e+01,4.901524000000000214e+00,
2.577322399999999902e+01,2.459020500000000098e+01,6.601219999999999644e+00,
C572: 3.027357999999999905e+01,2.661678300000000164e+01,6.096815999999999569e+00,
2.992350199999999916e+01,2.759827900000000156e+01,6.398400999999999783e+00,
3.112345499999999987e+01,2.672517200000000059e+01,5.430487000000000286e+00,
2.947532700000000006e+01,2.608827600000000047e+01,5.584755000000000358e+00,
3.057546899999999823e+01,2.604991800000000168e+01,6.972249999999999837e+00,
C573: 3.414551399999999859e+01,2.561200900000000047e+01,5.908957000000000015e+00,
3.480984999999999729e+01,2.538080199999999920e+01,6.734568999999999583e+00,
3.463331099999999907e+01,2.631262200000000107e+01,5.238779000000000075e+00,
3.323452499999999787e+01,2.605680200000000113e+01,6.296097999999999750e+00,
3.390534799999999649e+01,2.470008299999999934e+01,5.373255000000000337e+00,
C574: 3.769537900000000263e+01,2.620038500000000070e+01,5.996040999999999954e+00,
3.697104900000000072e+01,2.686611399999999961e+01,6.453813000000000244e+00,
3.858435000000000059e+01,2.676032800000000123e+01,5.723892000000000202e+00,
3.726336100000000329e+01,2.574507499999999993e+01,5.111449999999999605e+00,
3.796690300000000207e+01,2.542194399999999987e+01,6.702535000000000132e+00,
C575: 4.213749399999999667e+01,2.555328000000000088e+01,6.078255999999999659e+00,
4.261518399999999929e+01,2.504845500000000058e+01,6.912606000000000250e+00,
4.255511800000000022e+01,2.518839699999999837e+01,5.145489999999999675e+00,
4.230838299999999919e+01,2.662273000000000067e+01,6.156857999999999720e+00,
4.106992999999999938e+01,2.535601399999999828e+01,6.098978999999999928e+00,
C576: 4.594481499999999841e+01,2.580708900000000128e+01,5.903923999999999950e+00,
4.674552599999999813e+01,2.653369500000000158e+01,5.806181999999999732e+00,
4.587015699999999896e+01,2.522455700000000078e+01,4.992373999999999867e+00,
4.500675700000000035e+01,2.632221600000000095e+01,6.082843000000000444e+00,
4.615848600000000346e+01,2.514488100000000159e+01,6.736136000000000124e+00,
C577: 1.211480099999999993e+01,2.956681700000000035e+01,5.909740000000000215e+00,
1.229260599999999926e+01,2.894908099999999962e+01,6.785031000000000034e+00,
1.276051299999999955e+01,2.924048799999999915e+01,5.101808000000000121e+00,
1.232683899999999966e+01,3.060274400000000128e+01,6.152320999999999707e+00,
1.107661300000000004e+01,2.947199000000000028e+01,5.606364000000000125e+00,
C578: 1.567327200000000076e+01,2.921578600000000137e+01,5.855368000000000350e+00,
1.524275300000000044e+01,2.956136400000000108e+01,6.790531999999999790e+00,
1.672923199999999966e+01,2.946466600000000113e+01,5.830131999999999870e+00,
1.516700200000000009e+01,2.969533300000000153e+01,5.024013000000000062e+00,
1.555312499999999964e+01,2.813992199999999855e+01,5.778703000000000145e+00,
C579: 1.998346700000000098e+01,2.966806599999999960e+01,5.992765000000000342e+00,
1.905305500000000052e+01,2.952554900000000160e+01,5.452626999999999668e+00,
2.004383599999999888e+01,3.069071299999999880e+01,6.347565999999999597e+00,
2.082570099999999869e+01,2.945925300000000036e+01,5.340696999999999584e+00,
2.000921100000000052e+01,2.899087700000000112e+01,6.840626999999999569e+00,
C580: 2.406180600000000069e+01,2.948145600000000144e+01,5.851754999999999818e+00,
2.461870100000000150e+01,2.877841199999999944e+01,6.463740999999999737e+00,
2.460328700000000168e+01,3.041963399999999851e+01,5.791890999999999678e+00,
2.308882699999999843e+01,2.965396900000000002e+01,6.301140000000000185e+00,
2.393231000000000108e+01,2.906954800000000105e+01,4.856416000000000288e+00,
C581: 2.751892899999999997e+01,2.933770499999999970e+01,5.892867999999999995e+00,
2.710788799999999910e+01,2.974448100000000039e+01,6.811828000000000216e+00,
2.856644100000000108e+01,2.961144499999999979e+01,5.813312999999999953e+00,
2.697431299999999865e+01,2.973810800000000043e+01,5.043616000000000099e+00,
2.742698000000000036e+01,2.825593299999999886e+01,5.903970000000000162e+00,
C582: 3.216051699999999869e+01,2.977979799999999955e+01,5.930238000000000120e+00,
3.286110200000000248e+01,2.978528700000000029e+01,5.102433000000000440e+00,
3.239010499999999837e+01,2.894857100000000116e+01,6.589368000000000336e+00,
3.114970800000000040e+01,2.966998999999999853e+01,5.550138999999999712e+00,
3.224204100000000039e+01,3.071183699999999916e+01,6.479377000000000386e+00,
C583: 3.581070499999999868e+01,2.948980200000000096e+01,5.851583999999999897e+00,
3.650650600000000168e+01,2.996691099999999963e+01,6.534925000000000317e+00,
3.636286700000000138e+01,2.898584400000000016e+01,5.065434999999999910e+00,
3.515925699999999665e+01,3.023913399999999996e+01,5.415600999999999665e+00,
3.521268599999999793e+01,2.876428500000000099e+01,6.394997000000000043e+00,
C584: 3.968617299999999659e+01,2.956736000000000075e+01,5.989580000000000126e+00,
3.937615900000000124e+01,2.906042899999999918e+01,6.898016000000000147e+00,
3.882543600000000339e+01,2.970840099999999850e+01,5.343599000000000210e+00,
4.043028100000000080e+01,2.896546000000000021e+01,5.477437000000000111e+00,
4.011292600000000164e+01,3.053276299999999921e+01,6.241219000000000072e+00,
C585: 4.403240900000000124e+01,2.937320400000000120e+01,5.941476999999999897e+00,
4.409512999999999749e+01,3.030007399999999862e+01,6.501754000000000033e+00,
4.469349299999999658e+01,2.942060199999999881e+01,5.082423999999999609e+00,
4.301123299999999716e+01,2.922238199999999964e+01,5.604667000000000066e+00,
4.432672699999999821e+01,2.854694500000000090e+01,6.580888999999999989e+00,
C586: 4.767153299999999660e+01,2.949390199999999851e+01,5.832863999999999827e+00,
4.846619799999999856e+01,2.876334800000000058e+01,5.714231999999999978e+00,
4.810427099999999712e+01,3.047124300000000119e+01,6.024537999999999727e+00,
4.703993200000000030e+01,2.920810799999999929e+01,6.668740999999999808e+00,
4.707771300000000281e+01,2.953178300000000078e+01,4.924890000000000434e+00,
C587: 1.002269399999999955e+01,3.270456000000000074e+01,5.895805000000000184e+00,
1.079263699999999915e+01,3.333669799999999839e+01,5.463758999999999588e+00,
9.070192999999999728e+00,3.322543000000000291e+01,5.871159999999999712e+00,
1.028243900000000011e+01,3.247331599999999696e+01,6.923879000000000339e+00,
9.946714999999999307e+00,3.178330700000000064e+01,5.327570999999999835e+00,
C588: 1.432066299999999970e+01,3.268667500000000103e+01,5.938541999999999987e+00,
1.482111199999999940e+01,3.359217399999999998e+01,5.608783999999999992e+00,
1.422413599999999967e+01,3.200156499999999937e+01,5.102403999999999940e+00,
1.333444599999999980e+01,3.293745799999999946e+01,6.317695999999999756e+00,
1.490245200000000025e+01,3.221801399999999660e+01,6.726449999999999818e+00,
C589: 1.807745500000000050e+01,3.277999599999999703e+01,5.852473999999999954e+00,
1.847805599999999870e+01,3.285836700000000121e+01,6.858426999999999829e+00,
1.888374200000000158e+01,3.289559799999999967e+01,5.135774999999999757e+00,
1.733893499999999932e+01,3.356039499999999975e+01,5.696954999999999991e+00,
1.761179200000000122e+01,3.180793500000000051e+01,5.725310999999999595e+00,
C590: 2.194865899999999925e+01,3.280030500000000160e+01,5.935283000000000087e+00,
2.115597500000000153e+01,3.318212100000000220e+01,6.571204999999999963e+00,
2.259589100000000172e+01,3.361788599999999860e+01,5.632423000000000179e+00,
2.151398599999999917e+01,3.233365899999999726e+01,5.057269999999999932e+00,
2.252855999999999881e+01,3.206551499999999777e+01,6.484020000000000117e+00,
C591: 2.618953899999999990e+01,3.287485300000000166e+01,5.982992999999999562e+00,
2.659515899999999888e+01,3.386596999999999724e+01,5.805632000000000126e+00,
2.617243300000000161e+01,3.231766100000000108e+01,5.051618999999999637e+00,
2.517921199999999970e+01,3.296241100000000301e+01,6.371277000000000079e+00,
2.681048300000000140e+01,3.235439999999999827e+01,6.705752999999999631e+00,
C592: 2.993681600000000032e+01,3.275752099999999700e+01,5.859077000000000091e+00,
2.981867400000000146e+01,3.172794499999999829e+01,5.537643000000000093e+00,
3.091659800000000047e+01,3.312143799999999771e+01,5.567071000000000325e+00,
2.984125999999999834e+01,3.281343100000000135e+01,6.937409999999999854e+00,
2.916927000000000092e+01,3.337177199999999999e+01,5.399859000000000187e+00,
C593: 3.413795100000000105e+01,3.295797100000000057e+01,6.045605000000000118e+00,
3.321062599999999776e+01,3.317770199999999647e+01,6.565967999999999805e+00,
3.464486399999999833e+01,3.388674100000000067e+01,5.801376999999999562e+00,
3.392100500000000096e+01,3.241196500000000214e+01,5.132614000000000232e+00,
3.477598400000000112e+01,3.235674999999999812e+01,6.686282000000000281e+00,
C594: 3.821118799999999993e+01,3.291250500000000301e+01,5.930957000000000257e+00,
3.896717499999999745e+01,3.306210200000000299e+01,6.695784999999999876e+00,
3.867374300000000176e+01,3.249552400000000318e+01,5.042284000000000432e+00,
3.774511400000000094e+01,3.386332500000000323e+01,5.691404999999999603e+00,
3.745638600000000196e+01,3.222519799999999890e+01,6.299731999999999665e+00,
C595: 4.203518100000000146e+01,3.276956200000000052e+01,5.868682999999999872e+00,
4.116133700000000317e+01,3.302925499999999914e+01,5.280238999999999905e+00,
4.281258700000000061e+01,3.350979000000000241e+01,5.708148000000000444e+00,
4.239383600000000030e+01,3.179041799999999895e+01,5.571236999999999995e+00,
4.176596700000000340e+01,3.274898499999999757e+01,6.920079000000000313e+00,
C596: 4.579673900000000231e+01,3.269475899999999768e+01,5.965201000000000420e+00,
4.519423799999999858e+01,3.353509999999999991e+01,5.635272999999999755e+00,
4.681989899999999949e+01,3.302407099999999929e+01,6.120327999999999768e+00,
4.577939500000000095e+01,3.191590700000000069e+01,5.209421999999999997e+00,
4.539761200000000230e+01,3.230696700000000021e+01,6.897369000000000305e+00,
C597: 1.151937799999999967e+01,3.674746100000000126e+01,5.950890000000000235e+00,
1.193673099999999998e+01,3.773744800000000055e+01,6.102329000000000114e+00,
1.228618099999999913e+01,3.608696999999999666e+01,5.557673999999999559e+00,
1.069438199999999917e+01,3.680542700000000167e+01,5.247899999999999565e+00,
1.115936899999999987e+01,3.635816700000000168e+01,6.898479000000000028e+00,
C598: 1.618983199999999911e+01,3.678625199999999751e+01,6.022573000000000398e+00,
1.526895900000000061e+01,3.644560299999999842e+01,5.559173999999999616e+00,
1.699939300000000131e+01,3.674170300000000111e+01,5.301635000000000097e+00,
1.642563300000000126e+01,3.614716899999999811e+01,6.868017000000000039e+00,
1.606693200000000132e+01,3.780843600000000038e+01,6.363076000000000398e+00,
C599: 1.988259400000000099e+01,3.595724299999999829e+01,5.918453000000000408e+00,
1.948048400000000058e+01,3.696355499999999950e+01,5.857111999999999874e+00,
2.091536999999999935e+01,3.599987099999999884e+01,6.250195999999999863e+00,
1.983539800000000142e+01,3.548416499999999729e+01,4.944259999999999877e+00,
1.929969699999999833e+01,3.537859399999999965e+01,6.626915000000000333e+00,
C600: 2.412130200000000002e+01,3.692203599999999852e+01,6.096676000000000428e+00,

2.427583299999999866e+01,3.625468699999999700e+01,6.938791000000000153e+00,
2.491503000000000156e+01,3.677106799999999964e+01,5.372124999999999595e+00,
2.413439100000000082e+01,3.795066700000000282e+01,6.440291000000000210e+00,
2.316074700000000064e+01,3.670361400000000174e+01,5.640569000000000166e+00,
C601: 2.825480900000000162e+01,3.648913100000000043e+01,5.929406000000000176e+00,
2.719092900000000057e+01,3.644228400000000079e+01,5.722095999999999627e+00,
2.855425800000000081e+01,3.560236600000000351e+01,6.479815000000000325e+00,
2.846725899999999854e+01,3.737097099999999728e+01,6.525214000000000070e+00,
2.880560499999999990e+01,3.653908299999999798e+01,4.995726999999999585e+00,
C602: 3.181569999999999965e+01,3.633272699999999844e+01,5.941067000000000320e+00,
3.265931199999999990e+01,3.700259700000000151e+01,6.073564000000000185e+00,
3.217820900000000250e+01,3.532953400000000244e+01,5.740507000000000026e+00,
3.121192999999999884e+01,3.667252899999999727e+01,5.105739999999999945e+00,
3.121499000000000024e+01,3.632660099999999659e+01,6.845263000000000098e+00,
C603: 3.581812999999999647e+01,3.704103200000000129e+01,6.064734999999999765e+00,
3.673775499999999994e+01,3.672450099999999651e+01,5.582379000000000424e+00,
3.561085200000000128e+01,3.638144400000000189e+01,6.901678999999999675e+00,
3.498950099999999708e+01,3.699363900000000172e+01,5.365619999999999834e+00,
3.592866399999999771e+01,3.805700800000000328e+01,6.428511000000000308e+00,
C604: 4.009624399999999866e+01,3.606403300000000200e+01,5.946615999999999680e+00,
4.060756099999999691e+01,3.702078900000000061e+01,5.932324999999999626e+00,
4.057351500000000044e+01,3.540848799999999841e+01,6.667212000000000138e+00,
4.014565799999999740e+01,3.560881400000000241e+01,4.963796999999999571e+00,
3.905748499999999979e+01,3.621327500000000299e+01,6.224546000000000134e+00,
C605: 4.372705599999999748e+01,3.668893000000000352e+01,5.957428000000000168e+00,
4.322036299999999898e+01,3.631280600000000192e+01,6.840780999999999779e+00,
4.418494499999999903e+01,3.764704799999999807e+01,6.181548000000000265e+00,
4.300741599999999920e+01,3.681127200000000244e+01,5.154431999999999903e+00,
4.449450300000000169e+01,3.598391600000000068e+01,5.653133999999999659e+00,
C606: 4.822148399999999668e+01,3.638019700000000256e+01,6.075045000000000250e+00,
4.878091700000000230e+01,3.730402999999999736e+01,6.188536000000000037e+00,
4.860943400000000025e+01,3.582295599999999780e+01,5.228123000000000076e+00,
4.717298000000000258e+01,3.660955700000000235e+01,5.908924999999999983e+00,
4.832123899999999850e+01,3.578202399999999983e+01,6.975615999999999595e+00,
C607: 9.754896000000000456e+00,3.989931700000000347e+01,5.862967000000000262e+00,
9.262850999999999502e+00,4.086559700000000106e+01,5.807020999999999766e+00,
1.034493400000000030e+01,3.973773899999999770e+01,4.966680000000000206e+00,
9.007296999999999443e+00,3.911669599999999747e+01,5.950765999999999778e+00,
1.040555600000000069e+01,3.987571200000000005e+01,6.732287000000000354e+00,
C608: 1.396558100000000024e+01,3.993993999999999866e+01,5.921448999999999963e+00,
1.300397399999999948e+01,3.997100100000000111e+01,5.418797999999999782e+00,
1.404092600000000068e+01,3.902539800000000270e+01,6.500522000000000133e+00,
1.405375800000000019e+01,4.079476700000000022e+01,6.582594000000000278e+00,
1.476248499999999986e+01,3.997103400000000306e+01,5.185342000000000340e+00,
C609: 1.812271300000000096e+01,3.980742999999999654e+01,5.863715000000000011e+00,
1.871490800000000121e+01,4.068535500000000127e+01,5.626509000000000427e+00,
1.806246000000000151e+01,3.916344000000000136e+01,4.992125999999999841e+00,
1.712390699999999910e+01,4.011552799999999763e+01,6.157430999999999877e+00,
1.858841800000000077e+01,3.926662400000000019e+01,6.682240000000000180e+00,
C610: 2.167647499999999994e+01,3.968353400000000164e+01,5.881931999999999938e+00,
2.136171200000000070e+01,4.024725500000000267e+01,6.754641999999999591e+00,
2.271520100000000042e+01,3.990835799999999978e+01,5.660871000000000208e+00,
2.105642299999999878e+01,3.995419100000000157e+01,5.033723000000000170e+00,
2.156894099999999881e+01,3.862212900000000104e+01,6.082213000000000314e+00,
C611: 2.613460600000000156e+01,4.006465699999999686e+01,5.905084000000000444e+00,
2.518746900000000011e+01,3.999604899999999930e+01,5.379424000000000206e+00,
2.608699800000000124e+01,4.086846700000000254e+01,6.630917000000000172e+00,
2.693075800000000086e+01,4.026842400000000310e+01,5.196228999999999765e+00,
2.633595000000000041e+01,3.912626300000000157e+01,6.411421999999999954e+00,
C612: 3.006779900000000083e+01,3.974188500000000346e+01,5.823612999999999928e+00,
3.047991499999999832e+01,4.073027499999999890e+01,5.645004000000000133e+00,
2.993633000000000166e+01,3.922574999999999790e+01,4.877646999999999622e+00,
2.910897800000000046e+01,3.983625899999999831e+01,6.323655999999999722e+00,
3.074725799999999865e+01,3.917612199999999945e+01,6.453844000000000136e+00,
C613: 3.374230800000000130e+01,4.013111800000000073e+01,5.913100000000000023e+00,
3.382336399999999799e+01,4.106458099999999689e+01,6.459525000000000183e+00,
3.468370800000000287e+01,3.992086100000000215e+01,5.415372999999999770e+00,
3.295163099999999901e+01,4.021521599999999808e+01,5.174865999999999744e+00,
3.350962400000000230e+01,3.932636000000000109e+01,6.602636999999999645e+00,
C614: 3.834037099999999754e+01,3.984913699999999892e+01,5.863303000000000154e+00,
3.860913899999999899e+01,4.059344099999999855e+01,6.606090000000000018e+00,
3.896214599999999706e+01,3.997498699999999872e+01,4.982676999999999801e+00,
3.729630499999999671e+01,3.996932199999999824e+01,5.591342000000000034e+00,
3.849529700000000076e+01,3.885663399999999967e+01,6.275596000000000174e+00,
C615: 4.186335900000000265e+01,3.976585599999999943e+01,5.882615999999999623e+00,
4.131094699999999875e+01,4.069096100000000149e+01,5.751789999999999736e+00,
4.183738199999999807e+01,3.919169800000000237e+01,4.962582000000000271e+00,
4.141425600000000173e+01,3.918794100000000213e+01,6.684682999999999709e+00,
4.289390399999999914e+01,3.999350299999999692e+01,6.137445999999999735e+00,
C616: 4.611892199999999775e+01,4.004335700000000031e+01,5.893087999999999660e+00,
4.528863799999999884e+01,3.982238499999999704e+01,5.229541000000000217e+00,
4.596521400000000313e+01,4.101261300000000176e+01,6.354140000000000121e+00,
4.704608499999999793e+01,4.005267500000000069e+01,5.328173999999999744e+00,
4.617726199999999892e+01,3.928165099999999654e+01,6.664289000000000129e+00,
C617: 1.189260900000000021e+01,4.301525399999999877e+01,5.950056000000000012e+00,
1.259792099999999948e+01,4.371664499999999975e+01,6.384612999999999872e+00,
1.219576099999999919e+01,4.277449000000000012e+01,4.937738000000000405e+00,
1.090396800000000077e+01,4.346411799999999914e+01,5.934032000000000195e+00,
1.186716400000000071e+01,4.210969000000000051e+01,6.548157999999999923e+00,
C618: 1.561407299999999942e+01,4.323626999999999754e+01,5.897114000000000189e+00,
1.641836599999999891e+01,4.396210099999999699e+01,5.972565000000000346e+00,
1.531929700000000061e+01,4.291867500000000035e+01,6.891828000000000287e+00,
1.595510400000000040e+01,4.237462599999999924e+01,5.333558000000000021e+00,
1.476436299999999946e+01,4.368775099999999867e+01,5.396384000000000292e+00,
C619: 2.040995099999999951e+01,4.320682699999999699e+01,6.023622999999999728e+00,
2.086752699999999905e+01,4.413403499999999724e+01,5.694157999999999831e+00,
2.031774800000000170e+01,4.252810499999999649e+01,5.181608999999999909e+00,
1.942390699999999981e+01,4.341480099999999709e+01,6.428480000000000416e+00,
2.102685400000000016e+01,4.275155000000000172e+01,6.791800000000000281e+00,
C620: 2.404425700000000177e+01,4.311800099999999958e+01,5.877142000000000088e+00,
2.496118399999999937e+01,4.356519699999999773e+01,5.509204999999999686e+00,
2.378948099999999855e+01,4.225639699999999976e+01,5.269842999999999833e+00,
2.324546499999999938e+01,4.385065199999999663e+01,5.829288000000000025e+00,
2.418430800000000147e+01,4.280074100000000215e+01,6.904678999999999789e+00,
C621: 2.783280099999999990e+01,4.331057100000000304e+01,6.027581999999999773e+00,
2.702856399999999937e+01,4.366840400000000244e+01,6.662765000000000271e+00,
2.852057500000000090e+01,4.412499600000000299e+01,5.820452999999999655e+00,
2.742328300000000141e+01,4.293503199999999964e+01,5.096181999999999768e+00,
2.836387500000000017e+01,4.251113200000000347e+01,6.535464000000000162e+00,
C622: 3.221526599999999974e+01,4.357914300000000196e+01,6.062237999999999793e+00,
3.178790100000000152e+01,4.279763899999999666e+01,6.683262000000000036e+00,
3.303214700000000192e+01,4.405537600000000253e+01,6.594693000000000360e+00,
3.145180500000000023e+01,4.431758700000000317e+01,5.836318000000000339e+00,
3.258458999999999861e+01,4.314361099999999993e+01,5.139297000000000004e+00,
C623: 3.594912699999999717e+01,4.314362500000000011e+01,5.862326999999999622e+00,
3.596320999999999657e+01,4.309882199999999841e+01,6.944830999999999754e+00,
3.673828600000000222e+01,4.380410899999999685e+01,5.519778999999999769e+00,
3.499289600000000178e+01,4.352748199999999912e+01,5.526919000000000359e+00,
3.610474099999999709e+01,4.214919100000000185e+01,5.456563000000000052e+00,
C624: 3.960455600000000231e+01,4.344926099999999991e+01,6.062883000000000244e+00,
4.052055599999999913e+01,4.387679899999999833e+01,6.459164999999999601e+00,
3.984879000000000104e+01,4.266684200000000260e+01,5.350817000000000156e+00,
3.903166099999999972e+01,4.422447199999999867e+01,5.565358999999999945e+00,
3.901928099999999944e+01,4.303174200000000127e+01,6.875957999999999792e+00,
C625: 4.376627299999999821e+01,4.300812499999999972e+01,5.996125000000000149e+00,
4.399642800000000165e+01,4.406823899999999838e+01,6.043817999999999913e+00,
4.424660699999999736e+01,4.257191900000000118e+01,5.127350999999999992e+00,
4.269172900000000226e+01,4.287450599999999667e+01,5.922894000000000325e+00,
4.413060099999999863e+01,4.251835700000000173e+01,6.892953000000000330e+00,
C626: 4.750550599999999690e+01,4.345442200000000099e+01,5.864874000000000365e+00,
4.721042899999999776e+01,4.317280000000000229e+01,6.870610000000000106e+00,
4.824087099999999850e+01,4.425186200000000269e+01,5.914162000000000141e+00,
4.663430900000000179e+01,4.379819499999999977e+01,5.316853000000000051e+00,
4.793599900000000247e+01,4.259497900000000215e+01,5.360877000000000336e+00,
C627: 1.027482799999999941e+01,4.707945600000000042e+01,5.982681999999999611e+00,
9.727874999999999162e+00,4.628472099999999756e+01,5.484455999999999776e+00,
1.067283100000000040e+01,4.670845800000000025e+01,6.921560999999999630e+00,
9.607108000000000203e+00,4.791406599999999827e+01,6.173583999999999961e+00,
1.109279000000000082e+01,4.740760000000000218e+01,5.349370999999999654e+00,
C628: 1.393565399999999954e+01,4.663013000000000119e+01,5.945060999999999929e+00,
1.491694700000000040e+01,4.666279699999999764e+01,5.486345000000000027e+00,
1.359166800000000030e+01,4.763882699999999915e+01,6.151552999999999827e+00,
1.399252099999999999e+01,4.607033500000000004e+01,6.873456000000000010e+00,
1.323817200000000049e+01,4.613865299999999792e+01,5.274856999999999907e+00,
C629: 1.772965100000000049e+01,4.731103300000000189e+01,5.994352000000000125e+00,
1.875315000000000154e+01,4.705265500000000145e+01,5.739316999999999780e+00,
1.708179200000000009e+01,4.710229600000000261e+01,5.149892999999999610e+00,
1.767517799999999895e+01,4.836479400000000339e+01,6.246076999999999657e+00,
1.741004200000000068e+01,4.671765800000000013e+01,6.845391000000000226e+00,
C630: 2.232758400000000165e+01,4.694576299999999947e+01,5.920728000000000435e+00,
2.212924299999999889e+01,4.797509800000000268e+01,6.201560999999999879e+00,
2.309904300000000177e+01,4.691895600000000144e+01,5.157879999999999576e+00,
2.141839699999999880e+01,4.649631699999999768e+01,5.533876000000000239e+00,
2.266104500000000144e+01,4.639034099999999938e+01,6.792070999999999970e+00,
C631: 2.594668300000000016e+01,4.662878400000000312e+01,5.984558999999999962e+00,
2.692381400000000014e+01,4.623116699999999923e+01,6.239911000000000207e+00,
2.601691699999999940e+01,4.770550000000000068e+01,5.873349000000000153e+00,
2.524339700000000164e+01,4.639305499999999682e+01,6.776222999999999885e+00,
2.560666099999999901e+01,4.618314800000000275e+01,5.055642999999999887e+00,
C632: 2.993153200000000069e+01,4.737093399999999832e+01,6.022403999999999868e+00,
2.906930300000000145e+01,4.718328300000000297e+01,5.390505000000000102e+00,
3.086148400000000080e+01,4.726810400000000101e+01,5.472250999999999976e+00,
2.993139899999999898e+01,4.665072599999999881e+01,6.834590000000000387e+00,
2.986672700000000091e+01,4.836462300000000170e+01,6.449142000000000152e+00,
C633: 3.414578499999999650e+01,4.686579199999999901e+01,5.914470999999999812e+00,
3.480879900000000049e+01,4.695571199999999834e+01,5.060412999999999606e+00,
3.403631599999999935e+01,4.783316599999999852e+01,6.393716999999999651e+00,
3.456269499999999795e+01,4.615714499999999987e+01,6.623553000000000246e+00,
3.317178499999999985e+01,4.651732400000000212e+01,5.586903000000000397e+00,
C634: 3.773596799999999973e+01,4.688906899999999922e+01,5.967791000000000068e+00,
3.752764499999999970e+01,4.795173599999999681e+01,6.025872999999999813e+00,
3.879886299999999721e+01,4.673903200000000169e+01,5.804286000000000278e+00,
3.717721199999999726e+01,4.644808400000000148e+01,5.149085999999999608e+00,
3.744476900000000086e+01,4.641077599999999848e+01,6.897473999999999883e+00,
C635: 4.227544699999999978e+01,4.708330300000000079e+01,6.006872999999999685e+00,
4.301894899999999922e+01,4.707162100000000038e+01,5.216442999999999941e+00,
4.202730300000000341e+01,4.810922399999999755e+01,6.257509999999999906e+00,
4.267456599999999867e+01,4.658201499999999839e+01,6.883657000000000359e+00,
4.138145500000000254e+01,4.656638199999999728e+01,5.671175999999999995e+00,
C636: 4.603628299999999740e+01,4.681443600000000060e+01,5.883968000000000309e+00,
4.545765300000000053e+01,4.609485000000000099e+01,5.313695000000000057e+00,
4.624935599999999880e+01,4.640725700000000131e+01,6.867513999999999896e+00,
4.546952799999999684e+01,4.773355899999999963e+01,5.989567000000000085e+00,
4.697050800000000237e+01,4.702001500000000078e+01,5.370472999999999608e+00,
C637: 1.156512099999999954e+01,5.046833099999999916e+01,5.880841000000000207e+00,
1.170769400000000005e+01,4.989166600000000074e+01,6.790057000000000009e+00,
1.212844699999999953e+01,5.139423699999999684e+01,5.948688999999999893e+00,
1.051004900000000042e+01,5.069351799999999741e+01,5.756560000000000343e+00,
1.191493900000000039e+01,4.989223899999999645e+01,5.029533999999999949e+00,
C638: 1.533655599999999986e+01,5.008728700000000345e+01,5.860407000000000366e+00,
1.534473700000000029e+01,5.109678000000000253e+01,6.260472000000000037e+00,
1.442164700000000011e+01,4.992889600000000172e+01,5.298998000000000097e+00,
1.539016499999999965e+01,4.937453899999999862e+01,6.677692999999999657e+00,
1.619036399999999887e+01,4.995194800000000157e+01,5.203536999999999857e+00,
C639: 1.996429799999999943e+01,5.027467599999999948e+01,5.878465000000000273e+00,
2.035994600000000077e+01,4.953571999999999775e+01,5.189631999999999579e+00,
1.896235700000000080e+01,5.055894299999999930e+01,5.570846000000000409e+00,
2.060664600000000135e+01,5.115021899999999988e+01,5.879241999999999635e+00,
1.992833500000000058e+01,4.985231000000000279e+01,6.877608999999999639e+00,
C640: 2.423198100000000110e+01,5.006554299999999813e+01,5.861966999999999928e+00,
2.480744800000000083e+01,5.088814099999999740e+01,5.449482999999999855e+00,
2.410107800000000111e+01,4.929924700000000115e+01,5.105192999999999870e+00,
2.325904600000000144e+01,5.042922399999999783e+01,6.178745000000000154e+00,
2.475605200000000039e+01,4.964800699999999978e+01,6.716313999999999673e+00,
C641: 2.788057900000000089e+01,5.034213499999999897e+01,5.928129000000000204e+00,
2.880909000000000120e+01,5.080942600000000198e+01,6.240260000000000140e+00,
2.807019899999999879e+01,4.967245100000000235e+01,5.095044999999999824e+00,
2.717697400000000130e+01,5.111068699999999865e+01,5.624003000000000085e+00,
2.746330199999999877e+01,4.977826199999999801e+01,6.757083999999999868e+00,
C642: 3.176701800000000020e+01,5.050060400000000271e+01,5.867689999999999628e+00,
3.137626699999999857e+01,5.028708900000000170e+01,6.857798999999999978e+00,
3.222319300000000197e+01,5.148594400000000348e+01,5.864639000000000379e+00,
3.095695200000000114e+01,5.047138499999999794e+01,5.145976000000000106e+00,
3.251201799999999764e+01,4.975567499999999654e+01,5.606340000000000323e+00,

C643: 3.578203299999999842e+01,5.017433100000000223e+01,5.884083000000000396e+00,
3.667784199999999828e+01,5.078775600000000168e+01,5.903938000000000130e+00,
3.584291199999999833e+01,4.947287299999999988e+01,5.057590000000000252e+00,
3.491142599999999874e+01,5.081032600000000343e+01,5.755830999999999698e+00,
3.569757200000000097e+01,4.962884400000000085e+01,6.819365999999999595e+00,
C644: 3.991655999999999693e+01,5.025295700000000210e+01,5.878820000000000157e+00,
4.089211999999999847e+01,5.014535500000000212e+01,5.415723999999999982e+00,
3.987945700000000215e+01,4.965590499999999707e+01,6.784647999999999790e+00,
3.914826699999999704e+01,4.991320600000000240e+01,5.191641999999999868e+00,
3.974539299999999997e+01,5.129649400000000270e+01,6.125199000000000282e+00,
C645: 4.394954299999999847e+01,5.035110999999999848e+01,5.917971999999999788e+00,
4.478003900000000215e+01,5.097681000000000040e+01,5.606787999999999883e+00,
4.360656900000000036e+01,4.975862399999999752e+01,5.075657999999999781e+00,
4.313794500000000198e+01,5.097961999999999705e+01,6.272135999999999711e+00,
4.427096199999999726e+01,4.969316599999999795e+01,6.719179999999999708e+00,
C646: 4.765114499999999964e+01,5.012536500000000217e+01,5.892220000000000013e+00,
4.727814999999999657e+01,5.113736300000000057e+01,5.766677999999999749e+00,
4.871760499999999894e+01,5.015550199999999847e+01,6.094721999999999973e+00,
4.747180300000000130e+01,4.955689399999999978e+01,4.984900999999999804e+00,
4.713877399999999795e+01,4.965221599999999717e+01,6.724705000000000155e+00,
C647: 8.192325999999999553e+00,1.055196899999999971e+01,9.372058000000000888e+00,
8.722799000000000191e+00,1.006124299999999927e+01,1.018262499999999982e+01,
8.879388999999999754e+00,1.074297499999999950e+01,8.553373000000000559e+00,
7.779682000000000208e+00,1.149192799999999970e+01,9.726138000000000616e+00,
7.387055000000000149e+00,9.910845000000000127e+00,9.026092000000000226e+00,
C648: 1.194907500000000056e+01,1.059153799999999990e+01,9.585178000000000864e+00,
1.186239600000000038e+01,1.166988599999999998e+01,9.673780000000000712e+00,
1.299865600000000043e+01,1.031322300000000070e+01,9.576017000000000223e+00,
1.148030200000000001e+01,1.026622200000000085e+01,8.661222000000000421e+00,
1.145624100000000034e+01,1.011761300000000041e+01,1.042880500000000055e+01,
C649: 1.635055499999999995e+01,1.060108899999999998e+01,9.462626000000000204e+00,
1.650483399999999889e+01,9.876523000000000607e+00,8.668630999999999531e+00,
1.546553800000000045e+01,1.119151600000000002e+01,9.245473999999999748e+00,
1.721361500000000078e+01,1.125579800000000041e+01,9.525610999999999606e+00,
1.621721799999999902e+01,1.008101199999999942e+01,1.040641600000000011e+01,
C650: 1.996912499999999824e+01,1.017344399999999993e+01,9.338938999999999879e+00,
2.096706400000000059e+01,9.754611999999999838e+00,9.426671999999999940e+00,
1.933325699999999969e+01,9.482801000000000258e+00,8.793143999999999849e+00,
2.001837099999999836e+01,1.111816299999999913e+01,8.805407999999999902e+00,
1.955790700000000015e+01,1.033850799999999914e+01,1.033025899999999986e+01,
C651: 2.396314399999999978e+01,1.105444100000000063e+01,9.616331999999999880e+00,
2.494382099999999980e+01,1.086682000000000059e+01,9.189861000000000502e+00,
2.320223199999999864e+01,1.088349999999999973e+01,8.860951999999999273e+00,
2.390850999999999971e+01,1.208378300000000038e+01,9.955830000000000624e+00,
2.379728899999999925e+01,1.038479099999999988e+01,1.045486799999999938e+01,
C652: 2.802246099999999984e+01,1.021390199999999915e+01,9.429092000000000695e+00,
2.869378499999999832e+01,1.030168100000000031e+01,1.027772500000000022e+01,
2.855566699999999969e+01,9.781181000000000125e+00,8.587851000000000568e+00,
2.765277800000000141e+01,1.119743800000000000e+01,9.155115000000000336e+00,
2.718584800000000001e+01,9.574697000000000457e+00,9.694990000000000663e+00,
C653: 3.174800499999999914e+01,1.034605099999999922e+01,9.370176999999999978e+00,
3.142122399999999871e+01,1.006909699999999930e+01,1.036797400000000025e+01,
3.257072800000000257e+01,1.105115299999999934e+01,9.440410999999999220e+00,
3.092459799999999959e+01,1.080551700000000004e+01,8.832898999999999390e+00,
3.207702199999999948e+01,9.458826999999999430e+00,8.837512000000000256e+00,
C654: 3.594450599999999696e+01,1.031021600000000049e+01,9.591101999999999350e+00,
3.589754200000000139e+01,1.139445399999999964e+01,9.553798000000000457e+00,
3.626239799999999747e+01,9.929622000000000170e+00,8.624962999999999269e+00,
3.496277400000000313e+01,9.913372000000000739e+00,9.831578000000000372e+00,
3.665541100000000085e+01,1.000392599999999987e+01,1.035268499999999925e+01,
C655: 4.000763299999999845e+01,1.010655200000000065e+01,9.354872000000000298e+00,
4.030215199999999953e+01,1.101822699999999955e+01,8.843438000000000798e+00,
4.077730400000000088e+01,9.351872999999999436e+00,9.223836999999999620e+00,
3.907218300000000255e+01,9.745556000000000552e+00,8.938026999999999944e+00,
3.987684500000000298e+01,1.031130600000000008e+01,1.041321499999999922e+01,
C656: 4.362367799999999818e+01,1.077014199999999988e+01,9.458771999999999736e+00,
4.409150700000000001e+01,1.164447799999999944e+01,9.899902000000000868e+00,
4.435341700000000031e+01,1.023483899999999913e+01,8.858598999999999890e+00,
4.279829399999999850e+01,1.108468300000000006e+01,8.828231999999999857e+00,
4.325357499999999789e+01,1.011922799999999967e+01,1.024515899999999924e+01,
C657: 4.812525200000000325e+01,1.049191700000000083e+01,9.581398999999999333e+00,
4.865279000000000309e+01,1.105820399999999992e+01,1.034327799999999975e+01,
4.884388700000000227e+01,9.992136000000000351e+00,8.938732999999999151e+00,
4.751588699999999932e+01,1.116657799999999945e+01,8.987076999999999316e+00,
4.748742399999999719e+01,9.752444000000000557e+00,1.005649700000000024e+01,
C658: 9.667018000000000555e+00,1.403639300000000034e+01,9.317645000000000621e+00,
8.713824000000000680e+00,1.403309899999999999e+01,9.837704999999999700e+00,
9.634327000000000751e+00,1.475873900000000027e+01,8.507839999999999847e+00,
9.862902999999999309e+00,1.304899400000000043e+01,8.912362999999999147e+00,
1.045734400000000086e+01,1.430293799999999926e+01,1.001071800000000067e+01,
C659: 1.379044200000000053e+01,1.436251399999999911e+01,9.506752000000000535e+00,
1.386339500000000058e+01,1.510140299999999947e+01,1.029884099999999947e+01,
1.392598599999999998e+01,1.484821900000000028e+01,8.544954000000000605e+00,
1.281333399999999934e+01,1.389135199999999948e+01,9.538667999999999481e+00,
1.456236200000000025e+01,1.360728100000000040e+01,9.642452000000000467e+00,
C660: 1.804271599999999864e+01,1.416225799999999957e+01,9.329409999999999314e+00,
1.710392900000000083e+01,1.384365999999999985e+01,9.088186000000000320e+00,
1.852147000000000077e+01,1.457564299999999946e+01,8.448285999999999518e+00,
1.862292400000000114e+01,1.332367299999999943e+01,9.700941000000000258e+00,
1.797665900000000150e+01,1.492677999999999927e+01,1.009601299999999924e+01,
C661: 2.157290800000000175e+01,1.406345300000000087e+01,9.355508999999999631e+00,
2.236904099999999929e+01,1.358835299999999968e+01,8.790905000000000413e+00,
2.098177899999999951e+01,1.330299399999999999e+01,9.855036999999999381e+00,
2.094128699999999910e+01,1.462568699999999922e+01,8.677509000000000583e+00,
2.200506000000000029e+01,1.473331600000000030e+01,1.009174499999999952e+01,
C662: 2.626324899999999829e+01,1.431221299999999985e+01,9.454257999999999384e+00,
2.605104599999999948e+01,1.506620999999999988e+01,1.020595900000000000e+01,
2.687716199999999844e+01,1.474316299999999913e+01,8.671117999999999881e+00,
2.533054699999999926e+01,1.395756500000000067e+01,9.025964000000000098e+00,
2.679077900000000056e+01,1.348144199999999948e+01,9.912017999999999773e+00,
C663: 2.998293500000000122e+01,1.380751500000000043e+01,9.303867000000000331e+00,
2.919172899999999871e+01,1.310100000000000087e+01,9.532292999999999239e+00,
2.961697699999999855e+01,1.454300600000000010e+01,8.594680999999999571e+00,
3.082519299999999873e+01,1.327842500000000037e+01,8.869814999999999117e+00,
3.029885300000000115e+01,1.430638000000000076e+01,1.021313699999999969e+01,
C664: 3.369396400000000114e+01,1.415878700000000023e+01,9.462222000000000577e+00,
3.456062000000000012e+01,1.358380000000000010e+01,9.149972999999999246e+00,
3.401094599999999701e+01,1.495169399999999982e+01,1.013272000000000084e+01,
3.299420500000000089e+01,1.350681900000000013e+01,9.975281999999999982e+00,
3.321522600000000125e+01,1.459063800000000022e+01,8.589444000000000301e+00,
C665: 3.833955799999999670e+01,1.387400399999999934e+01,9.404505999999999588e+00,
3.793437399999999826e+01,1.434053699999999942e+01,1.029565500000000000e+01,
3.875488599999999906e+01,1.463736899999999963e+01,8.757531000000000176e+00,
3.754473399999999828e+01,1.335128800000000027e+01,8.881090999999999624e+00,
3.911387799999999970e+01,1.316657599999999917e+01,9.682259000000000171e+00,
C666: 4.189222900000000038e+01,1.420736100000000057e+01,9.304913000000000878e+00,
4.188909499999999753e+01,1.507549700000000037e+01,9.955659999999999954e+00,
4.133400799999999720e+01,1.443082099999999990e+01,8.402870000000000061e+00,
4.143622700000000236e+01,1.336481299999999983e+01,9.814298000000000854e+00,
4.291563000000000017e+01,1.395719300000000018e+01,9.042761999999999745e+00,
C667: 4.623401900000000353e+01,1.441671000000000014e+01,9.478296999999999528e+00,
4.604570999999999970e+01,1.512111200000000011e+01,1.028216100000000033e+01,
4.714740199999999959e+01,1.386672300000000035e+01,9.681834000000000273e+00,
4.633513500000000107e+01,1.495614999999999917e+01,8.541655999999999693e+00,
4.540298099999999692e+01,1.372196699999999936e+01,9.405309000000000808e+00,
C668: 5.032334199999999669e+01,1.386369999999999969e+01,9.372977000000000558e+00,
5.043335600000000341e+01,1.494015699999999924e+01,9.462526000000000437e+00,
5.117661600000000277e+01,1.345592500000000058e+01,8.839266999999999541e+00,
4.941319699999999671e+01,1.363521899999999931e+01,8.827123000000000275e+00,
5.027096099999999979e+01,1.342143399999999964e+01,1.036342999999999925e+01,
C669: 8.129282999999999149e+00,1.740592799999999940e+01,9.451150999999999414e+00,
8.123684000000000793e+00,1.846697299999999942e+01,9.682026000000000465e+00,
8.695824999999999250e+00,1.723711099999999874e+01,8.540210999999999331e+00,
7.109440000000000204e+00,1.705988500000000130e+01,9.312217000000000411e+00,
8.588224999999999554e+00,1.685966399999999865e+01,1.026978100000000005e+01,
C670: 1.179669600000000074e+01,1.732847399999999993e+01,9.370492999999999739e+00,
1.242505700000000068e+01,1.751471099999999836e+01,1.023584199999999989e+01,
1.125906699999999994e+01,1.823507299999999987e+01,9.110713999999999757e+00,
1.108795699999999940e+01,1.654103299999999876e+01,9.600647000000000375e+00,
1.241811900000000080e+01,1.702613500000000002e+01,8.533295000000000741e+00,
C671: 1.600792399999999915e+01,1.737627300000000119e+01,9.373281000000000418e+00,
1.590841900000000031e+01,1.787673699999999855e+01,1.033103499999999997e+01,
1.605837199999999854e+01,1.630410799999999938e+01,9.529294999999999405e+00,
1.691424599999999856e+01,1.771319099999999835e+01,8.879255000000000564e+00,
1.514941999999999922e+01,1.760845799999999883e+01,8.750733999999999568e+00,
C672: 2.006280399999999986e+01,1.732977899999999849e+01,9.403162000000000020e+00,
2.001044999999999874e+01,1.676519000000000048e+01,8.478137999999999508e+00,
2.096034500000000023e+01,1.705421000000000120e+01,9.948173000000000599e+00,
1.918713199999999830e+01,1.711501600000000067e+01,1.000720699999999930e+01,
2.009192600000000084e+01,1.838962199999999925e+01,9.172897000000000745e+00,
C673: 2.410413600000000045e+01,1.745047599999999832e+01,9.327567000000000164e+00,
2.385228599999999943e+01,1.801055699999999860e+01,1.022249099999999977e+01,
2.518350300000000175e+01,1.737772199999999856e+01,9.236990000000000848e+00,
2.370229000000000141e+01,1.795861000000000018e+01,8.456132999999999456e+00,
2.367905500000000174e+01,1.645364500000000163e+01,9.392381000000000313e+00,
C674: 2.845246799999999965e+01,1.722579700000000003e+01,9.375363000000000113e+00,
2.757202500000000001e+01,1.734723400000000026e+01,9.999038999999999788e+00,
2.885421399999999892e+01,1.820313099999999906e+01,9.125049999999999883e+00,
2.818103500000000139e+01,1.670445099999999883e+01,8.464363999999999777e+00,
2.920061700000000116e+01,1.665524399999999972e+01,9.915210000000000079e+00,
C675: 3.209737499999999955e+01,1.732967199999999863e+01,9.399606000000000350e+00,
3.284753899999999760e+01,1.725940999999999903e+01,1.018126200000000026e+01,
3.258664199999999767e+01,1.745286099999999863e+01,8.438477000000000672e+00,
3.145506800000000069e+01,1.818408600000000064e+01,9.590197999999999112e+00,
3.150244899999999859e+01,1.642247199999999907e+01,9.385360000000000369e+00,
C676: 3.613333500000000242e+01,1.741951399999999950e+01,9.335380000000000678e+00,
3.606547299999999723e+01,1.790644700000000000e+01,1.030320999999999998e+01,
3.674006800000000084e+01,1.802343000000000117e+01,8.667341000000000406e+00,
3.513951399999999836e+01,1.730398299999999878e+01,8.914346000000000103e+00,
3.658851899999999802e+01,1.644114199999999926e+01,9.453507999999999356e+00,
C677: 3.978907999999999845e+01,1.728451499999999896e+01,9.382289999999999353e+00,
3.896740700000000146e+01,1.683354800000000040e+01,9.928034000000000248e+00,
4.000056099999999759e+01,1.670025899999999908e+01,8.492779999999999774e+00,
4.067115400000000136e+01,1.731233100000000036e+01,1.001329100000000061e+01,
3.951655099999999976e+01,1.829376999999999853e+01,9.091701999999999728e+00,
C678: 4.398781499999999767e+01,1.731539700000000082e+01,9.371648999999999674e+00,
4.397982100000000116e+01,1.631183899999999909e+01,8.959205000000000751e+00,
4.408484200000000186e+01,1.803453899999999877e+01,8.563917999999999253e+00,
4.482571300000000036e+01,1.741926399999999830e+01,1.005400900000000064e+01,
4.306074799999999669e+01,1.749405600000000049e+01,9.906890999999999892e+00,
C679: 4.835350400000000093e+01,1.730966499999999897e+01,9.388042999999999694e+00,
4.743543199999999871e+01,1.726631499999999875e+01,9.966077999999999548e+00,
4.847891299999999859e+01,1.638344599999999929e+01,8.836349000000000231e+00,
4.919610000000000127e+01,1.744829000000000008e+01,1.005886500000000083e+01,
4.830513700000000199e+01,1.814098200000000105e+01,8.691067999999999572e+00,
C680: 1.028775199999999934e+01,2.116897000000000162e+01,9.527084000000000330e+00,
9.650622000000000256e+00,2.046691900000000075e+01,8.997757000000000005e+00,
9.682372000000000867e+00,2.176629600000000053e+01,1.020202800000000032e+01,
1.078014800000000051e+01,2.181811499999999882e+01,8.810750000000000526e+00,
1.103413300000000064e+01,2.062105199999999883e+01,1.009297699999999942e+01,
C681: 1.392224099999999964e+01,2.050614099999999951e+01,9.268392999999999660e+00,
1.310041000000000011e+01,2.082689699999999888e+01,8.636293999999999471e+00,
1.484909399999999913e+01,2.056807900000000089e+01,8.706956999999999169e+00,
1.375839099999999959e+01,1.948113400000000084e+01,9.582344000000000861e+00,
1.398261300000000062e+01,2.115378600000000020e+01,1.013706999999999958e+01,
C682: 1.773584400000000016e+01,2.072995299999999830e+01,9.527096000000000231e+00,
1.788701800000000119e+01,2.167225799999999936e+01,1.004486999999999952e+01,
1.691683599999999998e+01,2.018901699999999977e+01,9.989699999999999136e+00,
1.864413800000000165e+01,2.013919599999999832e+01,9.582350999999999175e+00,
1.749689400000000106e+01,2.092521999999999949e+01,8.486487000000000336e+00,
C683: 2.221725599999999901e+01,2.068998500000000007e+01,9.440329999999999444e+00,
2.285083500000000001e+01,2.053543900000000022e+01,1.030761000000000038e+01,
2.269815900000000042e+01,2.138539400000000157e+01,8.759624999999999773e+00,
2.126018699999999839e+01,2.109543899999999894e+01,9.752164000000000499e+00,
2.206024599999999936e+01,1.974230500000000177e+01,8.935864000000000473e+00,
C684: 2.588385399999999947e+01,2.057249699999999848e+01,9.325409999999999755e+00,
2.554646299999999925e+01,2.108706300000000056e+01,1.021882899999999950e+01,
2.637400999999999840e+01,1.964161400000000057e+01,9.591521000000000186e+00,
2.658472599999999986e+01,2.120539499999999933e+01,8.789362000000000563e+00,
2.503215799999999902e+01,2.036170299999999855e+01,8.686915000000000830e+00,
C685: 2.991976000000000013e+01,2.142071999999999932e+01,9.574768999999999863e+00,
2.999897299999999944e+01,2.237882400000000160e+01,1.007792599999999972e+01,
2.974125899999999945e+01,2.158427199999999857e+01,8.516688999999999510e+00,
2.909429700000000096e+01,2.085401299999999836e+01,9.994265000000000398e+00,

3.084272199999999842e+01,2.086402199999999851e+01,9.702830000000000510e+00,
C686: 3.407336500000000257e+01,2.041546900000000164e+01,9.323622000000000298e+00,
3.420740299999999934e+01,2.108152000000000115e+01,1.016924999999999990e+01,
3.412299600000000055e+01,1.938369300000000095e+01,9.650463000000000235e+00,
3.485269199999999756e+01,2.059933799999999948e+01,8.591412000000000049e+00,
3.310639799999999866e+01,2.060120200000000068e+01,8.866203999999999752e+00,
C687: 3.765912200000000354e+01,2.100071900000000014e+01,9.441038999999999959e+00,
3.718126800000000287e+01,2.121414199999999894e+01,8.489895000000000636e+00,
3.860518600000000333e+01,2.049987099999999884e+01,9.262862999999999403e+00,
3.701636500000000041e+01,2.036055199999999843e+01,1.003699600000000025e+01,
3.783897699999999986e+01,2.193004799999999932e+01,9.971759000000000484e+00,
C688: 4.183188899999999677e+01,2.056189099999999925e+01,9.528717000000000326e+00,
4.172321399999999869e+01,2.093519200000000069e+01,8.514974999999999739e+00,
4.269111000000000189e+01,1.990192899999999909e+01,9.580280999999999381e+00,
4.197721800000000059e+01,2.139911199999999880e+01,1.020413100000000028e+01,
4.093496400000000079e+01,2.002117900000000006e+01,9.811019999999999186e+00,
C689: 4.601509999999999678e+01,2.038948399999999950e+01,9.281527000000000527e+00,
4.502251700000000056e+01,2.042127599999999887e+01,8.842802000000000717e+00,
4.602846900000000119e+01,2.098929499999999848e+01,1.018489899999999970e+01,
4.673160800000000137e+01,2.079300599999999832e+01,8.573843000000000103e+00,
4.627381499999999903e+01,1.936287000000000091e+01,9.516071999999999420e+00,
C690: 4.953449599999999720e+01,2.126768600000000120e+01,9.485951000000000022e+00,
4.888901500000000055e+01,2.064116699999999938e+01,1.009397500000000036e+01,
5.037559100000000001e+01,2.068025000000000091e+01,9.130103000000000080e+00,
4.990085400000000249e+01,2.209749100000000155e+01,1.008286200000000044e+01,
4.897737099999999799e+01,2.165052899999999880e+01,8.636445999999999401e+00,
C691: 7.950345999999999691e+00,2.463753300000000124e+01,9.448394000000000403e+00,
8.816598000000000823e+00,2.446584100000000106e+01,1.008054899999999954e+01,
7.378608999999999973e+00,2.547476800000000097e+01,9.837533999999999779e+00,
7.328574999999999839e+00,2.374728500000000153e+01,9.437530000000000641e+00,
8.279495999999999967e+00,2.486173000000000144e+01,8.437972999999999502e+00,
C692: 1.208956099999999978e+01,2.445758599999999916e+01,9.325481999999999161e+00,
1.122071200000000069e+01,2.422420899999999833e+01,8.717613999999999308e+00,
1.178147099999999980e+01,2.505844499999999897e+01,1.017452800000000046e+01,
1.280509999999999948e+01,2.501147100000000023e+01,8.728300000000000836e+00,
1.254480000000000040e+01,2.353629600000000011e+01,9.675148000000000081e+00,
C693: 1.567366400000000048e+01,2.416787700000000072e+01,9.323926999999999410e+00,
1.486841100000000004e+01,2.418111199999999883e+01,1.004910399999999981e+01,
1.662800999999999974e+01,2.420972099999999827e+01,9.839804000000000883e+00,
1.558476699999999937e+01,2.502260300000000015e+01,8.661879000000000772e+00,
1.561781000000000041e+01,2.325192699999999846e+01,8.744498000000000104e+00,
C694: 2.018238699999999852e+01,2.449470799999999926e+01,9.483914999999999651e+00,
2.006311000000000178e+01,2.523165399999999892e+01,1.027233099999999943e+01,
2.046238800000000069e+01,2.499178600000000117e+01,8.559962000000000515e+00,
1.924528499999999909e+01,2.396526300000000020e+01,9.339498000000000744e+00,
2.095726200000000006e+01,2.378762299999999996e+01,9.763607999999999620e+00,
C695: 2.409437499999999943e+01,2.425919999999999987e+01,9.295325000000000060e+00,
2.376647900000000035e+01,2.477616000000000085e+01,1.019100399999999951e+01,
2.453387599999999935e+01,2.497262299999999868e+01,8.606263999999999470e+00,
2.324043400000000048e+01,2.378262399999999843e+01,8.824730000000000629e+00,
2.482981699999999847e+01,2.350521699999999825e+01,9.557242000000000459e+00,
C696: 2.778563700000000125e+01,2.453726899999999844e+01,9.395431999999999562e+00,
2.804969300000000132e+01,2.516753900000000144e+01,1.023869700000000016e+01,
2.868904799999999966e+01,2.424246000000000123e+01,8.870015000000000427e+00,
2.714089500000000044e+01,2.508687199999999962e+01,8.717753999999999337e+00,
2.726760099999999909e+01,2.365149699999999910e+01,9.748981999999999815e+00,
C697: 3.246781099999999753e+01,2.428650400000000076e+01,9.389080999999999122e+00,
3.214726600000000190e+01,2.493611399999999989e+01,1.019758500000000012e+01,
3.309721300000000355e+01,2.484283200000000136e+01,8.702415000000000234e+00,
3.159608800000000173e+01,2.391902800000000084e+01,8.856317000000000661e+00,
3.302359700000000231e+01,2.344698299999999946e+01,9.794620000000000104e+00,
C698: 3.597816600000000165e+01,2.433979499999999874e+01,9.295080999999999705e+00,
3.683265999999999707e+01,2.418973899999999944e+01,9.947018999999999167e+00,
3.537763100000000094e+01,2.343594500000000025e+01,9.271653000000000588e+00,
3.633045899999999762e+01,2.456466199999999844e+01,8.293836000000000652e+00,
3.538198200000000071e+01,2.516831799999999930e+01,9.663050000000000139e+00,
C699: 4.017915800000000104e+01,2.458630300000000091e+01,9.467470999999999748e+00,
3.987234000000000123e+01,2.520567399999999836e+01,1.030476700000000001e+01,
4.117714900000000000e+01,2.419896200000000164e+01,9.649324000000000012e+00,
4.018104399999999998e+01,2.517997700000000094e+01,8.558414000000000854e+00,
3.948512399999999900e+01,2.375878200000000007e+01,9.355845999999999663e+00,
C700: 4.443114200000000125e+01,2.388235099999999989e+01,9.352669999999999817e+00,
4.484160500000000127e+01,2.414645399999999853e+01,9.383689000000000391e+00,
4.361950300000000169e+01,2.317373399999999961e+01,9.218840999999999397e+00,
4.405420199999999653e+01,2.477498800000000045e+01,8.841661000000000215e+00,
4.520682899999999904e+01,2.343211000000000155e+01,9.963050000000000192e+00,
C701: 4.800367899999999821e+01,2.459394500000000150e+01,9.336911999999999878e+00,
4.794237900000000252e+01,2.502584999999999837e+01,1.033048900000000003e+01,
4.757963000000000164e+01,2.528422899999999984e+01,8.615043999999999258e+00,
4.745674600000000254e+01,2.365700700000000012e+01,9.308481000000000449e+00,
4.904466500000000195e+01,2.441072199999999946e+01,9.088447999999999638e+00,
C702: 9.709645000000000081e+00,2.783128400000000013e+01,9.310726000000000724e+00,
1.052301800000000043e+01,2.832849699999999871e+01,9.829696000000000211e+00,
9.505727999999999511e+00,2.834943399999999869e+01,8.378590000000000870e+00,
8.820902000000000243e+00,2.784336199999999906e+01,9.934518999999999878e+00,
9.992117999999999611e+00,2.680432800000000171e+01,9.102297999999999334e+00,
C703: 1.394311599999999984e+01,2.757215499999999864e+01,9.432562000000000779e+00,
1.421216599999999985e+01,2.862014699999999934e+01,9.519311999999999330e+00,
1.379753099999999932e+01,2.732492299999999830e+01,8.385733999999999355e+00,
1.302378599999999942e+01,2.738704800000000006e+01,9.979464999999999364e+00,
1.474080999999999975e+01,2.696185499999999990e+01,9.842109000000000663e+00,
C704: 1.780496000000000123e+01,2.747591800000000006e+01,9.361148000000000025e+00,
1.873989900000000119e+01,2.745037299999999902e+01,9.911922999999999817e+00,
1.793523199999999918e+01,2.805611299999999986e+01,8.452586000000000155e+00,
1.703715000000000046e+01,2.793576600000000099e+01,9.975108000000000530e+00,
1.750979600000000147e+01,2.646343900000000104e+01,9.107357999999999620e+00,
C705: 2.180583299999999980e+01,2.767255499999999913e+01,9.350517999999999219e+00,
2.121644799999999975e+01,2.774941099999999850e+01,1.025832800000000056e+01,
2.245485899999999901e+01,2.853863700000000136e+01,9.263593000000000188e+00,
2.114108099999999979e+01,2.763071100000000158e+01,8.493411000000000044e+00,
2.240882900000000078e+01,2.677086699999999908e+01,9.383485999999999549e+00,
C706: 2.575064700000000073e+01,2.758875799999999856e+01,9.456562999999999164e+00,
2.666577200000000047e+01,2.737460899999999953e+01,9.999928999999999846e+00,
2.580455100000000002e+01,2.714868399999999937e+01,8.465858000000000771e+00,
2.562854199999999949e+01,2.866370200000000068e+01,9.366137000000000157e+00,
2.490420500000000104e+01,2.717300200000000032e+01,9.994058000000000774e+00,
C707: 2.993981300000000090e+01,2.766110600000000019e+01,9.308799999999999741e+00,
2.978331899999999877e+01,2.822073800000000077e+01,1.022570100000000082e+01,
3.056443200000000004e+01,2.824129100000000037e+01,8.636981999999999715e+00,
2.898138499999999951e+01,2.747251500000000135e+01,8.834543999999999286e+00,
3.042512200000000178e+01,2.671578500000000034e+01,9.530730000000000146e+00,
C708: 3.355413800000000180e+01,2.784578099999999878e+01,9.426823999999999870e+00,
3.289882399999999762e+01,2.737265199999999865e+01,1.015138100000000065e+01,
3.435138299999999845e+01,2.836773900000000026e+01,9.946626999999999441e+00,
3.298693000000000097e+01,2.855461000000000027e+01,8.833014000000000365e+00,
3.398340199999999811e+01,2.709137799999999885e+01,8.774915999999999272e+00,
C709: 3.781509599999999693e+01,2.752738499999999888e+01,9.362002000000000379e+00,
3.777145800000000264e+01,2.826087100000000163e+01,8.562682999999999822e+00,
3.854797899999999800e+01,2.784017700000000062e+01,1.009869400000000006e+01,
3.810026899999999728e+01,2.656379099999999838e+01,8.953625000000000611e+00,
3.683801700000000068e+01,2.744694099999999892e+01,9.828077000000000396e+00,
C710: 4.188234700000000288e+01,2.769071100000000030e+01,9.329454000000000136e+00,
4.124404100000000284e+01,2.756782099999999858e+01,1.019889000000000046e+01,
4.255800299999999936e+01,2.852466700000000088e+01,9.490031999999999357e+00,
4.126900499999999994e+01,2.788422100000000097e+01,8.545454999999999387e+00,
4.245864300000000213e+01,2.678380100000000041e+01,9.173076999999999259e+00,
C711: 4.559842900000000299e+01,2.744827400000000139e+01,9.380732999999999322e+00,
4.485131299999999754e+01,2.738218499999999977e+01,1.016525900000000071e+01,
4.544275999999999982e+01,2.664685700000000068e+01,8.666463000000000250e+00,
4.659019599999999883e+01,2.736301100000000019e+01,9.814011000000000706e+00,
4.550705700000000320e+01,2.840514299999999892e+01,8.875633000000000550e+00,
C712: 5.011433799999999650e+01,2.762201800000000063e+01,9.356412999999999869e+00,
5.078195199999999687e+01,2.847850000000000037e+01,9.361145000000000493e+00,
5.050698400000000277e+01,2.685212200000000138e+01,1.001399400000000028e+01,
5.003448999999999813e+01,2.723008499999999898e+01,8.346735999999999933e+00,
4.913176800000000100e+01,2.792751600000000067e+01,9.703753000000000739e+00,
C713: 8.216108000000000189e+00,3.111320800000000020e+01,9.377309000000000339e+00,
8.610008999999999801e+00,3.056509399999999843e+01,1.022770500000000027e+01,
9.010115000000000762e+00,3.128745999999999938e+01,8.657920999999999978e+00,
7.815457999999999572e+00,3.206443900000000014e+01,9.714223999999999748e+00,
7.426231999999999722e+00,3.053357400000000155e+01,8.909017999999999660e+00,
C714: 1.200234500000000004e+01,3.124512500000000159e+01,9.569421999999999429e+00,
1.187566499999999969e+01,3.170467100000000116e+01,8.594046999999999770e+00,
1.114780900000000052e+01,3.061266600000000082e+01,9.784798000000000329e+00,
1.208212699999999984e+01,3.202010299999999887e+01,1.032475099999999912e+01,
1.290767199999999981e+01,3.064640699999999995e+01,9.568547000000000580e+00,
C715: 1.639849600000000152e+01,3.142003300000000010e+01,9.459274000000000626e+00,
1.688319999999999865e+01,3.166339500000000129e+01,8.519057000000000102e+00,
1.545450899999999983e+01,3.092289299999999841e+01,9.257573999999999970e+00,
1.621141499999999880e+01,3.233220899999999887e+01,1.001676199999999994e+01,
1.703558400000000006e+01,3.076121699999999848e+01,1.004069499999999948e+01,
C716: 1.984322600000000136e+01,3.067479099999999903e+01,9.281321000000000154e+00,
2.084643499999999960e+01,3.060035399999999939e+01,8.873557999999999168e+00,
1.950553499999999829e+01,2.969195900000000066e+01,9.587974000000000885e+00,
1.917985200000000034e+01,3.106248000000000076e+01,8.515506999999999493e+00,
1.984659200000000112e+01,3.135036699999999854e+01,1.012983900000000048e+01,
C717: 2.380426100000000034e+01,3.152955599999999947e+01,9.588817000000000590e+00,
2.295222100000000154e+01,3.098180199999999829e+01,9.978697000000000372e+00,
2.395937999999999946e+01,3.242828300000000041e+01,1.017780800000000063e+01,
2.361739100000000136e+01,3.180302299999999960e+01,8.555256999999999223e+00,
2.469228899999999882e+01,3.090718299999999985e+01,9.641209999999999170e+00,
C718: 2.824031400000000147e+01,3.139736200000000110e+01,9.393992000000000786e+00,
2.780355399999999833e+01,3.232787600000000339e+01,9.740888999999999243e+00,
2.880701699999999832e+01,3.157428000000000168e+01,8.486508000000000607e+00,
2.744785100000000000e+01,3.068399000000000143e+01,9.188598000000000710e+00,
2.889619899999999930e+01,3.099455999999999989e+01,1.015890100000000018e+01,
C719: 3.180856800000000106e+01,3.129042700000000110e+01,9.396763999999999228e+00,
3.123015799999999942e+01,3.040780399999999872e+01,9.649162000000000461e+00,
3.283991100000000074e+01,3.100775399999999848e+01,9.208223999999999521e+00,
3.177481500000000025e+01,3.199714200000000019e+01,1.021882899999999950e+01,
3.139343300000000170e+01,3.175205700000000064e+01,8.506747999999999976e+00,
C720: 3.640895900000000296e+01,3.133100900000000166e+01,9.569831999999999894e+00,
3.722832600000000269e+01,3.081643599999999950e+01,1.006173500000000054e+01,
3.559702999999999662e+01,3.063271800000000056e+01,9.389789000000000385e+00,
3.675327599999999961e+01,3.173419799999999924e+01,8.622543999999999542e+00,
3.605751300000000015e+01,3.214123000000000019e+01,1.020134700000000016e+01,
C721: 4.016836700000000349e+01,3.083523399999999981e+01,9.320947999999999567e+00,
4.055148899999999657e+01,3.125100099999999870e+01,1.024675399999999925e+01,
3.948023299999999836e+01,3.154013099999999881e+01,8.864779999999999660e+00,
3.964934900000000084e+01,2.990465500000000176e+01,9.523977000000000359e+00,
4.099242900000000134e+01,3.064714199999999877e+01,8.639901000000000053e+00,
C722: 4.379623699999999786e+01,3.140133799999999908e+01,9.489454000000000278e+00,
4.394637600000000077e+01,3.233496800000000349e+01,1.002216199999999979e+01,
4.474473900000000270e+01,3.088065299999999880e+01,9.397339000000000553e+00,
4.340156499999999795e+01,3.161098399999999842e+01,8.500201999999999813e+00,
4.309311999999999898e+01,3.078052100000000024e+01,1.003418300000000052e+01,
C723: 4.863296100000000166e+01,3.133818499999999929e+01,9.440737999999999630e+00,
4.953230800000000045e+01,3.102645700000000062e+01,9.963469999999999160e+00,
4.890589099999999689e+01,3.185206499999999963e+01,8.523808999999999969e+00,
4.805934100000000342e+01,3.200834499999999849e+01,1.007421800000000012e+01,
4.803265600000000290e+01,3.046569600000000122e+01,9.200037999999999272e+00,
C724: 9.674528999999999712e+00,3.453674099999999925e+01,9.312445999999999557e+00,
8.761793000000000831e+00,3.445725199999999688e+01,9.895234999999999559e+00,
1.035485300000000031e+01,3.522856600000000071e+01,9.799127000000000365e+00,
9.438375999999999877e+00,3.490145299999999651e+01,8.317256000000000427e+00,
1.014407699999999934e+01,3.356125800000000226e+01,9.238222000000000378e+00,
C725: 1.363889099999999921e+01,3.490904299999999694e+01,9.402627999999999986e+00,
1.380959900000000040e+01,3.558609200000000072e+01,1.023372200000000021e+01,
1.354481700000000011e+01,3.547890900000000158e+01,8.482929000000000386e+00,
1.272653099999999959e+01,3.434730499999999864e+01,9.575998999999999484e+00,
1.447549199999999914e+01,3.422191999999999723e+01,9.318118000000000123e+00,
C726: 1.796473100000000045e+01,3.470603700000000202e+01,9.311866000000000199e+00,
1.704983599999999910e+01,3.445540100000000194e+01,8.783543999999999130e+00,
1.860075099999999892e+01,3.382823100000000238e+01,9.366203999999999752e+00,
1.772024299999999997e+01,3.504373400000000061e+01,1.031336399999999998e+01,
1.847999199999999931e+01,3.549650199999999955e+01,8.777834000000000358e+00,
C727: 2.157215899999999920e+01,3.448572699999999713e+01,9.335615000000000663e+00,
2.248979200000000134e+01,3.420600600000000213e+01,8.827114999999999156e+00,
2.101313199999999881e+01,3.359158599999999950e+01,9.591962999999999795e+00,
2.097519399999999834e+01,3.510927000000000220e+01,8.678416999999999604e+00,
2.181603899999999996e+01,3.503716399999999709e+01,1.023809600000000053e+01,
C728: 2.609767000000000081e+01,3.493714700000000306e+01,9.388161000000000200e+00,
2.519987599999999972e+01,3.513556100000000271e+01,9.965505999999999531e+00,
2.615301200000000037e+01,3.562628899999999987e+01,8.550983999999999696e+00,

2.606684600000000174e+01,3.391823500000000280e+01,9.014449000000000822e+00,
2.697007199999999827e+01,3.506401799999999724e+01,1.002115900000000082e+01,
C729: 3.007416699999999921e+01,3.466260499999999922e+01,9.311904999999999433e+00,
3.076826499999999953e+01,3.410929000000000144e+01,8.687614999999999199e+00,
2.911618899999999854e+01,3.415563199999999711e+01,9.331927000000000305e+00,
2.994256000000000029e+01,3.566067100000000067e+01,8.905315999999999121e+00,
3.047242400000000018e+01,3.473593300000000283e+01,1.031793900000000086e+01,
C730: 3.385124900000000281e+01,3.485323199999999844e+01,9.401856999999999687e+00,
3.391015300000000110e+01,3.553987200000000257e+01,1.024033000000000015e+01,
3.483486200000000110e+01,3.443795800000000185e+01,9.203920999999999353e+00,
3.349850500000000153e+01,3.538302300000000145e+01,8.522126000000000090e+00,
3.316176399999999802e+01,3.404986099999999993e+01,9.641130999999999673e+00,
C731: 3.834139100000000155e+01,3.459420800000000185e+01,9.347080000000000055e+00,
3.740287299999999959e+01,3.412448499999999996e+01,9.070304000000000144e+00,
3.872456499999999835e+01,3.515396499999999946e+01,8.500173000000000201e+00,
3.905885200000000168e+01,3.383215400000000272e+01,9.632396999999999210e+00,
3.817330400000000168e+01,3.526946600000000132e+01,1.018017399999999917e+01,
C732: 4.193555800000000033e+01,3.460158899999999704e+01,9.308745999999999299e+00,
4.279473999999999734e+01,3.451263399999999848e+01,8.650854000000000710e+00,
4.149011099999999885e+01,3.362242200000000025e+01,9.452168000000000347e+00,
4.120767000000000024e+01,3.526698999999999984e+01,8.859747000000000483e+00,
4.225386900000000168e+01,3.500231699999999790e+01,1.026557200000000059e+01,
C733: 4.598697399999999647e+01,3.478477699999999828e+01,9.418831000000000842e+00,
4.671847100000000097e+01,3.500353900000000351e+01,1.019033600000000028e+01,
4.613007999999999953e+01,3.376847899999999925e+01,9.064121000000000095e+00,
4.611004599999999698e+01,3.547708000000000084e+01,8.591350999999999516e+00,
4.498786599999999680e+01,3.488596199999999925e+01,9.831023999999999319e+00,
C734: 5.028658099999999820e+01,3.465095900000000029e+01,9.342492000000000019e+00,
5.058887000000000000e+01,3.553504199999999713e+01,9.895981000000000805e+00,
5.042000600000000077e+01,3.482615499999999997e+01,8.279101000000000710e+00,
4.924152699999999783e+01,3.443686900000000151e+01,9.545206000000000301e+00,
5.089505100000000226e+01,3.380556200000000189e+01,9.649627000000000621e+00,
C735: 8.323836999999999264e+00,3.788645999999999958e+01,9.517267999999999617e+00,
8.024324999999999264e+00,3.891056499999999829e+01,9.718982999999999706e+00,
7.460380999999999929e+00,3.731315299999999925e+01,9.193303999999999476e+00,
8.733321000000000112e+00,3.744447100000000006e+01,1.042047699999999999e+01,
9.077826999999999202e+00,3.787750700000000137e+01,8.735673999999999495e+00,
C736: 1.221242799999999917e+01,3.823525800000000174e+01,9.366329999999999600e+00,
1.295034799999999997e+01,3.815521400000000085e+01,1.015826999999999991e+01,
1.271583200000000069e+01,3.838579599999999914e+01,8.416881000000000057e+00,
1.155702800000000074e+01,3.907756700000000194e+01,9.563143000000000171e+00,
1.162547900000000034e+01,3.732311299999999932e+01,9.323095999999999606e+00,
C737: 1.590079700000000074e+01,3.790019099999999952e+01,9.324588000000000321e+00,
1.513946999999999932e+01,3.815003000000000100e+01,8.592855000000000132e+00,
1.687929000000000102e+01,3.814832899999999682e+01,9.924675000000000580e+00,
1.585859199999999980e+01,3.683839100000000144e+01,9.542911000000000143e+00,
1.572739400000000032e+01,3.846919499999999914e+01,1.023159300000000016e+01,
C738: 2.002282900000000154e+01,3.781833100000000059e+01,9.481077000000000865e+00,
2.008954999999999913e+01,3.890175800000000095e+01,9.508850999999999942e+00,
2.003858999999999924e+01,3.748395699999999664e+01,8.448722999999999317e+00,
1.909688500000000033e+01,3.750338500000000153e+01,9.951475999999999544e+00,
2.086723399999999984e+01,3.739251099999999894e+01,1.001342700000000008e+01,
C739: 2.384027400000000085e+01,3.788009699999999924e+01,9.303216000000000818e+00,
2.311465499999999906e+01,3.833294300000000021e+01,8.634245999999999199e+00,
2.478606500000000068e+01,3.777262600000000248e+01,8.784197999999999951e+00,
2.348191800000000029e+01,3.690241199999999822e+01,9.609165000000000845e+00,
2.397265499999999960e+01,3.851742600000000039e+01,1.017186700000000066e+01,
C740: 2.753616200000000092e+01,3.827328299999999928e+01,9.421319999999999695e+00,
2.682940299999999922e+01,3.801122000000000156e+01,1.020254699999999914e+01,
2.820315499999999886e+01,3.905020300000000333e+01,9.781586000000000780e+00,
2.699882799999999961e+01,3.863600000000000279e+01,8.551614999999999966e+00,
2.811734500000000025e+01,3.739780799999999772e+01,9.148493999999999460e+00,
C741: 3.251830700000000007e+01,3.823971199999999726e+01,9.413247000000000142e+00,
3.320868600000000015e+01,3.808505600000000157e+01,1.023648099999999950e+01,
3.301749800000000334e+01,3.802592299999999881e+01,8.473760999999999655e+00,
3.217166699999999935e+01,3.926829699999999690e+01,9.414739000000000857e+00,
3.166659500000000094e+01,3.757557599999999809e+01,9.523011000000000337e+00,
C742: 3.618690200000000345e+01,3.780035500000000326e+01,9.301885999999999655e+00,
3.635387099999999805e+01,3.844389100000000070e+01,1.015977099999999922e+01,
3.706976300000000180e+01,3.781537800000000260e+01,8.669985999999999748e+00,
3.534502299999999764e+01,3.817679600000000306e+01,8.731044999999999945e+00,
3.599103399999999908e+01,3.678145700000000318e+01,9.618337000000000359e+00,
C743: 4.015361300000000000e+01,3.784451700000000329e+01,9.475818999999999548e+00,
3.932915799999999962e+01,3.768284799999999990e+01,1.016315200000000019e+01,
4.025293200000000127e+01,3.890735600000000005e+01,9.277976999999999919e+00,
3.995443300000000164e+01,3.732433799999999735e+01,8.544985999999999748e+00,
4.107493000000000194e+01,3.747164399999999773e+01,9.912107999999999919e+00,
C744: 4.435774800000000084e+01,3.802864900000000148e+01,9.327294000000000196e+00,
4.515380900000000253e+01,3.783757700000000312e+01,1.004006599999999949e+01,
4.477642199999999661e+01,3.846145899999999784e+01,8.424466000000000676e+00,
4.364229600000000175e+01,3.872023999999999688e+01,9.761200000000000543e+00,
4.385632600000000281e+01,3.709677500000000094e+01,9.085618999999999446e+00,
C745: 4.810568099999999703e+01,3.780556599999999889e+01,9.364219000000000293e+00,
4.768814900000000279e+01,3.822328100000000006e+01,1.027490099999999984e+01,
4.906920099999999962e+01,3.826476699999999909e+01,9.164407999999999888e+00,
4.743226700000000307e+01,3.800383300000000020e+01,8.536009999999999209e+00,
4.823281300000000016e+01,3.673483000000000231e+01,9.479179000000000244e+00,
C746: 9.684874000000000649e+00,4.202919599999999889e+01,9.534288000000000096e+00,
9.711845000000000283e+00,4.277362000000000108e+01,1.032387199999999972e+01,
9.709455000000000169e+00,4.252411599999999936e+01,8.568011999999999517e+00,
8.772489000000000203e+00,4.144643299999999897e+01,9.617938999999999794e+00,
1.054307099999999942e+01,4.137146599999999808e+01,9.624418000000000362e+00,
C747: 1.373820100000000011e+01,4.171421800000000246e+01,9.322407999999999362e+00,
1.284996699999999947e+01,4.124654799999999710e+01,9.733458999999999861e+00,
1.424022000000000077e+01,4.228111799999999931e+01,1.009757699999999936e+01,
1.345499200000000073e+01,4.237874000000000052e+01,8.512548000000000670e+00,
1.440510899999999950e+01,4.094534300000000115e+01,8.945237999999999801e+00,
C748: 1.735470099999999860e+01,4.143650800000000345e+01,9.464453999999999922e+00,
1.658462199999999953e+01,4.091941899999999777e+01,1.002775600000000011e+01,
1.783265300000000053e+01,4.217808600000000041e+01,1.009754500000000021e+01,
1.690861100000000050e+01,4.192589000000000254e+01,8.604086999999999819e+00,
1.809675299999999964e+01,4.071935400000000271e+01,9.126257999999999981e+00,
C749: 2.219460499999999925e+01,4.165435200000000293e+01,9.446327999999999392e+00,
2.215261599999999831e+01,4.258740000000000236e+01,9.998934000000000211e+00,
2.260870200000000096e+01,4.183598099999999675e+01,8.459671000000000163e+00,
2.119235700000000122e+01,4.124826500000000351e+01,9.347262999999999877e+00,
2.282281199999999899e+01,4.094407900000000211e+01,9.974057999999999424e+00,
C750: 2.579304000000000130e+01,4.158470100000000258e+01,9.328079999999999927e+00,
2.511171699999999873e+01,4.077594200000000058e+01,9.082819000000000642e+00,
2.551326200000000100e+01,4.202237399999999923e+01,1.027814799999999984e+01,
2.575114999999999910e+01,4.234354900000000299e+01,8.553660000000000707e+00,
2.680401000000000167e+01,4.119668599999999969e+01,9.393643000000000853e+00,
C751: 3.000459199999999882e+01,4.214632499999999737e+01,9.515059000000000822e+00,
3.085439600000000127e+01,4.147696899999999687e+01,9.603884000000000754e+00,
3.002935300000000041e+01,4.263830500000000256e+01,8.547409000000000034e+00,
3.004794599999999960e+01,4.289249699999999876e+01,1.030253100000000011e+01,
2.908625100000000074e+01,4.157559200000000033e+01,9.608361999999999625e+00,
C752: 3.418281600000000253e+01,4.160492099999999738e+01,9.346901000000000792e+00,
3.459516399999999692e+01,4.064685699999999713e+01,9.646746999999999517e+00,
3.474157000000000295e+01,4.198207500000000181e+01,8.497825000000000628e+00,
3.425101899999999944e+01,4.230813200000000052e+01,1.016928599999999960e+01,
3.314284099999999711e+01,4.147964999999999947e+01,9.063463999999999743e+00,
C753: 3.778993599999999731e+01,4.171757999999999811e+01,9.415912000000000504e+00,
3.793571099999999774e+01,4.247018800000000027e+01,1.018379000000000012e+01,
3.874319400000000062e+01,4.125406399999999962e+01,9.180058000000000717e+00,
3.738525899999999780e+01,4.218279299999999665e+01,8.523343999999999809e+00,
3.709959299999999871e+01,4.096050600000000230e+01,9.774150000000000560e+00,
C754: 4.228188999999999709e+01,4.162041299999999922e+01,9.544639000000000095e+00,
4.302027199999999851e+01,4.113626099999999752e+01,1.017411099999999990e+01,
4.135005600000000214e+01,4.106493900000000252e+01,9.585525999999999769e+00,
4.264028299999999660e+01,4.164572400000000130e+01,8.520621999999999474e+00,
4.211144099999999924e+01,4.263331500000000318e+01,9.895780000000000243e+00,
C755: 4.603500799999999771e+01,4.144830600000000231e+01,9.320069999999999411e+00,
4.682292300000000296e+01,4.079867399999999833e+01,8.951878000000000668e+00,
4.517032799999999781e+01,4.084901800000000094e+01,9.580987000000000364e+00,
4.576236000000000104e+01,4.215984699999999918e+01,8.547710999999999615e+00,
4.638407699999999977e+01,4.198389399999999938e+01,1.019509200000000071e+01,
C756: 4.963792800000000227e+01,4.179572100000000034e+01,9.476848999999999634e+00,
5.051574699999999751e+01,4.125932699999999897e+01,9.129177000000000319e+00,
4.994884600000000319e+01,4.265996599999999717e+01,1.005587200000000081e+01,
4.903822699999999912e+01,4.113927999999999940e+01,1.010022799999999954e+01,
4.905251799999999704e+01,4.212091199999999702e+01,8.622101000000000681e+00,
C757: 7.674485999999999919e+00,4.505085499999999854e+01,9.380706999999999240e+00,
8.158868000000000009e+00,4.499153700000000100e+01,1.035087500000000027e+01,
8.429038999999999554e+00,4.504644700000000057e+01,8.599479999999999791e+00,
7.096458000000000155e+00,4.596819899999999848e+01,9.320211999999999719e+00,
7.015498000000000012e+00,4.419733099999999837e+01,9.252242000000000743e+00,
C758: 1.184523500000000062e+01,4.500582500000000152e+01,9.353279999999999816e+00,
1.280026900000000012e+01,4.477584900000000090e+01,9.814372000000000540e+00,
1.191773200000000088e+01,4.594389499999999771e+01,8.812663000000000579e+00,
1.108309399999999911e+01,4.508878599999999892e+01,1.012198500000000045e+01,
1.157729199999999992e+01,4.421259500000000031e+01,8.663223999999999592e+00,
C759: 1.577482400000000062e+01,4.485237800000000163e+01,9.319708000000000325e+00,
1.533035300000000056e+01,4.533058299999999718e+01,1.018568299999999915e+01,
1.611497999999999919e+01,4.561339600000000161e+01,8.624178000000000566e+00,
1.503612200000000065e+01,4.422625299999999982e+01,8.831970000000000098e+00,
1.662033100000000019e+01,4.424938499999999664e+01,9.633770999999999418e+00,
C760: 2.004225900000000138e+01,4.504896300000000053e+01,9.385032000000000707e+00,
1.936564600000000169e+01,4.538332900000000336e+01,1.016570600000000013e+01,
1.993104999999999905e+01,4.568360700000000207e+01,8.510756999999999906e+00,
1.980762100000000010e+01,4.402244999999999919e+01,9.119516000000000844e+00,
2.106435700000000111e+01,4.510426100000000105e+01,9.745635999999999299e+00,
C761: 2.406963000000000133e+01,4.486528799999999961e+01,9.317532999999999177e+00,
2.434041399999999911e+01,4.578609600000000057e+01,8.811768000000000711e+00,
2.351480400000000159e+01,4.422996499999999997e+01,8.635678000000000409e+00,
2.345140800000000070e+01,4.509637500000000188e+01,1.017854600000000076e+01,
2.496882799999999847e+01,4.435539599999999893e+01,9.645089999999999719e+00,
C762: 2.778201500000000124e+01,4.507092500000000257e+01,9.353201000000000320e+00,
2.787759199999999993e+01,4.555714799999999798e+01,1.031887099999999968e+01,
2.874493299999999962e+01,4.507265900000000158e+01,8.851326999999999501e+00,
2.705938799999999844e+01,4.560789599999999666e+01,8.747047000000000239e+00,
2.744952899999999829e+01,4.404752899999999727e+01,9.491752999999999219e+00,
C763: 3.224729099999999704e+01,4.507737300000000147e+01,9.359149999999999636e+00,
3.309133800000000036e+01,4.544881999999999778e+01,9.930329999999999657e+00,
3.211428899999999942e+01,4.568819599999999781e+01,8.471168999999999727e+00,
3.134950600000000165e+01,4.512308699999999817e+01,9.967762000000000455e+00,
3.243357499999999760e+01,4.404883300000000190e+01,9.067422999999999789e+00,
C764: 3.595761799999999653e+01,4.492642899999999884e+01,9.326802000000000703e+00,
3.592110000000000269e+01,4.581678999999999746e+01,8.707086999999999577e+00,
3.698116300000000223e+01,4.457095999999999947e+01,9.387843000000000160e+00,
3.532673700000000139e+01,4.416229299999999824e+01,8.888469000000000619e+00,
3.559547100000000341e+01,4.516852500000000248e+01,1.031985899999999923e+01,
C765: 4.013250000000000028e+01,4.512819900000000217e+01,9.369087999999999639e+00,
3.953430800000000289e+01,4.561127199999999959e+01,1.013502199999999931e+01,
4.117170000000000130e+01,4.510731200000000030e+01,9.682771999999999935e+00,
4.004565399999999897e+01,4.568151600000000201e+01,8.438655999999999935e+00,
3.977947600000000250e+01,4.411225900000000166e+01,9.221026999999999418e+00,
C766: 4.433365700000000231e+01,4.479369400000000212e+01,9.324787999999999855e+00,
4.375150800000000118e+01,4.542648299999999750e+01,9.987474000000000629e+00,
4.488723099999999988e+01,4.541290999999999656e+01,8.626042999999999239e+00,
4.366648200000000202e+01,4.413871100000000069e+01,8.774440999999999491e+00,
4.502695299999999889e+01,4.419949499999999887e+01,9.910726000000000369e+00,
C767: 4.797548599999999652e+01,4.498863099999999804e+01,9.339688999999999908e+00,
4.752865500000000054e+01,4.400805199999999928e+01,9.214674000000000476e+00,
4.889690499999999673e+01,4.490055100000000010e+01,9.907126999999999128e+00,
4.728483800000000059e+01,4.563514800000000093e+01,9.870917000000000385e+00,
4.819100699999999904e+01,4.541501600000000138e+01,8.364613999999999550e+00,
C768: 9.771933999999999898e+00,4.824164799999999786e+01,9.338962000000000430e+00,
9.542239000000000360e+00,4.884212500000000290e+01,1.021387700000000009e+01,
1.078488499999999917e+01,4.845417299999999727e+01,9.010410000000000252e+00,
9.074611000000000871e+00,4.848631999999999920e+01,8.543542000000000414e+00,
9.684381999999999380e+00,4.718850599999999673e+01,9.584357999999999933e+00,
C769: 1.398889299999999913e+01,4.808581199999999711e+01,9.473316999999999766e+00,
1.394435700000000011e+01,4.882648600000000272e+01,8.680578999999999823e+00,
1.314804999999999957e+01,4.822914500000000260e+01,1.014480799999999938e+01,
1.491965000000000074e+01,4.819957699999999789e+01,1.001994799999999941e+01,
1.394359299999999990e+01,4.709293900000000122e+01,9.040345999999999549e+00,
C770: 1.807084800000000158e+01,4.832806800000000180e+01,9.308134000000000796e+00,
1.713747400000000098e+01,4.875773000000000224e+01,8.957162000000000290e+00,
1.838549700000000087e+01,4.883776300000000248e+01,1.021249899999999933e+01,
1.883139900000000111e+01,4.845180700000000229e+01,8.544024000000000285e+00,
1.792997899999999944e+01,4.727052400000000176e+01,9.506125000000000824e+00,
C771: 2.175558900000000051e+01,4.826638100000000264e+01,9.384213000000000804e+00,
2.092527199999999965e+01,4.787556899999999871e+01,9.963229000000000113e+00,

2.226350000000000051e+01,4.903844500000000295e+01,9.954076000000000590e+00,
2.138229799999999869e+01,4.869010200000000310e+01,8.457300999999999291e+00,
2.245182799999999901e+01,4.746423099999999806e+01,9.160743999999999332e+00,
C772: 2.598164799999999985e+01,4.833516399999999891e+01,9.539286999999999850e+00,
2.684514100000000170e+01,4.789661499999999705e+01,1.002896299999999918e+01,
2.609407300000000163e+01,4.824694999999999823e+01,8.463499999999999801e+00,
2.590916599999999903e+01,4.938438699999999670e+01,9.808712999999999127e+00,
2.507924699999999874e+01,4.781949999999999790e+01,8.851924999999999599e+00,
C773: 2.995225200000000143e+01,4.810653400000000346e+01,9.244082000000000576e+00,
3.074646500000000060e+01,4.836661000000000143e+01,8.553117000000000303e+00,
2.901546300000000045e+01,4.818502500000000310e+01,8.701283000000000101e+00,
2.994657700000000133e+01,4.881073599999999857e+01,1.006943200000000083e+01,
3.008139699999999905e+01,4.708219700000000074e+01,9.575302999999999898e+00,
C774: 3.355740300000000076e+01,4.854583699999999880e+01,9.467364999999999142e+00,
3.312391099999999966e+01,4.884172999999999831e+01,8.516878000000000171e+00,
3.399658500000000316e+01,4.941455299999999795e+01,9.947696000000000538e+00,
3.433031799999999834e+01,4.780300100000000185e+01,9.294774999999999565e+00,
3.278671099999999683e+01,4.812838299999999947e+01,1.010746499999999948e+01,
C775: 3.808852900000000119e+01,4.821676699999999727e+01,9.418642000000000181e+00,
3.891619399999999729e+01,4.825084900000000232e+01,1.011885400000000068e+01,
3.835831600000000208e+01,4.875064499999999867e+01,8.512726000000000681e+00,
3.721469799999999850e+01,4.868192700000000173e+01,9.863955999999999946e+00,
3.786430899999999866e+01,4.718387700000000251e+01,9.175043999999999755e+00,
C776: 4.177469599999999872e+01,4.838445800000000219e+01,9.310325000000000628e+00,
4.130390200000000078e+01,4.859977200000000153e+01,1.026317500000000038e+01,
4.245794999999999675e+01,4.918837299999999857e+01,9.053824999999999790e+00,
4.101179799999999886e+01,4.830107499999999732e+01,8.542794000000000665e+00,
4.232250799999999913e+01,4.744971799999999718e+01,9.376727000000000700e+00,
C777: 4.541222900000000351e+01,4.835510899999999879e+01,9.483071999999999946e+00,
4.549642399999999753e+01,4.940144699999999744e+01,9.760486000000000217e+00,
4.508796099999999996e+01,4.828098399999999657e+01,8.450243000000000393e+00,
4.468316599999999994e+01,4.786819899999999706e+01,1.012179399999999951e+01,
4.637856500000000182e+01,4.787279000000000195e+01,9.592057999999999751e+00,
C778: 5.001917000000000257e+01,4.808488700000000193e+01,9.418917000000000428e+00,
5.067901100000000270e+01,4.893927999999999656e+01,9.536841000000000790e+00,
5.060439600000000127e+01,4.720669300000000135e+01,9.162803000000000253e+00,
4.930351999999999890e+01,4.828675499999999943e+01,8.627202999999999733e+00,
4.948725300000000260e+01,4.790709600000000279e+01,1.034901699999999991e+01,
C779: 7.950955999999999690e+00,5.179795200000000222e+01,9.381227000000000871e+00,
8.386189999999999145e+00,5.138178700000000276e+01,1.028508000000000067e+01,
8.384577000000000169e+00,5.130929799999999830e+01,8.513604000000000838e+00,
8.157700000000000173e+00,5.286315799999999854e+01,9.337455000000000283e+00,
6.877061999999999564e+00,5.163683000000000334e+01,9.388797000000000281e+00,
C780: 1.162235800000000019e+01,5.219879099999999994e+01,9.405846999999999625e+00,
1.106094900000000081e+01,5.273819499999999749e+01,1.016290099999999974e+01,
1.264426399999999973e+01,5.205628699999999753e+01,9.744649000000000783e+00,
1.162359200000000037e+01,5.276835299999999762e+01,8.481267000000000778e+00,
1.116087800000000030e+01,5.123100999999999772e+01,9.233192000000000732e+00,
C781: 1.612737399999999965e+01,5.217036300000000182e+01,9.459530000000000882e+00,
1.677727799999999903e+01,5.221037700000000115e+01,1.032865299999999920e+01,
1.663859499999999869e+01,5.260302099999999825e+01,8.604665999999999926e+00,
1.521895300000000084e+01,5.273033800000000326e+01,9.660546000000000078e+00,
1.587461000000000055e+01,5.113630299999999806e+01,9.243988999999999123e+00,
C782: 1.986823700000000059e+01,5.177956600000000265e+01,9.348744999999999195e+00,
2.078285299999999935e+01,5.122122800000000353e+01,9.523785000000000167e+00,
1.903358100000000164e+01,5.109156699999999773e+01,9.261855999999999867e+00,
1.996357100000000173e+01,5.234874500000000097e+01,8.428910000000000124e+00,
1.969315599999999833e+01,5.245924300000000073e+01,1.017731500000000011e+01,
C783: 2.408469799999999950e+01,5.247488299999999839e+01,9.457917000000000129e+00,
2.490611499999999978e+01,5.291693000000000069e+01,1.001396800000000020e+01,
2.386080499999999915e+01,5.308961599999999947e+01,8.591170999999999225e+00,
2.320739700000000028e+01,5.241361200000000053e+01,1.009514599999999973e+01,
2.436420000000000030e+01,5.147742600000000124e+01,9.131368999999999403e+00,
C784: 2.829474400000000145e+01,5.171014199999999761e+01,9.370765000000000455e+00,
2.882864999999999966e+01,5.211611400000000316e+01,1.022455500000000050e+01,
2.844874000000000080e+01,5.235390300000000252e+01,8.509947000000000372e+00,
2.723430400000000162e+01,5.165661699999999712e+01,9.597886000000000806e+00,
2.866741400000000084e+01,5.071571200000000346e+01,9.148701000000000860e+00,
C785: 3.187151000000000067e+01,5.209093099999999765e+01,9.362655999999999423e+00,
3.133115600000000001e+01,5.270102700000000340e+01,1.008021100000000025e+01,
3.288057400000000285e+01,5.191592800000000096e+01,9.723267999999999134e+00,
3.191278600000000054e+01,5.260648499999999927e+01,8.407861999999999725e+00,
3.136291800000000052e+01,5.113966400000000334e+01,9.238170000000000215e+00,
C786: 3.598524199999999951e+01,5.239254499999999837e+01,9.495938000000000656e+00,
3.535673100000000346e+01,5.285913599999999946e+01,1.024865999999999921e+01,
3.695665799999999734e+01,5.216550399999999854e+01,9.925174000000000163e+00,
3.610942299999999960e+01,5.306980399999999776e+01,8.656207000000000207e+00,
3.551833100000000343e+01,5.147365599999999830e+01,9.153537000000000035e+00,
C787: 4.024877200000000244e+01,5.172073300000000273e+01,9.359609000000000734e+00,
4.120231400000000122e+01,5.143356899999999854e+01,9.791968999999999923e+00,
4.042129200000000111e+01,5.226605500000000148e+01,8.436623000000000872e+00,
3.970970599999999706e+01,5.235385200000000339e+01,1.005800699999999992e+01,
3.966239499999999651e+01,5.083160300000000120e+01,9.150071000000000510e+00,
C788: 4.416974600000000351e+01,5.242875099999999833e+01,9.428563999999999723e+00,
4.353587199999999768e+01,5.285110499999999689e+01,1.020261600000000080e+01,
4.518804099999999835e+01,5.234889499999999884e+01,9.797477999999999909e+00,
4.415055600000000169e+01,5.307115199999999788e+01,8.553235000000000809e+00,
4.380442599999999942e+01,5.144175700000000262e+01,9.160553000000000168e+00,
C789: 4.852361499999999950e+01,5.182527900000000187e+01,9.454485000000000028e+00,
4.939551199999999653e+01,5.146141000000000076e+01,9.989948999999999302e+00,
4.883881300000000181e+01,5.230555199999999871e+01,8.532918999999999699e+00,
4.799112600000000128e+01,5.254177800000000076e+01,1.007286700000000046e+01,
4.786819400000000257e+01,5.099120700000000284e+01,9.221159999999999357e+00,

Au: 8.160183999999999216e+00,1.050324099999999916e+01,0.000000000000000000e+00,
Au: 1.108175699999999964e+01,1.050206499999999998e+01,0.000000000000000000e+00,
Au: 1.400398199999999882e+01,1.050007899999999950e+01,0.000000000000000000e+00,
Au: 1.692608300000000199e+01,1.049651099999999992e+01,0.000000000000000000e+00,
Au: 1.984907600000000016e+01,1.049448600000000020e+01,0.000000000000000000e+00,
Au: 2.277238700000000193e+01,1.049300199999999883e+01,0.000000000000000000e+00,
Au: 2.569604200000000205e+01,1.049365500000000040e+01,0.000000000000000000e+00,
Au: 2.861916900000000297e+01,1.049582399999999893e+01,0.000000000000000000e+00,
Au: 3.154272900000000135e+01,1.049544099999999958e+01,0.000000000000000000e+00,
Au: 3.446579400000000248e+01,1.049306900000000020e+01,0.000000000000000000e+00,
Au: 3.738810699999999798e+01,1.049425100000000022e+01,0.000000000000000000e+00,
Au: 4.031236600000000436e+01,1.049555599999999878e+01,0.000000000000000000e+00,
Au: 4.323659500000000122e+01,1.049861399999999989e+01,0.000000000000000000e+00,
Au: 4.615798399999999901e+01,1.050142099999999878e+01,0.000000000000000000e+00,
Au: 4.907931700000000319e+01,1.050375999999999976e+01,0.000000000000000000e+00,
Au: 9.623723000000000027e+00,1.303593199999999896e+01,0.000000000000000000e+00,
Au: 1.254449400000000026e+01,1.303235199999999949e+01,0.000000000000000000e+00,
Au: 1.546704500000000060e+01,1.302748500000000043e+01,0.000000000000000000e+00,
Au: 1.839079500000000067e+01,1.302548099999999920e+01,0.000000000000000000e+00,
Au: 2.131502000000000052e+01,1.302583399999999969e+01,0.000000000000000000e+00,
Au: 2.423572800000000171e+01,1.302340799999999987e+01,0.000000000000000000e+00,
Au: 2.715568900000000241e+01,1.302542599999999950e+01,0.000000000000000000e+00,
Au: 3.008069200000000265e+01,1.302627700000000033e+01,0.000000000000000000e+00,
Au: 3.300555400000000361e+01,1.302466499999999883e+01,0.000000000000000000e+00,
Au: 3.592627900000000096e+01,1.302497099999999897e+01,0.000000000000000000e+00,
Au: 3.884709300000000098e+01,1.302616100000000010e+01,0.000000000000000000e+00,
Au: 4.177032499999999970e+01,1.302658699999999925e+01,0.000000000000000000e+00,
Au: 4.469326099999999968e+01,1.303047999999999895e+01,0.000000000000000000e+00,
Au: 4.761594500000000352e+01,1.303451599999999999e+01,0.000000000000000000e+00,
Au: 5.053763100000000463e+01,1.303587199999999946e+01,0.000000000000000000e+00,
Au: 8.163611999999998758e+00,1.556669100000000050e+01,0.000000000000000000e+00,
Au: 1.108857199999999921e+01,1.556554599999999944e+01,0.000000000000000000e+00,
Au: 1.401160499999999942e+01,1.555965400000000010e+01,0.000000000000000000e+00,
Au: 1.693096700000000254e+01,1.555672299999999986e+01,0.000000000000000000e+00,
Au: 1.985324800000000067e+01,1.555701299999999954e+01,0.000000000000000000e+00,
Au: 2.277682100000000176e+01,1.555594299999999919e+01,0.000000000000000000e+00,
Au: 2.569811500000000137e+01,1.555582099999999990e+01,0.000000000000000000e+00,
Au: 2.861999400000000193e+01,1.555642600000000009e+01,0.000000000000000000e+00,
Au: 3.154290000000000305e+01,1.555674999999999919e+01,0.000000000000000000e+00,
Au: 3.446286500000000075e+01,1.555634599999999956e+01,0.000000000000000000e+00,
Au: 3.738370100000000207e+01,1.555789500000000025e+01,0.000000000000000000e+00,
Au: 4.030866400000000027e+01,1.555633699999999919e+01,0.000000000000000000e+00,
Au: 4.323029000000000366e+01,1.555814599999999892e+01,0.000000000000000000e+00,
Au: 4.615001200000000381e+01,1.556354499999999952e+01,0.000000000000000000e+00,
Au: 4.907258900000000068e+01,1.556739199999999990e+01,0.000000000000000000e+00,
Au: 9.629313999999999041e+00,1.809511300000000134e+01,0.000000000000000000e+00,
Au: 1.255276800000000037e+01,1.809336100000000158e+01,0.000000000000000000e+00,
Au: 1.547237599999999880e+01,1.809032700000000204e+01,0.000000000000000000e+00,
Au: 1.839310299999999998e+01,1.808731700000000231e+01,0.000000000000000000e+00,
Au: 2.131780900000000045e+01,1.808762700000000123e+01,0.000000000000000000e+00,
Au: 2.423921800000000104e+01,1.808624300000000318e+01,0.000000000000000000e+00,
Au: 2.715842600000000218e+01,1.808856000000000108e+01,0.000000000000000000e+00,
Au: 3.007993000000000094e+01,1.808924600000000282e+01,0.000000000000000000e+00,
Au: 3.300084499999999821e+01,1.808835200000000043e+01,0.000000000000000000e+00,
Au: 3.592171199999999942e+01,1.808807100000000290e+01,0.000000000000000000e+00,
Au: 3.884586600000000089e+01,1.808770100000000269e+01,0.000000000000000000e+00,
Au: 4.176784299999999917e+01,1.808829200000000270e+01,0.000000000000000000e+00,
Au: 4.468590499999999821e+01,1.809177100000000138e+01,0.000000000000000000e+00,
Au: 4.760859100000000410e+01,1.809478800000000120e+01,0.000000000000000000e+00,
Au: 5.053479000000000099e+01,1.809632700000000227e+01,0.000000000000000000e+00,
Au: 8.166242999999999697e+00,2.062337500000000290e+01,0.000000000000000000e+00,
Au: 1.109173999999999971e+01,2.062455700000000292e+01,0.000000000000000000e+00,
Au: 1.401534999999999975e+01,2.062253700000000123e+01,0.000000000000000000e+00,
Au: 1.693488400000000027e+01,2.062017000000000166e+01,0.000000000000000000e+00,
Au: 1.985547500000000198e+01,2.061826700000000301e+01,0.000000000000000000e+00,
Au: 2.277785900000000296e+01,2.061793600000000026e+01,0.000000000000000000e+00,
Au: 2.569795799999999986e+01,2.061979900000000043e+01,0.000000000000000000e+00,
Au: 2.862006000000000228e+01,2.062154800000000066e+01,0.000000000000000000e+00,
Au: 3.154220500000000271e+01,2.062171100000000123e+01,0.000000000000000000e+00,
Au: 3.446053500000000014e+01,2.061861900000000247e+01,0.000000000000000000e+00,
Au: 3.738126499999999908e+01,2.061836700000000278e+01,0.000000000000000000e+00,
Au: 4.030546700000000016e+01,2.061890200000000206e+01,0.000000000000000000e+00,
Au: 4.322729800000000466e+01,2.062148499999999984e+01,0.000000000000000000e+00,
Au: 4.614748800000000273e+01,2.062328000000000117e+01,0.000000000000000000e+00,
Au: 4.906985200000000447e+01,2.062409200000000098e+01,0.000000000000000000e+00,
Au: 9.628555999999999671e+00,2.315334700000000012e+01,0.000000000000000000e+00,
Au: 1.255154199999999953e+01,2.315341800000000205e+01,0.000000000000000000e+00,
Au: 1.547308899999999987e+01,2.315131300000000181e+01,0.000000000000000000e+00,
Au: 1.839547800000000066e+01,2.314953000000000216e+01,0.000000000000000000e+00,
Au: 2.131807200000000080e+01,2.315054800000000057e+01,0.000000000000000000e+00,
Au: 2.423686400000000063e+01,2.315017900000000139e+01,0.000000000000000000e+00,
Au: 2.715632000000000090e+01,2.315275400000000161e+01,0.000000000000000000e+00,
Au: 3.008052500000000151e+01,2.315301800000000298e+01,0.000000000000000000e+00,
Au: 3.300465400000000216e+01,2.315101300000000251e+01,0.000000000000000000e+00,
Au: 3.592449799999999982e+01,2.315008700000000275e+01,0.000000000000000000e+00,
Au: 3.884463800000000333e+01,2.315055700000000272e+01,0.000000000000000000e+00,
Au: 4.176534699999999845e+01,2.315075900000000075e+01,0.000000000000000000e+00,
Au: 4.468616700000000463e+01,2.315174100000000124e+01,0.000000000000000000e+00,
Au: 4.761023200000000344e+01,2.315379300000000029e+01,0.000000000000000000e+00,
Au: 5.053447900000000459e+01,2.315319000000000216e+01,0.000000000000000000e+00,
Au: 8.166537999999999187e+00,2.568358500000000078e+01,0.000000000000000000e+00,
Au: 1.108989199999999897e+01,2.568391400000000147e+01,0.000000000000000000e+00,
Au: 1.401321800000000017e+01,2.568112400000000051e+01,0.000000000000000000e+00,
Au: 1.693297400000000152e+01,2.568018200000000206e+01,0.000000000000000000e+00,
Au: 1.985338400000000192e+01,2.568221500000000290e+01,0.000000000000000000e+00,
Au: 2.277476100000000159e+01,2.568269300000000044e+01,0.000000000000000000e+00,
Au: 2.569467400000000268e+01,2.568192300000000117e+01,0.000000000000000000e+00,
Au: 2.861895600000000073e+01,2.568282200000000159e+01,0.000000000000000000e+00,
Au: 3.154447199999999896e+01,2.568269300000000044e+01,0.000000000000000000e+00,
Au: 3.446433199999999886e+01,2.568164400000000214e+01,0.000000000000000000e+00,
Au: 3.738417900000000316e+01,2.568280100000000132e+01,0.000000000000000000e+00,
Au: 4.030766600000000466e+01,2.568107800000000296e+01,0.000000000000000000e+00,
Au: 4.322911200000000065e+01,2.568065800000000110e+01,0.000000000000000000e+00,
Au: 4.614942400000000333e+01,2.568274500000000060e+01,0.000000000000000000e+00,
Au: 4.907186300000000045e+01,2.568405000000000271e+01,0.000000000000000000e+00,
Au: 9.628966999999999388e+00,2.821333800000000025e+01,0.000000000000000000e+00,
Au: 1.255247099999999882e+01,2.821241100000000301e+01,0.000000000000000000e+00,
Au: 1.547012699999999974e+01,2.821166300000000149e+01,0.000000000000000000e+00,
Au: 1.838947399999999988e+01,2.821279499999999985e+01,0.000000000000000000e+00,
Au: 2.131463500000000266e+01,2.821313000000000315e+01,0.000000000000000000e+00,
Au: 2.423655700000000124e+01,2.821269800000000316e+01,0.000000000000000000e+00,
Au: 2.715586400000000111e+01,2.821254200000000267e+01,0.000000000000000000e+00,
Au: 3.007946100000000200e+01,2.821240500000000040e+01,0.000000000000000000e+00,
Au: 3.300394800000000117e+01,2.821298800000000284e+01,0.000000000000000000e+00,
Au: 3.592560100000000034e+01,2.821316900000000061e+01,0.000000000000000000e+00,
Au: 3.884916499999999928e+01,2.821282100000000170e+01,0.000000000000000000e+00,
Au: 4.176938300000000481e+01,2.821147300000000158e+01,0.000000000000000000e+00,
Au: 4.468686200000000497e+01,2.821174000000000248e+01,0.000000000000000000e+00,
Au: 4.760966700000000174e+01,2.821414100000000147e+01,0.000000000000000000e+00,
Au: 5.053440100000000257e+01,2.821358900000000247e+01,0.000000000000000000e+00,
Au: 8.165599000000000274e+00,3.074216400000000249e+01,0.000000000000000000e+00,

Au: 1.109033299999999933e+01,3.074161199999999994e+01,0.000000000000000000e+00,
Au: 1.401313799999999965e+01,3.074401300000000248e+01,0.000000000000000000e+00,
Au: 1.693061700000000158e+01,3.074427999999999983e+01,0.000000000000000000e+00,
Au: 1.985083500000000001e+01,3.074293199999999970e+01,0.000000000000000000e+00,
Au: 2.277439900000000250e+01,3.074258400000000080e+01,0.000000000000000000e+00,
Au: 2.569605200000000167e+01,3.074276500000000212e+01,0.000000000000000000e+00,
Au: 2.862053900000000084e+01,3.074334800000000101e+01,0.000000000000000000e+00,
Au: 3.154413600000000173e+01,3.074321100000000229e+01,0.000000000000000000e+00,
Au: 3.446344299999999805e+01,3.074305500000000180e+01,0.000000000000000000e+00,
Au: 3.738536500000000018e+01,3.074262300000000181e+01,0.000000000000000000e+00,
Au: 4.031052600000000297e+01,3.074295800000000156e+01,0.000000000000000000e+00,
Au: 4.322987300000000488e+01,3.074408999999999992e+01,0.000000000000000000e+00,
Au: 4.614752899999999869e+01,3.074334200000000195e+01,0.000000000000000000e+00,
Au: 4.907103299999999990e+01,3.074241500000000116e+01,0.000000000000000000e+00,
Au: 9.628136999999998835e+00,3.327170300000000225e+01,0.000000000000000000e+00,
Au: 1.255057599999999951e+01,3.327300800000000436e+01,0.000000000000000000e+00,
Au: 1.547088800000000042e+01,3.327509500000000031e+01,0.000000000000000000e+00,
Au: 1.839233400000000174e+01,3.327467500000000200e+01,0.000000000000000000e+00,
Au: 2.131582099999999969e+01,3.327295200000000364e+01,0.000000000000000000e+00,
Au: 2.423566800000000043e+01,3.327410900000000282e+01,0.000000000000000000e+00,
Au: 2.715552800000000033e+01,3.327306000000000097e+01,0.000000000000000000e+00,
Au: 3.008104400000000211e+01,3.327293000000000234e+01,0.000000000000000000e+00,
Au: 3.300532600000000372e+01,3.327382899999999921e+01,0.000000000000000000e+00,
Au: 3.592523900000000481e+01,3.327305900000000349e+01,0.000000000000000000e+00,
Au: 3.884661600000000448e+01,3.327353800000000206e+01,0.000000000000000000e+00,
Au: 4.176702600000000132e+01,3.327557099999999934e+01,0.000000000000000000e+00,
Au: 4.468678200000000089e+01,3.327462900000000445e+01,0.000000000000000000e+00,
Au: 4.761010800000000387e+01,3.327183800000000247e+01,0.000000000000000000e+00,
Au: 5.053346200000000010e+01,3.327216800000000063e+01,0.000000000000000000e+00,
Au: 8.165521000000000029e+00,3.580256299999999925e+01,0.000000000000000000e+00,
Au: 1.108976799999999940e+01,3.580196000000000112e+01,0.000000000000000000e+00,
Au: 1.401383299999999998e+01,3.580401200000000017e+01,0.000000000000000000e+00,
Au: 1.693465300000000084e+01,3.580499400000000065e+01,0.000000000000000000e+00,
Au: 1.985536200000000306e+01,3.580519600000000224e+01,0.000000000000000000e+00,
Au: 2.277550200000000302e+01,3.580566600000000221e+01,0.000000000000000000e+00,
Au: 2.569534600000000069e+01,3.580474000000000245e+01,0.000000000000000000e+00,
Au: 2.861947500000000133e+01,3.580273499999999842e+01,0.000000000000000000e+00,
Au: 3.154368000000000194e+01,3.580299899999999980e+01,0.000000000000000000e+00,
Au: 3.446313599999999866e+01,3.580557400000000001e+01,0.000000000000000000e+00,
Au: 3.738192800000000204e+01,3.580520500000000084e+01,0.000000000000000000e+00,
Au: 4.030452199999999863e+01,3.580622300000000280e+01,0.000000000000000000e+00,
Au: 4.322691100000000120e+01,3.580443999999999960e+01,0.000000000000000000e+00,
Au: 4.614845799999999798e+01,3.580233400000000188e+01,0.000000000000000000e+00,
Au: 4.907144399999999962e+01,3.580240600000000484e+01,0.000000000000000000e+00,
Au: 9.630148000000000152e+00,3.833166100000000398e+01,0.000000000000000000e+00,
Au: 1.255251200000000011e+01,3.833247300000000024e+01,0.000000000000000000e+00,
Au: 1.547270199999999996e+01,3.833426800000000156e+01,0.000000000000000000e+00,
Au: 1.839453300000000269e+01,3.833685100000000290e+01,0.000000000000000000e+00,
Au: 2.131873500000000021e+01,3.833738600000000218e+01,0.000000000000000000e+00,
Au: 2.423946500000000270e+01,3.833713399999999893e+01,0.000000000000000000e+00,
Au: 2.715779500000000013e+01,3.833404200000000372e+01,0.000000000000000000e+00,
Au: 3.007994000000000057e+01,3.833420500000000430e+01,0.000000000000000000e+00,
Au: 3.300204200000000299e+01,3.833595400000000097e+01,0.000000000000000000e+00,
Au: 3.592214100000000343e+01,3.833781700000000114e+01,0.000000000000000000e+00,
Au: 3.884452500000000441e+01,3.833748599999999840e+01,0.000000000000000000e+00,
Au: 4.176511599999999902e+01,3.833558299999999974e+01,0.000000000000000000e+00,
Au: 4.468465000000000487e+01,3.833321600000000018e+01,0.000000000000000000e+00,
Au: 4.760826000000000136e+01,3.833119599999999849e+01,0.000000000000000000e+00,
Au: 5.053375700000000137e+01,3.833237799999999851e+01,0.000000000000000000e+00,
Au: 8.165210000000000079e+00,4.085942599999999914e+01,0.000000000000000000e+00,
Au: 1.109140900000000052e+01,4.086096500000000020e+01,0.000000000000000000e+00,
Au: 1.401409499999999930e+01,4.086398100000000255e+01,0.000000000000000000e+00,
Au: 1.693215700000000012e+01,4.086746099999999871e+01,0.000000000000000000e+00,
Au: 1.985413400000000195e+01,4.086805199999999871e+01,0.000000000000000000e+00,
Au: 2.277828799999999987e+01,4.086768200000000206e+01,0.000000000000000000e+00,
Au: 2.569915500000000108e+01,4.086740000000000350e+01,0.000000000000000000e+00,
Au: 2.862007000000000190e+01,4.086650699999999858e+01,0.000000000000000000e+00,
Au: 3.154157400000000422e+01,4.086719300000000032e+01,0.000000000000000000e+00,
Au: 3.446078200000000180e+01,4.086950999999999823e+01,0.000000000000000000e+00,
Au: 3.738219099999999884e+01,4.086812600000000373e+01,0.000000000000000000e+00,
Au: 4.030689699999999931e+01,4.086843600000000265e+01,0.000000000000000000e+00,
Au: 4.322762399999999872e+01,4.086542599999999936e+01,0.000000000000000000e+00,
Au: 4.614723200000000247e+01,4.086239199999999983e+01,0.000000000000000000e+00,
Au: 4.907068600000000202e+01,4.086063899999999904e+01,0.000000000000000000e+00,
Au: 9.627411000000000385e+00,4.338835999999999871e+01,0.000000000000000000e+00,
Au: 1.254998799999999903e+01,4.339220800000000366e+01,0.000000000000000000e+00,
Au: 1.546971000000000096e+01,4.339760700000000071e+01,0.000000000000000000e+00,
Au: 1.839133600000000257e+01,4.339941600000000221e+01,0.000000000000000000e+00,
Au: 2.131629900000000077e+01,4.339785799999999938e+01,0.000000000000000000e+00,
Au: 2.423713500000000209e+01,4.339940700000000362e+01,0.000000000000000000e+00,
Au: 2.715709999999999980e+01,4.339900200000000297e+01,0.000000000000000000e+00,
Au: 3.008000600000000091e+01,4.339932699999999954e+01,0.000000000000000000e+00,
Au: 3.300188500000000147e+01,4.339993199999999973e+01,0.000000000000000000e+00,
Au: 3.592317900000000463e+01,4.339981000000000222e+01,0.000000000000000000e+00,
Au: 3.884675200000000217e+01,4.339874000000000365e+01,0.000000000000000000e+00,
Au: 4.176903300000000030e+01,4.339903000000000333e+01,0.000000000000000000e+00,
Au: 4.468839499999999987e+01,4.339609899999999953e+01,0.000000000000000000e+00,
Au: 4.761142800000000364e+01,4.339020599999999916e+01,0.000000000000000000e+00,
Au: 5.053638800000000231e+01,4.338906099999999810e+01,0.000000000000000000e+00,
Au: 8.162368999999999986e+00,4.591988100000000372e+01,0.000000000000000000e+00,
Au: 1.108405499999999932e+01,4.592123700000000497e+01,0.000000000000000000e+00,
Au: 1.400673899999999961e+01,4.592527300000000423e+01,0.000000000000000000e+00,
Au: 1.692967500000000314e+01,4.592916600000000216e+01,0.000000000000000000e+00,
Au: 1.985290700000000186e+01,4.592959100000000205e+01,0.000000000000000000e+00,
Au: 2.277372100000000188e+01,4.593078200000000066e+01,0.000000000000000000e+00,
Au: 2.569444600000000278e+01,4.593108800000000258e+01,0.000000000000000000e+00,
Au: 2.861930800000000019e+01,4.592947600000000108e+01,0.000000000000000000e+00,
Au: 3.154431100000000043e+01,4.593032699999999835e+01,0.000000000000000000e+00,
Au: 3.446427200000000113e+01,4.593234499999999798e+01,0.000000000000000000e+00,
Au: 3.738497999999999877e+01,4.592991800000000069e+01,0.000000000000000000e+00,
Au: 4.030920499999999862e+01,4.593027200000000221e+01,0.000000000000000000e+00,
Au: 4.323295500000000402e+01,4.592826800000000276e+01,0.000000000000000000e+00,
Au: 4.615550600000000259e+01,4.592340099999999836e+01,0.000000000000000000e+00,
Au: 4.907627700000000459e+01,4.591982000000000141e+01,0.000000000000000000e+00,
Au: 9.620682999999999652e+00,4.845199200000000417e+01,0.000000000000000000e+00,
Au: 1.254201600000000028e+01,4.845433200000000085e+01,0.000000000000000000e+00,
Au: 1.546340499999999984e+01,4.845713899999999796e+01,0.000000000000000000e+00,
Au: 1.838763400000000203e+01,4.846019700000000086e+01,0.000000000000000000e+00,
Au: 2.131189300000000131e+01,4.846150099999999838e+01,0.000000000000000000e+00,
Au: 2.423420600000000036e+01,4.846268299999999840e+01,0.000000000000000000e+00,
Au: 2.715727100000000149e+01,4.846031200000000183e+01,0.000000000000000000e+00,
Au: 3.008083099999999988e+01,4.845992900000000247e+01,0.000000000000000000e+00,
Au: 3.300395800000000435e+01,4.846209800000000456e+01,0.000000000000000000e+00,
Au: 3.592761300000000091e+01,4.846275100000000435e+01,0.000000000000000000e+00,
Au: 3.885092399999999913e+01,4.846126699999999943e+01,0.000000000000000000e+00,
Au: 4.177391700000000441e+01,4.845924200000000326e+01,0.000000000000000000e+00,
Au: 4.469601800000000225e+01,4.845567400000000191e+01,0.000000000000000000e+00,
Au: 4.761824299999999965e+01,4.845368799999999965e+01,0.000000000000000000e+00,
Au: 5.053981600000000185e+01,4.845251199999999869e+01,0.000000000000000000e+00,
Au: 8.157738000000000156e+00,5.098219399999999979e+01,0.000000000000000000e+00,
Au: 1.107958900000000035e+01,5.098507500000000192e+01,0.000000000000000000e+00,
Au: 1.400069899999999912e+01,5.098809599999999875e+01,0.000000000000000000e+00,
Au: 1.692338100000000267e+01,5.098971500000000390e+01,0.000000000000000000e+00,
Au: 1.984731400000000079e+01,5.099145700000000403e+01,0.000000000000000000e+00,
Au: 2.277124900000000096e+01,5.099244900000000058e+01,0.000000000000000000e+00,
Au: 2.569578700000000282e+01,5.099076399999999865e+01,0.000000000000000000e+00,
Au: 2.861957700000000315e+01,5.099144700000000086e+01,0.000000000000000000e+00,
Au: 3.154210000000000491e+01,5.099191000000000429e+01,0.000000000000000000e+00,
Au: 3.446448699999999832e+01,5.099191900000000288e+01,0.000000000000000000e+00,
Au: 3.738978900000000039e+01,5.099222999999999928e+01,0.000000000000000000e+00,
Au: 4.031498100000000306e+01,5.099099999999999966e+01,0.000000000000000000e+00,
Au: 4.323794900000000041e+01,5.098771599999999893e+01,0.000000000000000000e+00,
Au: 4.615951900000000308e+01,5.098684400000000494e+01,0.000000000000000000e+00,
Au: 4.908076700000000159e+01,5.098486799999999874e+01,0.000000000000000000e+00,

A4.2 Preliminary Analysis of VENUS Trajectories

This section contains preliminary analysis of the VENUS trajectories in **Chapter 5**. During this analysis, the Lennard Jones parameters as part of the potential were further refined as discussed in **Subsection A4.1**. The sticking probabilities for CH_4 and CD_4 scattering off a CH_4 surface after this adjustment are plotted in **Figure A4.20**. Although the VENUS values are now offset more from the experimental data, at the highest velocity (4600 m/s), with the refined potential, there is now a $\sim$ 7% difference (0.77 for CD_4 and 0.69 for CH_4) compared to $\sim$ 4% from before (0.88 for CD_4 and 0.85 for CH_4). The larger separation should hopefully make it easier to discern how energy is efficiently dissipated.

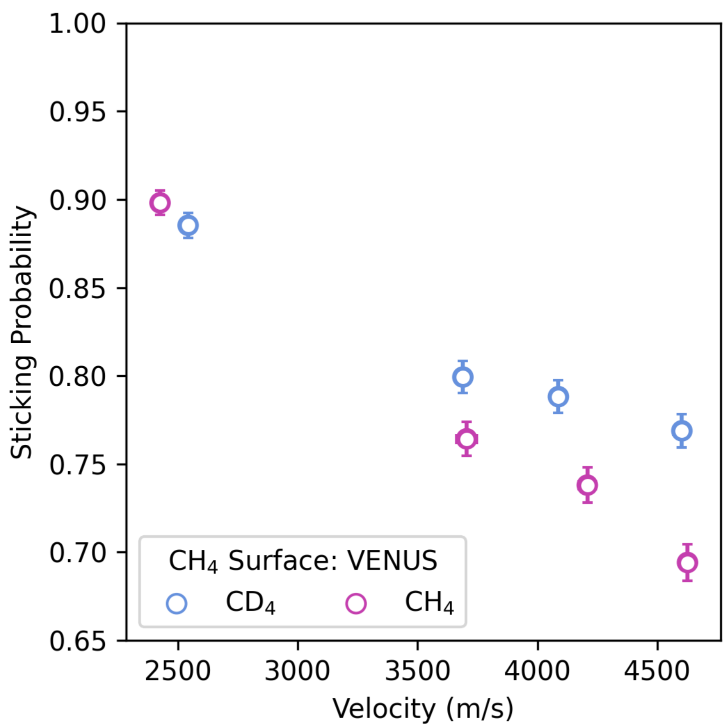

Figure A4.20: CH_4 and CD_4 sticking probabilities on a layered CH_4 surface at 20 K, refined potential. This figure replaces **Figure 5.5**. Error bars represent the standard error of at least 1900 trajectories for each velocity.

For each trajectory that does not stick on the surface, we further analyze to determine the energy distributions, residence time on the surface, and angle scattered from the surface. In the following figures, CD_4 is the top row and CH_4 is the bottom row. Each column is at the same incident velocity, which increases from 2500 m/s in the first column to 4600 m/s in the last column. However, due to different momenta, CH_4 and CD_4 have discrete kinetic energies.

To determine the total kinetic energy of the scattered CH_4 and CD_4, we use the final momenta and mass of the projectile and the equation $p^2/2m$ (**Figure A4.21**). The total kinetic energy is the sum of the vibrational, rotational, and translational energies evaluated at the final step. Ongoing analysis is focused on determining the internal energies of the CH_4 and CD_4 molecules and the final translational energy. The goal is to use the incident energy and final translational kinetic energy to examine how much energy is lost to the surface for each trajectory and explain the sticking probability results.

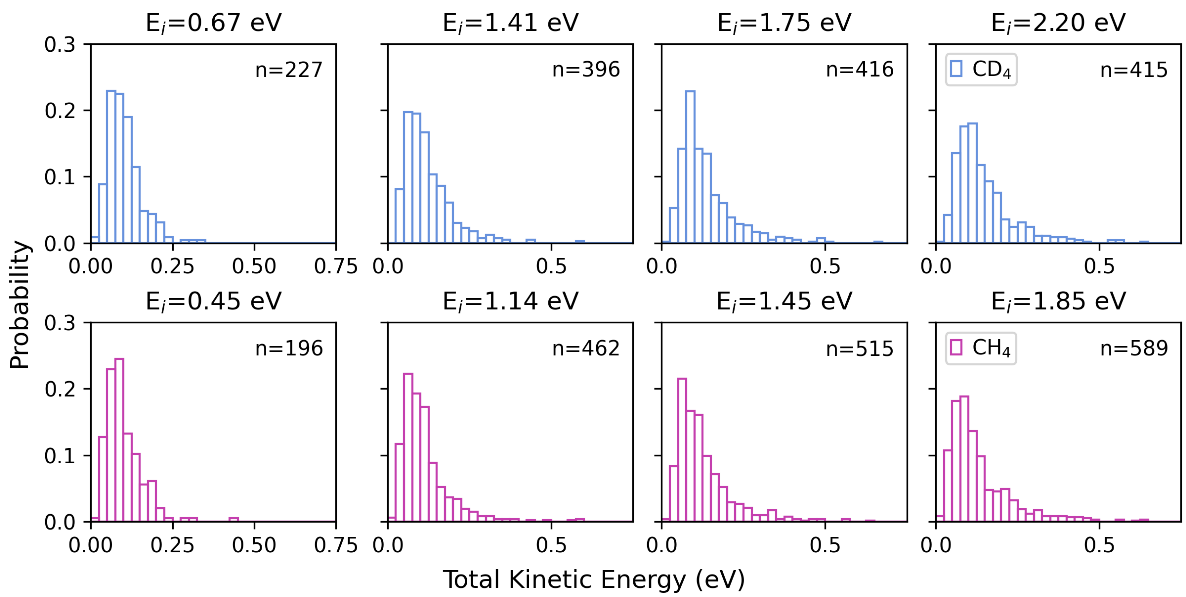

Figure A4.21: Total kinetic energy (eV) distribution of CH_4 and CD_4 scattering off a CH_4 surface at 20 K. The total kinetic energy for each trajectory is calculated using $p^2/2m$ where p is the final momenta and m is the mass of CH_4 or CD_4. The total kinetic energy is the sum of the final vibrational, rotational, and translational energies evaluated at the final step. Each bin is 0.025 eV.

The final scattering angle (θ_f) is defined as the angle between the final velocity vector of CH_4 or CD_4 and the surface normal. Thus, as seen in the distribution (**Figure A4.22**), projectiles scattering at 0° are coming off normal to the surface, while 90° are parallel to the surface. At higher energies, there are more trajectories coming off close to surface normal for both CH_4 and CD_4. Once calculated, the scattered angle will be plotted with the final translational kinetic energy.

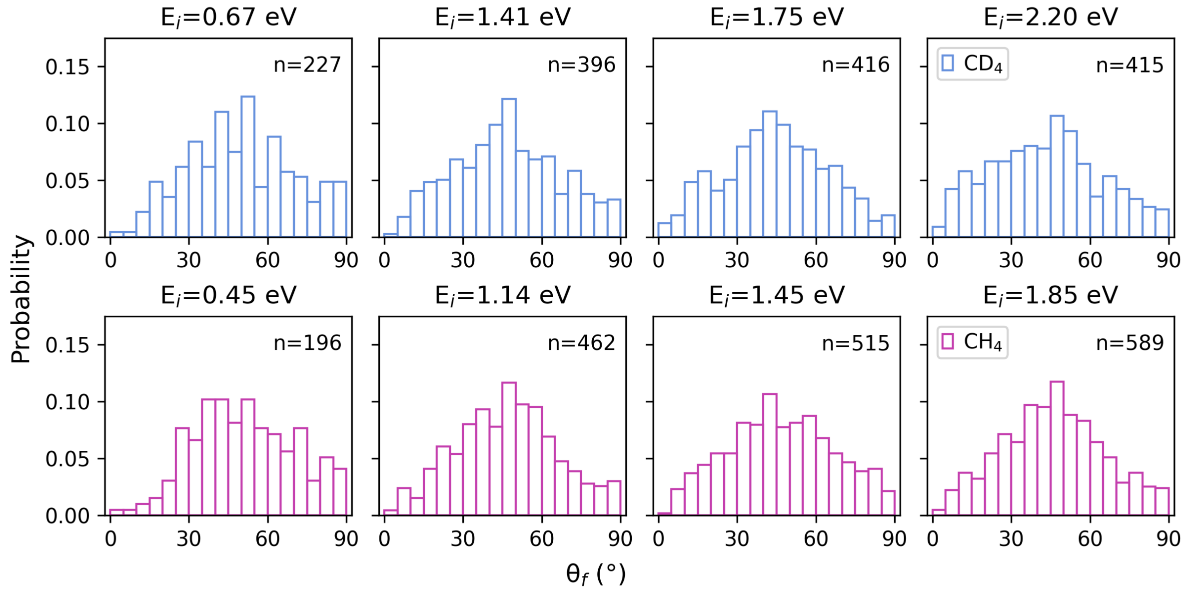

Figure A4.22: Angular (θ_f) Distribution of CH_4 and CD_4 scattering off a CH_4 surface at 20 K. The scattered angle is defined as the angle between the final velocity vector and the surface normal. Each bin is 5°.

To compare between the two projectiles at each incident velocity, these distributions will likely be curve fit.

The residence time is how long (in ps) the carbon of the incident projectile is within 5 Å of the surface. As shown in **Figure A4.23**, with increasing energy the CH_4 or CD_4 spend less time on the surface. Ongoing work is focused on plotting the number of residence species (N(t)/N(0) vs time in order to curve fit and directly compare different velocities as well as between CH_4 and CD_4 at each incident velocity.

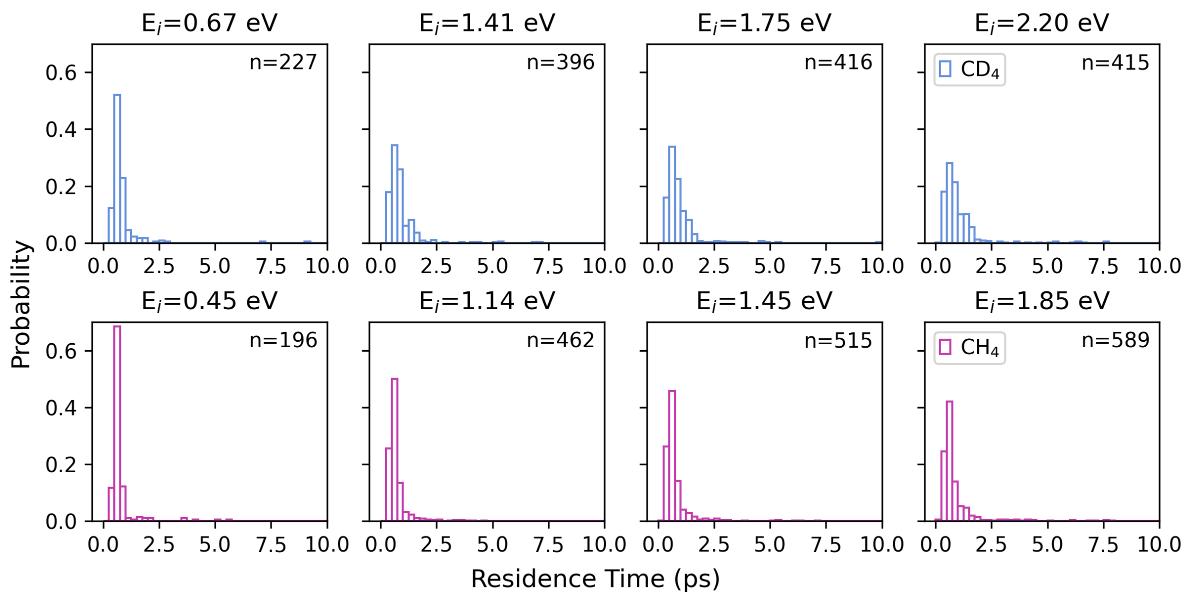

Figure A4.23: Residence time (ps) distribution of CH_4 and CD_4 prior to scattering off a CH_4 surface at 20 K. The residence time is the time in ps during which the carbon of the CH_4 or CD_4 is within 5Å of the surface. Each bin is 0.25 ps.

A5 Reaction Kinetics and Influence of Film Morphology on the Oxidation of Propene Thin Films by O(^{3}P) Atomic Oxygen (Chapter 6)

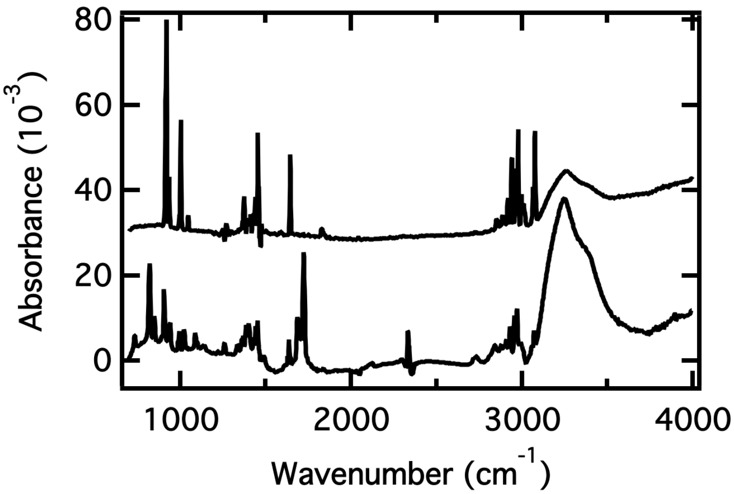

Figure A5.1: Raw RAIR spectrum for Figure 6.1. There two spectra correspond to a 66-layer propene film, deposited on the crystal at 59 K via the molecular beam. The "pristine" spectra was collected right after deposition, and the "reacted" spectrum after exposing the film to 1 $\times 10^{18}$ O(^{3}P) atoms cm^{-2} while the crystal is at 54 K. (*Data files: 040819A.IR02 (pristine, top), 040819A.IR16 (reacted, bottom)*)

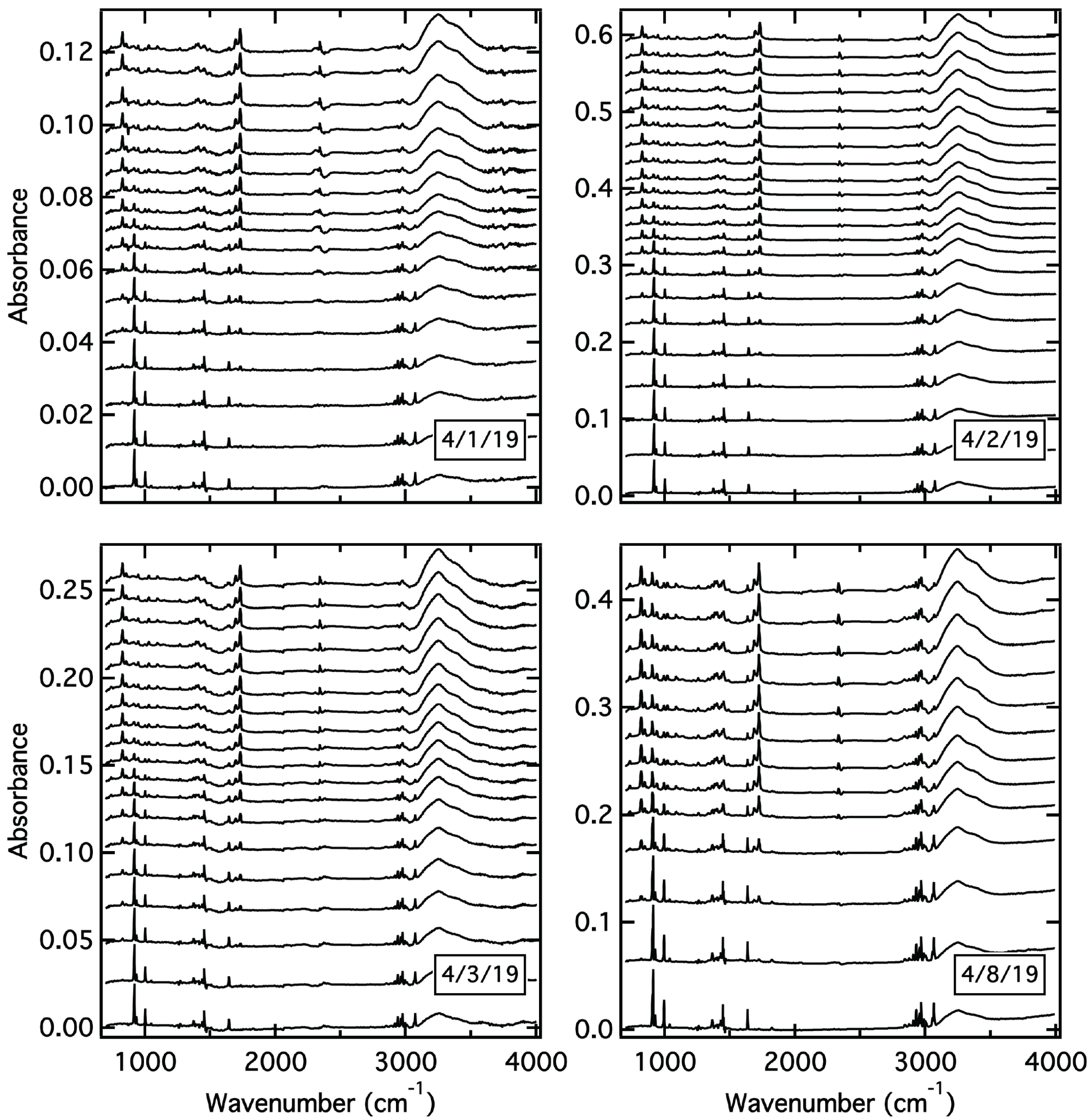

Figure A5.2: Raw RAIR spectrum for Figure 6.2 and 6.4. After depositing a propene film with a desired thickness on to the crystal at 59 K, we expose the film to O(^{3}P) at 54 K and take spectra at regular intervals. **Figure 6.2** contains the integrated areas of the 914 cm^{-1} - 919 cm^{-1} region, corresponding to the loss of propene's double bond. **Figure 6.4** contains the integrated area of the peaks at 827 cm^{-1} and 1730 cm^{-1}, corresponding to the appearance of propylene oxide and propanal, respectively. (*Data files: 040119B.IR02-18 (12 layers), 040319A.IR02-20 (24 layers), 040219A.IR02-23 (46 layers), 040819A.IR04-16(66 layers)*)

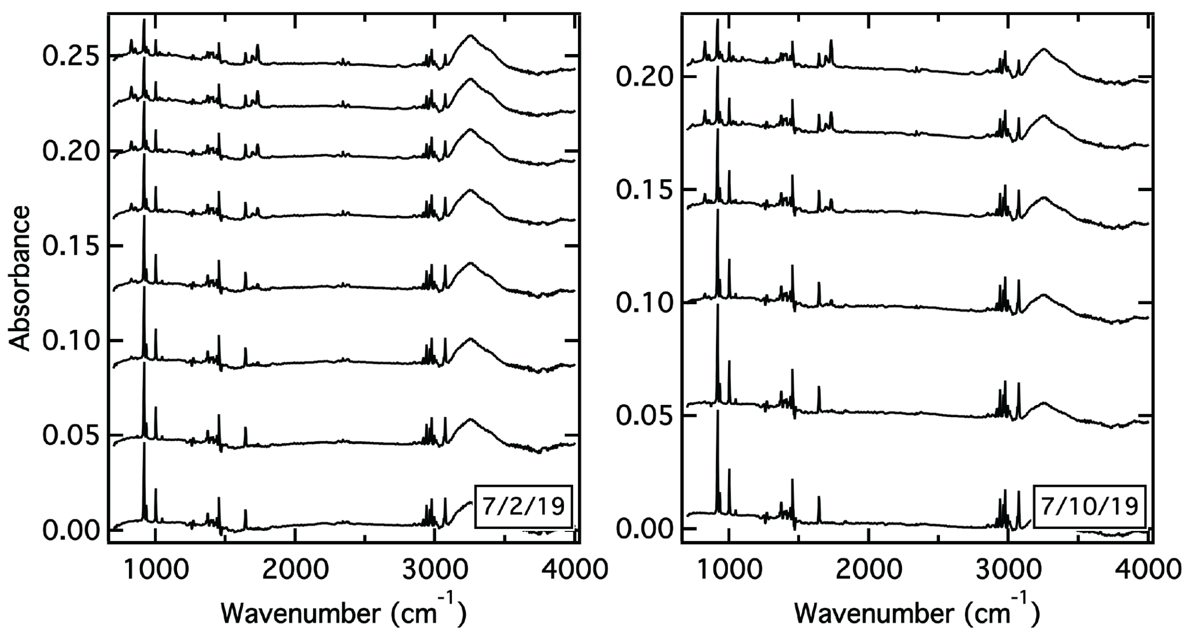

Figure A5.3: Raw RAIR spectrum for Figure 6.3 - 35-46 layers. As the propene film is exposed to $O(^3P)$ at 54 K (deposited at 59 K), we track the loss of spectral intensity in the 914 - 919 cm^{-1} region (corresponding to the loss of propene's double bond). We use the change in intensity to calculate an initial rate of reactivity. This figure is for trials with propene films between 35 and 46 layers thick. Note: **Figure 6.3** also includes the trials that are displayed in **Figure A5.2**. Data files: 070219A.IR02-09, 071019A.IR02-07)

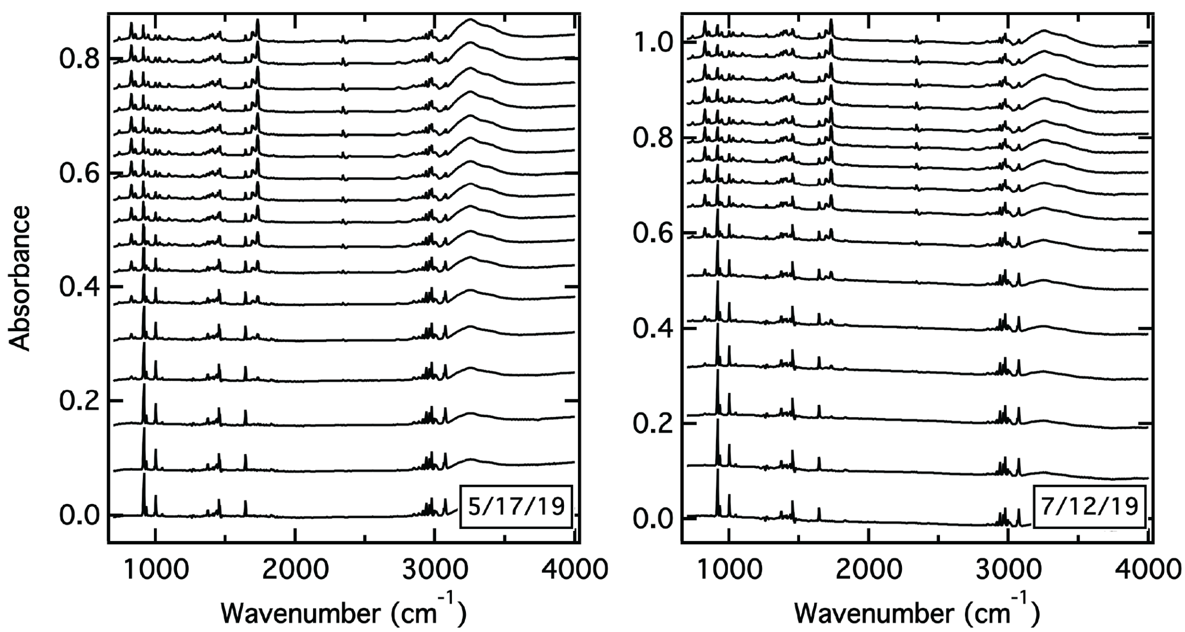

Figure A5.4: Raw RAIR spectrum for Figure 6.3 - 100 layers. As the propene film is exposed to O(^{3}P) at 54 K (deposited at 59 K), we track the loss of spectral intensity in the 914 - 919 cm^{-1} region (corresponding to the loss of propene's double bond). We use the change in intensity to calculate an initial rate of reactivity. This figure is for trials with propene films that are 100 layers thick. (*Data files: 051719A.IR04-20, 071219A.IR02-17*)

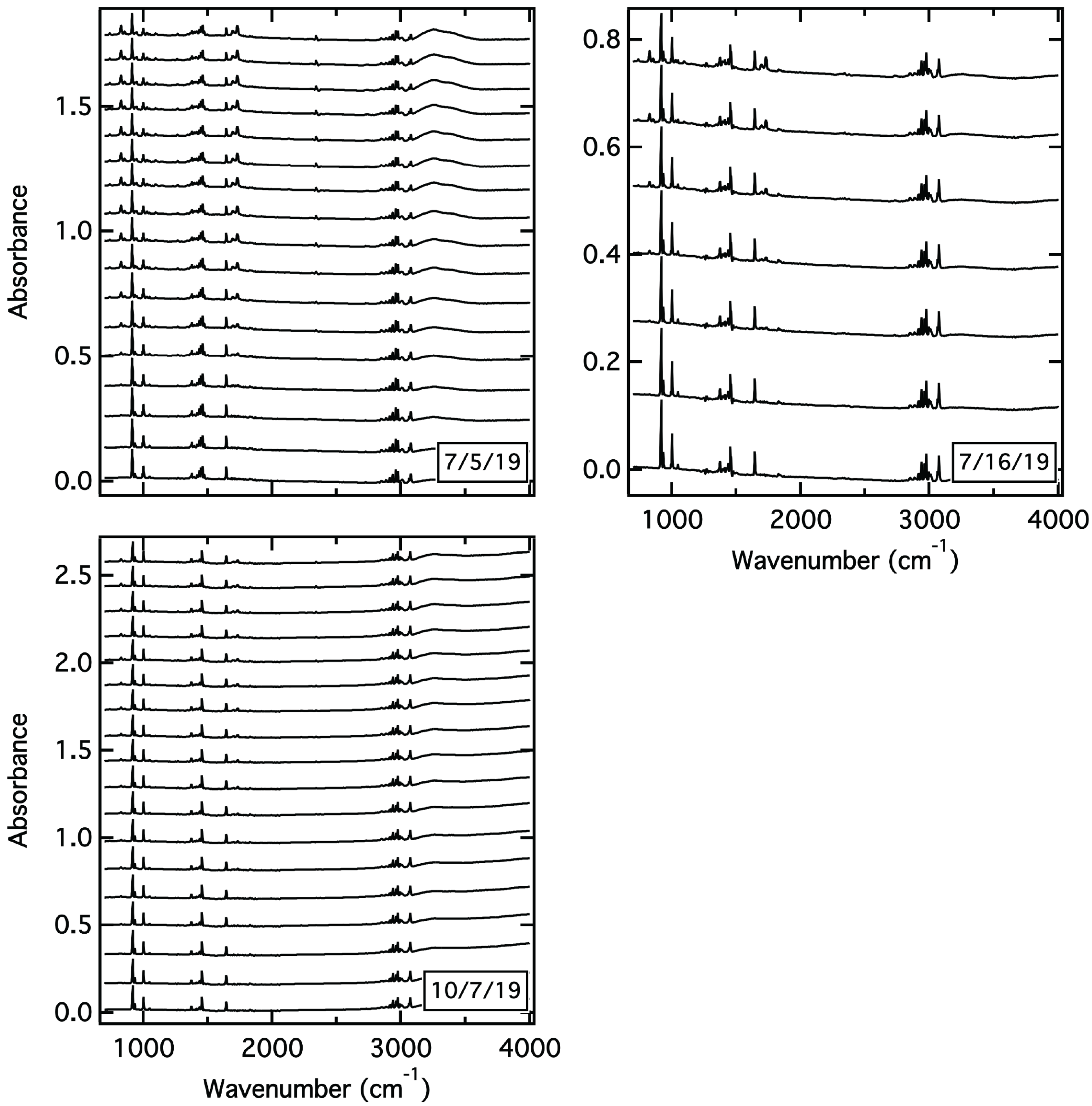

Figure A5.5: Raw RAIR spectrum for Figure 6.3 - 155-170 layers. As the propene film is exposed to O(^{3}P) at 54 K (deposited at 59 K), we track the loss of spectral intensity in the 914 - 919 cm^{-1} region (corresponding to the loss of propene's double bond). We use the change in intensity to calculate an initial rate of reactivity. This figure is for trials with propene films between 155 and 170 layers thick. (*Data files: 070519A.IR02-18, 071619A.IR02-08, 100719A.IR02-19*)

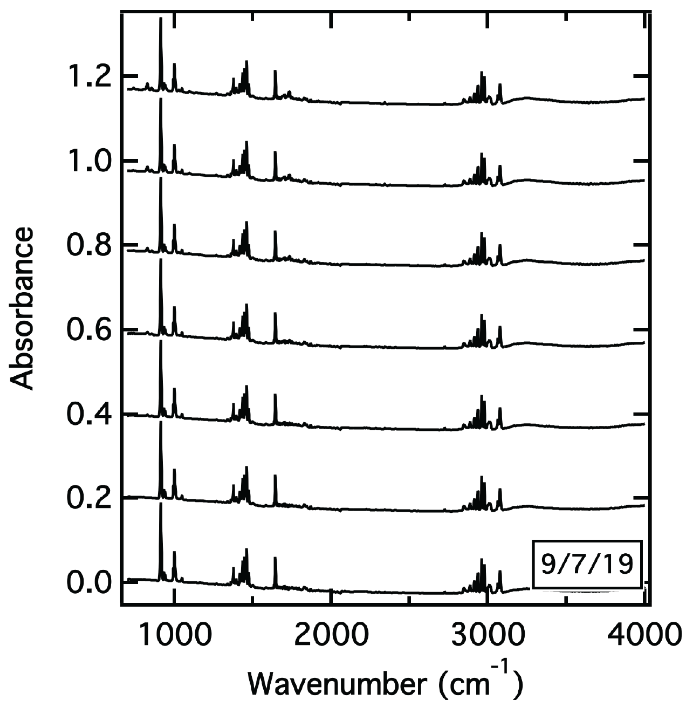

Figure A5.6: Raw RAIR spectrum for Figure 6.3 - 240 layers. As the propene film is exposed to O(^{3}P) at 54 K (deposited at 59 K), we track the loss of spectral intensity in the 914 - 919 cm^{-1} region (corresponding to the loss of propene's double bond). We use the change in intensity to calculate an initial rate of reactivity. This figure is for trials with propene films that are 240 layers thick.(*Data files: 090719A.IR02-08*)

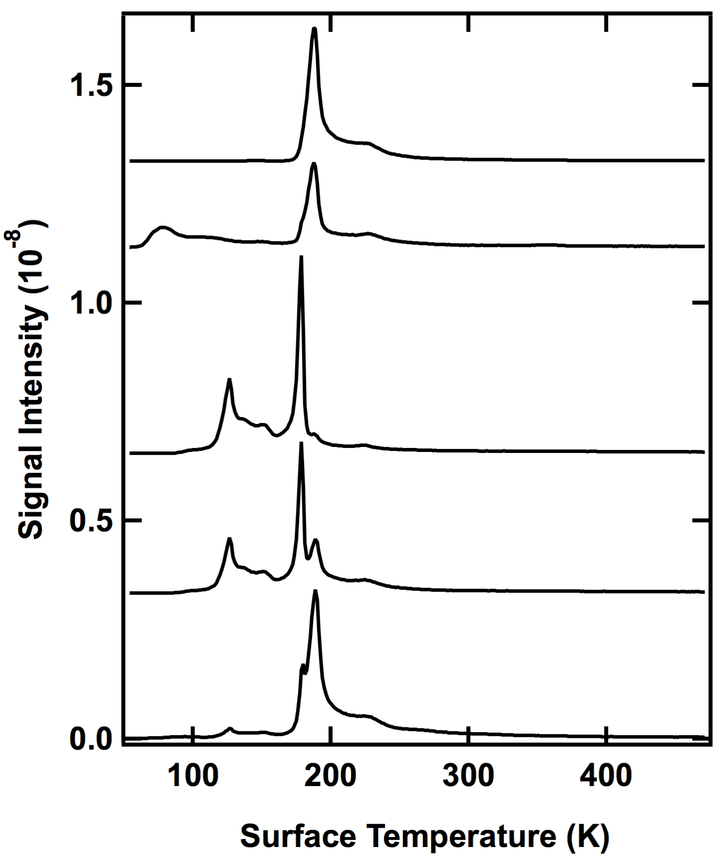

Figure A5.7: Raw TPD spectrum for Figure 6.5. After exposing at 46-layer propene film (see **Figure 6.2**) to 1 $\times 10^{18}$ atoms cm^{-2} $O(^3P)$, we track QMS signal as the surface is temperature is increased at a rate of $\approx$ 1 K s^{-1} (*Data file: 040219_TPD01.txt*)

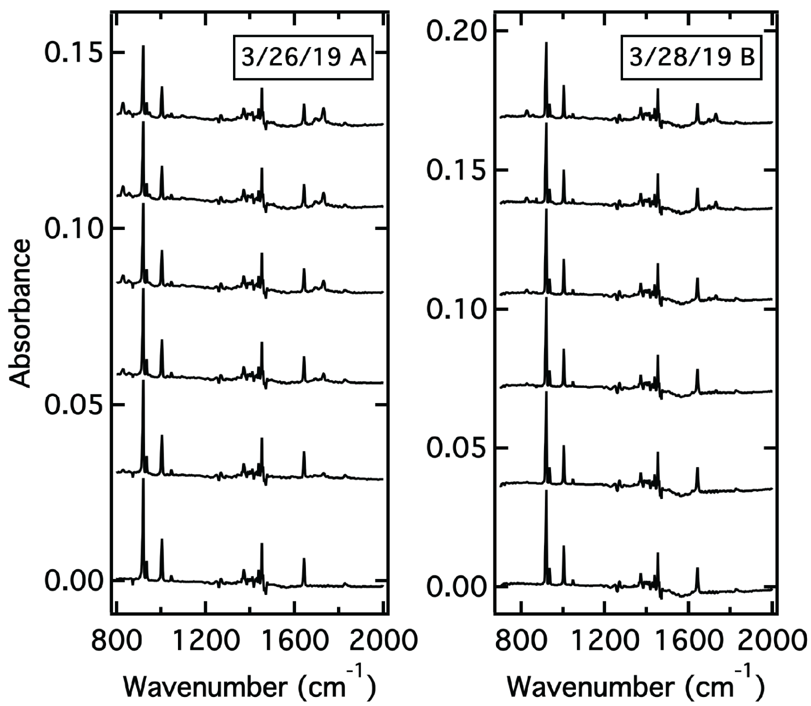

Figure A5.8: Raw RAIR spectrum for Figure 6.6 and 6.8 - 44 K. As the propene film is exposed to O(^{3}P), we track the loss of spectral intensity in the 914 - 919 cm^{-1} region (corresponding to the loss of propene's double bond, **Figure 6.6**). We also track the gain in spectral intensity for the 827 cm^{-1} and 1730 cm^{-1} peaks (corresponding to the appearance of propylene oxide and propanal respectively, **Figure 6.8**). All films are 30 layers thick, and the surface is held to 59 K during deposition and 44 K during exposure. (*Data files: 032619A.IR02-7 and 032819B.IR02-7*)

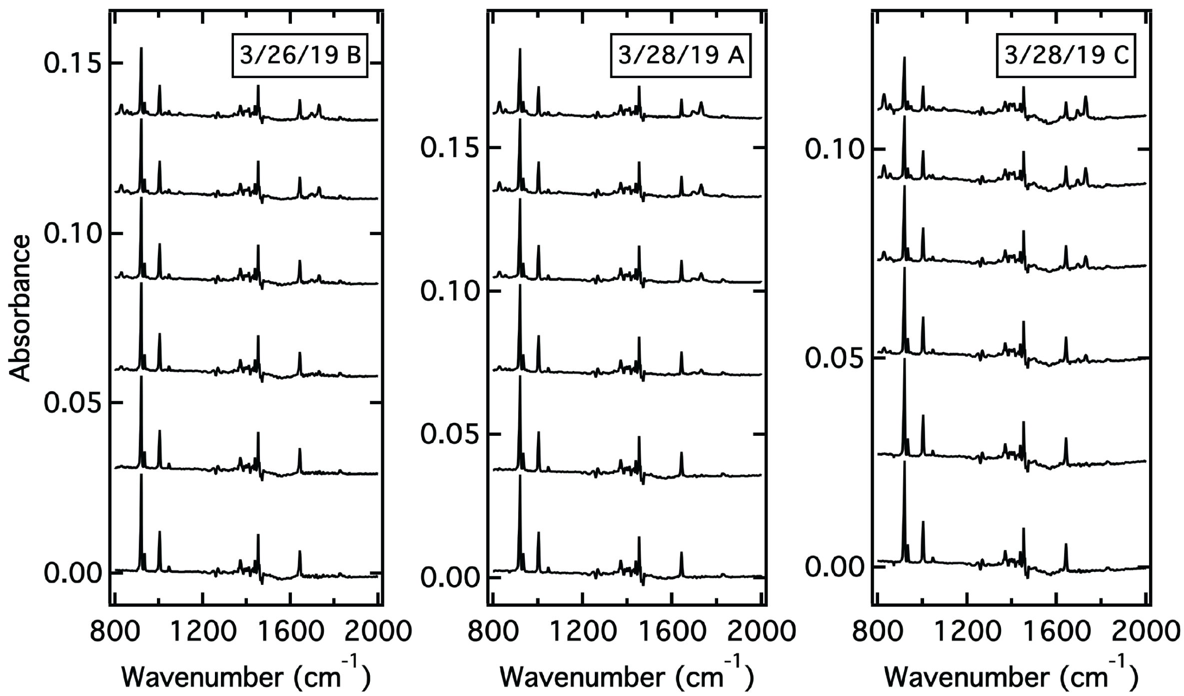

Figure A5.9: Raw RAIR spectrum for Figure 6.6 and 6.8 - 49 K. As the propene film is exposed to O(^{3}P), we track the loss of spectral intensity in the 914 - 919 cm^{-1} region (corresponding to the loss of propene's double bond, **Figure 6.6**). We also track the gain in spectral intensity for the 827 cm^{-1} and 1730 cm^{-1} peaks (corresponding to the appearance of propylene oxide and propanal respectively, **Figure 6.8**). All films are 30 layers thick, and the surface is held to 59 K during deposition and 49 K during exposure. (*Data files: 032619B.IR02-7, 032819A.IR02-7, and 032819C.IR02-7*)

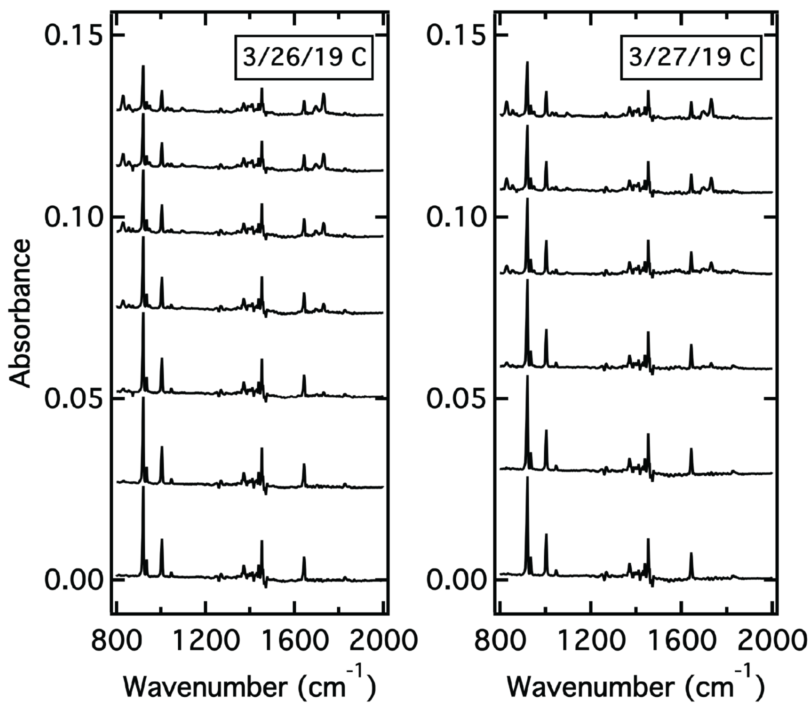

Figure A5.10: Raw RAIR spectrum for Figure 6.6 and 6.8 - 54 K. As the propene film is exposed to O(^{3}P), we track the loss of spectral intensity in the 914 - 919 cm^{-1} region (corresponding to the loss of propene's double bond, **Figure 6.6**). We also track the gain in spectral intensity for the 827 cm^{-1} and 1730 cm^{-1} peaks (corresponding to the appearance of propylene oxide and propanal respectively, **Figure 6.8**). All films are 30 layers thick, and the surface is held to 59 K during deposition and 54 K during exposure. (*Data files: 032619C.IR02-7 and 032819C.IR02-8*)

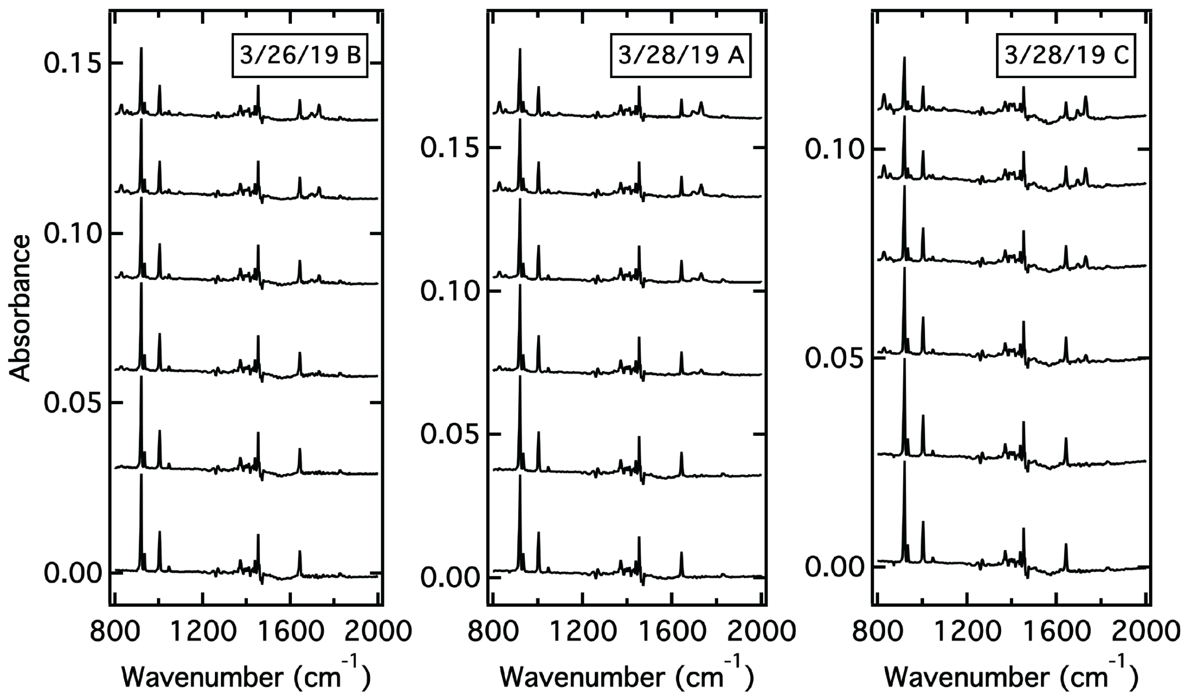

Figure A5.11: Raw RAIR spectrum for Figure 6.6 and 6.8 - 59 K. As the propene film is exposed to O(^{3}P), we track the loss of spectral intensity in the 914 - 919 cm^{-1} region (corresponding to the loss of propene's double bond, **Figure 6.6**). We also track the gain in spectral intensity for the 827 cm^{-1} and 1730 cm^{-1} peaks (corresponding to the appearance of propylene oxide and propanal respectively, **Figure 6.8**). All films are 30 layers thick, and the surface is held to 59 K during deposition and 59 K during exposure. (*Data files: 032619D.IR02-8, 032719A.IR02-6, and 040119A.IR02-7*)

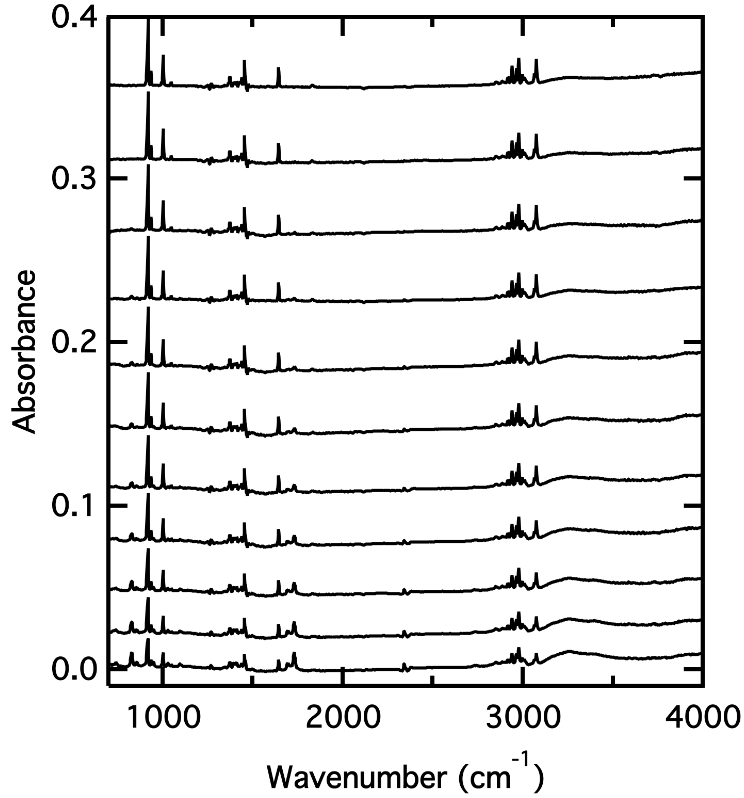

Figure A5.12: Raw RAIR spectrum for Figure 6.9. As a 46-layer propene film is exposed to O(^{3}P), we track changes and loss of spectral intensity of the CH peaks located at 2939, 2964, 2977, and 3075 cm^{-1}.(*Data files: 053119.IR03-13*)

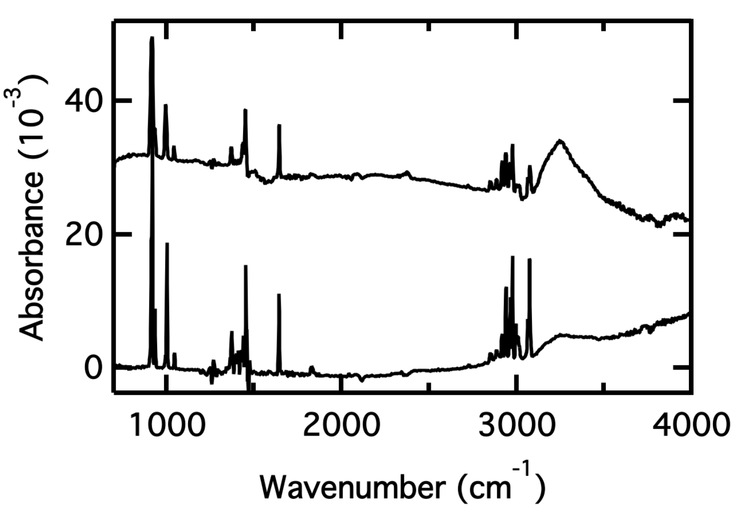

Figure A5.13: Raw RAIR spectrum for Figure 6.10. We collected spectra at 49 K of two "pristine", and 46-layer propene films: one deposited with the crystal held to 59 K, and one with the crystal at 44 K. (*Data files: 053019A.IR02 (44 K, top) and 053119.IR02 (59 K, bottom)*)

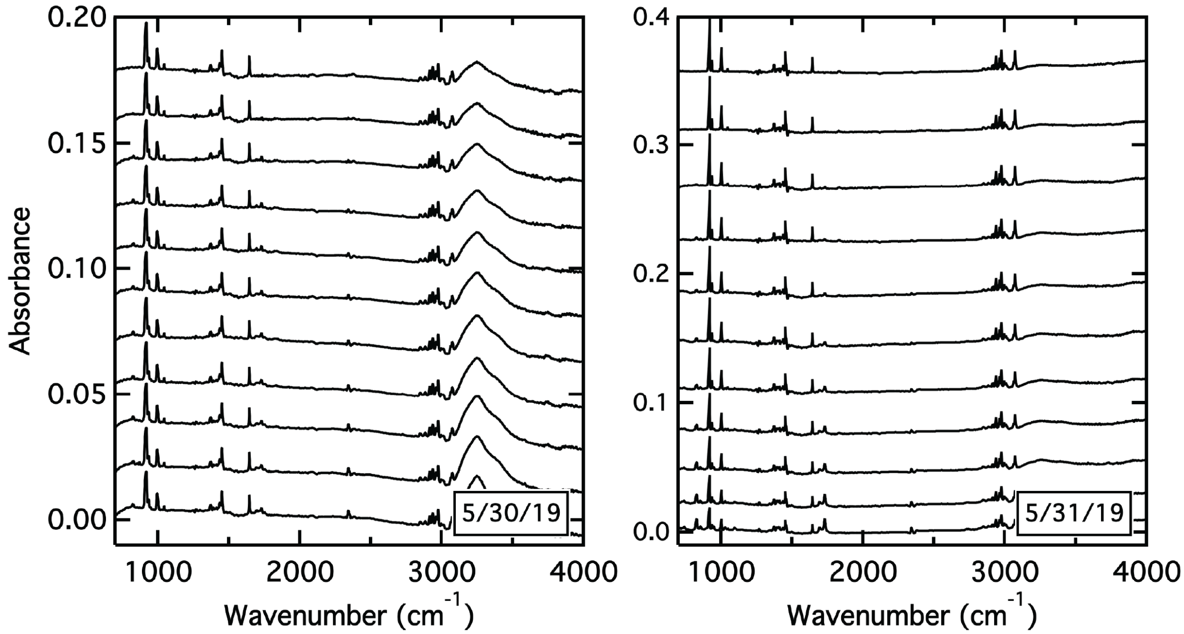

Figure A5.14: Raw RAIR spectrum for Figure 6.11. We collected spectra at regular time intervals as two 46-layer propene films are exposed to $O(^3P)$ at 49 K. We track the loss of spectral intensity in the 914 - 919 cm^{-1} region (corresponding to the loss of propene's double bond). One film was deposited with the crystal held to 59 K, and one with the crystal at 44 K. (*Data files: 053019A.IR02-12 (44 K) and 053119.IR03-13 (59 K)*)

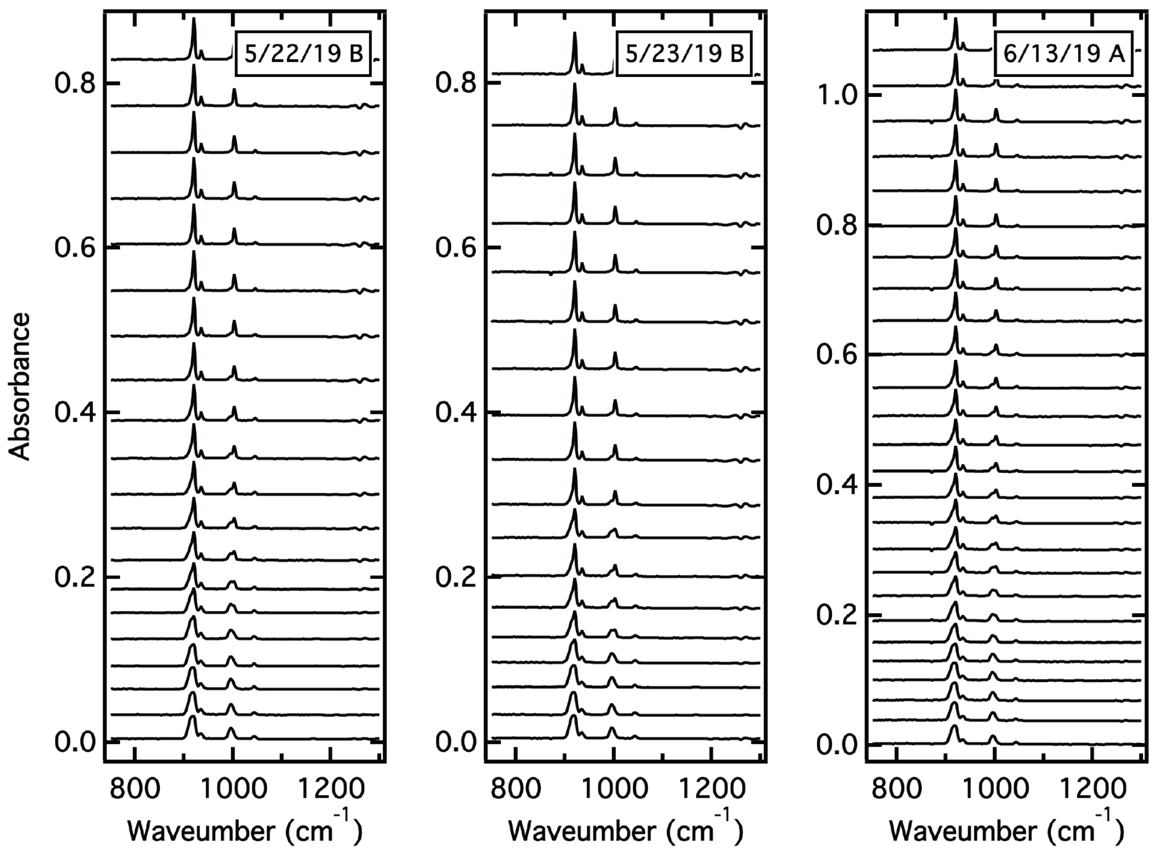

Figure A5.15: Raw RAIR spectrum for Figure 6.12 - 50 K. We collected spectra at regular time intervals as 24-layer propene films (deposited at 44 K) are isothermally annealed to 50 K. (*Data files: 052219B.IR02-21, 052319B.IR02-19, and 061319A.IR02-27*)

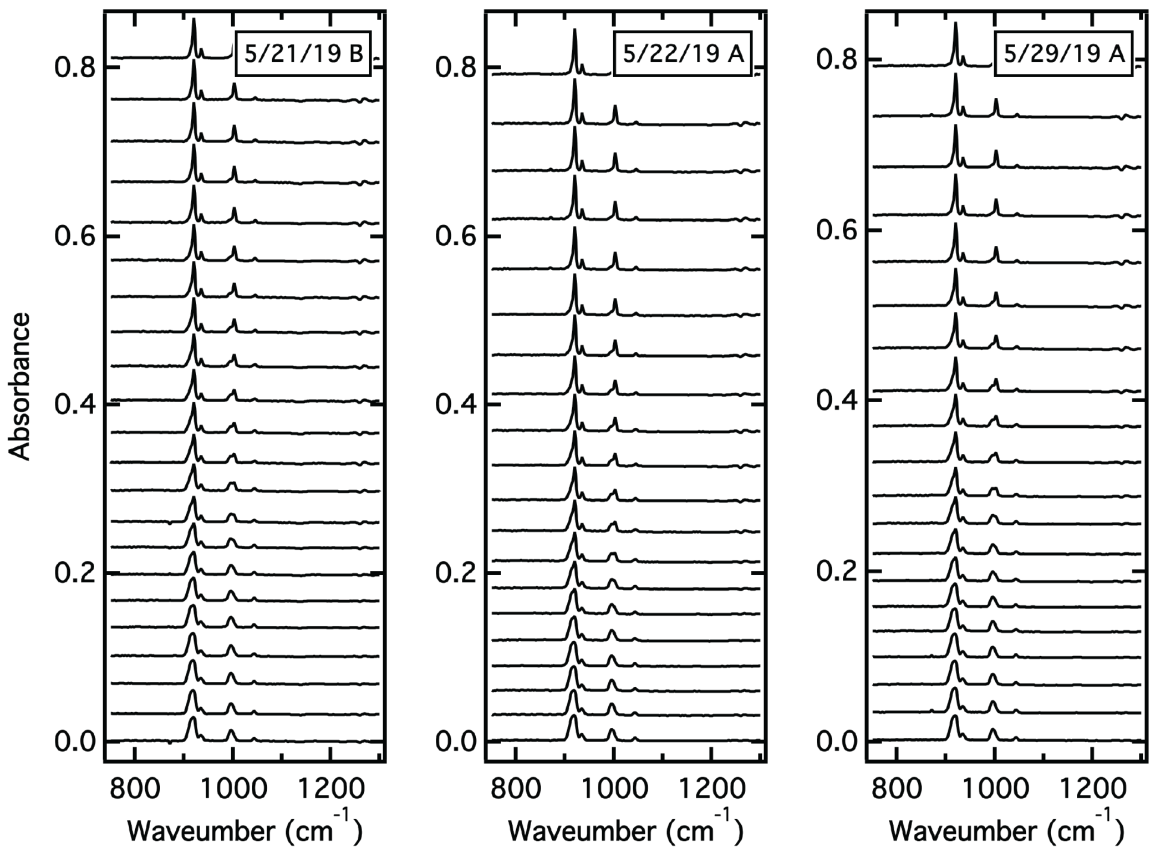

Figure A5.16: Raw RAIR spectrum for Figure 6.12 - 51 K. We collected spectra at regular time intervals as 24-layer propene films (deposited at 44 K) are isothermally annealed to 51 K.(*Data files: 052119B.IR02-24, 052219A.IR02-21, and 052919A.IR02-21*)

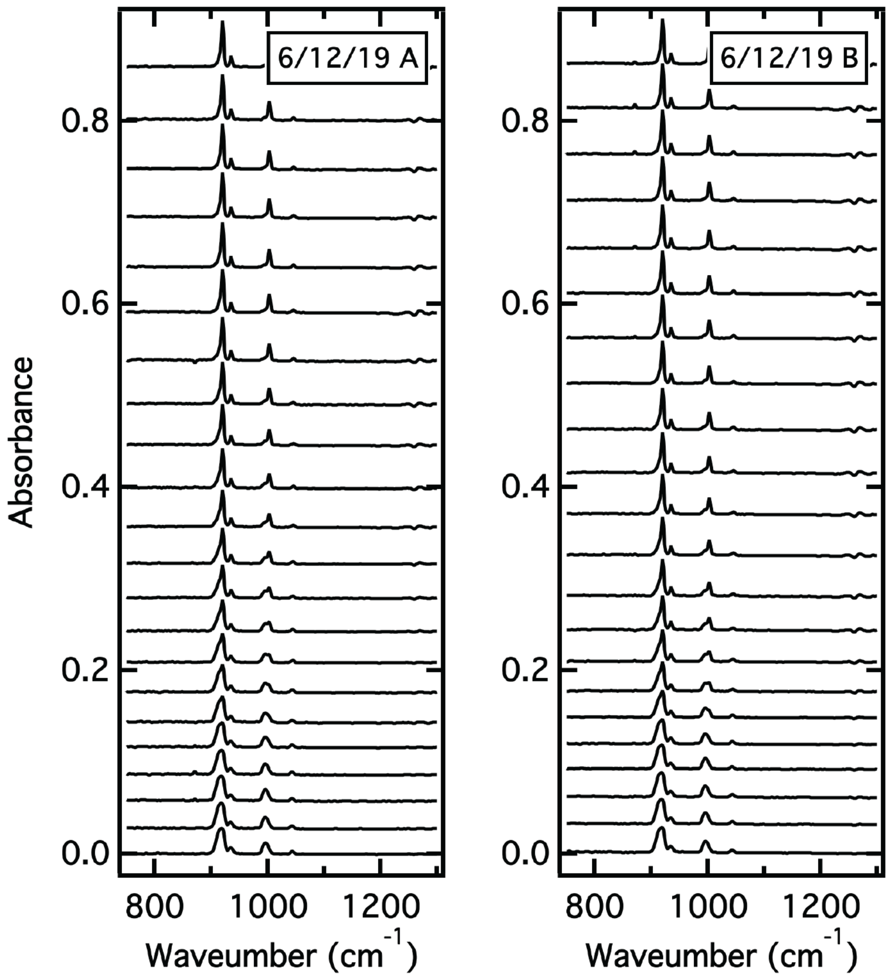

Figure A5.17: Raw RAIR spectrum for Figure 6.12 - 51.5 K. We collected spectra at regular time intervals as 24-layer propene films (deposited at 44 K) are isothermally annealed to 51.5 K. (*Data files: 061219A.IR02-23 and 061219A.IR02-23*)

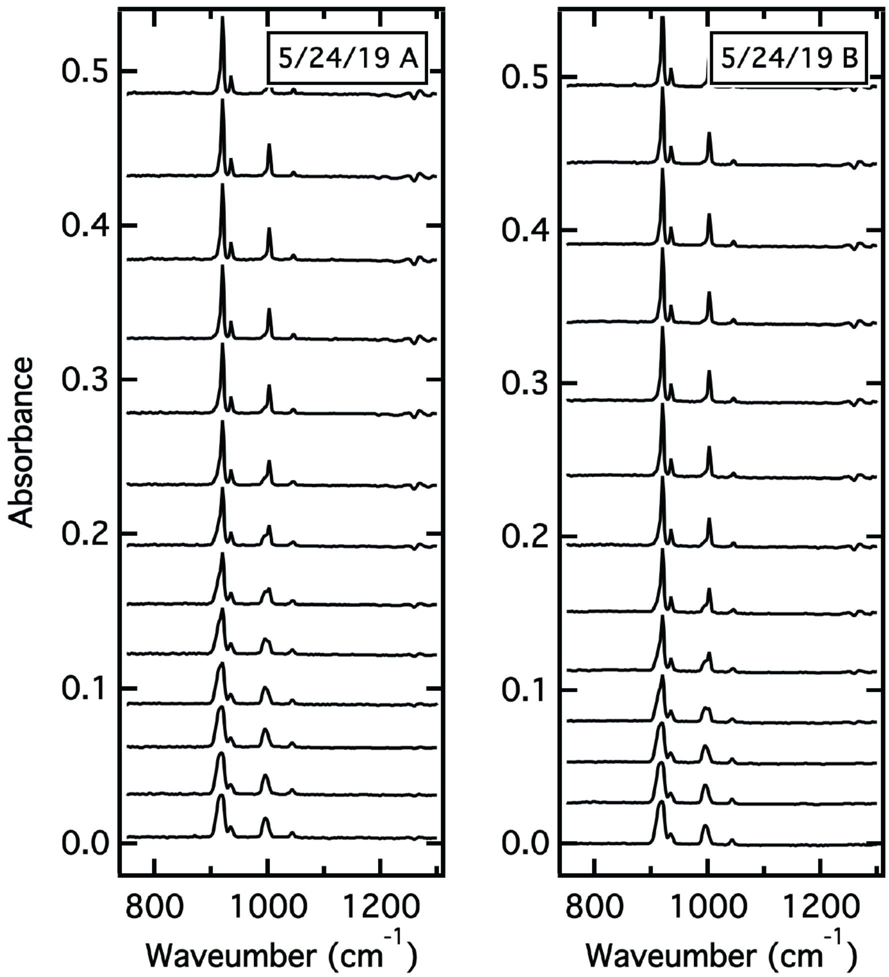

Figure A5.18: Raw RAIR spectrum for Figure 6.12 - 52 K. We collected spectra at regular time intervals as 24-layer propene films (deposited at 44 K) are isothermally annealed to 52 K. (*Data files: 052419A.IR02-14 and 052419B.IR02-14*)

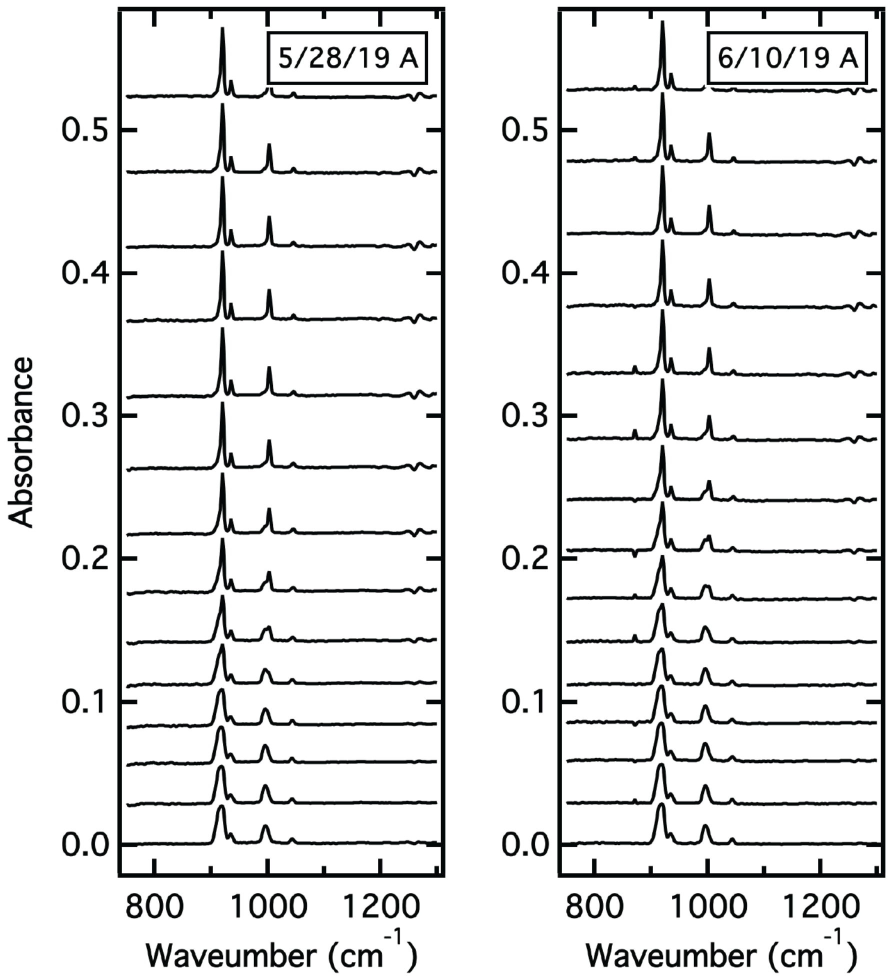

Figure A5.19: Raw RAIR spectrum for Figure 6.12 - 53 K. We collected spectra at regular time intervals as 24-layer propene films (deposited at 44 K) are isothermally annealed to 53 K. (*Data files: 052819A.IR02-18 and 061019A.IR02-16*)

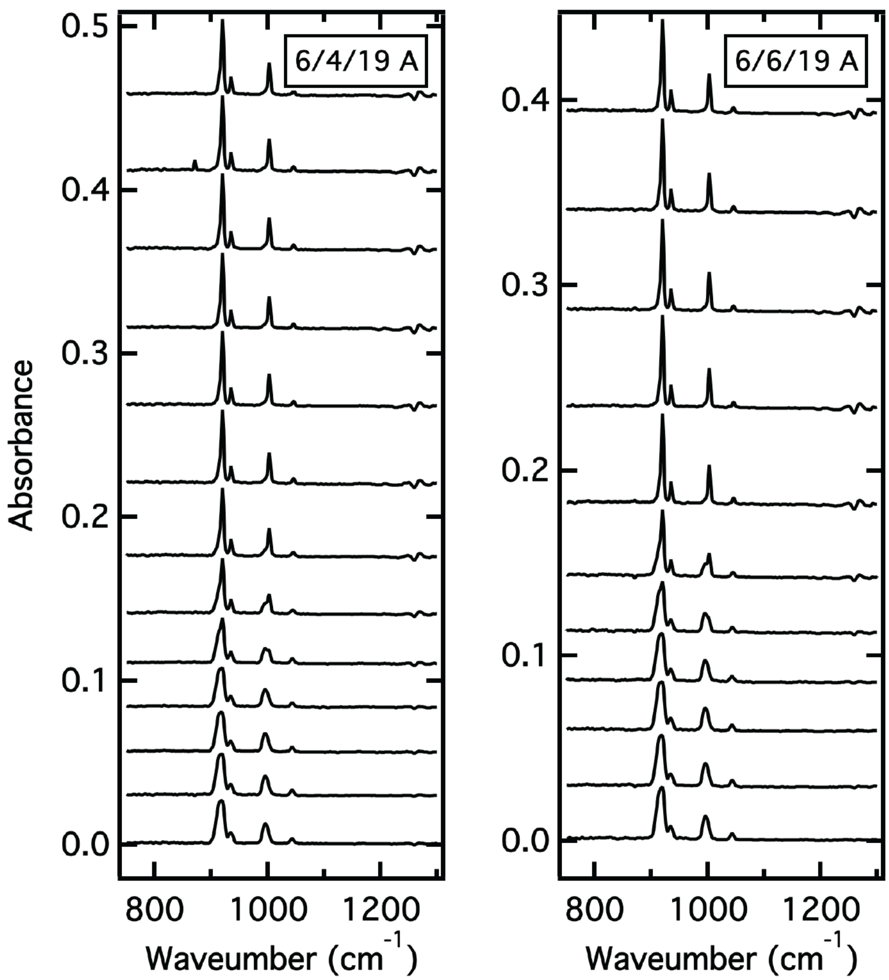

Figure A5.20: Raw RAIR spectrum for Figure 6.12 - 54 K. We collected spectra at regular time intervals as 24-layer propene films (deposited at 44 K) are isothermally annealed to 54 K. (*Data files: 060419A.IR02-14 and 060619A.IR02-14*)

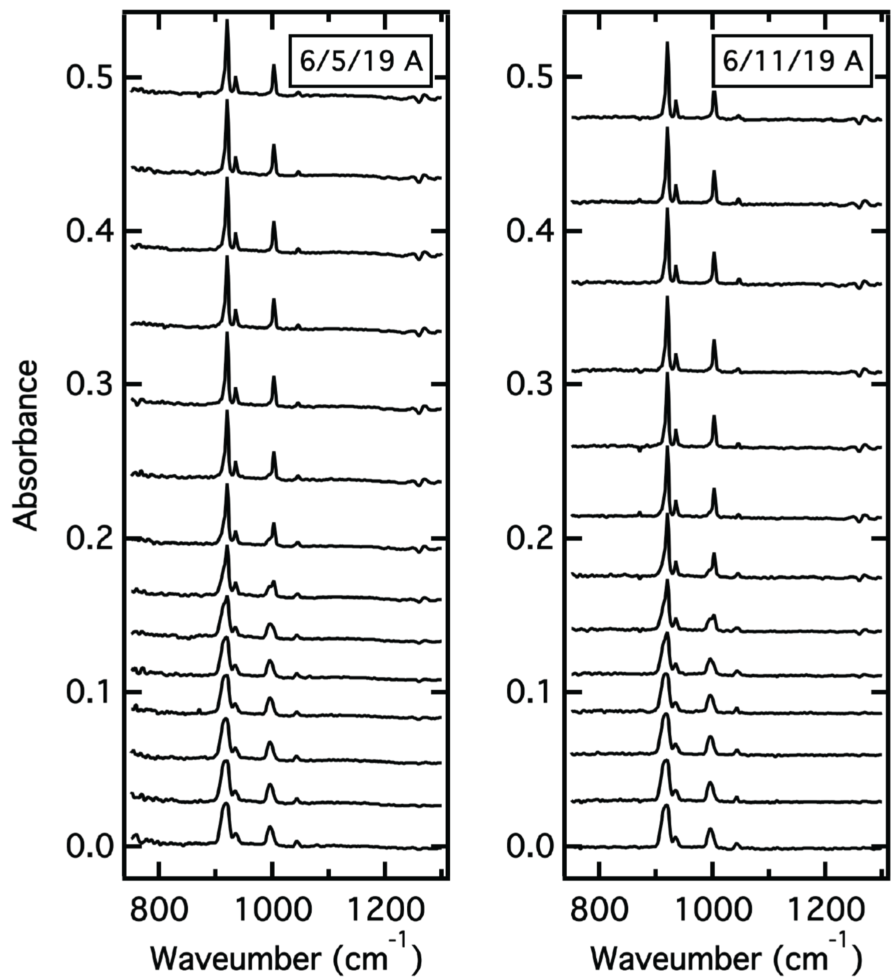

Figure A5.21: Raw RAIR spectrum for Figure 6.12 - 55 K. We collected spectra at regular time intervals as 24-layer propene films (deposited at 44 K) are isothermally annealed to 55 K.(*Data files: 060519A.IR02-15 and 061119A.IR02-14*)

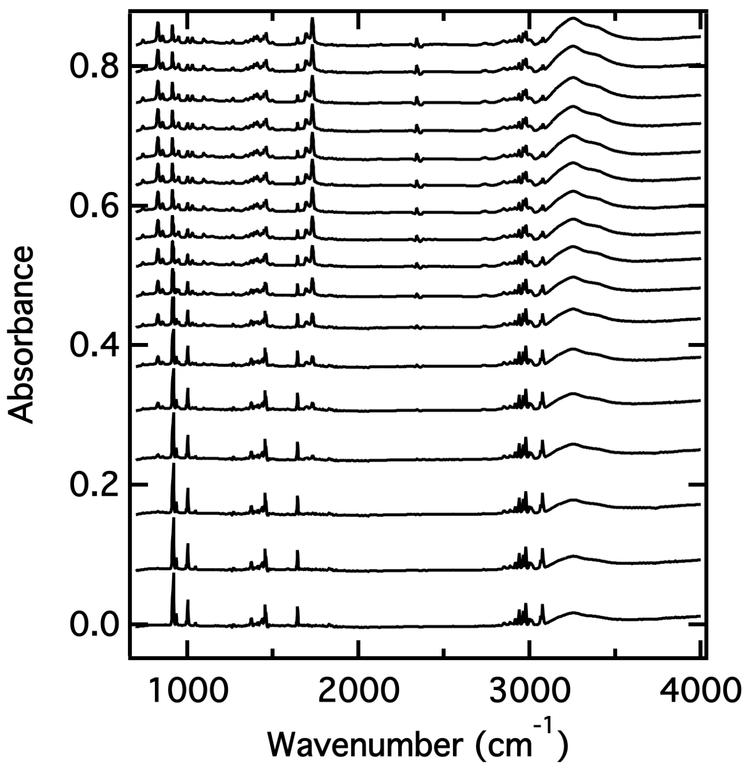

Figure A5.22: Raw RAIR spectrum for Figure 6.13. caption. (*Data files: 051719A.IR04-20*)

A6 Rapid Laser-Induced Temperature Jump Decomposition of the Nerve Agent Simulant Diisopropyl Methylphosphonate under Atmospheric Conditions (Chapter 7)

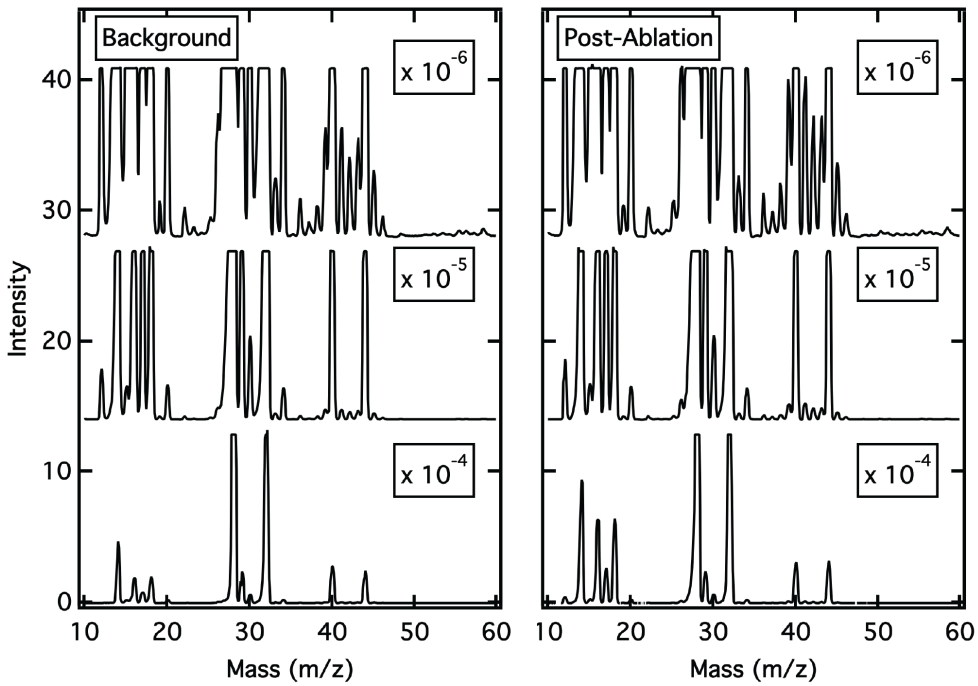

Figure A6.1: Raw MS spectrum for Figure 7.3. In order to get a full mass sweep over masses from 10 to 60 with proper resolution, we compile three separate spectra collected with three different magnifications ($\times10^{-4}$, $\times10^{-5}$, $\times10^{-6}$ Torr) into a single scan by scaling each scan to the same relative order of magnitude. Following DIMP ablation, we collect and compile three more spectra to get a full mass scan of the gaseous products. (*Data files: 073118F01-F03 (background), 073118F04-F06 (post-ablation)*)

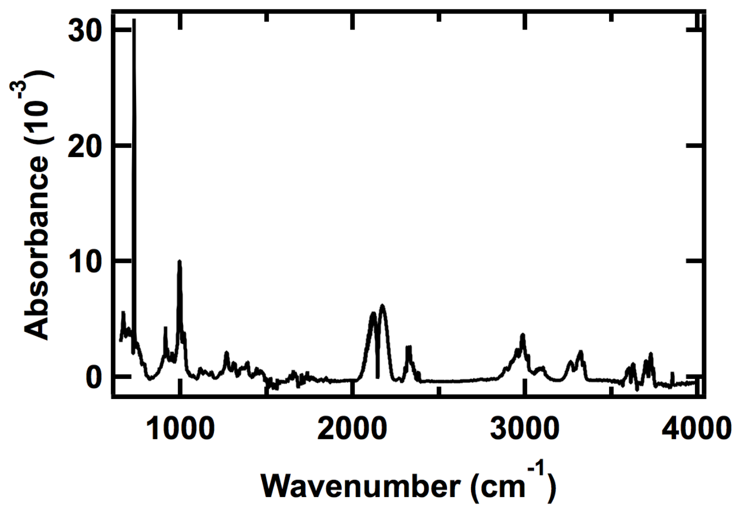

Figure A6.2: Raw FTIR spectrum for Figure 7.4. Following laser ablation under atmospheric conditions, gaseous products are transferred via a leak valve to a purged cell with ZnSe windows for FT-IR spectra collection. This representative spectra is for a DIMP sample ablated to 2720 K. (*Data file: 072718A.IR03*)

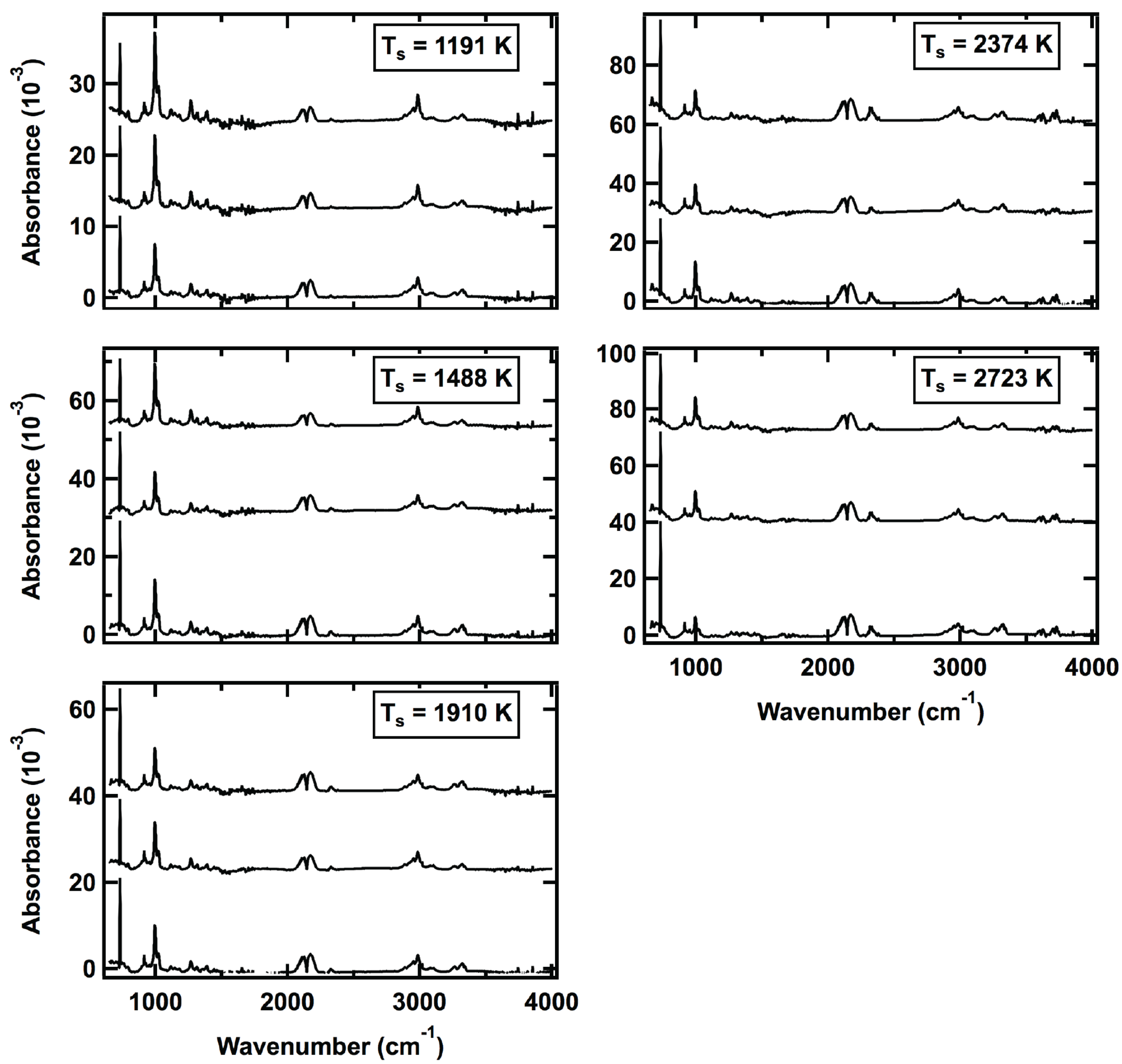

Figure A6.3: Raw FTIR spectra for Figure 7.5. We ablated DIMP at five different temperatures and collected FTIR spectra of the gaseous products. **Figure 7.5a** shows one spectra from each temperature, while **Figure 7.5b** contains the average of the integrated areas (propene's $=CH_2$ wagging mode and ethylene's bending mode) plotted vs temperature. (*Data files: 072518A.IR02-04 (1191 K), 072518A.IR05-07 (1488 K), 072618A.IR02-03 and 072718B.IR01 (1910 K), 0727618A.IR05-06 and 072718B.IR02 (2374 K), 072718A.IR01-03 (2723 K)*)

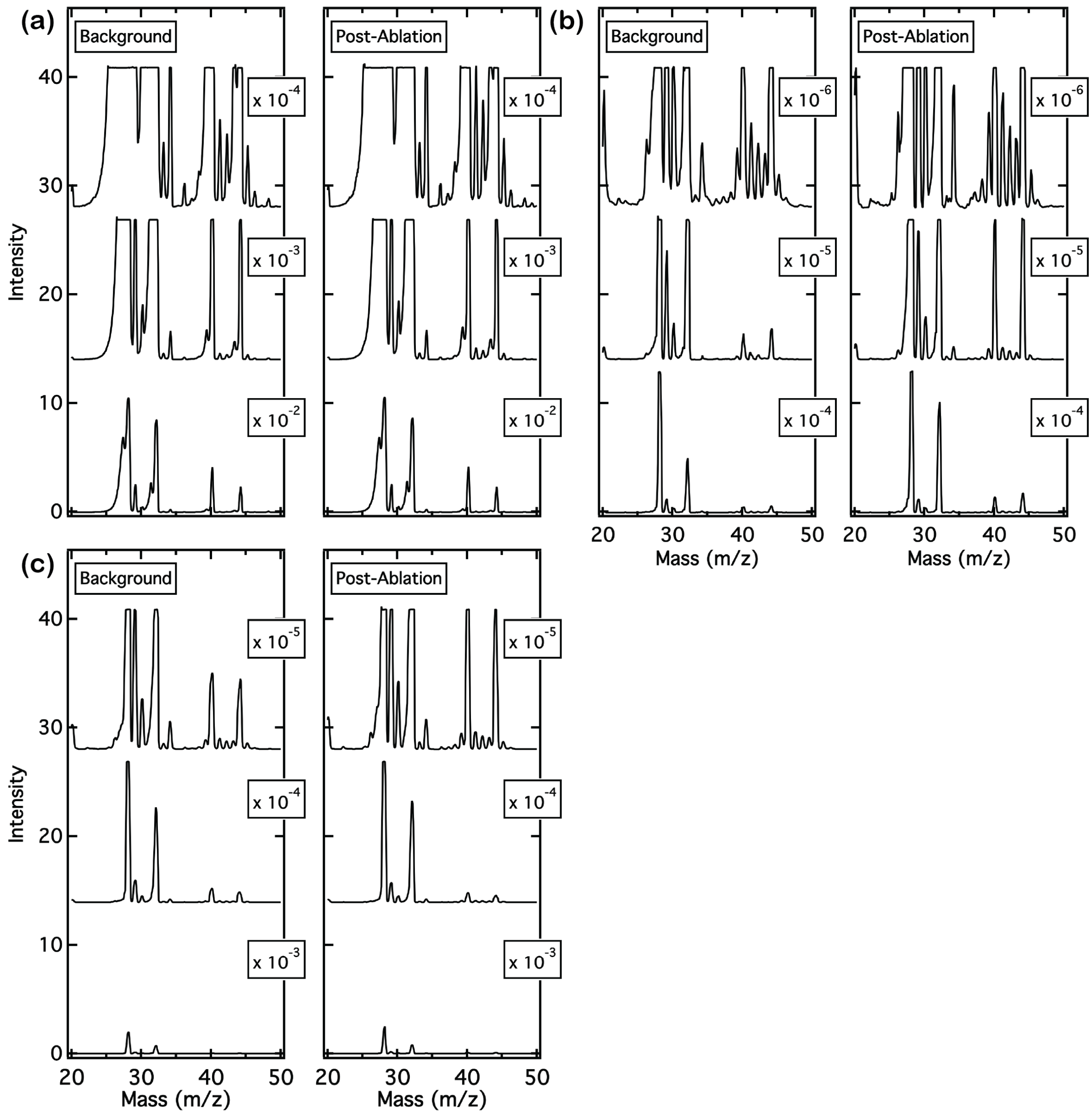

Figure A6.4: Raw MS for Figure 7.6 -1440 K. We ablated DIMP at three different temperatures and collected mass spectra of the associated gaseous products. **Figure 7.6a** contains the least square fit to the *080318B* data and the 1440 K data points in **Figure 7.6b** are the average amounts of propene and acetylene/ethylene present in the spectra at this ablation temperature. (*Data files: 061318S01-06 (a), 080218E01-06 (b), 080318B01-06 (c)*)

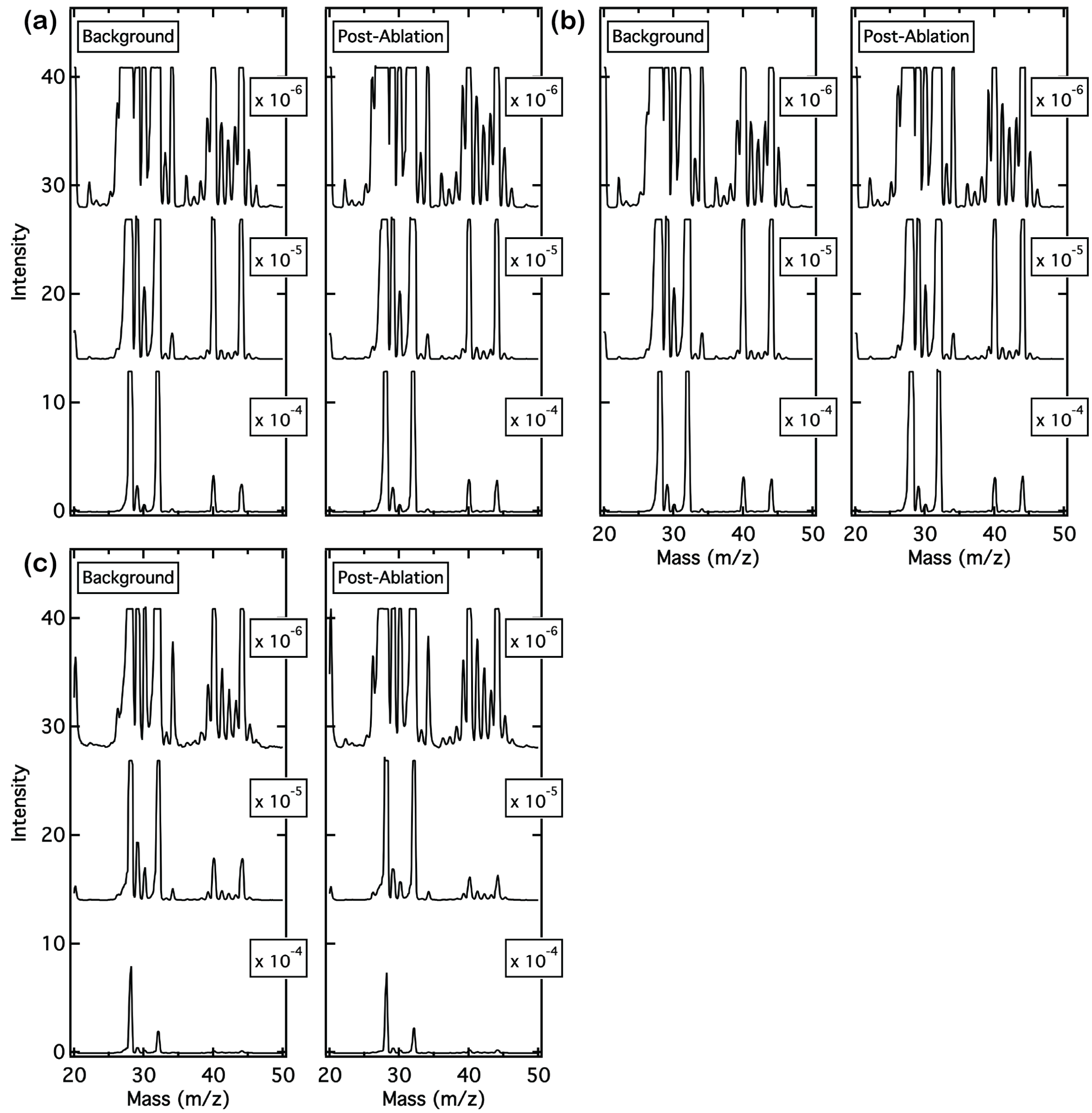

Figure A6.5: Raw MS for Figure 7.6 - 2140 K. We ablated DIMP at three different temperatures and collected mass spectra of the associated gaseous products. **Figure 7.6a** contains the least square fit to the *073118G* data and the 2140 K data points in **Figure 7.6b** are the average amounts of propene and acetylene/ethylene present in the spectra at this ablation temperature. (*Data files: 073118G01-06 (a), 073118H01-06 (b), 080218D01-06 (c)*)

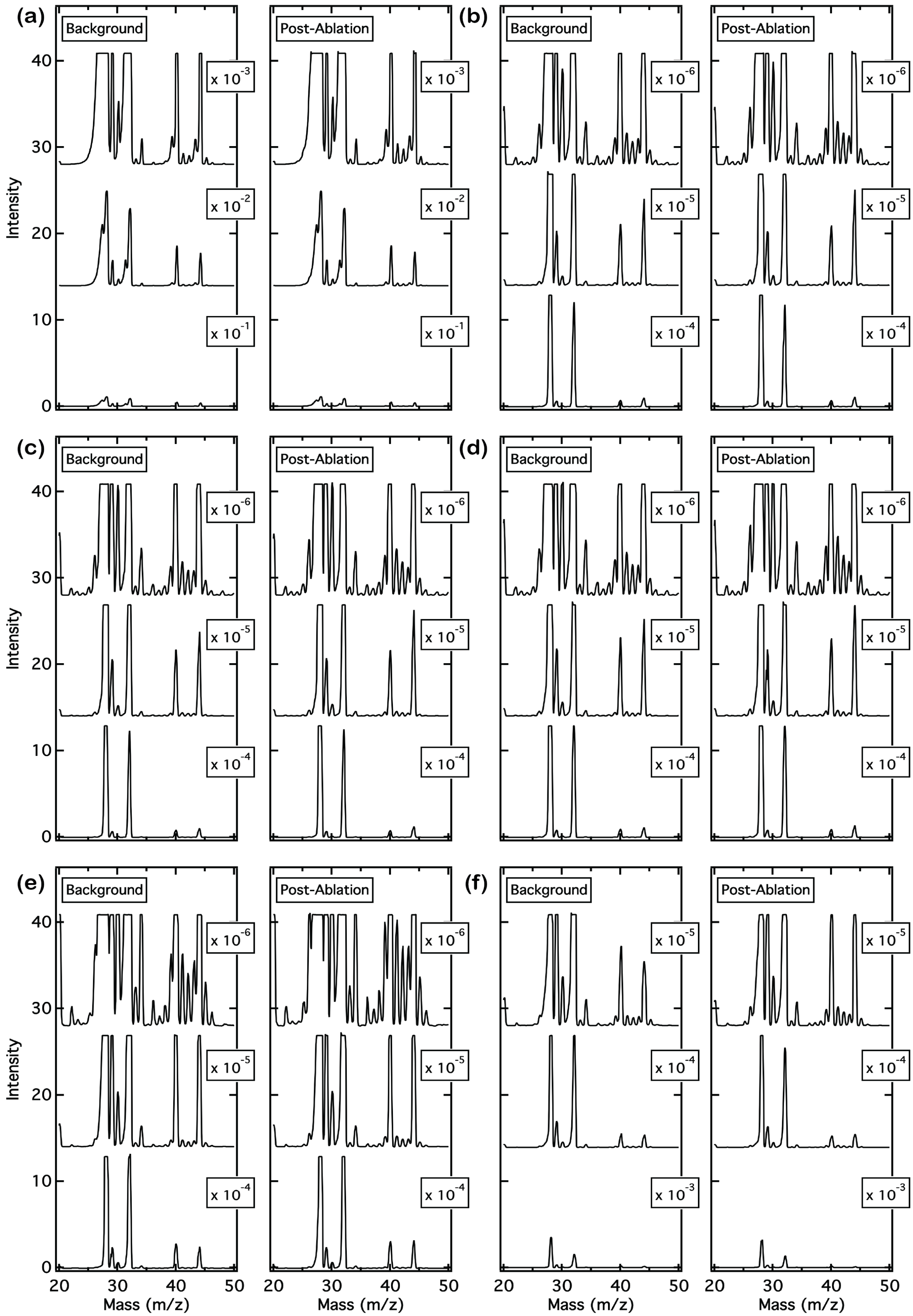
(a)
Background
Post-Ablation
(b)
Background
Post-Ablation
(c)
Background
Post-Ablation
(d)
Background
Post-Ablation
(e)
Background
Post-Ablation
(f)
Background
Post-Ablation
Intensity
Mass (m/z)
x 10^-1
x 10^-2
x 10^-3
x 10^-4
x 10^-5
x 10^-6

Figure A6.6: Raw MS for Figure 7.6 - 2830 K and Figure 7.7 - 1×10^{-6} Torr. We ablated DIMP at three different temperatures and collected mass spectra of the associated gaseous products. **Figure 7.6a** contains the least square fit to the *073118B* data and the 2830 K data points in **Figure 7.6b** are the average amounts of propene and acetylene/ethylene present in the spectra at this ablation temperature. Note: This data is also the atmospheric data in **Figure7.7** (*Data files: 061319S09-15 (a), 072718B01-06 (b), 072718C01-06 (c), 072718D01-06 (d), 073118F01-06 (e), 080318A01-06 (f)*)

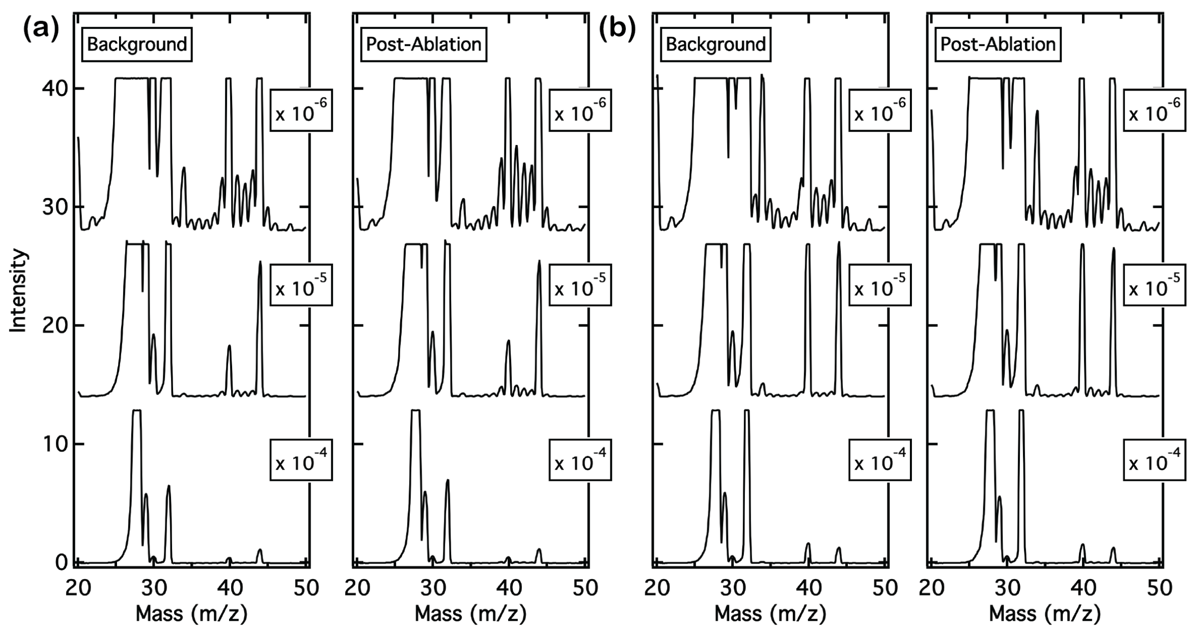

Figure A6.7: Raw MS for Figure 7.7 - 2×10^{-7}. We ablated DIMP at three atmospheric oxygen pressures and collected mass spectra of the associated gaseous products. **Figure 7.7a** contains the least square fit to the *081418B* data and the 2×10^{-7} Torr data points in **Figure 7.7b** are the average amounts of propene, acetone, and isopropyl alcohol present in the spectra under these conditions. (*Data files: 061318F01-06 (a), 081418B01-06 (b)*)

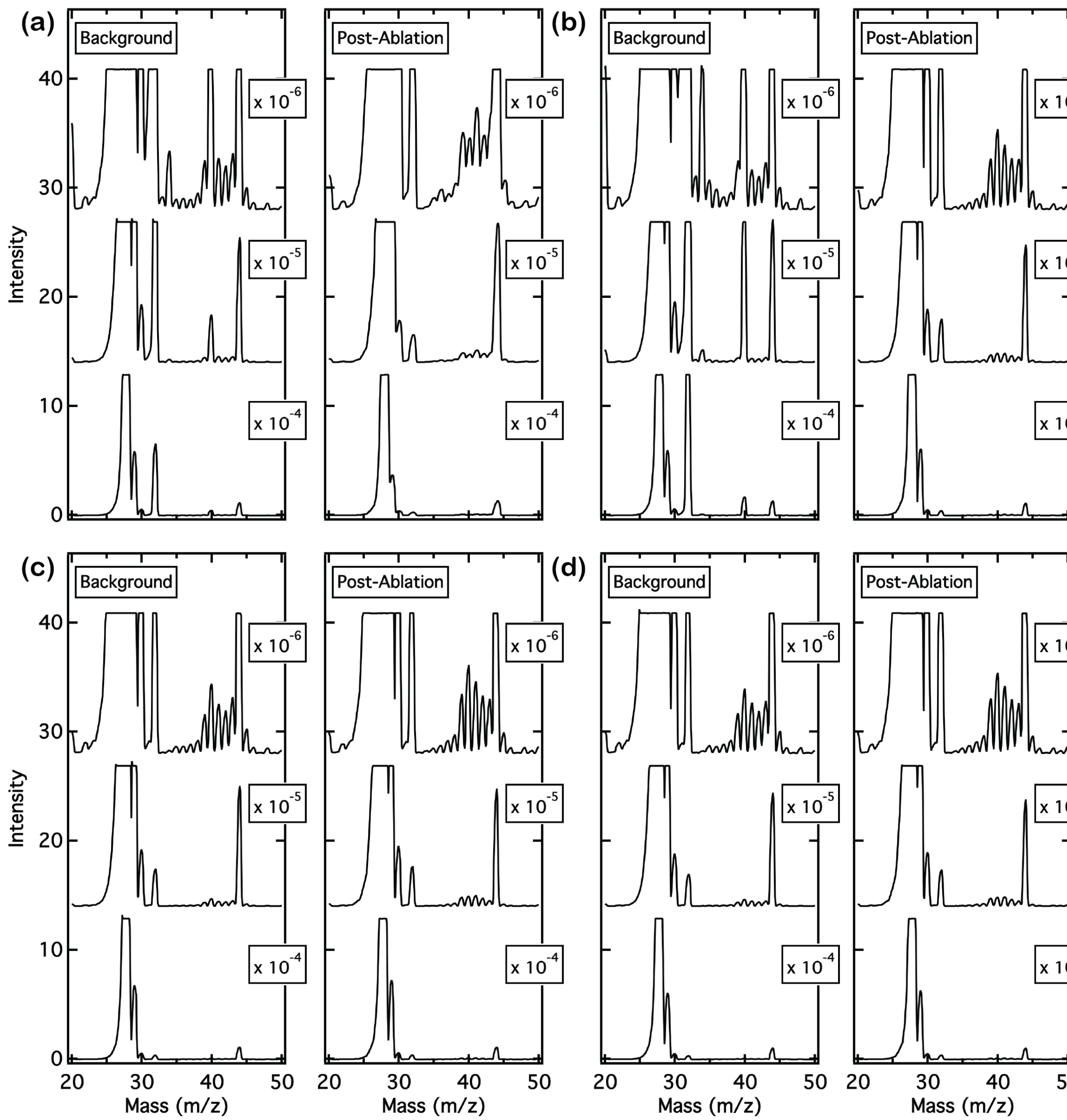

Figure A6.8: Raw MS for Figure 7.7 - 3×10^{-9}. We ablated DIMP at three atmospheric oxygen pressures and collected mass spectra of the associated gaseous products. **Figure 7.7a** contains the least square fit to the *08098H* data and the 3×10^{-9} Torr data points in **Figure 7.7b** are the average amounts of propene, acetone, and isopropyl alcohol present in the spectra under these conditions. (*Data files: 080918H01-06 (a), 081318C01-06 (b), 081318D01-06 (c), 081318E01-06 (d)*)

A7 Copyright Attribution

Chapter 3 is adapted with permission from Thompson, R. S.; **Brann, M. R.**; Sibener, S. J. Sticking Probability of High-Energy Methane on Crystalline, Amorphous, and Porous Amorphous Ice Films. *The Journal of Physical Chemistry C* **2019**, *123*, 17855–17863. Copyright 2019 American Chemical Society.[113]

Chapter 4 is adapted with permission from **Brann, M. R.**; Hansknecht, S.P.; Muir, M.; Sibener, S. J. Acetone-Water Interactions in Crystalline and Amorpous Ice Environments. *The Journal of Physical Chemistry A*. **2022** *127*, 2729–2738. Copyright 2022 American Chemical Society.[333]

Chapter 5 is adapted with permission from **Brann, M. R.**; Hansknecht, S.P.; Ma, X.; Sibener, S. J. Differential Condensation of Methane Isotopologues Leading to Isotopic Enrichment Under Non-equilibrium Gas-Surface Collision Conditions. *The Journal of Physical Chemistry A*. **2021** *125*, 9405-9413. Copyright 2021 American Chemical Society.[334]

Chapter 6 is adapted with permission from **Brann, M. R.**; Thompson, R. S.; Sibener, S. J. Reaction Kinetics and Influence of Film Morphology on the Oxidation of Propene Thin Films by O(^{3}P) Atomic Oxygen. *The Journal of Physical Chemistry C*. **2020** *124*, 7205-7215. Copyright 2020 American Chemical Society.[135]

Chapter 7 is adapted with permission from Thompson, R. S.*; **Brann, M. R.***; Purdy, E. H.; Graham, J. D.; McMillan, A. A.; Sibener, S. J. Rapid Laser-Induced Temperature Jump Decomposition of the Nerve Agent Simulant Diisopropyl Methylphosphonate under Atmospheric Conditions. *The Journal of Physical Chemistry C* **2019**, *123*, 21564–21570. Copyright 2019 American Chemical Society.[335]

RST and* ***MRB* *are co-first authors of this manuscript*

References

(1) Langlois, G. G.; Thompson, R. S.; Li, W.; Sibener, S. J. Oxidation, Destruction, and Persistence of Multilayer Dimethyl Methylphosphonate Films during Exposure to O(^{3}P) Atomic Oxygen. *The Journal of Physical Chemistry C* **2016**, *120*, 16863–16870.

(2) Thompson, R. S.; Langlois, G. G.; Sibener, S. J. Oxidative Destruction of Multilayer Diisopropyl Methylphosphonate Films by O(^{3}P) Atomic Oxygen. *The Journal of Physical Chemistry B* **2018**, *122*, 455–463.

(3) Suëtaka, W.; Yates, J. T. In *Surface Infrared and Raman Spectroscopy*; Springer US: Boston, MA, 1995, pp 13–116.

(4) Christy, A. A.; Ozaki, Y.; Gregoriou, V. G. In *Modern Fourier Transform Infrared Spectroscopy*, 1st ed.; Elsevier Science: New York, NY, 2001; Chapter 7, pp 143–147.

(5) Pemble, M. E.; Gardner, P. In *Surface Analysis– The Principal Techniques*; John Wiley & Sons, Ltd: Chichester, UK, 2009, pp 333–390.

(6) Greenler, R. G. Reflection Method for Obtaining the Infrared Spectrum of a Thin Layer on a Metal Surface. *The Journal of Chemical Physics* **1963**, *50*, 1963–1968.

(7) Greenler, R. G. Infrared Study of Adsorbed Molecules on Metal Surfaces by Reflection Techniques. *The Journal of Chemical Physics* **1966**, *44*, 310–315.

(8) Park, R. L.; Lagally, M. G. In *Solid State Physics: Surfaces*; Academic Press: 1985, p 543.

(9) Griffiths, D. J. In *Introduction to Electrodynamics*; Prentice-Hall: Englewood Cliffs, NJ, 2012, p 599.

(10) Greenler, R. G. In *Vibrations at Surfaces*; Springer US: Boston, MA, 1982, pp 255–264.

(11) Walsh, J. J.; Forster, R. J.; Keyes, T. E. In *Springer Handbook of Electrochemical Energy*; Springer: Berlin, Heidelberg, 2017, pp 365–421.

(12) Aroca, R. In *Surface-Enhanced Vibrational Spectroscopy*; John Wiley & Sons, Ltd: Hoboken, NJ, 2007, pp 35–71.

(13) Urban, M. W., *Vibrational Spectroscopy of Molecules and Macromolecules on Surfaces*; Wiley: New York, NY, 1993, p 384.

(14) Moulder, J. F.; Stickle, W. F.; Sobol, P. E.; Bomben, K. D. In *Handbook of X-ray Photoelectron Spectroscopy*, Chastain, J., Ed.; Perkin-Elmer Corporation: Eden Prairie, MN, 1981, pp 1–29.

(15) Ratner, B. D.; Castner, D. G. In *Surface Analysis – The Principal Techniques*, Vickerman, J. C., Gilmore, I. S., Eds.; John Wiley & Sons, Ltd: Chichester, UK, 2009, pp 47–112.

(16) B. Vincent Crist Handbooks of Monochromatic XPS Spectra Volume 1 - The Elements and Native Oxides. *Handbook of The Elements and Native Oxides* **1999**, *1*, 1–43.

(17) King, D. A.; Wells, M. G. Molecular beam investigation of adsorption kinetics on bulk metal targets: Nitrogen on tungsten. *Surface Science* **1972**, *29*, 454–482.

(18) Matar, E.; Bergeron, H.; Dulieu, F.; Chaabouni, H.; Accolla, M.; Lemaire, J. L. Gas temperature dependent sticking of hydrogen on cold amorphous water ice surfaces of interstellar interest. *The Journal of Chemical Physics* **2010**, *133*, 104507\1–10.

(19) Kay, B. D.; Lykke, K. R.; Creighton, J. R.; Ward, S. J. The influence of adsorbate-absorbate hydrogen bonding in molecular chemisorption: NH_3, HF, and H_2O on Au(111). *The Journal of Chemical Physics* **1989**, *91*, 5120–5121.

(20) Scoles, G. In *Atomic and Molecular Beam Methods, Volume 1*, Bassi, D., Buck, U., Laine, D., Eds.; Oxford University Press: New York, 1988, pp 14–53.

(21) Anderson, J. B.; Fenn, J. B. Velocity distributions in molecular beams from nozzle sources. *Physics of Fluids* **1965**, *8*, 780–787.

(22) Livesey, R. G. In *Foundations of vacuum science and technology*, Lafferty, J. M., Ed.; Wiley: New York, 1998, pp 81–105.

(23) Zheng, S. *Conductance Calculation - Molecular Flow, Long Tube of Circular Cross Section*; tech. rep.; 1993, pp 1–4.

(24) Saksaganskiĭ, G. L. In *Molecular flow in complex vacuum systems*; Gordon and Breach Science Publishers: New York, 1988, pp 1–31.

(25) Sibener, S. J.; Buss, R. J.; Cheuk Yiu Ng; Yuan, T. L. Development of a supersonic $O(^3P_J)$, $O(^1D_2)$ atomic oxygen nozzle beam source. *Review of Scientific Instruments* **1980**, *51*, 167–182.

(26) Garton, D. J.; Minton, T. K.; Alagia, M.; Balucani, N.; Casavecchia, P.; Volpi, G. G. Reactive scattering of ground-state and electronically excited oxygen atoms on a liquid hydrocarbon surface. *Faraday Discussions* **1997**, *108*, 387–399.

(27) Sibener, S. J.; Buss, R. J.; Casavecchia, P.; Hirooka, T.; Lee, Y. T. A crossed molecular beams investigation of the reactions $O(^3P)$ + C_6H_6, C_6D_6. *The Journal of Chemical Physics* **1980**, *72*, 4341–4349.

(28) Callen, B.; Griffiths, K.; Memmert, U.; Harrington, D.; Bushby, S.; Norton, P. The adsorption of water on Ni(110): Monolayer, bilayer and related phenomena. *Surface Science* **1990**, *230*, 159–174.

(29) Stevenson, K. P.; Kimmel, G. A.; Dohnalek, Z.; Smith, R. S.; Kay, B. D. Controlling the morphology of amorphous solid water. *Science* **1999**, *283*, 1505–1507.

(30) Gibson, K. D.; Langlois, G. G.; Li, W.; Killelea, D. R.; Sibener, S. J. Molecular interactions with ice: Molecular embedding, adsorption, detection, and release. *The Journal of Chemical Physics* **2014**, *141*, 18C514\1–11.

(31) Henderson, M. A. The interaction of water with solid surfaces: fundamental aspects revisited. *Surface Science Reports* **2002**, *46*, 1–308.

(32) Owen, T. The Contributions of Comets to Planets, Atmospheres, and Life: Insights from Cassini-Huygens, Galileo, Giotto, and Inner Planet Missions. *Space Science Reviews* **2008**, *138*, 301–316.

(33) Burke, D. J.; Brown, W. A. Ice in space: surface science investigations of the thermal desorption of model interstellar ices on dust grain analogue surfaces. *Physical Chemistry Chemical Physics* **2010**, *12*, 5947–5969.

(34) Ayotte, P.; Smith, R. S.; Stevenson, K. P.; Dohnálek, Z.; Kimmel, G. A.; Kay, B. D. Effect of porosity on the adsorption, desorption, trapping, and release of volatile gases by amorphous solid water. *Journal of Geophysical Research: Planets* **2001**, *106*, 33387–33392.

(35) Al-Halabi, A.; Van Dishoeck, E. F. Hydrogen adsorption and diffusion on amorphous solid water ice. *Monthly Notices of the Royal Astronomical Society* **2007**, *382*, 1648–1656.

(36) Hama, T.; Watanabe, N. Surface Processes on Interstellar Amorphous Solid Water: Adsorption, Diffusion, Tunneling Reactions, and Nuclear-Spin Conversion. *Chem. Rev* **2013**, *113*, 8783–8839.

(37) Al-Halabi, A.; van Dishoeck, E. F.; Kroes, G. J. Sticking of CO to crystalline and amorphous ice surfaces. *The Journal of Chemical Physics* **2004**, *120*, 3358–3367.

(38) Jenniskens, P.; Blake, D. F. Crystallization of Amorphous Water Ice in the Solar System. *The Astrophysical Journal* **1996**, *473*, 1104–1113.

(39) Jenniskens, P.; Blake, D. F.; Kouchi, A. In *Solar System Ices, Astrophysics and Space Science Library*; Springer, Dordrecht: Toulouse, France, 1998, pp 139–155.

(40) Angell, C. A. Amorphous Water. *Annu. Rev. Phys. Chem* **2004**, *55*, 559–83.

(41) Smith, R. S.; Petrik, N. G.; Kimmel, G. A.; Kay, B. D. Thermal and Nonthermal Physiochemical Processes in Nanoscale Films of Amorphous Solid Water. *Accounts of Chemical Research* **2012**, *45*, 33–42.

(42) Isokoski, K.; Bossa, J.-B.; Triemstra, T.; Linnartz, H. Porosity and thermal collapse measurements of H_2O, CH_3OH, CO_2, and H_2O:CO_2 ices. *Phys. Chem. Chem. Phys* **2014**, *16*, 3456–3465.

(43) Bossa, J.-B.; Isokoski, K.; Paardekooper, D. M.; Bonnin, M.; van der Linden, E. P.; Triemstra, T.; Cazaux, S.; Tielens, A. G. G. M.; Linnartz, H. Porosity measurements of interstellar ice mixtures using optical laser interference and extended effective medium approximations. *Astronomy & Astrophysics* **2014**, *561*, A136\1–8.

(44) Bartels-Rausch, T. et al. Ice structures, patterns, and processes: A view across the icefields. *Reviews of Modern Physics* **2012**, *84*, 885–944.

(45) Noble, J. A.; Martin, C.; Fraser, H. J.; Roubin, P.; Coussan, S. IR selective irradiations of amorphous solid water dangling modes: Irradiation vs annealing effects. *The Journal of Physical Chemistry C* **2014**, *118*, 20488–20495.

(46) He, J.; Acharyya, K.; Vidali, G. Sticking of Molecules on Nonporous Amorphous Water Ice. *The Astrophysical Journal* **2016**, *823*, 1–10.

(47) Batista, E. R.; Ayotte, P.; Bilić, A.; Kay, B. D.; Jónsson, H. What Determines the Sticking Probability of Water Molecules on Ice? *Physical Review Letters* **2005**, *95*, 223201\1–4.

(48) Watanabe, N.; Kouchi, A. Ice surface reactions: A key to chemical evolution in space. *Progress in Surface Science* **2008**, *83*, 439–489.

(49) Cardillo, M.; Balooch, M.; Stickney, R. Detailed balancing and quasi-equilibrium in the adsorption of hydrogen on copper. *Surface Science* **1975**, *50*, 263–278.

(50) Clark, R. N. In *The Science of Solar System Ices*, Gudipati, M. S., Castillo-Rogez, J., Eds.; Astrophysics and Space Science Library, Vol. 356; Springer: New York, NY, 2013, pp 3–46.

(51) Mousis, O.; Chassefière, E.; Holm, N. G.; Bouquet, A.; Waite, J. H.; Geppert, W. D.; Picaud, S.; Aikawa, Y.; Ali-Dib, M.; Charlou, J.-L.; Rousselot, P. Methane Clathrates in the Solar System. *Astrobiology* **2015**, *15*, 308–326.

(52) Dartois, E.; Muñoz Caro, G. M.; Deboffle, D.; Montagnac, G.; D'Hendecourt, L. Ultraviolet photoproduction of ISM dust. *Astronomy & Astrophysics* **2005**, *432*, 895–908.

(53) Langlois, G. G.; Li, W.; Gibson, K. D.; Sibener, S. J. Capture of Hyperthermal CO_2 by Amorphous Water Ice via Molecular Embedding. *The Journal of Physical Chemistry A* **2015**, *119*, 12238–12244.

(54) Gibson, K.; Killelea, D. R.; Becker, J. S.; Yuan, H.; Sibener, S. Energetic ballistic deposition of volatile gases into ice. *Chemical Physics Letters* **2012**, *531*, 18–21.

(55) Gibson, K. D.; Killelea, D. R.; Yuan, H.; Becker, J. S.; Sibener, S. J. Determination of the Sticking Coefficient and Scattering Dynamics of Water on Ice Using Molecular Beam Techniques. *J. Chem. Phys.* **2011**, *134*, 34703.

(56) Huthwelker, T.; Ammann, M.; Peter, T. The uptake of acidic gases on ice. *Chemical Reviews* **2006**, *106*, 1375–1444.

(57) Zubkov, T.; Smith, R. S.; Engstrom, T. R.; Kay, B. D. Adsorption, desorption, and diffusion of nitrogen in a model nanoporous material. I. Surface limited desorption kinetics in amorphous solid water. *The Journal of Chemical Physics* **2007**, *127*, 184707\1–11.

(58) Herrero, V. J.; Gaívez, S.; Mateánd Rafael Escribano, B. Interaction of CH_4 and H_2O in ice mixtures. *Phys. Chem. Chem. Phys* **2010**, *12*, 3164–3170.

(59) Rowland, B.; Devlin, J. P. Spectra of dangling OH groups at ice cluster surfaces and within pores of amorphous ice. *The Journal of Chemical Physics* **1991**, *94*, 812.

(60) Gálvez, Ó.; Maté, B.; Herrero, V. J.; Escribano, R. Spectroscopic Effects in CH_4/H_2O Ices. *The Astrophysical Journal* **2009**, *703*, 2101–2107.

(61) Killelea, D. R.; Gibson, K. D.; Yuan, H.; Becker, J. S.; Sibener, S. J. Dynamics of the sputtering of water from ice films by collisions with energetic xenon atoms. *The Journal of Chemical Physics* **2012**, *136*, 144705\1–8.

(62) Engquist, I.; Liedberg, B. D_2O Ice on Controlled Wettability Self-Assembled Alkanethiolate Monolayers: Cluster Formation and Substrate-Adsorbate Interaction. *J Phys Chem* **1996**, *100*, 20089–20096.

(63) Bergren, M. S.; Schuh, D.; Sceats, M. G.; Rice, S. A. The OH stretching region infrared spectra of low density amorphous solid water and polycrystalline ice Ih. *The Journal of Chemical Physics* **1978**, *69*, 3477–3482.

(64) Accolla, M.; Congiu, E.; Dulieu, F.; Manicò, G.; Chaabouni, H.; Matar, E.; Mokrane, H.; Lemaire, J. L.; Pirronello, V. Changes in the morphology of interstellar ice analogues after hydrogen atom exposure. *Physical Chemistry Chemical Physics* **2011**, *13*, 8037–8045.

(65) Maté, B.; Rodríguez-Lazcano, Y.; Herrero, V. J. Morphology and crystallization kinetics of compact (HGW) and porous (ASW) amorphous water ice. *Physical Chemistry Chemical Physics* **2012**, *14*, 10595–10602.

(66) Raut, U.; Famá, M.; Teolis, B. D.; Baragiola, R. A. Characterization of porosity in vapor-deposited amorphous solid water from methane adsorption. *The Journal of Chemical Physics* **2007**, *127*, 204713\1–6.

(67) Kimmel, G. A.; Stevenson, K. P.; Dohnálek, Z.; Smith, R. S.; Kay, B. D.; Smith, R. S.; Kay, B. D. Control of amorphous solid water morphology using molecular beams. I. Experimental results. *The Journal of Chemical Physics* **2001**, *114*, 5284–5294.

(68) Dohnálek, Z.; Kimmel, G. A.; Ayotte, P.; Smith, R. S.; Kay, B. D. The deposition angle-dependent density of amorphous solid water films. *The Journal of Chemical Physics* **2003**, *118*, 364–372.

(69) Smith, R. S.; Zubkov, T.; Dohnálek, Z.; Kay, B. D. The Effect of the Incident Collision Energy on the Porosity of Vapor-Deposited Amorphous Solid Water Films. *The Journal of Physical Chemistry B* **2009**, *113*, 4000–4007.

(70) Buch, V.; Devlin, J. P. Spectra of dangling OH bonds in amorphous ice: Assignment to 2- and 3-coordinated surface molecules. *The Journal of Chemical Physics* **1991**, *94*, 4091–4092.

(71) Cholette, F.; Zubkov, T.; Smith, R. S.; Dohnálek, Z.; Kay, B. D.; Ayotte, P. Infrared Spectroscopy and Optical Constants of Porous Amorphous Solid Water. *The Journal of Physical Chemistry B* **2009**, *113*, 4131–4140.

(72) Gibson, K. D.; Langlois, G. G.; Li, W.; Killelea, D. R.; Sibener, S. J. Molecular Interactions with Ice: Molecular Embedding, Adsorption, Detection, and Release. *J. Chem. Phys.* **2014**, *141*, 18C514.

(73) Itikawa, Y. Cross Sections for Electron Collisions with Nitrogen Molecules. *Journal of Physical and Chemical Reference Data* **2006**, *35*, 31–35.

(74) Orient, O. J.; Strivastava, S. K. Electron impact ionisation of H_2O, CO, CO_2 and CH_4. *Journal of Physics B: Atomic and Molecular Physics* **1987**, *20*, 3923–3936.

(75) Poll, H.; Winkler, C.; Margreiter, D.; Grill, V.; Märk, T. Discrimination effects for ions with high initial kinetic energy in a Nier-type ion source and partial and total electron ionization cross-sections of CF_4. *International Journal of Mass Spectrometry and Ion Processes* **1992**, *112*, 1–17.

(76) Smith, R. S.; May, R. A.; Kay, B. D. Desorption Kinetics of Ar, Kr, Xe, N_2, O_2, CO, Methane, Ethane, and Propane from Graphene and Amorphous Solid Water Surfaces. *The Journal of Physical Chemistry B* **2016**, *120*, 1979–1987.

(77) Morten Hundt, P.; Bisson, R.; Beck, R. D. The sticking probability of D_2O-water on ice: Isotope effects and the influence of vibrational excitation. *The Journal of Chemical Physics* **2012**, *137*, 074701–1–6.

(78) Fayolle, E. C.; Öberg, K. I.; Cuppen, H. M.; Visser, R.; Linnartz, H. Laboratory H_2O:CO_2 ice desorption data: entrapment dependencies and its parameterization with an extended three-phase model. *Astronomy & Astrophysics* **2011**, *529*, 1–11.

(79) Sandford, S. A.; Allamandola, L. J. The volume- and surface-binding energies of ice systems containing CO, CO_2 and H_2O. *Icarus* **1990**, *87*, 188–192.

(80) He, J.; Acharyya, K.; Vidali, G. Binding Energy of Molecules on Water Ice: Laboratory Measurements and Modeling. *The Astrophysical Journal* **2016**, *825*, 1–10.

(81) Hudson, R. L.; Gerakines, P. A.; Loeffler, M. J. Activation of weak IR fundamentals of two species of astrochemical interest in the T_d point group – the importance of amorphous ices. *Physical Chemistry Chemical Physics* **2015**, *17*, 12545–12552.

(82) Grundy, W.; Schmitt, B.; Quirico, E. The Temperature-Dependent Spectrum of Methane Ice I between 0.7 and 5 μm and Opportunities for Near-Infrared Remote Thermometry. *Icarus* **2002**, *155*, 486–496.

(83) Drobyshev, A.; Aldiyarov, A.; Sokolov, D. IR spectrometric studies of thin film cryovacuum condensates of methane and methane-water mixtures. *Low Temperature Physics* **2017**, *43*, 409–415.

(84) Laufer, D.; Kochavi, E.; Bar-Nun, A. Structure and dynamics of amorphous water ice. *Physical Review B* **1987**, *36*, 9219–9227.

(85) Kroes, G. J.; Andersson, S. Theory of Molecular Scattering from and Photochemistry at Ice Surfaces. *Proceedings of the International Astronomical Union* **2005**, *1*, 427–442.

(86) Pratihar, S.; Kohale, S. C.; Yang, L.; Manikandan, P.; Gibson, K. D.; Killelea, D. R.; Yuan, H.; Sibener, S. J.; Hase, W. L. Chemical Dynamics Simulations of High Energy Xenon Atom Collisions with the {0001} Surface of Hexagonal Ice. *The Journal of Physical Chemistry C* **2013**, *117*, 2183–2193.

(87) Johnson, R.; Famá, M.; Liu, M.; Baragiola, R.; Sittler, E.; Smith, H. Sputtering of ice grains and icy satellites in Saturn's inner magnetosphere. *Planetary and Space Science* **2008**, *56*, 1238–1243.

(88) Baragiola, R.; Vidal, R.; Svendsen, W.; Schou, J.; Shi, M.; Bahr, D.; Atteberrry, C. Sputtering of water ice. *Nuclear Instruments and Methods in Physics Research Section B: Beam Interactions with Materials and Atoms* **2003**, *209*, 294–303.

(89) Baragiola, R.; Atteberry, C.; Dukes, C.; Famá, M.; Teolis, B. Atomic collisions in solids: Astronomical applications. *Nuclear Instruments and Methods in Physics Research Section B: Beam Interactions with Materials and Atoms* **2002**, *193*, 720–726.

(90) Russo, M. F. J.; Szakal, C.; Kozole, J.; Winograd, N.; Garrison, B. J. Sputtering Yields for C_{60} and Au_3 Bombardment of Water Ice as a Function of Incident Kinetic Energy. *Analytical Chemistry* **2007**, *79*, 4493–4498.

(91) Palumbo, M. E.; Baratta, G. A.; Rangel, C.; Da Cruz, N. C.; Fulvio, D.; Garozzo, M.; Gomis, O.; Leto, G.; Spinella, F.; Strazzulla, G. Ion irradiation of astrophysical ices. *Journal of Physics Conference Series* **2008**, *101*, 1–8.

(92) Dartois, E.; Ding, J. J.; de Barros, A. L.; Boduch, P.; Brunetto, R.; Chabot, M.; Domaracka, A.; Godard, M.; Lv, X. Y.; Mejía Guamán, C. F.; Pino, T.; Rothard, H.; da Silveira, E. F.; Thomas, J. C. Swift heavy ion irradiation of water ice from MeV to GeV energies. *Astronomy & Astrophysics* **2013**, *557*, 1–8.

(93) Mejía, C.; de Barros, A.; Seperuelo Duarte, E.; da Silveira, E.; Dartois, E.; Domaracka, A.; Rothard, H.; Boduch, P. Compaction of porous ices rich in water by swift heavy ions. *Icarus* **2015**, *250*, 222–229.

(94) Raut, U.; Teolis, B. D.; Loeffler, M. J.; Vidal, R. A.; Famá, M.; Baragiola, R. A. Compaction of microporous amorphous solid water by ion irradiation. *The Journal of Chemical Physics* **2007**, *126*, 244511\1–5.

(95) Kimmel, G. A.; Dohnálek, Z.; Stevenson, K. P.; Smith, R. S.; Kay, B. D. Control of amorphous solid water morphology using molecular beams. II. Ballistic deposition simulations. *The Journal of Chemical Physics* **2001**, *114*, 5295–5303.

(96) Manca, C.; Martin, C.; Roubin, P. Spectroscopic and volumetric characterization of a non-microporous amorphous ice. *Chemical Physics Letters* **2002**, *364*, 220–224.

(97) Noble, J. A.; Congiu, E.; Dulieu, F.; Fraser, H. J. Thermal desorption characteristics of CO, O_2 and CO_2 on non-porous water, crystalline water and silicate surfaces at submonolayer and multilayer coverages. *Monthly Notices of the Royal Astronomical Society* **2012**, *421*, 768–779.

(98) Fillion, J.-H.; Amiaud, L.; Congiu, E.; Dulieu, F.; Momeni, A.; Lemaire, J.-L. D_2 desorption kinetics on amorphous solid water: from compact to porous ice films. *Physical Chemistry Chemical Physics* **2009**, *11*, 4396–4402.

(99) Hornekaer, L.; Baurichter, A.; Petrunin, V. V.; Luntz, A. C.; Kay, B. D.; Al-Halabi, A. Influence of surface morphology on D_2 desorption kinetics from amorphous solid water. *The Journal of Chemical Physics* **2005**, *122*, 124701\1–11.

(100) Al-Halabi, A.; Kleyn, A. W.; Kroes, G. J. Sticking of HCl to ice at hyperthermal energies: Dependence on incidence energy, incidence angle, and surface temperature. *The Journal of Chemical Physics* **2001**, *115*, 482–491.

(101) Paldor, A.; Toker, G.; Lilach, Y.; Asscher, M. Xe interacting with porous silicon. *Physical Chemistry Chemical Physics* **2010**, *12*, 6774–6781.

(102) Villalba, S.; Failache, H.; Lezama, A. Light-induced atomic desorption and diffusion of Rb from porous alumina. *Physical Review A* **2010**, *81*, 032901\1–8.

(103) Vidali, G.; Roser, J. E.; Ling, L.; Congiu, E.; Manic, G.; Pirronello, V. The formation of interstellar molecules via reactions on dust grain surfaces. *Faraday Discussions* **2006**, *133*, 125–135.

(104) Hornekaer, L.; Baurichter, A.; Petrunin, V. V.; Field, D.; Luntz, A. C. Importance of surface morphology in interstellar H_2 formation. *Science* **2003**, *302*, 1943–1946.

(105) Picaud, S.; Hoang, P. N. Adsorption of acetone molecules on proton ordered ice. A molecular dynamics study. *The Journal of Chemical Physics* **2000**, *112*, 9898–9908.

(106) Solomon, S. The mystery of the Antarctic Ozone "Hole". *Reviews of Geophysics* **1988**, *26*, 131–148.

(107) Orlando, J. J.; Tyndall, G. S. Laboratory Studies of Organic Peroxy Radical Chemistry: An Overview with Emphasis on Recent Issues of Atmospheric Significance. *Chem. Soc. Rev.* **2012**, *41*, 6294–6317.

(108) Zeits; Ortiz-Avilla, C. Y.; Squattrino, P. J.; Shieh, M.; Clearfield, A. Surface ozone depletion in Arctic spring sustained by bromine reactions on aerosols. *Nature* **1992**, *359*, 522–524.

(109) Finlayson-Pitts, B. J.; Livingston, F. E.; Berko, H. N. Ozone destruction and bromine photochemistry at ground level in the Arctic spring. *Nature* **1990**, *343*, 622–625.

(110) Pershin, A. A.; Torbin, A. P.; Mikheyev, P. A.; Kaiser, R. I.; Mebel, A. M.; Azyazov, V. N. Ozone destruction due to the recombination of oxygen atoms. *The Journal of Chemical Physics* **2021**, *155*.

(111) Brasseur, G.; Granier, C. Mount Pinatubo aerosols, chlorofluorocarbons, and ozone depletion. *Science* **1992**, *257*, 1239–1242.

(112) Bossa, J.-B. .-B.; Isokoski, K.; Paardekooper, D. M.; Bonnin, M.; van der Linden, E. P.; Triemstra, T.; Cazaux, S.; Tielens, a. G. G. M.; Linnartz, H. Porosity measurements of interstellar ice mixtures using optical laser interference and extended effective medium approximations. *Astronomy & Astrophysics* **2014**, *561*, A136.

(113) Thompson, R. S.; Brann, M. R.; Sibener, S. J. Sticking Probability of High-Energy Methane on Crystalline, Amorphous, and Porous Amorphous Ice Films. *The Journal of Physical Chemistry C* **2019**, *123*, 17855–17863.

(114) Almeida, G. C.; Pilling, S.; Andrade, D. P.; Castro, N. L. S.; Mendoza, E.; Boechat-Roberty, H. M.; Rocco, M. L. M. Photodesorption and photostability of acetone ices: Relevance to solid phase astrochemistry. *The Journal of Physical Chemistry C* **2014**, *118*, 6193–6200.

(115) Millar, T. J.; Herbst, E.; Charnley, S. B. The formation of oxygen-containing organic molecules in the Orion compact ridge. *Astrophysical Journal* **1991**, *369*, 147–156.

(116) Schaff, J. E.; Roberts, J. T. The adsorption of acetone on thin films of amorphous and crystalline ice. *Langmuir* **1998**, *14*, 1478–1486.

(117) Schaff, J. E.; Roberts, J. T. Toward an Understanding of the Surface Chemical Properties of Ice: Differences between the Amorphous and Crystalline Surfaces. *The Journal of Physical Chemistry* **1996**, *100*, 14151–14160.

(118) Schaff, J. E.; Roberts, J. T. Structure sensitivity in the surface chemistry of ice: Acetone adsorption on amorphous and crystalline ice films. *The Journal of Physical Chemistry* **1994**, *98*, 6900–6902.

(119) Zhang, X. K.; Lewars, E. G.; March, R. E.; Parnis, J. M. Vibrational spectrum of the acetone-water complex: a matrix isolation FTIR and theoretical study. *The Journal of Physical Chemistry* **2002**, *97*, 4320–4325.

(120) Mitlin, S.; Leung, K. T. Film Growth of Ice by Vapor Deposition at 128-185 K Studied by Fourier Transform Infrared Reflection-Absorption Spectroscopy: Evolution of the OH Stretch and the Dangling Bond with Film Thickness. *The Journal of Physical Chemistry B* **2002**, *106*, 6234–6247.

(121) Marinelli, F.; Allouche, A. An ab initio study of acetone and formaldehyde monolayers adsorbed on ice. *Chemical Physics* **2001**, *272*, 137–147.

(122) Souda, R. Adsorption, diffusion, dewetting, and entrapment of acetone on Ni(111), surface-modified silicon, and amorphous solid water studied by time-of-flight secondary ion mass spectrometry and temperature programmed desorption. *The Journal of Chemical Physics* **2011**, *135*, 164703.

(123) Smith, R. S.; Petrik, N. G.; Kimmel, G. A.; Kay, B. D. Thermal and Nonthermal Physiochemical Processes in Nanoscale Films of Amorphous Solid Water. *Accounts of Chemical Research* **2011**, *45*, 33–42.

(124) Accolla, M.; Congiu, E.; Dulieu, F.; Manicò, G.; Chaabouni, H.; Matar, E.; Mokrane, H.; Lemaire, J. L.; Pirronello, V. Changes in the morphology of interstellar ice analogues after hydrogen atom exposure. *Physical Chemistry Chemical Physics* **2011**, *13*, 8037–8045.

(125) Horimoto, N.; Kato, H. S.; Kawai, M. Stepwise morphological change of porous amorphous ice films observed through adsorption of methane. *The Journal of Chemical Physics* **2002**, *116*, 4375–1378.

(126) Pastega, D. F.; Lange, E.; Ameixa, J.; Barbosa, A. S.; Blanco, F.; Garcia, G.; Bettega, M. H. F.; Limão-Vieira, P.; Ferreira de Silva, F. Combined experimental and theoretical study on the differential elastic scattering cross sections for acetone by electron impact energy of 7.0-50 eV. *Physical Review A* **2016**, *93*, 032708–1–7.

(127) Max, J. J.; Chapados, C. Infrared spectroscopy of acetone-water liquid mixtures. I. Factor analysis. *The Journal of Chemical Physics* **2003**, *119*, 5632–5643.

(128) Rogers, J. D.; Rub, B.; Goldman, S.; Person, W. B. Measurement of infrared intensities for fundamental vibrations of gaseous acetone. *The Journal of Physical Chemistry* **2002**, *85*, 3727–3729.

(129) Syomin, D.; Koel, B. E. IRAS studies of the orientation of acetone molecules in monolayer and multilayer films on Au(111) surfaces. *Surface Science* **2002**, *498*, 53–60.

(130) Hudson, R. L.; Gerakines, P. A.; Ferrante, R. F. IR spectra and properties of solid acetone, an interstellar and cometary molecule. *Spectrochimica Acta Part A: Molecular and Biomolecular Spectroscopy* **2018**, *193*, 33–39.

(131) Andrade, D. P.; De Barros, A. L.; Ding, J.; Rothard, H.; Boduch, P.; da Silveira, E. F. Acetone degradation by cosmic rays in the solar neighbourhood and in the Galactic Centre. *Monthly Notices of the Royal Astronomical Society* **2014**, *444*, 3792–3801.

(132) Shin, S.; Kang, H.; Kim, J. S.; Kang, H. Phase Transitions of Amorphous Solid Acetone in Confined Geometry Investigated by Reflection Absorption Infrared Spectroscopy. *The Journal of Physical Chemistry B* **2014**, *118*, 13349–13356.

(133) Shin, S.; Kim, Y.; Kang, H.; Kang, H. Effect of Electric Field on Condensed-Phase Molecular Systems. I. Dipolar Polarization of Amorphous Solid Acetone. *The Journal of Physical Chemistry C* **2015**, *119*, 15588–15595.

(134) Vannice, M.; Erley, W.; Ibach, H. A RAIRS and HREELS study of acetone on Pt(111). *Surface Science* **1991**, *254*, 1–11.

(135) Brann, M. R.; Thompson, R. S.; Sibener, S. J. Reaction Kinetics and Influence of Film Morphology on the Oxidation of Propene Thin Films by O(^{3}P) Atomic Oxygen. *The Journal of Physical Chemistry C* **2020**, *124*, 7205–7215.

(136) Nagasawa, T.; Sato, R.; Hasegawa, T.; Numadate, N.; Shioya, N.; Shimoaka, T.; Hasegawa, T.; Hama, T. Absolute Absorption Cross Section and Orientation of Dangling OH Bonds in Water Ice. *The Astrophysical Journal Letters* **2021**, *923*, L3.

(137) Bahr, S.; Toubin, C.; Kempter, V. Interaction of methanol with amorphous solid water. *The Journal of Chemical Physics* **2008**, *128*, 134712-1–12.

(138) Narten, A. H.; Venkatesh, C. G.; Rice, S. A. Diffraction Pattern and Structure of Amoprhous Solid Water at 10 and 77 K. *The Journal of Chemical Physics* **2008**, *64*, 1106.

(139) Stähler, J.; Mehlhorn, M.; Bovensiepen, U.; Meyer, M.; Kusmierek, D. O.; Morgenstern, K.; Wolf, M. Impact of ice structure on ultrafast electron dynamics in D_2O clusters on Cu(111). *Physical Review Letters* **2007**, *98*, 206105.

(140) Rowland, B.; Devlin, J. P. Spectra of dangling OH groups at ice cluster surfaces and within pores of amorphous ice Infrared spectra of ice surfaces and assignment of surface-localized modes from simulated spectra of cubic ice Spectra of dangling OH groups at ice cluster surfaces an. *The Journal of Chemical Physics* **1991**, *941*, 812–813.

(141) Collings, M. P.; Anderson, M. A.; Chen, R.; Dever, J. W.; Viti, S.; Williams, D. A.; McCoustra, M. R. S. A laboratory survey of the thermal desorption of astrophysically relevant molecules. *Monthly Notices of the Royal Astronomical Society* **2004**, *354*, 1133–1140.

(142) Bolina, A. S.; Brown, W. A. Studies of physisorbed ammonia overlayers adsorbed on graphite. *Surface Science* **2005**, *598*, 45–56.

(143) Licandro, J.; Grundy, W. M.; Pinilla-Alonso, N.; Leisy, P. Visible spectroscopy of 2003 UB313: Evidence for N_2 ice on the surface of the largest TNO? *Astronomy & Astrophysics* **2006**, *458*, L5–8.

(144) Merlin, F.; Alvarez-Candal, A.; Delsanti, A.; Fornasier, S.; Barucci, M. A.; Demeo, F. E.; De Bergh, C.; Doressoundiram, A.; Quirico, E.; Schmitt, B. Stratification of methane ice on Eris' surface. *Astronomical Journal* **2009**, *137*, 315–328.

(145) Licandro, J.; Pinilla-Alonso, N.; Pedani, M.; Oliva, E.; Tozzi, G. P.; Grundy, W. M. The methane ice rich surface of large TNO 2005 FY9: A Pluto-twin in the trans-neptunian belt? *Astronomy & Astrophysics* **2006**, *445*, L35–38.

(146) Brown, M. E.; Trujillo, C. A.; Rabinowitz, D. L. Discovery of a Planetary-Sized Object in the Scattered Kuiper Belt. *The Astrophysical Journal* **2005**, *635*, 97–100.

(147) Dumas, C.; Merlin, F.; Barucci, M. A.; De Bergh, C.; Hainault, O.; Guilbert, A.; Vernazza, P.; Doressoundiram, A. Surface composition of the largest dwarf planet 136199 Eris (2003UB 313). *Astronomy & Astrophysics* **2007**, *471*, 331–334.

(148) Tokano, T.; McKay, C. P.; Neubauer, F. M.; Atreya, S. K.; Ferri, F.; Fulchignoni, M.; Niemann, H. B. Methane drizzle on Titan. *Nature* **2006**, *442*, 432–435.

(149) Owen, T.; Encrenaz, T. Element Abundances and Isotope Ratios in the Giant Planets and Titan. *Space Science Reviews* **2003**, *106*, 121–138.

(150) Merlin, F. New constraints on the surface of Pluto. *Astronomy & Astrophysics* **2015**, *39*, 1–9.

(151) Di, A.; Liberti, A. Isotope Effect on Physical Adsorption. *Transactions of the Faraday Society* **1970**, *66*, 967–975.

(152) Bossa, J. B.; Paardekooper, D. M.; Isokoski, K.; Linnartz, H. Methane ice photochemistry and kinetic study using laser desorption time-of-flight mass spectrometry at 20 K. *Physical Chemistry Chemical Physics* **2015**, *17*, 17346–17354.

(153) Wang, X.; Schultz, A. J.; Halpern, Y. Kinetics of methane hydrate formation from polycrystalline deuterated ice. *The Journal of Physical Chemistry A* **2002**, *106*, 7304–7309.

(154) Lanzerotti, L. J.; Brown, W. L.; Marcantonio, K. J. Experimental study of erosion of methane ice by energetic ions and some considerations for astrophysics. *The Astrophysical Journal* **1987**, *313*, 910–919.

(155) Jones, B. M.; Kaiser, R. I. Application of reflectron time-of-flight mass spectroscopy in the analysis of astrophysically relevant ices exposed to ionization radiation: Methane (CH_4) and D4-methane (CD_4) as a case study. *The Journal of Physical Chemistry Letters* **2013**, *4*, 1965–1971.

(156) Boogert, A. C.; Gerakines, P. A.; Whittet, D. C. Observations of the icy universe. *Annual Review of Astronomy and Astrophysics* **2015**, *53*, 541–581.

(157) Niemann, H. B. et al. The abundances of constituents of Titan's atmosphere from the GCMS instrument on the Huygens probe. *Nature* **2005**, *438*, 779–784.

(158) Abplanalp, M. J.; Góbi, S.; Kaiser, R. I. On the formation and the isomer specific detection of methylacetylene (CH_3CCH), propene (CH_3CHCH_2), cyclopropane (c-C_3H_6), vinylacetylene (CH_2CHCCH), and 1,3-butadiene ($CH_2CHCHCH$) from interstellar methane ice analogues. *Physical Chemistry Chemical Physics* **2019**, *21*, 5378–5393.

(159) Dartois, E.; Deboffle, D. Methane clathrate hydrate FTIR spectrum Implications for its cometary and planetary detection. *Astronomy & Astrophysics* **2008**, *490*, 19–22.

(160) He, J.; Gao, K.; Vidali, G.; Bennett, C. J.; Kaiser, R. I. Formation of Molecular Hydrogen from Methane Ice. *The Astrophysical Journal* **2010**, *721*, 1656–1662.

(161) Sakai, N.; Shirley, Y. L.; Sakai, T.; Hirota, T.; Watanabe, Y.; Yamamoto, S. Tentative detection of deuterated methane toward the low-mass protostar iras 04368+2557 in L1527. *The Astrophysical Journal Letters* **2012**, *758*, L4.

(162) Sakagami, H.; Tachikawa, M.; Ishimoto, T. Theoretical study of the H/D isotope effect of CH_4/CD_4 adsorption on a Rh(111) surface using a combined plane wave and localized basis sets method. *RSC Advances* **2021**, *11*, 10253–10257.

(163) Yaris, R.; Sams, J. R. Quantum treatment of the physical adsorption of isotopic species. *The Journal of Chemical Physics* **1962**, *37*, 571–576.

(164) Park, G. B.; Krüger, B. C.; Borodin, D.; Kitsopoulos, T. N.; Wodtke, A. M. Fundamental mechanisms for molecular energy conversion and chemical reactions at surfaces. *Reports on Progress in Physics* **2019**, *82*, 096401.

(165) Sibener, S. J.; Lee, Y. T. The internal and translational energy dependence of molecular condensation coefficients: SF_6 and CCl_4. *The Journal of Chemical Physics* **1994**, *101*, 1693–1703.

(166) Carlsson, A. F.; Madix, R. J. Alkane trapping onto structured alkane monolayers on Pt(111) at low temperature. *The Journal of Physical Chemistry B* **2000**, *104*, 12237–12249.

(167) Carlsson, A. F.; Madix, R. J. Trapping of Ar on well ordered Ar, Kr, and Xe overlayers on Pt(1 1 1) at 30 K. *Surface Science* **2000**, *470*, 62–80.

(168) Carlsson, A. F.; Madix, R. J. Dynamics of argon and methane trapping on Pt(111) at 30 and 50 K: energy scaling and coverage dependence. *Surface Science* **2000**, *458*, 91–105.

(169) Head-Gordon, M.; Tully, J. C. Competition between static and dynamical effects in adsorption: sticking of Ar on Ar-covered Ru(001). *Surface Science* **1992**, *268*, 113–126.

(170) Chesters, M. A.; De La Cruz, C.; Gardner, P.; McCash, E. M.; Prentice, J. D.; Sheppard, N. Infrared spectroscopic comparison of the chemisorbed species from ethene, propene, but-1-ene and cis- and trans-but-2-ene on Pt(111) and on a platinum/silica catalyst. *Journal of the Chemical Society, Faraday Transactions* **1990**, *86*, 2757–2763.

(171) Kao, C. L.; Carlsson, A.; Madix, R. J. Mass and lattice effects in trapping: Ar, Kr, and Xe on Pt(111), Pd(111), and Ni(111). *Surface Science* **2004**, *565*, 70–80.

(172) Krivchikov, A. I.; Stachowiak, P.; Pisarska, E.; Jezowski, A. Orientational isotopic effects in the thermal conductivity of CH_4/CD_4 solid solutions. *Low Temperature Physics* **2007**, *33*, 1061.

(173) Celli, V.; Himes, D.; Tran, P.; Toennies, J. P.; Wöll, C.; Zhang, G. Multiphonon processes in atom-surface scattering. *Physical Review Letters* **1991**, *66*, 3160–3163.

(174) Braun, J.; Glebov, A.; Graham, A. P.; Menzel, A.; Toennies, J. P. Structure and Phonons of the Ice Surface. *Physical Review Letters* **1998**, *80*, 2638–2641.

(175) Hu, X.; Hase, W. L.; Pirraglia, T. Vectorization of the general Monte Carlo classical trajectory program VENUS. *Journal of Computational Chemistry* **1991**, *12*, 1014–1024.

(176) Hase, W. L.; Duchovic, R. J.; Hu, X.; Komornicki, A.; Lim, K. F.; Lu, D.-H.; Peslherbe, G. H.; Swamy, K. N.; Vande Linde, S. R.; Varandas, A.; Wang, H.; Wolf, R. J. VENUS96: A general chemical dynamics computer program. *Quantum Chemistry Program Exchange (QCPE) Bulletin* **1996**, *16*, 43.

(177) Hase, W. L.; Date, N.; Bhuiyan, L. B.; Buckowski, D. G. Energy transfer in collisions of Ar with highly excited water and methane. *The Journal of Physical Chemistry* **1985**, *89*, 2502–2507.

(178) Duchovic, R. J.; Hase, W. L.; Bernhard Schlegel, H.; Frisch, M. J.; Raghavachari, K. Ab initio potential energy curve for CH bond dissociation in methane. *Chemical Physics Letters* **1982**, *89*, 120–125.

(179) Maynard-Casely, H. E.; Bull, C. L.; Guthrie, M.; Loa, I.; McMahon, M. I.; Gregoryanz, E.; Nelmes, R. J.; Loveday, J. S. The distorted close-packed crystal structure of methane A. *The Journal of Chemical Physics* **2010**, *133*, 064504\1–10.

(180) Heinz, H.; Vaia, R. A.; Farmer, B. L.; Naik, R. R. Accurate Simulation of Surfaces and Interfaces of Face-Centered Cubic Metals Using 12-6 and 9-6 Lennard-Jones Potentials. *The Journal of Physical Chemistry C* **2008**, *112*, 17281–17290.

(181) Darling, S. B.; Rosenbaum, A. W.; Wang, Y.; Sibener, S. J. Coexistence of the $(23 \times \sqrt{3})$ Au(111) Reconstruction and a Striped Phase Self-Assembled Monolayer. *Langmuir* **2002**, *18*, 7462–7468.

(182) Hellmann, R.; Bich, E.; Vogel, E. Ab Initio Intermolecular Potential Energy Surface and Second Pressure Virial Coefficients of Methane. *The Journal of Chemical Physics* **2008**, *128*, 214303\1–9.

(183) Severin, E. S. A Methane Molecule Adsorbed on a Graphite Surface. *Molecular Physics* **1980**, *41*, 1401–1418.

(184) Phillips, J. M.; Hammerbacher, M. D. Methane Adsorbed on Graphite. I. Intermolecular Potentials and Lattice Sums. *Physical Review B* **1984**, *29*, 5859–5864.

(185) Hirschfelder, J.; Curtiss, C.; Bird, R., *Molecular theory of gases and liquids*; 83; Wiley: New York, 1956; Vol. 17.

(186) Gibson, K. D.; Killelea, D. R.; Yuan, H.; Becker, J. S.; Pratihar, S.; Manikandan, P.; Kohale, S. C.; Hase, W. L.; Sibener, S. J. Scattering of High-Incident-Energy Kr and Xe from Ice: Evidence that a Major Channel Involves Penetration into the Bulk. *The Journal of Physical Chemistry C* **2012**, *116*, 14264–14273.

(187) Ma, X.; Paul, A. K.; Hase, W. L. Chemical Dynamics Simulations of Benzene Dimer Dissociation. *The Journal of Physical Chemistry A* **2015**, *119*, 6631–6640.

(188) Hariharan, S.; Majumder, M.; Edel, R.; Grabnic, T.; Sibener, S. J.; Hase, W. L. Exploratory Direct Dynamics Simulations of $^3O_2$ Reaction with Graphene at High Temperatures. *The Journal of Physical Chemistry C* **2018**, *122*, 29368–29379.

(189) Majumder, M.; Gibson, K. D.; Sibener, S. J.; Hase, W. L. Chemical Dynamics Simulations and Scattering Experiments for O_2 Collisions with Graphite. *The Journal of Physical Chemistry C* **2018**, *122*, 16048–16059.

(190) Furue, H.; LeBlanc, J. F.; Pacey, P. D.; Whalen, J. M. Analytical Potential Energy Surface for Methane in Terms of Interatomic Forces. *Chemical Physics* **1991**, *154*, 425–435.

(191) Maki, K.; Klein, M. L. Phonon Spectra of Methane Physisorbed on Graphite. *The Journal of Chemical Physics* **1981**, *74*, 1488–1494.

(192) Thomas, R. K. Neutron Scattering From Adsorbed Systems. *Progress in Solid State Chemistry* **1982**, *14*, 1–93.

(193) Saecker, M. E.; Nathanson, G. M. Collisions of Protic and Aprotic Gases with Hydrogen Bonding and Hydrocarbon Liquids. *The Journal of Chemical Physics* **1998**, *99*, 7056.

(194) DeSimone, A. J.; Olanrewaju, B. O.; Grieves, G. A.; Orlando, T. M. Photodissociation of Methyl Iodide Adsorbed on Low-Temperature Amorphous Ice Surfaces. *The Journal of Chemical Physics* **2013**, *138*, 084703.

(195) Owen, T.; Maillard, J. P.; De Bergh, C.; Lutz, B. L. Deuterium on mars: The abundance of HDO and the value of D/H. *Science* **1988**, *240*, 1767–1770.

(196) McCubbin, F. M.; Barnes, J. J. Origin and Abundances of H_2O in the Terrestrial Planets, Moon, and Asteroids. *Earth and Planetary Science Letters* **2019**, *526*, 115771\1–13.

(197) Davis, S.; Law, C.; Wang, H. Propene pyrolysis and oxidation kinetics in a flow reactor and laminar flames. *Combustion and Flame* **1999**, *119*, 375–399.

(198) Lissianski, V. V.; Zamansky, V. M.; Gardiner, W. C. In *Gas-phase combustion chemistry*, Gardiner, W. y., Ed.; Springer: New York, 2000, pp 1–123.

(199) Nguyen, T. L.; Peeters, J.; Vereecken, L. Quantum Chemical and Statistical Rate Study of the Reaction of O(^{3}P) with Allene: O-Addition and H-Abstraction Channels. *The Journal of Physical Chemistry A* **2006**, *110*, 12166–12176.

(200) Kahlich, D.; Wiechern, U.; Linder, J. In *Ullmann's Encyclopedia of Industrial Chemistry*; Wiley: Deerfield Beach, FL, 2012; Vol. 30, pp 313–335.

(201) Lambert, R. M.; Williams, F. J.; Cropley, R. L.; Palermo, A. Heterogeneous alkene epoxidation: past, present and future. *Journal of Molecular Catalysis A: Chemical* **2005**, *228*, 27–33.

(202) Kirschner, E. M. Production of Top 50 Chemicals Increased Substantially in 1994. *Chemical & Engineering News* **1995**, *73*, 16–20.

(203) Manz, T. A.; Yang, B. Selective oxidation passing through η3 -ozone intermediates: applications to direct propene epoxidation using molecular oxygen oxidant. *RSC Advances* **2014**, *4*, 27755–27774.

(204) Cavani, F. Catalytic selective oxidation: The forefront in the challenge for a more sustainable chemical industry. *Catalysis Today* **2010**, *157*, 8–15.

(205) Lee, H.-J.; Shi, T.-P.; Busch, D. H.; Subramaniam, B. A greener, pressure intensified propylene epoxidation process with facile product separation. *Chemical Engineering Science* **2007**, *62*, 7282–7289.

(206) Koda, S.; Endo, Y.; Tsuchiya, S.; Hirota, E. Branching Ratios in O(^{3}P) Reactions of Terminal Olefins Studied by Kinetic Microwave Absorption Spectroscopy. *J. Phys. Chem* **1991**, *95*, 1241–1244.

(207) Quandt, R.; Min, Z.; Wang, X.; Bersohn, R. Reactions of O(^{3}P) with Alkenes: H, CH_2CHO, CO, and OH Channels. *The Journal of Physical Chemistry A* **1998**, *102*, 60–64.

(208) Savee, J. D.; Welz, O.; Taatjes, C. A.; Osborn, D. L. New mechanistic insights to the O(^{3}P) + propene reaction from multiplexed photoionization mass spectrometry. *Physical Chemistry Chemical Physics* **2012**, *14*, 10410–10423.

(209) Cvetanović, R. J. In *Advances in Photochemistry*; John Wiley & Sons, Ltd: New York, 1963, pp 115–182.

(210) Morin, J.; Bedjanian, Y.; Romanias, M. N. Rate Constants of the Reactions of O(^{3}P) Atoms with Ethene and Propene over the Temperature Range 230-900 K. *International Journal of Chemical Kinetics* **2017**, *49*, 53–60.

(211) Leonori, F.; Balucani, N.; Nevrly, V.; Bergeat, A.; Falcinelli, S.; Vanuzzo, G.; Casavecchia, P.; Cavallotti, C. Experimental and Theoretical Studies on the Dynamics of the O(^{3}P) + Propene Reaction: Primary Products, Branching Ratios, and Role of Intersystem Crossing. *The Journal of Physical Chemistry C* **2015**, *119*, 14632–14652.

(212) Cavallotti, C.; Leonori, F.; Balucani, N.; Nevrly, V.; Bergeat, A.; Falcinelli, S.; Vanuzzo, G.; Casavecchia, P. Relevance of the Channel Leading to Formaldehyde + Triplet Ethylidene in the O(^{3}P) + Propene Reaction under Combustion Conditions. *The Journal of Physical Chemistry Letters* **2014**, *5*, 4213–4218.

(213) Hughes, A. N.; Scheer, M. D.; Klein, R. The Reaction between O(^{3}P) and Condensed Olefins below 100 K. *The Journal of Physical Chemistry* **1966**, *70*, 798–805.

(214) Klein, R.; Scheer, M. D. Mechanism of O(^{3}P) Addition to Condensed Films. II. Propene, 1-Butene, and Their Mixtures. *The Journal of Physical Chemistry* **1968**, *72*, 617–622.

(215) Cvetanović, R. J. Mechanism of the Interaction of Oxygen Atoms with Olefins. *The Journal of Chemical Physics* **1956**, *25*, 376–377.

(216) Atkinson, R.; Cvetanović, R. J. Activation Energies of the Addition of O(^{3}P) Atoms to Olefins. *The Journal of Chemical Physics* **1972**, *56*, 432–437.

(217) Ward, M. D.; Price, S. D. Thermal Reactions of Oxygen Atoms with Alkenes at Low Temperatures on Interstellar Dust. *The Astrophysical Journal* **2011**, *741*, 121–1–9.

(218) Herbst, E. Chemistry in the Interstellar Medium. *Annual Review of Physical Chemistry* **1995**, *46*, 27–54.

(219) Hickson, K. M.; Wakelam, V.; Loison, J.-C. Methylacetylene (CH_3CCH) and propene (C_3H_6) formation in cold dense clouds: A case of dust grain chemistry. *Molecular Astrophysics* **2016**, *3-4*, 1–9.

(220) Marcelino, N.; Cernicharo, J.; Agúndez, M.; Roueff, E.; Gerin, M.; Martín-Pintado, J.; Mauersberger, R.; Thum, C. Discovery of Interstellar Propylene (CH_2CHCH_3): Missing Links in Interstellar Gas-Phase Chemistry. *The Astrophysical Journal* **2007**, *665*, L127–L130.

(221) Nixon, C. A.; Jennings, D. E.; Bézard, B.; Vinatier, S.; Teanby, N. A.; Sung, K.; Ansty, T. M.; Irwin, P. G. J.; Gorius, N.; Cottini, V.; Coustenis, A.; Flasar, F. M. Detection of Propene in Titan's Stratosphere. *The Astrophysical Journal* **2013**, *776*, L14\1–6.

(222) Rawlings, J. M. C.; Williams, D. A.; Viti, S.; Cecchi-Pestellini, C. A radical route to interstellar propylene formation. *Monthly Notices of the Royal Astronomical Society: Letters* **2013**, *436*, L59–L63.

(223) Garrod, R. T.; Wakelam, V.; Herbst, E. Non-thermal desorption from interstellar dust grains via exothermic surface reactions. *Astronomy & Astrophysics* **2007**, *467*, 1103–1115.

(224) McGuire, B. A.; Carroll, P. B.; Loomis, R. A.; Finneran, I. A.; Jewell, P. R.; Remijan, A. J.; Blake, G. A. Discovery of the interstellar chiral molecule propylene oxide (CH_3CHCH_2O). *Science* **2016**, *352*, 1449–1452.

(225) Bergantini, A.; Abplanalp, M. J.; Pokhilko, P.; Krylov, A. I.; Shingledecker, C. N.; Herbst, E.; Kaiser, R. I. A Combined Experimental and Theoretical Study on the Formation of Interstellar Propylene Oxide (CH_3CHCH_2O)—A Chiral Molecule. *The Astrophysical Journal* **2018**, *860*, 108\1–15.

(226) Bergner, J. B.; Öberg, K. I.; Rajappan, M. Methanol Formation via Oxygen Insertion Chemistry in Ices. *The Astrophysical Journal* **2017**, *845*, 29\1–13.

(227) Bergner, J. B.; Öberg, K. I.; Rajappan, M. Oxygen Atom Reactions with C_2H_6, C_2H_4, and C_2H_2 in Ices. *The Astrophysical Journal* **2019**, *874*, 115\1–16.

(228) Nakao, F. Determination of the ionization gauge sensitivity using the relative ionization cross-section. *Vacuum* **1975**, *25*, 431–435.

(229) Stein, S. E. In *NIST Chemistry WebBook, NIST Standard Reference Database Number 69*, Linstrom, P. J., Mallard, W. G., Eds.; NIST standard reference database; National Institute of Standards and Technology: Gaithersburg MD.

(230) Sharpe, S. W.; Johnson, T. J.; Sams, R. L.; Chu, P. M.; Rhoderick, G. C.; Johnson, P. A. Gas-Phase Databases for Quantitative Infrared Spectroscopy. *Applied Spectroscopy* **2004**, *58*, 1452–1461.

(231) Es-sebbar, E.-t.; Alrefae, M.; Farooq, A. Infrared cross-sections and integrated band intensities of propylene: Temperature-dependent studies. *Journal of Quantitative Spectroscopy and Radiative Transfer* **2014**, *133*, 559–569.

(232) Sung, K.; Toon, G. C.; Drouin, B. J.; Mantz, A. W.; Smith, M. A. H. FT-IR measurements of cold propene (C_3H_6) cross-sections at temperatures between 150 and 299 K. *Journal of Quantitative Spectroscopy and Radiative Transfer* **2018**, *213*, 119–132.

(233) Alagia, M.; Aquilanti, V.; Ascenzi, D.; Balucani, N.; Cappelletti, D.; Cartechini, L.; Casavecchia, P.; Pirani, F.; Sanchini, G.; Volpi, G. G. Magnetic Analysis of Supersonic Beams of Atomic Oxygen, Nitrogen, and Chlorine Generated from a Radio-Frequency Discharge. *Israel Journal of Chemistry* **1997**, *37*, 329–342.

(234) Casavecchia, P.; Balucani, N.; Volpi, G. G. In *The Chemical Dynamics and Kinetics of Small Radicals*, Wagner, A., Liu, K., Eds.; World Scientific Publishing Company: Singapore, 1996; Chapter 9, pp 365–426.

(235) Itikawa, Y. Cross Sections for Electron Collisions with Nitrogen Molecules. *Journal of Physical and Chemical Reference Data* **2006**, *35*, 31–53.

(236) Itikawa, Y. Cross Sections for Electron Collisions with Oxygen Molecules. *Journal of Physical and Chemical Reference Data* **2009**, *38*, 1.

(237) Huang, W.; White, J. Propene adsorption on Ag(111): a TPD and RAIRS study. *Surface Science* **2002**, *513*, 399–404.

(238) Radziszewski, J. G.; Downing, J. W.; Gudipati, M. S.; Balaji, V.; Thulstrup, E. W.; Michl, J. How predictable are IR transition momemt directions? Vibrational transitions in propene and deuterated propenes. *Journal of the American Chemical Society* **1996**, *118*, 10275–10284.

(239) Barnes, A. J.; Howells, J. D. R. Infra-red cryogenic studies. Part 12.—Alkenes in argon matrices. *Journal of the Chemical Society, Faraday Transactions* **1973**, *69*, 532–539.

(240) Silvi, B.; Labarbe, P.; Perchard, J. Spectres de vibration et coordonnées normales de quatre espèces isotopiques de propène. *Spectrochimica Acta Part A: Molecular Spectroscopy* **1973**, *29*, 263–276.

(241) Huang, W.; White, J. Propene Oxidation on Ag(111): Spectroscopic Evidence of Facile Abstraction of Methyl Hydrogen. *Catalysis Letters* **2002**, *84*, 143–146.

(242) Davis, K. A.; Goodman, D. W. Propene Adsorption on Clean and Oxygen-Covered Au(111) and Au(100) Surfaces. *The Journal of Physical Chemistry B* **2000**, *104*, 8557–8562.

(243) McKean, D. CH stretching frequencies, bond lengths and strengths in acetone, acetaldehyde, propene and isobutene. *Spectrochimica Acta Part A: Molecular Spectroscopy* **1975**, *31*, 861–870.

(244) Tobin, M. The infrared spectrum of propylene oxide. *Spectrochimica Acta* **1960**, *16*, 1108–1110.

(245) Brown, N. F.; Barteau, M. A. Epoxides as probes of oxametallacycle chemistry on Rh(111). *Surface Science* **1993**, *298*, 6–17.

(246) Stacchiola, D.; Burkholder, L.; Tysoe, W. T. Enantioselective Chemisorption on a Chirally Modified Surface in Ultrahigh Vacuum: Adsorption of Propylene Oxide on 2-Butoxide-Covered Palladium(111). *Journal of the American Chemical Society* **2002**, *124*, 8984–8989.

(247) Dinger, A.; Lutterloh, C.; Biener, J.; Küppers, J. Adsorption of propylene oxide on Pt(111) surfaces and its reactions with gaseous and adsorbed H atoms. *Surface Science* **2000**, *449*, 1–18.

(248) Davis, J. L.; Barteau, M. A. Polymerization and decarbonylation reactions of aldehydes on the Pd(111) surface. *Journal of the American Chemical Society* **1989**, *111*, 1782–1792.

(249) Brown, N. F.; Barteau, M. A. Reactions of unsaturated oxygenates on rhodium(111) as probes of multiple coordination of adsorbates. *Journal of the American Chemical Society* **1992**, *114*, 4258–4265.

(250) Esan, D. A.; Trenary, M. Surface chemistry of propanal, 2-propenol, and 1-propanol on Ru(001). *Physical Chemistry Chemical Physics* **2017**, *19*, 10870–10877.

(251) Stacchiola, D.; Burkholder, L.; Tysoe, W. Structure and reactivity of propylene on clean and hydrogen-covered Pd(111). *Surface Science* **2003**, *542*, 129–141.

(252) Hudson, R.; Gerakines, P.; Moore, M. Infrared spectra and optical constants of astronomical ices: II. Ethane and ethylene. *Icarus* **2014**, *243*, 148–157.

(253) Dostert, K.-H.; O'Brien, C. P.; Mirabella, F.; Ivars-Barceló, F.; Schauermann, S. Adsorption of acrolein, propanal, and allyl alcohol on Pd(111): a combined infrared reflection–absorption spectroscopy and temperature programmed desorption study. *Physical Chemistry Chemical Physics* **2016**, *18*, 13960–13973.

(254) Browarzik, R.; Stuhl, F. Temperature Dependence of the Rate Constants for the Reactions of Oxygen Atoms with Ethene, Propene, and 1-Butene. *The Journal of Physical Chemistry* **1984**, *88*, 6004–6009.

(255) Atkinson, R.; Pitts, J. N. Absolute rate constants for the reaction of $O(^3P)$ atoms with a series of olefins over the temperature range 298–439 K. *The Journal of Chemical Physics* **1977**, *67*, 38–43.

(256) Ashford, R. D.; Ogryzlo, E. A. Temperature dependence of some reactions of singlet oxygen with olefins in the gas phase. *Journal of the American Chemical Society* **1975**, *97*, 3604–3607.

(257) Cvetanovic, R. J.; Singleton, D. L. Reaction of oxygen atoms with olefins. *Reviews of Chemical Intermediates* **1984**, *5*, 183–226.

(258) Cvetanović, R. J. The biradical intermediate in the addition of the ground state oxygen atoms, O(^{3}P), to olefins. *The Journal of Physical Chemistry* **1970**, *74*, 2730–2732.

(259) Leonori, F.; Occhiogrosso, A.; Balucani, N.; Bucci, A.; Petrucci, R.; Casavecchia, P. Crossed Molecular Beam Dynamics Studies of the O(3 P) + Allene Reaction: Primary Products, Branching Ratios, and Dominant Role of Intersystem Crossing. *The Journal of Physical Chemistry Letters* **2012**, *3*, 75–80.

(260) Rajak, K.; Maiti, B. Trajectory surface hopping study of the O(^{3}P) + C_2H_2 reaction dynamics: Effect of collision energy on the extent of intersystem crossing. *The Journal of Chemical Physics* **2014**, *140*, 44314.

(261) Atkinson, R. Gas-Phase Tropospheric Chemistry of Volatile Organic Compounds: 1. Alkanes and Alkenes. *Journal of Physical and Chemical Reference Data* **1997**, *26*, 215–290.

(262) Audouin, L.; Langlois, V.; Verdu, J.; de Bruijn, J. C. M. Role of oxygen diffusion in polymer ageing: kinetic and mechanical aspects. *Journal of Materials Science* **1994**, *29*, 569–583.

(263) Fairgrieve, S. P.; MacCallum, J. R. Diffusion-controlled oxidation of polymers: A mathematical model. *Polymer Degradation and Stability* **1985**, *11*, 251–265.

(264) Yousif, E., *Photostabilization of PVC: principles and applications*; Elsevier Applied Science: 2012, p 595.

(265) Pawela-Crew, J.; Madix, R. J. Anomalous effects of weak chemisorption on desorption kinetics of alkenes: The desorption of propylene and propane from Ag(110). *The Journal of Chemical Physics* **1996**, *104*, 1699–1708.

(266) Baker, T. A.; Xu, B.; Jensen, S. C.; Friend, C. M.; Kaxiras, E. Role of defects in propene adsorption and reaction on a partially O-covered Au(111) surface. *Catalysis Science & Technology* **2011**, *1*, 1166–1174.

(267) Nart, F. C.; Kelling, S.; Friend, C. M. Oxygen Lability on Thin Oxide Films on Mo(110). *The Journal of Physical Chemistry B* **2000**, *104*, 3212–3218.

(268) Giussani, E.; Fazzi, D.; Brambilla, L.; Caironi, M.; Castiglioni, C. Molecular Level Investigation of the Film Structure of a High Electron Mobility Copolymer via Vibrational Spectroscopy. *Macromolecules* **2013**, *46*, 2658–2670.

(269) Yates, J. T.; Madey, T. E., *Vibrational spectroscopy of molecules on surfaces*; Wiley: New York, 1987, p 468.

(270) Hudson, R.; Ferrante, R.; Moore, M. Infrared spectra and optical constants of astronomical ices: I. Amorphous and crystalline acetylene. *Icarus* **2014**, *228*, 276–287.

(271) Paz, Y.; Trakhtenberg, S.; Naaman, R. Reaction between O(^{3}P) and Organized Organic Thin-Films. *The Journal of Physical Chemistry* **1994**, *98*, 13517–13523.

(272) Paz, Y.; Trakhtenberg, S.; Naaman, R. Phase transitions in organized organic thin films as detected by their reactivity. *The Journal of Physical Chemistry* **1993**, *97*, 9075–9077.

(273) Paz, Y.; Trakhtenberg, S.; Naaman, R. Destruction of organized organic monolayers by oxygen atoms. *The Journal of Physical Chemistry* **1992**, *96*, 10964–10967.

(274) Gerakines, P. A.; Hudson, R. L. Infrared Spectra and Optical Constnats of Elusive Amorphous Methane. *The Astrophysical Journal* **2015**, *805*, L20\1–5.

(275) Alentiev, A.; Drioli, E.; Gokzhaev, M.; Golemme, G.; Ilinich, O.; Lapkin, A.; Volkov, V.; Yampolskii, Y. Gas permeation properties of phenylene oxide polymers. *Journal of Membrane Science* **1998**, *138*, 99–107.

(276) Tian Zhao, C.; Do Rosário Ribeiro, M.; De Pinho, M. N.; Subrahmanyam, V. S.; Gil, C. L.; De Lima, A. P. Structural characteristics and gas permeation properties of polynorbornenes with retained bicyclic structure. *Polymer* **2001**, *42*, 2455–2462.

(277) Kilburn, D.; Townrow, S.; Meunier, V.; Richardson, R.; Alam, A.; Ubbink, J. Organization and mobility of water in amorphous and crystalline trehalose. *Nature Materials* **2006**, *5*, 632–635.

(278) Smith, R. S.; Matthiesen, J.; Knox, J.; Kay, B. D. Crystallization Kinetics and Excess Free Energy of H_2O and D_2O Nanoscale Films of Amorphous Solid Water. *The Journal of Physical Chemistry A* **2011**, *115*, 5908–5917.

(279) Avrami, M. Kinetics of Phase Change. I General Theory. *The Journal of Chemical Physics* **1939**, *7*, 1103–1112.

(280) Rao, C. N. R.; Rao, K. J., *Phase transitions in solids: an approach to the study of the chemistry and physics of solids*; McGraw-Hill: 1978, p 330.

(281) Doremus, R. H., *Rates of phase transformations*; Academic Press: 1985, p 176.

(282) Pradell, T.; Crespo, D.; Clavaguera, N.; Clavaguera-Mora, M. T. Diffusion controlled grain growth in primary crystallization: Avrami exponents revisited. *Journal of Physics: Condensed Matter* **1998**, *10*, 3833–3844.

(283) Tait, S. L.; Dohnálek, Z.; Campbell, C. T.; Kay, B. D. n-alkanes on MgO(100). II. Chain length dependence of kinetic desorption parameters for small n-alkanes. *The Journal of Chemical Physics* **2005**, *122*, 164708\1–13.

(284) Dounce, S. M.; Mundy, J.; Dai, H.-L. Crystallization at the glass transition in supercooled thin films of methanol. *The Journal of Chemical Physics* **2007**, *126*, 191111\1–4.

(285) Safarik, D. J.; Meyer, R. J.; Mullins, C. B. Thickness dependent crystallization kinetics of sub-micron amorphous solid water films. *The Journal of Chemical Physics* **2003**, *118*, 4660–4671.

(286) Korobeinichev, O. P.; Chernov, A. A.; Sokolov, V. V.; Krasnoperov, L. N. Kinetics of destruction of diisopropyl methylphosphonate in corona discharge. *International Journal of Chemical Kinetics* **2002**, *34*, 331–337.

(287) Korobeinichev, O. P.; Ilyin, S. B.; Shvartsberg, V. M.; Chernov, A. A. The destruction chemistry of organophosphorus compounds in flames—I: quantitative determination of final phosphorus-containing species in hydrogen-oxygen flames. *Combustion and Flame* **1999**, *118*, 718–726.

(288) Ganesan, K.; Raza, S. K.; Vijayaraghavan, R. Chemical warfare agents. *Environmental Toxicology and Pharmacology* **2010**, *2*, 166–178.

(289) Jang, Y. J.; Kim, K.; Tsay, O. G.; Atwood, D. A.; Churchill, D. G. Destruction and Detection of Chemical Warfare Agents. *Chemical Reviews* **2011**, *111*, 5345–5403.

(290) Munro, N. B.; Talmage, S. S.; Griffin, G. D.; Waters, L. C.; Watson, A. P.; King, J. F.; Hauschild, V. The sources, fate, and toxicity of chemical warfare agent degradation products. *Environmental health perspectives* **1999**, *107*, 933–74.

(291) Council, N. R. In *Review of Acute Human-Toxicity Estimates for Selected Chemical-Warfare Agents*. National Academies Press: Washington, D.C., 1997, pp 28–34.

(292) Szinicz, L. History of chemical and biological warfare agents. *Toxicology* **2005**, *214*, 167–181.

(293) Aschmann, S. M.; Tuazon, E. C.; Atkinson, R. Atmospheric Chemistry of Diethyl Methylphosphonate, Diethyl Ethylphosphonate, and Triethyl Phosphate. *J. Phys. Chem. A* **2005**, *109*, 2282.

(294) Davis, E. D.; Gordon, W. O.; Wilmsmeyer, A. R.; Troya, D.; Morris, J. R. Chemical Warfare Agent Surface Adsorption: Hydrogen Bonding of Sarin and Soman to Amorphous Silica. *The Journal of Physical Chemistry Letters* **2014**, *5*, 1393–1399.

(295) Wilmsmeyer, A. R.; Gordon, W. O.; Davis, E. D.; Troya, D.; Mantooth, B. A.; Lalain, T. A.; Morris, J. R. Infrared spectra and binding energies of chemical warfare nerve agent simulants on the surface of amorphous silica. *The Journal of Physical Chemistry C* **2013**, *117*, 15685–15697.

(296) Zegers, E.; Fisher, E. Gas-Phase Pyrolysis of Diisopropyl Methylphosphonate. *Combustion and Flame* **1998**, *115*, 230–240.

(297) Kuiper, A. E. T.; van Bokhoven, J. J. G. M.; Medema, J. The role of heterogeneity in the kinetics of a surface reaction. I. Infrared characterization of the adsorption structures of organophosphonates and their decomposition. *Journal of Catalysis* **1976**, *43*, 154–167.

(298) Zegers, E. J. P.; Fisher, E. M. Gas-Phase Pyrolysis of Diethyl Methylphosphonate. *Combustion Science and Technology* **1996**, *116-117*, 69–89.

(299) Paciorek, K. J. L.; Kratzer, R. H.; Kaufman, J.; Nakahara, J. H.; Christos, T.; Hartstein, A. M. Thermal oxidative degradation studies of phosphate esters. *American Industrial Hygiene Association Journal* **1978**, *39*, 633–639.

(300) Lhomme, V.; Bruneau, C.; Soyer, N.; Brault, A. Thermal behavior of some organic phosphates. *Industrial & Engineering Chemistry Product Research and Development* **1984**, *23*, 98–102.

(301) Higgins, C. E.; Baldwin, W. H. The Thermal Decomposition of Tributyl Phosphate 1. *The Journal of Organic Chemistry* **1961**, *26*, 846–850.

(302) Bruneau, C.; Soyer, N.; Brault, A.; Kerfanto, M. Thermal degradation of tri-n-butyl phosphate. *Journal of Analytical and Applied Pyrolysis* **1981**, *3*, 71–81.

(303) Yang, L.; Shroll, R. M.; Zhang, J.; Lourderaj, U.; Hase, W. L. Theoretical investigation of mechanisms for the gas-phase unimolecular decomposition of DMMP. *The Journal of Physical Chemistry A* **2009**, *113*, 13762–71.

(304) Glaude, P.; Curran, H.; Pitz, W.; Westbrook, C. Kinetic study of the combustion of organophosphorus compounds. *Proceedings of the Combustion Institute* **2000**, *28*, 1749–1756.

(305) Glaude, P.; Melius, C.; Pitz, W.; Westbrook, C. Detailed chemical kinetic reaction mechanisms for incineration of organophosphorus and fluoroorganophosphorus compounds. *Proceedings of the Combustion Institute* **2002**, *29*, 2469–2476.

(306) Langlois, G. G.; Thompson, R. S.; Li, W.; Sibener, S. J. Oxidation, Destruction, and Persistence of Multilayer Dimethyl Methylphosphonate Films during Exposure to O(^{3}P) Atomic Oxygen. *The Journal of Physical Chemistry C* **2016**, *120*, 16863–16870.

(307) Thompson, R. S.; Langlois, G. G.; Sibener, S. J. Oxidative Destruction of Multilayer Diisopropyl Methylphosphonate Films by O(^{3}P) Atomic Oxygen. *The Journal of Physical Chemistry B* **2017**, *122*, 455–463.

(308) Gibson, K. D.; Sibener, S. J. Fate of Some Chemical Warfare Simulants Adsorbed on an Inert Surface when Exposed to Rapid Laser Initiated Heating. *The Journal of Physical Chemistry C* **2018**, *122*, 24684–24689.

(309) Oppelt, E. T. Incineration Of Hazardous Waste. *Journal of Air & Waste Management Association* **1987**, *37*, 558–586.

(310) Bulgakova, N.; Bulgakov, A. Pulsed laser ablation of solids: transition from normal vaporization to phase explosion. *Applied Physics A Materials Science & Processing* **2001**, *73*, 199–208.

(311) Smausz, T.; Kondász, B.; Gera, T.; Ajtai, T.; Utry, N.; Pintér, M.; Kiss-Albert, G.; Budai, J.; Bozóki, Z.; Szabó, G.; Hopp, B. Determination of UV–visible–NIR absorption coefficient of graphite bulk using direct and indirect methods. *Applied Physics A* **2017**, *123*, 633.

(312) Schultrich, B. In *Tetrahedrally Bonded Amorphous Carbon Films*; Springer, Berlin, Heidelberg: 2018, pp 585–631.

(313) Kononenko, V. V.; Kononenko, T. V.; Pimenov, S. M.; Sinyavskii, M. N.; Konov, V. I.; Dausinger, F. Effect of the pulse duration on graphitisation of diamond during laser ablation. *Quantum Electronics* **2005**, *35*, 252–256.

(314) Ready, J. F., *Effects of High-Power Laser Radiation*; Academic Press: New York, NY, 1971, pp 68–125.

(315) Windholz, R.; Molian, P. A. Nanosecond pulsed excimer laser machining of chemically vapour-deposited diamond and graphite: Part II Analysis and modelling. *Journal of Materials Science* **1998**, *33*, 523–528.

(316) Gibb, S.; Strimmer, K. MALDIquant: a versatile R package for the analysis of mass spectrometry data. *Bioinformatics* **2012**, *28*, 2270–2271.

(317) Savitzky, A.; Golay, M. J. E. Smoothing and Differentiation of Data by Simplified Least Squares Procedures. *Analytical Chemistry* **1964**, *36*, 1627–1639.

(318) Korobeinichev, O. P.; Shvartsberg, V. M.; Shmakov, A. G. The Chemistry of Combustion of Organophosphorus Compounds. *Russ. Chem. Rev.* **2007**, *76*, 1094.

(319) Radziemski, L. J. Laser-induced photodestruction of the organo-phosphates: DIMP and DMMP. *Journal of Environmental Science and Health, Part B* **1981**, *16*, 337–361.

(320) Templeton, M.; Weinberg, W. Decomposition of phosphonate esters adsorbed on aluminum oxide. *Journal of the American Chemical Society* **1985**, *107*, 774–779.

(321) Guilbault, G. G.; Scheide, E.; Das, J. An Experimental Technique for Studying the Infrared Spectrum of Chemisorbed Compounds. *Spectroscopy Letters* **1968**, *1*, 167–175.

(322) Crooks, R. M.; Yang, H. C.; McEllistrem, L. J.; Thomas, R. C.; Ricco, A. J. Interactions between self-assembled monolayers and an organophosphonate Detailed study using surface acoustic wave-based mass analysis, polarization modulation-FTIR spectroscopy and ellipsometry. *Faraday Discussions* **1997**, *107*, 285–305.

(323) Van Hest, M. F. A. M.; de Graaf, A.; van de Sanden, M. C. M. Use of in situ FTIR spectroscopy and mass spectrometry in an expanding hydrocarbon plasma. *Plasma Sources Science and Technology* **2000**, *9*, 615–624.

(324) Kaiser, R. I.; Roessler, K. Theoretical and Laboratory Studies on the Interaction of Cosmic-Ray Particles with Interstellar Ices. III. Suprathermal Chemistry–Induced Formation of Hydrocarbon Molecules in Solid Methane (CH_4), Ethylene (C_2H_4), and Acet. *The Astrophysical Journal* **1998**, *503*, 959–975.

(325) Yuan, B.; Eilers, H. T-jump pyrolysis and combustion of diisopropyl methylphosphonate. *Combustion and Flame* **2019**, *199*, 69–84.

(326) Shan, X.; Vincent, J. C.; Kirkpatrick, S.; Walker, M. D.; Sambrook, M. R.; Clary, D. C. A Combined Theoretical and Experimental Study of Sarin (GB) Decomposition at High Temperatures. *The Journal of Physical Chemistry A* **2017**, *121*, 6200–6210.

(327) Ash, T.; Debnath, T.; Banu, T.; Das, A. K. Exploration of Unimolecular Gas-Phase Detoxication Pathways of Sarin and Soman: A Computational Study from the Perspective of Reaction Energetics and Kinetics. *Chemical Research in Toxicology* **2016**, *29*, 1439–1457.

(328) Hahn, D. K.; RaghuVeer, K. S.; Ortiz, J. V. Computational Tests of Models for Kinetic Parameters of Unimolecular Reactions of Organophosphorus and Organosulfur Compounds. *The Journal of Physical Chemistry A* **2011**, *115*, 14143–14152.

(329) Hidaka, Y.; Nakamura, T.; Tanaka, H.; Jinno, A.; Kawano, H.; Higashihara, T. Shock tube and modeling study of propene pyrolysis. *International Journal of Chemical Kinetics* **1992**, *24*, 761–780.

(330) Milne, G. S.; Steel, C. The Gas-Phase Oxidation of Photochemically Generated Isopropyl Radicals. *The Journal of Physical Chemistry* **1968**, *72*, 3754–3761.

(331) Atkinson, R.; Carter, W. P. L. Reactions of alkoxy radicals under atmospheric conditions: The relative importance of decomposition versus reaction with O_2. *Journal of Atmospheric Chemistry* **1991**, *13*, 195–210.

(332) Wijnen, M. J. H. Reactions of Alkoxy Radicals. VI. Photolysis of Isopropyl Propionate. *Journal of the American Chemical Society* **1960**, *28*, 1847–1849.

(333) Brann, M. R.; Hansknecht, S. P.; Muir, M.; Sibener, S. J. Acetone–Water Interactions in Crystalline and Amorphous Ice Environments. *The Journal of Physical Chemistry A* **2022**, *126*, 2729–2738.

(334) Brann, M. R.; Hansknecht, S. P.; Ma, X.; Sibener, S. J. Differential Condensation of Methane Isotopologues Leading to Isotopic Enrichment under Non-equilibrium Gas–Surface Collision Conditions. *The Journal of Physical Chemistry A* **2021**, *125*, 9405–9413.

(335) Thompson, R. S.; Brann, M. R.; Purdy, E. H.; Graham, J. D.; McMillan, A. A.; Sibener, S. J. Rapid Laser-Induced Temperature Jump Decomposition of the Nerve Agent Simulant Diisopropyl Methylphosphonate under Atmospheric Conditions. *The Journal of Physical Chemistry C* **2019**, *123*, 21564–21570.